UNIVERSIDAD AUTÓNOMA DE MADRID

Facultad de Ciencias

Departamento de Química-Física Aplicada

Carbohidratos prebióticos: mecanismos de digestión, modulación de la microbiota y síntesis de nuevos oligosacáridos

PABLO GALLEGO LOBILLO

Tesis Doctoral

Madrid, 2021

CONSEJO SUPERIOR DE INVESTIGACIONES CIENTÍFICAS

INSTITUTO DE INVESTIGACIÓN EN CIENCIAS DE LA ALIMENTACIÓN

UNIVERSIDAD AUTÓNOMA DE MADRID

Facultad de Ciencias

Departamento de Química-Física Aplicada

Carbohidratos prebióticos: mecanismos de digestión, modulación de la microbiota y síntesis de nuevos oligosacáridos

PABLO GALLEGO LOBILLO

Tesis Doctoral presentada en cumplimiento
de los requisitos para optar al grado de Doctor
por la Universidad Autónoma de Madrid (UAM)
Madrid, 2021

Directores de Tesis:

Dra. María del Mar Villamiel Guerra

Dr. Oswaldo Hernández Hernández

(Consejo Superior de Investigaciones Científicas, CIAL, CSIC-UAM)

El tiempo me dijo que
era hora de bajarme del tren
y el tiempo, sólo el tiempo,
me empujó a volver

AGRADECIMIENTOS

Cuando te das cuenta que la ardua tarea de la Tesis Doctoral está llegando al final, el sinfín de sentimientos que aparecen son inexplicables. Al ver cómo mis compañeros y amigos del laboratorio iban doctorándose uno a uno, siempre me costaba imaginarme a mi mismo allí arriba, como una tarea inalcanzable. Sin embargo, al parecer, estoy aquí, he conseguido sobrevivir y llegar al final, o al menos lo parece. Y durante este camino, muchas personas han estado ahí y jamás se me ocurriría finalizar la tesis sin dedicarles unas palabras.

Como mis progenitores científicos, en primera posición y como grandes mentores, tienen que estar mis directores de tesis, **Mar y Oswaldo**. Quién diría que ese dificultoso TFM iba dar lugar a esto, a pesar de todos los óbstaculos, los cambios de temática, los infinitos papeles y becas, siempre habéis confiado en mi, apostastéis como nadie. Qué suerte tuve. **Mar**, la guía, la capitana del barco, el motivo por el cual me interesé por el grupo, y su calentamiento óhmico por supuesto. Siempre creíste en mi, me insististe a pesar de los problemas que surgieron, porque sabías que valía para ello. Esto es una carrera de fondo. **Oswaldo**, el primero de a bordo, al pie del cañón en el laboratorio, gracias por enseñarme a ser resolutivo, a no quedarme parado viendo cómo se solucionaban los problemas, a ser uno con el laboratorio. A pesar de ser tan meticuloso, todas las cuantificaciones siempre quedaron de 10. Gracias por todo, la tesis corta ha resultado ser única.

Al resto del grupo de Carbohidratos: gracias **Toñi**, por apostar por mi en ese pequeño comienzo de ciencia. Gracias **Javi, Nieves y Agustín**, por el apoyo durante todos estos años y por tenerme siempre en cuenta.

Pero durante estos años, en el barco, en el laboratorio, grandes amigos han estado junto a mi. Qué decir de mis dos grandes pilares, esas dos chicas que son en realidad gigantes, que trabajan como nadie y han sido imprescindibles. Nunca dudaron de mi. **Paloma**, experta en su trabajo, experta en cine, nadie ha valorado mi trabajo tanto como tú y tú también deberías hacer lo mismo. Esos debates sobre la vida y los papers y nuestras peleas para ser los reyes del gases. Y **Nerea**, mi ídolo a seguir, siempre dispuesta a

ayudar, siempre pendiente de todo y de todos, reina del HPLC. Por ser capaz de entenderme, por enseñarme ciencia y conocimiento popular. No hay nadie como tú. Mi **Pablo**, como tú ninguno, compañero nutri, de Amaral y hasta de bata, por toda esa energía positiva que transmites y por ser mi único rey**. Álvaro**, mi tercer director, gracias por enseñarme todo lo que sabes y por estar ahí en cada protocolo y procedimiento, somos los reyes de la digestión. **Paula, Agustina e Inés**, por los buenos momentos y por todo vuestro apoyo; y no olvidar a **Mayte, Cristina y Ana**, por estar siempre dispuestas a ayudar.

Después de cada día en el laboratorio, las risas y la tranquilidad estaban aseguradas. **Javier y Luzia**, por las tardes de juegos y vídeos chorras, por ayudarme a desconectar y disfrutar. Y **MA**, por ser el apoyo incodicional en todos los momentos, buenos y malos, y por ayudarme a crecer y a encontrarme a mí mismo.

Qué suerte que, al volver a mi ciudad, a Sevilla, siempre podía sentirme como en casa, como en ningún sitio. Los que saben perfectamente cómo estoy sin ni siquiera verme la cara. A mis padres, **Alberto y Rosario**, mi hermano, **Sergio**, y mi abuela, **Mª Jesús**, por ser mis superhéroes, por ser capaz de afrontar toda dificultad e incertidumbre constante. Los ánimos nunca faltaron, me salvaron cuando estaba en lo más bajo y gracias a ellos, pude volver a construir mi camino y estar aquí ahora. Familia no hay más que una, y no puedo describir lo afortunado que soy por ello. Gracias. Y al nombrar a **Sergio, Eva** tampoco puede faltar, por simplemente aguantarme. Y cómo no agradecer a mi tío, **Pepe**, el gran impulsor de mi carrera científica, esas conversaciones que me hiceron enamorarme de la ciencia, esos artículos científicos que parecía que no tenían fin y por ser mi referente. No me olvido de nombrar al resto de mi familia, mis padrinos, primos, tíos y amigos, **Grecia, Álvaro, Javi**, que nunca dudaron de mi.

También quería dedicar unas palabras a aquellas personas que ya no están, mis abuelos, que nos cuidan cada día y velan por nosotros. Ha costado muchísimo, pero estamos aquí, las caídas y los errores permanecen, y el objetivo final lo he podido alcanzar.

Por todos vosotros, GRACIAS.

Pablo

ÍNDICE DE CONTENIDOS

Índice de Tablas

.

Índice de Figuras

Abreviaturas y Acrónimos

ABREVIATURAS Y ACRÓNIMOS

α-GOS	Alfa-galactooligosacáridos
Ara	Arabinosa
AOAC	(*Association of Official Analytical Chemists*) Asociación Oficial de Química Analítica
AOM	Azoximetano
BBMV	(*Brush Border Membrane Vesicles*) Vesículas de la membrana del borde en cepillo
CP	(*Citrus Pectin*) Pectina de Cítricos
DM	(*Degree of methyl-esterification*) Grado de metil-esterificación
DP	(*Degree of polimerization*) Grado de polimerización
DSS	Dextrano Sulfato de Sodio
ECV	Enfermedades Cardiovasculares
EFSA	(*European Food Safety Authority*) Agencia Europea de Seguridad Alimentaria
ELA	Esclerosis Lateral Amiotrófica
ELSD	(*Evaporative Light Scattering Detector*) Detector Evaporativo de Dispersión de Luz
FAO	(*Food and Agriculture Organization of the United Nations*) Organización de las Naciones Unidas para la Alimentación y la Agricultura
FOS	Fructooligosacáridos
Fru	Fructosa
GalA	Ácido Galacturónico
Gal	Galactosa
GC-FID	(*Gas Chromatography with Flame Ionization Detector*) Cromatografía de Gases con Detector de Ionización de Llama
GC-MS	(*Gas Chromatography-Mass Spectrometry*) Cromatografía de Gases-Espectrometría de Masas
GI	Gastrointestinal
GOS	Galactooligosacáridos
Glc	Glucosa
HG	Homogalacturonano

HDMS	(*Hexamethyldisylazane*) Hexametildisilazano
HILIC	(*Hydrophilic Interaction Liquid Chromatography*) Cromatografía Líquida de Interacción Hidrofílica
HPLC	(*High Performance Liquid Chromatography*) Cromatografía Líquida de Alta Eficiencia
HPSEC	(*High Performance Size Exclusion Chromatography*) Cromatografía de Exclusión Molecular de Alta Eficiencia
IS	(*Internal Standard*) Patrón Interno
ISAPP	(*International Scientific Association for Probiotics and Prebiotics*) Asociación Científica Internacional para Probióticos y Prebióticos
$\mathbf{k_{obt}}$	Constante de hidrólisis enzimática
Lac	Lactosa
Lu	Lactulosa
Mal	Maltosa
Man	Manosa
MCP	(*Modified Citrus Pectin*) Pectina Modificada de Cítricos
MP	(*Modified Pectin*) Pectina Modificada
$\mathbf{M_w}$	(*Molecular Weight*) Peso Molecular
NMR	(*Nuclear Magnetic Resonance*) Resonancia Magnética Nuclear
OMS	Organización Mundial de la Salud
OsLu	Oligosacáridos derivados de Lactulosa
RFOs	(*Raffinose Family Oligosaccharides*) Oligosacáridos de la familia de la rafinosa
RG-I	Ramnogalacturonano-I
RG-II	Ramnogalacturonano-II
Rha	Ramnosa
RID	(*Refractive Index Detector*) Detector de Índice de Refracción
RMN	Resonancia Magnética Nuclear
RSIE	(*Rat Small Intestine Extract*) Extracto de Intestino Delgado de Rata
Sac	Sacarosa
SCFA	(*Short-Chain Fatty Acids*) Ácidos Grasos de Cadena Corta

SD	(*Standard Deviation*) Desviación Estándar
$t_{1/2}$	Tiempo de vida media
TFA	(*Trifluoroacetic Acid*) Ácido Trifluoroacético
TMSO	(*Trimethylsilylated Oximes*) Trimetilsilil Oximas
Tre	Trehalosa
UV	Ultravioleta
Xyl	Xilosa

Resumen / Abstract

Resumen

Dado el papel esencial de la microbiota intestinal en el organismo humano, su modulación resulta imprescindible, siendo los prebióticos unos de los compuestos más importantes que contribuyen a mantener su equilibrio y estado de salud. Aunque se han llevado a cabo numerosas investigaciones sobre los prebióticos y la microbiota, no ha sido hasta muy recientemente cuando se ha prestado atención a su digestión. Los métodos tradicionales de digestión de ingredientes y alimentos se centran principalmente en proteínas y almidón, siendo el protocolo InfoGest, basado en el empleo de soluciones digestivas, el más ampliamente aceptado. Además, existen otros tales como el método oficial de la Asociación Oficial de Química Analítica, más específico para fibra dietética. Las limitaciones de estos métodos para la digestión de carbohidratos podrían sustentarse en la ausencia de las enzimas disacaridasas presentes en la membrana del borde en cepillo de los enterocitos, no permitiendo distinguir entre carbohidratos digeribles y no digeribles. Estudios previos de nuestro grupo de investigación demostraron la idoneidad de un método *in vitro* basado en la utilización de un extracto acétonico de intestino delgado de rata para evaluar la digestibilidad de carbohidratos de la dieta y prebióticos reconocidos. A pesar de los resultados prometedores, no se estudió la cinética enzimática y su aplicación a carbohidratos más complejos.

El primer bloque de la presente Tesis Doctoral se basa en la ampliación del conocimiento sobre este método *in vitro* con extracto de intestino delgado de rata para evaluar la digestibilidad de carbohidratos prebióticos, y su comparación con el protocolo InfoGest (*Capítulos 1-3*). En primer lugar, se realizó un estudio cinético de las enzimas intestinales de dicho extracto de rata, optimizándose las condiciones de máxima hidrólisis de un disacárido digerible (lactosa). Además, se observó la elevada resistencia a las enzimas intestinales de la lactulosa, prebiótico reconocido, remarcando la importancia de la estructura química. Seguidamente, dado que la mayoría de carbohidratos prebióticos estudiados en la literatura eran de baja masa molecular, se analizaron mezclas complejas de prebióticos comerciales de mayor masa molecular, como fructanos y oligosacáridos emergentes, como α-galactooligosacáridos. Los

resultados indicaron una potencial versatilidad enzimática por parte de las disacaridasas, ya que fueron capaces de hidrolizar diferentes enlaces químicos de los prebióticos. A continuación, se consideró necesario hacer una comparación con el protocolo InfoGest en polisacáridos, como almidón y pectinas. Mediante el método InfoGest apenas se consiguió degradación de los carbohidratos en las diferentes fases del proceso. En cambio, la hidrólisis intestinal de todos los compuestos se vio siempre incrementada significativamente en presencia del extracto de intestino delgado de rata, lo que podría suponer una aproximación más real a la digestión intestinal.

El efecto de las pectinas sobre la microbiota intestinal fue evaluado mediante un ensayo *in vivo*, tanto en ratas sanas como con cáncer colorrectal, tal y como se muestra en el segundo bloque de la Tesis Doctoral (*Capítulo 4*). En las ratas enfermas se detectó un estado de disbiosis en la microbiota intestinal que no mejoró con la ingestión de pectinas de cítricos; sin embargo, sí se encontró un efecto positivo en cuanto al nivel de triglicéridos en sangre y glucemia.

Por otra parte, el creciente interés en la obtención de nuevos prebióticos con propiedades bioactivas adicionales dio lugar al tercer bloque de la Tesis, que abarca la síntesis de derivados de la trehalosa (*Capítulo 5*). La trehalosa, ingrediente alimentario ampliamente utilizado, posee efectos beneficiosos en la salud metabólica y frente a enfermedades neurodegenerativas. Sin embargo, puede llegar al colon y ejercer efectos negativos, en el caso de infecciones por *Clostridium difficile.* En este último capítulo se llevó a cabo la síntesis, purificación y caracterización de nuevos oligosacáridos derivados de trehalosa con potencial prebiótico.

Los resultados obtenidos en esta Tesis Doctoral amplian los conocimientos existentes en el campo de los prebióticos, con especial énfasis en la aplicación de métodos de digestión específicos y válidos para carbohidratos digeribles y no digeribles de diferente grado de polimerización y enlaces glicosídicos; y en la síntesis de nuevas moléculas, teóricamente más resistentes a la digestión, con importantes propiedades, no sólo a nivel intestinal.

ABSTRACT

Given the essential role of the intestinal microbiota in the human organism, its modulation is essential, and prebiotics are one of the most important compounds that contribute to maintaining its balance and state of health. Although several investigations have been carried out on prebiotics and microbiota, it is, nowadays, when more attention has been paid to their digestion. Traditional methods of ingredients and food digestion focus mainly on protein and starch, being the InfoGest protocol, the most widely accepted, and based on the use of digestion solutions. In addition, there are others such as the official method of the Association of Official Analytical Chemists, which is more specific for dietary fiber. The limitations of these methods for carbohydrate digestion could be due toon the absence of the disaccharidases enzymes present in the brush border membrane of the enterocytes, and therefore, they do not allow to distinguish between digestible and non-digestible carbohydrates. Previous work of our research group demonstrated the suitability of an *in vitro* method based on the use of an acetonic powder extract from rat small intestine to assess the digestibility of dietary carbohydrates and recognized prebiotics. Despite promising results, enzyme kinetics and their application to more complex carbohydrates were not investigated.

The first part of the present PhD Thesis is based on the extension of knowledge about this *in vitro* method with rat small intestine extract to evaluate the digestibility of prebiotic carbohydrates, and its comparison with the InfoGest protocol (*Chapters 1-3*). Firstly, a kinetic assay of the intestinal enzymes of this rat extract was performed, optimizing the conditions of maximum hydrolysis of a digestible disaccharide (lactose). In addition, lactulose, a recognized prebiotic, showed high resistance to intestinal enzymes, highlighting the high dependence on the chemical structure. Then, since most of the tested prebiotic carbohydrates had low molecular weight, complex mixtures of commercial prebiotics of higher molecular weight, such as fructans; and emerging oligosaccharides, such as α-galactooligosaccharides, were analyzed. Results indicated a potential enzymatic versatility by the intestinal disaccharidases, as they were able to hydrolyze different chemical bonds of prebiotic components. Following this, it seems

imperative to perform a comparison with the InfoGest protocol on those compounds with higher molecular weight, such as starch and pectins. Using the InfoGest method, hardly any carbohydrate digestion was achieved in the different stages of digestion. By contrast, intestinal hydrolysis in all compounds was always significantly increased in the presence of the rat small intestine extract, which may suggest a more realistic more realistic approach to ileal digestion.

The effect of pectins on the intestinal microbiota was evaluated by an *in vivo* assay, both in healthy rats and in rats with colorectal cancer, as it is shown in the second part of this PhD Thesis (*Chapter 4*). In diseased rats, a general dysbiosis data was detected in the intestinal microbiota that did not improve with the intake of citrus pectins; however, a positive effect was found in terms of blood triglyceride and glycaemia levels.

On the other hand, the growing interest in obtaining new prebiotics with additional bioactive properties gave rise to the third part of this PhD Thesis, involving the synthesis of trehalose derivatives (*Chapter 5*). Trehalose, a widely used food ingredient, has beneficial effects on metabolic health and against neurodegenerative diseases. This compound can reach the colon and cause adverse effects, due to the *Clostridium difficile* infections. In this last chapter, the synthesis, purification and characterization of new trehalose-derived oligosaccharides with prebiotic potential was carried out.

Results obtained in this PhD Thesis spread the existing knowledge in the field of prebiotics, with special emphasis on the application of specific and valid digestion methods for digestible and non-digestible carbohydrates of different degree of polymerization and glycosidic bonds; and in the synthesis of new molecules, theoretically more resistant to digestion, with important properties, not only at the intestinal level.

Introducción General

1. INTRODUCCIÓN GENERAL

1.1 La microbiota en el aparato digestivo

El cuerpo humano contiene alrededor de 10-100 trillones de microorganismos repartidos por las diferentes zonas del organismo, íntimamente relacionados entre sí y, a su vez, con las células humanas. El microbioma se conoce como el conjunto de microorganismos y su material genético presentes en el cuerpo, formado mayoritariamente por bacterias, aunque también aparecen otros tipos, tales como hongos, virus o arqueas (Ursell *et al.*, 2012). La mayor cantidad de éstos se encuentra a lo largo del tracto gastrointestinal (GI), considerado una de las zonas más relevantes, conocida como microbiota o flora intestinal (Thursby & Juge, 2017).

El tracto GI representa una de las mayores superficies de interacción entre el organismo humano y el entorno (medio ambiente, antígenos…), comprendiendo un total de, aproximadamente, 300 m^2 (Candela *et al.*, 2010; Thursby & Juge, 2017). La constante relación entre el ser humano y su microbiota ha permitido generar una relación de simbiosis, crucial para la homeostasis y el correcto funcionamiento de ambos. La cantidad aproximada de microorganismos presentes en el aparato digestivo es de 10^{14}, siendo 10 veces mayor que el número de células humanas (Thursby & Juge, 2017). Los principales *phylum* presentes en la microbiota intestinal son Firmicutes (género *Lactobacillus, Enterococcus* y *Clostridium*) y Bacteroidetes (género *Prevotella* y *Bacteroides*), representando un 65% y un 25% del total, respectivamente. El resto está comprendido por Proteobacteria, Actinobacteria y Fusobacteria con una abundancia del 8%, 5% y 1%, respectivamente. Además, al menos 1800 especies de microorganismos se han identificado a lo largo del tracto GI (Candela *et al.*, 2010). A pesar de la gran variabilidad inter-individual en cuanto a la microbiota, se ha observado que ésta se puede categorizar en 3 variantes principales, denominadas "enterotipos": *Prevotella, Bacteroides* y *Ruminococcus*, caracterizadas por la mayor presencia de uno de estos géneros, independientemente del sexo, edad, procedencia o índice de masa corporal

(Arumugam *et al.*, 2011; Power *et al.*, 2014; Yong, 2012). Este campo aún está en proceso de investigación, sin embargo, podría actuar como una herramienta útil para el estudio del ecosistema microbiano individual y su relación con el desarrollo de enfermedades crónicas (Malard *et al.*, 2021).

A lo largo del aparato digestivo, la microbiota se reparte de manera diferente debido a las condiciones fisiológicas (pH y O_2) de cada componente. La **Figura 1** muestra el contenido y la composición microbiana en las partes del aparato digestivo.

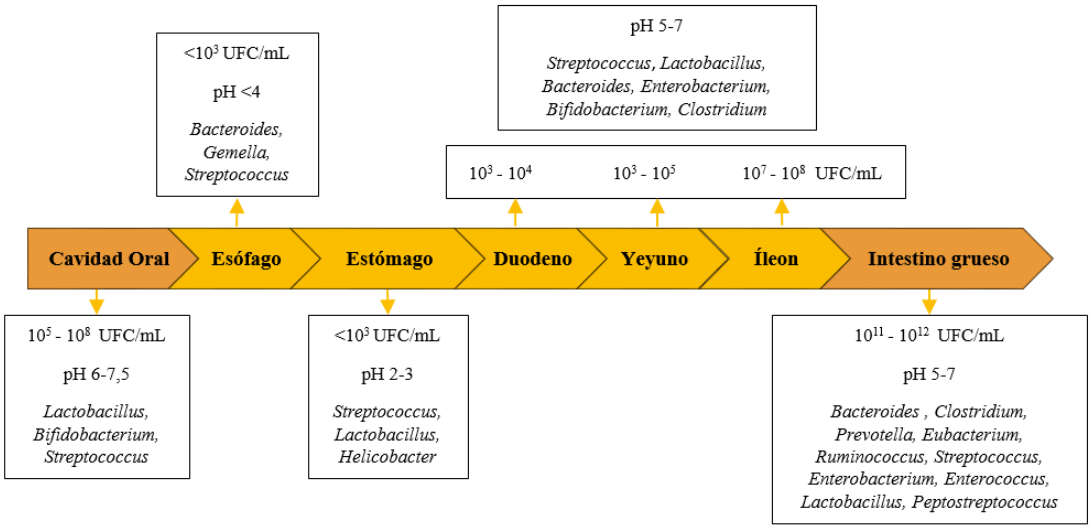

Figura 1. Microorganismos predominantes, cantidad y pH en cada sección del aparato digestivo. UFC: unidades formadoras de colonias. Adaptado de Jandhyala *et al.* (2015) y Power *et al.* (2014).

Las primeras porciones del aparato digestivo presentan menor cantidad de microorganismos, debido principalmente al rápido flujo de los alimentos por estas zonas (cavidad oral y esófago) y al pH ácido del estómago, impidiendo la supervivencia y actuación microbiana. El tiempo de tránsito a través del duodeno es rápido (~10 min), lo que, junto con la segregación del jugo pancreático y las sales biliares, disminuye la actuación de bacterias (Ferreira-Lazarte, 2019; Jandhyala *et al.*, 2015). En el yeyuno, el tiempo de tránsito es mayor (~120 min), implicando una cantidad creciente de

microorganismos (Nokhodchi *et al.*, 2012). La concentración de bacterias aumenta conforme se llega al íleon, hasta alcanzar el máximo en el colon, que comprende el 70% de la microbiota intestinal (10^{12} UFC/mL). El tiempo de tránsito lento, las condiciones anaeróbicas y la presencia de nutrientes favorecen la intervención microbiana (Hérnandez-Hérnandez, 2012).

La microbiota intestinal se ha convertido actualmente en un elemento clave en la salud humana, donde los microorganismos beneficiosos son bastante más predominantes y activos que aquellos potencialmente perjudiciales. Su correcto mantenimiento puede ocasionar numerosos beneficios, ilustrados a modo de resumen en la **Figura 2**.

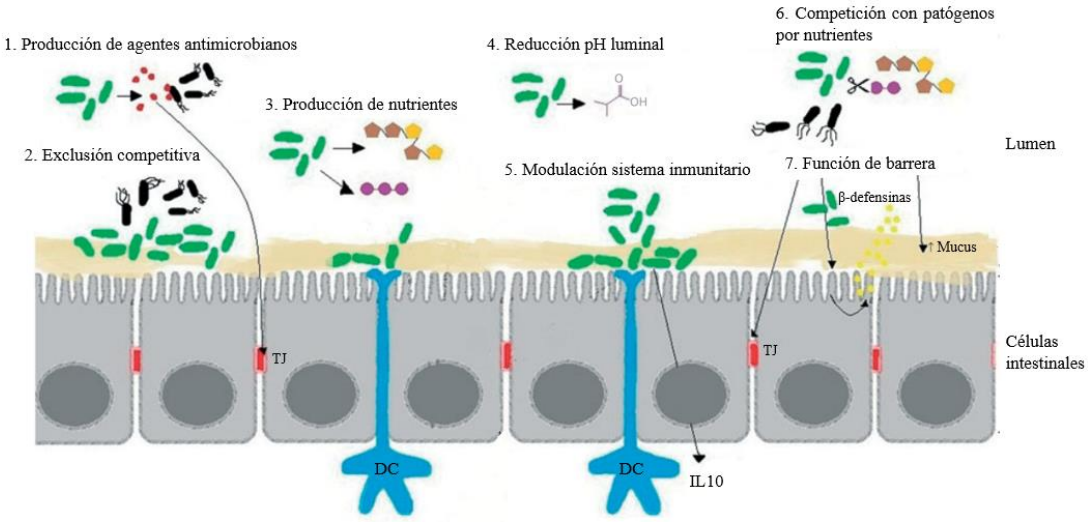

Figura 2. Esquema de los principales efectos beneficiosos de la microbiota intestinal de una persona sana. TJ: *Tight junction*, uniones estrechas entre las células, DC: células dendríticas, IL10: interleuquina-10. Adaptado de Power *et al.* (2014).

Entre las funciones beneficiosas de la microbiota se encuentran (Corebima *et al.*, 2019; Jandhyala *et al.*, 2015; Power *et al.*, 2014):

- Producción de nutrientes: vitaminas y, sobre todo, ácidos grasos de cadena corta (SCFA), favoreciendo el desarrollo de los enterocitos.
- Disminución del crecimiento de agentes patógenos mediante producción de agentes antimicrobianos (bacteriocinas), exclusión competitiva por la adhesión

al epitelio intestinal, competición por nutrientes y disminución del pH luminal (debido a SCFA).

- Mejora de la barrera intestinal: aumento de la producción de mucus, secreción de *β*-defensinas y modulación del citoesqueleto.
- Modulación de la respuesta inmune.

Una desregulación de la microbiota intestinal, también conocida como disbiosis, está asociada con determinadas enfermedades, tales como trastornos metabólicos (obesidad y diabetes), cardiovasculares o alérgicos, entre otros (Jandhyala *et al.*, 2015; Lynch & Pedersen, 2016). Por todo ello, el correcto mantenimiento y modulación de la microbiota intestinal es imprescindible para gozar de una buena salud.

Actualmente, la población general es cada vez más consciente del binomio alimentación-salud, siendo fundamental tomar decisiones correctas en cuanto a los hábitos alimentarios. La Organización Mundial de la Salud (OMS) establece las 10 primeras causas de muerte en el mundo, siendo las primeras las enfermedades cardiovasculares (ECV). La cardiopatía isquémica y el infarto provocaron un total de, aproximadamente, 15 millones de muertes en 2019 (World Health Organization, 2019). En cuanto al resto, destacan las enfermedades respiratorias, neonatales, diarreicas, cáncer y diabetes *mellitus*. El aumento de la incidencia de las enfermedades crónicas, especialmente ECV y diabetes, se debe principalmente al estilo de vida y la alimentación. Es por esta razón por la que surgieron los alimentos funcionales. Un alimento funcional se puede considerar como tal si, "además de su contenido nutricional, posee un efecto beneficioso en una o varias funciones del organismo, ya sea mejorando la salud en general y/o disminuyendo el riesgo de padecer una enfermedad" (Contor, 2001). El mercado de estos alimentos está creciendo rápidamente y seguirá creciendo en el futuro, con un incremento anual global del 8-16% (Butnariu & Sarac, 2019). Algunos de los más consumidos son aquellos enriquecidos con ácidos grasos funcionales o fibra. De este modo, la fibra dietética se considera como uno de los factores clave para la disminución del riesgo de ECV, diabetes tipo II y cáncer (Dahl & Stewart, 2015).

1.2 Fibra dietética

La fibra dietética se define, según el *Códex Alimentarius*, como "polímeros de carbohidratos con 3 o más unidades monoméricas, que no son hidrolizados por las enzimas endógenas en el intestino delgado humano y, a su vez pertenecen a una de estas categorías: a) Carbohidratos comestibles presentes naturalmente en los alimentos; b) Carbohidratos que han sido obtenidos a partir de materia prima alimentaria mediante procedimiento físico, químico o enzimático, y que muestran un efecto beneficioso para la salud, demostrado por estudios científicos competentes; c) Carbohidratos sintéticos que muestran un efecto beneficioso para la salud, demostrado por estudios científicos competentes" (Codex Alimentarius Comission, 2010). Además, también se incluyen otros compuestos no carbohidratos, como la lignina (Soliman, 2019). Generalmente, son componentes de la parte comestible de las plantas y algunos tipos pueden ser total o parcialmente fermentados por la microbiota intestinal, generando gases y SCFA. La fibra dietética se puede clasificar de diversas maneras: según su estructura, diferenciando entre polisacáridos estructurales, no estructurales, oligosacáridos y componentes no carbohidratos; y según su solubilidad, siendo esta última la más comúnmente utilizada (Qi *et al.*, 2018).

En función de la solubilidad, se pueden distinguir dos tipos de fibra dietética (**Figura 3**). La fibra soluble es total o parcialmente fermentada en el colon, mientras que la fibra insoluble apenas es digerida por las bacterias del intestino grueso (Soliman, 2019). La fibra insoluble incluye aquellos polisacáridos más complejos, tales como celulosa y algunas hemicelulosas, junto con la lignina. Sus principales efectos en el organismo son la disminución del tiempo de tránsito intestinal y el aumento de la consistencia de las heces (Mudgil & Barak, 2013; Perry & Ying, 2016; Soliman, 2019). Por otro lado, la fibra soluble está compuesta por almidón resistente, pectinas, algunas hemicelulosas mucílagos, gomas, β-glucanos y numerosos oligosacáridos. Sus funciones se basan en la reducción de la glucosa postprandial, de los lípidos en sangre, retraso del vaciado gástrico, actuación de diversas hormonas intestinales y disminución de la absorción de

ciertos macronutrientes, como el almidón, generando sensación de saciedad (Perry & Ying, 2016; Qi *et al.*, 2018; Sun *et al.*, 2021).

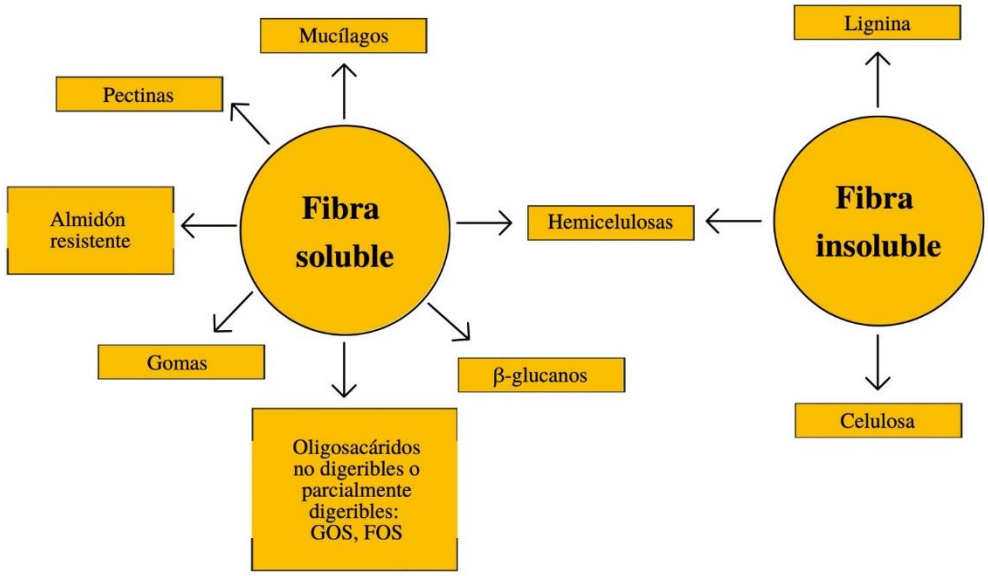

Figura 3. Clasificación de la fibra dietética según su solubilidad.

En general, la fibra dietética aporta numerosos beneficios a la salud humana, observándose una disminución del riesgo de obesidad, diabetes, ECV y cáncer, además del mantenimiento de la función gastrointestinal. Ello implica un consumo de 25-30 g de fibra por día, siendo la fibra soluble la que provoca un efecto más marcado (Sun *et al.*, 2021). Dentro de la fibra soluble, cabe destacar un tipo de componentes muy estudiado, los carbohidratos prebióticos, no sólo por su efecto directo sobre el aparato digestivo sino también por su efecto sistémico.

1.3 Prebióticos

1.3.1 *Definición*

Los prebióticos son ingredientes funcionales que están cobrando gran importancia en los últimos años, debido a su llegada directa al intestino grueso con un efecto selectivo en la microbiota del colon. El concepto de prebiótico ha ido variando a lo largo del tiempo.

En 1995, Gibson y Roberfroid introdujeron por primera vez el concepto de prebiótico definiéndolo como "un ingrediente alimentario no digerible que produce un efecto beneficioso en el organismo mediante la estimulación selectiva del crecimiento o la actividad de una o un número limitado de bacterias presentes en el colon" (Gibson & Roberfroid, 1995). Sin embargo, muchos componentes beneficiosos para la flora quedaban excluidos al hacer referencia exclusivamente a "un número limitado de bacterias". Conforme avanzaban las investigaciones científicas, el concepto de prebiótico también fue evolucionando. En 2004, se modificó como sigue: "ingredientes fermentados selectivamente que provocan cambios selectivos en la composición y/o actividad de la flora intestinal, confiriendo un beneficio a la salud" (Gibson *et al.*, 2004). Posteriormente, la Organización de las Naciones Unidas para la Alimentación y la Agricultura (FAO) elaboró otra definición eliminado el concepto de "fermentación selectiva" (Pineiro *et al.*, 2008) que fue duramente criticada. Gibson *et al.* (2010) formularon una definición adicional, no obstante, ésta se limitaba demasiado a la microbiota del intestino grueso, sin distinguir otros lugares extraintestinales. Con todo lo indicado, se hizo necesario un consenso para establecer una completa y conjunta definición del término prebiótico.

Así, la Asociación Científica Internacional de Probióticos y Prebióticos (ISAPP), en 2017, lo definió como "un sustrato que es selectivamente utilizado por la microbiota del organismo, otorgando un beneficio en la salud del individuo" (Gibson *et al.*, 2017). El efecto de los prebióticos en la salud debe estar estudiado y establecido mediante trabajos *in vitro*, *in vivo* y ensayos clínicos. Asimismo, aunque la mayoría de los prebióticos sean administrados oralmente, esta definición también incluye aquellos que se apliquen directamente a otras zonas con población microbiana, como la vagina o la piel. Además, a pesar de que los compuestos prebióticos predominantes son carbohidratos, otras sustancias, como ácidos grasos poliinsaturados o polifenoles, también se podrían considerar como tal, siempre que exista evidencia científica suficiente sobre su efecto en la microbiota (Gibson *et al.*, 2017).

1.3.2 *Ingredientes prebióticos*

Teniendo en cuenta la definición del ISAPP (Gibson *et al.*, 2017), un ingrediente alimentario puede ser considerado como prebiótico si:

- Es utilizado selectivamente por la microbiota del huésped.
- Otorga un beneficio en la salud humana, demostrado por estudios científicos.
- No es digerido por el huésped.

El uso selectivo de los prebióticos no implica que sólo puedan ser objetivo de una única especie bacteriana, sino que también pueden ser utilizados por numerosas especies, entre las que se incluyen *Bifidobacterium, Lactobacillus, Eubacterium, Faecalibacterium* o *Roseburia* (Gibson *et al.*, 2017; Vandeputte *et al.*, 2017). Las propiedades del consumo de estos componentes son muy variadas, otorgando un efecto positivo en la salud o reduciendo el riesgo de padecer diferentes patologías (**Tabla 1**).

Como se ha dicho anteriormente, la mayoría de prebióticos establecidos o reconocidos son carbohidratos, componentes de la fibra soluble, y caracterizados por su alta resistencia a las enzimas gastrointestinales, evitando su absorción. Entre todos los carbohidratos prebióticos, los oligosacáridos son los que están desempeñando uno de los papeles más importantes en la alimentación funcional, siendo su utilización cada vez más extendida entre la población. Los oligosacáridos se definen como carbohidratos con bajo grado de polimerización (DP) (entre 2 y 20 unidades) utilizados selectivamente por la microbiota del colon (Cardelle-Cobas *et al.*, 2016; Martínez-Villaluenga & Frías, 2014; Villamiel *et al.*, 2014). Existen numerosos tipos de carbohidratos prebióticos, con un efecto fisiológico investigado en la salud humana y, generalmente, bien establecidos en el mercado mundial: fructanos y fructooligosacáridos (FOS), galactooligosacáridos (GOS) y lactulosa. Pectinas y derivados, α-galactooligosacáridos (α-GOS) fructosilados y no fructosilados, almidón resistente, galactooligosacáridos derivados de la lactulosa (OsLu), xilooligosacáridos, isomaltooligosacáridos, lactosacarosa, entre otros, aún se pueden considerar en fase de estudio, a falta de ensayos clínicos que lo avalen.

Tabla 1. Efectos en la salud del consumo de prebióticos en la alimentación, estudiado mediante ensayos clínicos en humanos. GOS: galactooligosacáridos, FOS: fructooligosacáridos, OsLu: galactooligosacáridos derivados de lactulosa. Adaptado de Gibson *et al.* (2017).

Efecto en la salud	Mecanismo y prebiótico usado	Referencias
Saciedad	Reducción ingesta calórica y glucosa postprandial, aumento hidrógeno espirado, secreción glucagón y grelina. FOS, GOS.	Cani *et al.* (2009); Hume *et al.* (2017)
Salud ósea	Mejora absorción calcio y magnesio, aumento mineralización ósea. Inulina, FOS.	McCabe *et al.* (2015)
Salud capilar	Reducción niveles fenoles, queratinización y prevención de la sequedad de la piel. GOS.	Miyazaki *et al.* (2014)
Salud metabólica: obesidad, diabetes tipo II, síndrome metabólico y dislipemia	Saciedad, mejora sensibilidad insulina y perfil lipídico, reducción marcadores de inflamación. Inulina, FOS, GOS, OsLu (ensayos *in vivo*).	Barengolts (2016); Fernandes *et al.* (2017); Laparra *et al.* (2013)
Salud sanguínea	Mejora absorción hierro. OsLu (ensayos *in vivo*).	Laparra *et al.* (2014)
Síndrome del intestino irritable	Disminución de consistencia de heces, flatulencias y distensión abdominal. GOS.	Silk *et al.* (2009)
Enfermedad inflamatoria intestinal	Alivio síntomas. Inulina, lactulosa, OsLu (ensayos *in vivo*).	Algieri *et al.* (2014); Ghouri *et al.* (2014)
Enterocolitis necrotizante	Reducción incidencia en neonatos. FOS, GOS.	Armanian *et al.* (2014)
Estreñimiento	Aumento de la frecuencia y ablandamiento de las heces. Inulina, lactulosa.	Christodoulides *et al.* (2016)
Diarrea	Alivio síntomas. GOS, lactulosa.	Drakoularakou *et al.* (2010); Maltz *et al.* (2020)
Alergias	Modulación función inmunitaria e inflamatoria. FOS, GOS.	Cuello-Garcia *et al.* (2016); Vulevic *et al.* (2015)
Infecciones y respuesta a vacunas	Impacto en el desarrollo de las células inmunitarias. FOS, GOS.	Lohner *et al.* (2014); Valdez *et al.* (2014)
Estimulación de neurotransmisores	Supresión del estrés endocrino. GOS.	Schmidt *et al.* (2015)
Salud urogenital	Recuperación flora vaginal. GOS.	Coste *et al.* (2012)

1.4 Tipos de carbohidratos prebióticos

1.4.1 *Fructanos y fructooligosacáridos (FOS)*

Los fructanos son polisacáridos presentes naturalmente en numerosos alimentos, tales como cebolla, ajo, alcachofa, achicoria, plátano, puerro, trigo y avena. La inulina es el principal polisacárido de los fructanos, polímero lineal de monómeros de D-fructosa unidos por enlaces $\beta(2\rightarrow1)$, con una unidad de D-glucosa terminal a través del enlace $\alpha(1\rightarrow2)$ (GF_n). Además, también pueden estar formados únicamente por unidades de D-fructosas (FF_n) (Micka *et al.*, 2017). Su DP varía entre 2 y 60 monómeros, y pueden conocerse como oligofructosa cuando su valor es menor de 10. Igualmente, el levano también forma parte de este grupo, tratándose de un polisacárido lineal o ramificado de D-fructosas unidas por enlaces $\beta(2\rightarrow6)$ (Mensink *et al.*, 2015).

En la industria alimentaria, la inulina se utiliza como edulcorante hipocalórico, para formar geles o para incrementar la viscosidad de un alimento. Sin embargo, su principal función se basa en su efecto prebiótico. Debido a su configuración β, la inulina es resistente a las enzimas gastrointestinales humanas y fermentada selectivamente por la microbiota intestinal. Sin embargo, Ferreira-Lazarte, Olano, *et al.* (2017) observaron cierta digestión destacable en este tipo de compuestos. Sus efectos beneficiosos tales como saciedad (Parnell & Reimer, 2009), salud metabólica (Parnell & Reimer, 2009; Reimer *et al.*, 2020) o salud ósea (McCabe *et al.*, 2015), entre otros, han sido ampliamente estudiados. En concreto, la Agencia Europea de Seguridad Alimentaria (EFSA) ha aprobado una declaración de salud que concierne a la inulina de achicoria. La inulina "mejora la función intestinal mediante el incremento de la frecuencia de las deposiciones" (EFSA NDA Panel, 2015).

En cuanto a los oligosacáridos, los FOS son oligómeros compuestos por 2-9 monómeros de D-fructosa con una D-glucosa terminal. Pueden ser obtenidos a través de dos procedimientos diferentes: hidrólisis enzimática de inulina con inulinasas (EC 3.2.1.7), mediante la cual se fragmentan los enlaces $\beta(2\rightarrow1)$ intermedios, generando compuestos del tipo FF_n (inulobiosa DP2, inulotriosa DP3 o inulotetraosa DP4) o de los extremos de

la molécula, dando lugar a compuestos tipo GF_n (1-kestosa, nistosa…) (Singh *et al.*, 2017); y síntesis enzimática mediante la reacción de transfructosilación usando *β*-fructosidasas (EC 3.2.1.26) o *β*-fructosiltransferasas (EC 2.4.1.99) (Greg Kelly, 2008; Singh *et al.*, 2017). Este último proceso se realiza a partir de dos moléculas de sacarosa e implica una competencia entre la hidrólisis y la transfructosilación en el medio de reacción. El proceso consiste en la hidrólisis de sacarosa y posterior transferencia de la unidad de fructosa liberada a un aceptor, bien sacarosa o un FOS ya formado (Bali *et al.*, 2015; Flores-Maltos *et al.*, 2016). De esta manera, los monómeros de fructosa se unen a otros similares aumentando el DP y generando los diferentes tipos de FOS (**Figura 4**). Los FOS más comunes son: 1-kestosa (DP = 3), nistosa (DP = 4) y 1-fructosilnistosa (DP = 5) (Bali *et al.*, 2015).

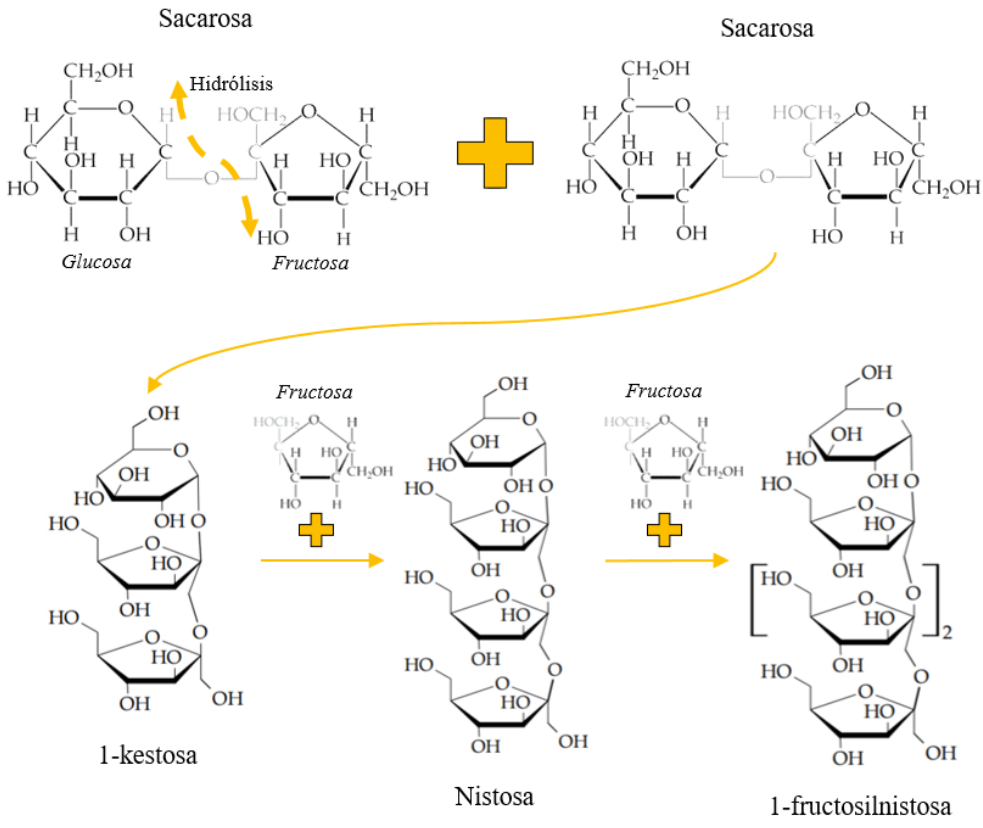

Figura 4. Reacción de transfructosilación para la síntesis enzimática de diferentes tipos de FOS. Adaptado de Bali *et al.* (2015).

Al igual que la inulina, los FOS son altamente resistentes a la digestión gastrointestinal, pudiendo observarse un 12% de hidrólisis intestinal (Ferreira-Lazarte, Olano, *et al.*, 2017), y una estimulación selectiva de la microbiota (Nobre *et al.*, 2018). Concretamente, los FOS fermentan en la zona proximal del colon favoreciendo el crecimiento de las bifidobacterias y lactobacilos y la producción de SFCA, lo que resulta beneficioso para la salud, tal y como se ha indicado con anterioridad (Fernandes *et al.*, 2017; Man *et al.*, 2021; Singh *et al.*, 2017). En el mercado actual, la inulina y los FOS son ampliamente comercializados, siendo Beneo Orafti (Bélgica) y Beghin-Meiji (Japón) algunas de las empresas más relevantes. Cabe destacar la producción de inulinas: Inulin Orafti® GR (92% inulina y 8% FOS) y Raftiline® High Performance (DP ≈ 25, sin compuestos con DP < 10). Asimismo, es importante nombrar los FOS comerciales obtenidos por hidrólisis de inulina (Raftilose®) o por síntesis enzimática (Actilight®) (Corzo *et al.*, 2015; Tsatsaragkou *et al.*, 2021).

1.4.2 *Galactooligosacáridos (GOS)*

Los GOS son mezclas complejas de oligosacáridos de galactosa con un DP entre 2 y 9, unidos entre sí mediante enlaces $\beta(1\rightarrow1)$, $\beta(1\rightarrow2)$, $\beta(1\rightarrow3)$, $\beta(1\rightarrow4)$ y $\beta(1\rightarrow6)$ y con una glucosa terminal, a través de un enlace $\beta(1\rightarrow4)$ (Rastall, 2010; Singh *et al.*, 2017). Se obtienen a través de la síntesis enzimática mediante una reacción de transgalactosilación, catalizada por β-galactosidasas, usando lactosa como aceptor y donante. Las enzimas β-galactosidasas más estudiadas son de origen microbiano: *Bacillus circulans, Aspergillus oryzae, Lactobacillus reuteri, Kluyveromyces lactis*, entre otras (Van Leeuwen *et al.*, 2016).

La enzima es una hidrolasa que ataca al enlace *o*-glicosídico de la lactosa. El mecanismo general es similar a la transfructosilación de los FOS, donde se genera una secuencia de reacciones de síntesis e hidrólisis con disacáridos y sacáridos de mayor DP. Esta síntesis consiste, principalmente, en dos mecanismos, uno intramolecular o directo, en el que la galactosa liberada es unida al mismo donante, aunque con diferente enlace (**Figura 5**, apartado **a**); y otro intermolecular o indirecto, donde los monómeros de galactosa se

unen a di-, tri- y tetrasacáridos aumentando el DP (**Figura 5**, apartado **b**) (Belorkar & Gupta, 2016; Torres *et al.*, 2010). La composición final de los GOS obtenidos dependerá del tipo de enzima utilizado, de la concentración y tipo de sustrato y de las condiciones de reacción (temperatura, pH y tiempo).

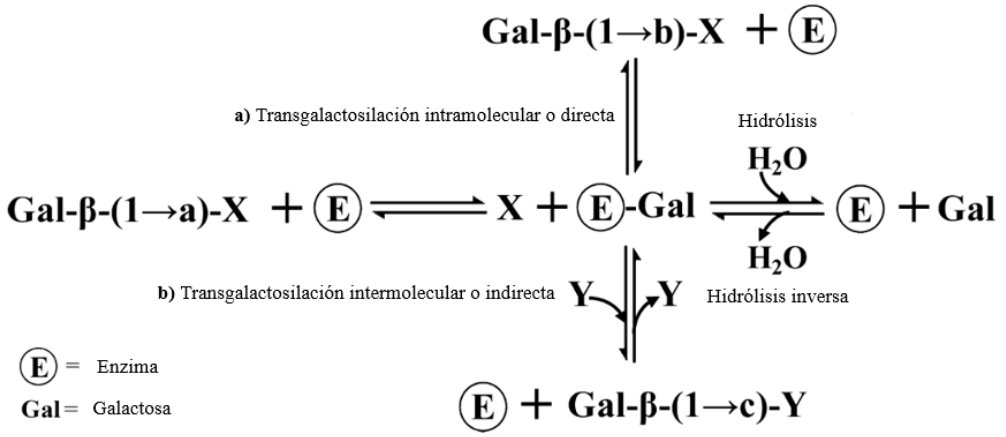

Figura 5. Mecanismos de transgalactosilación enzimática para la producción de GOS a partir de lactosa. X: Glucosa; Y: aceptor de galactosa; a,b,c: 2, 3, 4, 6, tipo de enlace glicosídico. Adaptado de Torres *et al.* (2010).

El efecto prebiótico de los GOS está sobradamente reconocido ya que favorecen y estimulan selectivamente a la microbiota, especialmente bacterias ácido lácticas y bifidobacterias (Roberfroid *et al.*, 2010). Los GOS son considerados como carbohidratos no digeribles, sin embargo, determinados estudios han observado una digestión parcial en este tipo de moléculas. El grado de hidrólisis intestinal varía dependiendo de la estructura química y del tipo de enlace (Ferreira-Lazarte, 2019; Ferreira-Lazarte, Olano, *et al.*, 2017; Hernández-Hernández *et al.*, 2012).

1.4.3 *Lactulosa y oligosacáridos derivados de la lactulosa (OsLu)*

La lactulosa (Lu) es un disacárido sintético compuesto por una molécula de D-fructosa y otra de D-galactosa, unidas mediante un enlace *β*(1→4) (**Figura 6**) (Rastall, 2010). Se obtiene por procedimientos químicos de isomerización de la lactosa, o por procesos enzimáticos, usando *β*-glucosidasas, en un proceso de bioconversión, o *β*-galactosidasas

en una reacción de transgalactosilación en presencia de fructosa (Panesar & Kumari, 2011; Villamiel *et al.*, 2014).

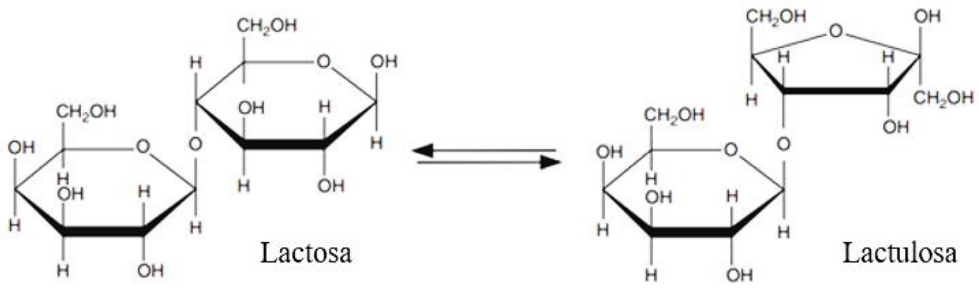

Figura 6. Estructura química de la lactulosa. Adaptado de Villamiel *et al.* (2014).

La lactulosa posee un efecto prebiótico reconocido, ya que estimula el crecimiento de las bacterias gastrointestinales e inhibe otras patógenas como *Salmonella* (Panesar & Kumari, 2011). No obstante, debido a su pequeño tamaño molecular, produce distensión abdominal al ser fermentado rápidamente en las partes más proximales del colon. Se utiliza para el tratamiento del estreñimiento crónico y la encefalopatía hepática o encefalopatía portal sistémica (Ferreira *et al.*, 2019; Zhang *et al.*, 2021). Por ello, se han buscado alternativas a la lactulosa, como sus oligosacáridos derivados (OsLu), con potencial efecto prebiótico (Cardelle-Cobas *et al.*, 2016; Martínez-Villaluenga, Cardelle-Cobas, Olano, *et al.*, 2008). De esta manera, los compuestos pueden llegar al colon distal y ser fermentados más lentamente, mostrando mejores propiedades prebióticas que la lactulosa y los GOS. El mecanismo de obtención es por transgalactosilación, de forma similar a los GOS pero, en este caso a partir de lactulosa y sintetizando oligómeros de DP 3-5 con enlaces mayoritariamente del tipo $\beta(1\rightarrow6)$ (Hernández-Hernández *et al.*, 2011; Villamiel *et al.*, 2014). Algunas de las estructuras ya elucidadas son: β-D-Gal-(1→6)-β-D-Gal-(1→4)-D-Fru, β-D-Gal-(1→4)-D-Fru-(1→1)-β-D-Gal, β-D-Gal-(1→5)-β-D-Gal-(1→4)-D-Fru, β-D-Gal-(1→4)-D-Fru-(1→6)-β-D-Gal, etcétera (Hernández-Hernández *et al.*, 2011; Martínez-Villaluenga, Cardelle-Cobas, Olano, *et al.*, 2008; Yin *et al.*, 2018).

Al igual que con el resto de prebióticos, para ejercer su efecto, la lactulosa y los OsLu no deben ser digeridos a lo largo del aparato digestivo. Sin embargo, su total resistencia a la digestión no está del todo clara, observándose un 24% y un 13% de hidrólisis de lactulosa y OsLu, respectivamente, tras 3 horas de digestión (Ferreira-Lazarte, Gallego-Lobillo, *et al.*, 2019). En este sentido, es necesario seguir profundizando en la digestión parcial de diferentes prebióticos, ampliando los estudios a otros carbohidratos emergentes, con el fin de conocer cómo pueden influir las diferentes estructuras químicas de los carbohidratos en la relación estructura-función.

1.4.4 *Alfa-galactooligosacáridos (α-GOS)*

En contraposición a los GOS nombrados en el apartado 1.4.2, existen otro tipo de GOS, de origen vegetal, que contienen enlaces tipo *α* en lugar de *β*. Se encuentran de forma abundante en las legumbres, tales como soja, lentejas, garbanzos, alubias y guisantes, siendo conocidos comúnmente como oligosacáridos de la familia de la rafinosa (RFOs) (Van den Ende, 2013). A diferencia del resto de oligosacáridos, la forma de obtención de los RFOs es la extracción directa a partir de la soja. Son carbohidratos solubles formados por monómeros de D-galactosa unidos por enlaces *α*(1→6) con una unidad de sacarosa terminal. Sus oligosacáridos más importantes son el trisacárido rafinosa [*α*-D-Gal-(1→6)-*α*-D-Glu-(1→2)-*β*-D-Fru], el tetrasacárido estaquiosa [*α*-D-Gal-(1→6)-*α*-D-Gal-(1→6)-*α*-D-Glu-(1→2)-*β*-D-Fru] y el pentasacárido vesbascosa [*α*-D-Gal-(1→6)-*α*-D-Gal-(1→6)-*α*-D-Gal-(1→6)-*α*-D-Glu-(1→2)-*β*-D-Fru] (Crittenden, 2012). Debido a la ausencia de la *α*-galactosidasa en el intestino delgado, los RFOs son fermentados por la microbiota pudiendo mostrar efecto prebiótico (Nakamura *et al.*, 2012; Van den Ende, 2013). No obstante, la presencia de la fructosa en los RFOs puede originar flatulencias, distensión y malestar abdominal al ser ingeridos y fermentados (Martins *et al.*, 2019).

Por ello, se obtuvieron los *α*-GOS no fructosilados, compuestos por melibiosa, maninotriosa y verbascotetraosa que, básicamente, son rafinosa, estaquiosa y verbascosa, sin la unidad de fructosa terminal (**Figura 7**). Este producto se comercializa como AlphaGOS® y es obtenido mediante enzimas *β*-fructosidasas, capaces de

fragmentar la sacarosa de los *α*-GOS, liberando la fructosa (Marín-Manzano *et al.*, 2020). Los *α*-GOS no fructosilados se metabolizan de manera total por las bacterias del colon y han mostrado actividad bifidogénica en estudios *in vitro*, de forma similar a los *β*-GOS, aumentando la población de *Bifidobacterium longum* y *Bifidobacterium catenulatum* (Marín-Manzano *et al.*, 2020). Asimismo, los AlphaGOS® también han mostrado un efecto de reducción de glucosa postprandial, alegación recientemente aprobada por la EFSA (EFSA NDA Panel, 2014).

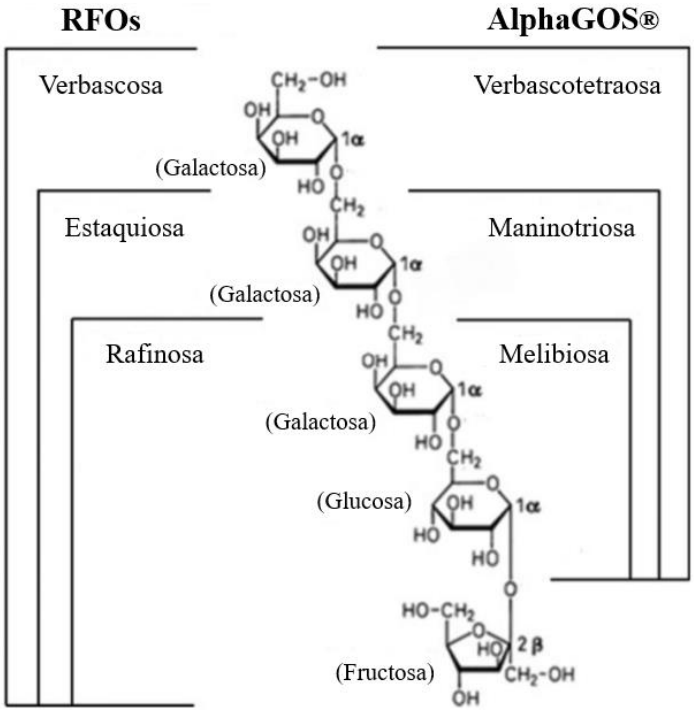

Figura 7. Estructura química de los oligosacáridos de la familia de la rafinosa (RFOs) y sus derivados, los AlphaGOS®. La fructosa terminal ha sido eliminada para producir estos compuestos. Adaptado de Kruger *et al.* (2017).

Todos estos efectos beneficiosos tienen lugar una vez los carbohidratos llegan "intactos" al colon y son fermentados por la microbiota. La ausencia de *α*-galactosidasa en mamíferos implica la no digestibilidad de los *α*-GOS y, por tanto, su total fermentación. Sin embargo, otros compuestos considerados completamente indigeribles, como los *β*-GOS o lactulosa, han mostrado cierta hidrólisis en ensayos con extractos intestinales de

mamíferos (Ferreira-Lazarte, 2019; Hernández-Hernández *et al.*, 2019). Partiendo de esta base, investigaciones sobre la digestión de los *α*-GOS permitirían conocer de manera más realista el comportamiento de estos carbohidratos hasta su llegada al colon.

1.4.5 *Pectinas y pectinas modificadas*

Las pectinas son un complejo grupo de polisacáridos de elevada masa molecular, muy heterogéneo y presentes en la pared celular de la célula vegetal. A pesar de que su estructura química exacta está aún en proceso de investigación, en el modelo mayoritariamente aceptado se distinguen tres tipos de dominios: homogalacturonano (HG), ramnogalacturonano I (RG-I) y ramnogalactorunonano II (RG-II) (**Figura 8**) (Chan *et al.*, 2017).

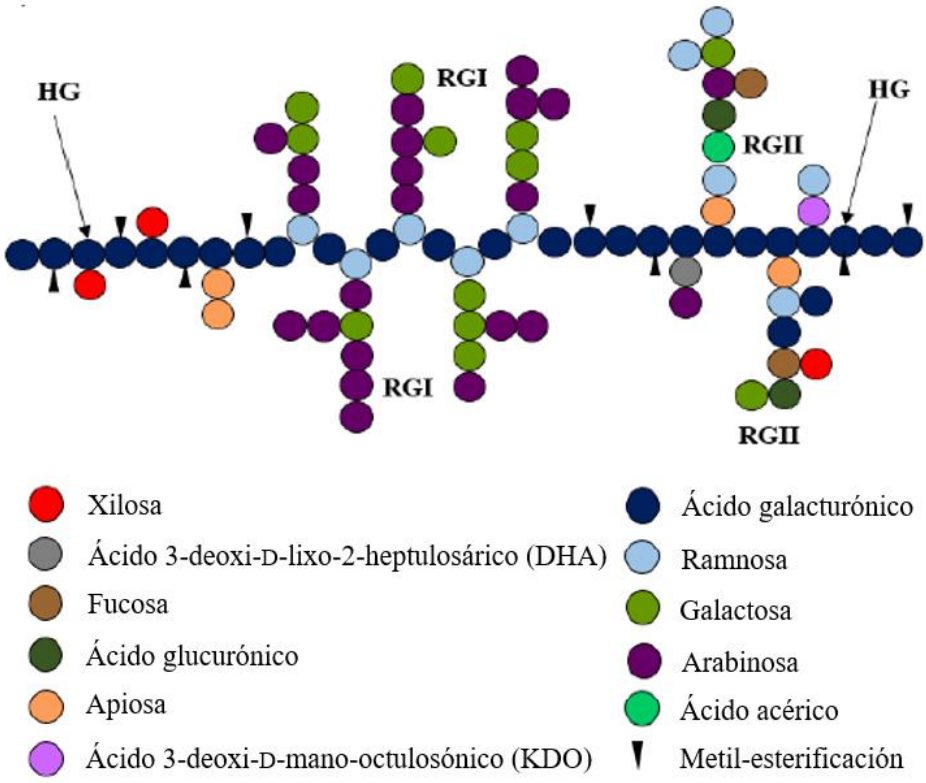

Figura 8. Estructura química de la pectina según el modelo mayoritariamente aceptado, conteniendo homogalacturonano (HG) y ramnogalacturonano (RGI y RGII). Adaptado de Muñoz-Almagro (2019).

El principal dominio y más abundante es el HG (~65%), constituido por una cadena lineal de monómeros de ácido galacturónico (GalA), conectados mediante enlaces *α*(1→4), en los que, a su vez, sus grupos carboxilo pueden estar parcialmente esterificados (Ciriminna *et al.*, 2016). De esta manera, se diferencian dos tipos de pectinas según su grado de metil-esterificación (DM): alto-metoxilo (HM), con más del 50% de los grupos carboxilo esterificados, y bajo-metoxilo (LM), con menos del 50% de los grupos esterificados (Adetunji *et al.*, 2017). La ramnosa (Rha) interrumpe el esqueleto de HG para dar lugar al RG-I (~20-35%), basado en una cadena compuesta por la repetición del disacárido [→4)-*α*-D-GalA-(1→2)-*α*-L-Rha-(1-], que, a su vez, contiene ramificaciones de azúcares neutros, como galactosa, arabinosa o arabinogalactanos (Muñoz-Almagro, 2019). RG-II (~1-8%) es la estructura más compleja y menos abundante, formada por un esqueleto de HG, con ramificaciones de ramnosa, xilosa, galactosa, fucosa, apiosa y ácido acérico (Chan *et al.*, 2017; Muñoz-Almagro, 2019).

En la industria agroalimentaria, las pectinas se obtienen fundamentalmente a partir de subproductos de cítricos (~85%). Sin embargo, han surgido fuentes alternativas como subproductos derivados del girasol o de la alcachofa debido a la búsqueda de otras estructuras con nuevas o mejoradas propiedades (Muñoz-Almagro, Rico-Rodriguez, Wilde, *et al.*, 2018; Sabater *et al.*, 2020). Se considera un aditivo alimentario (E-440), siempre y cuando su contenido en GalA sea mayor del 65%, y se utiliza principalmente como emulsificante, texturizante, estabilizante y espesante (EU Commission, 2012). Una de sus principales propiedades biológicas es su potencial efecto prebiótico, basado en su baja digestibilidad en el intestino delgado y posterior fermentación en el colon, con la consiguiente estimulación del crecimiento de la microbiota beneficiosa y producción de SCFA (Ferreira-Lazarte *et al.*, 2018; Ferreira-Lazarte, Moreno, *et al.*, 2019; Holck *et al.*, 2014). Asimismo, también se han estudiado otras propiedades tales como los efectos hipocolesterolémico, antiinflamatorio y antitumoral (Morris *et al.*, 2013; Zhang *et al.*, 2015).

Este tipo de propiedades pueden verse incrementadas en las pectinas modificadas (MP), cuyo interés está creciendo actualmente, debido a su mayor solubilidad en agua y su menor masa molecular, lo que facilitaría su metabolismo en el intestino grueso y su absorción al torrente sanguíneo. Se trata de MP mayoritariamente procedentes de subproductos cítricos, que se obtienen por diferentes métodos físicos o químicos, modificando su estructura química, lo cual, generalmente, provoca un aumento en el contenido en azúcares neutros y, por consiguiente, una mejora de la bioactividad (Ferreira-Lazarte *et al.*, 2018; Muñoz-Almagro, 2019; Zhang *et al.*, 2015). Estos azúcares neutros confieren un papel clave en el efecto prebiótico, tanto en el efecto bifidogénico como en la producción de SCFA (Ho *et al.*, 2017; Khodaei *et al.*, 2016). Además, al igual que en el caso de las pectinas, cabe destacar su repercusión en el cáncer, que está cobrando gran importancia gracias a las numerosas investigaciones realizadas.

En este sentido, la galectina-3 (Gal-3) es una proteína implicada en varias fases del cáncer, como adhesión celular, migración, crecimiento, diferenciación y metástasis. Se ha estudiado que las pectinas con alta cantidad de azúcares neutros (MP), concretamente los galactanos, son capaces de unirse e inhibir la proteína metastásica Gal-3, dando lugar a la disminución de la proliferación celular, adhesión y metástasis (Bernardino *et al.*, 2019; Maxwell *et al.*, 2015; Morris *et al.*, 2013). Este efecto en la salud ha sido investigado en estudios *in vitro* y, en menor proporción, *in vivo*, en diferentes fases de la metástasis, mostrando efectividad en cáncer de próstata, colon y piel (Bernardino *et al.*, 2019; Maxwell *et al.*, 2016). Otros efectos positivos de las MP son la modulación del sistema inmunitario (Holck *et al.*, 2014) o el efecto antioxidante (Ramachandran *et al.*, 2017). Las MP se consideran como unos compuestos con alto potencial para la salud, aunque sus principales efectos aún están en fase de investigación, requiriendo investigaciones *in vivo,* ensayos clínicos y estudios sobre su digestibilidad.

1.5 Tendencias actuales en los estudios sobre prebióticos

Actualmente, el mercado de los prebióticos se encuentra en auge. Está valorado en 3,4 billones de dólares en 2018 y se espera que alcance los 8,34 billones para el año 2026 con una tasa de crecimiento anual compuesto (CAGR) del 10,1%, siendo en Europa y en América del Norte donde el volumen es mayor (Grand View Research, 2018; Reports and Data, 2019). El aumento de la demanda de alimentos para la salud y la inmensa variedad de aplicaciones de los prebióticos han contribuido a este incremento de mercado. Dada la gran cantidad de investigaciones acerca de los mismos y sus diferentes tipos, existe un creciente interés a la hora de elaborar nuevos componentes con un mayor número de efectos beneficiosos y mayor conocimiento con respecto a su digestibilidad. Algunos potenciales prebióticos son las pectinas, las MP y los pectooligosacáridos, tal y como se ha indicado. También se está prestando atención hacia la búsqueda de nuevas fuentes de carbohidratos, como las algas marinas o el café (Khangwal & Shukla, 2019; Lopez-Santamarina *et al.*, 2020). Otra de las tendencias es la investigación de derivados de carbohidratos, cuya molécula original tenga efectos beneficiosos para la salud. En este sentido, la trehalosa es un disacárido con un amplio rango de aplicaciones alimentarias y diferentes propiedades bioactivas.

La trehalosa (Tre), *α*-D-Glc-(1→1)-*α*-D-Glc, es un carbohidrato usado en la industria alimentaria como edulcorante, estabilizante y humectante, en cosmética y en farmacia. Además, posee alta estabilidad en cuanto a temperatura, pH y ácidos (Ohtake & Wang, 2011; Peng *et al.*, 2017). Se han investigado diversas propiedades beneficiosas tales como disminución de la glucosa postprandial (Yaribeygi *et al.*, 2019), mejora de la resistencia a insulina (Arai *et al.*, 2010; Yoshizane *et al.*, 2017), disminución de la resorción ósea (Nishizaki *et al.*, 2000) e inducción de la autofagia (DeBosch *et al.*, 2016; Emanuele, 2014). Esta última es la más estudiada, permitiendo el tratamiento de enfermedades raras como el Párkinson, Alzheimer o la Esclerosis Lateral Amiotrófica (ELA) (Di Natale *et al.*, 2018; Emanuele, 2014; Massenzio *et al.*, 2018). Para observar estos efectos en el organismo, la trehalosa debe absorberse, permitiendo la circulación por el torrente sanguíneo. La enzima trehalasa, presente la membrana de los enterocitos,

es la encargada de hidrolizar este disacárido, sin embargo, su cantidad es bastante menor en comparación con el resto de enzimas intestinales (Hooton *et al.*, 2015; Kluch *et al.*, 2020). Teniendo esto en cuenta, la cantidad de trehalosa consumida no sería absorbida al completo, alcanzando así el intestino grueso y, además de servir de sustrato a la microbiota intestinal, podría alimentar a cepas virulentas de *Clostridium difficile*. Se ha observado que la alimentación de estas cepas con trehalosa provoca un aumento del riesgo de muerte en situaciones de diarreas graves (Cao *et al.*, 2019; Collins *et al.*, 2018).

Por tanto, es imprescindible conocer el grado de digestibilidad de este carbohidrato. Asimismo, la síntesis de derivados de trehalosa podría ser una solución para estos efectos adversos, debido a las modificaciones en la estructura química. Usando un proceso de transgalactosilación muy similar al expuesto en la **Sección 1.4.2**, con la trehalosa como molécula aceptora, se han obtenido derivados de trehalosa con un mayor grado de polimerización. Los métodos enzimáticos son los más fiables y rentables, de esta manera, Kim *et al.* (2007) obtuvieron trisacáridos derivados de trehalosa, como β-Gal-(1→4)-Tre y β-Gal-(1→6)-Tre. A su vez, estas moléculas mostraron un efecto potencialmente prebiótico debido al tipo de enlace generado, muy similar al de algunos tipos de GOS. Por consiguiente, el estudio de β-galactosidasas de diferente origen y la optimización del proceso de transgalactosilación permitiría la síntesis de oligosacáridos potencialmente prebióticos derivados de trehalosa con diversos tipos de enlace. Se debería conocer también la digestibilidad de los mismos, al igual que con el resto de prebióticos, para así observar qué cantidad real es capaz de llegar intacta al intestino grueso.

1.6 Digestibilidad de carbohidratos

Como se ha indicado anteriormente, uno de los requerimientos de los carbohidratos para ser considerados como prebióticos es su nula digestibilidad y absorción. Desde que se formuló la primera definición de prebiótico, la gran mayoría de los estudios científicos han ido enfocados sobre la estimulación selectiva de la microbiota, sin hacer apenas referencia al proceso de digestión anterior. Ha sido recientemente cuando se ha planteado la hipótesis de su hidrólisis parcial en el tracto GI (Ferreira-Lazarte, 2019).

El proceso de digestión de carbohidratos es complejo y comienza en la cavidad oral con la enzima *α*-amilasa salival. La función principal de esta fase es la conversión del alimento en una masa homogénea durante la masticación. La actuación de la enzima es muy limitada debido al corto período de tiempo que permanece el alimento en la boca y a que rápidamente es inactivada por el pH ácido al llegar al estómago (Feher, 2017; Hernández-Hernández *et al.*, 2019). La digestión principal de los carbohidratos ocurre en el intestino delgado, donde el jugo pancreático, que contiene la *α*-amilasa pancreática, se encarga de fragmentar el almidón y producir una mezcla de maltosa [*α*-D-Glc-(1→4)-*α*-D-Glc], maltotriosa [*α*-D-Glc-(1→4)-*α*-D-Glc-(1→4)-*α*-D-Glc] y *α*-dextrinas (compuestos de menor tamaño que contienen las ramificaciones del almidón) (Feher, 2017). Posteriormente, el resto de carbohidratos de la dieta, de menor masa molecular, como la sacarosa o la lactosa, se digieren por la acción de las enzimas de la membrana de las células con borde en cepillo de la mucosa intestinal.

Esta membrana contiene cuatro complejos enzimáticos, esenciales para el último paso de la digestión luminal, tratándose de la producción de monosacáridos, paso previo a la absorción. Las enzimas, también conocidas como disacaridasas, son: lactasa-floricina hidrolasa, sacarasa-isomaltasa, maltasa-glucoamilasa y trehalasa (Hooton *et al.*, 2015). Estas enzimas son responsables de la digestión completa de los carbohidratos de la dieta (**Tabla 2**). El complejo sacarasa-isomaltasa posee dos centros activos: a) Sacarasa, que fragmenta la sacarosa en glucosa y fructosa; y b) Isomaltasa o *α*-dextrinasa, rompe el enlace *α*(1→4) de la maltosa, y el enlace *α*(1→6) de las dextrinas, generando maltosa y maltotriosa. La maltasa-glucoamilasa también posee dos subunidades que hidrolizan los enlaces *α*(1→4) de las maltotriosas y maltosas, y a su vez, los enlaces *α*(1→6) terminales. La trehalasa, en cambio, sólo hidroliza el enlace *α*(1→1) entre las glucosas. La única *β*-glucosidasa presente es la lactasa-floricina hidrolasa, que genera glucosa y galactosa a partir de lactosa, mostrando además actividad en celobiosa, celulosa y *β*-GOS (Ferreira-Lazarte, Olano, *et al.*, 2017; Hooton *et al.*, 2015; Picariello *et al.*, 2016).

Tabla 2. Enzimas humanas encargadas de la digestión de los carbohidratos de la dieta. Adaptado de Hernández-Hernández *et al.* (2019).

Carbohidrasas digestivas	Tipo de enzima	Órgano de producción	Lugar de actuación	Sustratos	Enlace glicosídico afectado	Productos
α-amilasa salival	Secreción: α-glucosidasa	Glándulas salivares	Cavidad oral	Almidón, maltooligosacáridos (DP > 6)	Glc-α(1→4)-Glc	Maltosa, maltotriosa, α-dextrinas
α-amilasa pancreática	Secreción: α-glucosidasa	Páncreas	Intestino delgado			
Lactasa-floricina hidrolasa	Mucosa: β-glucosidasa	Intestino delgado	Microvellosidades del intestino delgado	Lactosa	Glc-β(1→4)-Gal Glc-β(1→4)-Glc	Glucosa, galactosa
Sacarasa-isomaltasa	Mucosa: α-glucosidasa			Sacarosa, isomaltosa, maltosa, maltotriosa, α-dextrinas	Glc-α(1↔2)β-Fru Glc-α(1→4)-Gl Glc-α(1→6)-Glc	Glucosa, fructosa
Maltasa-glucosamilasa				Maltooligosacáridos (DP 2-9)	Glc-α(1→4)-Glc Glc-α(1→6)-Glc	Glucosa
Trehalasa				Trehalosa	Glc-α(1↔1)α-Glc	Glucosa

El proceso de digestión de carbohidratos es gradual y complejo y todas las fases del mismo deben estar involucradas en los protocolos de digestibilidad. A pesar de los estudios disponibles en la bibliografía, el conocimiento de la digestión de carbohidratos prebióticos es aún limitado, debido en parte a que, aunque existen algunos protocolos estandarizados de digestión, no reflejan lo que ocurre *in vivo*. También destacan otros métodos aún en fase de investigación, pero que muestran resultados relevantes, tal y como se indica a continuación.

1.6.1 *Métodos para el análisis de la digestibilidad de carbohidratos*

La mayoría de los protocolos de digestibilidad de alimentos están enfocados en proteínas o almidón, permitiendo distinguir entre almidón rápidamente absorbible o resistente (Englyst *et al.*, 2018; Han *et al.*, 2018). Este tipo de métodos están bien caracterizados y estandarizados y se suelen aplicar a todos los tipos de carbohidratos, sin existir uno específicamente para estos compuestos.

Los modelos de digestión *in vitro* pueden llegar a ser útiles y fiables, permitiendo simular las condiciones fisiológicas del aparato digestivo (pH, temperatura, tiempo de tránsito, peristaltismo, concentración de sales), para así determinar y estudiar la hidrólisis de los carbohidratos (Kopf-Bolanz *et al.*, 2012). Se distinguen modelos de digestión estáticos y continuos. Éstos últimos son multicompartimentales, imitando cada una de las partes del proceso, como un flujo continuo del alimento pasando de órgano a órgano, cada uno con sus condiciones y funciones fisiológicas hasta la fermentación en el intestino grueso. Investigaciones realizadas en estos modelos han mostrado digestión parcial de ingredientes prebióticos, como pectinas. Ferreira-Lazarte, Moreno, *et al.* (2019) observaron un 12% de digestión de pectina de cítricos utilizando un Simulador Gastrointestinal Dinámico (simgi®), mientras que Khodaei *et al.* (2016) reportaron un 20% de hidrólisis de RG-I de patata usando otro sistema dinámico (TIM-1, *TNO GastroIntestinal Model*). Sin embargo, son altamente complejos y costosos para instalar y mantener en un laboratorio convencional y, por ello, son menos utilizados.

Los modelos estáticos *in vitro* son más simples y económicos y con una alta fiabilidad. El método más ampliamente conocido, aceptado y estandarizado es el protocolo InfoGest. Fue desarrollado en 2014 y mejorado en 2019, como un consenso internacional en cuanto a la digestión de alimentos y macronutrientes (Brodkorb *et al.*, 2019; Minekus *et al.*, 2014). Este método se basa fundamentalmente en la utilización de fluidos simulados para cada fase digestiva (**Figura 9**). Haciendo referencia a los carbohidratos, las enzimas que se emplean son la α-amilasa salival y un extracto de jugo pancreático, que contiene la α-amilasa pancreática, lipasas, peptidasas y nucleasas. No obstante, posee limitaciones al no incluir las disacaridasas de la mucosa intestinal.

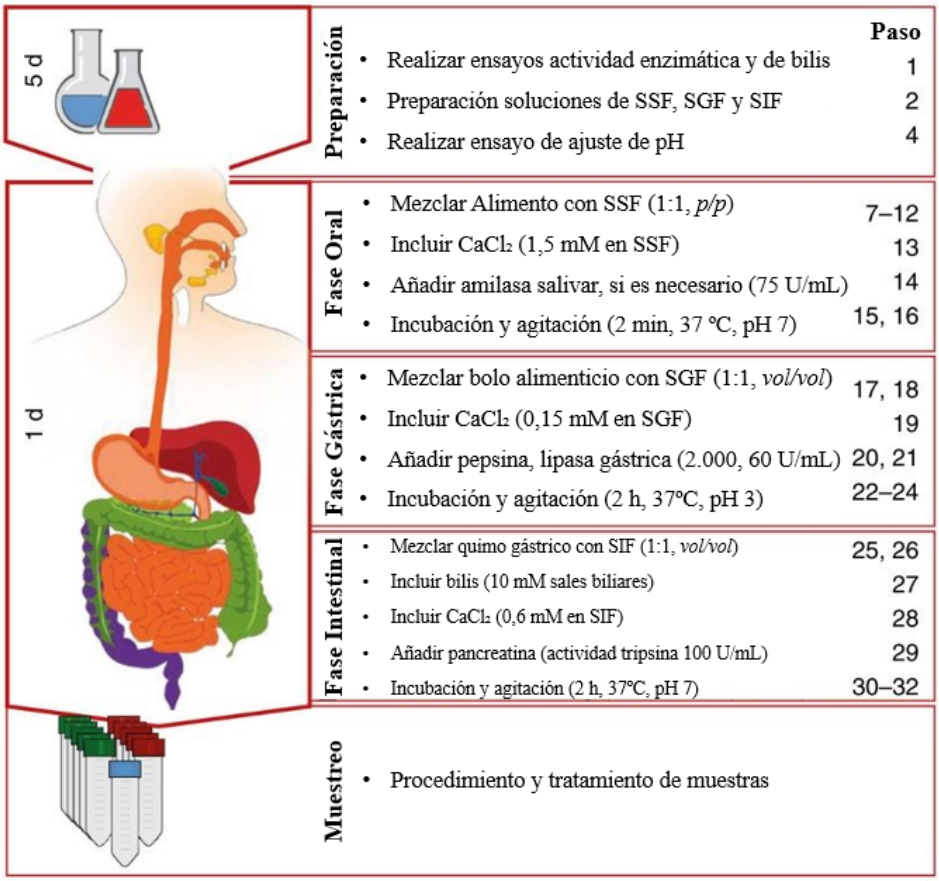

Figura 9. Diagrama de flujo del modelo de digestión INFOGEST 2.0 dividido por las etapas del proceso gastrointestinal. SSF: Fluido salival simulado, SGF: Fluido gástrico simulado, SIF: Fluido intestinal simulado. Adaptado de Brodkorb *et al.* (2019).

En este sentido, Ferreira-Lazarte, Montilla, *et al.* (2017) realizaron un estudio de digestibilidad de GOS y OsLu añadidos a leche, comparando el protocolo InfoGest y un método basado en la utilización de extracto comercial de intestino delgado de rata. Los resultados apuntaron a las posibles limitaciones del método InfoGest en cuanto a la hidrólisis de carbohidratos prebióticos.

Por otro lado, la Asociación Oficial de Química Analítica (AOAC 2009.01) desarrolló un método para evaluar la digestibilidad de la fibra dietética, basado en el uso de enzimas digestivas aisladas (McCleary *et al.*, 2010). Sin embargo, el modelo no permitía la distinción de carbohidratos digeribles y no digeribles al no contener las enzimas de la mucosa intestinal. Los azúcares de la dieta, como la lactosa, eran considerados como no digeribles, lo que puso de manifiesto la clara limitación de este tipo de ensayos (Tanabe *et al.*, 2014). Al igual que ocurre con el protocolo InfoGest, el uso de enzimas de manera individual no refleja la complejidad y el comportamiento real de los carbohidratos durante su digestión en el organismo.

Ha sido recientemente cuando se ha propuesto un método integral y específico para estudiar la digestibilidad de carbohidratos, que distinga los tipos e incluya los complejos enzimáticos de las membranas de las células del borde en cepillo de la mucosa intestinal, así como otras enzimas luminales. Ferreira-Lazarte, Olano, *et al.* (2017) demostraron que el método *in vitro* que emplea un extracto comercial acetónico de intestino delgado de rata es un método simple, eficaz y económico, que permite la distinción entre carbohidratos digeribles y no digeribles con un DP hasta 4, con la ventaja de usar, además, una mínima cantidad de compuesto (0,5 mg). Mediante este procedimiento de digestión se puso de manifiesto la hidrólisis eficaz de azúcares de la dieta (maltosa, lactosa y sacarosa) y la hidrólisis parcial de ingredientes prebióticos, supuestamente indigeribles. Por tanto, la inclusión de las enzimas de la mucosa intestinal proporciona una visión más realista del medio digestivo (Hernández-Hernández, 2019; Hernández-Hernández *et al.*, 2019). Se observó hasta un 34,2% de hidrólisis en diferentes tipos de GOS, un 12% en FOS y un 11,1% en lactulosa y derivados (**Figura 10**) (Ferreira-

Lazarte, Olano, *et al.*, 2017). Esto concuerda con lo obtenido por Hernández-Hernández *et al.* (2012) quienes, mediante un estudio *in vivo*, comprobaron una digestión considerable de GOS y OsLu, resaltando el papel clave de las enzimas de la mucosa y, también, de la microbiota del intestino delgado. A pesar de la digestión parcial en el intestino delgado, el efecto prebiótico en el colon seguía estando presente, sin embargo, dependerá de la cantidad de carbohidrato que sea capaz de alcanzar el colon.

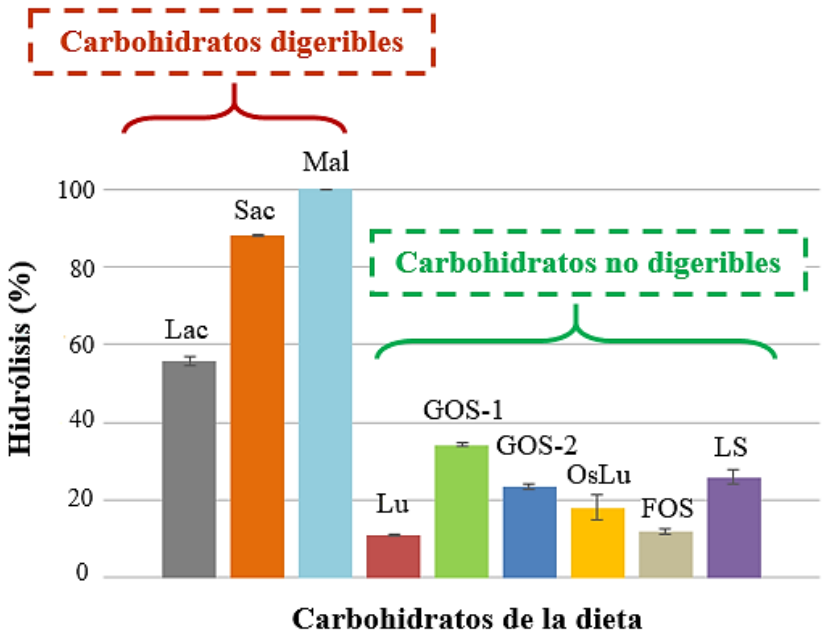

Figura 10. Grado de hidrólisis (%) de carbohidratos digeribles y no digeribles tras la digestión *in vitro* usando extracto de intestino delgado de rata. Lac: lactosa, Sac: sacarosa, Mal: maltosa, Lu: lactulosa, GOS: *β*-galactooligosacáridos, OsLu: galactooligosacáridos derivados de la lactulosa, LS: lactosacarosa. Adaptado de Ferreira-Lazarte, Olano, *et al.* (2017).

En los estudios previamente indicados se puso de manifiesto la importancia de la estructura del carbohidrato para su potencial digestión. La presencia de aldosas o cetosas y el tipo de enlace químico influye de manera determinante en la digestión de este tipo de compuestos. Es evidente que existe digestión parcial de aquellos componentes considerados en otros estudios como no digeribles, principalmente debido a las limitaciones de los métodos actuales y a su falta de estandarización (Ferreira-Lazarte *et*

al., 2020; Hernández-Hernández, 2019). A pesar de las investigaciones realizadas, no se ha realizado un estudio de la cinética de hidrólisis de carbohidratos empleando las enzimas del extracto intestinal. La velocidad de la digestión intestinal de carbohidratos adquiere especial relevancia al relacionarlo con el Índice Glicémico y su protección frente a enfermedades metabólicas. Una hidrólisis lenta de los mismos generaría una absorción más lenta, un aplanamiento de la curva de glucosa y por tanto, una menor liberación de insulina (Fernandes *et al.*, 2017; Mudgil & Barak, 2013).

Siguiendo esta misma línea de investigación, se ha publicado otro modelo de digestión integral, pero con extracto enzimático proveniente del intestino delgado de cerdo, concretamente un extracto purificado que contenía sólo las disacaridasas procedentes de las células del borde en cepillo del intestino delgado. Los resultados obtenidos por Ferreira-Lazarte, Gallego-Lobillo, *et al.* (2019) mostraron similitud con los anteriores, subrayando la influencia de la estructura química y del tipo de enlace en la digestión de oligosacáridos prebióticos. El mayor grado de hidrólisis se observó en los GOS, especialmente en los enlaces $\beta(1\rightarrow3)$ y $\beta(1\rightarrow4)$ (25% y 19,5%, respectivamente), seguido de la lactulosa (12%), los GOS con enlaces $\beta(1\rightarrow6)$ (10,9%) y, por último, los OsLu (10,5%). La similitud enzimática entre las disacaridasas humanas y de rata ha sido estudiada en ensayos *in vitro* por Oku *et al.* (2011). Todo ello, unido a múltiples estudios *in vitro* e *in vivo* que usan extractos de intestino delgado de mamíferos, subraya los resultados prometedores en cuanto patrones de digestión de oligosacáridos y sitúa este tipo de métodos como una herramienta eficaz (Ferreira-Lazarte, Olano, *et al.*, 2017; Hernández-Hernández *et al.*, 2012; Julio-Gonzalez *et al.*, 2019; Lin *et al.*, 2016). Sin embargo, hasta el momento no se ha llevado a cabo ninguna investigación en la que se empleen estos procedimientos más específicos de carbohidratos para estudiar el comportamiento de moléculas de mayor masa molecular y el de otros prebióticos emergentes altamente consumidos, tales como fructanos, pectinas o α-GOS.

Justificación y Objetivos de la Investigación

2. Justificación y Objetivos de la Investigación

El binomio dieta-salud está cada vez más presente en el estilo de vida cotidiano de los individuos, cobrando especial importancia los carbohidratos prebióticos. Este tipo de productos permiten y favorecen el mantenimiento y la modulación de una microbiota intestinal saludable. De esta manera, se contribuye a la homeostasis del organismo y a la reducción del riesgo de enfermedades metabólicas, intestinales y cardiovasculares, como la obesidad, diabetes o enfermedad inflamatoria intestinal. El avance en la investigación en el campo de los prebióticos ha incrementado el conocimiento sobre los mismos en otras patologías, existiendo compuestos más variados y accesibles, en forma de alimento o de nutracéutico. Prebióticos en fase de estudio, como las pectinas (intactas y modificadas) pueden poseer, además, actividad antiproliferativa en determinados tipos de cáncer, según lo investigado en estudios *in vitro*. Sin embargo, en el cáncer de colon los estudios existentes son limitados y contradictorios; en este caso, su digestión y posterior fermentación jugarían un papel esencial. En línea con la obtención de nuevos derivados prebióticos que puedan ejercer efectos beneficiosos más allá de los observados en el intestino grueso, podrían destacar los derivados de trehalosa, cuyas aplicaciones a nivel neurológico, entre otras, incrementarían las posibilidades en el campo de las Ciencias de la Salud.

Dada la repercusión de los prebióticos en la microbiota intestinal, se hace necesario conocer lo que ocurre en la digestión previa empleando modelos realistas. Por definición, la baja o nula hidrólisis de los carbohidratos prebióticos permite su llegada al intestino grueso y su consiguiente modulación de la microbiota. Sin embargo, la mayoría de trabajos relacionados con este tipo de ingredientes han estado enfocados en su efecto sobre las bacterias intestinales y sobre el organismo en general. Escasos estudios se han realizado sobre su digestibilidad.

La aplicación de modelos estandarizados de digestión ha mostrado diversas limitaciones, entre ellas la ausencia de las enzimas presentes en la membrana de las células del borde

en cepillo de la mucosa intestinal. Recientemente, el desarrollo de nuevos métodos de digestión usando extractos de intestino delgado de mamíferos ha reflejado una aproximación más real al entorno intestinal en cuanto a hidrólisis de carbohidratos, observándose digestión parcial de ciertos componentes prebióticos, previamente considerados indigeribles. La inclusión de las disacaridasas en los modelos de digestibilidad es imprescindible para obtener resultados fiables. La ampliación y la validación de este tipo de métodos supone, por tanto, un importante reto de investigación. La mayoría de las investigaciones se realizaron con carbohidratos digeribles y no digeribles de pequeña masa molecular, sin incidir en la cinética de hidrólisis de estos compuestos a nivel intestinal, ni en el estudio de otros carbohidratos prebióticos ampliamente utilizados, algunos de ellos de mayor grado de polimerización. Así, se hace necesario ampliar la idoneidad de estos nuevos métodos de digestión y de aquellos ya establecidos con otro tipo de carbohidratos.

Por ello, teniendo en cuenta los antecedentes previamente expuestos, el objetivo general de la presente Tesis Doctoral es **la síntesis y evaluación de la bioactividad y digestibilidad de diferentes polisacáridos y oligosacáridos con potencial prebiótico.** Por lo tanto, se establecen los siguientes objetivos parciales:

I. **Validación y aplicación de un modelo de digestión *in vitro* basado en un extracto acetónico de intestino delgado de rata en polisacáridos y oligosacáridos prebióticos, y su comparación con el método InfoGest.**

II. **Estudio *in vivo* del efecto de polisacáridos prebióticos en la microbiota intestinal en un modelo de cáncer colorrectal.**

III. **Obtención y caracterización de nuevos carbohidratos potencialmente prebióticos derivados de la trehalosa.**

Plan de Trabajo y Estructura de la Tesis

3. Plan de Trabajo y Estructura de la Tesis

Con el objetivo de lograr los objetivos anteriormente mostrados, el plan de trabajo de la presente Tesis Doctoral está representado esquemáticamente en la página 50. En este sentido, el diagrama proporciona una visión general de los estudios llevados a cabo, organizados en tres bloques principales, coincidentes con los objetivos parciales.

Bloque I. Validación y aplicación de un modelo de digestión *in vitro* basado en un extracto acetónico de intestino delgado de rata en polisacáridos y oligosacáridos prebióticos, y su comparación con el método InfoGest.

a) Estudiar la cinética de hidrólisis enzimática de lactosa y lactulosa mediante las enzimas presentes en el extracto comercial de intestino delgado de rata.
b) Validar y aplicar el modelo establecido de digestión *in vitro* con extracto de intestino delgado de rata en polisacáridos (fructanos) y oligosacáridos prebióticos comerciales (α-GOS y FOS).
c) Validar y comparar la digestibilidad *in vitro* de polisacáridos convencionales (almidón y dextrano) y prebióticos (pectina y pectina modificada) combinando, tanto el modelo de digestión de extracto intestinal de rata establecido, como el protocolo estandarizado InfoGest.

Bloque II. Estudio *in vivo* del efecto de polisacáridos prebióticos en la microbiota intestinal en un modelo de cáncer colorrectal.

a) Investigar *in vivo* el efecto de la pectina de cítricos y la pectina modificada de cítricos en los cambios que se producen en la microbiota intestinal, y sus consecuencias en el cáncer colorrectal, empleando un modelo animal de rata (*Rattus norvegicus* F344).

Bloque III. Obtención y caracterización de nuevos carbohidratos potencialmente prebióticos derivados de la trehalosa.

1. Sintetizar nuevos oligosacáridos derivados de trehalosa a través de reacciones de transgalactosilación usando *β*-galactosidasas de diferentes especies microbianas.
2. Caracterizar estructuralmente los nuevos compuestos obtenidos.

En el primer bloque, según el método de digestibilidad *in vitro* establecido basado en la utilización de extracto de intestino delgado de rata, se realizó el estudio de la actividad enzimática del extracto y de la cinética de hidrólisis de lactosa y lactulosa. Se evaluaron las condiciones de máxima hidrólisis de lactosa y posteriormente, de lactulosa (*Capítulo 1*). La optimización del método permitió la evaluación de la digestibilidad y validación del método, con poli- y oligosacáridos comerciales (*Capítulo 2*). También, se evaluó la digestión de polisacáridos convencionales (almidón y dextrano) y prebióticos (pectina y pectina modificada) con el extracto intestinal de rata, en combinación con el protocolo estandarizado InfoGest (*Capítulo 3*).

En la segunda parte, dada la parcial digestibilidad y el carácter bioactivo de las pectinas, su impacto sobre la microbiota intestinal en relación a su potencial efecto anticancerígeno, se ha evaluado mediante un estudio *in vivo.* El efecto de estos carbohidratos se comprobó en ratas (*Rattus norvegicus F344*) con cáncer inducido mediante combinación de azoximetano y dextrano sulfato de sodio (AOM/DSS), analizando parámetros tumorales, metabólicos, fisiológicos y metagenómicos (*Capítulo 4*).

La tercera parte se basó en la aplicación de enzimas *β*-galactosidasas de diversas fuentes microbianas para la síntesis de nuevos carbohidratos potencialmente prebióticos derivados de trehalosa, con objeto de disponer de compuestos de mayor DP que resitieran a la digestión y alcanzaran porciones más distales del colon. La estructura de los nuevos compuestos se caracterizó mediante RMN (*Capítulo 5*).

Como resultado de la presente Tesis Doctoral, cada uno de los capítulos se corresponde con un trabajo científico, publicados en revistas de alto índice de impacto. Todos ellos se presentan al estilo convencional de un artículo científico (Resumen, Introducción, Materiales y métodos, Resultados y Discusión y Conclusiones). El Resumen integra el objetivo de cada estudio, los resultados más relevantes y las principales conclusiones. La Introducción expone los antecedentes del tema principal del artículo y los objetivos del mismo. La sección de Materiales y métodos muestra el material utilizado y los métodos usados para llevar a cabo el trabajo de investigación. La sección de Resultados y Discusión (combinados o no) indica la relevancia de los resultados obtenidos en la investigación en comparación con la bibliografía. Las Conclusiones principales se presentan en una sección breve y concisa. Tras los capítulos, una sección de Discusión general engloba los resultados de toda la investigación de la Tesis Doctoral, su relación entre sí y con la literatura. Por último, las referencias de cada capítulo se sitúan al final del manuscrito. Además, el material suplementario de los capítulos (*Anexos A-C*) y las publicaciones científicas obtenidas a partir del trabajo desarrollado (*Anexo D*) se sitúan al término de la Tesis Doctoral.

Carbohidratos prebióticos: Mecanismos de digestión, modulación de la microbiota y síntesis de nuevos oligosacáridos

BLOQUE 1

Validación y Aplicación de un Modelo de Digestión *In Vitro* basado en un Extracto Acetónico de Intestino Delgado de Rata en Polisacáridos y Oligosacáridos Prebióticos, y su Comparación con el Método InfoGest.

Capítulo 1. Cinética de hidrólisis enzimática del RSIE.

- Digestión *in vitro* de lactosa a diferentes concentraciones
- Optimización de las condiciones de máxima hidrólisis de lactosa
- Digestión *in vitro* de lactulosa

Capítulo 2. Validación y aplicación del método de digestión de RSIE con polisacáridos.

- Digestión *in vitro* de polisacáridos (fructanos) y oligosacáridos prebióticos (FOS, α-GOS y melibiosa)
- Monitorización del contenido en carbohidratos: GC-FID

Capítulo 3. Combinación de los métodos de digestión de RSIE e InfoGest.

- Digestión gástrica *in vitro* de polisacáridos (almidón, dextrano, pectina y pectina modificada de cítricos) según InfoGest
- Digestión intestinal *in vitro* de polisacáridos según InfoGest y con RSIE
- Comparación entre ambos métodos y su combinación

BLOQUE 2

Estudio *In Vivo* del Efecto de Polisacáridos Prebióticos en la Microbiota Intestinal en un Modelo de Cáncer Colorrectal.

Capítulo 4. Efecto de la pectina y pectina modificada de cítricos en la microbiota intestinal de ratas con cáncer colorrectal.

- Experimento *in vivo* con ratas (*Rattus norvegicus* F344) con cáncer inducido por AOM/DSS alimentadas con pectina y pectina modificada
- Análisis de la microbiota intestinal
- Monitorización del peso e ingesta
- Análisis de los parámetros metabólicos (SCFA, glucemia y triglicéridos) y tumorales (tamaño,número y área)

BLOQUE 3

Obtención y Caracterización de Nuevos Carbohidratos Potencialmente Prebióticos Derivados de la Trehalosa

Capítulo 5. Síntesis y caracterización de oligosacáridos derivados de trehalosa.

- Barrido de β-galactosidasas de diferentes fuentes microbianas
- Síntesis de oligosacáridos de trehalosa catalizado por β-galactosidasas de *Bacillus circulans* y *Aspergillus oryzae*
- Análisis, purificación y aislamiento de los oligosacáridos sintetizados
- Caracterización estructural: GC-MS y RMN

Resultados y Discusión de la Investigación

BLOQUE I

VALIDACIÓN Y APLICACIÓN DE UN MODELO DE DIGESTIÓN *IN VITRO* BASADO EN UN EXTRACTO ACETÓNICO DE INTESTINO DELGADO DE RATA EN POLISACÁRIDOS Y OLIGOSACÁRIDOS PREBIÓTICOS, Y SU COMPARACIÓN CON EL MÉTODO INFOGEST

PREFACIO I

Como ha quedado patente en las secciones anteriores, existen evidencias científicas previas que ponen de manifiesto la necesidad de disponer de métodos de digestión específicos de carbohidratos, así como reconsiderar, en los requisitos que definen a los prebióticos, su "digestión intacta", si bien algunos aspectos necesitan ser clarificados y ampliados. Así, en el primer bloque de la presente Tesis Doctoral se engloban tres capítulos que tratan de arrojar luz sobre la cinética de digestión de carbohidratos empleando un extracto comercial de intestino delgado de rata (*Capítulo 1*), la aplicación de dicho método a compuestos de mayor masa molecular (*Capítulo 2*) y la comparación y complementación con el método armonizado InfoGest (no específico para carbohidratos) (*Capitulo 3*), con el fin de proporcionar conocimientos que permiten una mayor aproximación a la realidad de lo que ocurre con los prebióticos en el tracto gastrointestinal.

Capítulo 1

Kinetic study on the digestibility of lactose and lactulose using small intestinal glycosidases

Pablo Gallego-Lobillo, Alvaro Ferreira-Lazarte, Oswaldo Hernández-Hernández y Mar Villamiel

Instituto de Investigación en Ciencias de la Alimentación, CIAL (CSIC-UAM). C/Nicolás Cabrera, 9, Campus de la Universidad Autónoma de Madrid, 28049 Madrid, España.

Reproducido a partir de Elsevier
Food Chemistry
2020, 316, 126326
DOI: https://doi.org/10.1016/j.foodchem.2020.126326

Abstract

Lactose is mostly hydrolyzed in the small intestine, whereas lactulose, recognized prebiotic carbohydrate, reaches the colon to be fermented by the intestinal microbiota. Digestibility of these substrates was investigated by an *in vitro* digestion model using a Rat Small Intestine Extract (RSIE). A kinetic study of lactose digestion showed levels of hydrolysis (82.8%) at 0.2 mg/mL and the highest hydrolysis rate constant (k_{obt}). Considering these conditions, lactulose showed high resistance to intestinal digestion by RSIE, resulting in low hydrolysis degrees (20.4%) after 5 h reaction. These results underline the suitability of these intestinal extracts under the studied conditions, as a reliable tool to evaluate carbohydrate digestion and support the evidences towards the higher resistance of galactosyl-fructose linkages during its intestinal degradation.

Introduction

Lactose (*β*-D-galactopyranosyl-(1→4)-D-glucopyranose) is produced by the mammary gland in mammals, being the major carbohydrate in milk (4–7%) and the main source of nutrition until weaning. Lactose is hydrolyzed in the small intestine and the resulting monosaccharides (glucose and galactose) are absorbed by the intestinal enterocytes in the blood-stream. Glucose is finally used as a source of energy, and galactose, in the liver, is converted into components of glycolipids and glycoproteins. The hydrolysis of lactose normally occurs in the initial part of the small intestine (jejunum) where the concentration of microorganisms is very low and hardly any amount of lactose is fermented. The hydrolysis of lactose is catalyzed by the enzyme lactasephlorizin hydrolase (*β*-galactosidase or lactase), located in the brush border of the intestinal villi. Most of the individuals are born with the capability to digest lactose, but this activity drops after weaning (around 75% of the world's inhabitants) to an undetectable concentration as a consequence of normal maturational down-regulation of lactase expression. The exceptions to this rule are descendants of people that by tradition practiced cattle domestication and keep the capacity to hydrolyze milk and other dairy foods during adulthood (Belitz *et al.*, 2009; Di Rienzo *et al.*, 2013).

When lactose is not well digested in the small intestine, different symptoms can take place, including abdominal pain, bloating, flatulence, and diarrhea with a considerable intra-individual and inter-individual variability in severity. These symptoms are due to the increased osmotic load that raises the intestinal water content and the fermentation of lactose by the colonic microbiota leading to production of short chain fatty acids and gas (H_2, CO_2, and CH_4) (Bayless *et al.*, 2017). Taking into account these antecedents, it is of importance to know under which circumstances lactose is worse hydrolyzed causing discomfort in the body.

Hardly any research has been done on the lactose hydrolysis during intestinal digestion. Recently, a reliable and simple *in vitro* method using Rat Small Intestine Extract (RSIE)

has been developed for digestion of non-digestible and digestible carbohydrates, such as maltose, sucrose, and lactose. However, that study focused only on a ratio extract/ substrate (20 mg/0.5 mg) and maximum time (2 h), obtaining lactose hydrolysis levels of no more than 56% (Ferreira-Lazarte, Olano, *et al.*, 2017) The aim of the present investigation is to carry out a kinetic study on the digestion of lactose with the RSIE in order to know the conditions that predicate the maximum level of hydrolysis. Moreover, the use of these conditions on the digestion of the recognized prebiotic, lactulose is also intended in order to validate the method as well as to obtain more information of the structure/function of carbohydrates during digestion.

Materials and methods

Chemicals and reagents

In the present work, the following standards have been provided by Sigma-Aldrich (St. Louis, MO): D-galactose (Gal), D-glucose (Glc), sucrose (*β*-D-Fru-(2→1)-*α*-D-Glc), trehalose (*α*-D-Glc-(1→1)-*α*-D-Glc), lactulose (Lu) (*β*-D-Gal-(1→4)-D-Fru), phenyl-*β*-glucoside, *o*-nitrophenyl (o-NP), *p*-nitrophenyl (*p*-NP), *o*-nitrophenyl-*β*-D-glucopyranoside (*o*-NPG), *p*-nitrophenyl-*α*-glucopyranoside (*p*-NPG) and intestinal acetone powders from rat (RSIE), as well as standards for Bradford method (Bio-Rad Laboratories Gmbh, Múnich, Alemania) and for 3,5-dinitrosalicylic acid (DNS) method. Lactose (Lac) (*β*-D-Gal-(1→4)-D-Glc) was obtained from ACROS Organics (Geel, Belgium) and fructose (Fru) from Fluka Analytical (St. Gallen, Switzerland). All standards carbohydrates were of analytical grade (greater than 95%).

Rat Small Intestine Extract characterization

A solution of RSIE (10 mg/mL) was prepared in 0.05 M sodium phosphate buffer at 4 °C following the method of Olaokun *et al.* (2013), with minor changes. Subsequently, centrifugation at 6,000 rpm for 15 min was carried out and the supernatant was used for the complete characterization of RSIE.

Protein content

Protein quantification was done through the Bradford method (1976). Bovine Serum Albumin (BSA) was used as standard and absorbance was measured at 595 nm.

β-galactosidase and maltase activities

The enzymatic activity was determined following the method of Ferreira-Lazarte, Olano, *et al.* (2017) and Warmerdam *et al.* (2014). A spectrophotometer (Specord Plus, Analytik Jena) at 420 nm coupled to a temperature controller (Jumo dTRON 308, Jumo Instrument Co.) was used to obtain *β*-galactosidase activity of RSIE. Reactions of 1,900 µL of an *o*-NPG solution (0.5 mg/mL in phosphate buffer, pH 7) and 100 µL of the solution of RSIE was monitored every 20 s, during 2 h at 37 °C. Then, specific enzymatic activities (U) of RSIE were calculated and expressed in µmol/min*g protein as the amount of enzyme which released 1 µmol of *o*-NP in 1 min of incubation (n = 3).

The same assay was done to obtain the maltase activity, except for the use of a *p*-NPG solution (0.5 mg/mL in phosphate buffer, pH 6.8), measuring the release of *p*-NP during 2 h at 37 °C (n = 3).

Sucrase and trehalose activities

The determination of these enzymatic activities was carried out according to the method of Ferreira-Lazarte, Olano, *et al.* (2017). Two solutions of sucrose and trehalose 5 mg/mL (0.5%, w/w) in sodium phosphate buffer pH 6.8 were prepared. Independently, 500 µL of solution of sucrose and trehalose were mixed with 100 µL of enzymatic solution of RSIE (10 mg/mL) and incubated for 2 h at 37 °C. Aliquots were taken at different times (blank, 5, 15, 30, 60, 90 and 120 min). Reaction was ended with the subsequent addition of 650 µL of DNS. The liberation of the reducing sugars was measured at 540 nm, following the DNS method thus calculating the specific enzymatic activity (U/g protein) (n = 3).

In vitro digestion assays

Firstly, a preliminary assay was conducted to determine the lactose concentration, in which maximum hydrolysis existed, using RSIE. For this purpose, 10 mg/mL RSIE solution was prepared in potassium phosphate buffer 50 mM at pH 6.8. Subsequently, different concentrations of lactose were added to the enzyme mixture: 5, 2, 1, 0.6, 0.2 and 0.1 mg/mL. Digestion was carried out in agitation at 750 rpm and 37 °C for 5 h in a Thermomixer comfort Eppendorf®. Different aliquots were taken at different times (0, 0.5, 1, 2, 3, 4 and 5 h of digestion), which immediately afterwards were heated with boiling water for 5 min to stop the reaction. For the digestion of lactulose with RSIE (10 mg/mL) the same procedure was performed being 0.2 mg/mL the concentration of the disaccharide. In all cases, reaction blanks were performed with RSIE (10 mg/mL) under the same conditions to avoid overestimation of the carbohydrate content.

In addition, lactose control digestions were carried out to confirm the total hydrolysis. Two enzymes were used: Lactozym® 6500 L HP G and Saphera® 2500 L. In the former, a solution of the enzyme at a concentration of 2 µL/mL in potassium phosphate buffer 50 mM with 2 mM of MgCl2 at pH 6.5 was prepared. In the case of Saphera® 2500 L, the concentration was 5 µL/mL in potassium phosphate buffer 50 mM with 2 mM of MgCl2 at pH 6.0. Lactose 0.2 mg/mL was added to this mixture and the reaction was carried out on the Thermomixer at 750 rpm and 40 °C for 5 h. Aliquots were taken at the same time as above indicated for RSIE reactions.

Carbohydrate analysis using gas chromatography

GC-FID was used to analyze the fraction of carbohydrates in each digestion with intestinal extracts. Before the analysis, it was necessary to carry out the derivatization, obtaining trimethylsilyl derivatives from oximes (TMSO) of carbohydrates, according to Ruiz-Matute *et al.* (2011). Firstly, an aliquot of 500 µL of each intestinal digestion was taken (0.1 mg/mL of carbohydrates) and 500 µL of the internal standard solution (*β*-phenyl-glucoside, 0.5 mg/mL) were added and evaporated to dryness. Secondly, for

carbohydrate oximes, 300 µL of hydroxylamine chloride (2.5%, w/v) in pyridine were added, incubated at 70 °C for 30 min. Subsequently, 300 µL of hexamethyldisylazan (HDMS) and 30 µL of trifluoroacetic acid (TFA) were added, allowing to be reacted for 30 min to 50 °C with agitation. Finally, the samples were centrifuged for 2 min at 10,000 rpm. The supernatant (1 µL) was injected into the gas chromatograph.

The analysis was performed on a gas chromatograph (GC7890A), coupled to a flame ionization detector (FID) and an automatic injector 7693 (Agilent Technologies Ing., Palo Alto, CA). Separation was performed in a capillary column of molten silica DB-5HT (30 m × 0.32 mm× 0.10 m) (J&W Scientific, Folson, California, USA), using N_2 at a flow of 1 mL/min as the carrier gas. The temperature of the injector and detector was 280 °C and 385 °C, respectively. The oven temperature was programmed from 150 °C to 380 °C with an increase of 3 °C/min. The sample was injected in split mode 1:20.

Data processing and integration were carried out using an Agilent ChemStations software (Washington, DE, USA). Quantitative analysis was performed using the internal standard method calculating the response factors of the standard carbohydrates (D-fructose, D-galactose, D-glucose and lactose) previously injected at known concentrations (0.005 to 1 mg/mL) with respect to the *β*-phenyl-glucoside.

Statistical analysis

The digestions were done in duplicate and the characterization in triplicate by GC-FID. The results of the GC-FID analysis were statistically compared using variance analysis (ANOVA) for parametric testing in the SPSS software (IBM, Chicago, II), whereby the values are considered to be statistically significant at $p < 0.05$.

Results and discussion

Enzymatic activities of the rat small intestine extract

Table 1 shows the enzymatic activities under the conditions described above. For the determination of the specific enzymatic activity (U/g protein), the protein content of the extract was calculated being 6.1 ± 0.9% (*w/w*). Maltase was found to be the highest enzymatic activity, being twice the sucrase and *β*-galactosidase and 3-fold the trehalase activity. Similar trends were observed in previous reports by Ferreira-Lazarte, Olano, *et al.* (2017) and Oku *et al.* (2011), where the difference between maltase and the other enzymes were almost four times higher. These dissimilarities may be ascribed to the great variability that exists between the different extracts of the small rat intestine. The sucrose activity was slightly higher than the activity of *β*-galactosidase, with no significant differences, as also evidenced by Oku *et al.* (2011) and Semenza & Auricchio (1965).

In the case of the *β*-galactosidase, the activity was very close to that found by Ferreira-Lazarte, Olano, *et al.* (2017). The observed variability between the enzymatic activities of *β*-galactosidase could be due to the fact that these enzymes are gradually degraded with the age of the rat (Alexandre *et al.*, 2013). The trehalase activity was the least active, showing significant differences with the rest of the disaccharidases ($p < 0.05$), similarly to data of Ferreira-Lazarte, Olano, *et al.* (2017) and Oku *et al.* (2011).

Table 1.
Specific enzymatic activities of Rat Small Intestine Extract

Enzymatic activity	Substrate	U (µmol / min*g protein)
β-galactosidase	*o*-NPG	24.76 ± 2.01 [b]
Maltase	*p*-NPG	40.37 ± 0.14 [c]
Sucrase	Sucrose	28.39 ± 2.31 [b]
Trehalase	Trehalose	15.48 ± 1.55 [a]

Protein content of RSIE: 6.1±0.9% (*w/w*). [a-c] Different letters indicate statistical differences ($p<0.05$). Values are expressed as means ± SD (n=3).

Lactose and lactulose digestibility with RSIE

Firstly, digestions of control samples, based on the incubation of RSIE without carbohydrates, were performed under the same experimental conditions of digestions (5 h, pH 6.8, 37 °C, and 750 rpm). The results reflected a limited rise in fructose and galactose (data not shown), while glucose increased significantly during the 5 h digestion. These values were adequately considered to avoid overestimation of the content in monosaccharides.

Fig. 1 shows the evolution of lactose hydrolysis and, consequently, the release of galactose and glucose during intestinal digestion at the different substrate concentrations used (5, 2, 1, 0.6, 0.2, and 0.1 mg/mL of lactose) with RSIE.

The ln (C/C_0) versus time plot of lactose (**Fig. 2**) gave straight lines at each concentration value, indicating the substrate-concentration dependence nature of the reaction, suggesting, therefore, that hydrolysis followed in the first- or pseudo-first- order kinetics (Logan, 1996):

$$C = C_0 \cdot e^{-k_{obt}t}$$

where t represents the incubation time in hours, C is the concentration of lactose at time t, C_0 is the initial concentration in mg 100/mg total carbohydrates and k_{obt} (min^{-1}), the obtained rate constant of the reaction.

Hydrolysis percentages, as well as the hydrolysis rate constant (k_{obt}) and half-life ($t_{1/2} = \ln 0.5/k_{obt}$) values, obtained for lactose are shown in **Table 2**. Higher lactose hydrolysis values were correlated with lower initial contents of this substrate compared to enzymatic extract used (higher E:S ratio), which was maintained constant in all assays. In this sense, the maximum hydrolysis of lactose was 82.8% at a concentration of 0.2 mg/mL, without reaching total carbohydrate degradation. The hydrolysis observed at the lowest concentration, 0.1 mg/mL, was slightly lower (77%), indicating that the maximum RSIE activity was reached at 0.2 mg/mL concentration.

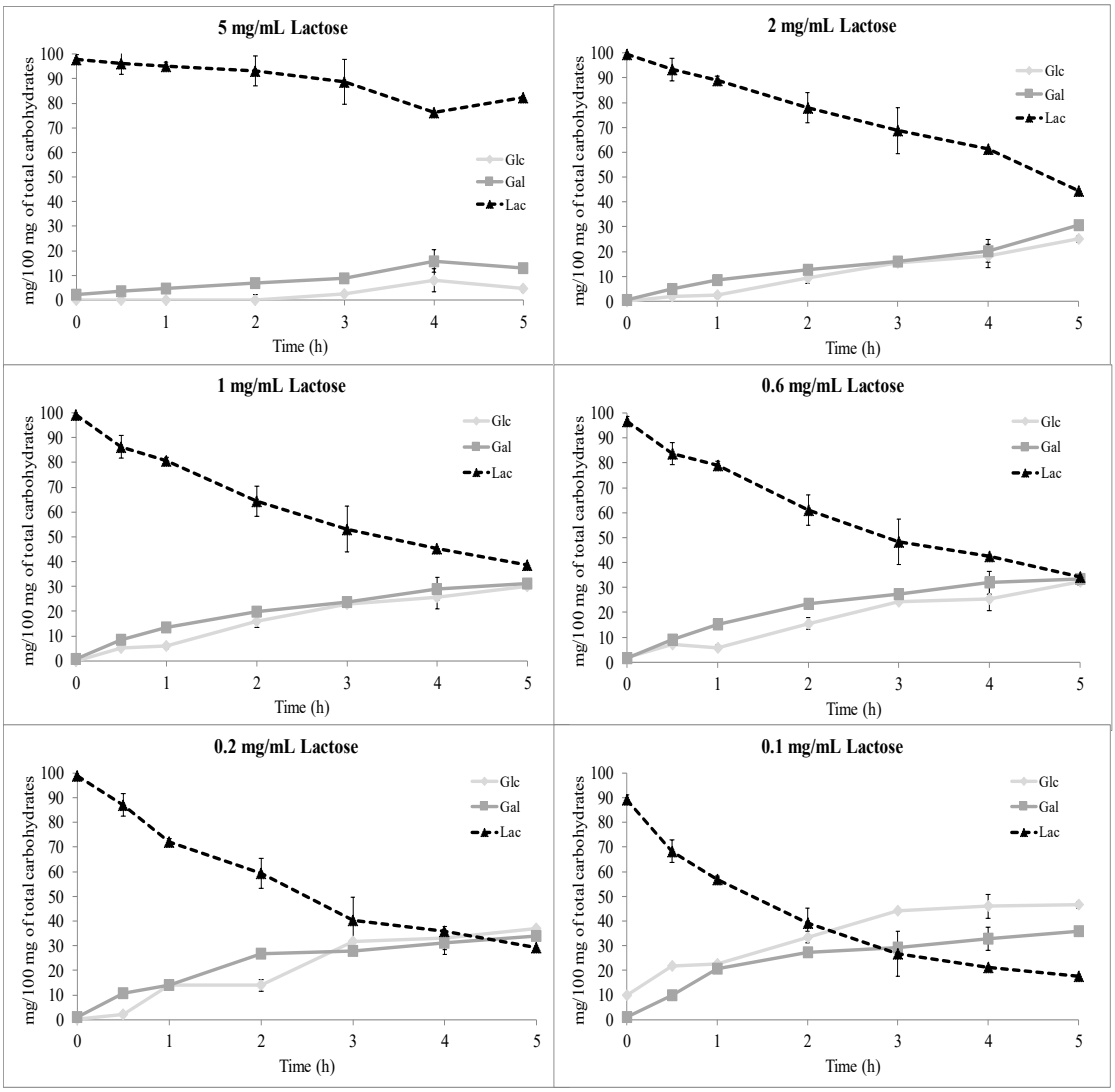

Figure 1. Evolution of the carbohydrate content in the digestion of lactose at different concentrations: 5 (A), 2 (B), 1 (C), 0.6 (D), 0.2 (E) and 0.1 (F) mg/mL during 5 h of small intestinal digestion using RSIE at 37ºC, pH 6.8

Table 2.

Table 2a. Hydrolysis degree (%) of lactose at different concentrations and lactulose (0.2 mg/mL) using Rat Small Intestine Extract at 37 ºC, pH 6.8

Digestion time (h)	Lactose concentration						**Lactulose**
	5 mg/mL	2 mg/mL	1 mg/mL	0.6 mg/mL	**0.2 mg/mL***	0.1 mg/mL	**0.2 mg/mL***
0.5	1.48 ± 1.93	16.03 ± 1.81	11.15 ± 0.10	13.71 ± 0.75	**42.95 ± 1.00**	28.30 ± 0.01	**2.05 ± 2.32**
1	2.51 ± 1.00	18.13 ± 0.78	25.60 ± 5.70	42.90 ± 2.45	**60.04 ± 5.31**	47.25 ± 0.82	**4.27 ± 3.70**
2	4.74 ± 1.55	28.05 ± 6.68	35.07 ± 5.04	45.79 ± 3.51	**64.61 ± 5.40**	59.38 ± 0.81	**10.20 ± 4.20**
3	9.10 ± 1.60	40.62 ± 1.50	45.24 ± 3.20	53.99 ± 2.16	**74.07 ± 5.92**	64.88 ± 0.29	**20.17 ± 0.01**
4	22.09 ± 2.21	46.01 ± 0.20	51.98 ± 3.48	65.59 ± 2.63	**78.54 ± 5.12**	72.67 ± 0.44	**19.32 ± 0.04**
5	15.84 ± 0.10	64.44 ± 1.10	53.77 ± 2.54	68.96 ± 1.68	**82.81 ± 4.99**	76.95 ± 0.42	**20.41 ± 0.09**

*Digestion of lactulose was done in the conditions of the highest hydrolysis of lactose (0.2 mg/mL).
Values are expressed as means ± SD (n=2).

Table 2b. Hydrolysis rate constants obtained (k_{obt}) and half-lives ($t_{1/2}$) after 2 and 5 hours digestion at the different concentrations of lactose

	2 hours		5 hours	
Lactose concentration (mg /mL)	k_{obt} (min^{-1})	$t_{1/2}$ (min)	k_{obt} (min^{-1})	$t_{1/2}$ (min)
5	4.7×10^{-3}	146.77	3.0×10^{-3}	234.05
2	2.7×10^{-3}	252.69	3.4×10^{-3}	201.10
1	3.6×10^{-3}	192.62	2.6×10^{-3}	269.51
0.6	5.1×10^{-3}	135.84	3.9×10^{-3}	177.74
0.2	$\mathbf{8.7 \times 10^{-3}}$	**80.07**	$\mathbf{5.9 \times 10^{-3}}$	**118.09**
0.1	7.5×10^{-3}	92.32	4.9×10^{-3}	141.71

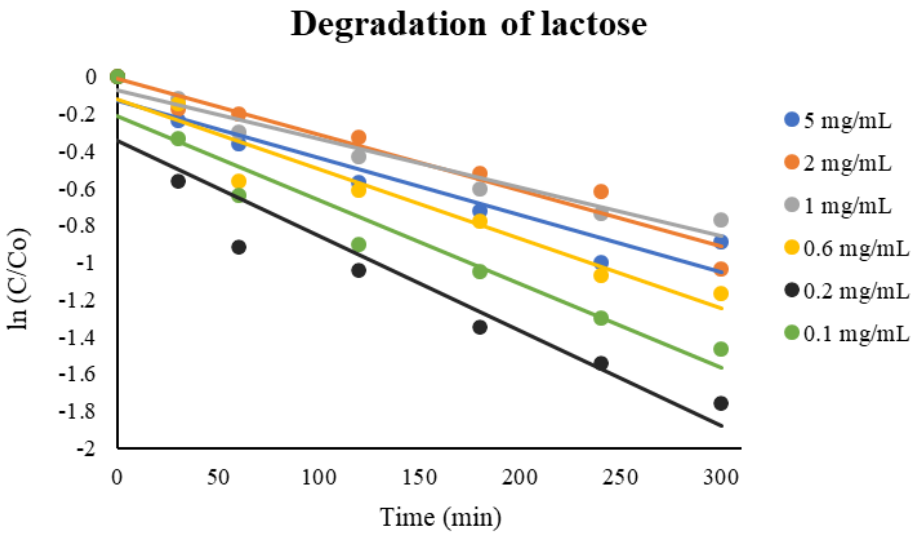

Figure 2. Kinetics of lactose hydrolysis at the different concentrations during small intestinal digestion using RSIE at 37ºC, pH 6.8.

Additionally, k_{obt} determined after 2 and 5 h of digestion showed the highest values for the reaction with 0.2 mg/mL and consequently the lowest $t_{1/2}$ at these conditions. Higher values of k_{obt} were observed after 2 h of digestion when compared to 5 h digestion, highlighting that the hydrolysis of the lactose was faster in the first stages of reaction due to higher presence of the disaccharide and lower concentration of monosaccharides that could inhibit the enzyme activity, which decreases over time.

Furthermore, lactose control digestions that were performed under the same conditions with *Kluyveromyces lactis* and *Bifidobacterium bifidum* commercial lactase (data not shown), showed a total degradation of lactose at 30 min of digestion in the case of *K. lactis*, and at 1 h in the case of *B. bifidum*, confirming its total hydrolysis, unlike the RSIE. Previous studies (Santibáñez *et al.*, 2016) have shown the high capacity of *K. lactis* and *B. bifidum* lactases to hydrolyze lactose, being used by the industry to obtain lactose-free milks. However, in the case of RSIE, total hydrolysis could not be obtained under the same conditions, probably due to the fact that the *β*-galactosidase activity, among all the disaccharidases present in the small intestine of the rat, was not the most relevant (Ferreira-Lazarte, Olano, *et al.*, 2017; Oku *et al.*, 2011; Prieto *et al.*, 1994).

Concretely, Ferreira-Lazarte, Olano, *et al.* (2017) obtained 55% of lactose hydrolysis at 2 h using a similar RSIE, with an E:S ratio of 20:0.5. The E:S ratio used in our study was 10:0.2 obtaining a slightly higher hydrolysis at 2 h (64%) probably due to the lower lactose presence.

Considering the obtained results, a subsequent assay was carried out with lactulose at the optimal conditions to evaluate the influence of a different structure in the digestion with RSIE. **Fig. 3** illustrates the evolution of lactulose over 5 h digestion, where a minimum hydrolysis of lactulose accompanied by a slight formation of galactose and fructose monosaccharides can be observed.

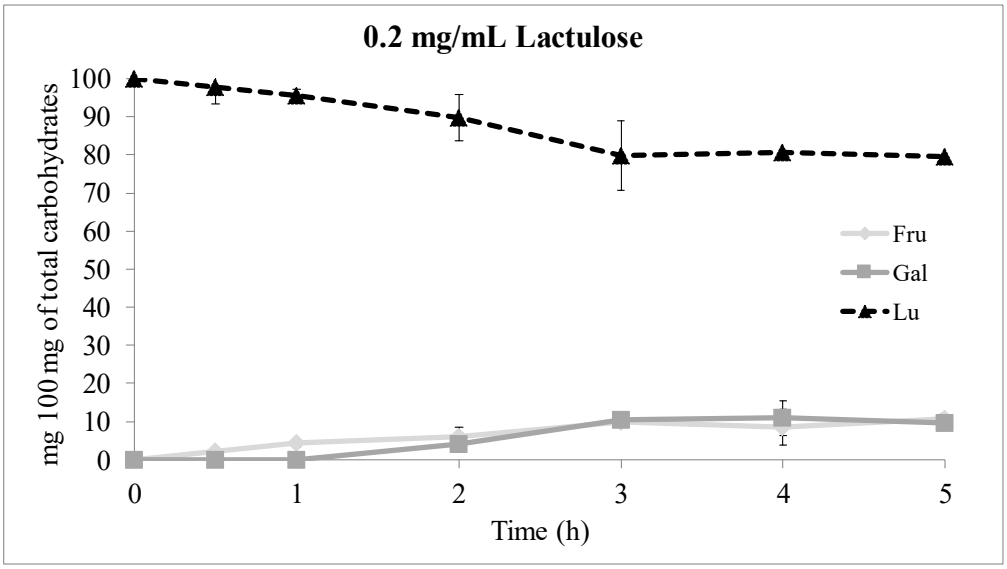

Figure 3. Evolution in the carbohydrate content of lactulose during the intestinal digestion of lactulose at 0.2 mg/mL during 5 h with RSIE at 37ºC, pH 6.8.

Table 2 also shows the percentages of lactulose hydrolysis as compared to lactose data obtained. Thus, a high resistance to intestinal digestion by lactulose can be observed, with only 20.4% hydrolysis after 5 h, showing meaningful differences with respect to lactose (82.8%) due to the different chemical linkages and/or the presence of a ketose (fructose) or aldose (glucose) in the structure (Ferreira-Lazarte, Olano, *et al.*, 2017; Hernández-Hernández *et al.*, 2011). Besides, 10% of lactulose hydrolysis was observed

after 2 h of digestion, which was very similar to a previous study (11%) by Ferreira-Lazarte, Olano, *et al.* (2017) using similar conditions.

Furthermore, GC-FID profiles of the optimal concentration are shown in the supplementary material (**Figs. S1 and S2**). In **Fig. S1**, lactose is identified as peak 3, illustrating the high hydrolysis of the disaccharide along the small intestinal digestion. Formation of monosaccharides is also observed (peaks 1 and 2). On the other hand, digestion of lactulose in **Fig. S2** shows the slight decrease of lactulose (peak 4) and the corresponding increase of fructose and galactose (peaks 1 and 2, respectively).

Kinetics of the reaction can also be observed in **Table 3**; low hydrolysis rate constants underline the high resistance of this substrate as compared to lactose resulting in higher $t_{1/2}$ values for the former, 700-900 min and 80-120 min, respectively. Hydrolysis evolution with RSIE of lactose and lactulose is heavily dependent on their chemical structure. Therefore, these data highlight the higher resistance to mammalian digestive enzymes of galactosyl-fructose (lactulose) as compared to galactosyl-glucose (lactose) (Hernández-Hernández *et al.*, 2012) and, although more studies are needed, reveal that this prebiotic carbohydrate can be partially digested in the small intestine before reaching the colon to be fermented by the colonic microbiota. This result reflect that very well-known prebiotic carbohydrates are not completely non-digested as proposed in the last prebiotic concept consensus (Gibson *et al.*, 2017), supporting the fact that prebiotic can be partially digested (Ferreira-Lazarte, Olano, *et al.*, 2017; Hernández-Hernández, 2019; Hernández-Hernández *et al.*, 2012).

Table 3. Kinetics of the degradation of lactulose during the digestion of lactulose at during 2 and 5 h with RSIE at 37ºC, pH 6.8.

Lactulose concentration (mg/mL)	**2 hours**		**5 hours**	
	k_{obt} (min^{-1})	$t_{1/2}$ (min)	k_{obt} (min^{-1})	$t_{1/2}$ (min)
0.2	9.0×10^{-4}	772.89	7.6×10^{-4}	911.07

Conclusions

Several limitations of traditional digestibility methods towards carbohydrates have been already shown in the literature (Ferreira-Lazarte, 2019; Hernández-Hernández, 2019). In this sense, according to the data obtained in the present work, RSIE has proved to be a reliable and efficient tool to evaluate the digestibility of a dietary carbohydrate (lactose) and a recognized prebiotic carbohydrate (lactulose). Conditions of maximum hydrolysis of lactose have been optimized and lactulose resistance to intestinal digestion was evaluated with a kinetic assay under these conditions. Lactose reached the maximum hydrolysis at 0.2 mg/mL with 10 mg/mL RSIE (82.8%) presenting the highest k_{obt} after 2 and 5 h digestion, indicating a major hydrolysis in the first stages of reaction probably due to the more quantity of substrate. Furthermore, in the same conditions, lactulose, was more resistant to digestion when compared to lactose, although could be slightly hydrolyzed (20.4%) by RSIE and, therefore, could not reach the colon intact, emphasizing the key role of the chemical structure in the digestion of carbohydrates.

Acknowledgments

Authors acknowledge the finance of this work by the Spanish Ministry of Economy, Industry and Competitiveness (Project AGL2017-84614-C2-1-R) and the Spanish Ministry of Science, Innovation and Universities (Project RTI2018-101273-J-I00).

Capítulo 2

Evaluation of the impact of a rat small intestinal extract on the digestion of four different functional fibers

Pablo Gallego-Lobillo, Alvaro Ferreira-Lazarte, Oswaldo Hernández-Hernández, Antonia Montilla y Mar Villamiel

Instituto de Investigación en Ciencias de la Alimentación, CIAL (CSIC-UAM). C/Nicolás Cabrera, 9, Campus de la Universidad Autónoma de Madrid, 28049 Madrid, España.

Reproducido a partir de Royal Society of Chemistry
Food & Function
2020, 11(5), 4081-4089
DOI: https://doi.org/10.1039/D0FO00236D

Abstract

The degree of digestion, modulated by rat small intestinal extract on different functional fibers was investigated. In general, inulin-type fructans and fructooligosaccharides were the most resistant to the enzymatic digestion. Results evidenced the high-resistance of fructosyl-fructose bonds. This fits well with the concept of prebiotic carbohydrates. However, the mixture of melibiose, manninotriose and verbascotetraose (α-GOS) from peas, with a considerably lower molecular weight (0.6 kDa) than the fructans studied, were highly digested (61.2%). Interestingly, the Gal-α(1→6)-Gal bonds present into the manninotriose and verbascotetraose were more prone to be hydrolyzed than Gal-α(1→6)-Glc (melibiose). However, when melibiose was the only disaccharide present in the reaction mixture, the hydrolysis was also high (67.7%). The use of small intestinal enzymatic preparations is a realistic approximation to evaluate the digestion of different carbohydrates, thus showing that recognized non-digestible carbohydrates can also be partially digested.

Introduction

The recommended daily allowances (RDAs) for total fiber consumption for healthy men and women (19–50 years old) are 38 g/day and 25 g/day, respectively, and these general needs can vary depending on the health status of the individual. Although fibers have revealed to possess numerous positive health effects on severe pathologies (obesity, diabetes, cardiovascular disease, among others), the mean daily intake for most people is much lower than the RDA. There is no superior acceptable amount for fiber consumption, although the tolerance depends mainly on the individual; bloating and abdominal pain being the most important consequences of excessive intake (Soliman, 2019; Van Hul & Cani, 2019).

In general, the total fiber consumption is the quantity of dietary fiber and functional fiber. Technically, dietary fiber is a complex group of carbohydrates and lignin, which are not digested nor absorbed, in the human body. They can be divided in two major groups: soluble and insoluble fiber according to their water solubility, both being indigestible in the small intestine (Abdul-Hamid & Luan, 2000; Champe & Harvey, 1994; Qi *et al.*, 2018).

Functional fibers constitute a wide range of non-digestible carbohydrates that are either isolated or synthesized from natural sources mainly agro-food by-products. Once the functional fiber is produced is added to food during processing with the aim of providing beneficial effects on human health. Functional fibers include polysaccharides such as β-glucans, cellulose, chitins and chitosan, fructans, gums, pectin, polydextrose, polyols, resistant dextrins, resistant starches and oligosaccharides that are resistant to digestion (Soliman, 2019).

According to previous studies, these carbohydrates can reach intact the large intestine, where they are hydrolyzed and fermented by the intestinal microbiota, thus causing the production of short chain fatty acids (SCFAs) that exert a beneficial effect not only in

the colon but also systemically (Cani & Jordan, 2018; Chambers *et al.*, 2018; Louis & Flint, 2017). However, few studies have been conducted on the digestive resistance of carbohydrates (also refereed as non-digestible carbohydrates), probably due to the lack of reliable digestion methods specifically designed for carbohydrates.

To date, the focus of the most common approach to simulate the small intestinal digestion is dedicated to proteins, lipids and starch, by using pancreatic enzymes from porcine origin, salivary enzymes and microbial enzymes, which could not reflex most of the carbohydrase activities of the whole small intestine (Brodkorb *et al.*, 2019). The Association of Official Analytical Chemist (AOAC) developed an integrated determination method for dietary fiber, including non-digestible oligosaccharides (NDOs) and resistant starch, which was modified later in 2015 (AOAC 2009.01) (McCleary *et al.*, 2010; 2015). Other methods, as well as this method, are based on the use of isolated digestive enzymes. Porcine pancreatic *α*-amylase and a fungal amyloglucosidase from *Aspergillus niger* are used to produce the complete hydrolysis of digestible saccharides, and therefore, to distinguish between digestible and non-digestible carbohydrates. However, similar to the InfoGest protocol, these enzymes cannot completely hydrolyze digestible saccharides since they do not represent the fully complex enzymatic environment of the small intestine, mainly because of the absence of the brush border enzymes of the enterocytes. As a result, digestible saccharides that are not fully degraded are detected as non-digestible carbohydrates, which lead to an inaccurate determination of the digestion resistance of these carbohydrates (Ferreira-Lazarte, 2019; Tanabe *et al.*, 2014). Recently, a promising *in vitro* digestibility method of dietary carbohydrates using rat small intestinal extract (RSIE) has questioned the belief that recognized prebiotics oligosaccharides derived from lactose (GOS) and fructooligosaccharides (FOS) reach the distal portions of colon without alterations (Ferreira-Lazarte, Gallego-Lobillo, *et al.*, 2019; Ferreira-Lazarte, Montilla, *et al.*, 2017; Ferreira-Lazarte, Olano, *et al.*, 2017). Therefore, with the aim of gain more insight on the benefits of non-digestible carbohydrates, in this work the digestibility of commercial

functional fiber, such as α-galactooligosaccharides derived from peas and different types of fructans have been tested using a rat small intestine extract.

Materials and methods

Chemicals and reagents

Fructose (Fru) standard was obtained from Fluka Analytical (St Gallen, Switzerland). Analytical standards of D-galactose (Gal), D-glucose (Glc), maltose (α-D-Glc-(1→4)-D-Glc), sucrose (β-D-Fru-(2→1)-α-D-Glc), phenyl-β-D-glucoside, pullulan set (805-0.34 kDa), as well as the reagents for Bradford method (Bio-Rad Laboratory Gmbh, Munich, Germany) and intestinal acetone powders from rat (Rat Small Intestine Extract, RSIE) were provided by Sigma-Aldrich (St Louis, MO). Lactose (β-D-Gal-(1→4)-D-Glc) standard was purchased from ACROS Organics (Geel, Belgium). Melibiose (α-D-Gal-(1→6)-D-Glc) standard was obtained from Thermo Fisher Scientific (Kandel, Germany). Analytical standards of kestose (β-D-Fru-(2→1)-β-D-Fru-(2→1)-α-D-Glc) and nystose (β-D-Fru-(2→1)-β-D-Fru-(2→1)-β-D-Fru-(2→1)-α-D-Glc) were supplied by FUJIFILM Wako Chemical Corporation (Neuss, Germany).

Prebiotic carbohydrates

Four types of commercial carbohydrates were used for the digestion assays: Orafti® GR (92% of inulin and 8% of FOS with a degree of polymerization (DP) up to 10), Raftiline® High Performance (inulin with an average DP up to 25), Raftilose® P95 (FOS; DP 3 to 7). These carbohydrates were obtained from Orafti S. A. (Oreye, Belgium). In addition, a commercial mixture of α-GOS with DP 2–4 (AlphaGOS® P) from Olygose (Venette, France) were tested.

Characterization of substrate by HPSEC-ELSD

The molecular weight (M_w) of each carbohydrate was obtained by High Performance Size Exclusion Chromatography (HPSEC) coupled to an Evaporative Light Scattering

Detector (ELSD), following the method described by Muñoz-Almagro, Rico-Rodriguez, Villamiel, *et al.* (2018). Analysis was carried out on a LC 1220 Infinity System (Agilent Technologies, Boebligen, Germany), using two TSK-GEL columns (G5000 PWXL, 7.8 × 300 mm, 10 µm; G2500 PWXL, 7.8 × 300 mm, 6 µm) linked with a TSK-Gel guard column (6.0 mm × 400 mm) (Tosoh Bioscience, Stuttgart, Germany). Diluted samples were filtered (0.45 µm) and eluted (20 µL) with 0.1 M $NH_4CH_3CO_2$, at a flow rate of 0.5 mL/min for 50 min at 30 °C. The detection was carried out on an ELSD System 1260 Infinity (Agilent Technologies, Boebligen, Germany). Pullulans of M_w 805, 200, 10, 1.3 and 0.34 kDa were used as calibration standards.

Enzymatic characterization of rat small intestine extract

Protein determination

Protein quantification was done through the Bradford method (1976). Bovine Serum Albumin (BSA) was used as a standard and absorbance was measured at 595 nm.

Enzymatic activities

Sucrase, melibiase and inulinase activities of RSIE were established by GC-FID. Firstly, solutions of sucrose, melibiose and inulin were incubated with RSIE (40 mg/mL) in distilled water (pH 6.8) during 180 min at 37 °C in an orbital Thermomixer comfort (Eppendorf®). Aliquots were taken in 0, 60, 120 and 180 min and inactivated in boiling water for 5 min.

The carbohydrate hydrolysis was measured through GC-FID as described below. Specific enzymatic activities (U) of RSIE were calculated and expressed in µmol per (min per g per protein). Each unit of specific enzymatic activity was defined as the amount of enzyme which released 1 µmol of the corresponding monosaccharides in 1 min of incubation (n = 4).

In vitro digestion of polysaccharides with RSIE

The digestibility of three types of inulin, a mixture of *α*-GOS and the corresponding blanks (no added carbohydrate sample) were digested with RSIE following the method used by Ferreira-Lazarte, Olano, *et al.* (2017) with slight changes. Initially, a solution of 0.5 mg/mL of prebiotic carbohydrate in distilled water was prepared, then 40 mg of RSIE was mixed with 1 mL of prebiotic solution and the mixture was incubated to perform the reactions. Digestions were carried out in an orbital Thermomixer comfort (Eppendorf®) at 37 °C during 3 h of reaction with continuous agitation (750 rpm). Duplicate of individual reactions were carried out for each time (0, 60, 120 and 180 min) in order to avoid any possible enzymes/substrate composition changes produced by taking aliquots, and reactions were stopped by heating in boiling water for 5 min.

Chromatographic analysis of carbohydrates

Gas chromatography, equipped with a flame ionization detector (GC-FID), was used to analyze the fraction of carbohydrates for each enzymatic characterization and digestion. Samples were derivatized, to obtain trimethylsilylated oximes (TSMO) of carbohydrates, according to the method of Brobst & Lott (1966). Samples solutions were prepared with 500 µL of digestion samples (0.25 mg of carbohydrates) and 250 µL of phenyl-*β*-D-glucoside (internal standard, 0.5 mg/mL), and were evaporated under vacuum. Three hundred µL of hydroxylamine chloride in pyridine (2.5%, *w/v*) were added to the samples and incubated at 70 °C for 30 min with agitation. Then, 300 µL of hexamethyldisilazane (HDMS) and 30 µL of trifluoroacetic acid (TFA) were added and heated at 50 °C for 30 min under continuous agitation. Finally, samples were centrifuged at 10 000 rpm for 3 min. Supernatants were injected in GC-FID.

GC-FID analysis was carried out in an Agilent Technologies 7820A gas chromatograph system. Separations of the compounds were achieved with a fused silica capillary column DB-5HT (5% phenyl methylpolysiloxane, 30 m × 0.25 mm × 0.1 µm, Agilent J&W Scientific, Folsom, CA, USA). The initial oven temperature was 150 °C, then

increased at a rate of 3 °C/min to 380 °C. The carrier gas used was nitrogen at a flow rate of 1 mL/min. Injector and detector temperatures were set at 280 and 385 °C, respectively. Split mode 1:20 were used for the injections.

Interpretation and identification of the TMSO derivatives were performed using Agilent ChemStation software (Washington, DE, USA). Quantitative analysis was obtained through the internal standard method, thus calculating the response factors of standards solutions of carbohydrates (D-fructose, D-galactose, D-glucose, sucrose, lactose, kestose, nystose) at known concentrations (0.005 to 1 mg/mL).

Statistical analysis

All digestions were made in duplicate and two GC-FID analysis (n = 2). For the statistical analysis, comparisons were made using analysis of variance (ANOVA) and Tukey's post hoc test with SPSS software for Windows (SPSS Inc., Chicago, II). Differences between content in carbohydrates were considered statistically significant when $p < 0.05$.

Results and discussion

Enzymatic characterization of RSIE

Table 1 shows the sucrase, inulinase and melibiase activities of RSIE analyzed by GC-FID in the same conditions of digestion. Sucrase activity (42.07 U) was the highest, being 2-fold higher than melibiase activity (26.56 U) and eight times higher than inulinase (5.46 U). Sucrase activity obtained was moderately higher than the values obtained in previous reports in rats by Ferreira-Lazarte, Olano, *et al.* (2017) (23.5 U). These differences could be due to the variability between the batches of commercial intestinal acetone powders from rat. Regarding inulinase and melibiase activity, no previous studies have reported these activities in these enzymatic substrates.

RSIE is a complex mixture of proteins, cells, lipids, enzymes and other carbohydrates contained in the small intestine. Sucrose (*β*-D-Fru-(2→1)-*α*-D-Glc) and melibiose (*α*-D-Gal-(1→6)-D-Glc) hydrolysis can be attributed to the sucrase-isomaltase complex (Feher, 2017). Sucrase site splits glucose and fructose, while isomaltase site splits Glc–Glc *α*(1→4) and *α*(1→6) linkages, being one of the most common complexes in the small intestine (Hooton *et al.*, 2015). Inulinase activity showed the lowest value, which could be related to the low digestibility of prebiotic fructans (Ferreira-Lazarte, Olano, *et al.*, 2017; Rastall, 2010).

Table 1. Specific enzymatic activities and protein content of Rat Small Intestine Extract (RSIE) at 37 ºC and pH 6.8

Activity	Substrate	U (µmol / min*g protein)
Sucrase	Sucrose	42.07 ± 2.6[a]
Inulinase	Inulin	5.46 ± 0.1[a]
Melibiase	Melibiose	26.56 ± 7.1[b]

Protein content of RSIE was 6.9 ± 0.5% (w/w).
Hydrolytic activities were calculated by measuring the carbohydrate evolution by GC-FID: [a] Increase of µmol of fructose. [b] Increase of µmol of galactose.

Characterization of prebiotic carbohydrates

The chromatographic profiles corresponding to the molecular weight (M_w) distribution of carbohydrates used in the digestion assays are showed in **Fig. 1**. Raftiline HP had the highest M_w (3.4 kDa – 19 DP), followed by Inulin Orafti GR (2.6 kDa; 14.5 DP); Raftilose P95 and AlphaGOS P presented similar values (0.6 and 0.7 kDa and 3.3 and 4.0 DP, respectively); and melibiose the lowest (0.4 kDa; 2.2 DP). Raftiline HP is reported to be a polysaccharide composed of mainly inulin, with a high DP (10–60) and higher M_w (Ávila-Fernández *et al.*, 2016; Franck, 2002; Mensink *et al.*, 2015; Schaller-Povolny *et al.*, 2000). A similar situation occurs with inulin Orafti GR, although a slightly lower M_w inulin was observed in this case (Ávila-Fernández *et al.*, 2016; Han *et al.*, 2013; *Product Sheet DOC.A4-03/001 Orafti ® GR*, 2016). Raftilose P95 and AlphaGOS P oligosaccharides showed the lowest M_w, 0.6 kDa (3.3 DP) and 0.7 kDa (4.0

DP), respectively (Blecker *et al.*, 2002; Franck, 2002; Han *et al.*, 2013; Mensink *et al.*, 2015; Nobre *et al.*, 2018).

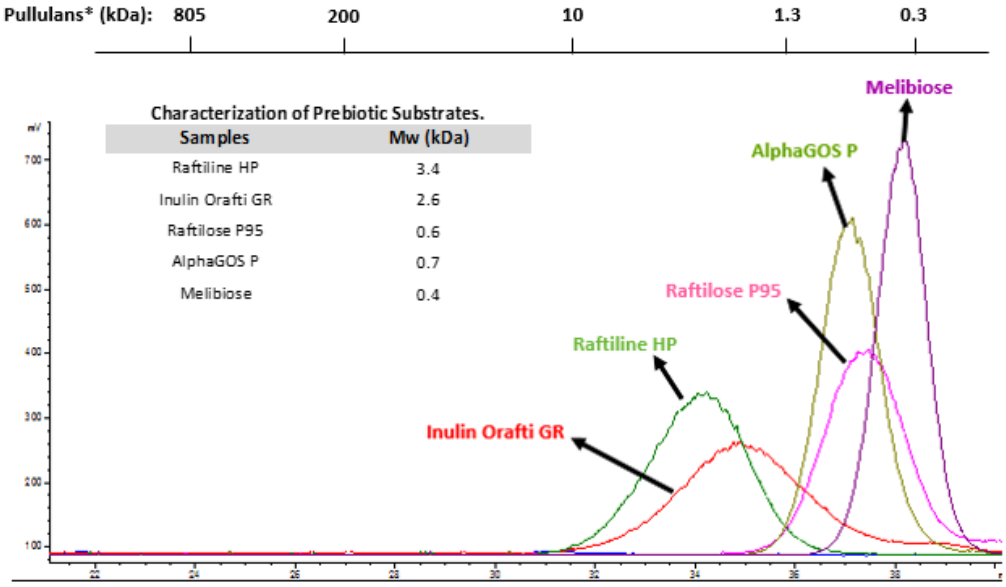

Figure 1. Molecular weight (M_w) and chromatographic profiles by HPSEC-ELSD of prebiotic carbohydrates used in the digestion assays. *M_w of standards of pullulans is indicated above.

Digestion of prebiotic carbohydrates using RSIE

The digestibility of three recognized prebiotics (Inulin Orafti GR, Raftiline HP and Raftilose P95) and two potential prebiotic carbohydrates (AlphaGOS P and melibiose) were tested using RSIE. Blank samples of digestion without carbohydrates were also carried out to measure possible matrix effects of this complex mixture (Pyner *et al.*, 2017).

Table 2 shows the individual composition of each carbohydrate incubated with RSIE, including mono-, di-, tri- and tetrasaccharide fractions. Before digestion treatments, Raftiline HP which is described as an inulin-type long-chain fructans, where DP below 10 is removed (Kelly, 2008), did not show any carbohydrate with DP < 4, apart from small amounts of fructose. On the other side, Inulin Orafti GR contains small amounts of FOS, detected as nystose, kestose and sucrose. Fructooligosaccharides (Raftilose P95)

showed higher contents of small compounds (DP < 4) due to their oligosaccharide composition. Inulobiose (*β*-D-Fru-(2→1)-*β*-D-Fru), inulotriose (*β*-D-Fru-(2→1)-*β*-D-Fru-(2→1)-*β*-D-Fru), inulotetraose (*β*-D-Fru-(2→1)-*β*-D-Fru-(2→1)-*β*-D-Fru-(2→1)-*β*-D-Fru) and nystose were detected in Raftilose P95 samples, in agreement with the data reported by Montilla *et al.* (2006). Interestingly, the analysis of AlphaGOS P showed that this commercial product contains melibiose (*α*-D-Gal-(1→6)-D-Glc), manninotriose (*α*-D-Gal-(1→6)-*α*-D-Gal-(1→6)-D-Glc) and verbascotetraose (*α*-D-Gal-(1→6)-*α*-D-Gal-(1→6)-*α*-D-Gal-(1→6)-D-Glc), defructosylated derivatives from the *α*-galactosides raffinose, stachyose and verbascose, respectively, compounds naturally present in peas (Moussou *et al.*, 2017). This different composition may be due to the fact that original *α*-galactosides could have been enzymatically treated with a fructosidase. Montilla *et al.* (2011), previously, found that this enzyme, under appropriate conditions, is able to completely eliminate the fructose from stachyose, forming manninotriose.

The evolution in the content of di-, tri- and tetrasaccharides in the samples was highly dependent on the structure during the RSIE digestion treatment. Inulin based samples such as Raftiline HP and Inulin Orafti GR exhibited the lowest changes in their composition due to the resistance of these substrates to intestinal enzymes. A minimum increase of fructose was observed in Raftiline HP possibly produced by the hydrolysis of high M_w inulin species and no bigger structures (DP < 4) were detected. Regarding Inulin Orafti GR sample, slight degradations, but not significant, in the high M_w structures such as nystose (24 to 19.5 mg nystose per g of sample) was registered after the digestion process (**Table 2a and 2b**), and increases in the trisaccharide fraction were observed. Sucrose was the most digested structure causing important increases in fructose content. A similar trend was observed by Ferreira-Lazarte, Olano, *et al.* (2017) after the digestion of FOS with RSIE exhibiting the tetrasaccharide structure the highest degradation (40%). The trisaccharide also increased, most likely, due to degradation of the tetrasaccharide. These changes are in line with the low inulinase activity measured in this extract (**Table 1**).

Table 2. Carbohydrate evolution during the small intestinal digestion with Rat Small Intestine Extract (RSIE) at 37 °C, pH 6.8, determined by GC-FID analysis (mg/g of sample)

Table 2a. Mono-, di- and trisaccharides

	Monosaccharides		Disaccharides			Trisaccharides		
Digestion time (min)	**Fructose**	**Galactose**	**Sucrose**	**Inulobiose**	**Melibiose[a]**	**Kestose**	**Inulotriose**	**Maninotriose[a]**
Raftiline HP								
0	0.0 ± 0.0	-	-	-	-	-	-	-
60	20.2 ± 1.8	-	-	-	-	-	-	-
120	32.0 ± 1.2	-	-	-	-	-	-	-
180	44.1 ± 4.5	-	-	-	-	-	-	-
Inulin Orafti GR								
0	0.0 ± 0.0	-	42.5 ± 1.8	-	-	20.1 ± 0.5	-	-
60	39.7 ± 3.0	-	17.6 ± 1.0	-	-	31.7 ± 2.2	-	-
120	56.5 ± 2.5	-	12.1 ± 3.0	-	-	31.6 ± 1.3	-	-
180	66.1 ± 3.7	-	10.1 ± 0.2	-	-	26.2 ± 1.8	-	-
Raftilose P95								
0	45.6 ± 1.7	-	-	49.1 ± 4.5	-	-	199.6 ± 3.0	-
60	81.6 ± 8.2	-	-	70.9 ± 6.8	-	-	226.2 ± 7.6	-
120	85.5 ± 5.3	-	-	72.8 ± 4.7	-	-	215.7 ± 7.8	-
180	117.6 ± 7.4	-	-	72.2 ± 2.0	-	-	172.3 ± 9.7	-

AlphaGOS P								
0	-	0.0 ± 0.0	-	-	37.2 ± 0.2	-	-	538.4 ± 15.0 *(0%)*
60	-	158.2 ± 3.1	-	-	69.9 ± 1.3	-	-	338.9 ± 1.7 *(37.1%)*
120	-	213.3 ± 3.8	-	-	75.7 ± 2.6	-	-	275.5 ± 8.1 *(48.8%)*
180	-	246.0 ± 5.9	-	-	80.9 ± 6.9	-	-	215.7 ± 15.4 *(59.9%)*
Melibiose								
0	-	0.0 ± 0.0	-	-	1013.6 ± 32.0 *(0%)*	-	-	-
60	-	158.2 ± 4.6	-	-	492.8 ± 19.8 *(51.3%)*	-	-	-
120	-	231.6 ± 20.7	-	-	403.7 ± 11.0 *(60.2%)*	-	-	-
180	-	280.8 ± 6.0	-	-	327.3 ± 14.7 *(67.7%)*	-	-	-

Data are expressed as the mean ± SD ($n = 4$).
[a] Hydrolysis degree (%) of isolated melibiose and maninotriose of AlphaGOS P are indicated in parentheses.

Table 2b. Tetrasaccharides

	Tetrasaccharides			
Digestion time (min)	**Nystose**	**Inulotetraose**	**Verbascotetraose[a]**	**Total OS[a, b]**
Raftiline HP				
0	-	-	-	-
60	-	-	-	-
120	-	-	-	-
180	-	-	-	-
Inulin Orafti GR				
0	24.0 ± 1.7	-	-	44.0 ± 1.0
60	20.0 ± 1.6	-	-	51.7 ± 1.9
120	19.8 ± 1.4	-	-	51.4 ± 1.4
180	19.5 ± 1.2	-	-	45.7 ± 1.5
Raftilose P95				
0	34.8 ± 2.2	121.0 ± 5.4	-	404.5 ± 3.8
60	27.5 ± 1.7	98.8 ± 5.6	-	423.4 ± 5.4
120	26.7 ± 1.6	97.3 ± 15.0	-	412.6 ± 7.3
180	29.6 ± 0.9	100.6 ± 8.2	-	374.7 ± 5.2

AlphaGOS P				
0	-	-	377.6 ± 11.0 (0%)	953.2 ± 8.7 (0%)
60	-	-	150.1 ± 5.1 (60.2%)	558.9 ± 2.7 (41.4%)
120	-	-	110.2 ± 7.3 (70.8%)	461.4 ± 6.0 (51.6%)
180	-	-	73.4 ± 2.5 (80.6%)	370.0 ± 8.3 (61.2%)
Melibiose				
0	-	-	-	-
60	-	-	-	-
120	-	-	-	-
180	-	-	-	-

Data are expressed as the mean ± SD (n = 4).
[a] Hydrolysis degree (%) of verbascotetraose and total OS of AlphaGOS P are indicated in parentheses.
[b] Total oligosaccharides was calculated by the sum of di-, tri- and tetrasaccharides of each carbohydrate.

Regarding Raftilose P95, both tetrasaccharides detected showed slight but not significant degradations, being inulotetraose more hydrolyzed than nystose. A consequent increase in the corresponding trisaccharide (inulotriose) was observed after 120 min digestion, probably due to the degradation of the former. Moreover, the presence of higher DP compounds in the sample could also produce tri- and tetrasaccharides during the digestion treatment (Nobre *et al.*, 2018). Increases in smaller structures such as disaccharides (inulobiose) and monosaccharides (fructose) were also observed due to the hydrolysis of the biggest compounds. These results underline the relevance of the higher M_w composition in terms of digestibility (Ferreira-Lazarte, Olano, *et al.*, 2017; Hernández-Hernández *et al.*, 2012). Higher hydrolysis in Inulin Orafti GR was observed in the tetrasaccharide fraction after 180 min of digestion, supporting the data obtained in the *in vivo* and *in vitro* studies by Ferreira-Lazarte, Olano, *et al.* (2017) and Molis *et al.* (1996), resulting in 12% and 11% of total digestion, respectively. In the case of Raftilose P95, a not significant decrease of tri- and tetrasaccharides was observed: hydrolysis being higher in the case of the linkage $\beta(2\rightarrow1)$ between fructose monomers (inulotriose and inulotetraose of Raftilose P95), when glucose is not present in the structure ending compared to sucrose oligosaccharides (kestose and nystose of Inulin Orafti GR) (**Table 2a and 2b**). This could suggest the lower resistance of the $\beta(2\rightarrow1)$ bonds to the action of the digestive enzymes (Ferreira-Lazarte, Olano, *et al.*, 2017).

With respect to oligosaccharides from galactose, chromatographic profiles by GC-FID of AlphaGOS P undigested and after digestion with RSIE are shown in **Fig. 2**. A decrease of verbascotetraose and manninotriose was observed (peaks 4 and 5) and, consequently, melibiose and galactose contents were increased after 180 min of digestion due to the degradation of the structures with higher M_w (**Table 2a and 2b**). However, decreases in the melibiose levels were detected when a standard of only melibiose was digested, showing the highest hydrolysis values (67.7%) after 180 min of digestion.

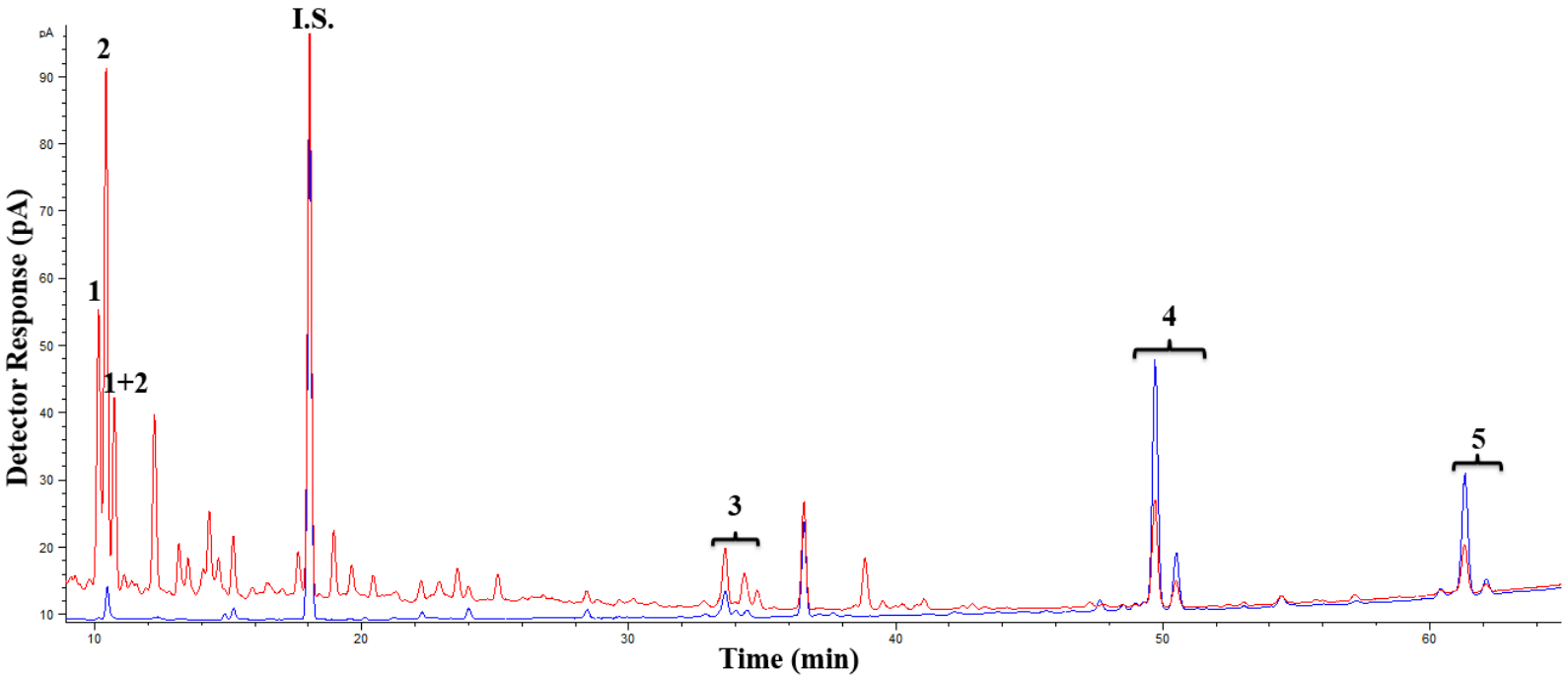

Figure 2. Chromatographic profiles obtained by GC-FID of TMSO derivatives of oligosaccharides present in AlphaGOS P before (blue) and after 180 min of small intestinal digestion with RSIE (red). Peaks: 1. Galactose, 2: Glucose, I.S.: Internal Standard, 3: Melibiose, 4: Maninotriose, 5: Verbascotetraose.

This degradation is in accordance with the considerable previous melibiase activity detected in the enzymatic extract, thus suggesting that the intestinal enzymes probably are more prone to hydrolyze higher M_w structures present in the sample (manninotriose and verbascotetraose) rather than the disaccharide.

Increases in galactose levels also suggest that linkages between galactose monomers are being broken by digestive enzymes, similar to the degradation of *β*-GOS derived from lactose and lactulose observed during small intestinal digestion in previous works (Ferreira-Lazarte, Gallego-Lobillo, *et al.*, 2019; Ferreira-Lazarte, Olano, *et al.*, 2017; Hernández-Hernández *et al.*, 2012; Julio-Gonzalez *et al.*, 2019; Shi *et al.*, 2018). Beneficial effect of the *α*-GOS on the modulation of the intestinal microbiota is well-known (Chen *et al.*, 2019; Yousefi *et al.*, 2018). Nevertheless, there is not enough information about their digestibility, even the expert scientific panel from the European Food Safety Authority (EFSA) claims that the *α*-GOS are non-digestible carbohydrates (EFSA NDA Panel on Dietetic Products Nutrition and Allergies, 2014). Considering the sum of total oligosaccharides of AlphaGOS P (manninotriose and verbascotetraose) the hydrolysis was considerably high (61.2%) (**Table 2b**), despite the lack of pancreatic *α*-galactosidase in mammals (LeBlanc *et al.*, 2004). However, Ferreira-Lazarte, Gallego-Lobillo, *et al.* (2019) showed meaningful hydrolysis degree of prebiotic *β*-GOS (53% for linkages *β*(1→3)) using brush border membrane vesicles of small intestine of pig. A possible explanation for this fact could be the promiscuous multienzymatic complexes in the rat small intestine extract (Ferreira-Lazarte, 2019). Carbohydrases of the small intestine, such as *α*-amylase, hydrolyze large starch structures, whereas complete digestion is done by the mucosal *α*-glucosidases (Lee & Hamaker, 2017; Shin *et al.*, 2019). In this sense, mucosal maltase-glucoamylase and sucrase-isomaltase complexes could hydrolyze to *α*(1→6) bonds between the monomers of both AlphaGOS P and melibiose (Dona *et al.*, 2010; Feher, 2017; Hooton *et al.*, 2015). These enzymatic structures could also have more versatility in terms of hydrolytic activity, as was showed elsewhere (Ferreira-Lazarte, Gallego-Lobillo, *et al.*, 2019; Lee *et al.*, 2016). To the best

of our knowledge, these data are the first evidence about digestibility of *α*-GOS with small intestine enzymes.

Some *in vivo* studies with rats have demonstrated a partial digestibility of prebiotic carbohydrates, showing a considerable high hydrolysis rate of *β*-GOS obtained from lactose and lactulose (Hernández-Hernández *et al.*, 2012; Jantscher-Krenn *et al.*, 2013). In the same way, an *in vitro* study with RSIE reported a hydrolysis degree of 12% of a mixture of FOS after 120 min of digestion (Ferreira-Lazarte, Olano, *et al.*, 2017). These reported data are consistent with this work, highlighting the key role of the mammalian intestinal enzymes on the digestibility of carbohydrates.

Conclusions

Limitations of traditional digestibility methods of carbohydrates have been shown in several works (Ferreira-Lazarte, 2019; Tanabe *et al.*, 2014). Therefore, results obtained in this work confirmed the usefulness and effectiveness of the use of a RSIE to evaluate the digestion of polysaccharides. Moreover, similarities between small intestinal enzymes of rat and human emphasized the viability of this extract (Oku *et al.*, 2011). Raftiline HP, which is mainly constituted by inulin, showed the highest resistance to the gastrointestinal enzymes, with only a slight increase of fructose. Inulin Orafti GR also showed high resistance, with a small hydrolysis of tetrasaccharides, followed by Raftilose P95, thus supporting the role of these substrates as prebiotic compounds. Finally, AlphaGOS P and melibiose showed a considerable high hydrolysis degree (61.2 and 67.7%, respectively), remarking the effect of the chemical structure (M_w and type of linkage) of prebiotic oligosaccharides with respect to their resistance to digestibility. According to the obtained results, mucosal enzymes complexes have versatile hydrolytic activities and contribute to the digestion of different types of functional fiber which is belief to reach intact the distal colon to be fermented by the microbiota exerting its beneficial effects. Therefore, although more studies are required, including *in vivo* analysis, the results obtained underline the need to use specific methods for

carbohydrates based on small intestinal extract of mammals, to test the resistance of these compounds to digestion.

In general, the well-known prebiotic activity of these fibers is aligned with their partial digestibility, since not all the carbohydrate fraction is digested. In consequence, it is important to highlight that not all prebiotic carbohydrates are non-digestible and can be partially digested, still exerting the beneficial effect in the large intestine, which, therefore, warrants a revision of the current assumption of non-digestibility of prebiotic carbohydrates, as recently was suggested by Hernández-Hernández (2019).

Acknowledgements

Authors acknowledge the finance of this work by the Spanish Ministry of Economy, Industry and Competitiveness (Project AGL2017-84614-C2-1-R) and the Spanish Ministry of Science, Innovation and Universities (Project RTI2018-101273-J-I00).

Capítulo 3

In vitro digestion of polysaccharides: InfoGest protocol and use of small intestinal extract from rat

Pablo Gallego-Lobillo, Alvaro Ferreira-Lazarte, Oswaldo Hernández-Hernández y Mar Villamiel

Instituto de Investigación en Ciencias de la Alimentación, CIAL (CSIC-UAM). C/Nicolás Cabrera, 9, Campus de la Universidad Autónoma de Madrid, 28049 Madrid, España.

Reproducido a partir de Elsevier
Food Research International
2021, 140, 110054
DOI: https://doi.org/10.1016/j.foodres.2020.110054

Abstract

Starch, dextran, pectin and modified citrus pectin were subjected to intestinal digestion following InfoGest protocol and a rat small intestine extract (RSIE) treatment. Gastric stage did not show any modification in the structure of the carbohydrates, except for modified pectin. Regarding intestinal phases, starch was hydrolyzed by different ways, resulting in a complementary behavior between InfoGest and RSIE. Contrarily, digestion of dextran was only observed using RSIE. Similar situation occurred in the case of pectins with RSIE, obtaining a partial hydrolysis, especially in the modified citrus pectin. However, citrus pectin was the less prone to hydrolysis by enzymes. The results demonstrated that InfoGest method underestimates the significance of the carbohydrates hydrolysis at the small intestine, thus indicating that RSIE is a very reliable and useful method for a more realistic study of polysaccharides digestion.

Introduction

Polysaccharides compose a wide group of carbohydrates that play different roles in the human body such as the storage of energy and the structural function in the cell, and these functions are determined by their digestibility in the small intestine (Hu *et al.*, 2018). Thus, polysaccharides can be considered as digestible or non-digestible depending on chemical structure as the most relevant factor (Li *et al.*, 2020; Zhu *et al.*, 2019). Among dietary polysaccharides, starch is the only one which can be hydrolyzed without the intervention of the intestinal microbiota (Cockburn & Koropatkin, 2016). Others, such as pectin could resist intestinal digestion and reach the colon to be fermented by the colonic bacteria, modulating intestinal metabolism. This effect on the microbiota is one of the reasons for that the interest towards pectin has aroused a great increase in recent years (Ferreira-Lazarte *et al.*, 2018; Ferreira-Lazarte, Moreno, *et al.*, 2019; Holck *et al.*, 2014). In this context, the majority of research has been focused on the benefits of pectin as dietary fiber and modulator of the microbiota and limited information is available on its digestion. Recently, digestion of pectin has been studied in a complex dynamic gastrointestinal simulator (simgi®) (Ferreira-Lazarte, Moreno, *et al.*, 2019). With this method, based on the use of digestive fluids including pancreatin, hardly any changes were observed along the gastric and small intestinal phases, resulting in a hydrolysis degree of 12%.

Majority of the digestibility methods are focused on proteins or starch allowing to distinguish between resistant and rapidly absorbable starch (Englyst *et al.*, 2018; Han *et al.*, 2018). The most common and accepted *in vitro* method for digestion is InfoGest protocol, developed in 2014 (Brodkorb *et al.*, 2019; Minekus *et al.*, 2014) and it is based on the use of simulated fluids of gastrointestinal enzymes. The Association of Official Analytical Chemist (AOAC) carried out another digestibility method for non-digestible carbohydrates, such as dietary fiber (McCleary *et al.*, 2010). Nevertheless, the use of isolated enzymes of both methods does not reflect the complexity of the digestion of carbohydrates at the small intestine (Ferreira-Lazarte *et al.*, 2020).

Beyond starch hydrolysis, there is a lack of standardized methods for carbohydrates digestion despite of their importance in human health (Hernández-Hernández, 2019; Hernández-Hernández *et al.*, 2019). Specifically, in the case of prebiotic carbohydrates is assumed that they are completely non-digestible (Hernández-Hernández, 2019). However, it has been described that some well-known prebiotic carbohydrates are partially degraded during small intestinal digestion (Ferreira-Lazarte *et al.*, 2020; Hernández-Hernández *et al.*, 2012).

Ferreira-Lazarte, Olano, *et al.* (2017) proposed a useful and simple *in vitro* method of digestibility using a rat small intestine extract (RSIE). A meaningful hydrolysis of *β*-galactooligosaccharides, previously considered as non-digestible with a degree of polymerization (DP) up to 4 was observed, similar to the *in vivo* results obtained by Hernández-Hernández *et al.* (2012). This GOS hydrolysis was not observed when InfoGest method was applied (Ferreira-Lazarte, Montilla, *et al.*, 2017). This could be ascribed to the lack of the disaccharidases present in the enterocyte brush border membranes in the InfoGest methodology (Hernández-Hernández, 2019; Hooton *et al.*, 2015). Indeed, it has been recently reported the hydrolysis of different kinds of dietary fiber such as non-fructosylated *α*-GOS and different types of inulin structures when RSIE was used (Gallego-Lobillo *et al.*, 2020).

The reported data on carbohydrates digestion emphasized the advantages of using mammal small intestinal digestive enzymes, which permit reducing uncertainties about the behavior of carbohydrates during the gastrointestinal process, and about the effect of carbohydrate chemical structure and the type of linkage on their digestibility (Ferreira-Lazarte, Olano, *et al.*, 2017; Hernández-Hernández *et al.*, 2012).

To the best of our knowledge, no investigation has been conducted on the impact of InfoGest protocol and subsequent application of RSIE for the evaluation of dietary polysaccharides. Thus, the aim of this work was to study the *in vitro* digestibility of polysaccharides by combining the standardized InfoGest protocol with the proposed digestion model using rat small intestine extract. The viability of these methods has been

proven with starch and dextran as glucose-based polysaccharides, and pectin and modified citrus pectin, as pectic polysaccharides.

Materials and methods

Chemicals and standards

The following analytical standards were supplied by Sigma-Aldrich (St. Louis, MO): D-galactose (Gal), D-glucose (Glc), D-arabinose (Ara), galacturonic acid (GalA), maltose (*α*-D-Glc-(1→4)-D-Glc), sucrose (*β*-D-Fru-(2→1)-*α*-D-Glc), maltotriose (*α*-D-Glc-(1→4)-*α*-D-Glc-(1→4)-D-Glc), phenyl-*β*-D-glucoside, as well as the intestinal acetone powders from rat (Rat Small Intestine Extract, RSIE). D-xylose (Xyl), L-rhamnose (Rha) and D-mannose (Man) standards were purchased from PanReac AppliChem (Darmstadt, Germany). Reagents for Bradford method were obtained from Bio-Rad Laboratory (Gmbh, Munich, Germany).

Polysaccharides studied

Two glucose-based polysaccharides were evaluated in this work: soluble starch and dextran from *Leuconostoc mesenteroides*, obtained from Sigma Aldrich. In addition, two commercial samples of pectin were also tested: commercial citrus pectin (CP) (Ceampectin®, ESS-4400), was supplied by CEAMSA (Porriño, Pontevedra, Spain); and a commercial pH-modified citrus pectin (MCP) was kindly provided by ecoNugenics (Santa Rosa, CA). Monomeric composition of CP was (percentages of total carbohydrates): traces of xylose, 6.7% arabinose, 4.4% rhamnose, 22.5% galactose, traces of mannose, 2.4% glucose and 64.0% galacturonic acid; and average M_w was 472 kDa (Muñoz-Labrador *et al.*, 2018). On the other hand, monosaccharides content of MCP were (percentages of total carbohydrates): traces of xylose, 3.9% arabinose, 2.3% rhamnose, 8.9% galactose, traces of mannose, 1.0% glucose and 83.9% galacturonic acid; and average M_w was 3.1–0.7 kDa.

Characterization of rat small intestine extract

Protein content

RSIE protein content was determined through the Bradford method (Bradford, 1976). The absorbance was measured at 595 nm and the standard used was bovine serum albumin.

Enzymatic activities

RSIE maltase, sucrase and pectinase activities (U/g protein) were evaluated by duplicate using GC-FID, according to the previously described methodology (Gallego-Lobillo *et al.*, 2020). Incubation of RSIE (40 mg/mL) with individual solutions of maltose, sucrose and citrus pectin in distilled water at pH 6.8 was carried out in an orbital Thermomixer comfort (Eppendorf®) at 37 ºC for 0, 60, 120 and 180 min and then, heated in boiling water during 5 min to stop the reaction.

Evolution of the carbohydrate content was analyzed through GC-FID, as described below, in order to calculate the specific enzymatic activity.

In vitro digestions

Fig. 1 shows the scheme followed in this work. The InfoGest protocol was used according to the literature (Brodkorb *et al.*, 2019). Digestions with RSIE were carried out following the method of Ferreira-Lazarte, Olano, *et al.* (2017)

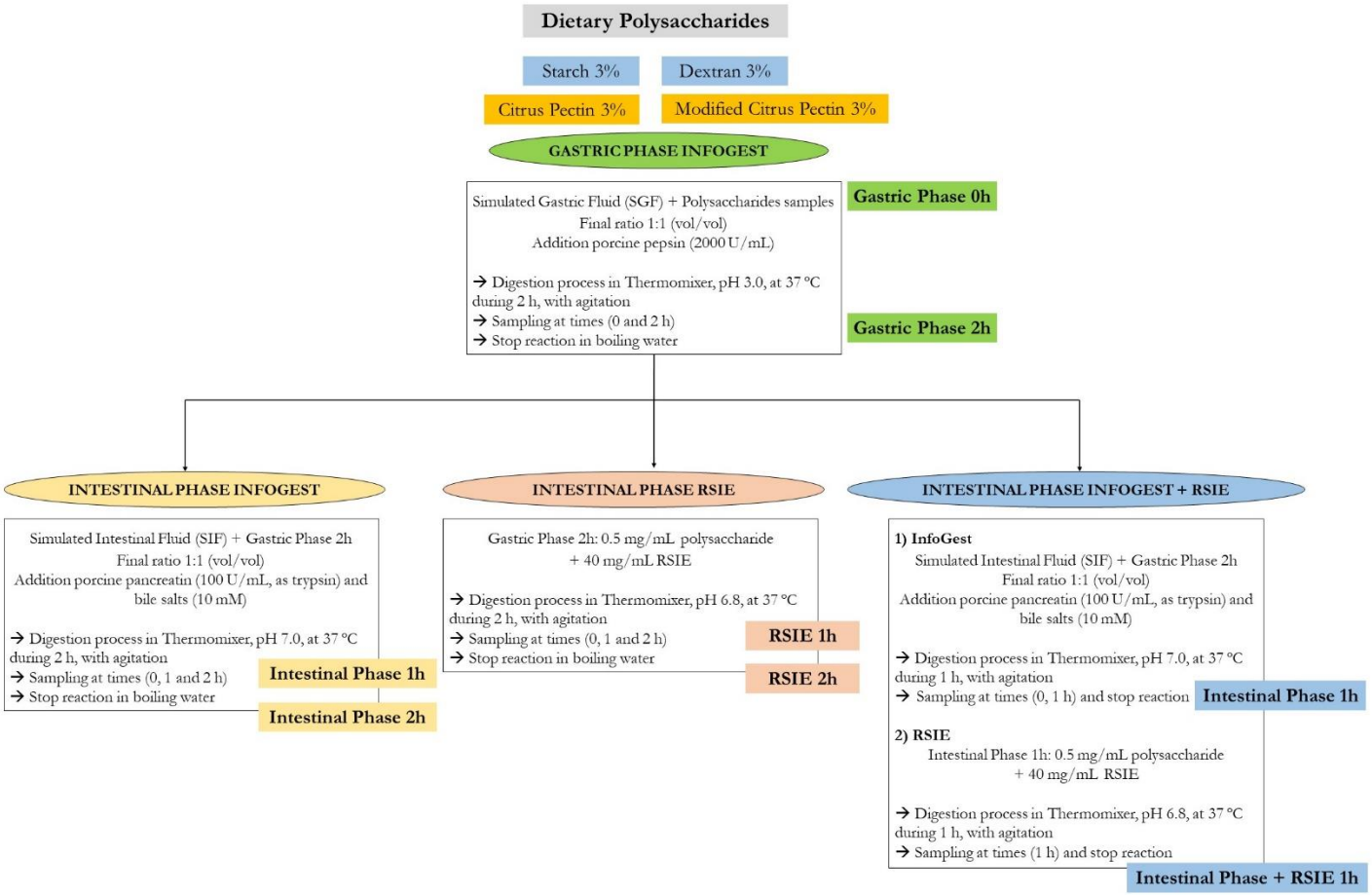

Figure 1. Scheme of the digestion assays with InfoGest protocol and RSIE.

Gastrointestinal digestion by InfoGest

The model and the simulated fluids preparation for the gastric and intestinal phases were based on the standardized InfoGest protocol reported by Brodkorb *et al.* (2019).

First, solutions of each polysaccharide with a concentration of 30 mg/mL (3%, w/w) in distilled water were prepared. For the stomach stage, solutions were mixed with an equal volume of simulated gastric fluid (SGF). Then, 2 mL of a porcine pepsin solution were added to obtain 2000 U/mL. Then, 5 µL of $CaCl_2$ 0.3 M and the pH was adjusted to 3.0. The mixture was incubated in an orbital Thermomixer at 37 ºC with continuous agitation. Samples were collected at 0 and 2 h, and the reaction was stopped by heating in boiling water for 5 min.

For the intestinal stage, solutions of the end of the gastric phase (Gastric Phase 2 h) of each carbohydrate were mixed with an equal volume of simulated intestinal fluid (SIF). Porcine pancreatin and bile salts were added to the digestion in order to achieve 100 U/mL (trypsin activity) and 10 mM, respectively. Then, 40 µL of $CaCl_2$ 0.3 M were added and the pH was adjusted to 7.0. Digestions were carried out in an orbital Thermomixer at 37 ºC with continuous agitation. Samples were taken at 0, 1 and 2 h of reaction, and inactivated in boiling water for 5 min. Samples of gastric and intestinal phases were analyzed by GC-FID.

Small intestinal digestion by RSIE

Samples of carbohydrates after Gastric Phase (2 h) and after 1 h of Intestinal Phase (InfoGest) (**Fig. 1**) were digested with RSIE according to the method of Ferreira-Lazarte, Olano, *et al.* (2017) with minor changes, to evaluate the digestibility of digested samples with RSIE and with the combined methods (InfoGest + RSIE), respectively. Firstly, a concentration of 0.5 mg/mL of each carbohydrate was prepared and mixed with RSIE (40 mg/mL). Reactions were performed in an orbital Thermomixer during 2 h at 37 ºC and 750 rpm. Samples were collected at different times (0, 1 and 2 h for only RSIE

digestion and after 1 h for InfoGest + RSIE digestion), stopping the digestion by heating. Analysis were carried out by GC-FID.

Assessment of digestion evolution by GC-FID

Gas chromatography coupled to a flame ionization detector (GC-FID) was used to analyze the evolution of polysaccharides in all digestion assays by means of the release of molecular species with lower polymerization degree (monosaccharides and oligosaccharides). Firstly, a derivatization process to obtain trimethylsilylated oximes (TSMO) was done, according to Brobst & Lott (1966). For that, samples obtained after digestions were mixed with 400 µL of phenyl-*β*-D-glucoside (internal standard, 0.5 mg/mL) and dried in a rotary evaporator (Büchi Labortechnik AG, Flawil, Switzerland). For the oxime formation, 300 µL of hydroxylamine chloride in pyridine (2.5%, w/v) were added, and the mixture was incubated at 70 ºC during 30 min. Then, silylation was performed with the addition of 300 µL of hexamethyldisilazane (HDMS) and 30 µL of TFA and incubated at 50 ºC for 30 min with agitation. Finally, TMSOs were centrifuged at 6,700 × *g* for 2 min, and the supernatants were injected into the GC-FID.

An Agilent Technologies 7820A gas chromatograph system was used for the analysis, equipped with a fused silica capillary column DB-5HT (5% phenyl methylpolysiloxane, 30 m × 0.25 mm × 0.1 µm, Agilent J&W Scientific, Folsom, CA, USA). Nitrogen was used as the carrier gas at 1 mL/min of flow rate. Heat oven program started in 150 ºC, and then, increased to 380 ºC at a rate of 3 ºC/min. Injector and detector temperature was 280 ºC and 385 ºC, respectively. Samples were analyzed in split mode 1:20.

Quantification in the content of carbohydrates were done calculating the response factors of standards solutions of carbohydrates (xylose, arabinose, rhamnose, galactose, mannose, glucose, galacturonic acid, maltose and maltotriose) at known concentrations (0.005 to 2 mg/mL). Data interpretation and integration were performed using Agilent ChemStation software (Washington, DE, USA).

Statistical analysis

All experiments were done in duplicate and two GC-FID analysis (n = 4). Statistical differences were analyzed using analysis of variance (ANOVA) and Scheffé's post hoc test, with the SPSS statistical package (Inc., Chicago, Il), considering significant values when $p \leq 0.05$.

Results and discussion

Enzymatic characterization of RSIE

Specific enzymatic activities of RSIE, measured under simulated physiological conditions (pH 6.8, 37 ºC) are shown in **Table 1**. Maltase was found to be the major activity (126.6 U) with a value 9- and 160-fold higher as compared to sucrose and pectinase activities, respectively. The considerable difference between activities with respect to maltase is in agreement with previous studies using the same commercial extract (Ferreira-Lazarte, Gallego-Lobillo, *et al.*, 2019; Ferreira-Lazarte, Olano, *et al.*, 2017; Gallego-Lobillo *et al.*, 2020; Oku *et al.*, 2011). Maltase activity, which is exerted by the maltase-glucoamylase and sucrase-isomaltase complexes present in the RSIE, is one of the main enzymes involved in the digestion of starch (Hooton *et al.*, 2015; Whistler & Daniel, 2000). Sucrase activity (14.3 U) coming from the sucrase-isomaltase complex was slightly lower than the data obtained by Ferreira-Lazarte, Olano, *et al.* (2017) and Gallego-Lobillo *et al.* (2020), probably, due to the variability among the different lot of intestinal extracts. Moreover, a low pectinase activity was also found in the RSIE (0.8 U), which can be explained by the resistance of this soluble fiber to digestion.

Table 1. Characterization of enzymatic activities in Rat Small Intestine Extract

Hydrolytic activity	Substrate	U/g protein
Maltase	Maltose	126.6 ± 0.1 [a]
Sucrase	Sucrose	14.1 ± 0.3 [b]
Pectinase	Citrus pectin	0.8 ± 0.1 [c]

Protein content of RSIE: 8.2±0.5% (*w/w*).
Activities were calculated evaluating the content of monosaccharides by GC-FID: [a] Release of glucose. [b] Release of fructose. [c] Release of galacturonic acid.
Data is expressed ± SD (n=4).

In vitro digestion assays

The effect of gastrointestinal digestion of four dietary polysaccharides (starch, dextran, CP and MCP) was evaluated using InfoGest and RSIE following the scheme indicated in **Fig. 1**. **Tables 2 and 3** indicate the quantitative evolution of the carbohydrate fraction in each polysaccharide analyzed during all the stages of the digestion process. **Tables 2a and 2b** are referred to the soluble starch and dextran, showing slight but no significant changes ($p \geq 0.05$) in the gastric digestion according to InfoGest protocol. Gastric juice contains hydrochloric acid and pepsin, with lack of carbohydrases (Feher, 2017). However, pepsin and acids can provoke alterations to the surface of the molecule of starch, as well as dextran, causing partial breakdown of the polysaccharide, with the consequent release of glucose (Fernandes *et al.*, 2020; Pérez & Bertoft, 2010). This effect is not overly strong (Freitas *et al.*, 2018). **Table 4** indicates the total hydrolysis degree of polysaccharides after each stage of digestion treatment. Low hydrolysis (1–2%) occurred during the gastric digestion of starch and dextran, which is in agreement with Tamura *et al.* (2016), who found no hydrolysis during gastric process using simulated digestion fluids.

Table 2. Digestion of glucose-based polysaccharides. Evolution in the content of carbohydrates of Starch and Dextran via InfoGest protocol and RSIE, determined by GC-FID (mg/g of sample)

Table 2a. Starch

		Glucose	Maltose	Maltotriose	Total CH
Gastric Phase InfoGest	0 h	18.3 ± 5.6 [a]	0.0 ± 0.0 [a]	0.0 ± 0.0 [a]	18.3 ± 5.6 [a]
	2 h	9.9 ± 3.6 [a]	0.0 ± 0.0 [a]	0.0 ± 0.0 [a]	9.9 ± 3.6 [a]
Intestinal Phase InfoGest	1 h	125.0 ± 4.7 [b]	325.5 ± 15.9 [b]	19.1 ± 1.1 [b]	469.6 ± 20.5 [b]
	2 h	178.5 ± 5.8 [c]	325.6 ± 22.1 [b]	45.4 ± 0.7 [c]	549.5 ± 27.7 [c]
Intestinal Phase RSIE	1 h	374.1 ± 20.3 [d]	0.0 ± 0.0 [a]	0.0 ± 0.0 [a]	374.1 ± 20.3 [d]
	2 h	584.7 ± 10.0 [e]	0.0 ± 0.0 [a]	0.0 ± 0.0 [a]	584.7 ± 10.0 [c]
Intestinal Phase InfoGest	1 h	125.0 ± 4.7 [b]	325.5 ± 15.9 [b]	19.1 ± 1.1 [b]	469.6 ± 20.5 [b]
Intestinal Phase InfoGest + RSIE	1 h	525.1 ± 15.0 [f]	0.0 ± 0.0 [a]	0.0 ± 0.0 [a]	525.1 ± 15.0 [c]

Values are expressed as means as ± SD (n=4)

Table 2b. Dextran

		Glucose	Maltose	Maltotriose	Total CH
Gastric Phase InfoGest	0 h	7.6 ± 2.0 [a]	N.D.	N.D.	7.6 ± 2.0 [a]
	2 h	10.8 ± 3.1 [a]	N.D.	N.D.	10.8 ± 3.1 [a]
Intestinal Phase InfoGest	1 h	10.1 ± 0.1 [a]	N.D.	N.D.	10.1 ± 0.1 [a]
	2 h	10.9 ± 0.6 [a]	N.D.	N.D.	10.9 ± 0.6 [a]
Intestinal Phase RSIE	1 h	149.3 ± 8.0 [b]	N.D.	N.D.	149.3 ± 8.0 [b]
	2 h	163.0 ± 10.6 [b]	N.D.	N.D.	163.0 ± 10.6 [b]
Intestinal Phase InfoGest	1 h	10.1 ± 0.1 [a]	N.D.	N.D.	10.1 ± 0.1 [a]
Intestinal Phase InfoGest + RSIE	1 h	205.9 ± 20.2 [c]	N.D.	N.D.	205.9 ± 20.2 [c]

Values are expressed as means as ± SD (n=4). Total CH: Total carbohydrates (glucose + maltose + maltotriose). N.D.: Not detected.
[a-f] Different letters indicate statistical differences between content of each column using ANOVA ($p \leq 0.05$)
LOD of Glc, Mal and Maltriose, respectively: 0.044, 0.043 and 0.059 mg
LOQ of Glc, Mal and Maltriose, respectively: 0.146, 0.144 and 0.195 mg

Table 3. Digestion of pectic polysaccharides. Evolution in the content of carbohydrates of Citrus Pectin and Modified Citrus Pectin via InfoGest protocol and RSIE, determined by GC-FID (mg/g of sample)

Table 3a. Citrus Pectin

		Galactose	Galacturonic Acid	Total CH
Gastric Phase InfoGest	0 h	0.0 ± 0.0 [a]	0.0 ± 0.0 [a]	0.0 ± 0.0 [a]
	2 h	0.7 ± 0.4 [a]	0.0 ± 0.0 [a]	0.7 ± 0.4 [a]
Intestinal Phase InfoGest	1 h	1.4 ± 0.1 [a]	0.0 ± 0.0 [a]	1.4 ± 0.1 [a]
	2 h	1.4 ± 0.1 [a]	0.0 ± 0.0 [a]	1.4 ± 0.1 [a]
Intestinal Phase RSIE	1 h	60.4 ± 4.1 [b]	43.9 ± 5.0 [b]	104.3 ± 6.5 [b]
	2 h	72.7 ± 5.5 [b]	56.4 ± 2.9 [b]	129.1 ± 6.3 [c]
Intestinal Phase InfoGest	1 h	1.4 ± 0.1 [a]	0.0 ± 0.0 [a]	1.4 ± 0.1 [a]
Intestinal Phase InfoGest + RSIE	1 h	148.2 ± 13.2 [c]	23.1 ± 3.2 [c]	172.3 ± 10.6 [d]

Values are expressed as means as ± SD (n=4)

Table 3b. Modified Citrus Pectin (MCP)

		Galactose	Galacturonic Acid	Total CH
Gastric Phase InfoGest	0 h	2.2 ± 1.2 [a]	37.5 ± 4.1 [a]	39.7 ± 9.7 [a]
	2 h	3.7 ± 1.7 [a]	86.6 ± 7.9 [b]	90.3 ± 10.2 [b]
Intestinal Phase InfoGest	1 h	2.6 ± 0.1 [a]	103.9 ± 3.7 [c]	106.5 ± 3.6 [b]
	2 h	3.0 ± 0.3 [a]	108.3 ± 5.9 [c]	111.3 ± 5.9 [b]
Intestinal Phase RSIE	1 h	53.4 ± 5.5 [b]	334.1 ± 7.8 [d]	387.5 ± 2.7 [c]
	2 h	75.2 ± 7.0 [c]	341.1 ± 18.5 [d]	416.3 ± 7.5 [c]
Intestinal Phase InfoGest	1 h	2.6 ± 0.1 [a]	103.9 ± 3.7 [c]	106.5 ± 3.6 [b]
Intestinal Phase InfoGest + RSIE	1 h	81.6 ± 11.4 [c]	340.9 ± 29.1 [d]	422.5 ± 36.5 [c]

Values are expressed as means as ± SD (n=4). Total CH: Total carbohydrates (galactose + galacturonic acid). N.D.: Not detected.
[a-d] Different letters indicate statistical differences between content of each column using ANOVA ($p \leq 0.05$)
LOD of Gal and GalA, respectively: 0.038 and 0.032 mg
LOQ of Gal and GalA, respectively: 0.126 and 0.106 mg

On the other hand, **Tables 3a and 3b** show the content of pectic carbohydrates. In first instance, MCP had a considerable content in galacturonic acid (GalA) due to the process of manufacture of the modified pectin, which involved enzymes-catalyzed reactions in the structure of the pectin (Holck *et al.*, 2014; Míguez *et al.*, 2016). Barely any hydrolysis was observed during gastric digestion of CP (**Table 3a**), highlighting their resistance to acidic gastric digestion. Nevertheless, a significant increase in GalA ($p \leq 0.05$) is observed in MCP (**Table 3b**), thus indicating the possible acidic hydrolysis effect in the lower M_w compounds (Holloway *et al.*, 1983; Thibault *et al.*, 1993). In addition, MCP is a de-esterified pectin, a simpler structure which permits an easier acidic-hydrolysis to the homogalacturonan (HG) backbone (Holck *et al.*, 2014).

Small intestinal digestion of starch

As it is very well-known, starch is the major dietary glycemic carbohydrate. Glucose molecules of starch are linked by $\alpha(1\rightarrow4)$ bonds for the amylose, and $\alpha(1\rightarrow6)$ and $\alpha(1\rightarrow4)$ for the amylopectin. In the gastrointestinal digestion, soluble starch is completely hydrolyzed to glucose by the action of different α-amylases and α-glucosidases (Englyst *et al.*, 1992).

After gastric digestion, a high and significant ($p \leq 0.05$) starch hydrolysis was observed in the first hour of InfoGest intestinal digestion (**Table 2a**), resulting in a significant increase of maltotriose, maltose and glucose content. After 2 h, although in minor proportion, a significant increase was obtained in the digestion of starch resulting in increases of glucose, maltotriose and total carbohydrates observed with respect to 1 h. These data are in line with the traditional hydrolytic activity of α-amylase towards $\alpha(1\rightarrow4)$ linkages presented in the starch, providing a mixture of low-molecular weight carbohydrates to be digested in the mucous membrane of the small intestine (Feher, 2017; Freitas & Le Feunteun, 2019). Starch digestion after RSIE treatment (**Table 2a**), indicates a different behavior with respect to the InfoGest small intestine protocol. RSIE treatment produced no disaccharides or trisaccharides presence, registering only a high and significant ($p \leq 0.05$) increase in glucose level after two hours of digestion, being

more pronounced in the first hour. This behavior is in agreement with the high maltase activity of RSIE observed (**Table 1**), underlining the action of the maltase-glucoamylase complex present in this extract (Ferreira-Lazarte, Olano, *et al.*, 2017; Hooton *et al.*, 2015; Lin *et al.*, 2016). Recently, Seo *et al.* (2020), which carried out a digestion assay using a solution of RSIE, observed a higher hydrolytic activities of the enzymes present in the RSIE compared to other digestive enzyme solutions, which is in good agreement with the highest hydrolysis degree of starch (58.5%, **Table 4**) and glucose generation observed.

The combination of both *in vitro* methods, InfoGest and RSIE, was also investigated (**Table 2a**). The effects of the two types of methodologies were complementary as pancreatic α-amylase hydrolyzed intra $\alpha(1\rightarrow4)$ linkages, resulting in di- and trisaccharides, whereas brush border enzymes hydrolyze by the reducing end of the chains of starch and the resulting di- and trisaccharides, generating more quantity of glucose when compare with the individual digestibility protocols (**Table 2a**).

In terms of hydrolysis degree (**Table 4**), the highest and significant value ($p \leq 0.05$) was observed with RSIE assay (58.5%), underlining the high importance of the enterocytes brush border enzymes for carbohydrate digestion (Ferreira-Lazarte, Olano, *et al.*, 2017; Gallego-Lobillo *et al.*, 2020; Lin *et al.*, 2016, 2012). Hydrolysis degree of starch via the combination of methods was slightly lower (55%, **Table 4**). Similar values were obtained by Bustos *et al.* (2017) and Fernandes *et al.* (2020) using InfoGest, with a 44.5% of hydrolysis of rice starch and 40% degradation of wheat starch observed by Selma-Gracia *et al.* (2020).

Table 4. Total hydrolysis degree (%) of polysaccharides after digestion treatment InfoGest protocol and RSIE

		Starch	Dextran	Citrus Pectin	Modified Citrus Pectin
Gastric Phase InfoGest	0 h	1.8 ± 0.6 [a]	0.8 ± 0.2 [a]	0.0 ± 0.0 [a]	4.0 ± 0.9 [a]
	2 h	0.9 ± 0.3 [a]	1.1 ± 0.3 [a]	0.0 ± 0.0 [a]	9.0 ± 1.0 [b]
Intestinal Phase InfoGest	1 h	47.0 ± 2.1 [b]	1.0 ± 0.0 [a]	0.1 ± 0.0 [a]	10.7 ± 0.4 [b]
	2 h	55.0 ± 2.8 [c]	1.1 ± 0.0 [a]	0.1 ± 0.0 [a]	11.1 ± 0.6 [b]
Intestinal Phase RSIE	1 h	37.4 ± 2.0 [d]	14.9 ± 0.8 [b]	10.4 ± 0.7 [b]	38.8 ± 0.3 [c]
	2 h	58.5 ± 1.0 [e]	16.3 ± 0.2 [c]	12.9 ± 0.6 [c]	41.6 ± 0.8 [d]
Intestinal Phase InfoGest	1 h	47.0 ± 2.1 [b]	1.0 ± 0.0 [a]	0.1 ± 0.0 [a]	10.7 ± 0.4 [b]
Intestinal Phase InfoGest + RSIE	1 h	52.5 ± 1.5 [c]	20.6 ± 0.2 [d]	17.2 ± 1.1 [d]	42.3 ± 3.7 [d]

Values are expressed as means as ± SD (n=4)

a-e Different letters indicate statistical differences between content of each column using ANOVA ($p \leq 0.05$)

Small intestinal digestion of dextran

Dextran is a glucose polymer mainly formed by $\alpha(1\rightarrow6)$ linkages (Naessens *et al.*, 2005; Sims *et al.*, 2001). Dextran contain short branches of two or three monomers of glucose linked by $\alpha(1\rightarrow3)$. No significant hydrolysis ($p \geq 0.05$) was observed during the intestinal digestion with InfoGest, compared to gastric digestion (**Table 2b**). This is consequence of the inability of α-amylase to hydrolyze $\alpha(1\rightarrow6)$ linkages (Whistler & Daniel, 2000).

Several works have reported a high resistance of dextran to the gastrointestinal digestion when simulated fluids are used, excluding the brush border enzymes (Fan *et al.*, 2017; Loyeau *et al.*, 2018; Meng *et al.*, 2018). In addition, Kothari *et al.* (2015) analyzed the behavior of the dextran used in this work with simulated digestion fluids, observing high resistance to digestion properties. Conversely, a significant increase of glucose ($p \leq 0.05$) was detected when RSIE was used, mainly after the first hour (**Table 2b**), reaching a total hydrolysis degree of 16.3% (**Table 4**). The $\alpha(1\rightarrow6)$ linkages were hydrolyzed by the sucrose-isomaltase complex, specifically, the isomaltase active site and also by the glucoamylase presented in the maltase-glucoamylase complex (Feher, 2017; Hooton *et al.*, 2015), confirming the effect of the chemical structure and type of linkage in the intestinal digestion (Ferreira-Lazarte, Gallego-Lobillo, *et al.*, 2019; Hernández-Hernández *et al.*, 2012). Lee *et al.* (2016) showed a hydrolysis rate of 24% of $\alpha(1\rightarrow6)$ disaccharides using rat enzymes, which was higher to the 16.3% observed in this study (**Table 3**), possibly due to the different methodology. In addition, these authors obtained 100% of hydrolysis of $\alpha(1\rightarrow4)$ carbohydrates (starch bonds), and a 52% for $\alpha(1\rightarrow3)$, emphasizing the effect of the glycosidic linkages and the capability of RSIE enzymes to hydrolyze different structures of carbohydrates (Gallego-Lobillo *et al.*, 2020; Lee *et al.*, 2016). Moreover, the considerable concentration of microorganisms in the small intestine, specially in the ileum (Kovatcheva-Datchary *et al.*, 2013), may also contribute to the hydrolysis of dextran. Thus, the complex environment of the small intestine concerns the activity of both types of enzymes: mammal and microbial. In this sense,

Hernández-Hernández *et al.* (2012) reported a high *in vivo* ileal digestion of *β*-GOS, considering the complete behavior of the small intestine in terms of carbohydrate digestion.

Concerning digestion assay of both methods, no significant modifications were obtained after the first small intestinal InfoGest hour, followed by a remarkable and significant hydrolysis during RSIE process (10.1 to 208.9 mg carbohydrates/g of sample, **Table 2b**; 20.6% hydrolysis degree, **Table 4**). Moreover, longer digestion times (6 h) with RSIE have demonstrated to reach higher degradation rates of dextran (44%) as observed in previous works (Poele *et al.*, 2020). Therefore, dextran could be mostly hydrolyzed by small intestinal enzymes present in the extract, showing a slight and significant increase when both methods are combined.

Small intestinal digestion of pectin and modified citrus pectin

Regarding non-digestible carbohydrates, the CP content along the different treatments is shown in **Table 3a**. CP is a heteropolysaccharide with a high M_w (472 kDa), mainly composed of GalA and galactose, as the most abundant neutral sugar. No hydrolysis by InfoGest method was observed, because of the resistance of this soluble fiber to the InfoGest simulated gastrointestinal digestion (Míguez *et al.*, 2016). The CP used in this study, had a degree of methylation of 70.7% (Muñoz-Labrador *et al.*, 2018), which increases the difficulty of the simulated fluids to hydrolyze this complex polysaccharide (Carnachan *et al.*, 2012), although, some authors have also reported slight hydrolysis with digestive solutions (10%) (Chen *et al.*, 2017), presumably due to the dynamic method used by them.

CP was partially hydrolyzed by RSIE, given a significant increase ($p \leq 0.05$) in GalA and galactose after the first hour of treatment (**Table 4**). These monomers are linked via *α*(1→4) in the CP backbone. As previously discussed, a complete ileal digestion with RSIE, regarding possible microbial and small intestine enzymes, might be able to hydrolyze *α*(1→4) bonds with monomers different to glucose (Gallego-Lobillo *et al.*,

2020; Hernández-Hernández *et al.*, 2012; Lee *et al.*, 2016; Marounek *et al.*, 1995), releasing GalA and galactose in significant proportions.

Digestion rate of the combined methods showed similar trend as these applied separately (**Table 3a**). Similarly, as occurred in dextran digestion with both methods, a higher and significant hydrolysis was observed in the combined method (20.6%, **Table 4**).

Galactose and galacturonic acid released in the digestion indicate the hydrolysis of the HG backbone and the lateral chains of galactose of RG-I (Ciriminna *et al.*, 2016). Furthermore, hydrolysis is related to the low pectinase activity obtained for this extract (**Table 1**). Different studies showed the low capability of the simulated digestion fluids to hydrolyze polysaccharides similar in structure to citrus pectin, obtaining percentages of low hydrolysis rate (8–10%) and observing limited modifications in the M_w (Chen *et al.*, 2017; Ferreira-Lazarte, Moreno, *et al.*, 2019; Huang *et al.*, 2019). With the combination of both methods, hydrolysis obtained is higher (17.2%) than literature. It is plausible that the combination of InfoGest and RSIE provides a more realistic approach on the digestion of these carbohydrates, nonetheless, the effect of the ileal microbiota present in the small intestine of the rat should also be considered in future studies to understand the complete environment of the digestive system (Hernández-Hernández *et al.*, 2012; Marounek *et al.*, 1995).

Evolution of the carbohydrate fraction of MCP is shown in **Table 3b**. MCP which has a lower M_w (3.1–0.7 kDa) than CP, it is also composed mainly by lineal GalA structures. A slight but significant increase ($p \leq 0.05$) in the GalA was observed after the first hour during the intestinal stage by InfoGest with no changes in the content of galactose. Hydrolysis degree (11.1%, **Table 4**), observed in this structure was similar to results reported by Khodaei *et al.* (2016), who digest a pectic polysaccharide rich in galactose and GalA, obtaining 14% of hydrolysis. Surprisingly, the incubation with RSIE significantly increase the concentration of GalA and galactose, resulting in a 41.6% of hydrolysis degree (**Table 4**). As indicated above, MCP is a non-methylated structure in contrast to the high methylation of CP (70.7). Therefore, the digestive enzymes might

have a better catalytic access to the HG backbone, providing a higher hydrolysis degree than in CP (Dongowski *et al.*, 2002). Furthermore, the better access may permit the intestinal enzymes, including the microbial and brush border complexes, to hydrolyze in major quantity the $\alpha(1\rightarrow4)$ bonds between GalA monomers, as it is observed in the higher and significant increase of this monosaccharide (**Table 3b**).

Concerning RSIE and the combination of InfoGest intestinal phase and RSIE, a significant increase in galactose and GalA was observed (**Table 3b**) and not significant differences between GalA concentration, resulting from these two methods, were found ($p \geq 0.05$). Similarly, the hydrolysis degree showed no statistical differences ($p \geq 0.05$) (42.3% InfoGest + RSIE vs. 41.6% RSIE, **Table 4**). In this context, the microbial enzymes present in the RSIE could also have an effect on the complete ileal carbohydrate digestion (Hernández-Hernández *et al.*, 2012; Marounek *et al.*, 1995). Thus, hydrolysis of MCP was higher than CP (**Table 3**), mainly due to the structural differences between the two types of pectins, such as the M_w and DP (Míguez *et al.*, 2016; Morris *et al.*, 2013).

Interestingly, in all samples, a more pronounced effect of intestinal digestion was observed after 1 h of InfoGest and RSIE treatment separately, while after 2 h digestion was lower. This fact also occurred in the combination (Intestinal Phase InfoGest + RSIE 1 h, **Table 2, 3 and 4**). An explanation for this fact might be the higher activity of pancreatic enzymes in their first approach, which is reduced in the second hour, probably reaching the maximum enzymatic activity (Freitas & Le Feunteun, 2019; Whistler & Daniel, 2000). Moreover, results in dextran and CP with the combination of InfoGest and RSIE are very similar in terms of hydrolysis degree (20.6% dextran vs. 17.2% CP, **Table 4**). These findings support the fact of the need of a complete method for the digestion of dietary polysaccharides.

According to these findings, the reliability of the RSIE as an *in vitro* digestion method is confirmed, showing meaningful differences with respect to InfoGest protocol as observed in previous reports. Although, the presence of small intestine microbial

enzymes in the digestion process could provide a more realistic simulation of the real process, a purification process should be considered in further studies. Although InfoGest is recognized as an international digestion model, the lack of the brush border enzymes and the inaccuracy to distinguish between digestible, partial non-digestible and non-digestible carbohydrates suggests the need of a revision and obtainment of a better method for the digestibility of carbohydrates (Ferreira-Lazarte, 2019; Hernández-Hernández, 2019), including brush border enzymes as was already reported in some works (Egger *et al.*, 2017; Ferreira-Lazarte, Gallego-Lobillo, *et al.*, 2019; Ferreira-Lazarte, Olano, *et al.*, 2017; Gallego-Lobillo *et al.*, 2020; Garcia-Campayo *et al.*, 2018; Mamone *et al.*, 2015; Tanabe *et al.*, 2015).

Conclusions

Digestibility of two glucose-based (starch and dextran) and two pectic polysaccharides (citrus pectin and modified citrus pectin) was investigated through the combination of two types of *in vitro* digestion methods: InfoGest protocol, method based on the use of simulated digestive fluids and RSIE, recently proposed as a useful model using a complete small intestine of rat. In the case of starch, the results confirmed the complementary effect of *α*-amylases and RSIE, with the hydrolysis rate higher than 50%. However, dextran was only hydrolyzed with RSIE. Citrus pectin was the least susceptible to the effect of digestive enzymes. In Modified Citrus Pectin, partial hydrolysis was observed, especially in the RSIE treatment and with the combination of the methods, resulting in a significant increase in GalA and galactose.

The data obtained in this work indicated the ineffectiveness of the InfoGest method as a versatile procedure for polysaccharides digestion. Although the presence of other enzymes different from *α*-amylase, including carbohydrases of the brush border enzymes of the enterocytes, is considered in this standardized method, they are still not used reducing the suitability of this method for carbohydrates digestion studies. Conversely, the reliability and usefulness of RSIE model has been proven. Going forward, standardized and specific methods for the digestibility of carbohydrates, realistically

mimicking the environment of the small intestine, are needed to understand the digestibility of different carbohydrates in the gastrointestinal tract.

Funding

This work was supported by the Spanish Ministry of Economy, Industry and Competitiveness (Project AGL2017-84614-C2-1-R) and the Spanish Ministry of Science, Innovation and Universities (Project RTI2018-101273-J-I00).

BLOQUE II

ESTUDIO *IN VIVO* DEL EFECTO DE POLISACÁRIDOS PREBIÓTICOS EN LA MICROBIOTA INTESTINAL EN UN MODELO DE CÁNCER COLORRECTAL

PREFACIO II

Dada la baja digestibilidad de la pectina, según se ha indicado en el *Bloque I, Capítulo 3*, es plausible que este compuesto llegue al intestino grueso donde ejerza su efecto sobre la microbiota intestinal. Por otro lado, existen investigaciones controvertidas sobre el efecto de la pectina en el cáncer colorrectal. Con estas premisas, en el *Capítulo 4* se planteó un estudio *in vivo* sobre el impacto de la ingestión de pectina y pectina modificada, ambas de cítricos, en la microbiota de animales sanos y con cáncer colorrectal en un modelo de rata (*Rattus norvegicus* F344) con cáncer inducido por azoximetano/dextrano sulfato de sodio (AOM/DSS). Además, se analizaron parámetros tumorales, fisiológicos y metabólicos.

Capítulo 4

Behaviour of citrus pectin and modified citrus pectin in an azoxymethane/dextran sodium sulfate (AOM/DSS)-induced rat colorectal carcinogenesis model

Alvaro Ferreira-Lazarte[a], Javier Fernández[b, c, d], Pablo Gallego-Lobillo[a], Claudio J. Villar[b, c, d], Felipe Lombó, F. Javier Moreno[a] y Mar Villamiel[a]

[a] Instituto de Investigación en Ciencias de la Alimentación, CIAL (CSIC-UAM). C/Nicolás Cabrera, 9, Campus de la Universidad Autónoma de Madrid, 28049 Madrid, España.
[b] Research Unit "Biotechnology in Nutraceuticals and Bioactive Compounds-BIONUC", Departamento de Biología Funcional, Área de Microbiología, Universidad de Oviedo.
[c] Instituto Universitario de Oncología del Principado de Asturias, Oviedo, España.
[d] Instituto de Investigación Sanitaria del Principado de Asturias, Oviedo, España.

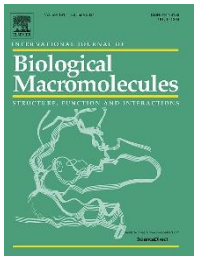

Reproducido a partir de Elsevier
International Journal of Biological Macromolecules
2021, 167, 1349-1360
DOI: https://doi.org/10.1016/j.ijbiomac.2020.11.089

Abstract

Large intestine cancer is one of the most relevant chronic diseases taking place at present. Despite therapies have evolved very positively, this pathology is still under deep investigation. One of the recent approaches is the prevention by natural compounds such as pectin. In this paper, we have assessed the impact of citrus pectin and modified citrus pectin on colorectal cancer in rats (*Rattus norvegicus F344*) to which azoxymethane and DSS were supplied. The lowest intake of food and body weight were detected in animals fed with citrus pectin, together with an increase in the caecum weight, probably due to the viscosity, water retention capacity and bulking properties of pectin. The most striking feature was that, neither citrus pectin nor modified citrus pectin gave rise to a tumorigenesis prevention. Moreover, in both, more than 50% of rats with cancer died, probably ascribed to a severe dysbiosis state in the gut, as shown by the metabolism and metagenomics studies carried out. This was related to a decrease of pH in caecum lumen and increase in acetate and lactic acid levels together with the absence of propionic and butyric acids. A relevant increase in *Proteobacteria* (*Enterobacteriaceae*) were thought to be one of the reasons for enteric infection that could have provoked the death of rats and the lack of cancer prevention. However, a reduction of blood glucose and triacylglycerides level and an increase of *Bifidobacterium* and *Lactobacillaceae* were found in animals that intake pectin, as compared to universal and modified citrus pectin feeding.

Introduction

Colorectal cancer (CRC) is the third most common malignancy in the world, being the second reason of cancer deaths in 2018 (Bray *et al.*, 2018). As it is known, CRC can imply severe health complications related to the illness itself and the side effects of surgery and/or therapy (C. K. H. Wong *et al.*, 2012). A recent study on the incidence and mortality of CRC in 39 countries has shown that the occurrence of colon and rectal cancers is increasing in countries with medium to high development degrees, mainly in the case of young people (M. C. S. Wong *et al.*, 2021); therefore, it is necessary to increase the early detection methods and to continue with the investigations that can shed light on the prevention and treatment of this pathology.

CRC usually is developed during several years when a sequence of genetic modifications (towards polyps, adenoma and carcinoma) gives rise to tumors that are more common in the distal large intestine, including the descending colon and rectum, as compared to the proximal sections. Although some CRC forms can be of genetic origin, most CRC cases have a relationship with the lifestyle and diet. In this sense, a diet based on dietary fiber and the use of cancer-therapeutic or cancer-preventive natural compounds are considered efficient and affordable approaches (Louis *et al.*, 2014).

A plethora of scientific articles has linked a high fiber consumption with a lower frequency of large intestine cancer. Particular interest has been sparked in the case of pectin, mainly derived from citrus, that is used as important technological food ingredient and also for its bioactivity (Maxwell *et al.*, 2012). Experimental studies have also showed a limited consistency on the effects of pectin on CRC with results of inhibition, no effect, or even tumor augmentation (Jacobasch *et al.*, 2008; Jacobs & Lupton, 1986; Nurdin *et al.*, 2018; Zhang *et al.*, 2015). Several factors related to pectin such as the source, extraction and purification methods can affect the effectiveness of the assays since the extracted pectin could have rather dissimilar structural features. This fact seems to play an important role in terms of molecular weight (M_w), methyl

esterification degree (DM), composition of galacturonic acid (GalA) and neutral sugars such as galactose and arabinose (Zhang *et al.*, 2015).

Pectin is a complex hetero-polysaccharide occurring in plant cell walls and its precise chemical structure is still under debate. The most recognized model combines the structural domains of homogalacturonan (HG), rhamnogalacturonan I (RG-I) and rhamnogalacturonan II (RG-II). HG corresponds to 65% of pectin molecules, with a linear backbone composed of *α*(1→4)-D-galacturonic acid, partially methyl-esterified in the C6, or acetylated in O-3 and/or O-2. RG-I corresponds to 20–35% of pectin molecules; this chain is composed of hundreds of repeating disaccharides [→4)*α*-D-galacturonic acid and (1–2)*α*-L-rhamnose(1→]n, and may present side chains of molecules of L-arabinose and D-galactose. RG-II represents 10% of pectin molecules and it is a well preserved and extremely complex molecule, where the main backbone is HG with four heteropolymer side chains with more than 17 rare monosaccharides and 20 different types of bonds (Marenda *et al.*, 2019).

Due to its highly branched complex, pectin is poorly soluble in water, limiting its use. Thus, Modified Citrus Pectin (MCP) has been developed by chemical, enzymatic or heat treatment of citrus pectin to produce a mixture of low M_w polysaccharides that could have a stronger therapeutic role against cancer as compared to full citrus pectin (Glinsky & Raz, 2009; Morris *et al.*, 2013).

In colon cancer cell lines, several studies have demonstrated the efficiency of different citrus pectin and MCP, and their fractions, and even different mechanisms of action have been postulated (Zhang *et al.*, 2015). Ai *et al.* (2018) assayed, against Caco-2 cells, different fractions obtained by an enzymatic treatment and subsequent ultrafiltration. Among the samples tested, the highest activity was found in the fraction of RG-II, probably due to its peculiar branched structure and low M_w. In the case of do Prado *et al.* (2019), the production of MCP fractions was by heat treatment and ultrafiltration. In HCT116 and HT29 colon cancer cells, the highest antiproliferative effect was observed

when HG oligomers were de-esterified and enriched in arabinogalactan I and poor in RG-I.

On the contrary, the limited *in vivo* information available on the effect of citrus pectin on CRC shows contradictory results using different animal models, different types of modified pectin and carcinogen doses. Scarce attention has been considered to effects on the microbiota and the relationship with the pectin structure. Moreover, in some cases, the effect of citrus pectin is considered together with other bioactive compounds (Odun-Ayo *et al.*, 2017; Zhang *et al.*, 2015). Ohkami *et al.* (1995) stated that the intake of 20% of citrus pectin in rats injected with azoxymethane (AOM) decreased the multiplicity of colon tumors and they hypothesized that a decrease of *β*-glucuronidase activity was the most important mechanism, although this effect was much higher in the case of apple pectin. According to Jacobasch *et al.* (2008), who used a model of animals with a genetic predisposition for intestinal neoplasia (APCMin/+ mice), pectins (with low and high DM) were ineffective for reduction of tumorigenesis in the small or large intestine and for suppressing COX-2 activity, an enzyme that plays a key role in the pathogenesis of tumor progression. These results were in line with those earlier obtained by Jacobs & Lupton (1986) who stated in Sprawe-Dawley rats that the intake of pectin and other soluble fiber could increase proximal colon tumorigenesis. However, Nangia-Makker *et al.* (2002) observed in BALB/c mice, with implanted tumors in the colon, that the daily oral administration of MCP reduced the growth of those implanted tumors and subsequent metastasis.

On the basis of this background, we have carried out an exhaustive study on the effect of commercial citrus pectin and Modified Citrus Pectin (MCP) in an animal model (*Rattus norvegicus* F344) developed for colorectal cancer using a combination of azoxymethane and DSS as carcinogenic compounds. Structural and physicochemical characteristics of both test substances have been considered in this animal model. Also, different tumorigenesis parameters (tumor size, number, area) have been analyzed, together with metabolic data (short-chain fatty acids, glycaemia, etc.), physiological

(food intake, weight, number of hyperplastic Peyer's patches, caecum weight) and metagenomics of gut microbiota.

Materials and methods

Manufacturing and samples

Commercial citrus pectin (trade name Ceampectin, ESS-4400) was kindly provided by CEAMSA® (Porriño, Pontevedra, Spain). Modified Citrus Pectin (MCP) was kindly provided by Econugenics®, Inc. (Santa Rosa, CA, USA).

Physicochemical characterization of substrates

A high M_w citrus pectin as well as MCP were used in this study. Physicochemical characterization of each substrate and the feed mixtures was carried out in samples before assays. Product composition was determined regarding carbohydrates, DM, M_w, water retention capacity (W_r) and pH (**Table 1**). Monomeric composition of pectins was analyzed after acid hydrolysis with 2 M trifluoroacetic acid (TFA) at 110 °C during 4 h. The released monosaccharides were derivatized by the formation of trimethylsilyl oximes, following a previous method (Brobst & Lott, 1966). Then, samples were analyzed by gas chromatography coupled to a flame ionization detector (GC-FID) and equipped with a fused silica capillary column DB-5HT (5% phenyl methylpolysiloxane, 30 m × 0.25 mm × 0.1 μm, Agilent J&W Scientific, Folsom, CA, USA). Oven temperature program started in 150 °C and increased to 165 °C at 1 °C/min and up to 300 °C in a rate of 10 °C/min. Injector and detector temperature were 280 and 350 °C, respectively. Nitrogen was used as the carrier gas at 1 mL/min of flow rate. Samples were injected in split mode 1:5. Quantification was done through the internal standard method (phenyl-*β*-D-glucoside).

Table 1. Physicochemical characterization of pectin and modified citrus pectin used in this study.

Sample	Monosaccharides composition (%)									
	Xyl	Ara	Rha	Gal	Man	Glc	GalA	GalA:Rha	Ara:Rha	Gal:Rha
Citrus pectin	tr.	6.7 ± 0.4	4.4 ± 0.3	22.5 ± 0.5	tr.	2.4 ± 0.1	64.0 ± 0.9	14.6 ± 1.2	1.5 ± 0.1	5.1 ± 0.4
Modified Citrus Pectin	tr.	3.9 ± 0.7	2.3 ± 0.1	8.9 ± 0.3	tr.	1.0 ± 0.0	83.9 ± 0.9	37.0 ± 1.1	1.7 ± 0.3	3.9 ± 0.2

	Wr (mL/mg)	Average M_w (kDa)	DM (%)
Citrus pectin	10 ± 0.0	472	70.7
Modified Citrus Pectin	0.7 ± 0.0	3.1-0.7	0

Analysis were carried out at least in duplicate (n = 2).
tr. = traces

Estimation of the M_w was conducted by HPSEC-ELSD (Muñoz-Almagro, Rico-Rodriguez, Wilde, *et al.*, 2018). Samples were filtered (0.45 μm), analyzed on a LC 1220 Infinity System (Agilent Technologies, Boebligen, Germany) and detected on an ELSD System 1260 Infinity (Agilent Technologies, Boebligen, Germany). Mobile phase used was 0.1 M $NH_4CH_3CO_2$, at a flow rate of 0.5 mL/min for 50 min at 30 °C. Pullulans of M_w 805, 200, 10, 3 and 0.3 kDa were used as standards.

DM of the samples was analyzed by Fourier transform infrared spectroscopy (FTIR) (Muñoz-Almagro *et al.*, 2017). The DM was determined as the average of the ratio of the peak area at 1747 cm^{-1} (COO-R) over the sum of the peaks 1747 cm^{-1} (COO-R) and 1632 cm^{-1} (COO^-).

W_r was determined following the method of Chau & Huang (2003). Pectins were incubated with distilled water (1:10, w/v) for 24 h with continuous agitation. Then, samples were centrifuged at 1006 ×g for 30 min. W_r was expressed as mL of water held by 1 g of pectin. In addition, pH of samples was measured using a pH-meter FE20 (Mettler Toledo GmBH, Schwerzenbach, Switzerland).

Animal and experimental design

In the inducted colorectal cancer model a total of 30 male Fischer 344 rats were maintained in the Animal Facilities at the University of Oviedo (authorised facility No. ES330440003591). All rat assays were approved by the Ethics Committee of the Principality of Asturias (authorization code PROAE 36/2018).

Rats (5 weeks old) were divided into 3 cohorts of 10 individuals each and fed ad libitum in individual cages. Cohort 1 was fed with universal feed (F cohort, 2014 Teklad Global 14% Protein Rodent Maintenance Harlan diet feed), which contained 6.7% protein, 5.8% fat, 53,6% carbohydrates, 20% fiber, 4.7% ashes (**Table 2**). Cohort 2 was fed with a mixture feed prepared from universal feed where cellulose (BW200) was substituted by citrus pectin (20%) (FP cohort) (Research Diets Inc., NJ, USA). In a similar way, cohort

3 was fed with a preparation where cellulose was substituted with the Modified Citrus Pectin (FMP cohort) (20%) (Research Diets Inc., NJ, USA).

Table 2.
Structural composition and characterization of feed mixtures utilized in the experiment.

	Universal Feed (F)	**Universal Feed + Pectin (FP)**	**Universal Feed + Modified Pectin (FMP)**
Protein (%)	16.7	16.7	16.7
Lipids (%)	5.8	5.8	5.8
Carbohydrates (%)	53.6	53.6	53.6
Fiber (%)	20	20	20
Ashes (%)	4.7	4.7	4.7
Pectin or MCP content	-	20	20
pH	6.67	6.50	6.7
Water retention (mL/mg)	0.8	4.5	0.7
kcal/g	3.33	3.33	3.33

Colorectal cancer induction and monitoring

The colorectal cancer inducing was carried out according to previously described methodology (Fernández, Moreno, *et al.*, 2018). Assay took place one week after the animals arrived at the facility when the diets started. After one week of eating the corresponding diet, CRC was induced in eight rats from each cohort. The two other rats were kept free of CRC induction as absolute control animals. CRC induction was carried out in those eight rats of each cohort using azoxymethane (AOM, Sigma-Aldrich, Madrid, Spain) dissolved in sterile saline solution (0.9% NaCl) at a concentration of 2 mg/mL. This AOM solution was injected intraperitoneally at a final concentration of 10 mg per kg body weight. This AOM treatment was repeated seven days after the first injection (weeks 2 and 3). The absolute control animals received sterile saline in both injections.

In weeks 4 and 15, rats received drinking water during seven days' treatment, containing 3% and 2% dextran sodium sulfate (DSS, 40000 g/mol, VWR), respectively. This

ulcerative colitis step was repeated twice because it enhances the pro-carcinogenic effect caused by AOM administration.

Rats were sacrificed by pneumothorax 21 weeks after the first administration of AOM. Throughout the entire process, rats were monitored for body weight and stool consistency/rectal bleeding.

Weight measurements

Rats were weighed regularly during the 21 experimental weeks; at reception of the animals (week 1), at each of the AOM administrations (week 2 and 3), and at weeks 6, 10, 13, 18 and 21.

Blood and tissue samples

Before being sacrificed (bilateral pneumothorax) at week 21, rats were anesthetized (isoflurane) for the extraction of blood (2 mL) from the heart, which was then centrifuged at 3000 rpm for 15 min, in order to collect and freeze the plasma at -20 °C.

Small intestines were fresh removed and the hyperplastic Peyer's patches were counted. Their number in the experimental animals was calculated and compared with respect to the two absolute control animals from each cohort (animals 9 and 10). Weight and length of small intestines was also measured in all cohort individuals. Caecums were weighed immediately after sacrifice using a precision scale and then frozen at -20 °C.

Finally, the colon was opened longitudinally and washed with PBS (phosphate buffer saline) before keeping it in 4% formaldehyde at 4 °C. Fixed colons were meticulously examined with a caliper in order to count the number of polyps larger than 1 mm on the inner mucosa surface. The largest detected polyps were 10 mm in diameter. The shape of the polyps was identified as pedunculated (a disc connected via a peduncle to the colon mucosa), plane irregular, plane circular and spherical. Finally, the total polyp-affected area was calculated.

Plasma glucose and triacylglycerides analysis

Plasma glucose levels were measured using a Accutrend Plus and the reactive strips 11447475 (Roche, Barcelona, Spain). Plasma triacylglycerides levels were measured using the same equipment, but with reactive strips 11538144 (Roche, Barcelona, Spain).

HPLC-UV quantification of SCFA in caecum samples

Prior to HPLC analysis, short chain fatty acids (SCFA) were extracted from rat caecum, according to the method of Joseph *et al.* (2019). Caecum samples (0.2 g) were added to distilled water (1.6 mL) in order to get a final ratio of 1:8 (w/v). Then, extraction was performed by mixing powerfully in vortex for 1 min. Finally, samples were centrifuged for 10 min at 10,000 × *g* and supernatant was filtered using a 0.22 µm syringe filter (Symta, Madrid, Spain). Samples were injected on a HPLC system (Agilent Technologies, Germany) equipped with a UV-975 detector. Separation was done through a Rezex ROA Organic Acids column (300 cm × 7.8 mm) (Phenomenex, Macclesfield, UK) at a flow rate of 0.5 mL/min (isocratic elution) at 50 °C. The mobile phase was 0.005 N H_2SO_4 and detection was performed at a wavelength of 210 nm. Identification and quantification of peaks were done through external standards solutions of SCFA (acetic, propionic, butyric, formic, lactic, valeric and isovaleric acid) in different concentrations (1-100 mM).

Genomic DNA extraction and 16S ribosomal RNA sequencing for metagenomics

Genomic DNA (gDNA) was extracted from 200 mg of frozen (-80 °C) caecum feces using E.Z.N.A.® DNA Stool kit (Omega BioTek Ref. D4015- 02, VWR, Madrid, Spain) and provided 200 µL of genomic DNA. These gDNA samples were then quantified using a BioPhotometer® (Eppendorf, Madrid, Spain) and their concentrations diluted to 6 ng/µL. Diluted samples were used for performing polymerase chain reactions (PCR) amplification, following the protocol of the Ion 16™ Metagenomic kit (Thermo Fischer Scientific, Madrid, Spain).

PCR amplification products were utilized to create a library using the Ion Plus Fragment Library kit for AB Library Builder™ System (Cat. No. 4477597, Thermo Fischer Scientific), with sample indexing using the Ion Xpress™ Barcode adapters 1–96 kit (Cat. No. 4474517, Thermo Fischer Scientific).

Template preparation was performed using the ION OneTouch™ 2 System and the ION PGM™Hi-Q™OT2 kit (Cat. No. A27739, Thermo Fischer Scientific). Metagenomics sequencing was performed using ION PGM™ Hi-Q™ Sequencing kit (Cat. No. A25592, Thermo Fischer Scientific) on the ION PGM™ System. The chips used were the ION 314 ™ v2, 316™ v2 or 318™ v2 Chips (Cat. No. 4482261, 4483188, 4484355, Thermo Fischer) with various barcoded samples per chip (Fernández, García, *et al.*, 2018).

Phylogenetic analysis

The consensus excel table for each metagenomics sequencing was downloaded from ION Reporter 5.6 software (Life Technologies Holdings Pte Ltd., Singapore). This excel table includes the percentages for each taxonomic level and was used for comparing frequencies between rat individuals and cohorts.

Taxonomic adscription up to species level was conducted using the QIIME-2 (v.2017.6.0) open-source bioinformatics pipeline. Analysis of the microbiome community was carried out using R software (v3.2.4): non-supervised multivariate analysis (PCA). The reference library used was the Curated MicroSEQ(R) 16S Reference Library v2013.1; Curated Greengenes v13.5. The number of mapped reads (after the ignored ones due to less than 10 copies) per sample was always over 80.000. Total number of reads was always over 110.000. Counts were normalized by sum scaling (Fernández *et al.*, 2020).

Statistical methods

Data were expressed as the mean value ± S.E.M. Statistical analyses were conducted using ANOVA test when the quantitative data presented normality and the variances were assumed equal. Normality was analyzed using Shapiro-Wilk. In the absence of normality, Kruskal-Wallis test was used. The graphical representation of all these data was generated using GraphPad Prism software (version 8, GraphPad Software, San Diego, CA, USA). In all cases, a p value < 0.05 was considered statistically significant (*p < 0.05; **p < 0.005; ***p < 0.0005; ****p < 0.0001) (Fernández *et al.*, 2020).

Results

Effect of pectin diets on body weight

Body weight was affected in all cohorts due to the different feeding after the AOM and DSS treatment. In general, all cohorts gained weight during the experiment after the DSS treatment maintaining a continuous gain along the experimental weeks. Rats with inducted CRC achieved a slightly lower weight values as compared to the control rats (**Fig. 1A and B**). It is noteworthy that cohort fed with pectin (FP) showed the lowest intake and body weights in all cohorts, followed by the cohort fed with modified pectin (FMP), whereas the cohort fed with the universal diet (F) showed the highest values.

Nevertheless, it should be noted that nine animals died during the assay; five in FP cohort and four in FMP cohort. They did not survive the DSS treatment, which was used to enhance the final production and size of the colon tumors, and died just after its administration. Five of them died during the next 10 days after finishing the first DSS treatment (mainly in FP cohort), three died one day after finishing the second DSS treatment and the last animal died 2 days before sacrifice day (mainly in FMP cohort).

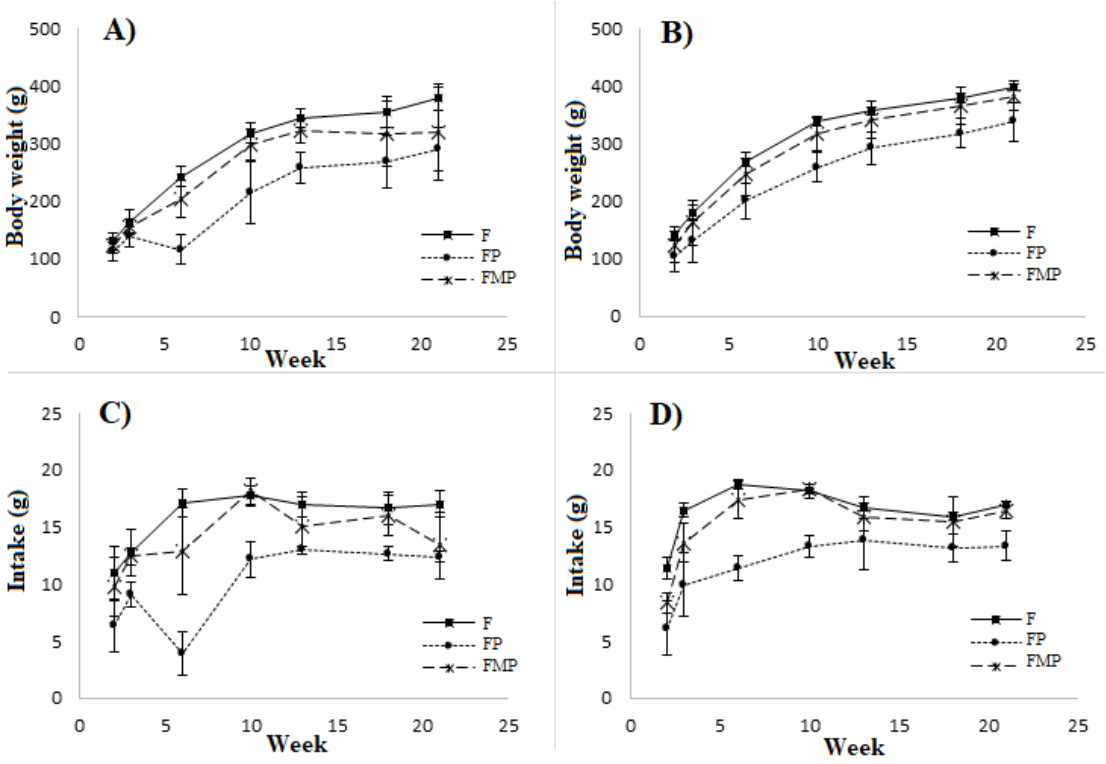

Figure 1. A) Evolution of body weight throughout the experiment for the eight rats with colorectal cancer (CRC) induction in the three cohorts, F = Universal Feed cohort; FP = Pectin + Universal Feed cohort; FMP = Modified Pectin + Universal Feed cohort. Body weight was measured at week 2, 3, 6, 10, 13, 18 and 21. When the animals were sacrificed, the mean value for the F cohort was 378.6 ± 20.4, and 290.7 ± 37, and 321.3 ± 63.2 g for FP and FMP cohorts, respectively. B) Evolution of body weight for the two rat controls (no CRC induction) in the three cohorts. The mean weight when the animals were sacrificed were 398.5 ± 6.4, 338.0 ± 33.9 and 383.5 ± 24.8 g for F, FP and FMP cohorts, respectively. C) Evolution of the intake of the feed by the rats throughout the experiments for the eight CRC rats. D) Intake evolution for the two rat controls (no CRC inducted).

Effect of pectin diets on caecum weight

Statistically significant differences in the caecum weight values between the three different cohorts were observed (**Fig. 2**). Highest weight was detected in the FP cohort (14.4 ± 1.4 g) as compared to FMP (9.4 ± 1.9) and F (3.8 ± 0.6) cohorts.

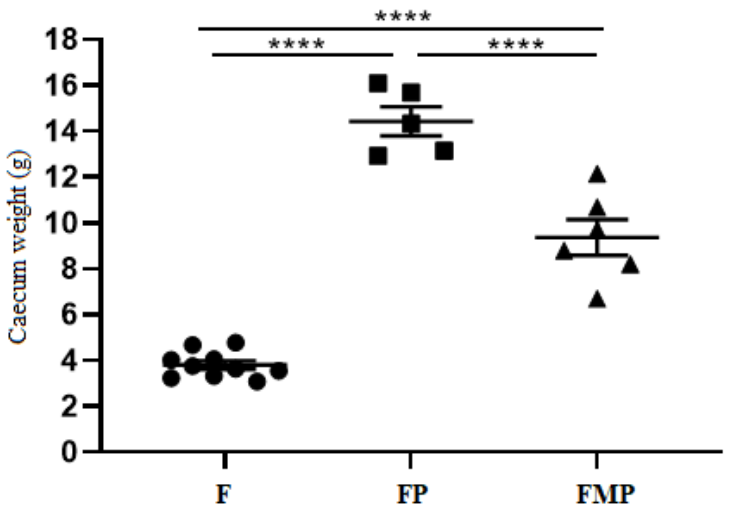

Figure 2. Mean cecum weight in grams for each cohort (all rats included) in the chemically induced CRC animal model. F = Universal Feed cohort, FP = Pectin + Universal Feed cohort, FMP = Modified Pectin + Universal Feed cohort.

Effect of pectin diets on hyperplastic Peyer's patches

The hyperplastic Peyer's patches in the small intestine was quantified when the animals were sacrificed. Peyer's patches contain high amounts of lymphocytes and are located in the mucosa layer of the small intestine. These lymphoid nodules can become hyperplastic and are, therefore, easily visible in the small intestine as rounded, protruding, white 2-3 mm ovals (Fernández, García, *et al.*, 2018).

In this work, differences in the Peyer's patch mean values were not statistically significant between the universal feed cohort and pectin and modified pectin cohorts (**Fig. 3**).

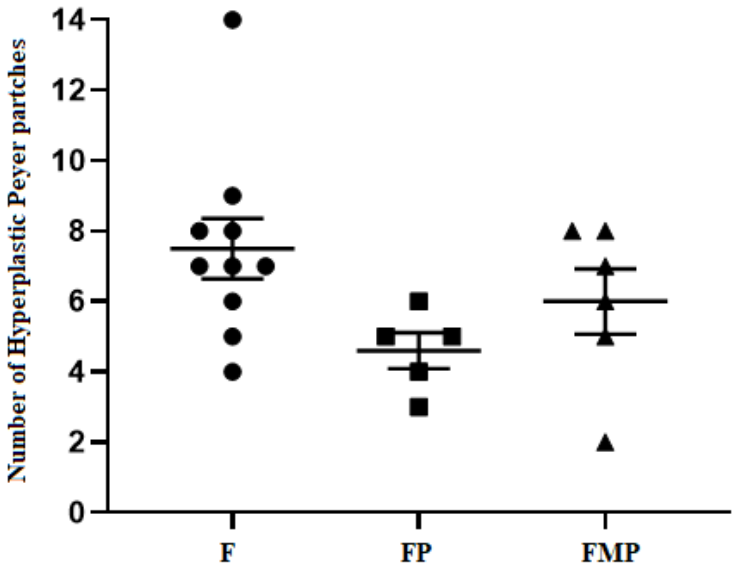

Figure 3. Mean number of hyperplastic Peyer patches in the small intestine from each cohort (all rats included. Rats from F cohort with CRC induced showed a mean of **7.4 ± 0.9** compared with rat F controls 4.5 ± 0.7. Rats from FP cohort with CRC induced showed values of **4.7 ± 1.5** and 4.5 ± 0.7 for control FP rats. FMP cohort showed values of **5.3 ± 2.5** and 7.5 ± 0.7 for CRC induced and control rats, respectively. In general, no significant differences were observed along all cohorts. F = Universal Feed cohort, FP = Pectin + Universal Feed cohort, FMP = Modified Pectin + Universal Feed cohort.

Effect of pectin diets on number of polyps and tumor-affected area

After sacrifice, colonic mucosa of each animal was analyzed for the number of polyps which diameter ranged from 1 to 10mm. Statistically differences were not observed in the number of polyps between rats from the different cohorts (**Fig. 4A**). Moreover, the area of each polyp present in a given colon mucosa was calculated according to its shape and the total polyp area was computed for each animal. Highest tumor area was measured

for F cohort (629.1 ± 270) with a reduction of 23.5% in FP cohort and 5% in FMP cohort, respectively; however, these reductions were not statistically significant (**Fig. 4B**).

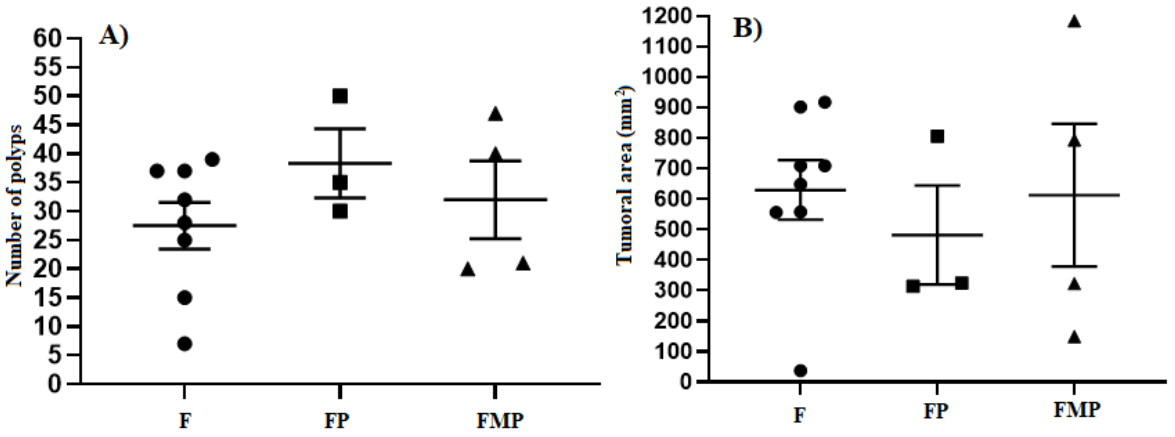

Figure 4. A) Mean number of colon polyps from each cohort in the animal CRC model (rats 1 to 8 in the three groups). Control rats in each cohort showed zero colon polyps (rats 9 and 10 in each cohort). B) Mean value in mm^2 of the sum of polyp area from all polyps in all rats from each cohort. F = Universal Feed cohort, FP = Pectin + Universal Feed cohort, FMP = Modified Pectin + Universal Feed cohort.

Effect of pectin diets on SCFAs production and blood glucose and triacylglyceride levels

Caecal production of SCFA is important since these compounds show interesting antitumor properties regarding CRC prevention. As it could be expected, acetate, which is the main product of saccharolytic fermentation of polysaccharides, was the highest SCFA detected in all samples (**Fig. 5A**). F cohort showed the lowest values of acetate (22.6 mM ± 5.5) as compared to FP (33.71 mM ± 7.4) and FMP (35.0 mM ± 6.3), respectively. Slight levels of lactic acid were also detected in all cohorts (0.4 mM ± 0.3; 1.9 mM ± 0.1 and 2.8 mM ± 1.4 for F, FP and FMP, respectively) (**Fig. 5B**). Although lactate is not a SCFA, it is usually considered in the metabolism of bacteria as a product of saccharolytic fermentation. Regarding other SCFA, no quantifiably values were found in the samples with the chromatographic method used. In general, total organic acids observed (acetate and lactate) showed an increase in FP and FMP cohorts (in line with

the lower pH observed in these groups; 6.33 ± 0.13 and 6.50 ± 0.15, respectively, *vs* F cohort 6.92 ± 0.19; **Fig. 5C**), although these increases did not show statistically significant differences.

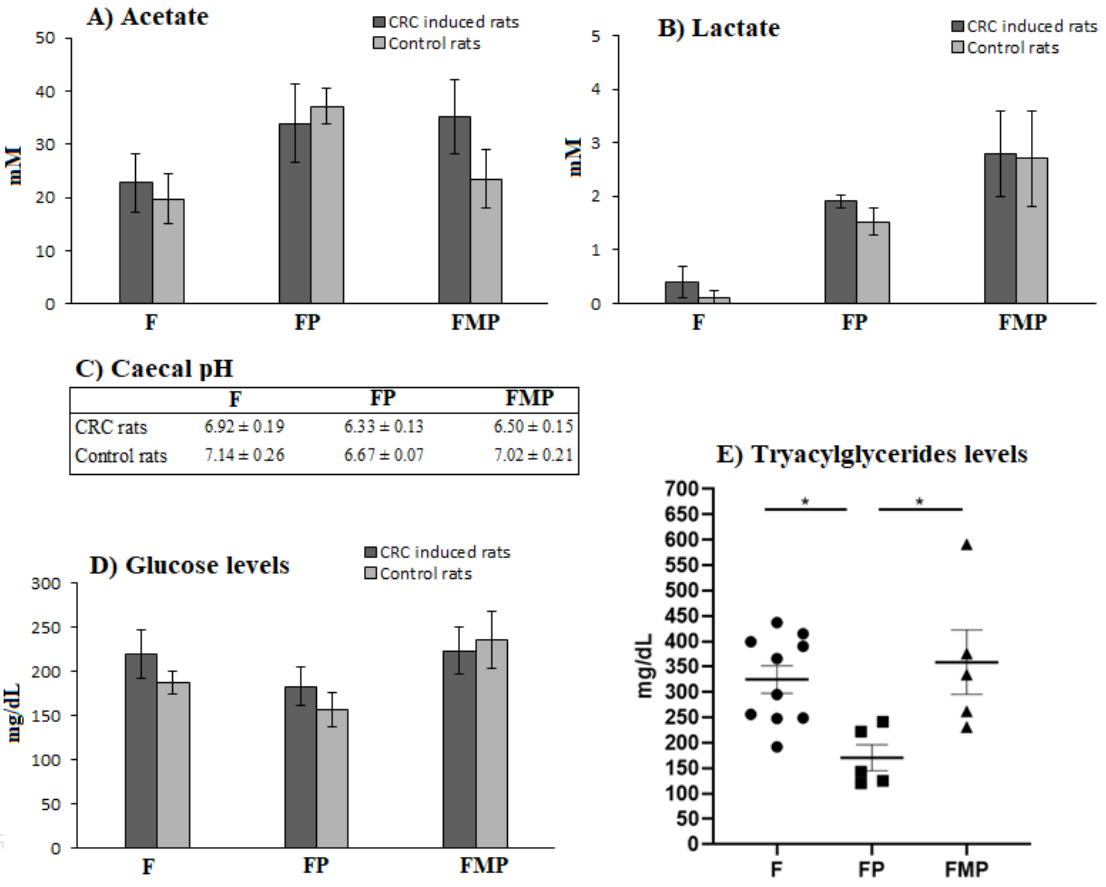

Figure 5. Caecal concentration of organic acids (A) acetate (B) lactate and pH measured in all three cohorts caecum (C). D) Glucose levels (mg/dL) measured in plasma of individuals in the three cohorts. E) Triacylglycerides levels in plasma for the three cohorts. F = Universal Feed cohort, FP = Pectin + Universal Feed cohort, FMP = Modified Pectin + Universal Feed cohort.

Regarding glucose levels determined in plasma (**Fig. 5D**), citrus pectin presence in the FP cohort provided lower levels of glucose in the animals, which is in accordance with its relation of a better control of the caloric intake given its high resistance to intestinal digestion. Conversely, FMP, which is mainly composed of oligosaccharides (average M_w = 3.1 kDa) did not show any decrease in the glucose levels compared to the F cohorts.

Nevertheless, all variations found in this analysis did not show any statistically significant differences.

Finally, plasma triacylglycerides levels showed a statistically significant reduction of this parameter in FP cohort (170.2 mg/dL ± 25.4) in comparison with F (324.7 mg/dL ± 27.3) and FMP (358.8 mg/dL ± 63.4) (**Fig. 5E**).

Effect of pectin diets on intestinal microbiota

Average phyla compositions showed important differences between the three animal cohorts with and without disease (**Table 3**). At this level, one of the main differences observed was the high increase in *Bacteroidetes* in the FP cohort with respect to F and FMP cohorts in both CRC and healthy rats. No-CRC rats showed higher increases in this phyla compared to CRC rats. Additionally, reduction in the *Firmicutes* levels was found in the FP cohort of CRC rats with respect to the F (20.7%) and FMP (19.9%) groups, where no-CRC animals showed decreases only in FP cohort, in a lesser extent, compared to F cohort (6.9%). Finally, the main difference observed in this level was the important increase in *Proteobacteria* in CRC rats, in FP (14.8%) and FMP (4.3%) groups compared to F group, whereas no-CRC animals showed a reduction of these bacteria, 3.1% and 2.3% reduction for FP and FMP cohorts compared to F, respectively.

At family level (**Fig. 6, Table 4**), in the F cohort, the most abundant families were *Clostridiaceae* (14.91%), *Lachnospiraceae* (13.60%), *Bacteroidaceae* (12.78%), *Porphyromonadaceae* (11.86%), *Ruminococcaceae* (11.75%), and *Desulfovibrionaceae* (10.70%). In the case of FP cohort, the most abundant ones were *Prevotellaceae* (25.42%), *Enterobacteriaceae* (13.04%), *Lachnospiraceae* (12.12%), *Bacteroidaceae* (12.08%), and *Clostridiacea* (8.12%). Highest values found in FMP were for *Lachnospiraceae* (20.39%), *Bacteroidaceae* (13.74%), *Porphyromonadaceae* (10.49%), *Clostridiaceae* (8.28%), *Desulfovibrionaceae* (6.85%), *Enterobacteriaceae* (5.37%), *Lactobacillaceae* (5.25%) and *Ruminococcaceae* (5.17%).

Table 3.
Average percentage composition of intestinal microbiota at phylum level for the three cohorts studied for CRC and no-CRC rats.

	CRC rats			No-CRC rats		
Percentage of:	**F**	**FP**	**FMP**	**F**	**FP**	**FMP**
Actinobacteria	0.06	0.27	0.42	0.02	0.18	0.03
Bacteroidetes	29.44	39.32	28.89	32.35	47.09	36.02
Deferribacteres	0.97	0.00	0.00	1.39	0.00	0.00
Firmicutes	51.51	30.78	50.72	42.94	36.02	46.49
Lentisphaerae	0.00	0.26	0.23	0.00	0.10	0.02
Nitrospinae	0.00	0.12	0.03	0.01	0.01	0.00
Proteobacteria	13.16	27.99	17.44	17.25	14.13	14.96
Spirochaetes	0.18	0.00	0.00	1.00	0.00	0.00
Synergistetes	0.06	0.02	0.02	0.10	0.04	0.04
Tenericutes	0.15	0.06	0.17	0.00	0.10	0.01
Verrucomicrobia	4.03	1.08	2.05	4.94	2.18	2.40
Unclasified bacteria	0.01	0.06	0.01	0.00	0.12	0.00
Firmicutes/Bacteroidetes	*1.75*	*0.78*	*1.76*	*1.33*	*0.76*	*1.29*

At this level, different statistically significant increases can be observed compared to the F cohort. For example, *Lactobacillaceae* increased from 0.27% to 2.01% and 5.25% in FP and FMP cohorts, respectively. *Prevotellaceae* increased from 1.77% to 25.42% in FP group. *Enterobacteriaceae* showed high increase in FP individuals (13.04%) and FMP (5.37%) vs 0.35% in F group. *Suterellaceae* increased from 1.12% in F cohort to 4.05% in FP animals. *Lachnospiraceae* family showed an increase in FMP cohort (20.39%) in comparison with F (13.60%) and FP animals (12.12%).

Additionally, significant reductions were observed in *Porphyromonadaceae* (3.91% in FP, 11.86% in F and 10.49% in FMP). *Clostridiaceae* in FP (8.12%) and FMP (8.28%) vs 14.91% in F cohort and *Desulfovibrionaceae* (3.18%, 6.85% for FP and FMP, vs 10.70% for F cohort). *Ruminococcaceae* showed a value of 4.48% in FP, 5.17% in FMP and 11.75% in F cohort (**Table 4**).

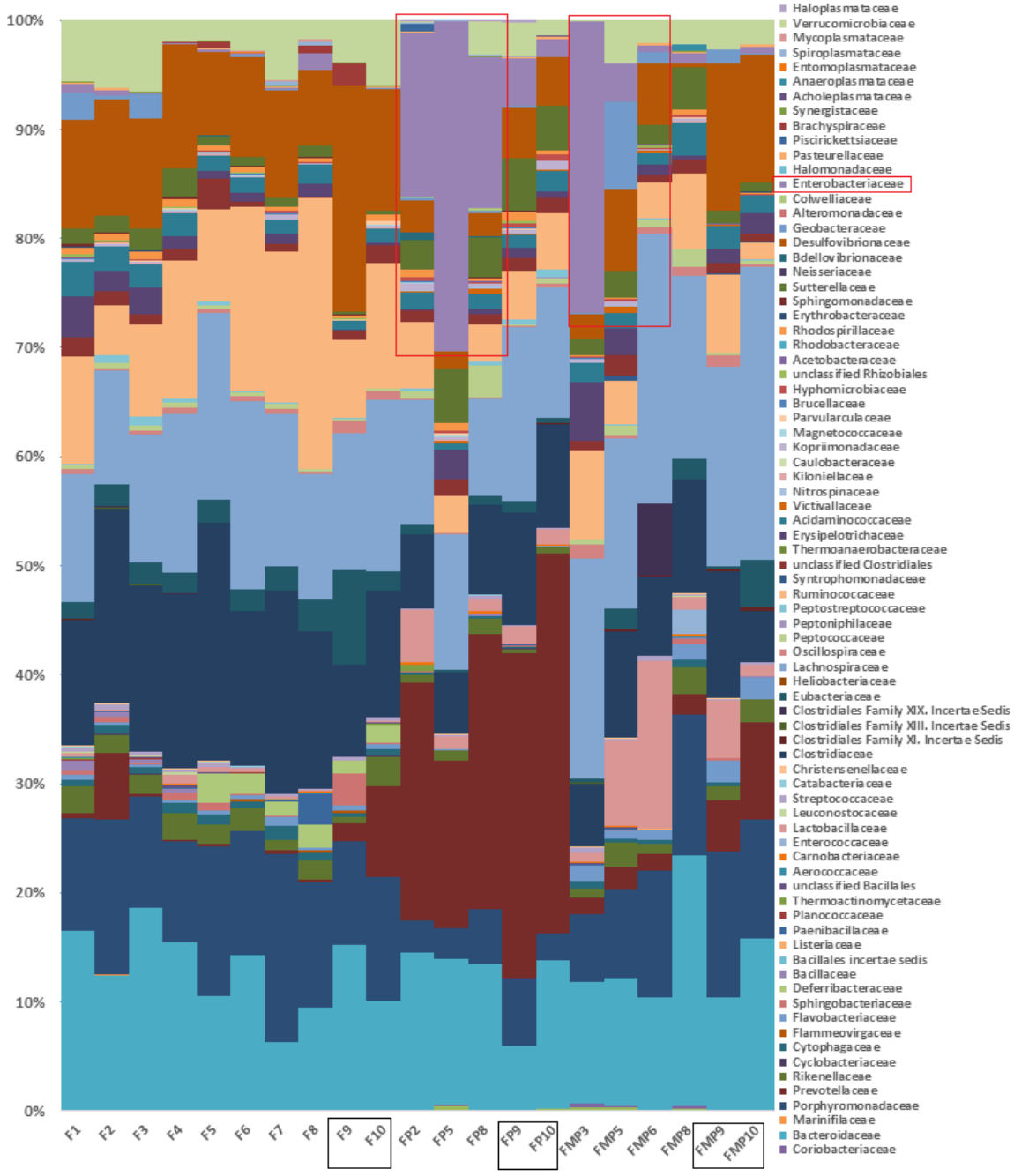

Figure 6. Intestinal microbiota composition at the family level in rats belonging to all tree cohorts. Rectangles remark results obtained for the no-CRC control rats (black) and the high levels of *Enterobacteria* observed in FP and FMP CRC-rats (red).

Table 4.
Average percentage composition of intestinal microbiota at family level for the three cohorts studied. *Indicate statistically significant differences between each pairs of compared cohorts

Percentage of:	**F**	**FP**	**FMP**	**F-FP**	**F-FMP**	**FP-FMP**
Bifidobacteriaceae	0.00	0.17	0.13	**	-	-
Porphyromonadaceae	11.86	3.91	10.49	****	-	***
Prevotellaceae	1.76	25.42	3.44	***	-	-
Rikenellaceae	1.80	0.79	1.64	*	-	-
Cytophagaceae	0.73	0.14	0.42	***	*	-
Flavobacteriaceae	0.40	0.03	1.41	***	*	**
Sphingobacteriaceae	0.56	0.03	0.12	*	-	-
Deferribacteraceae	1.04	0.00	0.00	-	-	*
Paenibacillaceae	0.31	0.00	0.05	-	-	-
Lactobacillaceae	0.27	2.01	5.25	**	**	-
Clostridiaceae	14.91	8.11	8.27	**	**	-
Clostridiales family XI	0.01	0.00	0.14	-	*	*
Eubacteriaceae	2.71	0.69	1.44	*	-	-
Lachnospiraceae	13.60	12.12	20.39	-	**	**
Oscillospiraceae	0.49	0.17	0.69	-	-	*
Ruminococcaceae	11.75	4.48	5.17	*	*	-
Victivallaceae	0.00	0.19	0.15	**	-	-
Kopriimonadaceae	0.16	0.43	0.16	*	-	*
Hyphomicrobiaceae	0.06	0.31	0.10	**	-	-
Rhodospirillaceae	0.49	0.54	0.16	-	*	*
Suterellaceae	1.12	4.05	1.89	****	-	**
Bdellovibrionaceae	0.03	0.15	0.00	-	*	-
Desulfovibrionaceae	10.70	3.17	6.84	**	-	-
Enterobacteriaceae	0.34	13.04	5.36	**	-	-
Verrumicrobiaceae	4.21	1.54	2.16	*	-	-

PCA analysis of gut microbiota composition at family level divided the animals in three clusters, indicating differences in the gut microbiota composition associated to these dietary interventions, where F and FMP animals are clustered closer than FP cohort (**Fig. 7**).

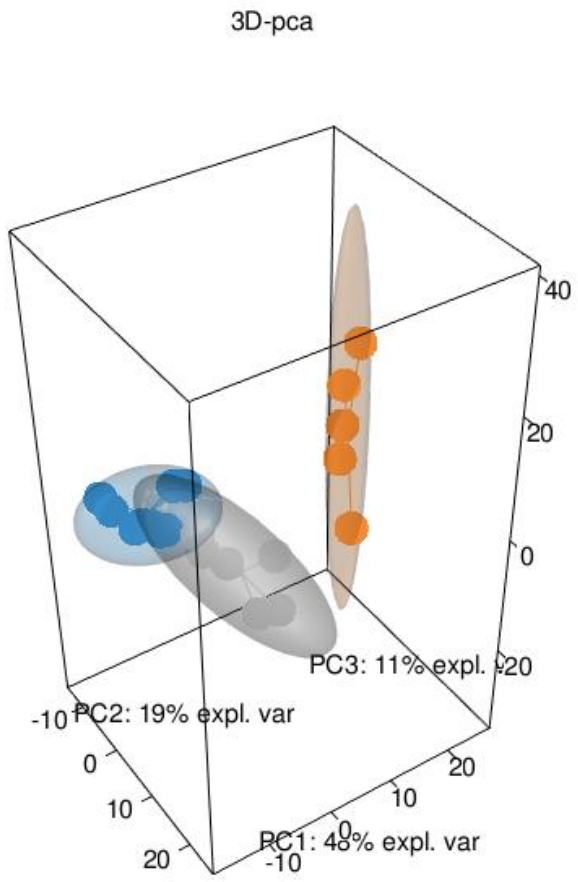

Figure 7. Gut microbiota PCA cluster analysis, showing that animals belonging to each of the three compared diet cohorts show very distinctive characteristics. Blue dots = Universal Feed cohort, Orange dots = Pectin + Universal Feed cohort, Grey dots = Modified Pectin + Universal Feed cohort.

Tables 5 and S1 show the percent abundance of the genera and species with statistically significant differences between the three cohorts in the assay. The main differences are associated with a higher proportion of some genera (such as *Lactobacillus*) in the pectin administration diets (FP, FMP), some of them involved in SCFAs biosynthesis (*Bifidobacterium, Paraprevotella, Bacteroides, Eubacterium, Parasutterella, Blautia*), and a reduction in the populations of other genera in these cohorts (*Prevotella, Clostridium, Blautia*), including a significant reduction in some pro-inflammatory genera (*Ruminococcus and Bilophila*).

Table 5.
Caecal microbiota composition (percentages) at the genus and species levels where statistically significant differences observed are marked as (*)

Genus	Species	F	FP	FMP	F-FP	F-FMP	FP-FMP
Bifidobacterium		0.000	0.174	0.135	**		
	animalis	0.000	0.090	0.007	*		
Bacteroides	*acidifaciens*	1.420	0.514	0.000		***	
	eggerthii	0.050	0.290	1.053		*	
	vulgatus	0.710	0.050	0.217	*		
Butyricimonas		0.342	0.138	0.278	*		
	virosa	0.157	0.048	0.090	**		
Parabacteroides		1.357	0.570	2.210			*
	merdae	0.200	0.116	0.662		**	**
Paraprevotella		0.001	0.306	0.358	**	**	
Prevotella		0.004	2.302	1.692	**		
Alistipes	*sp.*	0.072	0.010	0.158			*
Mucispirillum		1.049	0.000	0.000		*	
	schaedleri	1.049	0.000	0.000		*	
Lactobacillus		0.004	0.704	0.620	**	**	
Clostridium		4.296	3.000	2.643		*	
Eubacterium		0.015	0.274	0.055	*		
Anaerostipes		0.492	0.004	0.020	**	*	
Blautia		0.429	0.166	1.115			*
	producta	0.316	0.086	0.858			**
Dorea		0.145	0.008	0.037	*		
	Dorea	0.145	0.008	0.037	*		
	bolteae	0.003	0.000	0.360		*	**
LachnoClostridium							
Stomatobaculum		0.195	0.000	0.007	**	**	
	longum	0.195	0.000	0.007	**	**	
Faecalibacterium	*prausnitzii*	1.345	0.338	0.565	**	*	
		0.152	0.016	0.005	*	**	
RuminiClostridium							
Ruminococcus		2.503	0.342	0.242	*	**	
Bacteroides		0.000	0.366	0.000	***		***
Turicibacter		0.030	0.148	0.000			**
Victivallis		0.003	0.196	0.155	**		
	vadensis	0.003	0.196	0.155	**		
Parasutterella		1.123	4.058	1.895	****		**
	excrementihominis	1.026	3.370	1.657	****		**

Bilophila		9.832	3.042	6.687	*	
	wadsworthia	7.635	2.260	2.735	**	**
Escherichia		0.004	0.552	0.197	**	
	coli	0.004	0.532	0.195	**	
Akkermansia		4.208	1.518	2.165	*	
	muciniphila	4.208	1.518	2.165	*	

Discussion

Potential antitumor effects of commercial citrus pectin (CP) and Modified Citrus Pectin (MCP) were studied in an animal model where CRC was generated using AOM/DSS. Chemical composition of both test substrates demonstrated to be similar regarding the monomeric composition (**Table 1**). The higher M_w and methylation degree observed in pectin support the highly complex structure of this substrate with a high number of side chains, already observed in previous studies (Ferreira-Lazarte *et al.*, 2018), whereas MCP was mainly composed of a galacturonic acid backbone and free mono- and oligosaccharides, showing a lack of methylation degree (0%). Pectin structure provides an important water retention capacity being almost 15-fold higher than that of MCP (10 mL/mg vs 0.7 mL/mg). In this sense, pectin, as well as other dietary fibers, is known to impact on satiety and satiation due to its properties of producing viscosity (satiety) and adding bulk to the food (satiation). Pectin has been shown to significantly delay gastric emptying time, hence increasing satiety (Christiaens *et al.*, 2016; Lorenzo *et al.*, 1989; Mortensen *et al.*, 2017), which can explain the lower intake of food observed in the FP cohort (**Fig. 1C**) and, therefore, the lower body weight observed in all individuals (**Fig. 1A**), although the important food intake reduction observed at week 6 was also associated to the secondary effects of the ulcerative colitis episode due to DSS administration. Conversely, MCP, with a lower M_w and DM than pectin and similar physicochemical properties to the universal feed regarding water retention capacity, showed higher intake values during the assay (FMP cohort), with almost similar responses to the universal feed individuals (F cohort) (**Fig. 1C**). In addition, bacterial

pectate lyase has shown to hydrolyze preferably low DM pectin structures, such as MCP, contributing, therefore, to their high intake and absorption (Jacobasch *et al.*, 2008). Thus, higher body weight was observed in the FMP cohort as compared to pectin being almost as high as the F cohort was.

Regarding glucose content at the end of the study, high plasma levels were observed in F and FMP cohorts (>200 mg/dL) (**Fig. 5D**), whereas, pectin intake decreased glucose levels showing the lowest values (FP cohort) of all studied groups. The anti-diabetic and hypoglycemic effects of dietary fiber and pectin have been widely reported in previous *in vivo* and *in vitro* studies (Qilei Chen *et al.*, 2017; Cui *et al.*, 2015; Grunberger *et al.*, 2007). In this sense, the European Food Safety Authority (EFSA) has recognized a direct cause and effect relationship between the consumption of pectins and a reduction of postprandial glycemic responses in adults (EFSA Panel on Dietetic Products Nutrition and Allergies (NDA), 2010; Mortensen *et al.*, 2017). Studies with rats have demonstrated the effectiveness of pectin in reducing glucose levels in type 1 and type 2 diabetic rats (Liu *et al.*, 2016; Silva *et al.*, 2011). Conversely, the low M_w carbohydrates composition and low viscosity in FMP produced higher glucose levels, since it has been reported that a reduction in the viscosity of pectins can reduce significantly the effect on postprandial hyperglycaemia (Brenelli *et al.*, 1997). A plausible explanation for this is that glucose intake is reduced with a high viscosity possibly due to a combination of delayed gastric emptying, reducing macronutrient absorption and preventing diffusion of glucose through the lumen to the epithelium (Ou *et al.*, 2001; Weickert & Pfeiffer, 2018). In the same sense, plasma triacylglycerides showed a statistically significant reduction in the case of pectin cohort (FP) in comparison with the two other cohorts (**Fig. 5E**), due to a similar positive effect.

At the end of the experiment, all surviving animals were sacrificed. It has to be noted that FP diet caused the death of five CRC rats and four rats did not survive in the FMP cohort, whereas CRC control cohort rats (F) did not show any mortality. One possible explanation to this is the fact that these two diets based on pectins, caused a dysbiosis at

the intestinal microbiota level, with higher percentages of proinflammatory taxons, especially in the *Proteobacteria* phylum, which was not observed in the no-CRC rats (**Table 3**). This dysbiosis ismore extreme in the FP cohort (**Fig. 7**), where more animals' deaths took place, and also it took place during the first DSS challenge. However, dysbiosis in the FMP cohort is less accentuated and these animals' deaths took place closer to the last experimental weeks. DSS challenges are helpful for induction of a stronger CRC phenotype due to its ability to cause ulcerative colitis as pro-inflammatory trigger of CRC. This ulcerative colitis increases the intestinal permeability, enhancing the transfer of bacterial cells from lumen to intestinal submucosa tissue, inducing a proinflammatory status; and in FP and FMP animals this higher permeability is probably increasing the presence in intestinal submucosa of highly pro-inflammatory taxons (such as *E. coli*) (**Tables 5, S1, Fig. 6**). Remarkably, those rats fed with either pectin or modified citrus pectin but that were also kept free of CRC induction did not exhibit any increase in proinflammatory taxons. In a mouse model, virulent *E. coli* was accumulated after antibiotic treatment and can disseminate systematically when the intestinal epithelial barrier is breached by DSS, thereby inducing lethal inflammasome activation (Ayres *et al.*, 2012). In a similar way, DSS induced intestinal inflammation markedly increased the proliferation of *Citrobacter rodentium* in the intestine (Kamada *et al.*, 2012). Thus, the reduced barrier function, as could be taking place in our study, would enable more interaction with the epithelium, resulting in an increased delivery of mutagenic and/or proinflammatory metabolites produced by *Enterobacteriaceae* (Arthur *et al.*, 2012; Secher *et al.*, 2013).

To assess the effect of the pectin diets on CRC, histological parameters such as caecum weight, number of hyperplastic Peyer's patches, number of colon tumors, and total tumor area in the colon mucosa were measured.

Caecum weight was significantly increased in individuals from FP cohort, and, to a lesser extent, in the FMP animals (**Fig. 2**). This effect could be ascribed to a higher stimulation of bacterial cell growth (Fernández *et al.*, 2019) in the case of pectin. However, the most

plausible cause may be the physicochemical properties of pectin, such as the high viscosity, water retention capacity and bulking properties, which are higher in pectin in comparison with MCP (Christiaens *et al.*, 2016).

Concerning hyperplastic Peyer's patches, no statistically significant differences were found between all three cohorts (**Fig. 3**). Peyer's patches are abundant in lymphocytes and become hyperplastic when alterations in the digestive tract, which affect the animal's immune condition, take place, as may occur in response to some chemicals, pathogens or toxins (Bailey *et al.*, 2001; Mishra *et al.*, 2014). This parameter has been used as a marker of the general pro-inflammatory condition of the small intestine mucosa in all individuals in response to the CRC induction treatment (Fernández *et al.*, 2019; Jung *et al.*, 2010).

However, in our case, the absence of significant differences revealed that pectin does not affect the presence of these mucosal structures in the experimental model used.

Regarding the last histological parameters measured, number of colon tumors and the total tumor area in the colon mucosa (**Fig. 4**), any significant difference between all cohorts were found.

The limited available *in vivo* information on the effect of citrus pectin on CRC and the contradictory results makes it difficult to elucidate the mechanism of action of these substrates, where most studies have been carried out in *in vitro* assays (Ai *et al.*, 2018; Cheng *et al.*, 2011; Zhang *et al.*, 2015). However, there are *in vivo* reports that do not support the chemopreventive effect of these pectins in line with our work. Jacobs *et al.* (1986) reported that different fiber such as oat bran, guar and citrus pectin could increase by 4.5 to 5 times the yield of proximal colonic adenocarcinomas, providing stimulus to cell proliferation in a 1,2-dimethylhydrazine (DMH) colonic cancer model in rats. These authors attributed that a reduction in colonic luminal pH, similar to the observed in our work ($\geqslant$0.3), while not providing any protection, may even enhance colon tumorigenesis. In addition, Jacobasch *et al.* (2008) found that citrus pectins (with high

and low methylation degree, 70% and 37%, respectively) did not inhibit tumorigenesis regardless their DM in APC Min/+ mice. Moreover, those pectins seemed even to accelerate CRC carcinogenesis since all polyps found in pectin-fed animals were large adenocarcinomas whereas only 80% in control diet mice were large adenocarcinomas. As basic requirements for colorectal anticarcinogenic effect can be a sufficient high fermentative butyrate production and an adequate butyrate absorption. These authors attributed this behavior to an insufficient butyrate supply, since fermentation of pectin delivered only low amounts of butyrate. This might lead to a deficient energy metabolism and an ineffective function of butyrate as a promoter of normal cell differentiation and inducer of apoptosis in tumor cells, which could also explain the obtained results in the present study.

Thus, changes in the luminal pH may affect the uptake of luminal compounds by colonocytes and their action on these cells; increasing tumorigenesis as observed in our results (Blachier *et al.*, 2017). Decreases in the pH could increase hydrogen sulphide concentrations (pKa = 7.04) (Blachier *et al.*, 2010), which easily penetrates the biological membrane amplifying its deleterious and pro-inflammatory effect on colonocytes respiration at excessive concentration (Mimoun *et al.*, 2012). Moreover, modification of the luminal pH *per se* may affect colonic epithelial cell physiology where lower colonic luminal pH in patients with ulcerative colitis has been observed as compared to healthy patients (Nugent *et al.*, 2001). Low external pH has been shown to dramatically increase the expression of p-glycoproteins, related with multidrug resistance, in human colon carcinoma cell lines (Wei & Roepe, 1994), rendering these cells more resistant to chemotherapeutic agents.

Interestingly, an evaluation of the abilities to prevent colorectal cancer of different dietary fiber in an AOM rat model showed that pectin from green cincau (*Premna oblongifolia* Merr.) was able to increase butyrate levels, however, no antiproliferative properties were observed (Nurdin *et al.*, 2018). Despite the SCFA stimulation, feeding with pectin led to an increase in proliferation within the colon and an increase in

preneoplastic lesions, thus, appeared to be acting more like a pro-carcinogen. These authors maintained that it was possible that more pectin (>5%) needed to be consumed by rats to act as a protective, which was not confirmed in our work (20%), or that pectin may need to be delivered with other nutrients or fiber source to be protective in AOM/DSS models as observed in other studies (Cho *et al.*, 2012; Odun-Ayo *et al.*, 2015).

Analyses of organic acids showed important differences in acetate levels, as well in lactic acid amounts (**Fig. 5A and B**). Acetate has been previously reported as the main SCFA from pectin structures fermentation (Gómez *et al.*, 2016). The high presence of this metabolite can be justified due to that acetate is generated by many bacterial groups that inhabit the colon, with approximately one-third of the product coming from reductive acetogenesis (Fernández *et al.*, 2016; Miller & Wolin, 1996). Absence of propionic and butyric acids in our study is in line with the no protective effect against tumorigenesis observed, since the presence of these metabolites have been widely correlated with the inhibition of growth of different CRC lines, induction of apoptosis of tumor cells and enhancement of anti-inflammatory properties (Louis *et al.*, 2014; Zeng, 2014; W. Zhang *et al.*, 2015), whereas low levels of these metabolites can increase the risks of CRC and inflammatory gut diseases (Jacobasch *et al.*, 2008; Topping & Clifton, 2001; Wächtershäuser & Stein, 2000). Moreover, in line with our results, elevated concentrations of luminal lactic acid have been reported in active colitis and CRC cases (Hove & Mortensen, 1995; Uga *et al.*, 2019), a factor that could explain again that more animals died in our study during DSS challenges.

Analysis of microbiota of survival animals at phylum level showed significant differences between FP cohort versus F and FMP cohorts (**Table 3**). The *Firmicutes/Bacteroidetes* coefficient, which has been described as a parameter associated with obesity and type II diabetes (De Filippo *et al.*, 2010; Ley *et al.*, 2006), was reduced in FP (0.78) when compared to F and FMP cohorts (1.75 and 1.76,

respectively), due to the increase in *Bacteroidetes* and diminution in *Firmicutes*, supporting the hypoglycemic effect of high M_w citrus pectin.

Higher *Bacteroidetes* population in FP was mainly produced due to the significant increase in *Prevotellaceae* family (**Fig. 6, Table 4**). Species within genera *Bacteroides* and *Prevotella* are the primary pectin-degraders, possessing carbohydrate-active enzymes (CAZymes) within the polysaccharide utilization loci (Flint, Scott, Duncan, *et al.*, 2012; Larsen *et al.*, 2019; Martens *et al.*, 2011). However, the decrease in families, such as *Porphyromonadaceae*, observed in FP cohort might contribute to the absence of propionate production since these families contain numerous genera involved in propionate production (Louis *et al.*, 2014). The marked reduction in *Firmicutes* phylum was mainly produced by the decrease of the *Ruminococcaceae, Clostridiaceae* and *Eubacteriaceae* families, as it was observed in previous *in vitro* studies with pectin (Ferreira-Lazarte *et al.*, 2018; Ferreira-Lazarte, Moreno, *et al.*, 2019). The reduction observed in *Faecalibacterium* genus (especially *F. prausnitzii, Ruminococcaceae* family) could also contribute to the low anticarcinogenic properties observed in pectins cohorts, since its presence has been related with anti-inflammatory properties and it is described as a key bacteria species in promoting health (Ferreira-Lazarte, Moreno, *et al.*, 2019; Miquel *et al.*, 2013).

Strikingly, a massive increase in *Proteobacteria* phylum was also observed in FP cohort due to the increase in *Enterobacteriaceae* family (13.04%) (**Fig. 6**). This family did not show any increase in a previous *in vitro* study with the same pectin (Ferreira-Lazarte, Moreno, *et al.*, 2019). Higher *Proteobacteria* populations and, particularly, *Enterobacteriaceae* family (including *E. coli*) are found in the gut microbiota of patients with IBD, which is a known risk factor for CRC (Mukhopadhya *et al.*, 2012). In this sense, generally recognized pathogenic species, such as *E. coli, Salmonella* and *Serratia* increased in FP cohort compared to F cohort. This dysbiotic status has been correlated with various immune, metabolic and neurological disorders, in both intestinal and extra-intestinal sites (Donaldson *et al.*, 2016). As a consequence, susceptibility to enteric

infection can be markedly increased. *Salmonella enterica* for example, poorly colonize the mouse intestine in the presence of commensal microbiota, however, it can proliferate and induce inflammation if the resident bacterial community is disrupted (Endt *et al.*, 2010). Thus, the presence of inflammation or an altered bacterial community facilitates the overgrowth of potentially harmful bacteria by decreasing the production of protective mucins and antimicrobial peptides.

In contrast, certain beneficial effect can also be identified when pectin is present such as the reduction of *Desulfovibrionaceae* family (*Proteobacteria* phylum), whose high levels have been associated with damages at the mucosal level caused by reduction of the mucin barrier (Song *et al.*, 2018).

High levels of *Prevotellaceae* family, as observed in our study in the FP cohort (25.42%) (**Table 4**), have also been associated in some studies with a healthier status (Ferrario *et al.*, 2017; Flemer *et al.*, 2018). In this study, it has been also observed a significant increase in *Bifidobacteriaceae* family (*Actinobacteria* phylum) in both FP and FMP cohorts, mainly due to the increase of *Bifidobacterium*; as well as in *Lactobacillaceae* family (*Lactobacillus* genus, *Firmicutes* phylum). Both families have been associated to several health benefits (Donaldson *et al.*, 2016; Flint, Scott, Louis, *et al.*, 2012; Guinane & Cotter, 2013).

Conclusions

No previous studies have been carried out on the evaluation of the potential anticarcinogenic properties of citrus pectin and modified citrus pectin in *in vivo* models based on the use of azoxymethane/dextran sodium sulfate (AOM/DSS) to induce colorectal cancer in rats. Neither citrus pectin nor modified citrus pectin tested were able to inhibit tumorigenesis in this rat model. Of special relevance is the effect found in the intestinal microbiota. Strikingly, both pectins, particularly citrus pectin, seemed to induce a decrease of luminal pH of caecum and a huge dysbiosis degree in the CRC rats at the intestinal microbiota level, leading towards a potential proinflammatory status,

even causing the death of five and four animals (of a total of eight) in pectin and modified pectin cohorts, respectively. Thus, a high increase in *Proteobacteria* (proinflammatory bacteria) and a reduction in *Faecalibacterium* genus were observed mainly in the former. These results were in line with the absence of butyric and propionic acids and the levels of lactic and acetic acid. On the other hand, citrus pectin demonstrated an important impact in the decrease of glucose and triacylglycerides in plasma, probably related to the lower feeding and body weight as compared to modified citrus pectin and universal feed cohorts. These results agree to the low *Bacteroidetes/Firmicutes* ratio. Citrus pectin and modified citrus pectin also demonstrated to stimulate the growth of other positive bacteria such as *Prevotellaceae, Bifidobacteriaceae* and *Lactobacillaceae* families. Summing up, the consumption of pectin such as citrus pectin and modified citrus pectin could not be beneficial in an inflammatory-tumour status due to an important worsening of the pathology related to a severe unbalance of the intestinal microbiota. However, in a status of health, these pectins have relevant benefits not only in the gut but also at systemic level. Although the results obtained under the conditions assayed in this investigation seems to indicate the ineffectiveness of commercial citrus pectin and modified citrus pectin to exert a benefit in the prevention of CRC, more research is needed with other animal models in order to understand the intricate behavior of this polysaccharide in this severe pathology.

Acknowledgements

Authors acknowledge the finance of this work by the Spanish Ministry of Economy, Industry and Competitiveness (Projects AGL2017- 84614-C2-1-R and AGL2014-53445-R) and to the *Programa de Ayudas a Grupos de Investigación del Principado de Asturias* (IDI/2018/000120, Spain). Authors wish to thank Servicios Científico Técnicos from the University of Oviedo (Environmental Assays Unit, Sequencing Unit) and Biostatistical Unit from ISPA (Spain).

BLOQUE III

OBTENCIÓN Y CARACTERIZACIÓN DE NUEVOS CARBOHIDRATOS POTENCIALMENTE PREBIÓTICOS DERIVADOS DE LA TREHALOSA

PREFACIO III

Tal y como se ha mostrado en la Introducción General, otra de las principales tendencias en el campo de los prebióticos es la búsqueda de nuevas estructuras de carbohidratos con propiedades sobre la microbiota intestinal y, además, con actuación a nivel sistémico. En este contexto, la obtención de derivados de la trehalosa podría suponer un avance, no sólo por su potencial efecto prebiótico basado en la existencia de enlaces glicosídicos resistentes a la digestión intestinal, sino también por su efecto en determinadas patologías infecciosas y crónicas. Por ello, en el *Capítulo 5* se planteó la síntesis de nuevos carbohidratos derivados de la trehalosa mediante transgalactosilación, empleando lactosa como donante, trehalosa como aceptor y *β*-galactosidasas de diferentes fuentes microbianas, como catalizadores. La estructura de los oligosacáridos obtenidos se ha elucidado por técnicas cromatográficas, espectrométricas y espectroscópicas.

Capítulo 5

Enzymatic synthesis and structural characterization of novel trehalose-based oligosaccharides

Pablo Gallego-Lobillo[a], Elisa G. Doyagüez[b], María Luisa Jimeno[b], Mar Villamiel[a], Oswaldo Hernández-Hernández[a]

[a] Instituto de Investigación en Ciencias de la Alimentación, CIAL (CSIC-UAM). C/Nicolás Cabrera, 9, Campus de la Universidad Autónoma de Madrid, 28049, Madrid, España

[b] Centro de Química Orgánica "Lora Tamayo" (CSIC), c/Juan de la Cierva, 3, 28006, Madrid, España

Reproducido a partir de ACS Publications
Journal of Agricultural and Food Chemistry
2021, 69, 42, 12541–12553
DOI: https://doi.org/10.1021/acs.jafc.1c03768

Abstract

Trehalose, α-D-glucopyranosyl-(1↔1)-α-D-glucopyranoside, is a disaccharide with multiple effects on the human body. Synthesis of new trehalose derivatives was investigated through transgalactosylation reactions using β-galactosidase from four different species. β-galactosidases from *Bacillus circulans* and *Aspergillus oryzae* were observed to be the best biocatalysts, using lactose as donor and trehalose as the acceptor. Galactosyl-derivatives of trehalose were characterized using Nuclear Magnetic Resonance Spectroscopy. Trisaccharides were the most abundant oligosaccharides obtained, followed by the tetrasaccharide fraction (19.5% *vs* 8.2% carbohydrates). Interestingly, the pentasaccharide [β-Gal*p*-(1→4)]^3-Trehalose was characterized for the first time. Greater oligosaccharide production was observed using β-galactosidase from *B. circulans* than those obtained from *A. oryzae*, where the main structures were based on galactose monomers linked by β(1→6) and β(1→4) bonds with trehalose in the ending. These results indicate the feasibility of commercially available β-galactosidases for the synthesis of trehalose-derived oligosaccharides, which might have functional properties, excluding the adverse effects of the single trehalose.

Introduction

Trehalose, α-D-glucopyranosyl-(1↔1)-α-D-glucopyranoside, is a nonreducing disaccharide with a wide range of applications as a food additive as well as in cosmetics and pharmaceutical sciences (Acuña-Rodríguez *et al.*, 2020; Garcia & Gardner, 2021). Trehalose can be found in multiple sources such as invertebrates, fungi, and bacteria, holding a protective function against dryness and stress (Garcia & Gardner, 2021; Mijailovic *et al.*, 2021). This disaccharide was generally recognized as safe (GRAS) in 2000 by the Food & Drug Administration (FDA, USA), with an equivalent sweetness of 45% sucrose and being mainly used in the food industry as a sweetener, stabilizer, and moisturizer (Sokołowska *et al.*, 2021). In this context, it is important to emphasize its high stability in terms of temperature and pH. In addition, its α-bond is not hydrolyzed by the pancreatic α-amylase, and it has considerable resistance to acids (Khalifeh *et al.*, 2021; Peng *et al.*, 2017).

Multiple functionalities of trehalose such as a decrease in the postprandial glucose level (Yaribeygi *et al.*, 2019; Yoshizane *et al.*, 2017), improvement of the insulin resistance (Arai *et al.*, 2010; Yoshizane *et al.*, 2017), prevention of adipocyte hypertrophy (Arai *et al.*, 2010, 2013), suppression of bone resorption (Nishizaki *et al.*, 2000), and induction of autophagy (DeBosch *et al.*, 2016) have been reported. Regarding the latter, it is of paramount importance in the case of neurodegenerative and metabolic diseases. Autophagy is a conserved degradation mechanism of the cell, which can be regulated by trehalose, due to the chemical chaperone properties (Hosseinpour-Moghaddam *et al.*, 2018; Khalifeh *et al.*, 2021). This fact opens a new field in the development of some rare diseases, such as Huntington's and Parkinson's diseases (Emanuele, 2014; Khalifeh *et al.*, 2019, 2020). Furthermore, the latest studies have found promising results of trehalose in amyotrophic lateral sclerosis (ALS) (Massenzio *et al.*, 2018). All these beneficial properties occur in response to its absorption in the small intestine and then the transport to the target organs through the bloodstream (Emanuele, 2014; Khalifeh *et al.*, 2021).

Enzymatic complexes of disaccharidases are placed in the brush border membranes of the enterocytes, including the enzyme trehalase, which hydrolyzes the trehalose into two molecules of glucose (Hooton *et al.*, 2015). The content of trehalase in the small intestine is lower than other small-intestinal disaccharidases (Kluch *et al.*, 2020), and a considerable amount of the disaccharide (~75 g) is necessary to observe a real benefit in the organism (Higashiyama, 2002; Tan *et al.*, 2020). Then, a substantial quantity of the saccharide might not be hydrolyzed or absorbed in the small intestine, and therefore, it would reach the colon. This fact could become a drawback, especially due to the feeding of some species of pathogenic microorganisms, which can be present in the gut, such as *Clostridium difficile* (*C. difficile*). Recent findings have shown the development of genetic mechanisms by *C. difficile* species to metabolize trehalose (Collins *et al.*, 2018; Halstead *et al.*, 2019). It has been observed that these bacteria could increase significantly the risk of death when they were fed with trehalose, causing strong diarrhea (Cao *et al.*, 2019). Trehalose does not induce bacterial growth; nevertheless, it seems to increase the production of toxins that could exacerbate the infection (Collins *et al.*, 2018). Synthesis of trehalose derivatives might be a solution to reduce the adverse effects of this carbohydrate. These derivatives would suppose a change in the chemical structure of the classic trehalose; therefore, their behavior in the human body wouldbe different. In addition, these new compounds might have new beneficial properties.

Concerning the synthesis processes of new oligosaccharides, enzymatic procedures, such as the use of *β*-galactosidases (*β*-gal), are proven to be reliable, cost-effective, and environmentally friendly. *β*-Gal of *Escherichia coli* (*E. coli*) were used to produce trisaccharides from trehalose through transgalactosylation, obtaining structures such as *β*-Gal*p*-(1→4)-trehalose and *β*-Gal*p*-(1→6)-trehalose (Kim *et al.*, 2007). In previous works, *β*-gal activities from different microorganisms have shown an excellent ability to form lactose derivatives such as galactooligosaccharides (*β*-GOS) (Cardelle-Cobas *et al.*, 2008; C. W. Chen *et al.*, 2003; Hérnandez-Hérnandez, 2012; Martínez-Villaluenga, Cardelle-Cobas, Olano, *et al.*, 2008); however, to the best of our knowledge, few studies with trehalose as an acceptor have been carried out so far. A straightforward process of

synthesis may permit the obtainment of new bioactive molecules from trehalose, avoiding the negative effects by *C. difficile*. Therefore, the aim of this work was to study the usefulness of four commercial *β*-gal to synthesize new oligosaccharides derived from trehalose, through transgalactosylation reactions. Different sources of the enzymes have been tested: *Bacillus circulans* (*B. circulans*), *Aspergillus oryzae* (*A. oryzae*), *Bifidobacterium bifidum* (*B. bifidum*), and *Kluyveromyces lactis* (*K. lactis*). Syntheses were studied with lactose (as a galactosyl donor) and trehalose (as an acceptor). Trehalose derivatives were characterized by nuclear magnetic resonance spectroscopy (NMR spectroscopy).

Materials and methods

Chemicals and Standards

Standards of D-galactose (Gal), D-glucose (Glc), trehalose, lactose, raffinose, nystose, phenyl-*β*-D-glucoside, and activated charcoal were purchased from Sigma-Aldrich (St. Louis, MO, USA). Lactose was supplied by ACROS Organics (Geel, Belgium). HPLC-grade acetonitrile and ethanol (96%) were obtained from VWR (Barcelona, Spain). All reagents were of analytical grade (purity of > 95%). Standard GOS (3′-galactosyllactose, 4′-galactosyllactose, 6′-galactosyllactose, 3′-galactobiose, 4′-galactobiose, and 6′-galactobiose) were purchased from Biosynth Carbosynth (Reading, UK).

Commercial Enzyme Preparations

Four commercial *β*-gal preparations were evaluated in this work: Lactozym® Pure 6500 L [*Kluyveromyces lactis* (6500 U/g)] and Saphera® 2600 L [*Bifidobacterium bifidum* (2600 U/g)] were kindly provided by Novozymes A/S (Bagsvaerd, Denmark), Biolactase® [*Bacillus circulans* (1500 U/g)] was supplied by Biocon (Barcelona, Spain), and *β*-gal from *Aspergillus oryzae* (111,000 U/g) was provided by Sigma-Aldrich (St. Louis, MO, USA).

Enzymatic Synthesis of Trehalose Derivatives

Enzymatic synthesis with *K. lactis* and *B. bifidum* β-gal was performed in 50 mM sodium phosphate buffer with 2 mM $MgCl_2$ at pH 6.5. *A. oryzae* and *B. circulans* β-gal assays were carried out in 50 mM sodium acetate buffer at pH 4.5. The enzymatic activity used for the four enzymes was 15 U/mL.

Transgalactosylation reactions were carried out in an orbital Thermomixer comfort (Eppendorf) at 50 °C and 750 rpm using trehalose (25%, w/v), as an acceptor, and lactose (25%, w/v), as a donor. Reactions were incubated during 24 h, taking aliquots at 0, 2, 4, 6, and 24 h. Assays were stopped by heating in boiling water for 5 min. In all cases, reaction blanks using only lactose were performed under the same conditions. Transgalactosylation reactions were monitored through gas chromatography coupled to a flame ionization detector (GC-FID), as described below. After GC-FID analysis, β-gal from *K. lactis* and *B. bifidum* did not show any formation of new trehalose derivatives. For this reason, analysis, isolation, and characterization were carried out using *A. oryzae* and *B. circulans* β-gal.

Analysis of the Carbohydrate Content by Gas Chromatography (GC-FID)

Samples were derivatized to their corresponding trimethyl silylated oximes (TMSOs) according to Brobst and Lott (1966). Analysis was performed in an Agilent Technologies 7820A gas chromatograph system. Separation of the samples was carried out in a fused silica capillary column DB-5HT (5% phenyl methylpolysiloxane, 30 m × 0.25 mm × 0.1 µm) (Agilent J&W Scientific, Folsom, CA, USA). The oven temperature started at 150 °C and then increased to 380 °C at a rate of 3 °C/min. Injector and detector temperatures were 280 and 385 °C, respectively. Samples were analyzed in split mode 1:20 using nitrogen as the carrier gas at a 1 mL/min flow rate.

Data quantification was calculated through the internal standard method (phenyl-β-D-glucopyranoside, 0.5 mg/mL) and the corresponding response factors of standard

solutions of carbohydrates (galactose, glucose, trehalose, lactose, raffinose, and nystose) at known concentrations (0.005-1 mg/mL). All analyses were carried out in triplicate.

Purification and Isolation of Trehalose Derivatives

Activated Charcoal Treatment

With the objective to remove monosaccharides and concentrate the oligosaccharide fraction, synthesized samples after 6 (*A. oryzae*) and 24 h (*B. circulans*) were purified using activated charcoal according to Hernández-Hernández *et al.* (2009). First, 10 mL of the mixture of the reaction was mixed with 60 g of activated charcoal and 1 L of ethanol solution (5%, v/v). This solution was incubated for 30 min at 25 °C under continuous agitation. Then, it was filtered through Whatman No.1 paper. The desorption of oligosaccharides was carried out by mixing the activated charcoal with ethanolic solution (50%, v/v) during 30 min and filtering, and then, the ethanolic solution was evaporated for subsequent isolation.

Isolation by Semi-Preparative Chromatography

Trehalose-derived oligosaccharides were isolated by hydrophilic interaction liquid chromatography equipped with a refractive index detector (HILIC-RID), following the method of Julio-González *et al.* (2020) Sample separation was carried out by a semi-preparative ZORBAX NH2 column (PrepHT cartridge 250 × 21.2 mm, 7 µm particle size) (Agilent), using acetonitrile/water (70:30, v/v) as a mobile phase, at a flow rate of 21 mL/min for 45 min at 25 °C. Two milliliters was repeatedly injected. The main synthesized compounds were collected, evaporated, and freeze-dried for characterization by NMR and GC-MS.

Structural Characterization of Trehalose Derivatives

Gas Chromatography-Mass Spectrometry (GC-MS)

Trehalose-derived oligosaccharides were also studied by GC-MS. Analysis was performed by a fused silica capillary column DB-5HT (5% phenyl methylpolysiloxane; 30 m × 0.25 mm × 0.10 μm) (Agilent) in a 6890 gas chromatograph system coupled to a 5973 quadrupole mass detector (Agilent). Helium was used as the carrier gas at a flow of 0.8 mL/min. The oven temperature program was 150 °C, increased to 300 °C at 3 °C/min, and maintained for 10 min. Injections were done in split mode (1:20). Electron impact (EI) mode was used at 70 eV in the mass spectrometer, considering a range of 35-700 m/z. Interface and source temperatures were 280 and 230 °C, respectively.

Identification of known structures of GOS was done by comparison of standard solutions and their respective mass spectra.

Nuclear Magnetic Resonance Spectroscopy (NMR Spectroscopy)

Structure elucidation of the purified fractions was accomplished by nuclear magnetic resonance spectroscopy (NMR spectroscopy). NMR spectra were recorded at 298 K, using D_2O as a solvent, on an Agilent system 500 NMR spectrometer (^1H 500 MHz, ^{13}C 125 MHz) equipped with a 5 mm HCN cold probe. Chemical shifts of ^1H (δ_H) and ^{13}C (δ_C) in parts per million were determined relative to internal standards of sodium [2,2,3,3-$^2H_4$]-3-(trimethylsilyl)- propanoate in D_2O (δ_H 0.00) and 1,4-dioxane (δ_C 67.40) in D_2O, respectively. One-dimensional (1D) NMR experiments (^1H and $^{13}C\{^1H\}$) were performed using standard pulse sequences. Twodimensional (2D) [^1H, ^1H] NMR experiments [gradient correlation spectroscopy (gCOSY), total correlation spectroscopy (TOCSY), and rotating-frame Overhauser effect spectroscopy (ROESY)] were carried out with the following parameters: a delay time of 1 s, a spectral width of 2800 Hz in both dimensions, 2048 complex points in t2, 4 transients (24 or 32 for ROESY) for each of 128 (200 for TOCSY and ROESY) time increments, and linear prediction to 512. The mixing time used for ROESY was 0.3 ms. The data were zerofilled to 2048 × 2048 real

points. 2D [$^{1}H–^{13}C$] NMR experiments [gradient heteronuclear single-quantum coherence (gHSQC), hybrid experiment gHSQC-TOCSY, and selective 2D bsgHMBC (Gaillet *et al.*, 1999) used the same 1H spectral window, a ^{13}C spectral window of 7541.5 Hz, 1 s relaxation delay, 1024 data points, and 128 or 200 time increments, with a linear prediction to 256. The data were zero-filled to 2048 × 2048 real points. Typical numbers of transients per increment were 4 and 16. A mixing time of 80 ms was used for gHSQC-TOCSY experiments.

Results and discussion

Transgalactosylation of Trehalose by *β*-Galactosidase from *Bacillus circulans*

The reaction conditions are different from those most commonly used for *Bacillus circulans* *β*-gal due to the major presence of the *β*-gal isoforms II and III in the Biolactase® NTL Conc. **Figure 1** shows the chromatographic GC-FID profile during the transgalactosylation assay after 24 h of reaction using lactose and trehalose and only lactose. In the first instance, a considerable amount of monosaccharides (peaks 1 and 2) was observed in the chromatogram due to the hydrolytic activity of the *β*-gal. Moreover, the transgalactosylation reaction was also observed (**Figure 1A-D**).

In the lactose assays, di- and trisaccharide *β*-GOS fractions (**Figure 1A,B**, red) were obtained and identified by GC-MS profiles (peaks 6-8, 10, and 11). These structures are known, as they were obtained by reactions with *β*-gal of different sources (Cardelle-Cobas *et al.*, 2008; Gänzle, 2012). On the other hand, new oligosaccharides were synthesized using trehalose as a carbohydrate acceptor (**Figure 1**, blue). These compounds correspond to galactosylated trehalose (**Figure 1B**, peaks 9 and 12; **Figure 1C**, peaks 13, 14, 15, 16, and 17). Interestingly, although there was a low quantity, the pentasaccharide fraction was also observed in the chromatogram (**Figure 1D**, peak 18).

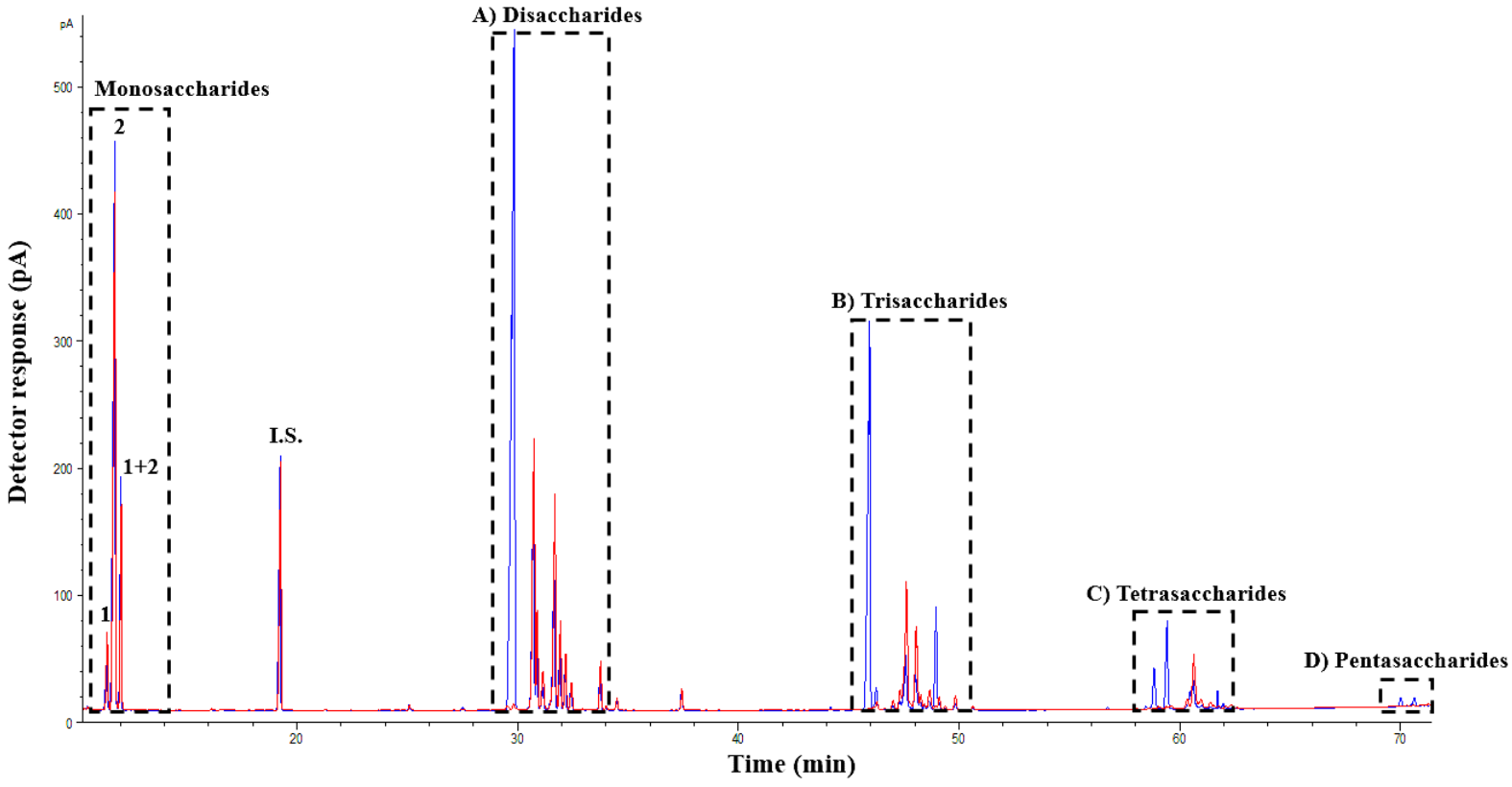
pA
500
400
300
200
100
0
Detector response (pA)
Monosaccharides
2
1+2
1
I.S.
A) Disaccharides
B) Trisaccharides
C) Tetrasaccharides
D) Pentasaccharides
20
30
40
50
60
70
Time (min)

Figure 1

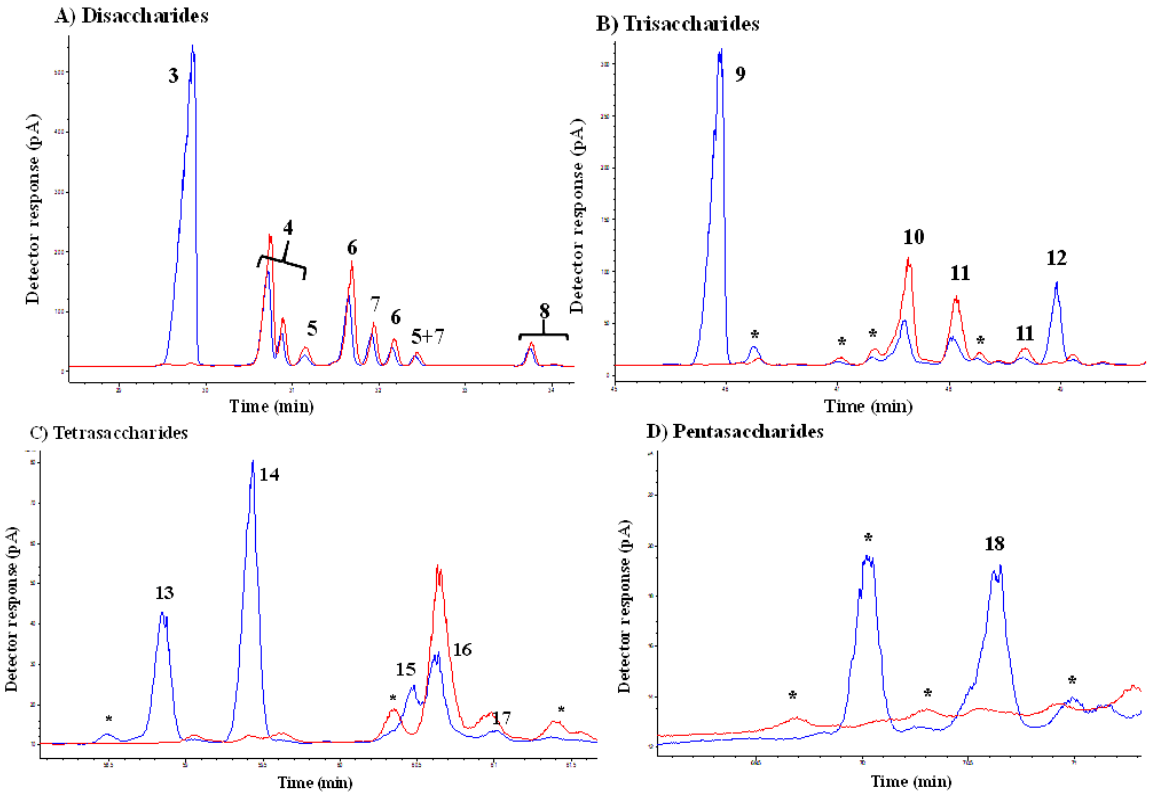

Figure 1. Chromatographic profiles obtained by GC-FID of TMSO derivatives of the transgalactosylation reaction after 24 h by *β*-galactosidase from *Bacillus circulans* using lactose/trehalose (blue) and lactose (red). Disaccharides (A), trisaccharides (B), tetrasaccharides (C) and pentasaccharides (D) fraction are shown for each reaction. Peaks: 1: Galactose, 2: Glucose, I.S.: Internal Standard, (A) 3: Trehalose, 4: Lactose, 5: *β*-D-galactopyranosyl-(1→4)-*β*-D-glucose, 6: *β*-D-galactopyranosyl-(1→3)-*β*-D-glucose , 7: *β*-D-galactopyranosyl-(1→2)-*β*-D-glucose, 8: *β*-D-galactopyranosyl-(1→6)-*β*-D-glucose, (B) 9: *β*-D-galactopyranosyl-(1→4)-D-trehalose, 10: *β*-D-galactopyranosyl-(1→4)-D-lactose, 11: *β*-D-galactopyranosyl-(1→6)-D-lactose, 12: *β*-D-galactopyranosyl-(1→6)-D-trehalose, (C) 13 and 15: *β*-D-galactopyranosyl-(1→4)-*β*-D-galactopyranosyl-(1→6)-D-trehalose or *β*-D-galactopyranosyl-(1→4)-*α*-D-glucopyranosyl-(1↔1)-[*β*-D-galactopyranosyl-(1→4)]-*α*-D-glucopyranoside, 14: *β*-D-galactopyranosyl-(1→4)-*β*-D-galactopyranosyl-(1→4)-D-trehalose, 16 and 17: *β*-D-galactopyranosyl-(1→4)-*α*-D-glucopyranosyl-(1↔1)-[*β*-D-galactopyranosyl-(1→6)]-*α*-D-glucopyranoside or *β*-D-galactopyranosyl-(1→6)-*α*-D-glucopyranosyl-(1↔1)-[*β*-D-galactopyranosyl-(1→6)]-*α*-D-glucopyranoside, (D) 18: *β*-D-galactopyranosyl-(1→4)-*β*-D-galactopyranosyl-(1→4)-*β*-D-galactopyranosyl-(1→4)-D-trehalose. *Other saccharides with unknown structures.

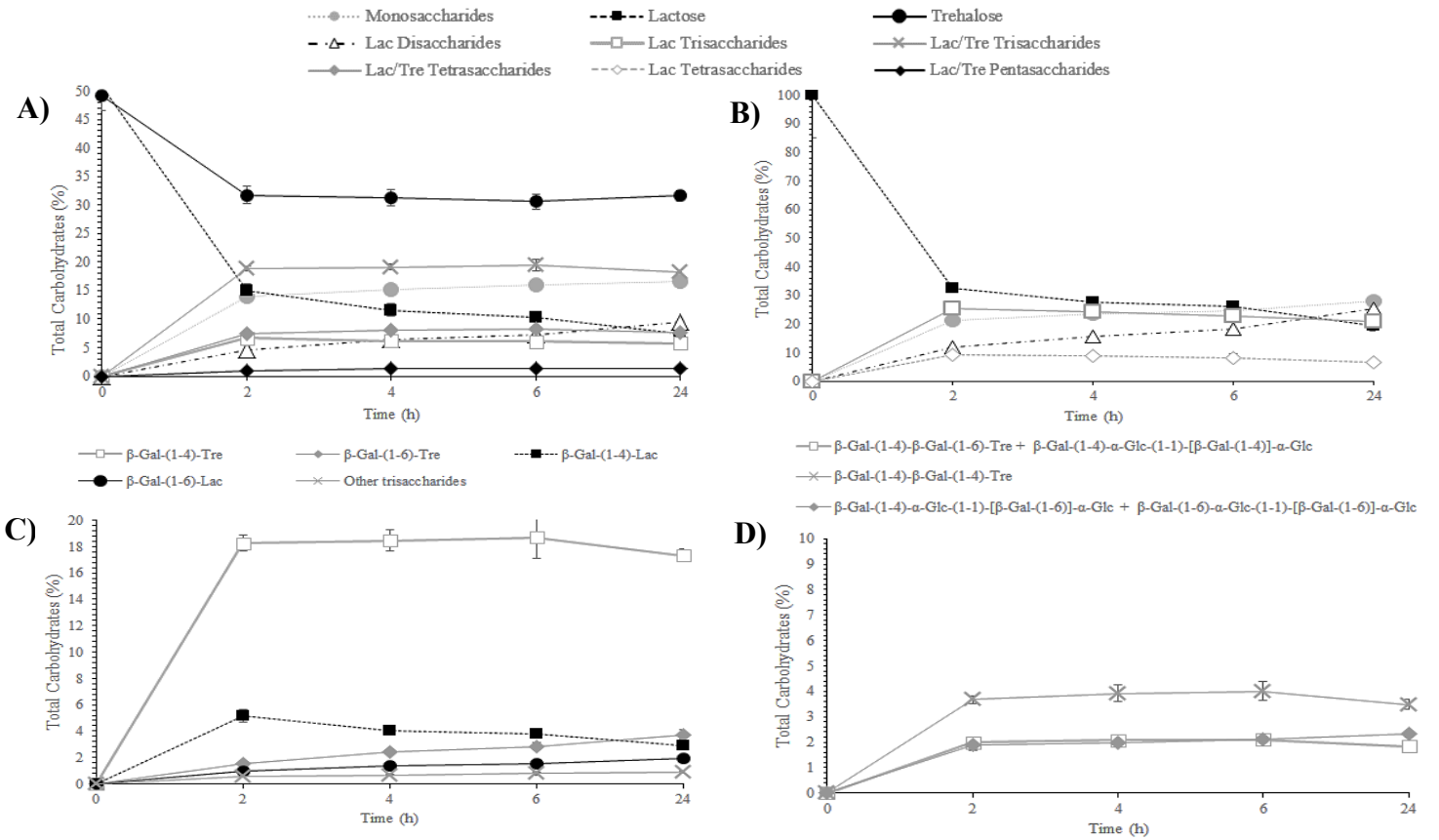

Figure 2. Evolution in the content of carbohydrates (%) during transgalactosylation reactions of lactose/trehalose (A) and lactose (B) solutions; and evolution of tri- (C) and tetrasaccharides (D) (%) of lactose/trehalose mixture. Reactions catalyzed by *β*-galactosidase from *Bacillus circulans* for 24 h at 50 ºC, pH 4.5.

The kinetic behavior of the reaction mixtures, lactose/trehalose and lactose, is indicated in **Figure 2A,B**, respectively; moreover, quantitative data are shown in **Table S1**. After 24 h, 85.3 (Lac/Tre, **Figure 2A**) and 80.8% (Lac, **Figure 2B**) lactose was hydrolyzed, whereas trehalose decreased by 35.8% (**Figure 2A**). Regarding disaccharide synthesis, only *β*-GOS disaccharides derived from lactose were observed in both reactions, being produced in a higher amount using the lactose only mixture (23.3%, **Figure 2B**).

Trisaccharides were the main oligosaccharides generated during the lactose/trehalose reaction, especially those derived from trehalose (19.5% after 6 h), in contrast to those derived using only lactose (6.1%) (**Figure 2A and Table S1**). This result indicates that trehalose is a better acceptor than lactose. Just tetrasaccharides from trehalose were identified in the lactose/trehalose reaction (8.2%). A similar situation occurred with pentasaccharides, which were only formed in the trehalose/lactose mixture (**Figure 2A**; 1.4% after 24 h). The maximum formation of the trehalose derivatives occurred between 6 and 24 h of the incubation time (**Figure 2A**). These data support the efficiency and the suitability of the *β*-gal to produce trehalose derivatives. *β*-GOS tri- and tetrasaccharide productions were 21.0 and 6.5% after 24 h, respectively, using lactose as the sole donor and acceptor (**Figure 2B**), which is in line with previously reported *β*-GOS production (Botvynko *et al.*, 2019; Martínez-Villaluenga, Cardelle-Cobas, Olano, *et al.*, 2008).

Tri-, tetra-, and pentasaccharide fractions were isolated by HILIC-RID and characterized by NMR. This characterization was accomplished by the combined use of 1D and 2D [^{1}H, ^{1}H] and [^{1}H, ^{13}C] NMR experiments (gCOSY, TOCSY, ROESY, multiplicity-edited gHSQC, bsgHMBC, and hybrid experiment gHSQC-TOCSY). ^{1}H and ^{13}C NMR chemical shifts were observed, and the structures of each compound are summarized and numbered in **Tables 1-4**. Full sets of spectra are available in the Supporting Information (**Figures S1-S43**).

Two compounds could be identified in the trisaccharide fraction (**Figure 1B**). Compound **1** (peak 12) was assigned as *β*-D-galactopyranosyl-(1→6)-*α*-D-glucopyranosyl-(1↔1)-*α*-D-glucopyranoside [*β*-D-galactopyranosyl-(1→6)-*α*,*α*-trehalose] (**Table 1**, compound

1). The 1D ^{1}H NMR spectrum of this compound (see Supporting Information, Figure S1) showed three doublets in the anomeric region (δ 5.19, $^{3}J_{H1,H2}$ = 3.8 Hz, δ 5.18, $^{3}J_{H1,H2}$ = 3.8 Hz and δ 4.43, $^{3}J_{H1,H2}$ = 8.1 Hz), corresponding to both *α*-glucoses and *β*-galactose, respectively. In addition, the 1D ^{13}C NMR spectrum showed signals corresponding to 18 carbons, including three anomeric carbons (δ 94.02, δ 93.97 and δ103.95). A multiplicity-edited gHSQC spectrum was used to link the carbon signals to the corresponding proton resonances. It showed three anomeric carbons, 12 CH, and three methylene carbons. In addition, COSY, TOCSY, and gHSQC-TOCSY experiments supported the presence of two *α*-glucose units and one *β*-galactose unit. The position of glycosidic linkages was analyzed from the bsgHMBC spectrum. It showed correlations between the two *α*-Glc anomeric positions, confirming the presence of a trehalose unit. In addition, relevant correlation bands between the *β*-Gal-3-C1 anomeric carbon and *α*-Glc-2-H6 and between the *α*-Glc-2-C6 methylene carbon and the *β*-Gal-3-H1 anomeric proton could be found. These results confirmed the proposed structure. This compound has been previously characterized through NMR by Ajisaka and Fujimoto (1990) and by Kim *et al.* (2007) Some differences in chemical shifts are found, but in the first case, acetonitrile was used as an internal reference in D_2O, and in the second one, DMSO-*d6* was used as a solvent, which could explain these little changes.

Regarding compound **2** (peak 9, **Figure 1B**), it was assigned as *β*-D-galactopyranosyl-(1→4)-*α*-D-glucopyranosyl-(1↔1)-*α*-D-glucopyranoside [*β*-D-galactopyranosyl-(1→4)-*α*,*α*-trehalose] (**Table 1**, compound **2**). 1D and 2D spectra were analyzed as in the previous case (**see Supporting Information, Figures S7-S11**), and they also supported the presence of two *α*-glucose units and one *β*-galactose unit. All ^{1}H and ^{13}C signals could be assigned (**Table 1**). The results confirmed the structure as *β*-D-galactopyranosyl-(1→4)-*α*-D-glucopyranosyl-(1↔1)-*α*-D-glucopyranoside, and they are in accordance with other data from Ishii *et al.* (2000).

Table 1. ^{1}H (500 MHz) and ^{13}C (125 MHz) NMR Chemical Shifts (δ, ppm) and Coupling Constants (*J* in Hz, in parentheses) Determined by 1D and 2D NMR Spectroscopy of Trisaccharides **1** and **2**.

		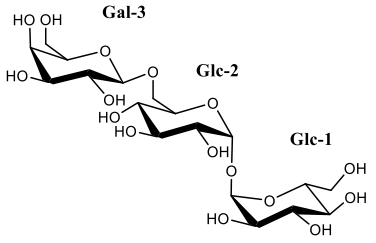 **1** *β*-D-Gal*p*-(1→6)-*α*-D-Glc*p*-(1↔1)-*α*-D-Glc*p*		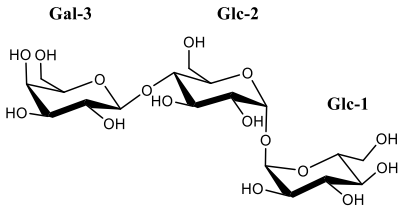 **2** *β*-D-Gal*p*-(1→4)-*α*-D-Glc*p*-(1↔1)-*α*-D-Glc*p*	
		δ_C	δ_H(*J*, Hz)	δ_C	δ_H(*J*, Hz)
α-Glc-1	1	94.02	5.19 (3.8)	94.07	5.186 (3.8)
	2	71.61	3.64	71.70	3.64
	3	73.13	3.84	73.17	3.84
	4	70.31	3.44	70.31	3.44
	5	72.83	3.80	72.82	3.83
	6	61.15	3.85, 3.76	61.15	3.84, 3.76
α-Glc-2	1	93.97	5.18 (3.8)	93.74	5.188 (3.8)
	2	71.66	3.65	71.38	3.70
	3	73.07	3.85	71.81	3.97
	4	69.97	3.58	79.08	3.69
	5	71.86	3.95	71.50	3.94
	6	68.74	4.17,3.88	60.49	3.89,3.85
Gal-3	1	103.95	4.43 (8.1)	103.57	4.46 (8.1)
	2	71.40	3.54	71.60	3.55
	3	73.34	3.65	73.15	3.66
	4	69.32	3.91	69.21	3.92
	5	75.81	3.69	76.02	3.73
	6	61.66	3.79,3.75	61.69	3.79, 3.75

In the case of tetrasaccharide fractions, we have been able to characterize two types of tetrasaccharides: two of them with a terminal trehalose in their structure (**Table 2**, compounds **3** and **4**) and three more where trehalose is situated in the center (**Table 3**, compounds **5, 6** and **7**).

Compound **3** (peak 14, **Figure 1C**) was assigned as *β*-D-galactopyranosyl-(1→4)-*β*-D-galactopyranosyl-(1→4)-*α*-D-glucopyranosyl-(1↔1)-*α*-D-glucopyranoside [*β*-D-galactopyranosyl-(1→4)-*β*-D-galactopyranosyl-(1→4)-*α*,*α*-trehalose] (**Table 2**, compound **3**). 1D ^{1}H NMR spectrum (**see Supporting Information, figure S12 and Table 2**) showed four doublets in the anomeric region (δ 5.17, $^{3}J_{H1,H2}$ = 3.7 Hz, δ 5.18, $^{3}J_{H1,H2}$ = 3.7 Hz, δ 4.48, $^{3}J_{H1,H2}$ = 7.8 Hz and δ 4.59, $^{3}J_{H1,H2}$ = 7.8 Hz), corresponding to both *α*-glucoses from trehalose units and two *β*-galactoses. The 1D ^{13}C NMR spectrum showed signals corresponding to 24 carbons, including four anomeric carbons (δ 94.04, δ 93.70, δ 103.53 and δ 104.84). 2D spectra also supported the presence of two *α*-glucose and two *β*-galactose units. The position of glycosidic linkages was analyzed from the bsgHMBC spectrum. It showed correlations between the two *α*-Glc anomeric positions, confirming the presence of a trehalose unit, and in addition, relevant correlations between the *β*-Gal-3-C1 anomeric carbon and *α*-Glc-2-H4 and between *α*-Glc-2-C4 and *β*-Gal-3-H1 anomeric protons were found. Moreover, key correlations between the *β*-Gal-4-C1 anomeric carbon and *β*-Gal-3-H4 and between *β*-Gal-3-C4 and *β*-Gal-4-H1 anomeric protons showed a (1→4) linkage between two galactose units, confirming the proposed structure.

Table 2. ^{1}H (500 MHz) and ^{13}C (125 MHz) NMR Chemical Shifts (δ , ppm) and Coupling Constants (*J* in Hz, in parentheses) Determined by 1D and 2D NMR Spectroscopy of Tetrasaccharides **3** and **4,** and Pentasaccharide **8**, with Terminal Trehalose.

		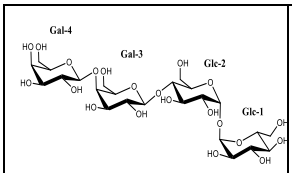 **3** *β*-D-Gal*p*-(1→4)-*β*-D-Gal*p*-(1→4)-*α*-D-Glc*p*-(1↔1)-*α*-D-Glc*p*		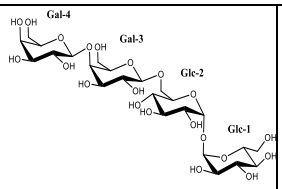 **4** *β*-D-Gal*p*-(1→4)-*β*-D-Gal*p*-(1→6)-*α*-D-Glc*p*-(1↔1)-*α*-D-Glc*p*		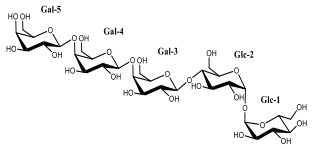 **8** *β*-D-Gal*p*-(1→4)-*β*-D-Gal*p*-(1→4)-*β*-D-Gal*p*-(1→4)-*α*-D-Glc*p*-(1↔1)-*α*-D-Glc*p*	
		δ_C	δ_H(*J*, Hz)	δ_C	δ_H(*J*, Hz)	δ_C	δ_H(*J*, Hz)
α-Glc-1	1	94.04	5.17 (3.7)	93.98	5.19 (3.7)	94.05	5.19 (3.7)
	2	71.69	3.63	71.66	3.64	71.70	3.65
	3	73.17	3.84	73.13	3.84	73.17	3.84
	4	70.31	3.43	70.30	3.44	70.31	3.45
	5	72.81	3.82	72.83	3.80	72.82	3.82
	6	61.14	3.85, 3.76	61.15	3.84, 3.75	61.14	3.84, 3.77
α-Glc-2	1	93.70	5.18 (3.7)	93.93	5.18 (3.7)	93.71	5.18 (3.7)
	2	71.33	3.68	71.61	3.62	71.35	3.68
	3	71.78	3.97	73.08	3.84	71.80	3.96
	4	79.14	3.67	70.06	3.54	79.17	3.68
	5	71.48	3.92	71.90	3.96	71.49	3.93
	6	60.44	3.88,3.85	68.87	4.15,3.87	60.47	3.90,3.85
Gal-3	1	103.53	4.48 (7.8)	103.88	4.46 (7.8)	103.57	4.49 (7.9)
	2	71.99	3.62	71.88	3.62	71.99	3.62
	3	73.58	3.77	73.75	3.75	73.67	3.77
	4	77.77	4.19	77.74	4.17	78.18	4.18
	5	75.16	3.75	74.93	3.72	75.25	3.76
	6	61.39	3.82, 3.80	61.19	3.83, 3.75	61.55	3.84, 3.77
Gal-4	1	104.84	4.59 (7.8)	104.89	4.58 (7.8)	104.90	4.65 (8.0)
	2	72.08	3.56	72.05	3.57	72.49	3.65
	3	73.45	3.66	73.40	3.65	73.93	3.77
	4	69.26	3.90	69.27	3.90	77.78	4.17
	5	75.77	3.67	75.76	3.67	75.09	3.71
	6	61.64	3.78, 3.75	61.65	3.78, 3.73	61.19	3.84, 3.77
Gal-5	1					104.95	4.59 (7.8)
	2					72.03	3.56
	3					73.41	3.65
	4					69.28	3.90
	5					75.77	3.68
	6					61.69	3.78, 3.75

Table 3. ^{1}H (500 MHz) and ^{13}C (125 MHz) NMR Chemical Shifts (δ , ppm) and Coupling Constants (J in Hz, in parentheses) Determined by 1D and 2D NMR Spectroscopy of Tetrasaccharides **5**, **6** and **7,** with Central Trehalose.

		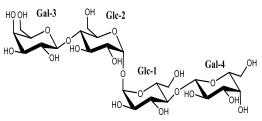 **5** *β*-D-Gal*p*-(1→4)-*α*-D-Glc*p*-(1↔1)-[*β*-D-Gal*p*-(1→4)]-*α*-D-Glc*p*		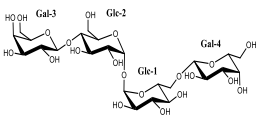 **6** *β*-D-Gal*p*-(1→4)-*α*-D-Glc*p*-(1↔1)-[*β*-D-Gal*p*-(1→6)]-*α*-D-Glc*p*		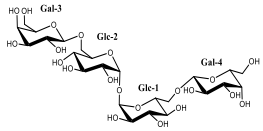 **7** *β*-D-Gal*p*-(1→6)-*α*-D-Glc*p*-(1↔1)-[*β*-D-Gal*p*-(1→6)]-*α*-D-Glc*p*	
		δ_C	δ_H(J, Hz)	δ_C	δ_H(J, Hz)	δ_C	δ_H(J, Hz)
α-Glc-1	1	93.93	5.18 (3.7)	94.17	5.19 (3.7)	94.13	5.19 (3.7)
	2	71.40	3.68	71.64	3.65	71.59	3.65
	3	71.82	3.96	73.09	3.84	73.05	3.84
	4	79.02	3.69	69.97	3.57	69.97	3.57
	5	71.53	3.94	71.89	3.96	71.92	3.96
	6	60.47	3.89,3.85	68.74	4.17, 3.88	68.74	4.17, 3.88
α-Glc-2	1	93.93	5.18 (3.7)	93.88	5.19 (3.7)	94.13	5.19 (3.7)
	2	71.40	3.68	71.35	3.70	71.59	3.65
	3	71.82	3.96	71.78	3.96	73.05	3.84
	4	79.02	3.69	79.05	3.68	69.97	3.57
	5	71.53	3.94	71.54	3.93	71.92	3.96
	6	60.47	3.89,3.85	60.47	3.90,3.85	68.74	4.17, 3.88
Gal-3	1	103.56	4.45 (7.8)	103.55	4.45 (7.9)	103.96	4.43 (7.9)
	2	71.59	3.54	71.59	3.54	71.40	3.54
	3	73.15	3.66	73.15	3.65	73.34	3.65
	4	69.21	3.92	69.20	3.92	69.32	3.92
	5	76.02	3.72	76.02	3.72	75.81	3.68
	6	61.70	3.78, 3.74	61.69	3.78, 3.73	61.66	3.78,3.73
Gal-4	1	103.56	4.45 (7.8)	103.95	4.43 (7.9)	103.96	4.43 (7.9)
	2	71.59	3.54	71.40	3.54	71.40	3.54
	3	73.15	3.66	73.34	3.65	73.34	3.65
	4	69.21	3.92	69.32	3.92	69.32	3.92
	5	76.02	3.72	75.81	3.69	75.81	3.68
	6	61.70	3.78, 3.74	61.66	3.78, 3.73	61.66	3.78,3.73

Compound **4** was obtained together with compound **5** by HILIC-RID, as a 1:1.5 mixture, but despite this, both compounds could be assigned by NMR unequivocally, differentiating signals of each one in the spectra (**see Supporting Information, Figures S18-S24**). Following the same procedure as before, compound **4** (peaks 13 and 15, **Figure 1C**) was assigned as *β*-D-galactopyranosyl-(1→4)-*β*-D-galactopyranosyl-(1→6)-*α*-D-glucopyranosyl-(1↔1)-*α*-D-glucopyranoside [*β*-D-galactopyranosyl-(1→4)-*β*-D-galactopyranosyl-(1→6)-*α*,*α*-trehalose] (**Table 2**, compound **4**). The position of glycosidic linkages was established, as in the previous case, with corresponding key correlations analyzed from bsgHMBC spectra. They showed a (1→4) linkage between the two galactose units, but in this case, the linkage between Gal-3 and the trehalose unit was (1→6).

As mentioned before, tetrasaccharides **5, 6** and **7** present a different structure, where the trehalose unit is situated in the center of the molecule. In these cases, every galactose unit is linked to a different glucose unit of the trehalose. Compound **5** (peaks 13 and 15, **Figure 1C**), assigned as *β*-D-galactopyranosyl-(1→4)-*α*-D-glucopyranosyl-(1↔1)-[*β*-D-galactopyranosyl-(1→4)]-*α*-D-glucopyranoside, is a symmetric compound, with a (1→4) linkage between every *β*-galactose and *α*-glucose (**Table 3**, compound 5). Due to its symmetry, chemical shifts are the same for both galactoses and for both glucoses in the molecule. It showed two doublets in the anomeric region (δ 5.18, $^{3}J_{H1,H2}$ = 3.7 Hz and δ 4.45, $^{3}J_{H1,H2}$ = 7.8 Hz), corresponding to both *α*-glucoses from the trehalose unit and two *β*-galactoses, respectively. The 1D ^{13}C NMR spectrum showed signals corresponding to 12 carbons (due to the symmetry of the molecule), including two anomeric carbons (δ 93.93 and δ 103.56). 2D spectra, together with ^{13}C chemical shifts and intensity of the signals (**see Supporting Information, Figures S19 and S21**), supported the presence of two *α*-glucose and two *β*-galactose units. The (1→4) linkage between every *β*-galactose and *α*-glucose was determined by the bsgHMBC spectrum showing correlations between the *β*-Gal-C1 anomeric carbons and *α*-Glc-H4 and between *α*-Glc-C4 and *β*-Gal-H1 anomeric protons. Correlations between the two *α*-Glc anomeric positions supported the presence of the trehalose unit.

Compounds **6, 7** and **8** were part of the same fraction obtained by HILIC-RID, as a 3.5:2.7:1 mixture; however, all compounds could be assigned by NMR unequivocally, differentiating signals of each one in the spectra (**see Supporting Information, Figures S25-S32**).

In compound **6** (peaks 16 and 17, **Figure 1C**), assigned as *β*-D-galactopyranosyl-(1→4)-*α*-D-glucopyranosyl-(1↔1)-[*β*-Dgalactopyranosyl-(1→6)]-*α*-D-glucopyranoside, three doublets in the anomeric region are shown (δ 5.19, $^{3}J_{H1,H2}$ = 3.7 Hz, δ 4.45, $^{3}J_{H1,H2}$ = 7.9 Hz and δ 4.43, $^{3}J_{H1,H2}$ = 7.9 Hz). They corresponded to both *α*-glucoses from the trehalose unit and two *β*-galactoses (**Table 3**, compound **6**). The 1D ^{13}C NMR spectrum showed signals corresponding to 24 carbons, including four anomeric carbons (δ 94.17, δ 93.88, δ 103.55 and δ 103.95). 2D spectra also supported the presence of two *α*-glucose and two *β*-galactose units, and according to correlations shown in the bsgHMBC spectra, it could be affirmed that one galactose was linked to position 4 of one of the glucose units of the central trehalose, and the other galactose was linked to position 6 of the other glucose unit.

Compound **7** (peaks 16 and 17, **Figure 1C**), assigned as *β*-D-galactopyranosyl-(1→6)-*α*-D-glucopyranosyl-(1↔1)-[*β*-D-galactopyranosyl-(1→6)]-*α*-D-glucopyranoside, is a symmetric compound, as compound **5**, and it was assigned following the same strategy (**Table 3**, compound **7**). This time, the bsgHMBC spectrum showed correlations between the *β*-Gal-C1 anomeric carbons and *α*-Glc-H6 and between *α*-Glc-C6 and *β*-Gal-H1 anomeric protons, besides correlations between the two *α*-Glc anomeric positions, supporting the proposed structure.

Compound **8** (peak 18, **Figure 1D**) was assigned as the pentasaccharide *β*-D-galactopyranosyl-(1→4)-*β*-D-galactopyranosyl-(1→4)-*β*-D-galactopyranosyl-(1→4)-*α*-D-glucopyranosyl-(1↔1)-*α*-D-glucopyranoside (*β*-D-galactopyranosyl-(1→4)-*β*-D-galactopyranosyl-(1→4)-*β*-D-galactopyranosyl-(1→4)-*α*,*α*-trehalose) (**Table 2**, compound **8**). In this case, the 1D ^{1}H NMR spectrum (**see Supporting Information, figure S25 and Table 2**) showed five doublets in the anomeric region (δ 5.19, $^{3}J_{H1,H2}$ =

3.7 Hz, δ 5.18, $^{3}J_{H1,H2}$ = 3.7 Hz, δ 4.49, $^{3}J_{H1,H2}$ = 7.9 Hz, δ 4.65, $^{3}J_{H1,H2}$ = 8.0 Hz, and δ 4.59, $^{3}J_{H1,H2}$ = 7.8 Hz), corresponding to both *α*-glucoses from the trehalose unit and three *β*-galactoses. The 1D ^{13}C NMR spectrum showed signals corresponding to 30 carbons, including five anomeric carbons (δ 94.05, δ 93.71, δ 103.57, δ 104.90, and δ 104.95). 2D spectra also supported the presence of two *α*-glucose and three *β*-galactose units. In this case, trehalose is situated at the end of the chain, and the position of glycosidic linkages was analyzed from bsgHMBC spectra, being always (1→4) between every galactose unit and the next one of the chains and between galactose-3 and trehalose. Relevant correlations to support this affirmation were *β*-Gal-5-C1 anomeric carbon and *β*-Gal-4-H4, *β*-Gal-4-C4 and *β*-Gal-5-H1 anomeric protons, *β*-Gal-4-C1 anomeric carbon and *β*-Gal-3-H4, *β*-Gal-3-C4 and *β*-Gal-4-H1 anomeric protons, *β*-Gal-3-C1 anomeric carbon and *α*-Glc-2- H4, *α*-Glc-2-C4 and *β*-Gal-3-H1 anomeric protons, and between the two *α*-Glc anomeric positions, confirming the presence of a trehalose unit.

These results sustained the obtainment of two new trisaccharides derived from trehalose. The structure was confirmed to be as *β*-D-galactopyranosyl-(1→6)-D-trehalose (**Table 1**, compound **1**) and *β*-D-galactopyranosyl-(1→4)-D-trehalose (**Table 1**, compound **2**). *β*-Gal of *E. coli* was used by Kim *et al.* (2007) to generate trehalose derivatives. That work revealed that the main products were *β*-Gal-(1→4)-Trehalose and *β*-Gal-(1→6)-Trehalose, which are in good agreement with the results of **Figure 1**. In addition, this type of linkage is very similar to the trisaccharides contained in commercial dietary *β*-GOS. Van Leeuwen *et al.* (2014) compared the structure of different commercially available GOS trisaccharides, indicating that bonds *β*(1→4) and *β*(1→6) were the most abundant, depending on the microbial enzyme used in the synthesis. Specifically, **Figure 2C** shows the individual evolution of the trisaccharides synthesized in the lactose/trehalose reaction.

The synthesis yield of each oligosaccharide increased with reaction time, observing the highest increase after 2 h of incubation and then reaching a plateau with a progressive

synthesis of trisaccharides. The main product obtained was *β*-Gal-(1→4)-Tre (∼18.7%) (**Figure 2C**). These results seem to indicate that *β*-gal from *Bacillus circulans* prioritize to join the galactose from lactose (used as a donor) in the trehalose with a linkage *β*(1→4) and in a lesser extent *β*(1→6). The same structures of trisaccharides derived from trehalose were also obtained by Ishii *et al.* (2000) using *B. circulans β*-gal. This indicates the effectiveness of transgalactosylation mechanisms of *β*-gal of *B. circulans* (Abdul Manas *et al.*, 2018).

New tetrasaccharides were found in this work [*β*-D-galactopyranosyl-(1→4)-*β*-D-galactopyranosyl-(1→4)-D-trehalose and *β*-D-galactopyranosyl-(1→4)-*β*-D-galactopyranosyl-(1→6)-D-trehalose] (**Table 2**). These results followed the same pattern as the trisaccharides synthesized, where the galactose monomers of lactose have been driven to the acceptor molecule galactosyl-trehalose and linked by *β*(1→6) and *β*(1→4) bonds. **Figure 2D** indicates that similar quantities of the different tetrasaccharides were obtained. Therefore, quantitative results (**Table S1**) show a greater production after 6 h of reaction (8.2%). Remarkably, an interesting mixture of structures where the trehalose unit is situated in the center of the molecule was also synthesized (**Table 3**, compounds **5, 6** and **7**). In this case, the trehalose has been galactosylated in both terminal endings resulting in three different tetrasaccharides distinguished by both types of bonds. This fact could indicate that the trisaccharides *β*-Gal-(1→4)-Tre and *β*-Gal-(1→6)-Tre also acted as acceptors. Furthermore, the slight differences between these chemical structures may be important in a possible production in a major scale.

The majority of the studies based on the synthesis of trehalose derivatives focused on the synthesis of disaccharides analogues, such as lactotrehalose or mannotrehalose (Walmagh *et al.*, 2015; Y. Zhang *et al.*, 2020), or trisaccharides, as the structures named above (Ishii *et al.*, 2000; Kim *et al.*, 2007); however, no tetra- or pentasaccharides were investigated. Chaube *et al.* (2016) were the first to synthesize tetrasaccharides trehalosederivatives from *Mycobacterium smegmatis* obtaining galactosyl and glucosyl structures linked by *α*(1→6) and *β*(1→6) to trehalose moieties, respectively.

Nevertheless, the process of synthesis was arduous and complex, using organic solvents. On the other hand, Wessel & Niggemann (1995) synthesized different types of trehalose oligosaccharides with glucose linked via $\beta(1\rightarrow4)$ and DP up to 5. To the best of our knowledge, our data are the first evidence on the synthesis of tetra- and pentasaccharide trehalose galactosylated using commercially available enzymes.

Transgalactosylation by *β*-Galactosidase from *Aspergillus oryzae*

Figure 3 shows the GC-FID chromatogram during the transgalactosylation assay after 6 h of reaction using the lactose/trehalose mixture and only lactose by *β*-gal from *A. oryzae*. The GC-FID profile of *A. oryzae* (**Figure 3**) shows a less complex mixture than *B. circulans*, as a result of the less formation of disaccharides (**Figure 3A**), trisaccharides (**Figure 3B**), and tetrasaccharides (**Figure 3C**), including *β*-GOS and trehalose derivatives. In the lactose assay (**Figure 3**, red), *β*-GOS di- (peaks 5−7; **Figure 3A**) and trisaccharides (peaks 8−10, **Figure 3B**) were detected, in a higher level than the lactose/trehalose mixture. Tetrasaccharides were found in both reactions, in a substantially low level (multiple peaks labeled as 11 and *; **Figure 3C**). Remarkably, a series of unknown compounds were also detected in the lactose/trehalose mixture (**Figure 3**, blue): saccharides labeled as 10 and 11 (**Figure 3**) were only synthesized when trehalose was present on the reaction.

The evolution in the content of carbohydrates for each reaction is observed in **Figure 4A** (lactose/trehalose) and **Figure 4B** (lactose). **Table S2** shows the quantitative data of the assays. A progressive and complete hydrolysis of lactose after 24 h was observed in both reactions, while the corresponding monosaccharides increased (peaks 1 and 2, **Figure 3A**) with the incubation time. In the lactose/trehalose mixture (**Figure 4A**), the maximum formation of the di- and trisaccharides occurred between 2 and 6 h of reaction. As observed in the reaction with *B. circulans*, only disaccharides from lactose were synthesized, reaching a maximum of 14.1% after 6 h in the lactose mixture versus 6.3% obtained when lactose/trehalose was used.

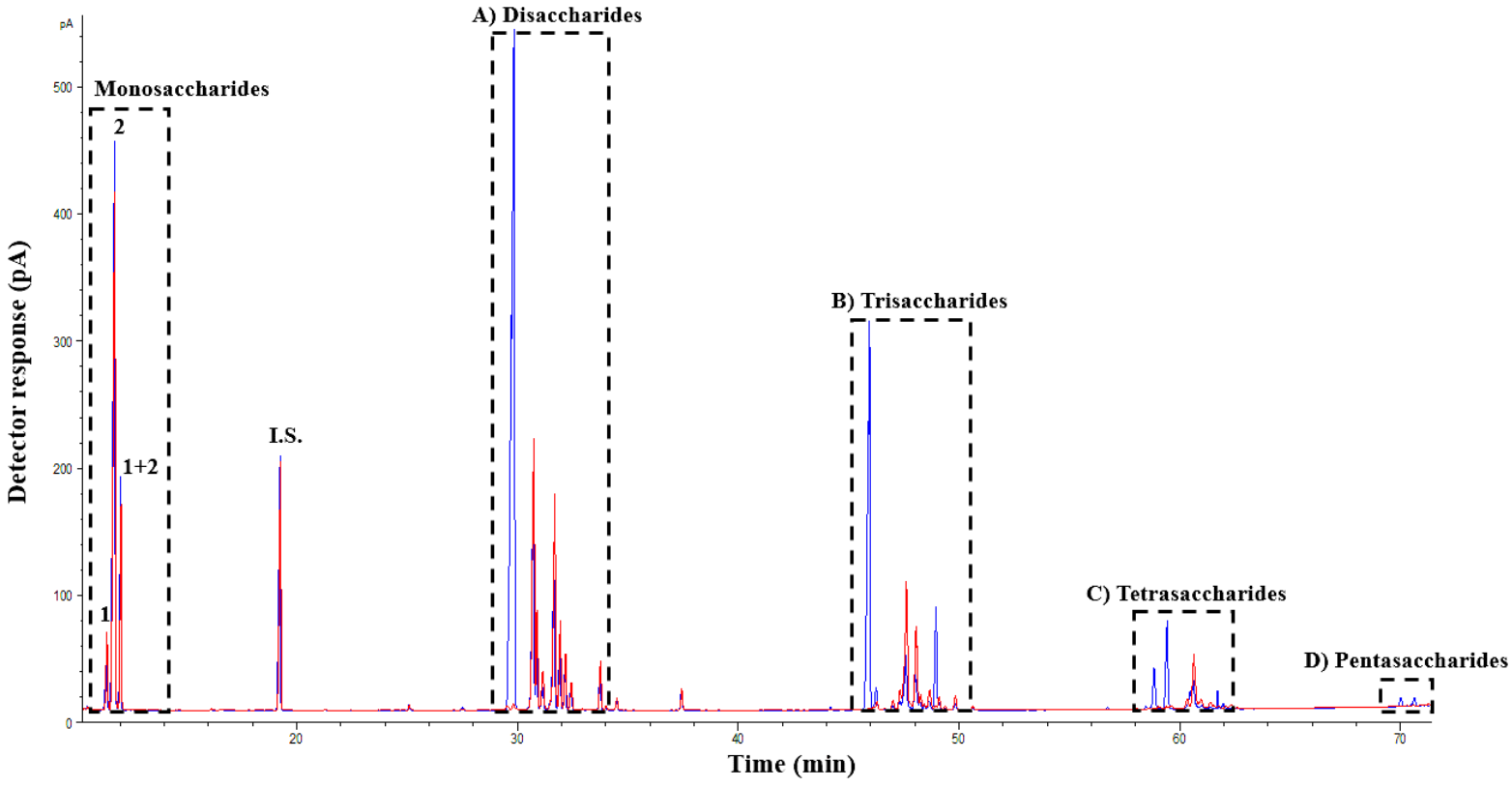
pA
Detector response (pA)
Time (min)
Monosaccharides
2
1+2
1
I.S.
A) Disaccharides
B) Trisaccharides
C) Tetrasaccharides
D) Pentasaccharides
0
100
200
300
400
500
20
30
40
50
60
70

Figure 3

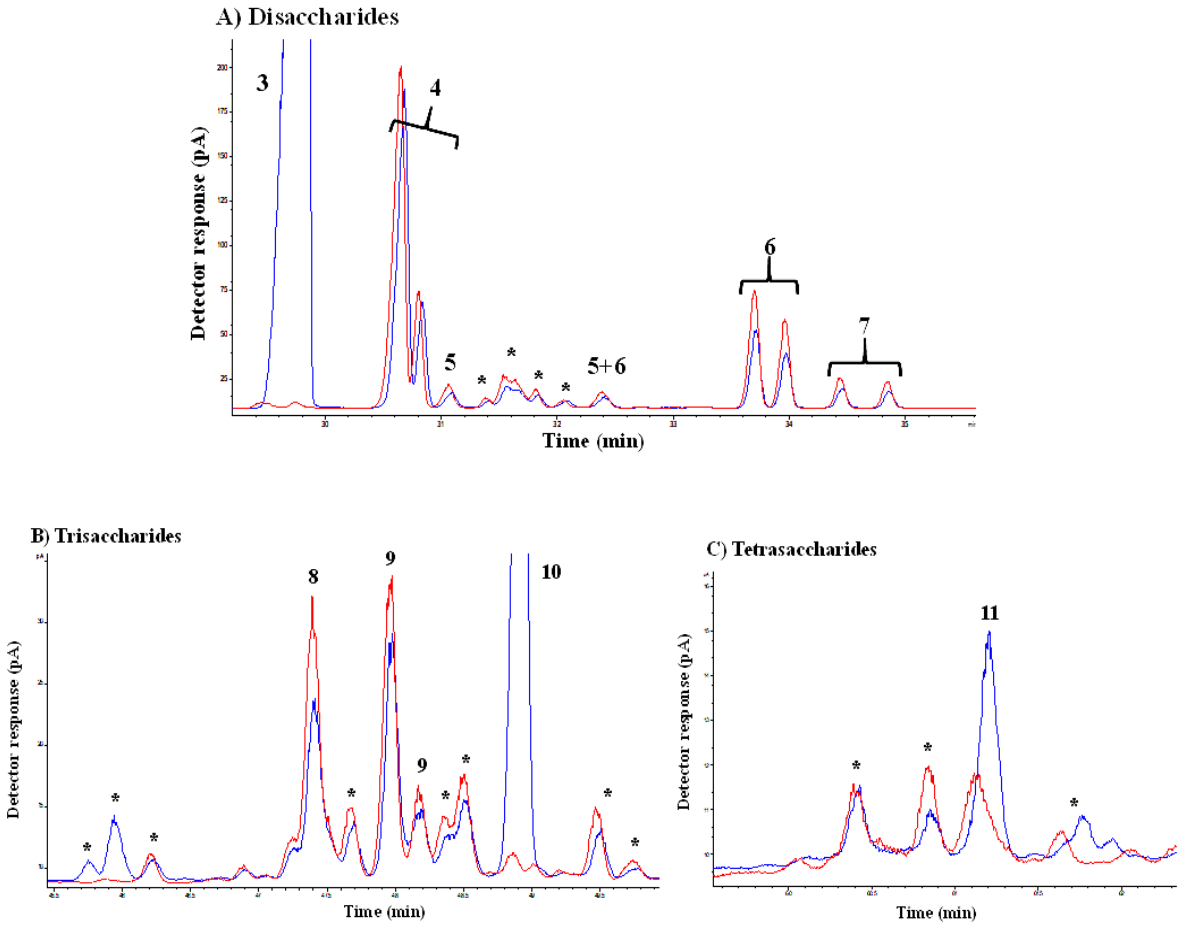

Figure 3. Chromatographic profiles obtained by GC-FID of TMSO derivatives of the transgalactosylation reaction after 6 h by *β*-galactosidase from *Aspergillus oryzae* using lactose/trehalose (blue) and lactose (red). Disaccharide (A), trisaccharide (B) and tetrasaccharide (C) fraction are shown for each reaction. Peaks: 1: Galactose, 2: Glucose, I.S.: Internal Standard, (A) 3: Trehalose, 4: Lactose, 5: *β*-D-galactopyranosyl-(1→4)-*β*-D-galactose, 6: *β*-D-galactopyranosyl-(1→6)-*β*-D-glucose, 7: *β*-D-galactopyranosyl-(1→6)-*β*-D-galactose, (B) 8: *β*-D-galactopyranosyl-(1→4)-[*β*-D-galactopyranosyl-(1→6)]-D-glucose, 9: *β*-D-galactopyranosyl-(1→6)-lactose, 10: *β*-galactopyranosyl-(1→6)-trehalose, (C) 11: *β*-galactopyranosyl-(1→6)-*β*-galactopyranosyl-(1→6)-trehalose. *Other saccharides with unknown structure.

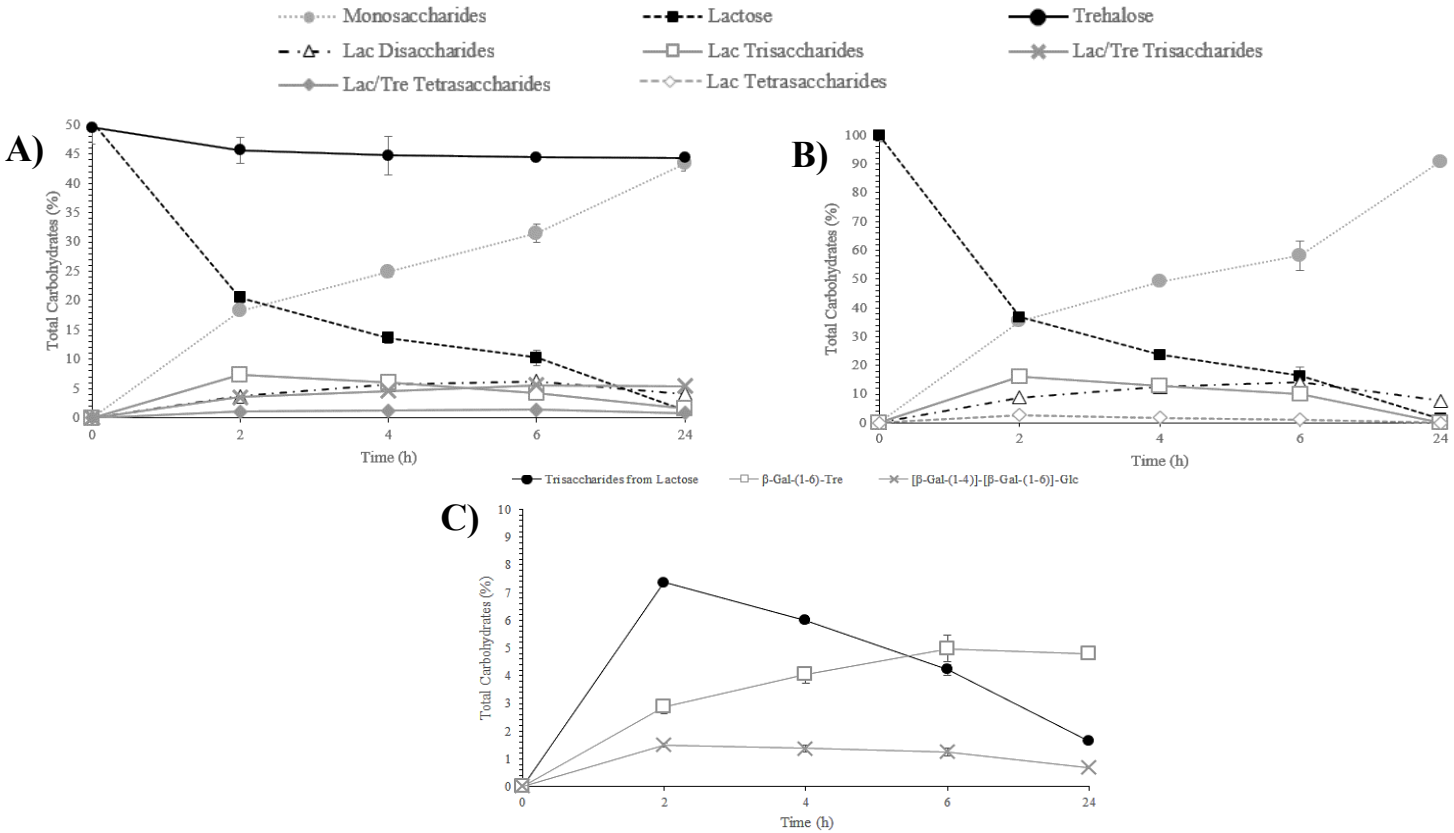

Figure 4. Evolution in the content of carbohydrates (%) during transgalactosylation reactions of lactose/trehalose (A) and lactose (B) solutions; and (C) evolution in the content of trisaccharides (%) of lactose/trehalose mixture. Reactions catalyzed by *β*-galactosidase from *Aspergillus oryzae* for 24 h at 50 ºC, pH 4.5.

The presence of trehalose appeared to decrease the *β*-GOS formation in favor to giving rise to the new oligosaccharides. The less formation of disaccharides in **Figure 4A** was balanced for the synthesis of the trehalose trisaccharides (5.6% after 6 h). Trehalose levels were diminished in a lower degree than the *B. circulans* reaction (**Figure 2A**); therefore, the synthesis of trehalose-derived oligosaccharides was lower. It has been reported that the transgalactosylation properties of *β*-gal from *A. oryzae* are less effective than those of *E. coli* and *B. circulans* in terms of trehalose analogues (Ajisaka & Fujimoto, 1990; Ishii *et al.*, 2000). Remarkably, despite the low quantity of tetrasaccharides (1.4%) observed in **Figure 4A**, new oligosaccharides were synthesized. The new oligosaccharides were isolated by HILIC-RID and characterized by NMR.

NMR characterization was accomplished as before by the combined use of 1D and 2D [^{1}H, ^{1}H] and [^{1}H, ^{13}C] NMR experiments (gCOSY, TOCSY, ROESY, multiplicity-edited gHSQC, bsgHMBC and hybrid experiment gHSQC-TOCSY). ^{1}H and ^{13}C NMR chemical shifts observed are summarized in **Tables 1 and 4**. Full sets of spectra are available in the Supporting Information (**Figures S1-S6 and S33-S43**). Peak 10 (**Figure 3B**) was identified as compound 1 [*β*-D-galactopyranosyl-(1→6)-*α*,*α*-trehalose]. All NMR spectra were identical to those for the trisaccharide already described in the previous section.

Interestingly, in the case of trisaccharide **9** (peak 8, **Figure 3B**), the *α*,*α*-trehalose moiety was not found. The 1D ^{1}H NMR spectrum spectrum (**see Supporting Information, Figure S33 and Table 4**) showed five doublets in the anomeric region. Theybelong to two sets of signals, corresponding to an equilibrium of the *α*:*β* anomers of the terminal glucose (δ 5.22, $^{3}J_{H1,H2}$ = 3.8 Hz, δ 4.44 or 4.45, $^{3}J_{H1,H2}$ = 7.8 Hz and δ 4.51, $^{3}J_{H1,H2}$ = 8.1 Hz for *α* anomer, and δ 4.67, $^{3}J_{H1,H2}$ = 8.0 Hz, δ δ 4.44 or 4.45, $^{3}J_{H1,H2}$ = 7.8 Hz and δ 4.51, $^{3}J_{H1,H2}$ = 8.1 Hz for the *β* anomer). The 1D ^{13}C NMR spectrum showed signals corresponding to 31 carbons (five of them including two carbons in the same signal). The gHSQC spectrum was used to link the carbon signals to the corresponding proton resonances. It showed six anomeric carbons (δ 92.55, δ 96.57, δ 103.79, δ 103.77, δ

103.44 and δ 103.48), 20 CH (four pairs occur under the same signal), and five methylene carbons (two of them are under the same signal). In addition, COSY, TOCSY, and gHSQC-TOCSY experiments supported the presence of two *β*-galactose units and one glucose unit (*α* and *β* forms) for each trisaccharide of the pair. The position of glycosidic linkages was analyzed from bsgHMBC spectra. In this case, it showed correlations between the anomeric carbons of the two *β*-Gal units with protons in positions 4 and 6 of the same glucose unit for each anomeric form. Therefore, relevant correlation bands between the *β*-Gal-3-C1 anomeric carbon and *α*/*β*-Glc-H4 and between *α*/*β*-Glc-C4 carbon and the *β*- Gal-3-H1 anomeric proton could be found. Also, it showed correlations between *β*-Gal-2-C1 anomeric carbon and *α*/*β*-Glc-H6 methylene protons and between *α*/*β*-Glc-C6 methylene carbon and the *β*-Gal-2-H1 anomeric proton. These results confirmed the structure as *β*-D-galactopyranosyl-(1→4)-[*β*-D-galactopyranosyl-(1→6)]-D-glucopyranose (**Table 4**, compound **9**).

Carrying out a similar analysis, compound **10** (peak 11, **Figure 3C**) was assigned as *β*-D-galactopyranosyl-(1→6)-*β*-D-galactopyranosyl-(1→6)-*α*-D-glucopyranosyl-(1↔1)-*α*-D-glucopyranoside [*β*-D-galactopyranosyl-(1→6)-*β*-D-galactopyranosyl-(1→4)-*α*,*α*-trehalose] (**see Supporting Information, Figures S39−S43 and Table 4**, compound **10**). Key correlations in 2D spectra confirmed the presence of a trehalose unit and also the position of glycosidic linkages.

It should be noted that compound **10** was obtained together with compound **11**, in a 2:1 mixture. In this case, not all signals for compound **11** could be assigned, but signals observed in all spectra were consistent with the assignation of this compound as previously described (Prakash *et al.*, 1989), the trisaccharide *β*-D-galactopyranosyl-(1→6)-*β*-D-galactopyranosyl-(1→4)-D-glucopyranose (**see Supporting Information, Figures S39-S43**).

Table 4. ^{1}H (500 MHz) and ^{13}C (125 MHz) NMR Chemical Shifts (δ , ppm) and Coupling Constants (J in Hz, in parentheses) Determined by 1D and 2D NMR Spectroscopy of Oligosaccharides **9** and **10**.

		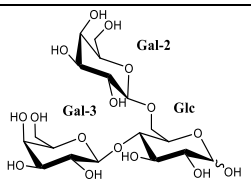 **9** *β*-D-Gal*p*-(1→4)-[*β*-D-Gal*p*-(1→6)]-D-Glc*p*				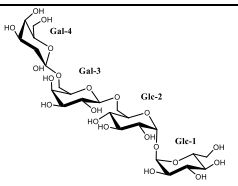 **10** *β*-D-Gal*p*-(1→6)-*β*-D-Gal*p*-(1→6)-*α*-D-Glc*p*-(1↔1)-*α*-D-Glc*p*	
		δ_C	δ_H(J, Hz)			δ_C	δ_H(J, Hz)
α-Glc	1	92.55	5.22 (3.8)	*α*-Glc-1	1	94.01	5.19 (3.9)
	2	71.77	3.60		2	71.65	3.64
	3	72.01	3.82		3	73.12	3.82
	4	78.41	3.79		4	70.31	3.44
	5	69.63	4.08		5	72.83	3.83
	6	68.08	4.21, 3.96		6	61.14	3.84,3.76
β-Glc	1	96.57	4.67 (8.0)	*α*-Glc-2	1	93.96	5.18 (3.9)
	2	74.36	3.31		2	71.62	3.64
	3	74.94	3.62		3	73.07	3.84
	4	78.44	3.79		4	69.99	3.57
	5	74.24	3.75		5	71.84	3.94
	6	68.14	4.29, 3.91		6	68.84	4.16,3.87
Gal-2(*α*) (1→6)	1	103.79	4.44 or 4.45 (7.8)	Gal-3	1	103.85	4.46 (7.9)
	2	71.28	3.54		2	71.33	3.53
	3	73.33	3.66		3	73.20	3.65
	4	69.33	3.92		4	69.34	3.95
	5	75.74	3.70		5	74.54	3.89
	6	61.65	3.78, 3.75		6	69.60	4.04,3.87
Gal-2(*β*) (1→6)	1	103.77	4.44 or 4.45 (7.8)	Gal-4	1	103.97	4.44 (7.9)
	2	71.28	3.54		2	71.38	3.53
	3	73.32	3.66		3	73.38	3.65
	4	69.32	3.92		4	69.26	3.91
	5	75.78	3.70		5	75.81	3.69
	6	61.65	3.78, 3.75		6	61.62	3.78,3.75

Gal-3(*α*) (1→4)	1	103.44	4.51 (7.8)	
	2	71.59	3.54	
	3	73.13	3.66	
	4	69.23 or 69.26	3.92	
	5	75.91	3.70	
	6	61.75	3.78, 3.75	
Gal-3(*β*) (1→4)	1	103.48	4.51 (7.8)	
	2	71.59	3.54	
	3	73.13	3.66	
	4	69.23 or 69.26	3.92	
	5	75.91	3.70	
	6	61.72	3.78, 3.75	

The synthesis of the lactose/trehalose mixture promoted considerably the formation of two trisaccharides, reaching maximum yields at 6 h of reaction (**Figure 4C**). *β*-D-galactopyranosyl-(1→4)-[*β*-D-galactopyranosyl-(1→6)]-D-glucopyranose (**Table 4**, compound **9**) was the main product obtained in the transgalactosylation assay; this *β*-GOS trisaccharide has been also found by Yin *et al.* (2017) using lactose as a donor and acceptor. The other trisaccharide was the same as that obtained by *B. circulans*, *β*-Gal*p*-(1→6)-Tre (**Table 4**, compound **1**), but in a lower quantity (**Figure 4C**). These data are in line with Urrutia *et al.* (2013) who observed a high preference of *β*-gal of *A. oryzae* for the formation of *β*(1→6) bonds, as well as for *B. circulans*. Moreover, the low level of production using the *A. oryzae* enzyme is in good agreement with Ajisaka and Fujimoto (1990) who carried out a total synthesis yield of 7%.

On the other hand, a new tetrasaccharide was obtained in the reaction, whose structure is shown in **Table 4** (Compound **10**). As well as in *B. circulans*, these are the first data reported of galactosylated trehalose tetrasaccharides synthesized by commercial enzymes. In addition, Ferreira-Lazarte, Gallego-Lobillo, *et al.* (2019) studied the digestibility of *β*-GOS with different types of bonds using brush border membrane vesicles from pig, which contains the disaccharidases responsible for the digestion of

dietary sugars. Their findings revealed that the *β*(1→6) linkage showed the highest resistance to digestion (12% after 3 h) followed by *β*(1→4) (26%) and *β*(1→3) (40%). This supports the hypothesis that the new trehalose tri- and tetrasaccharides could be less prone to hydrolysis.

The *B. circulans* enzyme seemed to have a greater production of potential new trehalose derivatives, including tri- and tetrasaccharides (19.5 and 8.2%, respectively). The main synthesized trisaccharides were *β*-Gal*p*-(1→4)-Tre and *β*-Gal*p*-(1→6)-Tre, obtained by both enzymes. On the other hand, tetrasaccharides were produced in a higher quantity while using the *B. circulans* enzyme and showed the most diverse structures. The *A. oryzae* enzyme only synthesized *β*-Gal*p*-(1→6)-*β*-Gal*p*-(1→6)-Tre in a lower amount. In addition, a tetrasaccharide was also found: *β*-Gal*p*-(1→6)-*β*-Gal*p*-(1→6)-Tre. *β*(1→6) and *β*(1→4) galactosyl linkages are minimally digested in the small intestine; therefore, the virulence mediated by negative microorganisms, such as *C. difficile*, in the gut could be reduced. In addition, these new structures could have a key role in the proper beneficial effects of trehalose, such as autophagy or glycemic control. Data obtained in this wok could be useful to the production of trehalose derivatives in a major scale, concerning the selectivity of each *β*-gal from different sources. In this context, increasing the knowledge in terms of the digestibility of this new compound is necessary to understand the real behavior of this carbohydrate in the digestive system.

Funding

This work was supported by the Spanish Ministry of Economy, Industry and Competitiveness (Project AGL2017-84614-C2-1-R) and the Spanish Ministry of Science, Innovation and Universities (Project RTI2018-101273-J-I00). O.H.H. has received funding from the European Union's Horizon 2020 research and innovation program under the Marie Skłodowska-Curie grant agreement no. 843950.

Discusión General

5. Discusión General

En las últimas décadas, los estudios sobre la modulación de la microbiota humana han despertado un enorme interés debido a su fuerte relación con la salud y el bienestar. Numerosas enfermedades crónicas (síndrome metabólico, cáncer, etc…) se han relacionado con alteraciones en la composición y en el funcionamiento de la microbiota intestinal, siendo la utilización de prebióticos una de las aproximaciones más eficaces para restaurar la homeostasis del colon. Son, por tanto, muy numerosas las investigaciones realizadas en los últimos años dentro del campo de los prebióticos. Se han alcanzado importantes avances en la síntesis y purificación de nuevos prebióticos, testándose sus propiedades bioactivas tanto en ensayos *in vitro* como *in vivo*, además de estudiar sus aplicaciones en diversos alimentos. Sin embargo, apenas se ha prestado atención a la digestión de los mismos, asumiendo erróneamente que llegan intactos a las porciones más distales del intestino grueso para ejercer su principal efecto modulador. En este sentido, la mayor parte de los estudios realizados sobre la digestión de carbohidratos han obviado la importancia de las disacaridasas presentes en la membrana de los enterocitos, poniendo de manifiesto la necesidad de disponer de protocolos específicos para entender la digestión de los carbohidratos prebióticos previa a su fermentación por la microbiota intestinal (Feher, 2017; Ferreira-Lazarte *et al.*, 2020; Picariello *et al.*, 2016).

Los métodos *in vitro* con extractos intestinales de mamíferos se muestran como posibles protocolos de digestión fiables y sencillos (Ferreira-Lazarte, Gallego-Lobillo, *et al.*, 2019; Ferreira-Lazarte, Olano, *et al.*, 2017). En estos trabajos se ha indicado cómo la estructura química y el tipo de enlace del carbohidrato pueden llegar a tener un impacto directo en su grado de digestión. Estos métodos *in vitro* se han ensayado en moléculas de bajo grado de polimerización, sin embargo, no se han realizado estudios cinéticos a través de los cuales se intuya la velocidad de digestión, parámetro muy relevante, ya que no solo es importante conocer si los prebióticos llegan o no al colon, sino cuánto tardarían en llegar.

Por todo ello, el primer enfoque de la presente Tesis Doctoral fue el estudio de la cinética de hidrólisis enzimática de carbohidratos digeribles y no digeribles con un método de digestión basado en la utilización de extracto de intestino delgado de rata (RSIE), (Ferreira-Lazarte, Olano, *et al.*, 2017), dada la similitud entre las enzimas de rata y de humanos (Lin *et al.*, 2016; Oku *et al.*, 2011) (*Capítulo 1*). Tras evaluar la hidrólisis de la lactosa (carbohidrato digerible) a diferentes concentraciones y tiempos, se observó, en general que, a menor cantidad de lactosa, existía mayor velocidad de hidrólisis, siendo 0,2 mg/mL y 2 h de digestión las condiciones de máxima hidrólisis de lactosa. Estos datos pueden ser de utilidad en los estudios sobre intolerancia a la lactosa, enfermedad con una alta prevalencia mundial (57%) (Catanzaro *et al.*, 2021). Una vez optimizadas las condiciones de máxima hidrólisis, se realizó el mismo ensayo con lactulosa (carbohidrato no digerible) en las mismas condiciones, y se compararon las cinéticas de la reacción. Los valores de los parámetros cinéticos pusieron de manifiesto la elevada resistencia de la lactulosa a la digestión en comparación con la lactosa, así como la alta dependencia de la estructura química. Así, estos resultados obtenidos mediante un método *in vitro* subrayan la elevada resistencia a las enzimas digestivas de galactosil-fructosas (lactulosa) en comparación con las galactosil-glucosas (lactosa), tal y como indicaron Hernández-Hernández *et al.* (2012) en un ensayo realizado con ratones en el que estudiaron GOS y oligosacáridos derivados de la lactulosa. Se establece, de esta manera, el método con RSIE como un procedimiento fiable, sencillo y eficiente para evaluar la digestibilidad de carbohidratos digeribles y no digeribles de pequeño tamaño, conteniendo, además, las enzimas del borde en cepillo del intestino delgado (Ferreira-Lazarte *et al.*, 2020; Hernández-Hernández, 2019).

Dado que hasta ese momento el método basado en el empleo de RSIE sólo se había empleado en di- y oligosacáridos, se consideró necesario testar la validez del método anteriormente indicado en prebióticos comerciales con distinto grado de polimerización y tipo de enlaces, compuestos por inulina (Orafti® GR y Raftiline® HP) y FOS (Raftilose® P95) y una mezcla de α-GOS (AlphaGOS® P) (*Capítulo 2*). Las condiciones de los ensayos fueron las mismas que las indicadas en el *Capítulo 1*, para continuar con

un acercamiento más real al comportamiento de los carbohidratos prebióticos en el intestino delgado. Los productos derivados de la inulina mostraron la mayor resistencia a las enzimas intestinales, con una mínima liberación de fructosa (~4%). En cambio, en Raftilose P95, de menor tamaño molecular, se observó una mayor degradación (~10%), especialmente en los tetrasacáridos (inulotetraosa y nistosa) y en menor medida en trisacáridos. Una vez más se pudo resaltar la importancia de la estructura química en la digestión, ya que la hidrólisis era mayor en aquellas moléculas donde la glucosa terminal no estaba presente (inulotriosa e inulotetraosa de Raftilose P95). Los resultados indicaron que los enlaces $\beta(2\rightarrow1)$ entre moléculas de fructosa son más propensos a la acción intestinal, en línea con lo mostrado previamente por Ferreira-Lazarte, Olano, *et al.* (2017). Por otro lado, este estudió mostró los primeros resultados de digestión intestinal de α-GOS alcanzándose valores por encima del 60%, similares a los de la digestión del disacárido melibiosa. Estos resultados no fueron los esperables debido a la ausencia de la enzima α-galactosidasa en el aparato digestivo humano. Sin embargo, los datos obtenidos parecen indicar que los complejos enzimáticos maltasa-glucoamilasa y sacarasa-isomaltasa podrían actuar sobre los enlaces $\alpha(1\rightarrow6)$ (Lee *et al.*, 2016), exhibiendo la versatilidad de las disacaridasas presentes en las microvellosidades de la membrana de los enterocitos. Asimismo, estos datos sugieren que las enzimas empiezan a hidrolizar desde las estructuras con mayor DP, generando compuestos más pequeños para producir una degradación progresiva de los carbohidratos. Una situación semejante con el método InfoGest y sin presencia de las disacaridasas ocurre en el estudio de Nobre *et al.* (2018), quienes realizaron un ensayo de digestibilidad con Raftilose P95, y el grado de hidrólisis obtenido fue muy bajo, observado sólo en la fracción de tetrasacáridos (1.4%).

Para acabar el primer bloque de la Tesis, una vez evaluado el método de digestión con RSIE en diferentes estructuras químicas correspondientes a diferentes tipos de carbohidratos, se consideró necesario hacer una comparación con el método de digestión InfoGest. Dicho método se estableció hace años como un protocolo internacional de digestión de macronutrientes (Brodkorb *et al.*, 2019; Minekus *et al.*, 2014), sin embargo,

no incluye las disacaridasas intestinales ni tampoco ha sido evaluado con carbohidratos prebióticos. Por tanto, el estudio sobre la comparación y la combinación del protocolo InfoGest y del modelo de digestión con RSIE en polisacáridos puede implicar un paso adelante para mejorar los métodos de digestibilidad, además de ampliar la información con carbohidratos de mayor tamaño. La viabilidad de ambos métodos se ha mostrado en el artículo correspondiente al *Capítulo 3*. En este caso los sustratos estudiados fueron: almidón y dextrano como polisacáridos de glucosa, y pectina de cítricos (CP) y pectina modificada de cítricos (MCP), como polisacáridos pécticos con potencial prebiótico.

El efecto de la fase gástrica, siguiendo el método InfoGest, en compuestos de alta masa molecular, apenas había sido estudiado, no obstante, la ausencia de carbohidrasas en el estómago señala una nula o baja digestión. Tanto almidón, como dextrano y CP no mostraron cambios en esta fase digestiva, a excepción de la MCP, con un incremento de ácido galacturónico, posiblemente debido al efecto del ácido en los compuestos de menor masa molecular (Holloway *et al.*, 1983). Ferreira-Lazarte, Montilla, *et al.* (2017) observaron mínimos cambios en GOS y OsLu en la digestión gástrica con InfoGest. Al llegar a la fase intestinal, como se ha mencionado en los *Capítulos 1* y *2*, las disacaridasas aparecen como una pieza clave en el proceso digestivo. A pesar de ello, no están presentes en el protocolo InfoGest, cuyo fluido intestinal contiene únicamente la α-amilasa presente en el jugo pancreático. Teniendo esto en cuenta, no se observaron cambios significativos en el contenido en carbohidratos durante la fase intestinal con InfoGest ni en el dextrano ni en ambas pectinas. Como era de esperar, el almidón se hidrolizó en un alto grado por la presencia de la α-amilasa pancreática. Por otro lado, usando el extracto de intestino delgado de rata (RSIE) y con la combinación de ambos métodos, se apreció un incremento significativo en la hidrólisis de todos los compuestos. En el almidón, el efecto complementario entre las enzimas de InfoGest y del RSIE se puso de manifiesto (52,5% de hidrólisis), ya que mediante el primer método se rompieron los enlaces $\alpha(1\rightarrow4)$ de la amilosa y la amilopectina, generando compuestos de menor masa molecular, entre ellos las dextrinas límite. Mientras que el RSIE hidrolizó estos oligosacáridos de menor masa molecular generados por la acción de la α-amilasa

pancreática. Esto coincide con lo estudiado en el *Capítulo 2*, resaltando la importancia de la estructura química y el mecanismo de hidrólisis.

En el caso del dextrano sólo se observó digestión en presencia del RSIE (20,6% de hidrólisis). El dextrano está compuesto por monómeros de glucosa unidos mediante enlaces $\alpha(1\rightarrow6)$, al igual que los α-GOS estudiados en el *Capítulo 2*, lo que implica la capacidad de las disacaridasas para hidrolizar diferentes tipos de carbohidratos. Lee *et al.* (2016) mostraron diferentes ratios de hidrólisis en carbohidratos con enlaces α, con resultados similares (24% para enlaces de dextrano). Con respecto a los compuestos pécticos, la digestión mediante InfoGest es prácticamente nula. Sin embargo, con RSIE se observó la hidrólisis de los enlaces $\alpha(1\rightarrow4)$ presentes en el esqueleto de HG y RG-I, subrayando la versatilidad de las enzimas anteriormente nombradas. Cuando ambos métodos son combinados, el grado de hidrólisis se incrementa significativamente, siendo 17,2% en CP y 42,3% en MCP. En el caso de MCP, la digestión es mayor debido probablemente a su menor masa molecular y menor grado de metil-esterificación (Dongowski *et al.*, 2002).

Además del relevante papel de las disacaridasas intestinales en la digestión de prebióticos, indicado previamente en el *Capítulo 2* y en línea con otros estudios (Ferreira-Lazarte, Gallego-Lobillo, *et al.*, 2019; Julio-Gonzalez *et al.*, 2019), el complejo entorno digestivo también incluye las enzimas microbianas. Tanto las enzimas digestivas de mamíferos como las microbianas forman parte de la digestión ileal completa (Hernández-Hernández *et al.*, 2012). Así, la utilización de RSIE contempla la combinación tanto de las disacaridasas presentes en las células del borde en cepillo como de las enzimas del lumen intestinal. Por tanto, los datos obtenidos en el *Capítulo 3* muestran un acercamiento más real al aparato digestivo humano, a la vez que se demuestra la eficacia y la utilidad del método del RSIE para polisacáridos. Asimismo, quedan de manifiesto las limitaciones del método InfoGest para la digestión de carbohidratos. Consecuentemente, una optimización en la combinación de los dos

métodos de digestión (InfoGest y RSIE) podría resultar en una aproximación más realista a la digestión intestinal completa.

Dado que los resultados del *Capítulo 3* arrojaron evidencia sobre la posible digestión parcial de pectinas, y como estos carbohidratos prebióticos (en estudio) son objeto de interés por su potencial efecto antitumoral, se planteó estudiar en qué medida podían afectar a la microbiota intestinal. De esta manera, se comprobó el efecto de la CP y MCP en un modelo animal de rata (*Rattus norvegicus* F344) con cáncer colorrectal inducido mediante combinación de azoximetano y dextrano sulfato de sodio (AOM/DSS) (*Bloque II, Capítulo 4*). El estudio se realizó con 3 cohortes diferentes (Universal, CP y MCP), cada una con su grupo control.

A pesar de observar un incremento de familias de bacterias beneneficiosas (*Prevotellaceae, Bifidobacteriaceae*), se observó una disbiosis general en la microbiota intestinal y una disminución del pH luminal en las cohortes de CP y MCP. Se detectó un incremento significativo en el *phylum* de *Proteobacteria*, concretamente, la familia de las enterobacterias, en las ratas con cáncer y alimentadas con CP y MCP. Se trata de bacterias proinflamatorias y su aumento se relaciona con numerosos trastornos inmunes y metabólicos, siendo además un factor de riesgo para la Enfermedad Inflamatoria Intestinal (EII) y para el propio cáncer (Arthur *et al.*, 2014; Baldelli *et al.*, 2021; Hernaiz-Leonardo *et al.*, 2017). Asimismo, aquellos grupos de bacterias productoras de SCFA y las relacionadas con propiedades anticarcinógenas y antiinflamatorias (género *Faecalibacterium y Fusobacterium*) (Ahn *et al.*, 2013; Ahn & Hayes, 2020; Tahara *et al.*, 2014) estaban disminuidos en las cohortes de pectina. Por otro lado, el coeficiente *Firmicutes/Bacteroidetes* era menor en la cohorte de pectina, poniendo de manifiesto su efecto hipoglucemiante en el organismo.

La familia *Porphyromonadaceae* también se encontraba reducida en los grupos pécticos, lo que explicaba la inexistente producción de SCFA en el intestino grueso, a excepción del ácido acético, principal componente de la fermentación de las pectinas. Al final del estudio, la mortalidad fue mayor en las ratas con cáncer pertenecientes a las cohortes de

CP (5 ratas) y MCP (4 ratas), mientras que en el grupo control no hubo ninguna muerte. No se observaron diferencias significativas en cuanto a número y tamaño de tumores; ni placas de Peyer entre cohortes; únicamente en el tamaño del ciego, encontrándose aumentado en los animales alimentados con CP y MCP. El motivo más probable está relacionado con la viscosidad de las pectinas. Las propiedades tecnológicas y funcionales de estos polisacáridos ejercen un papel fundamental en este incremento de la mortalidad. Las pectinas son moléculas de alto peso molecular, cuyo paso por el intestino es lento, generando un aplanamiento de la curva de glucemia (Christiaens *et al.*, 2016; Ferreira-Lazarte *et al.*, 2018), como muestra el coeficiente *Firmicutes/Bacteroidetes*. Esto unido a la baja digestibilidad de la misma, estudiada en el *Capítulo 3*, generó un aumento de la saciedad y de viscosidad en el intestino (Ferreira-Lazarte, Moreno, *et al.*, 2019) y, como consecuencia, una menor ingesta de alimentos. Esto incidió directamente en los efectos inflamatorios del DSS, lo que, junto con el cáncer, propició la mortalidad.

No obstante, esta digestibilidad y viscosidad característica de las pectinas también implica un efecto en la glucemia y en los triglicéridos. En la cohorte de CP, los niveles de glucosa en sangre y de triglicéridos eran los más bajos, en comparación con MCP y Universal. Esto se relaciona con su efecto antidiabético, hipoglucemiante y de retraso del vaciado gástrico (Brouns *et al.*, 2012; Liu *et al.*, 2016). A pesar de que el consumo de pectinas parece no contribuir a la prevención del cáncer colorrectal, con los efectos beneficiosos y perjudiciales observados en este trabajo, serían necesarias más investigaciones con nuevas condiciones y modelos de animal para comprender el complejo efecto de esta molécula en esta enfermedad.

Con el fin de ahondar en la relación de los carbohidratos prebióticos con algunas enfermedades crónicas, se planteó la búsqueda de compuestos que pudieran tener efecto sobre patologías degenerativas. En este sentido, la trehalosa ha demostrado ser una buena opción para el tratamiento de la ELA (Emanuele, 2014; Massenzio *et al.*, 2018), pero dada su cuestionable digestibilidad (Hooton *et al.*, 2015; Kluch *et al.*, 2020) y su efecto

negativo en el caso de infecciones intestinales por *Clostridium difficile* (Cao *et al.*, 2019), es necesario disponer de derivados de dicho carbohidrato con posibles efectos mejorados. Así, el último bloque (*Bloque III, Capítulo 5*) de la presente Tesis Doctoral se basa en la producción de nuevos oligosacáridos potencialmente prebióticos derivados de la trehalosa. El mecanismo de síntesis fue la transgalactosilación, basado en estudios previos para GOS y OsLu (Cardelle-Cobas *et al.*, 2016; Martínez-Villaluenga, Cardelle-Cobas, Corzo, *et al.*, 2008), utilizando lactosa como donante, trehalosa como aceptor y catalizado por *β*-galactosidasas de *Bacillus circulans* y *Aspergillus oryzae*. Las enzimas de ambos microorganismos sintetizaron nuevos compuestos, siendo la de *B. circulans* la que generó una mayor producción (22% trisacáridos y 8.3% tetrasacáridos). Los compuestos mayoritarios fueron *β*-Gal*p*-(1→6)-Tre y *β*-Gal*p*-(1→4)-Tre. En el caso de los tetrasacáridos, se hallaron resultados relevantes, ya que se obtuvieron estructuras donde la molécula de trehalosa se encontraba en un extremo: *β*-Gal*p*-(1→4)-*β*-Gal*p*-(1→4)-Tre y *β*-Gal*p*-(1→4)-*β*-Gal*p*-(1→6)-Tre; y en la posición central: *β*-Gal*p*-(1→4)-*α*-Glc*p*-(1↔1)-[*β*-Gal*p*-(1→4)]-*α*-Glc*p*, *β*-Gal*p*-(1→4)-*α*-Glc*p*-(1↔1)-[*β*-Gal*p*-(1→6)]-*α*-Glc*p* y *β*-Gal*p*-(1→6)-*α*-Glc*p*-(1↔1)-[*β*-Gal*p*-(1→6)]-*α*-Glc*p*. Asimismo, destaca la producción de un pentasacárido: [*β*-Gal*p*-(1→4)]^3-Tre. Los derivados de trehalosa con el disacárido en posición terminal han sido obtenidos en estudios anteriores empleando procedimientos más complejos y con solventes orgánicos (Chaube *et al.*, 2016; Kim *et al.*, 2007). No obstante, los resultados aquí hallados son los primeros datos de síntesis de tetra- y pentasacáridos con enzimas comerciales y con la trehalosa en posición central. La presencia de los enlaces galactosil *β*(1→6) y *β*(1→4) podría contribuir a la disminución de los efectos negativos del *C. difficile*, debido a su resistencia parcial a las enzimas gastrointestinales (Ferreira-Lazarte, Gallego-Lobillo, *et al.*, 2019; Julio-Gonzalez *et al.*, 2019; *Capítulo 1 y 2*). Estas nuevas moléculas podrían tener potenciales efectos beneficiosos (**Sección 1.5**), por lo que el uso de *β*-galactosidasas de diferente origen podrían generar unas moléculas u otras, favoreciendo una posible producción a gran escala. Asimismo, estudios *in vivo* y de digestibilidad son necesarios para desengranar el comportamiento real de estos componentes en el organismo.

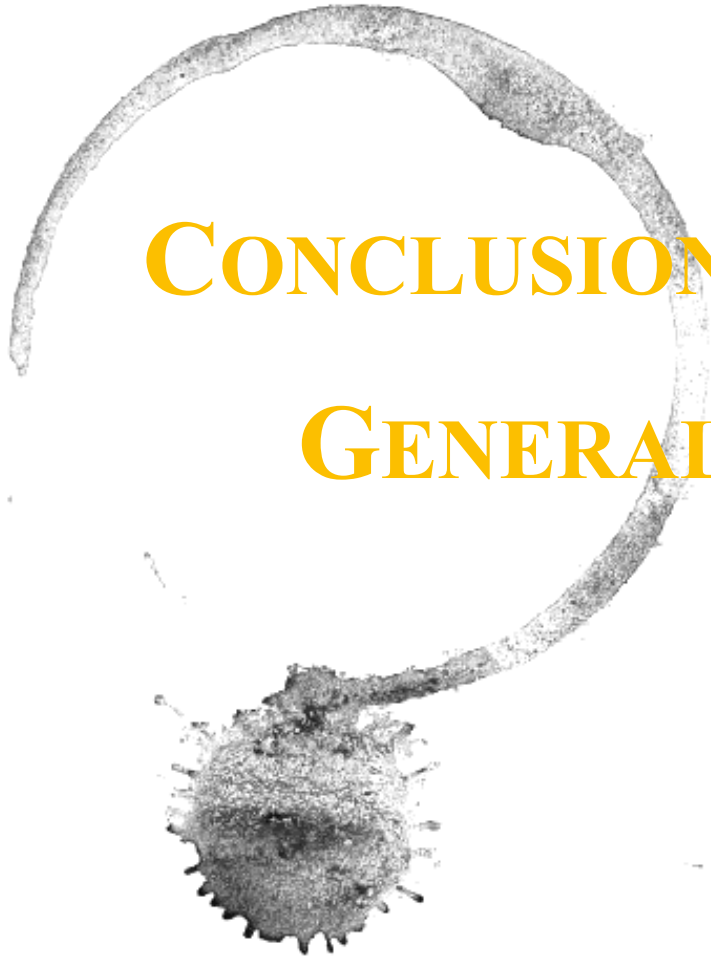

Conclusiones Generales

6. Conclusiones Generales

Los resultados obtenidos en la presente Tesis Doctoral, han derivado en las siguientes conclusiones:

I. El estudio cinético con el método de digestión *in vitro* con extracto de intestino delgado de rata (RSIE) permitió la optimización de las condiciones máximas de hidrólisis de la lactosa (0,2 mg/mL), obteniendo cerca de un 83% de hidrólisis tras 2 horas de digestión.

II. En las mismas condiciones que la lactosa, la lactulosa fue más resistente a la acción de las enzimas intestinales, obteniéndose un 20,4% de hidrólisis, así como una mayor resistencia digestiva de la segunda (galactosil-fructosa) en comparación con la lactosa (galactosil-glucosa).

III. En la digestión con extracto acetónico de intestino delgado de rata de polisacáridos y oligosacáridos prebióticos, la inulina y los fructanos fueron los más resistentes a la degradación intestinal, seguidos de los fructooligosacáridos (FOS) y los α-galactooligosacáridos (α-GOS) en último lugar.

IV. Los FOS con enlaces $\beta(2\rightarrow1)$ entre monómeros de fructosa (inulotriosa e inulotetraosa) fueron más susceptibles a la digestión intestinal que aquellos en los que la glucosa terminal estaba presente (kestosa y nistosa).

V. Se obtuvieron por primera vez datos relativos a la digestión de α-GOS, alcanzándose valores del 61,2% para la mezcla de α-GOS y 67,7% para el disacárido melibiosa.

VI. Con el protocolo InfoGest, la digestión de polisacáridos (almidón, dextrano y pectinas) fue muy escasa, sin cambios significativos en el contenido en carbohidratos, a excepción del almidón, debido a la acción de la α-amilasa pancreática.

VII. La incorporación del extracto de intestino delgado de rata, junto con el protocolo de digestión InfoGest, generó un aumento significativo en el grado de hidrólisis del dextrano (20,6%), la pectina modificada de cítricos (42,3%) y la pectina de

cítricos (17,2%), siendo esta última la más resistente al efecto de las enzimas digestivas. Estos resultados indicaron que la combinación del método *in vitro* con extracto acetónico de intestino delgado de rata y el protocolo InfoGest es una aproximación más real a la digestión en el intestino delgado.

VIII. En el estudio de la microbiota y el efecto del consumo de pectina y pectina modificada de cítricos en el cáncer colorrectal, se observó una disbiosis general de la microbiota intestinal en un modelo de rata (*Rattus norvegicus* F344) Destacó el incremento significativo del *phylum* de *Proteobacteria*; y de algunas familias beneficiosas (*Prevotellaceae, Bifidobacteriaceae*), no observándose ningún efecto positivo en la prevención de dicho cáncer.

IX. En la cohorte alimentada con pectina, las ratas presentaron niveles de glucosa postprandial y de triglicéridos en sangre menores con respecto a aquellos de los animales que no habían consumido dicho polisacárido.

X. El proceso de transgalactosilación, catalizado por *β*-galactosidasas de *Bacillus circulans* y *Aspergillus oryzae*, utilizando lactosa como donante y trehalosa como aceptor ha mostrado ser un proceso eficaz y útil para la síntesis de nuevos oligosacáridos derivados de la trehalosa.

XI. La producción de derivados de trehalosa fue mayor con la *β*-galactosidasa de *Bacillus circulans*. Los oligosacáridos predominantes fueron *β*-Gal*p*-(1→6)-Tre y *β*-Gal*p*-(1→4)-Tre. A su vez, se sintetizaron por primera vez tetrasacáridos con la trehalosa en posición central y el pentasacárido [*β*-Gal*p*-(1→4)]^3-Tre.

Teniendo en cuenta estos resultados, el trabajo llevado a cabo en la presente Tesis Doctoral ha permitido ahondar en el campo de la Nutrición y la Ciencia y Tecnología de los Alimentos, concretamente el de los carbohidratos prebióticos y su impacto dentro y fuera del aparato digestivo. Las limitaciones de los métodos tradicionales de digestibilidad de carbohidratos han quedado de manifiesto, por lo que un protocolo estandarizado y optimizado que unifique InfoGest y las disacaridasas del intestino delgado podría suponer una aproximación más real a la digestión ileal humana. Asimismo, la obtención de nuevos oligosacáridos resistentes a la digestión, como los derivados de trehalosa, podrían constituir una alternativa a la trehalosa, contribuyendo a la mejora de estados de disbiosis en la microbiota intestinal, especialmente en determinados procesos infecciosos.

Referencias

7. Referencias

Abdul-Hamid, A., & Luan, Y. S. (2000). Functional properties of dietary fibre prepared from defatted rice bran. *Food Chemistry*, *68*(1), 15-19.

Abdul Manas, N. H., Md. Illias, R., & Mahadi, N. M. (2018). Strategy in manipulating transglycosylation activity of glycosyl hydrolase for oligosaccharide production. *Critical Reviews in Biotechnology, 38*(2), 272-293.

Acuña-Rodríguez, I. S., Newsham, K. K., Gundel, P. E., Torres-Díaz, C., & Molina-Montenegro, M. A. (2020). Functional roles of microbial symbionts in plant cold tolerance. *Ecology Letters, 23*(6), 1034-1048.

Adetunji, L. R., Adekunle, A., Orsat, V., & Raghavan, V. (2017). Advances in the pectin production process using novel extraction techniques: A review. *Food Hydrocolloids, 62*, 239-250.

Ahn, J., & Hayes, R. B. (2020). Environmental Influences on the Human Microbiome and Implications for Noncommunicable Disease. *Annual Review of Public Health, 4*2, 277-292.

Ahn, J., Sinha, R., Pei, Z., Dominianni, C., Wu, J., Shi, J., Goedert, J. J., Hayes, R. B., & Yang, L. (2013). Human gut microbiome and risk for colorectal cancer. *Journal of the National Cancer Institute*, *105*(24), 1907-1911.

Ai, L., Chung, Y. C., Lin, S. Y., Lee, K. C., Lai, P. F. H., Xia, Y., Wang, G., & Cui, S. W. (2018). Active pectin fragments of high in vitro antiproliferation activities toward human colon adenocarcinoma cells: Rhamnogalacturonan II. *Food Hydrocolloids*, *83*, 239-245.

Ajisaka, K., & Fujimoto, H. (1990). Regioselective syntheses of trehalose-containing trisaccharides using various glycohydrolases. *Carbohydrate Research*, *199*(2),

227-234.

Alexandre, V., Even, P. C., Larue-Achagiotis, C., Blouin, J. M., Blachier, F., Benamouzig, R., Tomé, D., & Davila, A. M. (2013). Lactose malabsorption and colonic fermentations alter host metabolism in rats. *British Journal of Nutrition*, *110*(4), 625-631.

Algieri, F., Rodríguez-Nogales, A., Garrido-Mesa, N., Vezza, T., Garrido-Mesa, J., Utrilla, M. P., Montilla, A., Cardelle-Cobas, A., Olano, A., Corzo, N., Guerra-Hernández, E., Zarzuelo, A., Rodriguez-Cabezas, M. E., & Galvez, J. (2014). Intestinal anti-inflammatory effects of oligosaccharides derived from lactulose in the trinitrobenzenesulfonic acid model of rat colitis. *Journal of Agricultural and Food Chemistry*, *62*(19), 4285-4297.

Arai, C., Arai, N., Mizote, A., Kohno, K., Iwaki, K., Hanaya, T., Arai, S., Ushio, S., & Fukuda, S. (2010). Trehalose prevents adipocyte hypertrophy and mitigates insulin resistance. *Nutrition Research*, *30*(12), 840-848.

Arai, C., Miyake, M., Matsumoto, Y., Mizote, A., Yoshizane, C., Hanaya, Y., Koide, K., Yamada, M., Hanaya, T., Arai, S., & Fukuda, S. (2013). Trehalose prevents adipocyte hypertrophy and mitigates insulin resistance in mice with established obesity. *Journal of Nutritional Science and Vitaminology*, *59*(5), 393-401.

Armanian, A. M., Sadeghnia, A., Hoseinzadeh, M., Mirlohi, M., Feizi, A., Salehimehr, N., Saee, N., & Nazari, J. (2014). The effect of neutral oligosaccharides on reducing the incidence of necrotizing enterocolitis in preterm infants: A randomized clinical trial. *International Journal of Preventive Medicine*, *5*(11), 1387-1395.

Arthur, J. C., Gharaibeh, R. Z., Mühlbauer, M., Perez-Chanona, E., Uronis, J. M., McCafferty, J., Fodor, A. A., & Jobin, C. (2014). Microbial genomic analysis reveals the essential role of inflammation in bacteria-induced colorectal cancer. *Nature Communications*, *5*(1), 1-11.

Arthur, J. C., Perez-Chanona, E., Mühlbauer, M., Tomkovich, S., Uronis, J. M., Fan, T. J., Campbell, B. J., Abujamel, T., Dogan, B., Rogers, A. B., Rhodes, J. M., Stintzi, A., Simpson, K. W., Hansen, J. J., Keku, T. O., Fodor, A. A., & Jobin, C. (2012). Intestinal inflammation targets cancer-inducing activity of the microbiota. *Science*, *338*(6103), 120-123.

Arumugam, M., Raes, J., Pelletier, E., Le Paslier, D., Yamada, T., Mende, D. R., Fernandes, G. R., Tap, J., Bruls, T., Batto, J. M., Bertalan, M., Borruel, N., Casellas, F., Fernandez, L., Gautier, L., Hansen, T., Hattori, M., Hayashi, T., Kleerebezem, M., Kurokawa, K., Leclerc, M., Levenez, F., Manichanh, C., Nielsen, H. B., Nielsen, T., Pons, N., Poulain, J., Qin, J. J,. Sicheritz-Ponten, T., Tims, S., Torrents, D., Ugarte, E., Zoetendal, E. G., Wang, J., Guarner, F., Pedersen, O., de Vos, W. M., Brunak, S., Dore, J., Weissenbach, J., Ehrlich, S.D., & Bork, P. (2011). Enterotypes of the human gut microbiome. *Nature*, *473*(7346), 174-180.

Ávila-Fernández, Cuevas-Juárez, E., Rodríguez-Alegría, M. E., Olvera, C., & López-Munguía, A. (2016). Functional characterization of a novel *β*-fructofuranosidase from Bifidobacterium longum subsp. infantis ATCC 15697 on structurally diverse fructans. *Journal of Applied Microbiology*, *121*(1), 263-276.

Ayres, J. S., Trinidad, N. J., & Vance, R. E. (2012). Lethal inflammasome activation by a multidrug-resistant pathobiont upon antibiotic disruption of the microbiota. *Nature Medicine*, *18*(5), 799-806.

Bailey, M., Plunkett, F. J., Rothkötter, H. J., Vega-Lopez, M. A., Haverson, K., & Stokes, C. R. (2001). Regulation of mucosal immune responses in effector sites. *Proceedings of the Nutrition Society*, *60*(4), 427-435.

Baldelli, V., Scaldaferri, F., Putignani, L., & Del Chierico, F. (2021). The role of enterobacteriaceae in gut microbiota dysbiosis in inflammatory bowel diseases. *Microorganisms*, *9*(4), 1-15.

Bali, V., Panesar, P. S., Bera, M. B., & Panesar, R. (2015). Fructo-oligosaccharides: Production, Purification and Potential Applications. *Critical Reviews in Food Science and Nutrition*, *55*(11), 1475-1490.

Barengolts, E. (2016). Gut microbiota, prebiotics, probiotics, and synbiotics in management of obesity and prediabetes: Review of randomized controlled trials. *Endocrine Practice*, *22*(10), 1224-1234.

Bayless, T. M., Brown, E., & Paige, D. M. (2017). Lactase Non-persistence and Lactose Intolerance. *Current Gastroenterology Reports*, *19*(5), 23-34.

Belitz, H. D., Grosch, W., & Schieberle, P. (2009). Milk and dairy products. En *Food Chemistry* (pp. 498-545). Springer Berlin Heidelberg.

Belorkar, S. A., & Gupta, A. K. (2016). Oligosaccharides: A boon from nature's desk. *AMB Express*, *6*(1), 1-11.

Bernardino, S., Shiga, T. M., Harazono, Y., Hogan, V. A., Raz, A., Carpita, N. C., & Fabi, J. P. (2019). Migration and proliferation of cancer cells in culture are differentially affected by molecular size of modified citrus pectin. *Carbohydrate Polymers*, *211*, 141-151.

Blachier, F., Beaumont, M., Andriamihaja, M., Davila, A. M., Lan, A., Grauso, M., Armand, L., Benamouzig, R., & Tomé, D. (2017). Changes in the Luminal Environment of the Colonic Epithelial Cells and Physiopathological Consequences. *The American Journal of Pathology, 187*(3), 476-486.

Blachier, F., Davila, A. M., Mimoun, S., Benetti, P. H., Atanasiu, C., Andriamihaja, M., Benamouzig, R., Bouillaud, F., & Tomé, D. (2010). Luminal sulfide and large intestine mucosa: Friend or foe?. *Amino Acids, 39*(2), 335-347.

Blecker, C., Fougnies, C., Van Herck, J. C., Chevalier, J. P., & Paquot, M. (2002). Kinetic study of the acid hydrolysis of various oligofructose samples. *Journal of*

Agricultural and Food Chemistry, *50*(6), 1602-1607.

Botvynko, A., Bednářová, A., Henke, S., Shakhno, N., & Čurda, L. (2019). Production of galactooligosaccharides using various combinations of the commercial *β*-galactosidases. *Biochemical and Biophysical Research Communications*, *517*(4), 762-766.

Bradford, M. M. (1976). A rapid and sensitive method for the quantitation of microgram quantities of protein utilizing the principle of protein-dye binding. *Analytical Biochemistry*, *72*(1-2), 248-254.

Bray, F., Ferlay, J., Soerjomataram, I., Siegel, R. L., Torre, L. A., & Jemal, A. (2018). Global cancer statistics 2018: GLOBOCAN estimates of incidence and mortality worldwide for 36 cancers in 185 countries. *CA: A Cancer Journal for Clinicians*, *68*(6), 394-424.

Brenelli, S. L., Campos, S. D. S., & Saad, M. J. A. (1997). Viscosity of gums in vitro and their ability to reduce postprandial hyperglycemia in normal subjects. *Brazilian Journal of Medical and Biological Research*, *30*(12), 1437-1440.

Brobst, K. M., & Lott, C. E. J. (1966). Determination of some components in cron syrup by gas-liquid chromatography of the trimethylsilyl derivatives. *Cereal Chemistry*, *43*, 35-43.

Brodkorb, A., Egger, L., Alminger, M., Alvito, P., Assunção, R., Ballance, S., Bohn, T., Bourlieu-Lacanal, C., Boutrou, R., Carrière, F., Clemente, A., Corredig, M., Dupont, D., Dufour, C., Edwards, C., Golding, M., Karakaya, S., Kirkhus, B., Le Feunteun, S., Lesmes, U., Macierzanka, A., Mackie, A. R., Martins, C., Marze, S., McClements, D. J., Ménard, O., Minekus, M., Portmann, R., Santos, C. N., Souchon, I., Singh, R. P., Vegarud, G. E., Wickham, M. S. J., Weitschies, W., & Recio, I. (2019). INFOGEST static in vitro simulation of gastrointestinal food digestion. *Nature Protocols*, *14*(4), 991-1014.

Brouns, F., Theuwissen, E., Adam, A., Bell, M., Berger, A., & Mensink, R. P. (2012). Cholesterol-lowering properties of different pectin types in mildly hyper-cholesterolemic men and women. *European Journal of Clinical Nutrition*, *66*(5), 591-599.

Bustos, M. C., Vignola, M. B., Pérez, G. T., & León, A. E. (2017). In vitro digestion kinetics and bioaccessibility of starch in cereal food products. *Journal of Cereal Science*, *77*, 243-250.

Butnariu, M., & Sarac, I. (2019). Functional food. *International Journal of Nutrition*, *3*(3), 7-16.

Candela, M., Maccaferri, S., Turroni, S., Carnevali, P., & Brigidi, P. (2010). Functional intestinal microbiome, new frontiers in prebiotic design. *International Journal of Food Microbiology*, *140*(2-3), 93-101.

Cani, P. D., & Jordan, B. (2018). Gut microbiote-mediated inflammation in obesity: a link with gastrointestinal cancer. *Nature Reviews. Gastroenterology & Hepatology, 15*(11), 671-682.

Cani, P., Lecourt, E., Dewulf, E. M., Sohet, F. M., Pachikian, B. D., Naslain, D., De Backer, F., Neyrinck, A. M., & Delzenne, N. M. (2009). Gut microbiota fermentation of prebiotics increases satietogenic and incretin gut peptide production with consequences for appetite sensation and glucose response after a meal. *The American Journal of Clinical Nutrition*, *90*(5), 1236-1243.

Cao, H., Wong, S. C. Y., Yam, W. C., Liu, M. C. J., Chow, K. H., Wu, A. K. L., & Ho, P. L. (2019). Genomic investigation of a sequence type 67 *Clostridium* difficile causing community-acquired fulminant colitis in Hong Kong. *International Journal of Medical Microbiology*, *309*(5), 270-273.

Cardelle-Cobas, A., Olano, A., Irazoqui, G., Giacomini, C., Batista-Viera, F., Corzo, N.,

& Corzo-Martínez, M. (2016). Synthesis of Oligosaccharides Derived from Lactulose (OsLu) Using Soluble and Immobilized Aspergillus oryzae *β*-Galactosidase. *Frontiers in Bioengineering and Biotechnology*, *4*(21), 1-10.

Cardelle-Cobas, A., Villamiel, M., Olano, A., & Corzo, N. (2008). Study of galacto-oligosaccharide formation from lactose using Pectinex Ultra SP-L. *Journal of the Science of Food and Agriculture*, *88*(6), 954-961.

Carnachan, S. M., Bootten, T. J., Mishra, S., Monro, J. A., & Sims, I. M. (2012). Effects of simulated digestion in vitro on cell wall polysaccharides from kiwifruit (Actinidia spp.). *Food Chemistry*, *133*(1), 132-139.

Catanzaro, R., Sciuto, M., & Marotta, F. (2021). Lactose intolerance: An update on its pathogenesis, diagnosis, and treatment. *Nutrition Research, 89*, 23-34.

Chambers, E. S., Preston, T., Frost, G., & Morrison, D. J. (2018). Role of Gut Microbiota-Generated Short-Chain Fatty Acids in Metabolic and Cardiovascular Health. *Current Nutrition Reports, 7*(4), 198-206.

Champe, P. C., & Harvey, R. A. (1994). *Biochemistry (Lippincott's illustrated reviews)*. Lippincott Williams & Wilkins.

Chan, S. Y., Choo, W. S., Young, D. J., & Loh, X. J. (2017). Pectin as a rheology modifier: Origin, structure, commercial production and rheology. *Carbohydrate Polymers, 161*, 118-139.

Chau, C. F., & Huang, Y. L. (2003). Comparison of the chemical composition and physicochemical properties of different fibers prepared from the peel of citrus sinensis L. Cv. Liucheng. *Journal of Agricultural and Food Chemistry*, *51*(9), 2615-2618.

Chaube, M. A., Sarpe, V. A., Jana, S., & Kulkarni, S. S. (2016). First total synthesis of trehalose containing tetrasaccharides from: Mycobacterium smegmatis. *Organic*

and Biomolecular Chemistry, *14*(24), 5595-5598.

Chen, C. W., Ou-Yang, C. C., & Yeh, C. W. (2003). Synthesis of galactooligosaccharides and transgalactosylation modeling in reverse micelles. *Enzyme and Microbial Technology*, *33*(4), 497-507.

Chen, D., Chen, G., Wan, P., Hu, B., Chen, L., Ou, S., Zeng, X., & Ye, H. (2017). Digestion under saliva, simulated gastric and small intestinal conditions and fermentation in vitro of polysaccharides from the flowers of Camellia sinensis induced by human gut microbiota. *Food and Function*, *8*(12), 4619-4629.

Chen, Q., Liu, M., Zhang, P., Fan, S., Huang, J., Yu, S., Zhang, C., & Li, H. (2019). Fucoidan and galactooligosaccharides ameliorate high-fat diet–induced dyslipidemia in rats by modulating the gut microbiota and bile acid metabolism. *Nutrition*, *65*, 50-59.

Chen, Q., Zhu, L., Tang, Y., Zhao, Z., Yi, T., & Chen, H. (2017). Preparation-related structural diversity and medical potential in the treatment of diabetes mellitus with ginseng pectins. *Annals of the New York Academy of Sciences*, 1401(1), 75-89.

Cheng, H., Li, S., Fan, Y., Gao, X., Hao, M., Wang, J., Zhang, X., Tai, G., & Zhou, Y. (2011). Comparative studies of the antiproliferative effects of ginseng polysaccharides on HT-29 human colon cancer cells. *Medical Oncology*, *28*(1), 175-181.

Cho, Y., Turner, N. D., Davidson, L. A., Chapkin, R. S., Carroll, R. J., & Lupton, J. R. (2012). A chemoprotective fish oil/pectin diet enhances apoptosis via Bcl-2 promoter methylation in rat azoxymethane-induced carcinomas. *Experimental Biology and Medicine*, *237*(12), 1387-1393.

Christiaens, S., Van Buggenhout, S., Houben, K., Jamsazzadeh Kermani, Z., Moelants, K. R. N., Ngouémazong, E. D., Van Loey, A., & Hendrickx, M. E. G. (2016).

Process–Structure–Function Relations of Pectin in Food. *Critical Reviews in Food Science and Nutrition, 56*(6), 1021-1042.

Christodoulides, S., Dimidi, E., Fragkos, K. C., Farmer, A. D., Whelan, K., & Scott, S. M. (2016). Systematic review with meta-analysis: Effect of fibre supplementation on chronic idiopathic constipation in adults. *Alimentary Pharmacology and Therapeutics*, *44*(2), 103-116.

Ciriminna, R., Fidalgo, A., Delisi, R., Ilharco, L. M., & Pagliaro, M. (2016). Pectin production and global market. *Agro Food Industry Hi-Tech*, *27*(5), 17-20.

Cockburn, D. W., & Koropatkin, N. M. (2016). Polysaccharide Degradation by the Intestinal Microbiota and Its Influence on Human Health and Disease. *Journal of Molecular Biology, 428*(16), 3230-3252.

Codex Alimentarius Comission. Guidelines on nutrition labelling CAC/GL 2-1985 as Last Amended 2010. Joint FAO/WHO Food Standards Programme, Secretariat of the Codex Alimentarius Commission. Rome, Italy: FAO. 2010.

Collins, J., Robinson, C., Danhof, H., Knetsch, C. W., Van Leeuwen, H. C., Lawley, T. D., Auchtung, J. M., & Britton, R. A. (2018). Dietary trehalose enhances virulence of epidemic *Clostridium* difficile. *Nature*, *553*(7688), 291-294.

Contor, L. (2001). Functional Food Science in Europe. *Nutrition, Metabolism and Cardiovascular Diseases*, *11*(4 Suppl), 20-23.

Corebima, B. I. R. V., Rohsiswatmo, R., Gayatri, P., & Patole, S. (2019). Fecal human *β*-defensin-2 (hBD-2) levels and gut microbiota patterns in preterm neonates with different feeding patterns. *Iranian Journal of Microbiology*, *11*(2), 151-159.

Corzo, N., Alonso, J. L., Azpiroz, F., Calvo, M. A., Cirici, M., Leis, R., Lombó, F., Mateos-Aparicio, I., Plou, F. J., Ruas-Madiedo, P., Rúperez, P., Redondo-Cuenca, A., Sanz, M. L., & Clemente, A. (2015). Prebióticos; Concepto, propiedades y

efectos beneficiosos. *Nutricion Hospitalaria*, *31*, 99-118.

Coste, I., Judlin, P., Lepargneur, J.-P., & Bou-Antoun, S. (2012). Safety and Efficacy of an Intravaginal Prebiotic Gel in the Prevention of Recurrent Bacterial Vaginosis: A Randomized Double-Blind Study. *Obstetrics and Gynecology International*, *2012*, 1-7.

Crittenden, R. (2012). Emerging Prebiotic Carbohydrates. En B. Rastall & G. Gibson (Eds.), *Prebiotics: Development & Application* (pp. 111-133). John Wiley & Sons.

Cuello-Garcia, C. A., Fiocchi, A., Pawankar, R., Yepes-Nuñez, J. J., Morgano, G. P., Zhang, Y., Ahn, K., Al-Hammadi, S., Agarwal, A., Gandhi, S., Beyer, K., Burks, W., Canonica, G. W., Ebisawa, M., Kamenwa, R., Lee, B. W., Li, H., Prescott, S., Riva, J. J., Rosenwasser, L., Sampson, H., Spigler, M., Terracciano, L., Vereda, A., Waserman, S., Schünemann, H. J., & Brozek, J. L. (2016). World Allergy Organization-McMaster University Guidelines for Allergic Disease Prevention (GLAD-P): Prebiotics. *World Allergy Organization Journal*, *9*(1), 1-10.

Cui, J., Gu, X., Zhang, Q., Ou, Y., & Wang, J. (2015). Production and anti-diabetic activity of soluble dietary fiber from apricot pulp by Trichoderma viride fermentation. *Food and Function*, *6*(5), 1635-1642

Dahl, W. J., & Stewart, M. L. (2015). Position of the Academy of Nutrition and Dietetics: Health Implications of Dietary Fiber. *Journal of the Academy of Nutrition and Dietetics*, *115*(11), 1861-1870.

De Filippo, C., Cavalieri, D., Di Paola, M., Ramazzotti, M., Poullet, J. B., Massart, S., Collini, S., Pieraccini, G., & Lionetti, P. (2010). Impact of diet in shaping gut microbiota revealed by a comparative study in children from Europe and rural Africa. *Proceedings of the National Academy of Sciences of the United States of America*, *107*(33), 14691-14696.

DeBosch, B. J., Heitmeier, M. R., Mayer, A. L., Higgins, C. B., Crowley, J. R., Kraft, T. E., Chi, M., Newberry, E. P., Chen, Z., Finck, B. N., Davidson, N. O., Yarasheski, K. E., Hruz, P. W., & Moley, K. H. (2016). Trehalose inhibits solute carrier 2A (SLC2A) proteins to induce autophagy and prevent hepatic steatosis. *Science Signaling*, *9*(416), ra21-ra21.

Di Natale, G., Zimbone, S., Bellia, F., Tomasello, M. F., Giuffrida, M. L., Pappalardo, G., & Rizzarelli, E. (2018). Potential therapeutics of Alzheimer's diseases: New insights into the neuroprotective role of trehalose-conjugated beta sheet breaker peptides. *Peptide Science*, *110*(5), e24083.

Di Rienzo, T., D'Angelo, G., D'Aversa, F., Campanale, M. C., Cesario, V., Montalto, M., Gasbarrini, A., & Ojetti, V. (2013). Lactose intolerance: from diagnosis to correct management. *European Review for Medical and Pharmacological Sciences*, *17*(Suppl 2), 18-25.

do Prado, S. B. R., Shiga, T. M., Harazono, Y., Hogan, V. A., Raz, A., Carpita, N. C., & Fabi, J. P. (2019). Migration and proliferation of cancer cells in culture are differentially affected by molecular size of modified citrus pectin. *Carbohydrate Polymers*, *211*, 141-151.

Dona, A. C., Pages, G., Gilbert, R. G., & Kuchel, P. W. (2010). Digestion of starch: In vivo and in vitro kinetic models used to characterise oligosaccharide or glucose release. *Carbohydrate Polymers, 80*(3), 599-617.

Donaldson, G. P., Lee, S. M., & Mazmanian, S. K. (2016). Gut biogeography of the bacterial microbiota. *Nature Reviews Microbiology, 14*(1), 20-32.

Dongowski, G., Lorenz, A., & Proll, J. (2002). The Degree of Methylation Influences the Degradation of Pectin in the Intestinal Tract of Rats and In Vitro. *The Journal of Nutrition*, *132*(7), 1935-1944.

Drakoularakou, A., Tzortzis, G., Rastall, R. A., & Gibson, G. R. (2010). A double-blind, placebo-controlled, randomized human study assessing the capacity of a novel galacto-oligosaccharide mixture in reducing travellers' diarrhoea. *European Journal of Clinical Nutrition*, *64*(2), 146-152.

EFSA NDA Panel on Dietetic Products Nutrition and Allergies. (2014). Scientific Opinion on the substantiation of a health claim related to AlphaGOS® and a reduction of post-prandial glycaemic responses pursuant to Article 13(5) of Regulation (EC) No 1924/2006. *EFSA Journal*, *12*(10), 3838.

EFSA NDA Panel on Dietetic Products Nutrition and Allergies. (2015). Scientific Opinion on the substantiation of a health claim related to "native chicory inulin" and maintenance of normal defecation by increasing stool frequency pursuant to Article 13.5 of Regulation (EC) No 1924/2006. *EFSA Journal*, *13*(1), 3951.

EFSA Panel on Dietetic Products Nutrition and Allergies (NDA). (2010). Scientific Opinion on Dietary Reference Values for carbohydrates and dietary fibre. *EFSA Journal*, *8*(3), 1462.

Egger, L., Schlegel, P., Baumann, C., Stoffers, H., Guggisberg, D., Brügger, C., Dürr, D., Stoll, P., Vergères, G., & Portmann, R. (2017). Physiological comparability of the harmonized INFOGEST in vitro digestion method to in vivo pig digestion. *Food Research International*, *102*, 567-574.

Emanuele, E. (2014). Can Trehalose Prevent Neurodegeneration? Insights from Experimental Studies. *Current Drug Targets*, *15*(5), 551-557.

Endt, K., Stecher, B., Chaffron, S., Slack, E., Tchitchek, N., Benecke, A., van Maele, L., Sirard, J. C., Mueller, A. J., Heikenwalder, M., Macpherson, A. J., Strugnell, R., von Mering, C., & Hardt, W. D. (2010). The microbiota mediates pathogen clearance from the gut lumen after non-typhoidal salmonella diarrhea. *PLoS Pathogens*, *6*(9), e1001097.

Englyst, H. N., Kingman, S. M., & Cummings, J. H. (1992). Classification and measurement of nutritionally important starch fractions. *European Journal of Clinical Nutrition*, *46*(2), S33-50.

Englyst, K., Goux, A., Meynier, A., Quigley, M., Englyst, H., Brack, O., & Vinoy, S. (2018). Inter-laboratory validation of the starch digestibility method for determination of rapidly digestible and slowly digestible starch. *Food Chemistry*, *245*, 1183-1189.

EU Commission. (2012). Commission regulation (EU) Nº 231/2012 of 9 March 2012 laying down specifications for food additives listed in Annexes II and III to Regulation (EC) Nº 1333/2008 of the European Parliament and of the Council. *Official Journal of the European Union*, *55*, 1-295.

Fan, Y., Yi, J., Zhang, Y., Wen, Z., & Zhao, L. (2017). Physicochemical stability and in vitro bioaccessibility of *β*-carotene nanoemulsions stabilized with whey protein-dextran conjugates. *Food Hydrocolloids*, *63*, 256-264.

Feher, J. (2017). Digestion and Absorption of the Macronutrients. En *Quantitative Human Physiology* (pp. 821-833). Academic Press.

Fernandes, J. M., Madalena, D. A., Pinheiro, A. C., & Vicente, A. A. (2020). Rice in vitro digestion: application of INFOGEST harmonized protocol for glycemic index determination and starch morphological study. *Journal of Food Science and Technology*, *57*(4), 1393-1404.

Fernandes, R., do Rosario, V. A., Mocellin, M. C., Kuntz, M. G. F., & Trindade, E. B. S. M. (2017). Effects of inulin-type fructans, galacto-oligosaccharides and related synbiotics on inflammatory markers in adult patients with overweight or obesity: A systematic review. *Clinical Nutrition, 36*(5), 1197-1206.

Fernández, J., De La Fuente, V. G., Fernández García, M. T., Sánchez, G. J., Redondo,

B. I., Villar, C. J., & Lombó, F. (2020). A diet based on cured acorn-fed ham with oleic acid content promotes anti-inflammatory gut microbiota and prevents ulcerative colitis in an animal model. *Lipids in Health and Disease*, *19*(1), 1-19.

Fernández, J., García, L., Monte, J., Villar, C. J., & Lombó, F. (2018). Functional anthocyanin-rich sausages diminish colorectal cancer in an animal model and reduce pro-inflammatory bacteria in the intestinal microbiota. *Genes*, *9*(3), 133.

Fernández, Javier, Ledesma, E., Monte, J., Millán, E., Costa, P., de la Fuente, V. G., García, M. T. F., Martínez-Camblor, P., Villar, C. J., & Lombó, F. (2019). Traditional Processed Meat Products Re-designed Towards Inulin-rich Functional Foods Reduce Polyps in Two Colorectal Cancer Animal Models. *Scientific Reports*, *9*(1), 14783.

Fernández, J., Moreno, F. J., Olano, A., Clemente, A., Villar, C. J., & Lombó, F. (2018). A galacto-oligosaccharides preparation derived from lactulose protects against colorectal cancer development in an animal model. *Frontiers in Microbiology*, *9*(2004), 1-14.

Fernández, J., Redondo-Blanco, S., Gutiérrez-del-Río, I., Miguélez, E. M., Villar, C. J., & Lombó, F. (2016). Colon microbiota fermentation of dietary prebiotics towards short-chain fatty acids and their roles as anti-inflammatory and antitumour agents: A review. *Journal of Functional Food*s, 25, 511-522.

Ferrario, C., Statello, R., Carnevali, L., Mancabelli, L., Milani, C., Mangifesta, M., Duranti, S., Lugli, G. A., Jimenez, B., Lodge, S., Viappiani, A., Alessandri, G., Dall'Asta, M., Rio, D. Del, Sgoifo, A., van Sinderen, D., Ventura, M., & Turroni, F. (2017). How to feed the Mammalian gut microbiota: Bacterial and metabolic modulation by dietary fibers. *Frontiers in Microbiology*, *8*(1749), 1-11.

Ferreira-Lazarte, A. (2019). *In vitro digestibility and fermentability of selected prebiotics and functional carbohydrates with prebiotic potential*. [Tesis Doctoral,

Universidad Autónoma de Madrid]. Repositorio Institucional Universidad Autónoma de Madrid.

Ferreira-Lazarte, A., Gallego-Lobillo, P., Moreno, F. J., Villamiel, M., & Hernández-Hernández, O. (2019). In vitro digestibility of galactooligosaccharides: effect of the structural features on their intestinal degradation. *Journal of Agricultural and Food Chemistry*, *67*(16), 4662-4670.

Ferreira-Lazarte, A., Kachrimanidou, V., Villamiel, M., Rastall, R. A., & Moreno, F. J. (2018). In vitro fermentation properties of pectins and enzymatic-modified pectins obtained from different renewable bioresources. *Carbohydrate Polymers*, *199*, 482-491.

Ferreira-Lazarte, A., Montilla, A., Mulet-Cabero, A. I., Rigby, N., Olano, A., Mackie, A., & Villamiel, M. (2017). Study on the digestion of milk with prebiotic carbohydrates in a simulated gastrointestinal model. *Journal of Functional Foods*, *33*, 149-154.

Ferreira-Lazarte, A., Moreno, F. J., Cueva, C., Gil-Sánchez, I., & Villamiel, M. (2019). Behaviour of citrus pectin during its gastrointestinal digestion and fermentation in a dynamic simulator (simgi®). *Carbohydrate Polymers*, *207*, 382-390.

Ferreira-Lazarte, A., Moreno, F. J., & Villamiel, M. (2020). Bringing the digestibility of prebiotics into focus: update of carbohydrate digestion models. *Critical Reviews in Food Science and Nutrition, 61*(19), 1-12.

Ferreira-Lazarte, A., Olano, A., Villamiel, M., & Moreno, F. J. (2017). Assessment of in vitro digestibility of dietary carbohydrates using rat small intestinal extract. *Journal of Agricultural and Food Chemistry*, *65*(36), 8046-8053.

Ferreira, M. da F., Salavati Schmitz, S., Schoenebeck, J. J., Clements, D. N., Campbell, S. M., Gaylor, D. E., Mellanby, R. J., Gow, A. G., & Salavati, M. (2019). Lactulose drives a reversible reduction and qualitative modulation of the faecal microbiota

diversity in healthy dogs. *Scientific Reports*, *9*(1), 1-11.

Flemer, B., Herlihy, M., O'Riordain, M., Shanahan, F., & O'Toole, P. W. (2018). Tumour-associated and non-tumour-associated microbiota: Addendum. *Gut microbes*, *9*(4), 369-373.

Flint, H. J., Scott, K. P., Duncan, S. H., Louis, P., & Forano, E. (2012). Microbial degradation of complex carbohydrates in the gut. *Gut Microbes, 3*(4), 289-306.

Flint, H. J., Scott, K. P., Louis, P., & Duncan, S. H. (2012). The role of the gut microbiota in nutrition and health. *Nature Reviews Gastroenterology and Hepatology, 9*(10), 577-589.

Flores-Maltos, D. A., Mussatto, S. I., Contreras-Esquivel, J. C., Rodríguez-Herrera, R., Teixeira, J. A., & Aguilar, C. N. (2016). Biotechnological production and application of fructooligosaccharides. *Critical Reviews in Biotechnology*, *36*(2), 259-267.

Franck, A. (2002). Technological functionality of inulin and oligofructose. *British Journal of Nutrition*, *87*(S2), S287-S291.

Freitas, D., & Le Feunteun, S. (2019). Oro-gastro-intestinal digestion of starch in white bread, wheat-based and gluten-free pasta: Unveiling the contribution of human salivary *α*-amylase. *Food Chemistry*, *274*, 566-573.

Freitas, D., Le Feunteun, S., Panouillé, M., & Souchon, I. (2018). The important role of salivary *α*-amylase in the gastric digestion of wheat bread starch. *Food and Function*, *9*(1), 200-208.

Gaillet, C., Lequart, C., Debeire, P., & Nuzillard, J. M. (1999). Band-selective HSQC and HMBC experiments using excitation sculpting and PFGSE. *Journal of Magnetic Resonance*, *139*(2), 454-459.

Gallego-Lobillo, P., Ferreira-Lazarte, A., Hernández-Hernández, O., Montilla, A., & Villamiel, M. (2020). Evaluation of the impact of a rat small intestinal extract on the digestion of four different functional fibers. *Food and Function*, *11*(5), 4081-4089.

Gänzle, M. G. (2012). Enzymatic synthesis of galacto-oligosaccharides and other lactose derivatives (hetero-oligosaccharides) from lactose. *International Dairy Journal, 22*(2), 116-122.

Garcia-Campayo, V., Han, S., Vercauteren, R., & Franck, A. (2018). Digestion of food ingredients and food using an in vitro model integrating intestinal mucosal enzymes. *Food and Nutrition Sciences*, *9*(6), 711-734.

Garcia, C. A., & Gardner, J. G. (2021). Bacterial *α*-diglucoside metabolism: perspectives and potential for biotechnology and biomedicine. *Applied Microbiology and Biotechnology, 105*(10), 4033-4052.

Ghouri, Y. A., Richards, D. M., Rahimi, E. F., Krill, J. T., Jelinek, K. A., & DuPont, A. W. (2014). Systematic review of randomized controlled trials of probiotics, prebiotics, and synbiotics in infammatory bowel disease. *Clinical and Experimental Gastroenterology*, *7*, 473-487.

Gibson, G. R., & Roberfroid, M. B. (1995). Dietary modulation of the human colonic microbiota: Introducing the concept of prebiotics. *Journal of Nutrition, 125*(6), 1401-1412.

Gibson, Glenn R., Hutkins, R., Sanders, M. E., Prescott, S. L., Reimer, R. A., Salminen, S. J., Scott, K., Stanton, C., Swanson, K. S., Cani, P. D., Verbeke, K., & Reid, G. (2017). Expert consensus document: The International Scientific Association for Probiotics and Prebiotics (ISAPP) consensus statement on the definition and scope of prebiotics. *Nature Reviews Gastroenterology and Hepatology*, *14*(8), 491-502.

Gibson, Glenn R., Probert, H. M., Loo, J. Van, Rastall, R. A., & Roberfroid, M. B. (2004). Dietary modulation of the human colonic microbiota: updating the concept of prebiotics. *Nutrition Research Reviews*, *17*(2), 259-275.

Gibson, Glenn R, Scott, K. P., Rastall, R. A., Tuohy, K. M., Hotchkiss, A., Dubert-Ferrandon, A., Gareau, M., Murphy, E. F., Saulnier, D., Loh, G., Macfarlane, S., Delzenne, N., Ringel, Y., Kozianowski, G., Dickmann, R., Lenoir-Wijnkoop, I., Walker, C., & Buddington, R. (2010). Dietary prebiotics: current status and new definition. *Food Science & Technology Bulletin: Functional Foods*, *7*(1), 1-19.

Glinsky, V. V., & Raz, A. (2009). Modified citrus pectin anti-metastatic properties: one bullet, multiple targets. *Carbohydrate Research, 344*(14), 1788-1791.

Gómez, B., Gullón, B., Yáñez, R., Schols, H., & Alonso, J. L. (2016). Prebiotic potential of pectins and pectic oligosaccharides derived from lemon peel wastes and sugar beet pulp: A comparative evaluation. *Journal of Functional Foods*, *20*, 108-121.

Grand View Research. (2010). *Prebiotics market size, share & trends analysis by ingredients (FOS, Inulin, GOS, MOS), by application (food and beverages, dietary supplements, animal feed), by region, and segment forecasts, 2014 - 2024*. https://www.grandviewresearch.com/industry-analysis/prebiotics-market.

Greg Kelly, N. D. (2008). Inulin-Type Prebiotics - A Review: Part 1. *Alternative Medicine Review*, *13*(4), 315-329.

Grunberger, G., Jen, K. L. C., & Artiss, J. D. (2007). The benefits of early intervention in obese diabetic patients with FBCx™ - A new dietary fibre. *Diabetes/Metabolism Research and Reviews*, *23*(1), 56-62.

Guinane, C. M., & Cotter, P. D. (2013). Role of the gut microbiota in health and chronic gastrointestinal disease: Understanding a hidden metabolic organ. *Therapeutic Advances in Gastroenterology*, *6*(4), 295-308.

Halstead, F. D., Ravi, A., Thomson, N., Nuur, M., Hughes, K., Brailey, M., & Oppenheim, B. A. (2019). Whole genome sequencing of toxigenic *Clostridium* difficile in asymptomatic carriers: insights into possible role in transmission. *Journal of Hospital Infection*, *102*(2), 125-134.

Han, K. H., Tsuchihira, H., Nakamura, Y., Shimada, K. I., Ohba, K., Aritsuka, T., Uchino, H., Kikuchi, H., & Fukushima, M. (2013). Inulin-type fructans with different degrees of polymerization improve lipid metabolism but not glucose metabolism in rats fed a high-fat diet under energy restriction. *Digestive Diseases and Sciences*, *58*(8), 2177-2186.

Han, X., Xie, Y., Wu, Q., & Wu, S. (2018). A novel protein digestion method with the assistance of alternating current denaturation for high efficient protein digestion and mass spectrometry analysis. *Talanta*, *184*, 382-387.

Hernaiz-Leonardo, J. C., Golzarri, M. F., Cornejo-Juárez, P., Volkow, P., Velázquez, C., Ostrosky-Frid, M., & Vilar-Compte, D. (2017). Microbiology of surgical site infections in patients with cancer: A 7-year review. *American Journal of Infection Control*, *45*(7), 761-766.

Hernández-Hernández, O. (2019). In vitro Gastrointestinal Models for Prebiotic Carbohydrates: A Critical Review. *Current Pharmaceutical Design*, *25*(32), 3478-3483.

Hérnandez-Hérnandez, O. (2012). *Desarrollo de nuevos métodos para la caracterización estructural de carbohidratos prebióticos y péptidos funcionales de interés alimentario. Estudio de su bioactividad.* [Tesis Doctoral, Universidad Autónoma de Madrid]. Repositorio Institucional Universidad Autónoma de Madrid.

Hernández-Hernández, O., Marin-Manzano, M. C., Rubio, L. A., Moreno, F. J., Sanz, M. L., & Clemente, A. (2012). Monomer and linkage type of galacto-

oligosaccharides affect their resistance to ileal digestion and prebiotic properties in rats. *Journal of Nutrition*, *142*(7), 1232-1239.

Hernández-Hernández, O., Montañés, F., Clemente, A., Moreno, F. J., & Sanz, M. L. (2011). Characterization of galactooligosaccharides derived from lactulose. *Journal of Chromatography A*, *1218*(42), 7691-7696.

Hernández-Hernández, O., Olano, A., Rastall, R. A., & Moreno, F. J. (2019). In vitro digestibility of dietary carbohydrates: Toward a standardized methodology beyond amylolytic and microbial enzymes. *Frontiers in Nutrition*, *6*(61), 1-5.

Hernández-Hernández, O., Ruiz-Matute, A. I., Olano, A., Moreno, F. J., & Sanz, M. L. (2009). Comparison of fractionation techniques to obtain prebiotic galactooligosaccharides. *International Dairy Journal*, *19*(9), 531-536.

Higashiyama, T. (2002). Novel functions and applications of trehalose. *Pure and Applied Chemistry*, *74*(7), 1263-1269.

Ho, Y. Y., Lin, C. M., & Wu, M. C. (2017). Evaluation of the prebiotic effects of citrus pectin hydrolysate. *Journal of Food and Drug Analysis*, *25*(3), 550-558.

Holck, J., Hotchkiss, A. T., Meyer, A. S., Mikkelsen, J. D., & Rastall, R. A. (2014). Production and bioactivity of pectic oligosaccharides from fruit and vegetable biomass. En F. J. Moreno & M. L. Sanz (Eds.), *Food Oligosaccharides: Production, Analysis and Bioactivity* (pp. 76-87). John Wiley & Sons.

Holloway, W. D., Tasman-Jones, C., & Maher, K. (1983). Pectin digestion in humans. *The American Journal of Clinical Nutrition*, *37*(2), 253-255.

Hooton, D., Lentle, R., Monro, J., Wickham, M., & Simpson, R. (2015). The Secretion and Action of Brush Border Enzymes in the Mammalian Small Intestine. *Review in physiological Biochemistry Pharmacology*, *168*, 59-118.

Hosseinpour-Moghaddam, K., Caraglia, M., & Sahebkar, A. (2018). Autophagy induction by trehalose: Molecular mechanisms and therapeutic impacts. *Journal of Cellular Physiology, 233*(9), 6524-6543.

Hove, H., & Mortensen, P. B. (1995). Influence of intestinal inflammation (IBD) and small and large bowel length on fecal short-chain fatty acids and lactate. *Digestive Diseases and Sciences*, *40*(6), 1372-1380.

Hu, J. L., Nie, S. P., & Xie, M. Y. (2018). Antidiabetic mechanism of dietary polysaccharides based on their gastrointestinal functions. *Journal of Agricultural and Food Chemistry*, *66*(19), 4781-4786.

Huang, F., Liu, Y., Zhang, R., Bai, Y., Dong, L., Liu, L., Jia, X., Wang, G., & Zhang, M. (2019). Structural characterization and in vitro gastrointestinal digestion and fermentation of litchi polysaccharide. *International Journal of Biological Macromolecules*, *140*, 965-972.

Hume, M. P., Nicolucci, A. C., & Reimer, R. A. (2017). Prebiotic supplementation improves appetite control in children with overweight and obesity: A randomized controlled trial. *American Journal of Clinical Nutrition*, *105*(4), 790-799.

Ishii, T., Tanimoto, M., Itagaki, Y., Honda, Y., Win, T. T., Kawase, C., Kita, A., Onodera, S., Ito, H., Matsui, H., & Honma, M. (2000). Enzymatic synthesis of nonreducing trisaccharide containing lactose and trehalose as a part of the structure. *Journal of Applied Glycoscience*, *47*(2), 193-196.

Jacobasch, G., Dongowski, G., Florian, S., Müller-Schmehl, K., Raab, B., & Schmiedl, D. (2008). Pectin does not inhibit intestinal carcinogenesis in APC-deficient min/+ mice. *Journal of Agricultural and Food Chemistry*, *56*(4), 1501-1510.

Jacobs, L. R., & Lupton, J. R. (1986). Relationship between colonic luminal pH, cell proliferation, and colon carcinogenesis in 1,2-dimethylhydrazine treated rats fed

high fiber diets. *Cancer Research*, *46*(4 Part 1), 1727-1734.

Jandhyala, S. M., Talukdar, R., Subramanyam, C., Vuyyuru, H., Sasikala, M., & Reddy, D. N. (2015). Role of the normal gut microbiota. *World Journal of Gastroenterology*, *21*(29), 8836-8847.

Jantscher-Krenn, E., Marx, C., & Bode, L. (2013). Human milk oligosaccharides are differentially metabolised in neonatal rats. *British Journal of Nutrition*, *110*(4), 640-650.

Joseph, N., Vasodavan, K., Saipudin, N. A., Yusof, B. N. M., Kumar, S., & Nordin, S. A. (2019). Gut microbiota and short-chain fatty acids (SCFAs) profiles of normal and overweight school children in Selangor after probiotics administration. *Journal of Functional Foods*, *57*, 103-111.

Julio-González, L. C., Hernández-Hernández, O., Moreno, F. J., Jimeno, M. L., García Doyagüez, E., Olano, A., & Corzo, N. (2020). Hydrolysis and transgalactosylation catalysed by *β*-galactosidase from brush border membrane vesicles isolated from pig small intestine : A study using lactulose and its mixtures with lactose or galactose as substrates. *Food Research International*, *129*, 108811.

Julio-Gonzalez, L. C., Hernández-Hernández, O., Moreno, F. J., Olano, A., Jimeno, M. L., & Corzo, N. (2019). Trans-*β*-galactosidase activity of pig enzymes embedded in the small intestinal brush border membrane vesicles. *Scientific Reports*, *9*(1), 2-11.

Jung, C., Hugot, J.P., & Barreau, F. (2010). Peyer's Patches: The Immune Sensors of the Intestine. *International Journal of Inflammation*, *2010*, 1-12.

Kamada, N., Kim, Y. G., Sham, H. P., Vallance, B. A., Puente, J. L., Martens, E. C., & Núñez, G. (2012). Regulated virulence controls the ability of a pathogen to compete with the gut microbiota. *Science*, *336*(6086), 1325-1329.

Khalifeh, M., Barreto, G. E., & Sahebkar, A. (2019). Trehalose as a promising therapeutic candidate for the treatment of Parkinson's disease. *British Journal of Pharmacology, 176*(9), 1173-1189.

Khalifeh, M., Barreto, G., & Sahebkar, A. (2021). Therapeutic potential of trehalose in neurodegenerative diseases: The knowns and unknowns. *Neural Regeneration Research, 16*(10), 2026-2027.

Khalifeh, M., Read, M. I., Barreto, G. E., & Sahebkar, A. (2020). Trehalose against Alzheimer's disease: Insights into a potential therapy. *BioEssays*, *42*(8), 1900195.

Khangwal, I., & Shukla, P. (2019). Potential prebiotics and their transmission mechanisms: Recent approaches. *Journal of Food and Drug Analysis, 27*(3), 649-656

Khodaei, N., Fernandez, B., Fliss, I., & Karboune, S. (2016). Digestibility and prebiotic properties of potato rhamnogalacturonan I polysaccharide and its galactose-rich oligosaccharides/oligomers. *Carbohydrate Polymers*, *136*, 1074-1084.

Kim, B. G., Lee, K. J., Han, N. S., Park, K. H., & Lee, S. B. (2007). Enzymatic synthesis and characterization of galactosyl trehalose trisaccharides. *Food Science and Biotechnology*, *16*(1), 127-132.

Kluch, M., Socha-Banasiak, A., Pacześ, K., Borkowska, M., & Czkwianianc, E. (2020). The role of disaccharidases in the digestion-diagnosis and significance of their deficiency in children and adults. *Polski Merkuriusz Lekarski: Organ Polskiego Towarzystwa Lekarskiego*, *49*(286), 275-278.

Kopf-Bolanz, K. A., Schwander, F., Gijs, M., Vergéres, G., Portmann, R., & Egger, L. (2012). Validation of an in vitro digestive system for studying macronutrient decomposition in humans. *Journal of Nutrition*, *142*(2), 245-250.

Kothari, D., Tingirikari, J. M. R., & Goyal, A. (2015). In vitro analysis of dextran from

Leuconostoc mesenteroides NRRL B-1426 for functional food application. *Bioactive Carbohydrates and Dietary Fibre*, *6*(2), 55-61.

Kovatcheva-Datchary, P., Tremaroli, V., & Bäckhed, F. (2013). The gut microbiota. En E. Rosenberg, E. F. DeLong, S. Lory, E. Stackebrandt, & F. Thompson (Eds.), *The Prokaryotes – Human Microbiology* (pp. 3-24). Springer-Verlag.

Kruger, C., Beauchamp, N., Modeste, V., Morel-Despeisse, F., & Chappuis, E. (2017). Toxicological evaluation of alpha-galacto-oligosaccharides shows no adverse effects over a 90-day study in rats. *Toxicology Research and Application*, *1*, 1-7.

Laparra, J. M., Hernández-Hernández, O., Moreno, F. J., & Sanz, Y. (2013). Neoglycoconjugates of caseinomacropeptide and galactooligosaccharides modify adhesion of intestinal pathogens and inflammatory response(s) of intestinal (Caco-2) cells. *Food Research International*, *54*(1), 1096-1102.

Laparra, José Moisés, Díez-Municio, M., Herrero, M., & Moreno, F. J. (2014). Structural differences of prebiotic oligosaccharides influence their capability to enhance iron absorption in deficient rats. *Food and Function*, *5*(10), 2430-2437.

Larsen, N., De Souza, C. B., Krych, L., Cahú, T. B., Wiese, M., Kot, W., Hansen, K. M., Blennow, A., Venema, K., & Jespersen, L. (2019). Potential of pectins to beneficially modulate the gut microbiota depends on their structural properties. *Frontiers in Microbiology*, *10*(223), 1-13.

LeBlanc, J. G., Garro, M. S., Silvestroni, A., Connes, C., Piard, J. C., Sesma, F., & Savoy De Giori, G. (2004). Reduction of *α*-galactooligosaccharides in soyamilk by Lactobacillus fermentum CRL 722: In vitro and in vivo evaluation of fermented soyamilk. *Journal of Applied Microbiology*, *97*(4), 876-881.

Lee, B. H., & Hamaker, B. R. (2017). Number of branch points in *α*-limit dextrins impact glucose generation rates by mammalian mucosal *α*-glucosidases. *Carbohydrate*

Polymers, *157*, 207-213.

Lee, B. H., Rose, D. R., Lin, A. H. M., Quezada-Calvillo, R., Nichols, B. L., & Hamaker, B. R. (2016). Contribution of the individual small intestinal *α*-glucosidases to digestion of unusual *α*-linked glycemic disaccharides. *Journal of Agricultural and Food Chemistry*, *64*(33), 6487-6494.

Ley, R. E., Turnbaugh, P. J., Klein, S., & Gordon, J. I. (2006). Microbial ecology: Human gut microbes associated with obesity. *Nature*, *444*(7122), 1022-1023.

Li, X., Guo, R., Wu, X., Liu, X., Ai, L., Sheng, Y., Song, Z., & Wu, Y. (2020). Dynamic digestion of tamarind seed polysaccharide: Indigestibility in gastrointestinal simulations and gut microbiota changes in vitro. *Carbohydrate Polymers*, *239*, 116194.

Lin, A. H. M., Hamaker, B. R., & Nichols, B. L. (2012). Direct starch digestion by sucrase-isomaltase and maltase-glucoamylase. *Journal of Pediatric Gastroenterology and Nutrition*, *55*, S43-S45.

Lin, A. H. M., Lee, B. H., & Chang, W. J. (2016). Small intestine mucosal *α*-glucosidase: A missing feature of in vitro starch digestibility. *Food Hydrocolloids*, *53*, 163-171.

Liu, Y., Dong, M., Yang, Z., & Pan, S. (2016). Anti-diabetic effect of citrus pectin in diabetic rats and potential mechanism via PI3K/Akt signaling pathway. *International Journal of Biological Macromolecules*, *89*, 484-488.

Logan, S. R. (1996). *Fundamentals of Chemical Kinetics*. Longman.

Lohner, S., Küllenberg, D., Antes, G., Decsi, T., & Meerpohl, J. J. (2014). Prebiotics in healthy infants and children for prevention of acute infectious diseases: A systematic review and meta-analysis. *Nutrition Reviews*, *72*(8), 523-531.

Lopez-Santamarina, A., Miranda, J. M., Del Carmen Mondragon, A., Lamas, A.,

Cardelle-Cobas, A., Franco, C. M., & Cepeda, A. (2020). Potential use of marine seaweeds as prebiotics: A review. *Molecules*, *25*(4), 1-26.

Lorenzo, C., Williams, C., & Valenzuela, J. (1989). Pectin delays gastric emptying. *Nutrition Reviews*, *47*, 268-270.

Louis, P., & Flint, H. J. (2017). Formation of propionate and butyrate by the human colonic microbiota. *Environmental Microbiology, 19*(1), 29-41.

Louis, P., Hold, G. L., & Flint, H. J. (2014). The gut microbiota, bacterial metabolites and colorectal cancer. *Nature Reviews Microbiology, 12*(10), 661-672.

Loyeau, P. A., Spotti, M. J., Vanden Braber, N. L., Rossi, Y. E., Montenegro, M. A., Vinderola, G., & Carrara, C. R. (2018). Microencapsulation of Bifidobacterium animalis subsp. lactis INL1 using whey proteins and dextrans conjugates as wall materials. *Food Hydrocolloids*, *85*, 129-135.

Lynch, S. V., & Pedersen, O. (2016). The human ntestinal microbiome in health and disease. *New England Journal of Medicine*, *375*(24), 2369-2379.

Malard, F., Dore, J., Gaugler, B., & Mohty, M. (2021). Introduction to host microbiome symbiosis in health and disease. *Mucosal Immunology*, *14*(3), 547-554.

Maltz, C., Miskovitz, P. F., & Hajifathalian, K. (2020). Lactulose may reduce *Clostridium* difficile-related diarrhea among patients receiving antibiotics. *JGH Open*, *4*(6), 1088-1090.

Mamone, G., Nitride, C., Picariello, G., Addeo, F., Ferranti, P., & Mackie, A. (2015). Tracking the fate of pasta (T. Durum Semolina) immunogenic proteins by in vitro simulated digestion. *Journal of Agricultural and Food Chemistry*, *63*(10), 2660-2667.

Man, S., Liu, T., Yao, Y., Lu, Y., Ma, L., & Lu, F. (2021). Friend or foe? The roles of

inulin-type fructans. *Carbohydrate Polymers, 252*, 117155.

Marenda, F. R. B., Mattioda, F., Demiate, I. M., de Francisco, A., de Oliveira Petkowicz, C. L., Canteri, M. H. G., & Amboni, R. D. M. C. (2019). Advances in studies using vegetable wastes to obtain pectic substances: A review. *Journal of Polymers and the Environment*, *27*(3), 549-560.

Marín-Manzano, M. C., Hernández-Hernández, O., Diez-Municio, M., Delgado-Andrade, C., Moreno, F. J., & Clemente, A. (2020). Prebiotic properties of non-fructosylated *α*-galactooligosaccharides from PEA (Pisum sativum L.) using infant fecal slurries. *Foods*, *9*(7), 921.

Marounek, M., Vovk, S. J., & Skřivanová, V. (1995). Distribution of activity of hydrolytic enzymes in the digestive tract of rabbits. *British Journal of Nutrition*, *73*(3), 463-469.

Martens, E. C., Lowe, E. C., Chiang, H., Pudlo, N. A., Wu, M., McNulty, N. P., Abbott, D. W., Henrissat, B., Gilbert, H. J., Bolam, D. N., & Gordon, J. I. (2011). Recognition and degradation of plant cell wall polysaccharides by two human gut symbionts. *PLoS Biology*, *9*(12), 1001221.

Martínez-Villaluenga, C., Cardelle-Cobas, A., Corzo, N., Olano, A., & Villamiel, M. (2008). Optimization of conditions for galactooligosaccharide synthesis during lactose hydrolysis by *β*-galactosidase from Kluyveromyces lactis (Lactozym 3000 L HP G). *Food Chemistry*, *107*(1), 258-264.

Martínez-Villaluenga, C., Cardelle-Cobas, A., Olano, A., Corzo, N., Villamiel, M., & Jimeno, M. L. (2008). Enzymatic synthesis and identification of two trisaccharides produced from lactulose by transgalactosylation. *Journal of Agricultural and Food Chemistry*, *56*(2), 557-563.

Martínez-Villaluenga, C., & Frías, J. (2014). Production and bioactivity of

oligosaccharides in plants foods. En F. J. Moreno & M. L. Sanz (Eds.), *Food Oligosaccharides. Production, Analysis and Bioactivity.* (pp. 35-54). John Wiley & Sons.

Martins, G. N., Ureta, M. M., Tymczyszyn, E. E., Castilho, P. C., & Gomez-Zavaglia, A. (2019). Technological aspects of the production of fructo and galacto-oligosaccharides. Enzymatic synthesis and hydrolysis. *Frontiers in Nutrition, 6*(78), 1-24.

Massenzio, F., Peña-Altamira, E., Petralla, S., Virgili, M., Zuccheri, G., Miti, A., Polazzi, E., Mengoni, I., Piffaretti, D., & Monti, B. (2018). Microglial overexpression of fALS-linked mutant SOD1 induces SOD1 processing impairment, activation and neurotoxicity and is counteracted by the autophagy inducer trehalose. *Biochimica et Biophysica Acta - Molecular Basis of Disease*, *1864*(12), 3771-3785.

Maxwell, E. G., Belshaw, N. J., Waldron, K. W., & Morris, V. J. (2012). Pectin - An emerging new bioactive food polysaccharide. *Trends in Food Science and Technology, 24*(2), 64-73.

Maxwell, E. G., Colquhoun, I. J., Chau, H. K., Hotchkiss, A. T., Waldron, K. W., Morris, V. J., & Belshaw, N. J. (2015). Rhamnogalacturonan I containing homogalacturonan inhibits colon cancer cell proliferation by decreasing ICAM1 expression. *Carbohydrate Polymers*, *132*, 546-553.

Maxwell, E. G., Colquhoun, I. J., Chau, H. K., Hotchkiss, A. T., Waldron, K. W., Morris, V. J., & Belshaw, N. J. (2016). Modified sugar beet pectin induces apoptosis of colon cancer cells via an interaction with the neutral sugar side-chains. *Carbohydrate Polymers*, *136*, 923-929.

McCabe, L., Britton, R. A., & Parameswaran, N. (2015). Prebiotic and Probiotic Regulation of Bone Health: Role of the Intestine and its Microbiome. En *Current Osteoporosis Reports, 13*(6), 363-371.

McCleary, B, Rader, J., Champ, M., & Okuma, K. (2010). Determination of total dietary fiber (CODEX definition) by Enzymatic-Gravimetric method and liquid chromatography. *Journal of AOAC International*, *93*(1), 221-233.

McCleary, Barry V., Sloane, N., & Draga, A. (2015). Determination of total dietary fibre and available carbohydrates: A rapid integrated procedure that simulates in vivo digestion. *Starch/Staerke*, *67*(9-10), 860-883.

Meng, J., Kang, T. T., Wang, H. F., Zhao, B. Bin, & Lu, R. R. (2018). Physicochemical properties of casein-dextran nanoparticles prepared by controlled dry and wet heating. *International Journal of Biological Macromolecules*, *107*, 2604-2610.

Mensink, M. A., Frijlink, H. W., Van Der Voort Maarschalk, K., & Hinrichs, W. L. J. (2015). Inulin, a flexible oligosaccharide I: Review of its physicochemical characteristics. *Carbohydrate Polymers*, *130*, 405-419.

Micka, A., Siepelmeyer, A., Holz, A., Theis, S., & Schön, C. (2017). Effect of consumption of chicory inulin on bowel function in healthy subjects with constipation: a randomized, double-blind, placebo-controlled trial. *International Journal of Food Sciences and Nutrition*, *68*(1), 82-89.

Míguez, B., Gómez, B., Gullón, P., Gullón, B., & Alonso, J. L. (2016). Pectic oligosaccharides and other emerging prebiotics. En Rao, V., & Rao, L. (Eds.), *Probiotics and Prebiotics in Human Nutrition and Health*. InTech.

Mijailovic, N., Nesler, A., Perazzolli, M., Aït Barka, E., & Aziz, A. (2021). Rare sugars: Recent advances and their potential role in sustainable crop protection. *Molecules, 26*(6), 1720.

Miller, T. L., & Wolin, M. J. (1996). Pathways of acetate, propionate, and butyrate formation by the human fecal microbial flora. *Applied and Environmental Microbiology*, *62*(5), 1589-1592.

Mimoun, S., Andriamihaja, M., Chaumontet, C., Atanasiu, C., Benamouzig, R., Blouin, J. M., Tomé, D., Bouillaud, F., & Blachier, F. (2012). Detoxification of H2S by differentiated colonic epithelial cells: Implication of the sulfide oxidizing unit and of the cell respiratory capacity. En *Antioxidants and Redox Signaling, 17*(1), 1-10.

Minekus, M., Alminger, M., Alvito, P., Ballance, S., Bohn, T., Bourlieu, C., Carrière, F., Boutrou, R., Corredig, M., Dupont, D., Dufour, C., Egger, L., Golding, M., Karakaya, S., Kirkhus, B., Le Feunteun, S., Lesmes, U., MacIerzanka, A., MacKie, A., Marze, S., McClements, D J., Menard, O., Recio, I., Santos, C N., Singh, R P., Vegarud, G E., Wickham, M S J., & Brodkorb, A. (2014). A standardised static in vitro digestion method suitable for food-an international consensus. *Food and Function*, *5*(6), 1113-1124.

Miquel, S., Martín, R., Rossi, O., Bermúdez-Humarán, L. G., Chatel, J. M., Sokol, H., Thomas, M., Wells, J. M., & Langella, P. (2013). Faecalibacterium prausnitzii and human intestinal health. *Current Opinion in Microbiology, 16*(3), 255-261.

Mishra, S., Tripathi, A., Chaudhari, B. P., Dwivedi, P. D., Pandey, H. P., & Das, M. (2014). Deoxynivalenol induced mouse skin cell proliferation and inflammation via MAPK pathway. *Toxicology and Applied Pharmacology*, *279*(2), 186-197.

Miyazaki, K., Masuoka, N., Kano, M., & Iizuka, R. (2014). Bifidobacterium fermented milk and galacto-oligosaccharides lead to improved skin health by decreasing phenols production by gut microbiota. *Beneficial Microbes*, *5*(2), 121-128.

Molis, C., Flourié, B., Ouarne, F., Gailing, M. F., Lartigue, S., Guibert, A., Bornet, F., & Galmiche, J. P. (1996). Digestion, excretion, and energy value of fructooligosaccharides in healthy humans. *American Journal of Clinical Nutrition*, *64*(3), 324-328.

Montilla, A., Van De Lagemaat, J., Olano, A., & Del Castillo, M. D. (2006). Determination of oligosaccharides by conventional high-resolution gas

chromatography. *Chromatographia*, *63*(9-10), 453-458.

Montilla, Antonia, Olano, A., Martínez-Villaluenga, C., & Corzo, N. (2011). Study of influential factors on oligosaccharide formation by fructosyltransferase activity during stachyose hydrolysis by pectinex ultra SP-L. *Journal of Agricultural and Food Chemistry*, *59*(19), 10705-10711.

Morris, V. J., Belshaw, N. J., Waldron, K. W., & Maxwell, E. G. (2013). The bioactivity of modified pectin fragments. *Bioactive Carbohydrates and Dietary Fibre, 1*(1), 21-37.

Mortensen, A., Aguilar, F., Crebelli, R., Di Domenico, A., Dusemund, B., Frutos, M. J., Galtier, P., Gott, D., Gundert-Remy, U., Lambré, C., Leblanc, J. C., Lindtner, O., Moldeus, P., Mosesso, P., Oskarsson, A., Parent-Massin, D., Stankovic, I., Waalkens-Berendsen, I., Wright, M., Younes, M., Tobback, P., Ioannidou, S., Tasiopoulou, S., & Woutersen, R. A. (2017). Re-evaluation of pectin (E 440i) and amidated pectin (E 440ii) as food additives. *EFSA Journal*, *15*(7), 4866.

Moussou, N., Corzo-Martínez, M., Sanz, M. L., Zaidi, F., Montilla, A., & Villamiel, M. (2017). Assessment of Maillard reaction evolution, prebiotic carbohydrates, antioxidant activity and α-amylase inhibition in pulse flours. *Journal of Food Science and Technology*, *54*(4), 890-900.

Mudgil, D., & Barak, S. (2013). Composition, properties and health benefits of indigestible carbohydrate polymers as dietary fiber: A review. *International Journal of Biological Macromolecules, 61*, 1-6.

Mukhopadhya, I., Hansen, R., El-Omar, E. M., & Hold, G. L. (2012). IBD-what role do Proteobacteria play?. *Nature Reviews Gastroenterology and Hepatology*, 9(4), 219-230.

Muñoz-Almagro, N. (2019). *Innovative approaches in the production of low-glycemic*

index carbohydrates: structural and functional evaluation of pectin obtained from sunflower by-products. [Tesis Doctoral, Universidad Autónoma de Madrid]. Repositorio Institucional Universidad Autónoma de Madrid.

Muñoz-Almagro, N., Montilla, A., Moreno, F. J., & Villamiel, M. (2017). Modification of citrus and apple pectin by power ultrasound: Effects of acid and enzymatic treatment. *Ultrasonics Sonochemistry*, *38*, 807-819.

Muñoz-Almagro, N., Rico-Rodriguez, F., Villamiel, M., & Montilla, A. (2018). Pectin characterisation using size exclusion chromatography: A comparison of ELS and RI detection. *Food Chemistry*, *252*, 271-276.

Muñoz-Almagro, N., Rico-Rodriguez, F., Wilde, P. J., Montilla, A., & Villamiel, M. (2018). Structural and technological characterization of pectin extracted with sodium citrate and nitric acid from sunflower heads. *Electrophoresis*, *39*(15), 1984-1992.

Muñoz-Labrador, A., Moreno, R., Villamiel, M., & Montilla, A. (2018). Preparation of citrus pectin gels by power ultrasound and its application as an edible coating in strawberries. *Journal of the Science of Food and Agriculture*, *98*(13), 4866-4875.

Naessens, M., Cerdobbel, A., Soetaert, W., & Vandamme, E. J. (2005). Leuconostoc dextransucrase and dextran: Production, properties and applications. *Journal of Chemical Technology and Biotechnology*, *80*(8), 845-860.

Nakamura, T., Nagura, T., Sato, K., & Ohnishi, M. (2012). Evaluation of the effects of dietary organic germanium, Ge-132, and raffinose supplementation on caecal flora in rats. *Bioscience of Microbiota, Food and Health*, *31*(2), 37-45.

Nangia-Makker, P., Hogan, V., Honjo, Y., Baccarini, S., Tait, L., Bresalier, R., & Raz, A. (2002). Inhibition of human cancer cell growth and metastasis in nude mice by oral intake of modified citrus pectin. *Journal of the National Cancer Institute*, *94*(24),

1854-1862.

Nishizaki, Y., Yoshizane, C., Toshimori, Y., Arai, N., Akamatsu, S., Hanaya, T., Arai, S., Ikeda, M., & Kurimoto, M. (2000). Disaccharide-trehalose inhibits bone resorption in ovarieciomized mice. *Nutrition Research*, *20*(5), 653-664.

Nobre, C., Sousa, S. C., Silva, S. P., Pinheiro, A. C., Coelho, E., Vicente, A. A., Gomes, A. M. P., Coimbra, M. A., Teixeira, J. A., & Rodrigues, L. R. (2018). In vitro digestibility and fermentability of fructo-oligosaccharides produced by Aspergillus ibericus. *Journal of Functional Foods*, *46*, 278-287.

Nokhodchi, A., Raja, S., Patel, P., & Asare-Addo, K. (2012). The role of oral controlled release matrix tablets in drug delivery systems. *BioImpacts*, *2*(4), 175-187.

Nugent, S. G., Kumar, D., Rampton, D. S., & Evans, D. F. (2001). Intestinal luminal pH in inflammatory bowel disease: Possible determinants and implications for therapy with aminosalicylates and other drugs. *Gut, 48*(4), 571-577.

Nurdin, S. U., Le Leu, R. K., Aburto-Medina, A., Young, G. P., Stangoulis, J. C. R., Ball, A. S., & Abbott, C. A. (2018). Effects of dietary fibre from the traditional Indonesian food, green cincau (Premna oblongifolia merr.) on preneoplastic lesions and short chain fatty acid production in an azoxymethane rat model of colon cancer. *International Journal of Molecular Sciences*, *19*(9), 2593.

Odun-Ayo, F., Mellem, J., Naicker, T., & Reddy, L. (2015). Chemoprevention of azoxymethane-induced colonic carcinogenesis in Balb/c mice using a modified pectin alginate probiotic. *Anticancer Research*, *35*(9), 4765-4776.

Odun-Ayo, F., Mellem, J., & Reddy, L. (2017). The effect of modified citrus pectin-probiotic on faecal lactobacilli in Balb/c mice. *Food Science and Technology*, *37*(3), 478-482.

Ohkami, H., Tazawa, K., Yamashita, I., Shimizu, T., Murai, K., Kobashi, K., & Fujimaki,

M. (1995). Effects of Apple Pectin on Fecal Bacterial Enzymes in Azoxymethane-induced Rat Colon Carcinogenesis. *Japanese Journal of Cancer Research*, *86*(6), 523-529.

Ohtake, S., & Wang, Y. J. (2011). Trehalose: Current use and future applications. *Journal of Pharmaceutical Sciences*, *100*(6), 2020-2053.

Oku, T., Tanabe, K., Ogawa, S., Sadamori, N., & Nakamura, S. (2011). Similarity of hydrolyzing activity of human and rat small intestinal disaccharidases. *Clinical and Experimental Gastroenterology*, *4*(1), 155-161.

Olaokun, O. O., McGaw, L. J., Eloff, J. N., & Naidoo, V. (2013). Evaluation of the inhibition of carbohydrate hydrolysing enzymes, antioxidant activity and polyphenolic content of extracts of ten African Ficus species (Moraceae) used traditionally to treat diabetes. *BMC Complementary and Alternative Medicine*, *13*(1), 1-10.

Ou, S., Kwok, K. C., Li, Y., & Fu, L. (2001). In vitro study of possible role of dietary fiber in lowering postprandial serum glucose. *Journal of Agricultural and Food Chemistry*, *49*(2), 1026-1029.

Panesar, P. S., & Kumari, S. (2011). Lactulose: Production, purification and potential applications. *Biotechnology Advances, 29*(6), 940-948.

Parnell, J. A., & Reimer, R. A. (2009). Weight loss during oligofructose supplementation is associated with decreased ghrelin and increased peptide YY in overweight and obese adults. *American Journal of Clinical Nutrition*, *89*(6), 1751-1759.

Peng, B., Li, Y., Ding, S., & Yang, J. (2017). Characterization of textural, rheological, thermal, microstructural, and water mobility in wheat flour dough and bread affected by trehalose. *Food Chemistry*, *233*, 369-377.

Pérez, S., & Bertoft, E. (2010). The molecular structures of starch components and their

contribution to the architecture of starch granules: A comprehensive review. *Starch/Staerke*, *62*(8), 389-420.

Perry, J. R., & Ying, W. (2016). A Review of Physiological Effects of Soluble and Insoluble Dietary Fibers. *Journal of Nutrition & Food Sciences*, *6*(2). 476.

Picariello, G., Ferranti, P., & Addeo, F. (2016). Use of brush border membrane vesicles to simulate the human intestinal digestion. *Food Research International*, *88*, 327-335.

Pineiro, M., Asp, N. G., Reid, G., Macfarlane, S., Morelli, L., Brunser, O., & Tuohy, K. (2008). FAO Technical meeting on prebiotics. *Journal of clinical gastroenterology*, *42*(Suppl 3), S156-S159.

Poele, E., Corwin, S., Hamaker, B. R., Lamothe, L., Vafeiadi, C., & Dijkhuizen, L. (2020). Biotechnology and Biological Transformations Development of slowly digestible starch derived alpha-glucans with 4 , 6- # -glucanotransferase and branching sucrase enzymes. *Journal of Agricultural and Food Chemistry, 68*(24), 6664-6671.

Power, S. E., O'Toole, P. W., Stanton, C., Ross, R. P., & Fitzgerald, G. F. (2014). Intestinal microbiota, diet and health. *British Journal of Nutrition*, *111*(3), 387-402.

Prakash, B. S., Suyama, K., Itoh, T., & Adachi, S. (1989). Structure Elucidation of Major Galacto Oligosaccharides Formed by Growing Culture of Trichoderma harzianum. *Journal of Agricultural and Food Chemistry*, *37*(2), 334-337.

Prieto, R. M., Ferrer, M., Rayó, J. M., & Tur, J. A. (1994). Disaccharidase activities in pregnant and lactating rats. *Comparative Biochemistry and Physiology -- Part A: Physiology*, *109*(3), 741-747.

Product Sheet DOC.A4-03/001 Orafti ® GR. (2016). https://www.anna-gold.at/docs/ArtikelDocs/Spezifikationen/_yyyymmdd.pdf/17293_20160718.pdf

Pyner, A., Nyambe-Silavwe, H., & Williamson, G. (2017). Inhibition of human and rat sucrase and maltase activities to assess antiglycemic potential: Optimization of the assay using acarbose and polyphenols. *Journal of Agricultural and Food Chemistry*, *65*(39), 8643-8651.

Qi, X., Al-Ghazzewi, F. H., & Tester, R. F. (2018). Dietary Fiber, Gastric Emptying, and Carbohydrate Digestion: A Mini-Review. *Starch/Staerke*, *70*(9-10), 1-5.

Ramachandran, C., Wilk, B., Melnick, S. J., & Eliaz, I. (2017). Synergistic Antioxidant and Anti-Inflammatory Effects between Modified Citrus Pectin and Honokiol. *Evidence-based Complementary and Alternative Medicine*, *2017*.

Rastall, R. A. (2010). Functional Oligosaccharides: Application and Manufacture. *Annual Review of Food Science and Technology*, *1*(1), 305-339.

Reimer, R. A., Soto-Vaca, A., Nicolucci, A. C., Mayengbam, S., Park, H., Madsen, K. L., Menon, R., & Vaughan, E. E. (2020). Effect of chicory inulin-type fructan-containing snack bars on the human gut microbiota in low dietary fiber consumers in a randomized crossover trial. *American Journal of Clinical Nutrition*, *111*(6), 1286-1296.

Reports and Data. (2019). *Prebiotic Ingredients Market To Reach USD 8.34 Billion By 2026*. https://www.globenewswire.com/news-release/2019/10/16/1930796/0/en/Prebiotic-Ingredients-Market-To-Reach-USD-8-34-Billion-By-2026-Reports-And-Data.html

Roberfroid, M., Gibson, G. R., Hoyles, L., McCartney, A. L., Rastall, R., Rowland, I., Wolvers, D., Watzl, B., Szajewska, H., Stahl, B., Guarner, F., Respondek, F., Whelan, K., Coxam, V., Davicco, M. J., Léotoing, L., Wittrant, Y., Delzenne, N. M., Cani, P. D., Neyrinck, A. M., & Meheust, A. (2010). Prebiotic effects: Metabolic and health benefits. *British Journal of Nutrition, 104*, S1-S63.

Ruiz-Matute, A. I., Hernández-Hernández, O., Rodríguez-Sánchez, S., Sanz, M. L., & Martínez-Castro, I. (2011). Derivatization of carbohydrates for GC and GC-MS analyses. *Journal of Chromatography B: Analytical Technologies in the Biomedical and Life Sciences*, *879*(17-18), 1226-1240.

Sabater, C., Sabater, V., Olano, A., Montilla, A., & Corzo, N. (2020). Ultrasound-assisted extraction of pectin from artichoke by-products. An artificial neural network approach to pectin characterisation. *Food Hydrocolloids*, *98*, 105238.

Santibáñez, L., Fernández-Arrojo, L., Guerrero, C., Plou, F. J., & Illanes, A. (2016). Removal of lactose in crude galacto-oligosaccharides by *β*-galactosidase from Kluyveromyces lactis. *Journal of Molecular Catalysis B: Enzymatic*, *133*, 85-91.

Schaller-Povolny, L. A., Smith, D. E., & Labuza, T. P. (2000). Effect of water content and molecular weight on the moisture isotherms and glass transition properties of inulin. *International Journal of Food Properties*, *3*(2), 173-192.

Schmidt, K., Cowen, P. J., Harmer, C. J., Tzortzis, G., Errington, S., & Burnet, P. W. J. (2015). Prebiotic intake reduces the waking cortisol response and alters emotional bias in healthy volunteers. *Psychopharmacology*, *232*(10), 1793-1801.

Secher, T., Samba-Louaka, A., Oswald, E., & Nougayrède, J. P. (2013). Escherichia coli producing colibactin triggers premature and transmissible senescence in mammalian cells. *PLoS ONE*, *8*(10), 77157.

Selma-Gracia, R., Laparra, J. M., & Haros, C. M. (2020). Potential beneficial effect of hydrothermal treatment of starches from various sources on in vitro digestion. *Food Hydrocolloids*, *103*, 105687.

Semenza, G., & Auricchio, S. (1965). Multiplicity of human intestinal disaccharides. I. Chromatographic separation of maltases and two lactases. *Biochimica et biophysica acta*, *96*(1965), 487-497.

Seo, J. M., Lamothe, L. M., Shin, H., Austin, S., Yoo, S. H., & Lee, B. H. (2020). Determination of glucose generation rate from various types of glycemic carbohydrates by mammalian glucosidases anchored in the small intestinal tissue. *International Journal of Biological Macromolecules*, *154*, 751-757.

Shi, Y., Liu, J., Yan, Q., You, X., Yang, S., & Jiang, Z. (2018). In vitro digestibility and prebiotic potential of curdlan (1→3)-*β*-D-glucan oligosaccharides in Lactobacillus species. *Carbohydrate Polymers*, *188*, 17-26.

Shin, H., Seo, D. H., Seo, J., Lamothe, L. M., Yoo, S. H., & Lee, B. H. (2019). Optimization of in vitro carbohydrate digestion by mammalian mucosal *α*-glucosidases and its applications to hydrolyze the various sources of starches. *Food Hydrocolloids*, *87*, 470-476.

Silk, D. B. A., Davis, A., Vulevic, J., Tzortzis, G., & Gibson, G. R. (2009). Clinical trial: The effects of a trans-galactooligosaccharide prebiotic on faecal microbiota and symptoms in irritable bowel syndrome. *Alimentary Pharmacology and Therapeutics*, *29*(5), 508-518.

Silva, D. C., Freitas, A. L. P., Pessoa, C. D. S., Paula, R. C. M., Mesquita, J. X., Leal, L. K. A. M., Brito, G. A. C., Gonçalves, D. O., & Viana, G. S. B. (2011). Pectin from passiflora edulis shows anti-inflammatory action as well as hypoglycemic and hypotriglyceridemic properties in diabetic Rats. *Journal of Medicinal Food*, *14*(10), 1118-1126.

Sims, I. M., Thomson, A., Hubl, U., Larsen, N. G., & Furneaux, R. H. (2001). Characterisation of polysaccharides synthesised by Gluconobacter oxydans NCIMB 4943. *Carbohydrate Polymers*, *45*(3), 285-292.

Singh, S. P., Jadaun, J. S., Narnoliya, L. K., & Pandey, A. (2017). Prebiotic Oligosaccharides: Special focus on fructooligosaccharides, its biosynthesis and bioactivity. *Applied Biochemistry and Biotechnology*, *183*(2), 613-635.

Sokołowska, E., Sadowska, A., Sawicka, D., Kotulska-Bąblińska, I., & Car, H. (2021). A head-to-head comparison review of biological and toxicological studies of isomaltulose, d-tagatose, and trehalose on glycemic control. *Critical Reviews in Food Science and Nutrition*, 1-26.

Soliman, G. A. (2019). Dietary Fiber, Atherosclerosis, and Cardiovascular Disease. *Nutrients*, *11*(5), 1155.

Song, H., Wang, W., Shen, B., Jia, H., Hou, Z., Chen, P., & Sun, Y. (2018). Pretreatment with probiotic Bifico ameliorates colitis-associated cancer in mice: Transcriptome and gut flora profiling. *Cancer Science*, *109*(3), 666-677.

Sun, Y., Cheng, L., Zeng, X., Zhang, X., Liu, Y., Wu, Z., & Weng, P. (2021). The intervention of unique plant polysaccharides-Dietary fiber on depression from the gut-brain axis. *International Journal of Biological Macromolecules*, *170*, 336-342.

Tahara, T., Yamamoto, E., Suzuki, H., Maruyama, R., Chung, W., Garriga, J., Jelinek, J., Yamano, H. O., Sugai, T., An, B., Shureiqi, I., Toyota, M., Kondo, Y., Estecio, M. R. H., & Issa, J. P. J. (2014). Fusobacterium in colonic flora and molecular features of colorectal carcinoma. *Cancer Research*, *74*(5), 1311-1318.

Tamura, M., Singh, J., Kaur, L., & Ogawa, Y. (2016). Impact of structural characteristics on starch digestibility of cooked rice. *Food Chemistry*, *191*, 91-97.

Tan, S., Yang, S., Chen, G., Zhu, L., Sun, Z., & Chen, S. (2020). Trehalose alleviates apoptosis by protecting the autophagy-lysosomal system in alveolar macrophages during human silicosis. *Life Sciences*, *257*, 118043.

Tanabe, K., Nakamura, S., & Oku, T. (2014). Inaccuracy of AOAC method 2009.01 with amyloglucosidase for measuring non-digestible oligosaccharides and proposal for an improvement of the method. *Food Chemistry*, *151*, 539-546.

Tanabe, K., Nakamura, S., Omagari, K., & Oku, T. (2015). Determination trial of

nondigestible oligosaccharide in processed foods by improved AOAC method 2009.01 using porcine small intestinal enzyme. *Journal of Agricultural and Food Chemistry*, *63*(24), 5747-5752.

Thibault, J. F., Renard, C. M. G. C., Axelos, M. A. V., Roger, P., & Crépeau, M. J. (1993). Studies of the length of homogalacturonic regions in pectins by acid hydrolysis. *Carbohydrate Research*, *238*, 271-286.

Thursby, E., & Juge, N. (2017). Introduction to the human gut microbiota. *Biochemical Journal*, *474*(11), 1823-1836.

Topping, D. L., & Clifton, P. M. (2001). Short-chain fatty acids and human colonic function: Roles of resistant starch and nonstarch polysaccharides. *Physiological Reviews, 81*(3), 1031-1064.

Torres, D. P. M., Gonçalves, M. do P. F., Teixeira, J. A., & Rodrigues, L. R. (2010). Galacto-Oligosaccharides: Production, properties, applications, and significance as prebiotics. *Comprehensive Reviews in Food Science and Food Safety*, *9*(5), 438-454.

Tsatsaragkou, K., Methven, L., Chatzifragkou, A., & Rodriguez-Garcia, J. (2021). The functionality of inulin as a sugar replacer in cakes and biscuits; highlighting the influence of differences in degree of polymerisation on the properties of cake batter and product. *Foods*, *10*(5), 951.

Uga, A. H., Loganathan, P., Habeeb, A., Oyeka, M., & Farran, Y. (2019). An Unusual Case of Lactic Acidosis in Colon Cancer: A Case Report and Review of the Literature. *Annals of Clinical Case Reports*, *4*(1660), 1-2.

Urrutia, P., Rodriguez-Colinas, B., Fernandez-Arrojo, L., Ballesteros, A. O., Wilson, L., Illanes, A., & Plou, F. J. (2013). Detailed analysis of galactooligosaccharides synthesis with *β*-galactosidase from Aspergillus oryzae. *Journal of Agricultural*

and Food Chemistry, *61*(5), 1081-1087.

Ursell, L. K., Metcalf, J. L., Parfrey, L. W., & Knight, R. (2012). Defining the human microbiome. *Nutrition Reviews*, *70*(Suppl. 1), S38-S44.

Valdez, Y., Brown, E. M., & Finlay, B. B. (2014). Influence of the microbiota on vaccine effectiveness. *Trends in Immunology, 35*(11), 526-537.

Van den Ende, W. (2013). Multifunctional fructans and raffinose family oligosaccharides. *Frontiers in Plant Science, 4*(247), 1-11.

Van Hul, M., & Cani, P. D. (2019). Targeting Carbohydrates and Polyphenols for a Healthy Microbiome and Healthy Weight. *Current Nutrition Reports, 8*(4), 307-316.

Van Leeuwen, S. S., Kuipers, B. J. H., Dijkhuizen, L., & Kamerling, J. P. (2014). 1H NMR analysis of the lactose/*β*-galactosidase-derived galacto-oligosaccharide components of Vivinal® GOS up to DP5. *Carbohydrate Research*, *400*, 59-73.

Van Leeuwen, S. S., Kuipers, B. J. H., Dijkhuizen, L., & Kamerling, J. P. (2016). Comparative structural characterization of 7 commercial galacto-oligosaccharide (GOS) products. *Carbohydrate Research*, *425*, 48-58.

Vandeputte, D., Falony, G., Vieira-Silva, S., Wang, J., Sailer, M., Theis, S., Verbeke, K., & Raes, J. (2017). Prebiotic inulin-type fructans induce specific changes in the human gut microbiota. *Gut*, *66*(11), 1968-1974.

Villamiel, M., Montilla, A., Olano, A., & Corzo, N. (2014). Production and bioactivity of oligosaccharides derived from lactose. En F. J. Moreno & M. L. Sanz (Eds.), *Food Oligosaccharides. Production, Analysis and Bioactivity.* (pp. 137-167). John Wiley & Sons.

Vulevic, J., Juric, A., Walton, G. E., Claus, S. P., Tzortzis, G., Toward, R. E., & Gibson,

G. R. (2015). Influence of galacto-oligosaccharide mixture (B-GOS) on gut microbiota, immune parameters and metabonomics in elderly persons. *British Journal of Nutrition*, *114*(4), 586-595.

Wächtershäuser, A., & Stein, J. (2000). Rationale for the luminal provision of butyrate in intestinal diseases. *European Journal of Nutrition*, *39*(4), 164-171.

Walmagh, M., Zhao, R., & Desmet, T. (2015). Trehalose analogues: Latest insights in properties and biocatalytic production. *International Journal of Molecular Sciences, 16*(6), 13729-13745.

Warmerdam, A., Zisopoulos, F. K., Boom, R. M., & Janssen, A. E. M. (2014). Kinetic characterization of galacto-oligosaccharide (GOS) synthesis by three commercially important *β*-galactosidases. *Biotechnology Progress*, *30*(1), 38-47.

Wei, L. Y., & Roepe, P. D. (1994). Low external pH and osmotic shock increase the expression of human MDR protein. *Biochemistry*, *33*(23), 7229-7238.

Weickert, M. O., & Pfeiffer, A. F. H. (2018). Impact of dietary fiber consumption on insulin resistance and the prevention of type 2 diabetes. *Journal of Nutrition*, *148*(1), 7-12.

Wessel, H. P., & Niggemann, J. (1995). Synthesis of *α*-D-(l-»4)-Substituted trehalose oligosaccharides. *Journal of Carbohydrate Chemistry*, *14*(8), 1089-1100.

Whistler, R. L., & Daniel, J. R. (2000). Starch. En *Kirk-Othmer Encyclopedia of Chemical Technology* (p. 825). John Wiley & Sons.

Wong, C. K. H., Lam, C. L. K., Poon, J. T. C., McGhee, S. M., Law, W. L., Kwong, D. L. W., Tsang, J., & Chan, P. (2012). Direct medical costs of care for Chinese patients with colorectal neoplasia: A health care service provider perspective. *Journal of Evaluation in Clinical Practice*, *18*(6), 1203-1210.

Wong, M. C. S., Huang, J., Lok, V., Wang, J., Fung, F., Ding, H., & Zheng, Z. J. (2021). Differences in Incidence and Mortality Trends of Colorectal Cancer Worldwide Based on Sex, Age, and Anatomic Location. *Clinical Gastroenterology and Hepatology*, *19*(5), 955-966.e61.

World Health Organization. (2019). *WHO - The top 10 causes of death*. WHO.int. https://www.who.int/news-room/fact-sheets/detail/the-top-10-causes-of-death

Yaribeygi, H., Yaribeygi, A., Sathyapalan, T., & Sahebkar, A. (2019). Molecular mechanisms of trehalose in modulating glucose homeostasis in diabetes. *Diabetes and Metabolic Syndrome: Clinical Research and Reviews*, *13*(3), 2214-2218.

Yin, H., Bultema, J. B., Dijkhuizen, L., & van Leeuwen, S. S. (2017). Reaction kinetics and galactooligosaccharide product profiles of the *β*-galactosidases from Bacillus circulans, Kluyveromyces lactis and Aspergillus oryzae. *Food Chemistry*, *225*, 230-238.

Yin, H., Dijkhuizen, L., & van Leeuwen, S. S. (2018). Synthesis of galacto-oligosaccharides derived from lactulose by wild-type and mutant *β*-galactosidase enzymes from Bacillus circulans ATCC 31382. *Carbohydrate Research*, *465*, 58-65.

Yong, E. (2012). Gut microbial «enterotypes» become less clear-cut. *Nature News*.

Yoshizane, C., Mizote, A., Yamada, M., Arai, N., Arai, S., Maruta, K., Mitsuzumi, H., Ariyasu, T., Ushio, S., & Fukuda, S. (2017). Glycemic, insulinemic and incretin responses after oral trehalose ingestion in healthy subjects. *Nutrition Journal*, *16*(1), 1-6.

Yousefi, S., Hoseinifar, S. H., Paknejad, H., & Hajimoradloo, A. (2018). The effects of dietary supplement of galactooligosaccharide on innate immunity, immune related genes expression and growth performance in zebrafish (Danio rerio). *Fish and*

Shellfish Immunology, *73*, 192-196.

Zeng, H. (2014). Mechanisms linking dietary fiber, gut microbiota and colon cancer prevention. *World Journal of Gastrointestinal Oncology*, *6*(2), 41.

Zhang, W., Xu, P., & Zhang, H. (2015). Pectin in cancer therapy: A review. *Trends in Food Science and Technology, 44*(2), 258-271.

Zhang, X., Zheng, J., Jiang, N., Sun, G., Bao, X., Kong, M., Cheng, X., Lin, A., & Liu, H. (2021). Modulation of gut microbiota and intestinal metabolites by lactulose improves loperamide-induced constipation in mice. *European Journal of Pharmaceutical Sciences*, *158*, 105676.

Zhang, Y., Shaikh, N., Ferey, J. L., Wankhade, U. D., Chintapalli, S. V., Higgins, C. B., Crowley, J. R., Heitmeier, M. R., Stothard, A. I., Mihi, B., Good, M., Higashiyama, T., Swarts, B. M., Hruz, P. W., Shankar, K., Tarr, P. I., & DeBosch, B. J. (2020). Lactotrehalose, an Analog of Trehalose, Increases Energy Metabolism Without Promoting Clostridioides difficile Infection in Mice. *Gastroenterology*, *158*(5), 1402-1416.

Zhu, K., Yao, S., Zhang, Y., Liu, Q., Xu, F., Wu, G., Dong, W., & Tan, L. (2019). Effects of in vitro saliva, gastric and intestinal digestion on the chemical properties, antioxidant activity of polysaccharide from Artocarpus heterophyllus Lam. (Jackfruit) Pulp. *Food Hydrocolloids*, *87*, 952-959.

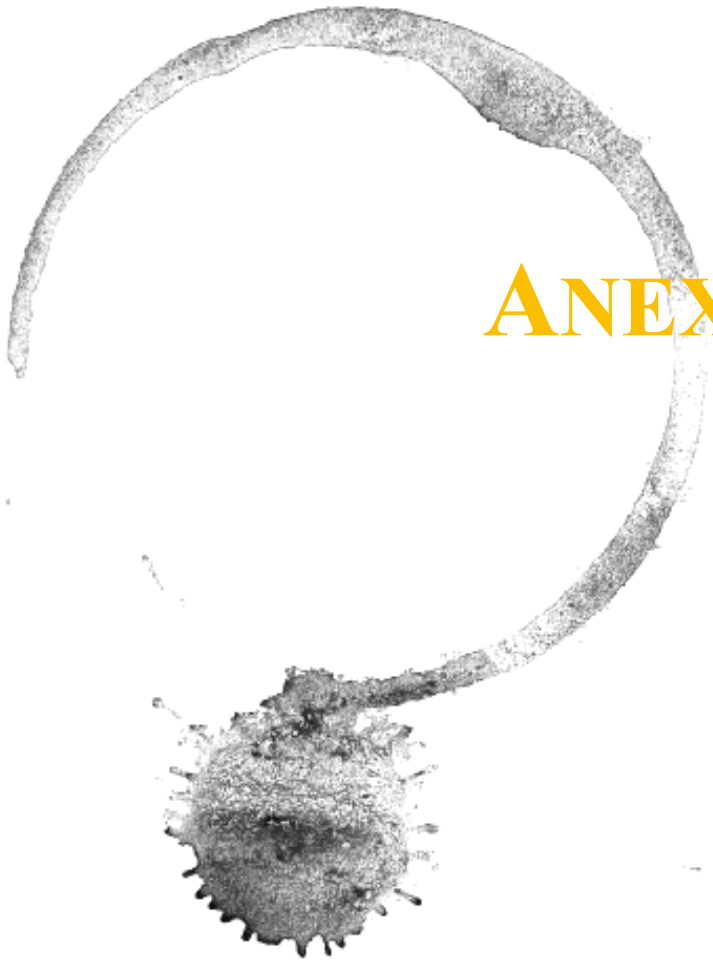

ANEXOS

ANEXOS

Anexo A: **Material Suplementario Capítulo 1. Kinetic study on the digestibility of lactose and lactulose using small intestinal glycosidases**

Anexo B: **Material Suplementario Capítulo 4. Behaviour of citrus pectin and modified citrus pectin in an azoxymethane/dextran sodium sulfate (AOM/DSS)-induced rat colorectal carcinogenesis model**

Anexo C: **Material Suplementario Capítulo 5. Enzymatic synthesis and structural characterization of novel trehalose-based oligosaccharides**

Anexo D: **Artículos científicos publicados**

ANEXO A

MATERIAL SUPLEMENTARIO CAPÍTULO 1

Kinetic study on the digestibility of lactose and lactulose using small intestinal glycosidases

Pablo Gallego-Lobillo, Alvaro Ferreira-Lazarte, Oswaldo Hernández-Hernández y Mar Villamiel

Instituto de Investigación en Ciencias de la Alimentación, CIAL (CSIC-UAM). C/Nicolás Cabrera, 9, Campus de la Universidad Autónoma de Madrid, 28049 Madrid, España.

Reproducido a partir de Elsevier
Food Chemistry
2020, 316, 126326
DOI: https://doi.org/10.1016/j.foodchem.2020.126326

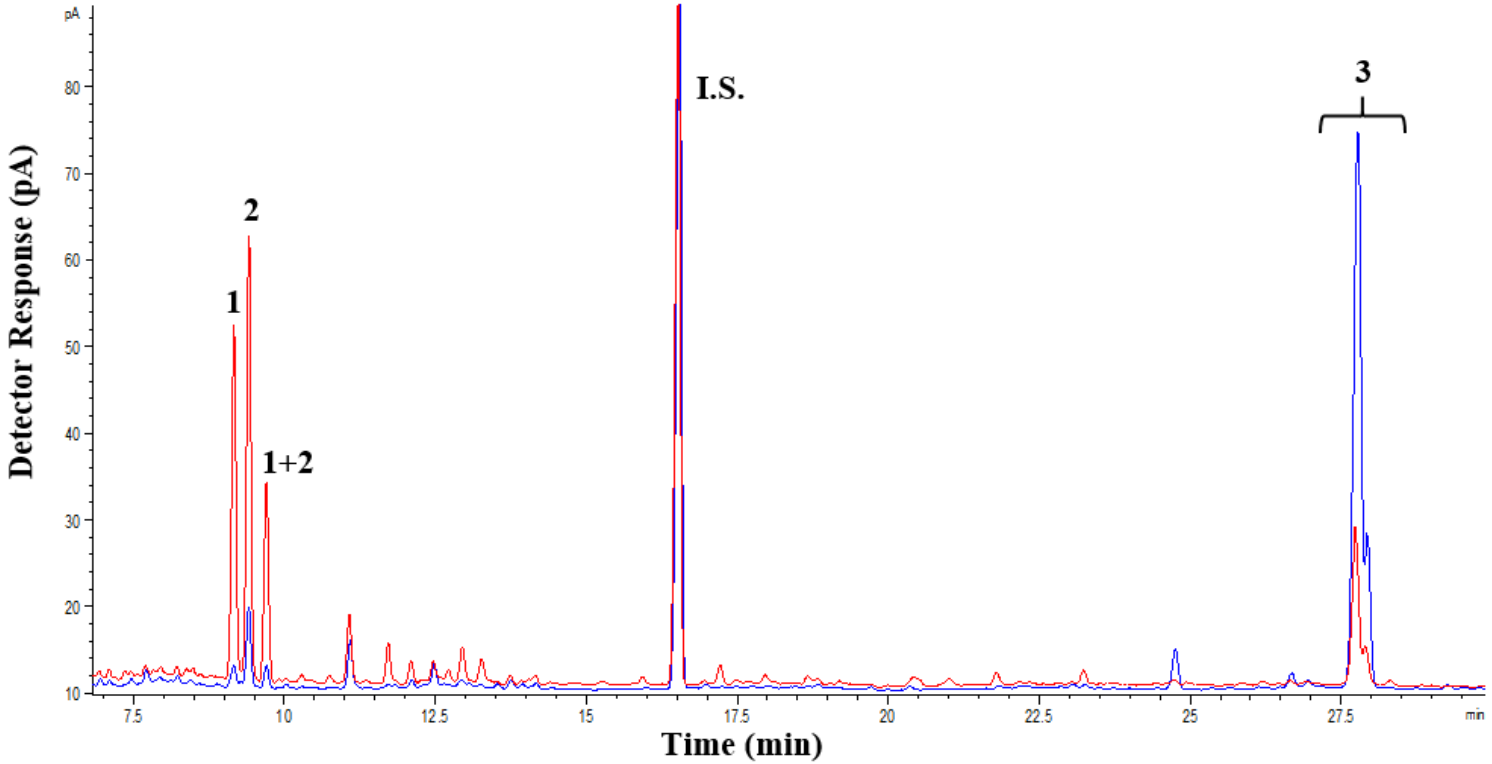

Figure S1. Chromatographic profiles obtained by GC-FID of TMSO derivatives of the digestion of lactose at 0.2 mg/mL before (blue) and after (red) 5 h of small intestinal digestion with RSIE. Peaks: 1: Galactose, 2: Glucose, I.S.: Internal Standard, 3: Lactose.

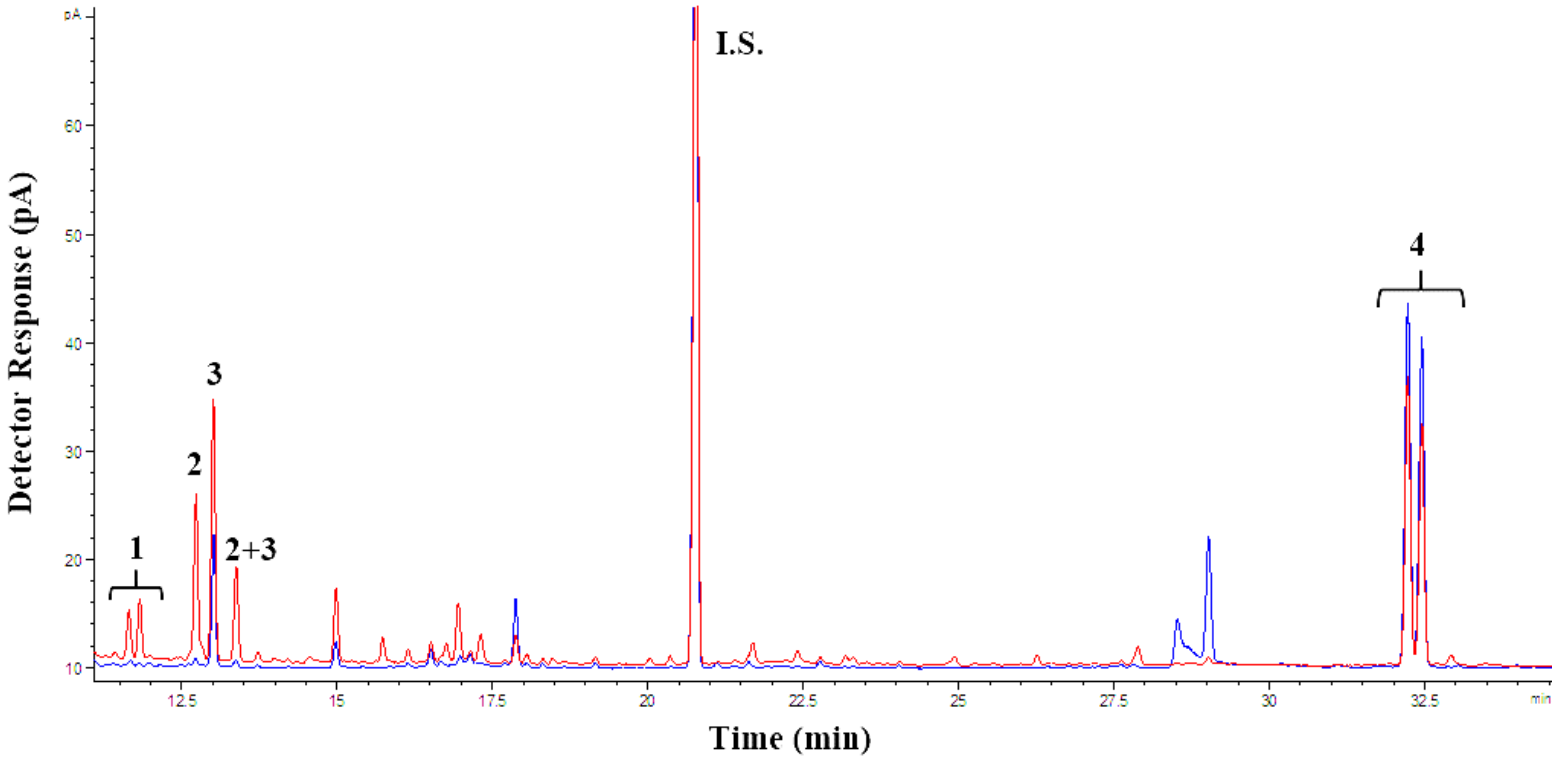

Figure S2. Chromatographic profiles obtained by GC-FID of TMSO derivatives of the digestion of lactulose at 0.2 mg/mL before (blue) and after (red) 5 h of small intestinal digestion with RSIE. Peaks: 1: Fructose, 2: Galactose, 3: Glucose, I.S.: Internal Standard, 4: Lactulose.

ANEXO B

MATERIAL SUPLEMENTARIO CAPÍTULO 4

Behaviour of citrus pectin and modified citrus pectin in an azoxymethane/dextran sodium sulfate (AOM/DSS)-induced rat colorectal carcinogenesis model

Alvaro Ferreira-Lazarte[a], Javier Fernández[b, c, d], Pablo Gallego-Lobillo[a], Claudio J. Villar[b, c, d], Felipe Lombó, F. Javier Moreno[a] y Mar Villamiel[a]

[a] Instituto de Investigación en Ciencias de la Alimentación, CIAL (CSIC-UAM). C/Nicolás Cabrera, 9, Campus de la Universidad Autónoma de Madrid, 28049 Madrid, España.
[b] Research Unit "Biotechnology in Nutraceuticals and Bioactive Compounds-BIONUC", Departamento de Biología Funcional, Área de Microbiología, Universidad de Oviedo.
[c] Instituto Universitario de Oncología del Principado de Asturias, Oviedo, España.
[d] Instituto de Investigación Sanitaria del Principado de Asturias, Oviedo, España.

Reproducido a partir de Elsevier
International Journal of Biological Macromolecules
2021, 167, 1349-1360
DOI: https://doi.org/10.1016/j.ijbiomac.2020.11.089

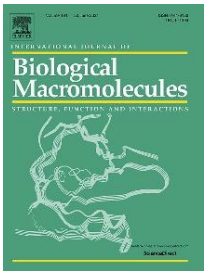

Table S1.
Caecal microbiota composition (percentages) at the genus and species levels for CRC-rats, no CRC-rats (control) and the sum of both groups.

		All individuals			CRC rats			No CRC rats (control cohort)		
Genus	**Species**	**F**	**FP**	**FMP**	**F**	**FP**	**FMP**	**F**	**FP**	**FMP**
Bifidobacterium		0.000	0.174	0.135	0.00	0.20	0.20	0.00	0.14	0.00
	animalis	0.000	0.090	0.007	0.00	0.14	0.01	0.00	0.02	0.00
	pseudolongum	0.000	0.010	0.028	0.00	0.01	0.04	0.00	0.02	0.00
Adlercreutzia		0.018	0.006	0.027	0.02	0.01	0.04	0.01	0.01	0.01
	equolifaciens	0.018	0.006	0.027	0.02	0.01	0.04	0.01	0.01	0.01
Atopobium		0.000	0.004	0.000	0.00	0.01	0.00	0.00	0.00	0.00
Bacteroides		9.174	8.460	10.607	9.46	10.09	11.19	8.05	6.01	9.45
	acidifaciens	1.420	0.514	0.000	1.06	0.70	0.00	2.88	0.24	0.00
	caccae	0.192	0.096	0.423	0.23	0.09	0.48	0.04	0.11	0.32
	eggerthii	0.050	0.290	1.053	0.06	0.41	1.50	0.00	0.12	0.17
	massiliensis	0.052	0.000	0.222	0.02	0.00	0.17	0.19	0.00	0.33
	nordii	0.086	0.020	0.003	0.09	0.00	0.01	0.06	0.05	0.00
	oleiciplenus	0.009	0.004	0.000	0.01	0.01	0.00	0.00	0.00	0.00
	intestinalis	0.000	0.020	0.012	0.00	0.03	0.00	0.00	0.01	0.04
	sp.	0.150	0.078	0.093	0.16	0.07	0.05	0.12	0.09	0.18
	stercorirosoris	0.801	0.740	0.508	0.94	1.11	0.62	0.25	0.18	0.29
	thetaiotaomicron	0.042	0.022	0.037	0.04	0.04	0.05	0.04	0.00	0.01
	uniformis	0.119	0.040	0.140	0.12	0.04	0.03	0.11	0.04	0.37
	vulgatus	0.710	0.050	0.217	0.78	0.03	0.19	0.42	0.09	0.28
Butyricimonas		0.342	0.138	0.278	0.33	0.12	0.32	0.40	0.16	0.20
	virosa	0.157	0.048	0.090	0.15	0.04	0.10	0.17	0.06	0.07
Parabacteroides		1.357	0.570	2.210	1.61	0.55	1.98	0.35	0.60	2.68
	distasonis	0.599	0.156	0.478	0.69	0.19	0.49	0.23	0.10	0.46
	merdae	0.200	0.116	0.662	0.25	0.10	0.58	0.01	0.14	0.83

Anexo B

Paraprevotella		0.001	0.306	0.358	0.00	0.29	0.41	0.00	0.33	0.27
Prevotella		0.004	2.302	1.692	0.01	2.23	0.05	0.00	2.41	4.99
	stercorea	0.000	0.002	0.000	0.00	0.00	0.00	0.00	0.01	0.00
Alistipes		1.252	0.682	1.080	1.33	0.88	1.04	0.93	0.39	1.16
	indistinctus	0.005	0.016	0.042	0.01	0.02	0.06	0.00	0.01	0.02
	shahii	0.000	0.032	0.097	0.00	0.02	0.06	0.00	0.05	0.17
	sp.	0.072	0.010	0.158	0.09	0.02	0.19	0.02	0.00	0.11
	timonensis	0.000	0.028	0.063	0.00	0.05	0.03	0.00	0.00	0.14
Mucispirillum		1.049	0.000	0.000	0.97	0.00	0.00	1.39	0.00	0.00
	schaedleri	1.049	0.000	0.000	0.97	0.00	0.00	1.39	0.00	0.00
Lactobacillus		0.004	0.704	0.620	0.01	0.74	0.77	0.00	0.65	0.32
	murinus	0.000	0.000	0.007	0.00	0.00	0.01	0.00	0.00	0.00
	reuteri	0.000	0.000	0.002	0.00	0.00	0.00	0.00	0.00	0.00
	johnsonii	0.000	0.002	0.000	0.00	0.00	0.00	0.00	0.00	0.00
Lactococcus		0.001	0.000	0.003	0.00	0.00	0.01	0.00	0.00	0.00
	garvieae	0.001	0.000	0.003	0.00	0.00	0.01	0.00	0.00	0.00
Streptococcus		0.002	0.000	0.000	0.00	0.00	0.00	0.00	0.00	0.00
	hyointestinalis	0.002	0.000	0.000	0.00	0.00	0.00	0.00	0.00	0.00
Clostridium		4.296	3.000	2.643	4.24	2.94	3.16	4.51	3.09	1.62
	hiranonis	0.033	0.036	0.003	0.04	0.03	0.01	0.00	0.05	0.00
	sp.	0.723	0.894	0.680	0.75	1.02	0.92	0.63	0.71	0.20
Eubacterium		0.015	0.274	0.055	0.02	0.04	0.02	0.00	0.63	0.13
	limosum	0.000	0.016	0.002	0.00	0.01	0.00	0.00	0.02	0.00
Acetatifactor		0.010	0.002	0.015	0.01	0.00	0.02	0.00	0.00	0.00
	muris	0.004	0.000	0.005	0.01	0.00	0.01	0.00	0.00	0.00
Anaerostipes		0.492	0.004	0.020	0.35	0.00	0.01	1.07	0.01	0.04
	sp.	0.005	0.000	0.015	0.01	0.00	0.01	0.00	0.00	0.04

Blautia		0.429	0.166	1.115	0.52	0.21	1.34	0.09	0.10	0.67
	glucerasea	0.080	0.002	0.010	0.09	0.00	0.02	0.03	0.00	0.00
	producta	0.316	0.086	0.858	0.38	0.12	1.09	0.05	0.03	0.40
Butyrivibrio		0.009	0.004	0.000	0.00	0.01	0.00	0.03	0.00	0.00
	crossotus	0.009	0.004	0.000	0.00	0.01	0.00	0.03	0.00	0.00
Dorea		0.145	0.008	0.037	0.18	0.00	0.05	0.01	0.02	0.01
	Dorea	0.145	0.008	0.037	0.18	0.00	0.05	0.01	0.02	0.01
Eubacterium		0.022	0.002	0.002	0.02	0.00	0.00	0.02	0.01	0.00
Lachnoanaerobaculum		0.021	0.000	0.125	0.03	0.00	0.19	0.01	0.00	0.00
	umeaense	0.018	0.000	0.115	0.02	0.00	0.17	0.01	0.00	0.00
LachnoClostridium		0.145	0.000	0.412	0.18	0.00	0.57	0.00	0.00	0.10
	aldenense	0.001	0.000	0.025	0.00	0.00	0.04	0.00	0.00	0.00
	asparagiforme	0.004	0.000	0.000	0.01	0.00	0.00	0.00	0.00	0.00
	bolteae	0.003	0.000	0.360	0.00	0.00	0.51	0.00	0.00	0.06
	lavalense	0.032	0.000	0.005	0.04	0.00	0.00	0.00	0.00	0.02
Marvinbryantia		0.002	0.000	0.082	0.00	0.00	0.12	0.00	0.00	0.00
	formatexigens	0.000	0.000	0.028	0.00	0.00	0.04	0.00	0.00	0.00
Robinsoniella		0.015	0.000	0.000	0.01	0.00	0.00	0.02	0.00	0.00
Roseburia		0.073	0.000	0.042	0.07	0.00	0.05	0.10	0.00	0.04
	faecis	0.069	0.000	0.033	0.06	0.00	0.03	0.10	0.00	0.04
	intestinalis	0.003	0.000	0.000	0.00	0.00	0.00	0.00	0.00	0.00
Stomatobaculum		0.195	0.000	0.007	0.18	0.00	0.01	0.26	0.00	0.00
	longum	0.195	0.000	0.007	0.18	0.00	0.01	0.26	0.00	0.00
Tyzzerella		0.088	0.012	0.005	0.07	0.00	0.01	0.15	0.03	0.00
	propionicum	0.082	0.000	0.000	0.07	0.00	0.00	0.13	0.00	0.00
[Ruminococcus]		3.866	3.550	4.748	3.92	3.56	5.61	3.64	3.54	3.03
	gnavus	0.556	2.834	3.942	0.58	2.72	4.64	0.47	3.01	2.55
	torques	0.002	0.000	0.000	0.00	0.00	0.00	0.00	0.00	0.00

Anexo B

Oscillibacter	*sp.*	0.112	0.092	0.230	0.07	0.07	0.21	0.29	0.12	0.28
PeptoClostridium		0.007	0.000	0.000	0.01	0.00	0.00	0.00	0.00	0.00
	difficile	0.007	0.000	0.000	0.01	0.00	0.00	0.00	0.00	0.00
Acetivibrio		0.057	0.000	0.000	0.01	0.00	0.00	0.26	0.00	0.00
	ethanolgignens	0.057	0.000	0.000	0.01	0.00	0.00	0.26	0.00	0.00
Anaerotruncus		0.126	0.030	0.063	0.13	0.00	0.02	0.10	0.08	0.16
Faecalibacterium		2.440	2.050	2.102	2.50	1.76	2.38	2.19	2.49	1.54
	prausnitzii	1.345	0.338	0.565	1.34	0.16	0.63	1.36	0.60	0.44
Oscillospira		0.014	0.076	0.093	0.01	0.02	0.06	0.05	0.17	0.17
	guilliermondii	0.014	0.076	0.093	0.01	0.02	0.06	0.05	0.17	0.17
RuminiClostridium		0.152	0.016	0.005	0.16	0.02	0.01	0.13	0.01	0.00
Ruminococcus		2.503	0.342	0.242	2.76	0.42	0.28	1.47	0.23	0.16
	bromii	0.073	0.004	0.027	0.05	0.00	0.02	0.19	0.01	0.05
	flavefaciens	0.823	0.214	0.090	0.77	0.29	0.14	1.06	0.10	0.00
	sp.	0.119	0.012	0.115	0.11	0.00	0.12	0.18	0.03	0.10
Subdoligranulum	*sp.*	0.072	0.004	0.035	0.09	0.01	0.04	0.00	0.00	0.02
Bacteroides		0.000	0.366	0.000	0.00	0.45	0.00	0.00	0.24	0.00
Flavonifractor		0.433	0.098	0.290	0.31	0.02	0.38	0.95	0.21	0.11
	plautii	0.022	0.002	0.015	0.03	0.00	0.02	0.00	0.00	0.01
Pseudoflavonifractor		0.184	0.164	0.100	0.21	0.16	0.11	0.10	0.18	0.09
[Eubacterium]		0.045	0.000	0.007	0.06	0.00	0.01	0.00	0.00	0.01
	dolichum	0.045	0.000	0.007	0.06	0.00	0.01	0.00	0.00	0.01
Clostridium		0.058	0.000	0.002	0.07	0.00	0.00	0.02	0.00	0.00
Holdemania		0.012	0.002	0.048	0.02	0.00	0.07	0.00	0.00	0.00
	filiformis	0.012	0.002	0.048	0.02	0.00	0.07	0.00	0.00	0.00
Turicibacter		0.030	0.148	0.000	0.04	0.12	0.00	0.00	0.19	0.00
Phascolarctobacterium		1.776	1.334	1.830	1.95	1.15	1.80	1.07	1.61	1.90
	succinatutens	1.513	1.124	1.465	1.69	1.00	1.53	0.83	1.32	1.34

Victivallis		0.003	0.196	0.155	0.00	0.26	0.23	0.00	0.10	0.02
	vadensis	0.003	0.196	0.155	0.00	0.26	0.23	0.00	0.10	0.02
Parasutterella		1.123	4.058	1.895	1.35	3.76	2.35	0.21	4.51	0.99
	excrementihominis	1.026	3.370	1.657	1.24	3.10	2.09	0.18	3.78	0.80
Bilophila		9.832	3.042	6.687	8.70	2.15	3.72	14.37	4.39	12.63
	wadsworthia	7.635	2.260	2.735	6.43	1.49	2.10	12.46	3.42	4.01
Desulfovibrio		0.179	0.072	0.072	0.14	0.04	0.11	0.33	0.13	0.00
	C21_c20	0.008	0.000	0.000	0.00	0.00	0.00	0.03	0.00	0.00
	sp.	0.171	0.072	0.072	0.14	0.04	0.11	0.30	0.13	0.00
Citrobacter		0.000	0.006	0.002	0.00	0.01	0.00	0.00	0.00	0.00
	farmeri	0.000	0.002	0.000	0.00	0.00	0.00	0.00	0.00	0.00
	sp.	0.000	0.004	0.002	0.00	0.01	0.00	0.00	0.00	0.00
Cronobacter		0.000	0.004	0.002	0.00	0.01	0.00	0.00	0.00	0.00
	sakazakii	0.000	0.004	0.002	0.00	0.01	0.00	0.00	0.00	0.00
Edwardsiella		0.000	0.002	0.000	0.00	0.00	0.00	0.00	0.00	0.00
	ictaluri	0.000	0.002	0.000	0.00	0.00	0.00	0.00	0.00	0.00
Enterobacter	*sp.*	0.000	0.002	0.000	0.00	0.00	0.00	0.00	0.00	0.00
Escherichia		0.004	0.552	0.197	0.01	0.88	0.29	0.00	0.07	0.01
	albertii	0.000	0.006	0.002	0.00	0.01	0.00	0.00	0.00	0.00
	coli	0.004	0.532	0.195	0.01	0.84	0.29	0.00	0.07	0.01
	sp.	0.000	0.008	0.000	0.00	0.01	0.00	0.00	0.00	0.00
Salmonella		0.000	0.050	0.010	0.00	0.08	0.02	0.00	0.00	0.00
	enterica	0.000	0.050	0.010	0.00	0.08	0.02	0.00	0.00	0.00
Serratia		0.007	0.022	0.017	0.01	0.02	0.02	0.00	0.02	0.01

Shigella		0.000	0.080	0.048	0.00	0.13	0.07	0.00	0.00	0.00
	dysenteriae	0.000	0.006	0.002	0.00	0.01	0.00	0.00	0.00	0.00
	flexneri	0.000	0.058	0.040	0.00	0.10	0.06	0.00	0.00	0.00
	sonnei	0.000	0.012	0.003	0.00	0.02	0.01	0.00	0.00	0.00
	sp.	0.000	0.002	0.002	0.00	0.00	0.00	0.00	0.00	0.00
Sodalis		0.000	0.002	0.000	0.00	0.00	0.00	0.00	0.00	0.00
	glossinidius	0.000	0.002	0.000	0.00	0.00	0.00	0.00	0.00	0.00
Trabulsiella		0.000	0.038	0.005	0.00	0.06	0.01	0.00	0.00	0.00
	farmeri	0.000	0.030	0.003	0.00	0.05	0.01	0.00	0.00	0.00
Aggregatibacter		0.004	0.002	0.013	0.01	0.00	0.02	0.00	0.01	0.01
	aphrophilus	0.004	0.002	0.013	0.01	0.00	0.02	0.00	0.01	0.01
Pasteurella		0.005	0.026	0.000	0.01	0.02	0.00	0.00	0.03	0.00
	sp.	0.001	0.000	0.000	0.00	0.00	0.00	0.00	0.00	0.00
Akkermansia		4.208	1.518	2.165	4.03	1.08	2.05	4.94	2.18	2.40
	muciniphila	4.208	1.518	2.165	4.03	1.08	2.05	4.94	2.18	2.40

ANEXO C

MATERIAL SUPLEMENTARIO CAPÍTULO 5

Enzymatic synthesis and structural characterization of novel trehalose-based oligosaccharides

Pablo Gallego-Lobillo[a], Elisa G. Doyagüez[b], María Luisa Jimeno[b], Mar Villamiel[a], Oswaldo Hernández-Hernández[a]

[a] Instituto de Investigación en Ciencias de la Alimentación, CIAL (CSIC-UAM). C/Nicolás Cabrera, 9, Campus de la Universidad Autónoma de Madrid, 28049 Madrid, España.

[b] Centro de Química Orgánica "Lora Tamayo" (CSIC), c/Juan de la Cierva, 3, E-28006, Madrid, España

Reproducido a partir de ACS Publications
Journal of Agricultural and Food Chemistry
2021, 69, 42, 12541–12553
DOI: https://doi.org/10.1021/acs.jafc.1c03768

Table S1. Carbohydrate Evolution during the Transgalactosylation Assay with Lactose/Trehalose and Lactose Solutions, by *β*-Galactosidase from *Bacillus circulans* at 50 °C, pH 4.5, Determined by GC-FID Analysis (% total carbohydrates)

		25% Lactose/25% Trehalose					25% Lactose				
Carbohydrate	**T_r**	**0 h**	**2 h**	**4 h**	**6 h**	**24 h**	**0 h**	**2 h**	**4 h**	**6 h**	**24 h**
Monosaccharides											
Galactose	11.4	0.0 ± 0.0	0.6 ± 0.1	0.7 ± 0.1	0.8 ± 0.0	1.1 ± 0.1	0.0 ± 0.0	1.8 ± 0.1	2.1 ± 0.2	2.4 ± 0.0	3.5 ± 0.3
Glucose	11.7	0.0 ± 0.0	13.4 ± 0.4	14.6 ± 0.4	15.2 ± 1.3	15.5 ± 0.6	0.0 ± 0.0	19.7 ± 0.2	21.3 ± 0.3	22.4 ± 1.3	24.7 ± 0.3
Disaccharides											
Trehalose	29.9	49.2 ± 2.7	31.8 ± 1.5	31.3 ± 1.4	30.6 ± 1.3	31.6 ± 1.0	-	-	-	-	-
Lactose	30.8	50.8 ± 2.5	15.0 ± 1.3	11.5 ± 1.2	10.2 ± 0.8	7.5 ± 0.3	100.0 ± 15.6	32.6 ± 0.0	27.6 ± 0.4	26.1 ± 1.2	19.2 ± 1.8
β-Gal-(1→4)-*β*-Glc	31.1	0.0 ± 0.0	0.3 ± 0.0	0.4 ± 0.0	0.5 ± 0.0	0.7 ± 0.3	0.0 ± 0.0	1.1 ± 0.0	1.4 ± 0.1	1.6 ± 0.1	2.4 ± 0.2
β-Gal-(1→3)-*β*-Glc	31.7	0.0 ± 0.0	2.8 ± 0.1	4.0 ± 0.1	4.4 ± 0.1	5.3 ± 0.1	0.0 ± 0.0	7.6 ± 0.2	10.1 ± 0.1	11.5 ± 0.5	14.7 ± 0.2
β-Gal-(1→2)-*β*-Glc	31.9	0.0 ± 0.0	1.1 ± 0.0	1.6 ± 0.0	1.8 ± 0.0	2.4 ± 0.1	0.0 ± 0.0	2.3 ± 0.2	3.3 ± 0.1	3.8 ± 0.3	5.8 ± 0.3
β-Gal-(1→6)-*β*-Glc	33.8	0.0 ± 0.0	0.4 ± 0.0	0.6 ± 0.0	0.7 ± 0.0	1.0 ± 0.0	0.0 ± 0.0	0.9 ± 0.1	1.1 ± 0.1	1.4 ± 0.1	2.5 ± 0.1
Trisaccharides											
β-Gal-(1→4)-Tre*	46.0	0.0 ± 0.0	18.3 ± 0.6	18.4 ± 0.8	18.7 ± 1.6	17.3 ± 0.5	-	-	-	-	-
β-Gal-(1→4)-Lac	47.6	0.0 ± 0.0	5.2 ± 0.5	4.1 ± 0.3	3.8 ± 0.3	3.0 ± 0.3	0.0 ± 0.0	21.1 ± 0.3	18.4 ± 0.7	16.4 ± 0.6	12.8 ± 1.5
β-Gal-(1→6)-Lac	48.0	0.0 ± 0.0	1.0 ± 0.0	1.4 ± 0.1	1.5 ± 0.1	1.9 ± 0.1	0.0 ± 0.0	4.3 ± 0.3	6.0 ± 0.4	6.3 ± 0.2	8.2 ± 0.6
β-Gal-(1→6)-Tre*	49.0	0.0 ± 0.0	1.5 ± 0.1	2.4 ± 0.1	2.9 ± 0.3	3.8 ± 0.3	-	-	-	-	-
Other trisaccharides	-	0.0 ± 0.0	0.6 ± 0.1	0.7 ± 0.0	0.8 ± 0.1	0.9 ± 0.1	-	-	-	-	-

Anexo C

Tetrasaccharides											
β-Gal-(1→4)-*β*-Gal-(1→6)-Tre* + *β*-Gal-(1→4)-*α*-Glc-(1→1)-[*β*-Gal-(1→4)]-*α*-Glc*	58.9	0.0 ± 0.0	2.0 ± 0.2	2.1 ± 0.2	2.1 ± 0.2	1.9 ± 0.2	-	-	-	-	-
β-Gal-(1→4)-*β*-Gal-(1→4)-Tre*	59.5	0.0 ± 0.0	3.7 ± 0.2	4.0 ± 0.3	4.0 ± 0.4	3.5 ± 0.2	-	-	-	-	-
β-Gal-(1→4)-*α*-Glc-(1↔1)-[*β*-Gal-(1→6)]-*α*-Glc* + *β*-Gal-(1→6)-*α*-Glc-(1↔1)-[*β*-Gal-(1→6)]-*α*-Glc*	60.6	0.0 ± 0.0	1.9 ± 0.2	2.0 ± 0.2	2.1 ± 0.1	2.3 ± 0.1	-	-	-	-	-
Other tetrasaccharides	-	-	-	-	-	-	0.0 ± 0.0	9.4 ± 0.3	9.0 ± 0.2	8.2 ± 0.7	6.5 ± 1.0
Pentasaccharides											
β-Gal-(1→4)-*β*-Gal-(1→4)-*β*-Gal-(1→4)-Tre*	70.0	0.0 ± 0.0	0.9 ± 0.0	1.3 ± 0.1	1.3 ± 0.1	1.4 ± 0.1	-	-	-	-	-

Data are expressed as the mean ± SD (n = 4). Tr: Retention time.
* Trehalose derivatives synthesized.

Table S2. Carbohydrate Evolution during the Transgalactosylation Assay with Lactose/Trehalose and Lactose Solutions, by *β*-Galactosidase from *Aspergillus oryzae* at 50 °C, pH 4.5, Determined by GC-FID Analysis (% total carbohydrates)

		25% Lactose/25% Trehalose					25% Lactose				
Carbohydrate	**T_r**	**0 h**	**2 h**	**4 h**	**6 h**	**24 h**	**0 h**	**2 h**	**4 h**	**6 h**	**24 h**
Monosaccharides											
Galactose	11.4	0.0 ± 0.0	6.0 ± 0.3	9.1 ± 0.7	12.3 ± 1.2	20.4 ± 0.5	0.0 ± 0.0	11.7 ± 0.3	18.5 ± 1.0	23.7 ± 4.1	43.5 ± 0.2
Glucose	11.7	0.0 ± 0.0	12.2 ± 0.6	15.7 ± 1.1	19.2 ± 1.9	23.0 ± 2.0	0.0 ± 0.0	23.7 ± 0.3	30.5 ± 1.3	34.6 ± 6.1	47.2 ± 0.1
Disaccharides											
Trehalose	29.9	49.5 ± 2.8	45.7 ± 2.2	44.8 ± 3.3	44.5 ± 0.5	44.3 ± 0.7	-	-	-	-	-
Lactose	30.8	50.5 ± 1.4	20.5 ± 0.9	13.7 ± 1.0	10.3 ± 1.3	1.3 ± 0.2	100.0 ± 2.1	36.8 ± 0.1	23.8 ± 0.4	16.4 ± 3.1	1.6 ± 0.2
β-Gal-(1→4)-Gal	31.1	0.0 ± 0.0	0.2 ± 0.0	0.4 ± 0.1	0.4 ± 0.0	0.3 ± 0.0	0.0 ± 0.0	0.6 ± 0.1	0.8 ± 0.0	0.9 ± 0.2	0.6 ± 0.0
β-Gal-(1→6)-Glc	33.7	0.0 ± 0.0	2.0 ± 0.1	3.1 ± 0.3	3.5 ± 0.4	2.2 ± 0.2	0.0 ± 0.0	4.8 ± 0.3	7.1 ± 0.3	8.1 ± 1.6	4.3 ± 0.4
β-Gal-(1→6)-Gal	34.4	0.0 ± 0.0	0.5 ± 0.0	0.7 ± 0.0	0.9 ± 0.0	0.6 ± 0.0	0.0 ± 0.0	1.2 ± 0.1	1.7 ± 0.1	1.9 ± 0.3	1.0 ± 0.1
Other disaccharides	-	0.0 ± 0.0	1.0 ± 0.0	1.4 ± 0.1	1.5 ± 0.2	1.0 ± 0.1	0.0 ± 0.0	2.3 ± 0.1	2.9 ± 0.0	3.2 ± 0.6	1.8 ± 0.1
Trisaccharides											
[*β*-Gal-(1→4)]-[*β*-Gal-(1→6)]-Glc	47.4	0.0 ± 0.0	1.5 ± 0.1	1.4 ± 0.1	1.2 ± 0.1	0.7 ± 0.0	0.0 ± 0.0	3.4 ± 0.1	3.5 ± 0.2	3.3 ± 0.6	0.0 ± 0.0
β-Gal-(1→6)-Lac	48.0	0.0 ± 0.0	4.1 ± 0.3	2.4 ± 0.2	1.3 ± 0.2	0.4 ± 0.0	0.0 ± 0.0	4.5 ± 0.3	3.1 ± 0.2	2.2 ± 0.3	0.0 ± 0.0
β-Gal-(1→6)-Tre*	49.0	0.0 ± 0.0	2.9 ± 0.2	4.0 ± 0.3	5.0 ± 0.5	4.8 ± 0.1	-	-	-	-	-
Other trisaccharides	-	0.0 ± 0.0	2.6 ± 0.3	2.9 ± 0.2	2.4 ± 0.3	1.3 ± 0.	0.0 ± 0.0	8.4 ± 0.2	6.2 ± 0.2	4.5 ± 0.4	0.0 ± 0.0
Tetrasaccharides											
β-Gal-(1→6)-*β*-Gal-(1→6)-Tre*	61.2	0.0 ± 0.0	1.1 ± 0.3	1.2 ± 0.3	1.4 ± 0.1	0.8 ± 0.0	-	-	-	-	-
Other tetrasaccharides	-	-	-	-	-	-	0.0 ± 0.0	2.8 ± 0.2	1.8 ± 0.2	1.2 ± 0.3	0.0 ± 0.0

Data are expressed as the mean ± SD (n = 4). Tr: Retention time.
* Trehalose derivatives synthesized.

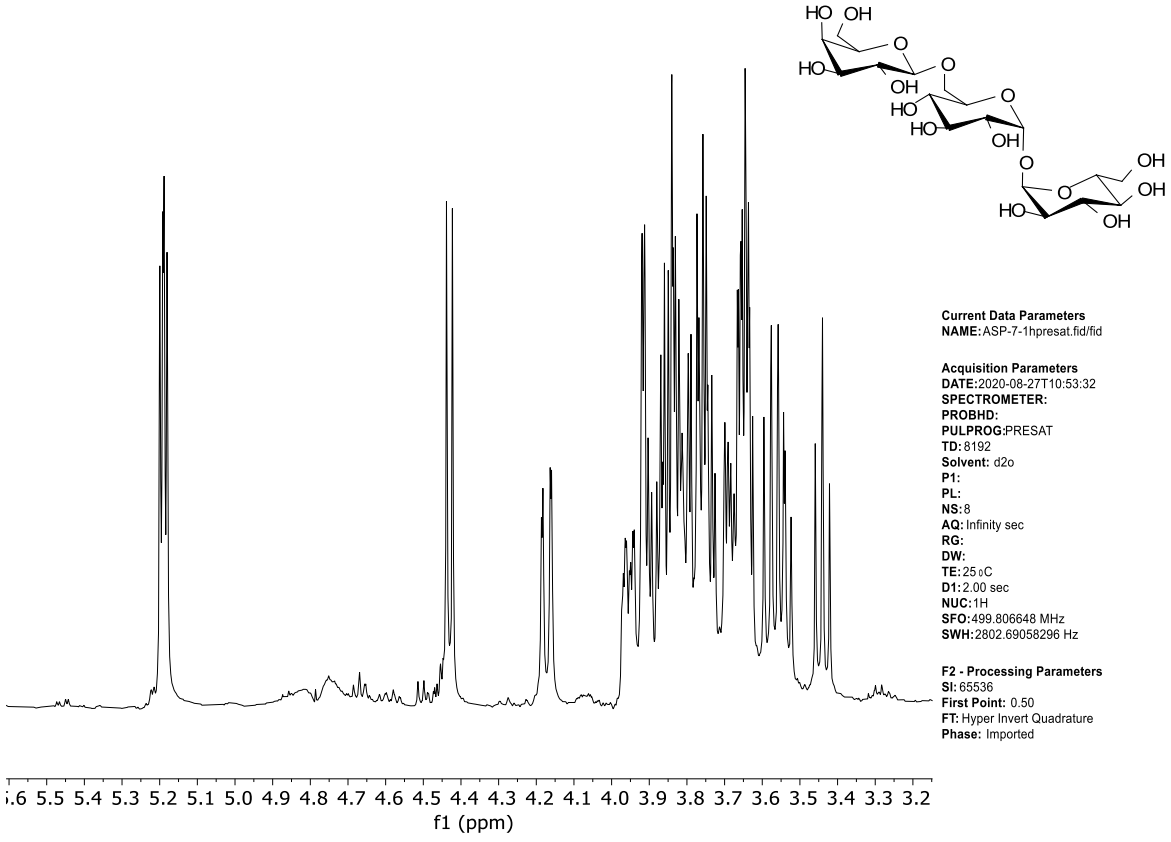

Figure S1. ^{1}H NMR (500 MHz, D_2O) of trisaccharide **1** derived from trehalose.

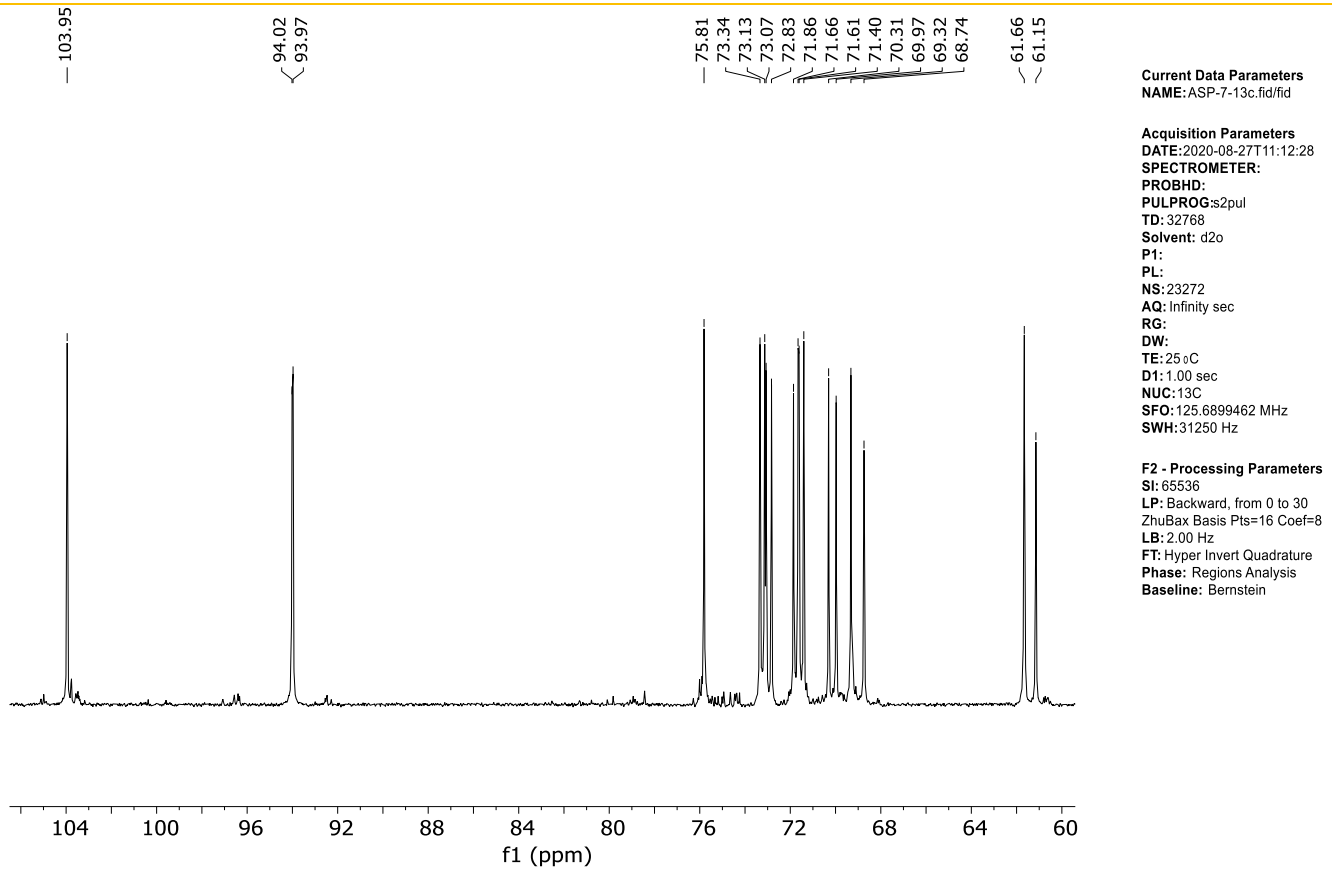

Figure S2. ^{13}C NMR (125 MHz, D_2O) of trisaccharide **1** derived from trehalose.

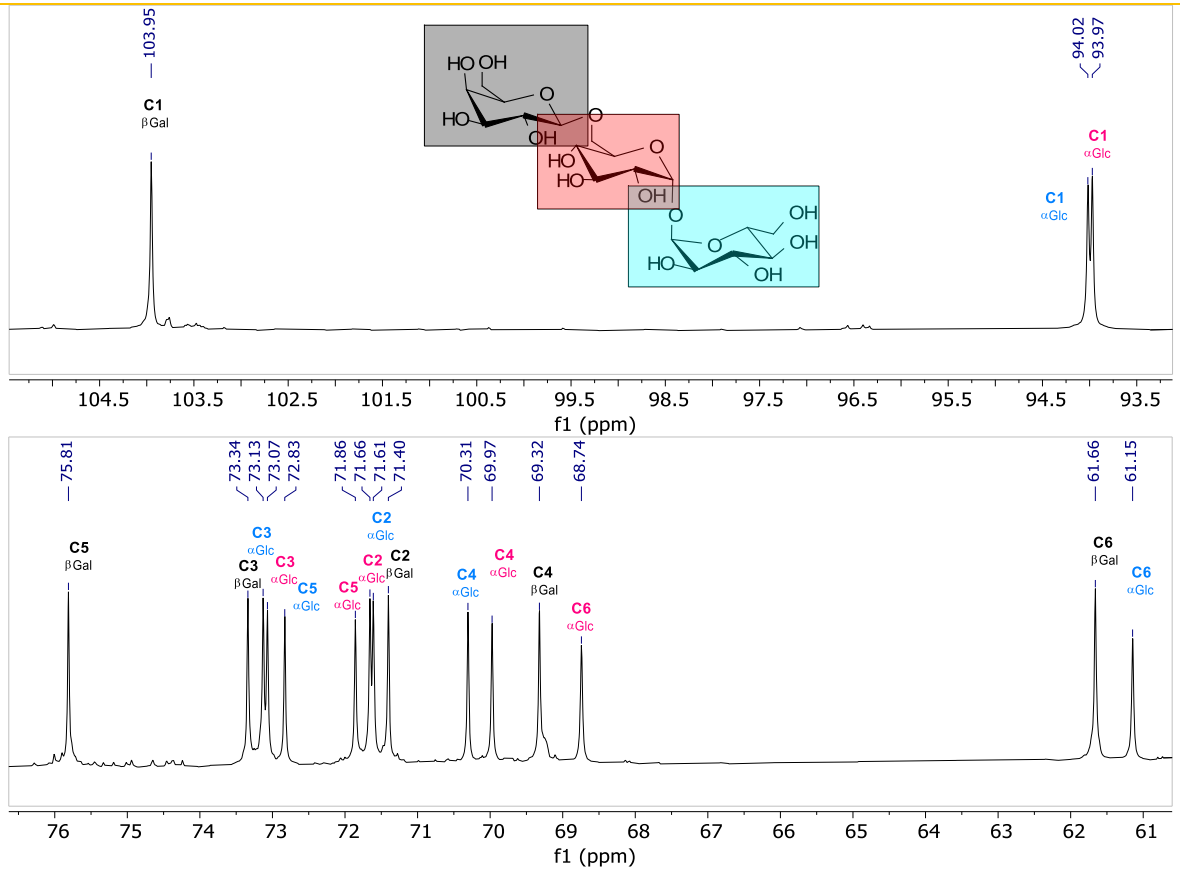

Figure S3. Complete assignment of ^{13}C NMR spectrum of trisaccharide **1** derived from trehalose.

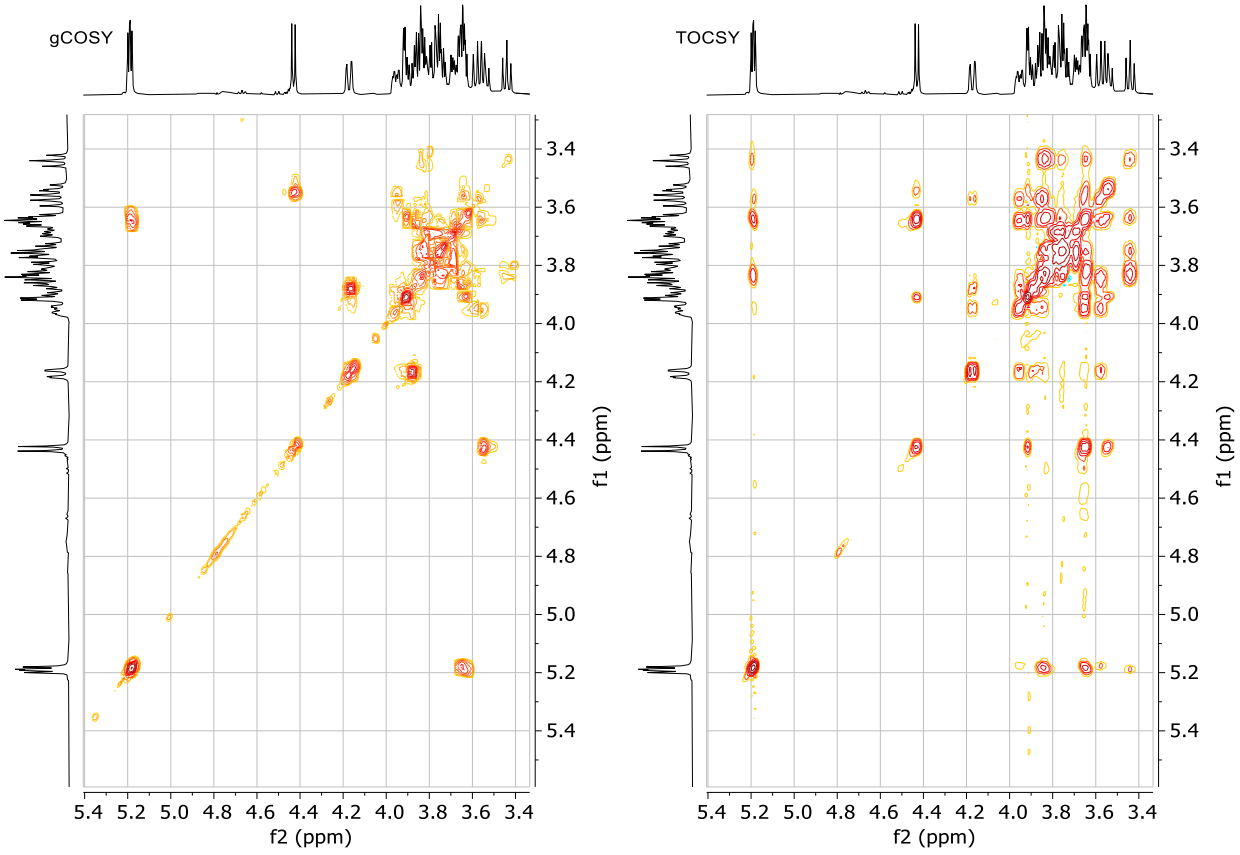

Figure S4. gCOSY and TOCSY (500 MHz, D_2O) of trisaccharide **1** derived from trehalose.

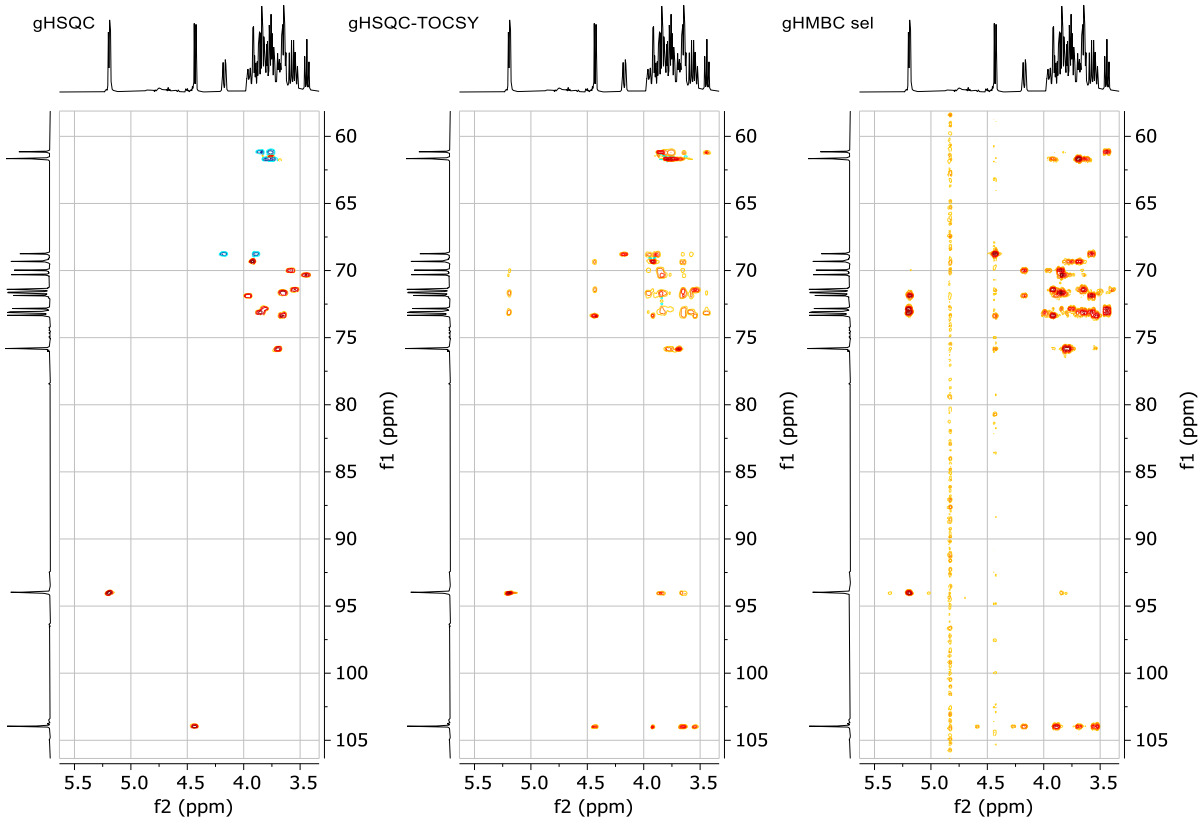

Figure S5. Multiplicity-edited gHSQC (methylene**:** blue cross peaks; methine**:** red cross peaks), gHSQC-TOCSY and gHMBC semiselective (500 MHz, D_2O) of trisaccharide **1** derived from trehalose.

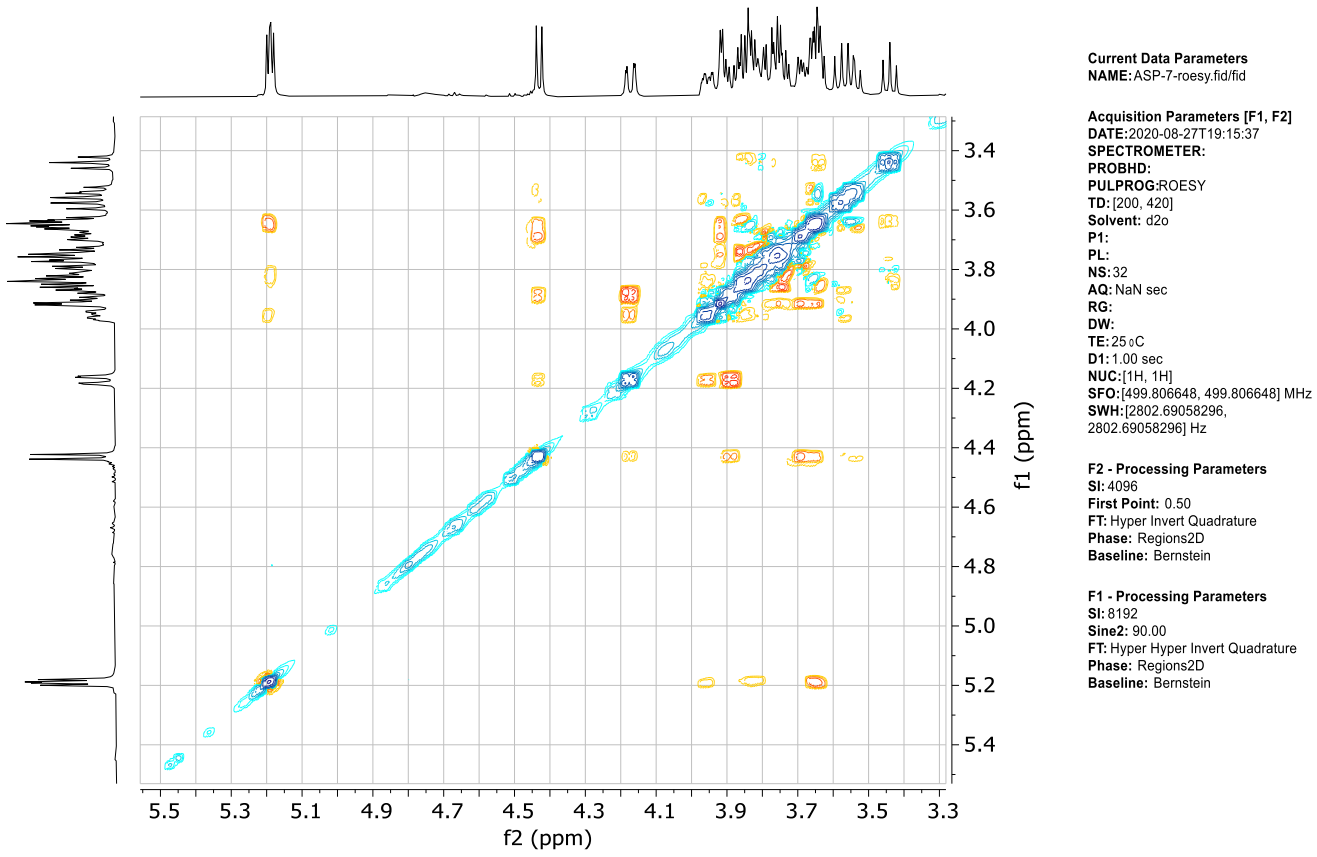

Figure S6. ROESY (500 MHz, D_2O) of trisaccharide **1** derived from trehalose.

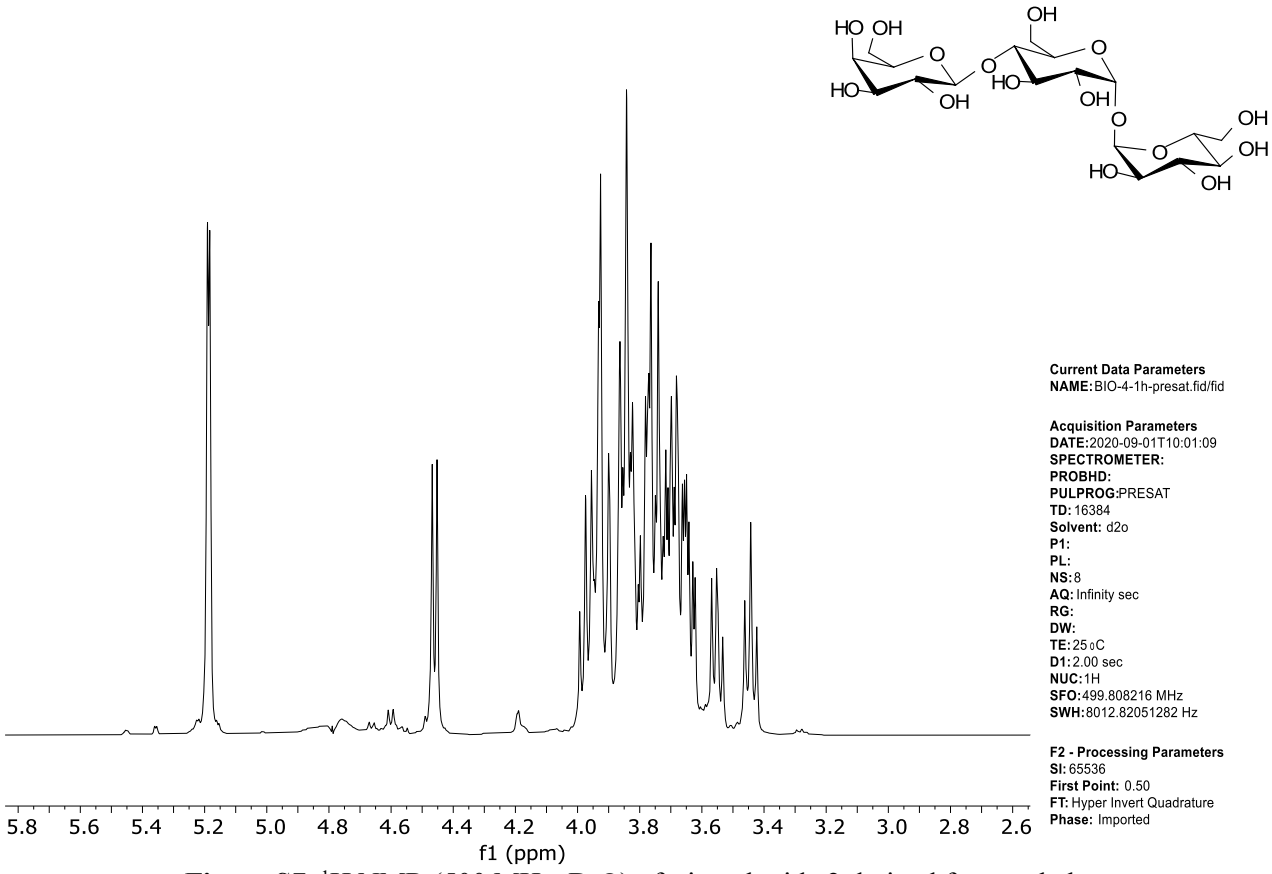

Figure S7. ^{1}H NMR (500 MHz, D_2O) of trisaccharide **2** derived from trehalose.

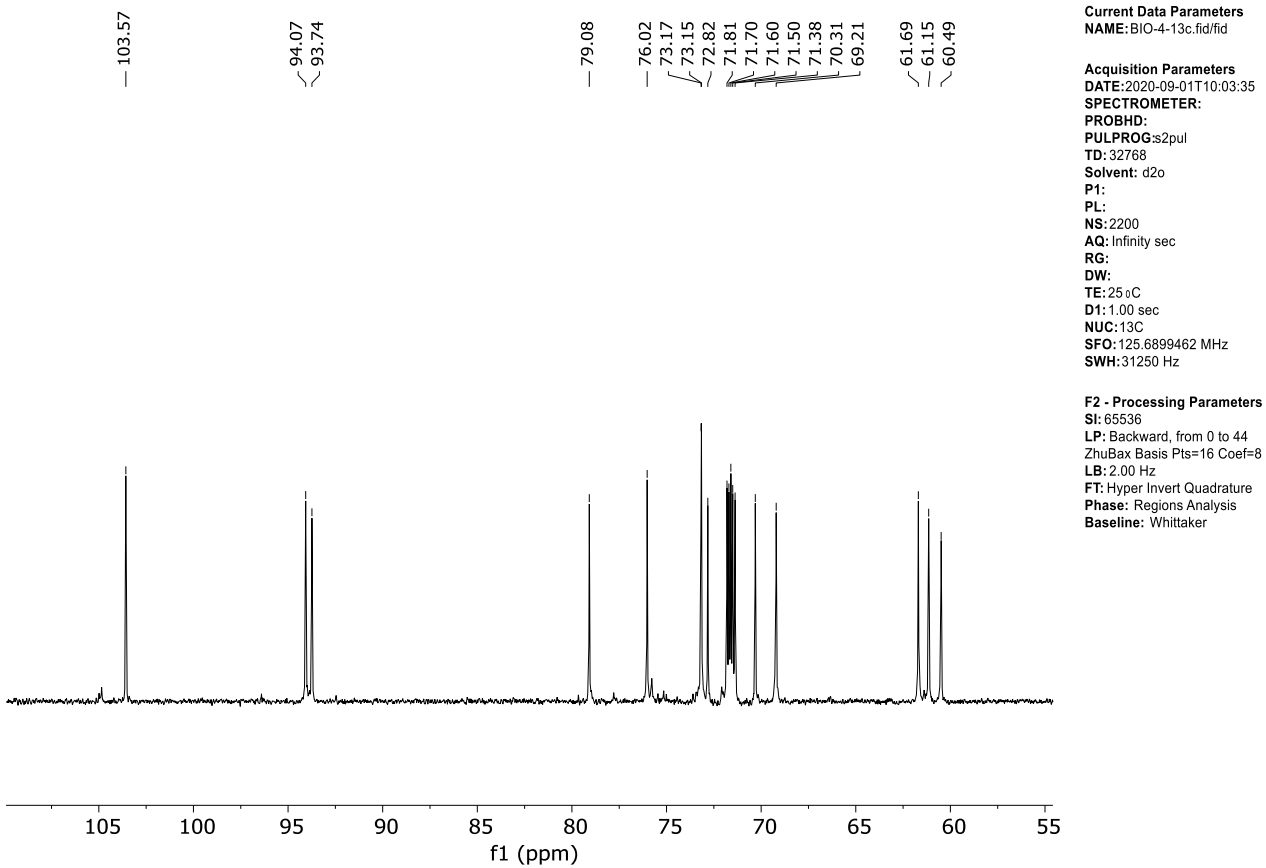

Figure S8. ^{13}C NMR (125 MHz, D_2O) of trisaccharide **2** derived from trehalose.

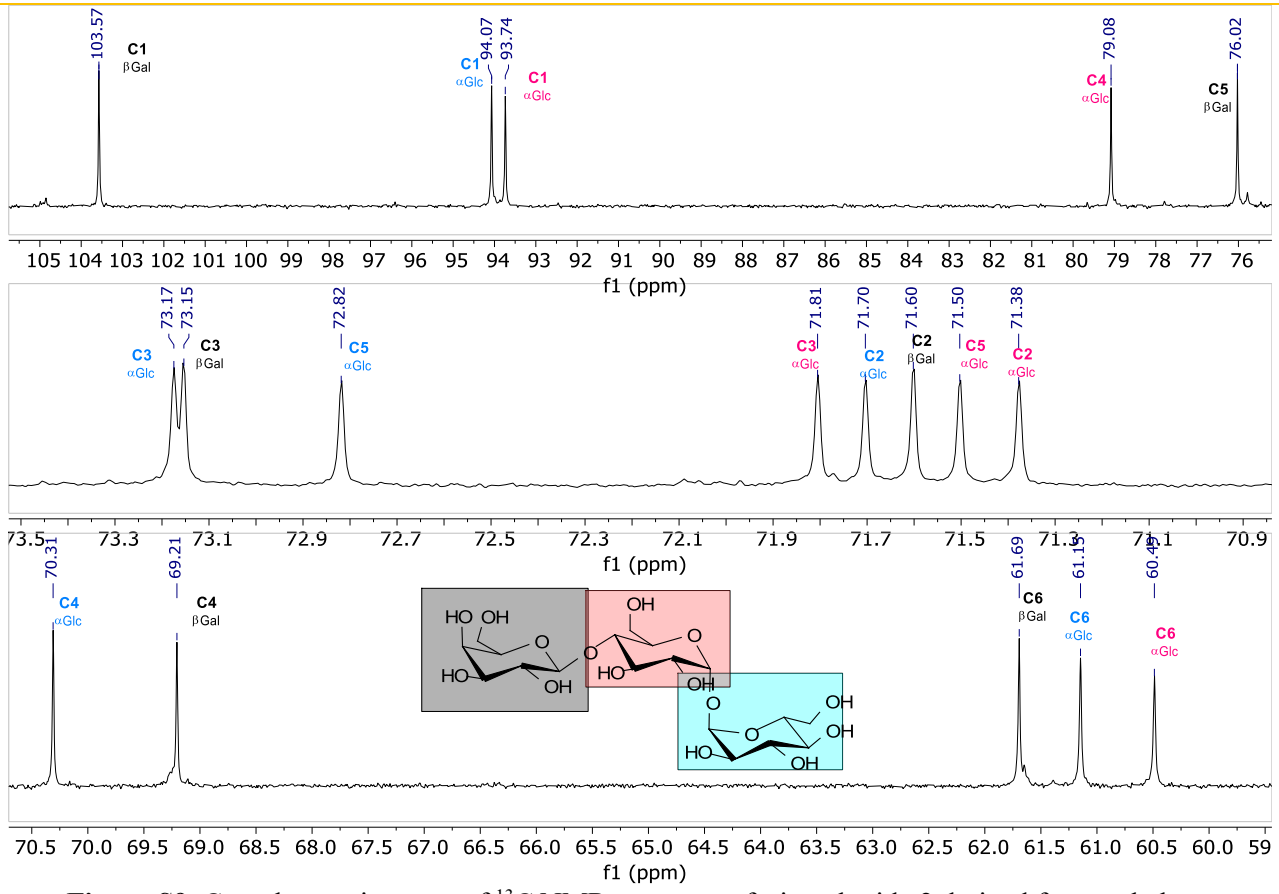

Figure S9. Complete assignment of ^{13}C NMR spectrum of trisaccharide **2** derived from trehalose.

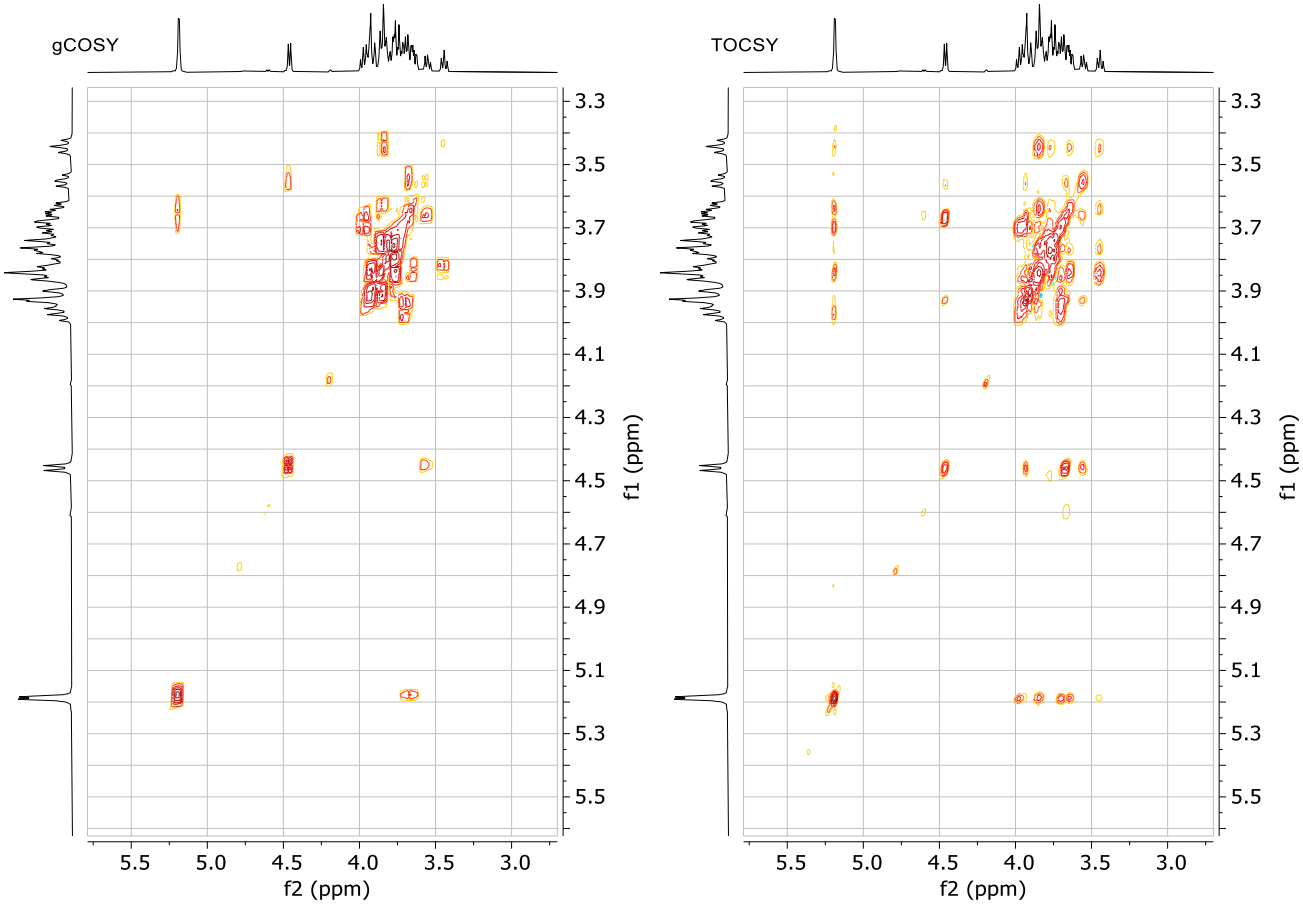

Figure S10. gCOSY and TOCSY (500 MHz, D_2O) of trisaccharide **2** derived from trehalose.

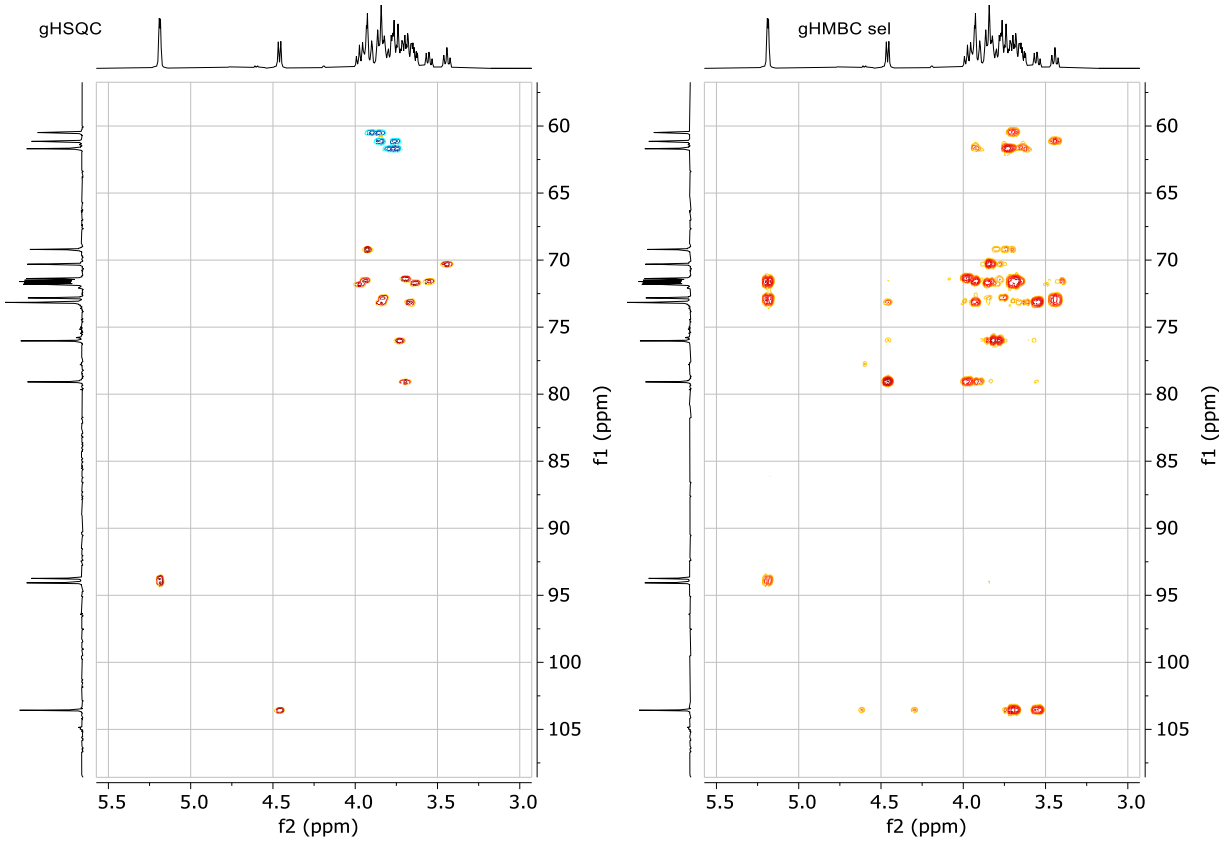

Figure S11. Multiplicity-edited gHSQC **(**methylene**:** blue cross peaks; methine**:** red cross peaks), and gHMBC semiselective (500 MHz, D_2O) of trisaccharide **2** derived from trehalose.

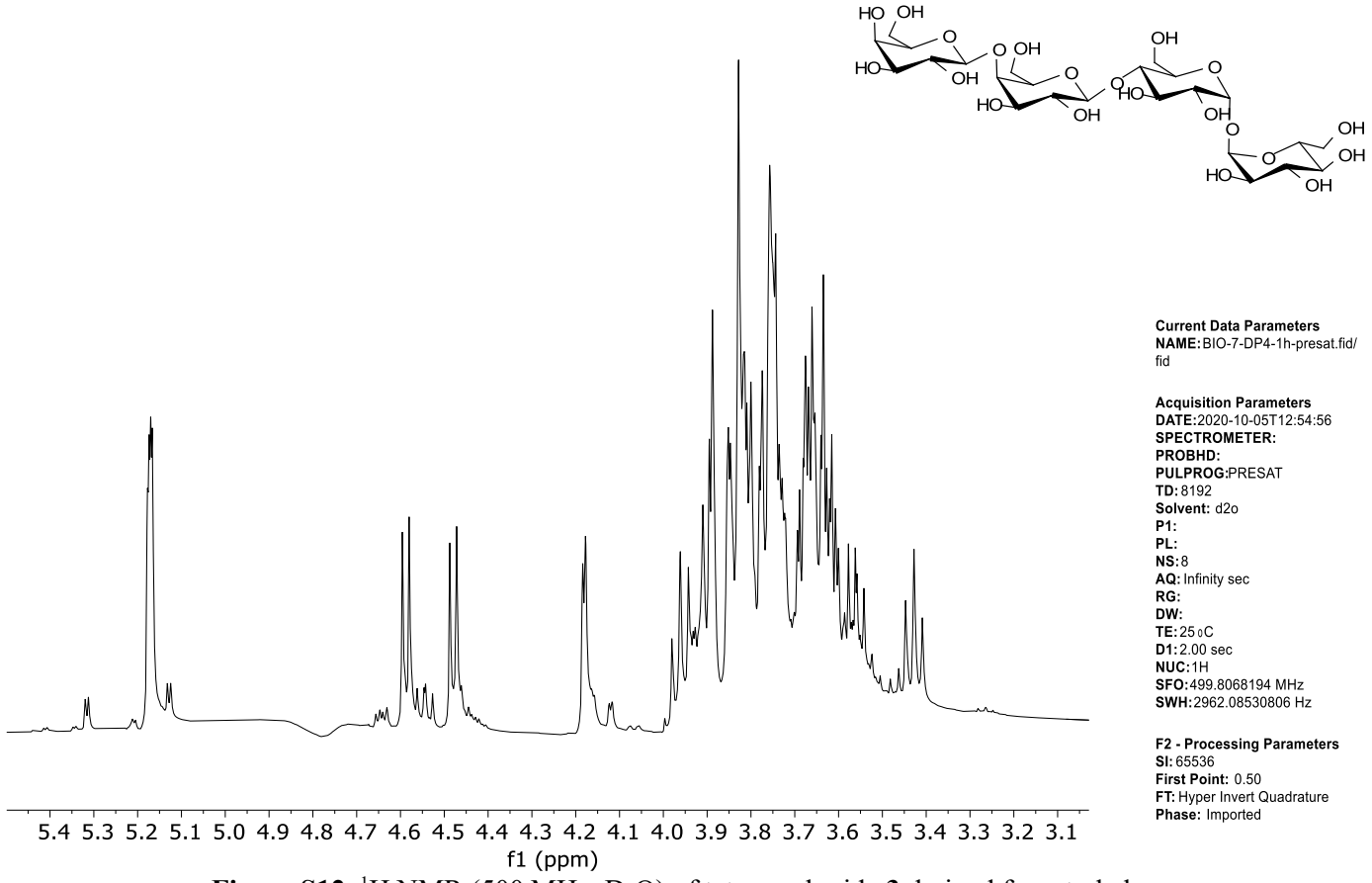

Figure S12. ^{1}H NMR (500 MHz, D_2O) of tetrasaccharide **3** derived from trehalose.

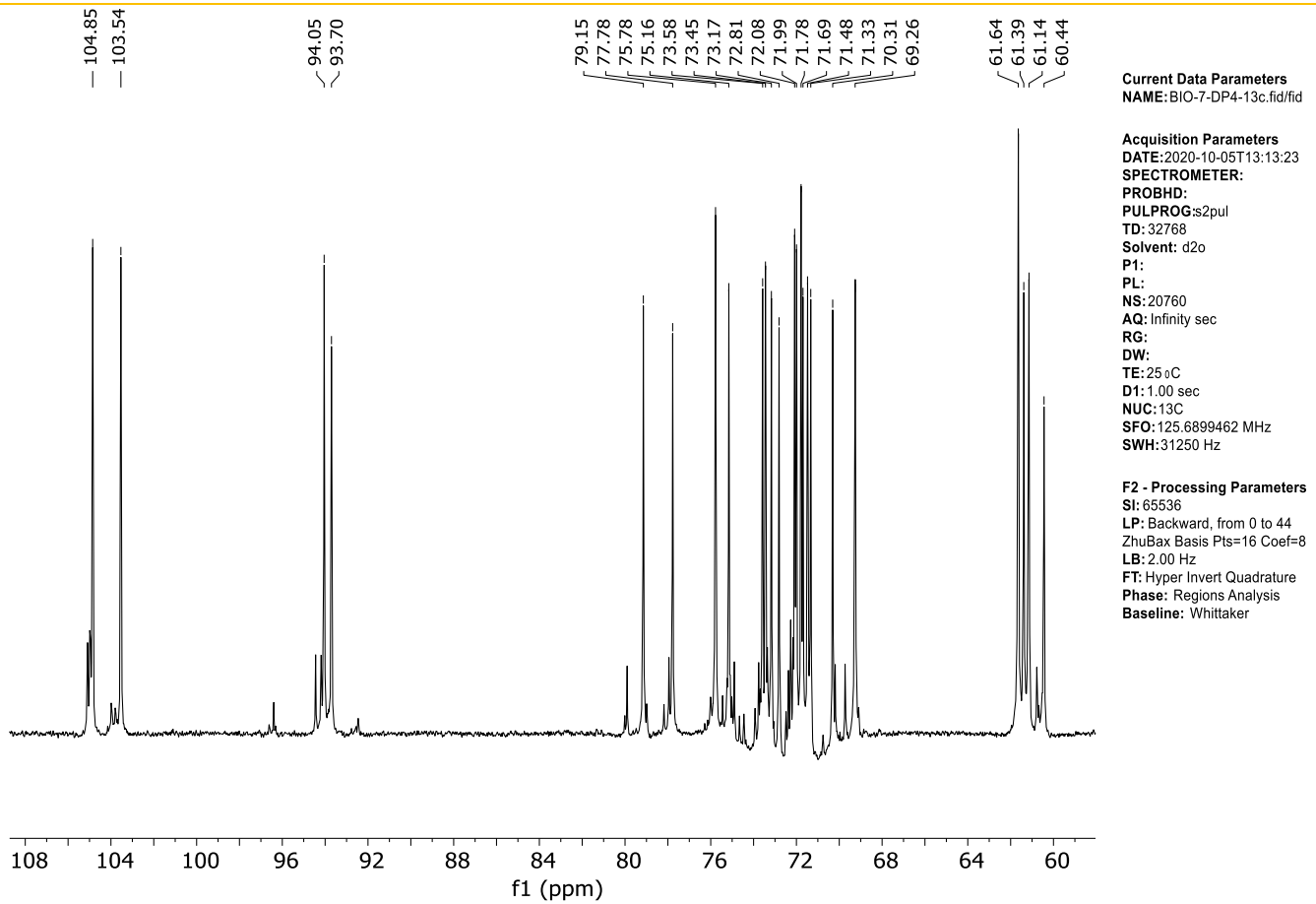

Figure S13. ^{13}C NMR (125 MHz, D_2O) of tetrasaccharide **3** derived from trehalose.

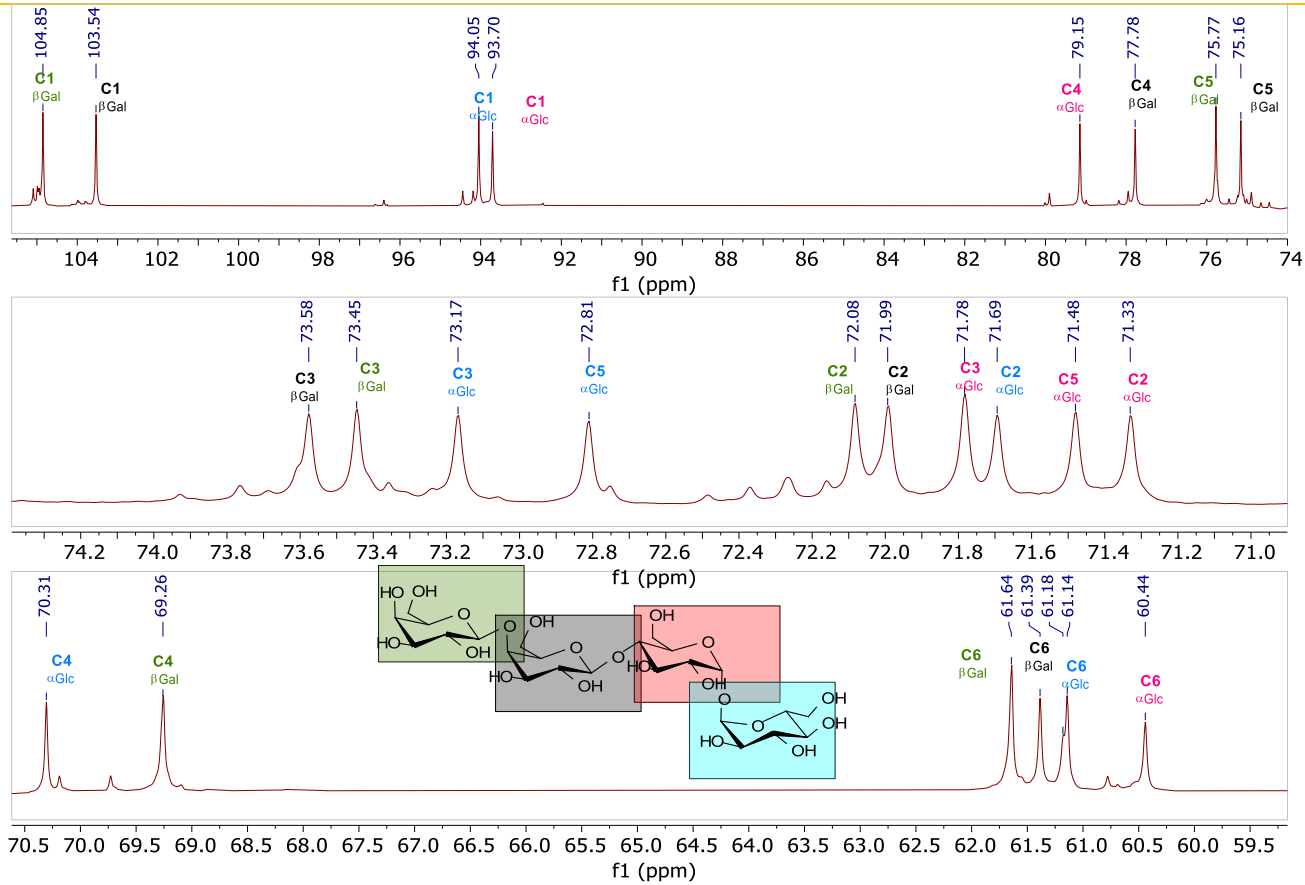

Figure S14. Complete assignment of ^{13}C NMR spectrum of tetrasaccharide **3** derived from trehalose.

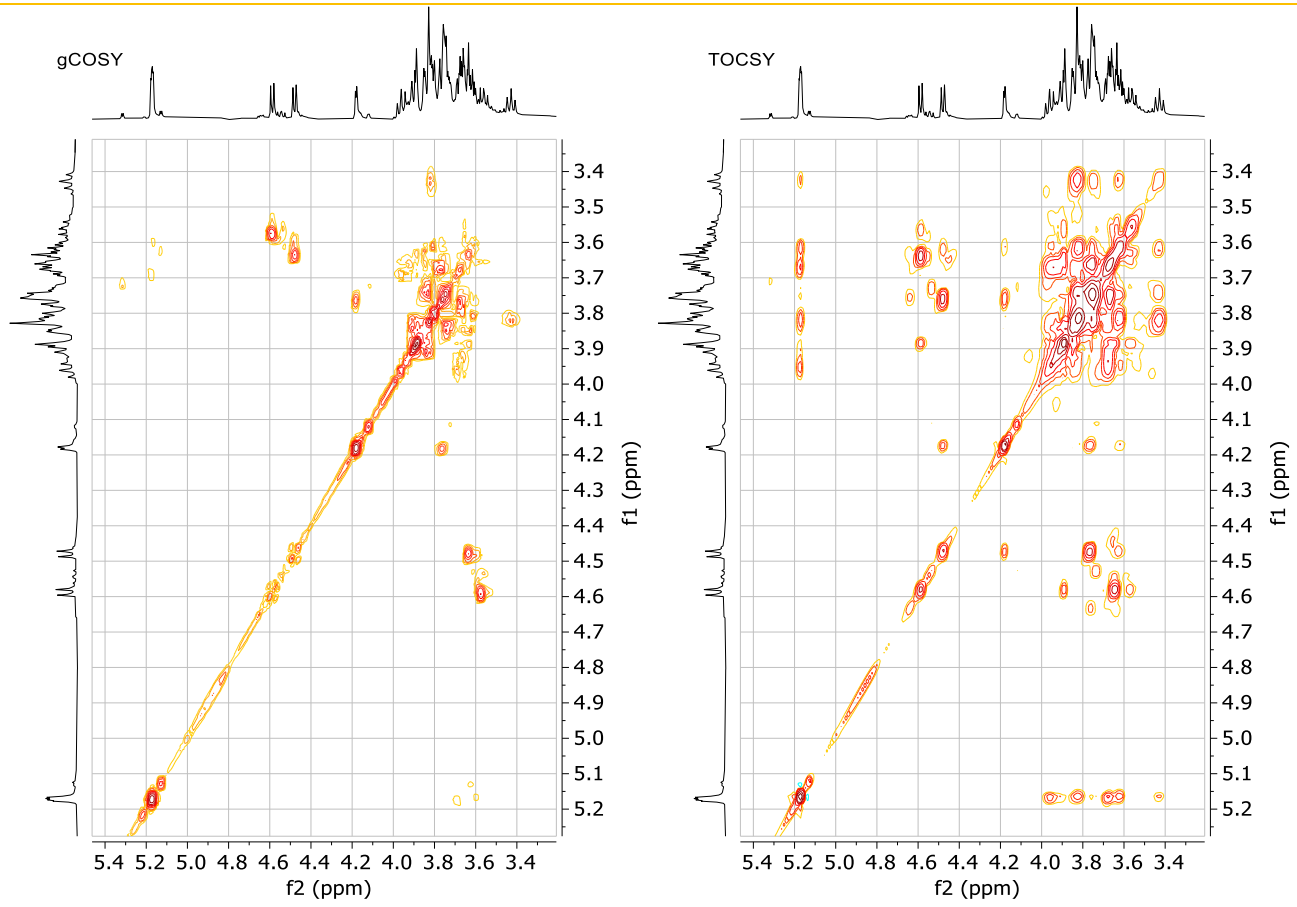

Figure S15. gCOSY and TOCSY (500 MHz, D_2O) of tetrasaccharide **3** derived from trehalose.

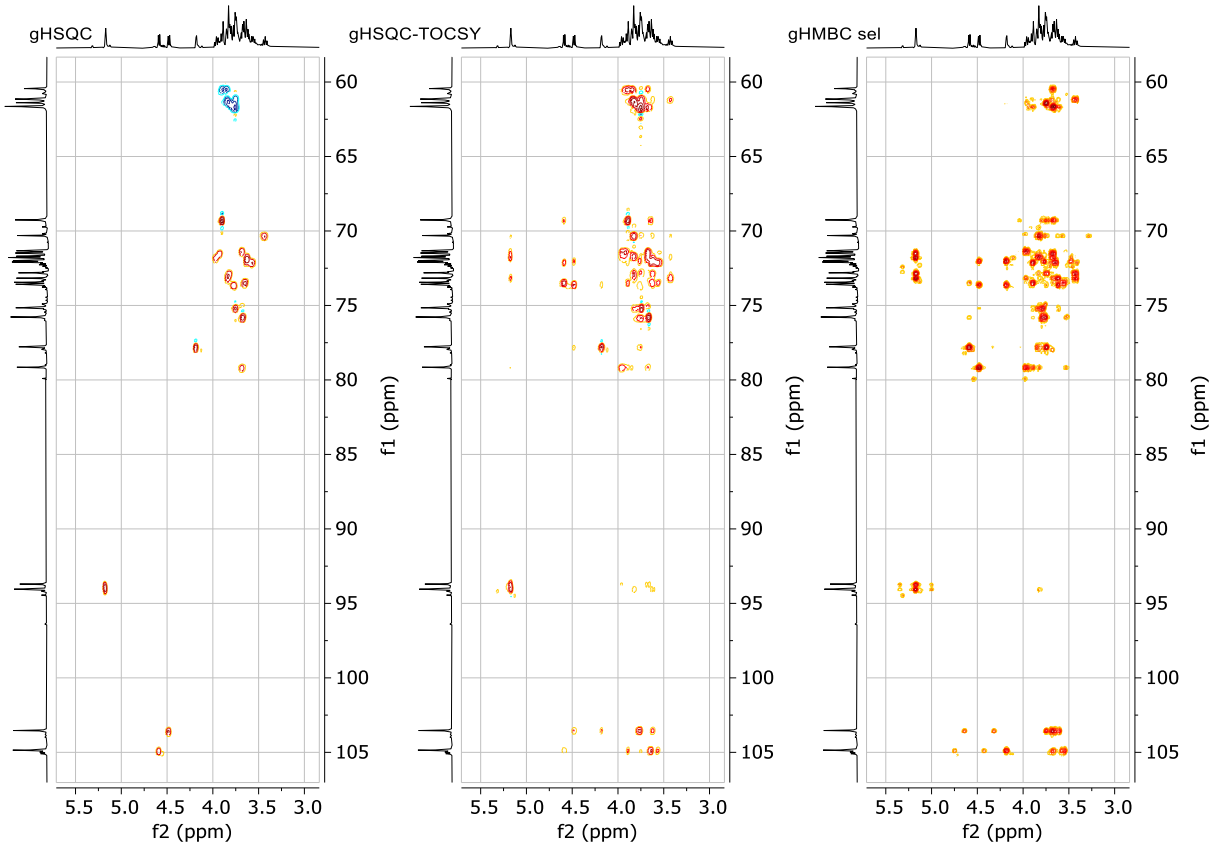

Figure S16. Multiplicity-edited gHSQC **(**methylene**:** blue cross peaks; methine**:** red cross peaks), gHSQC-TOCSY and gHMBC semiselective (500 MHz, D_2O) of tetrasaccharide **3** derived from trehalose.

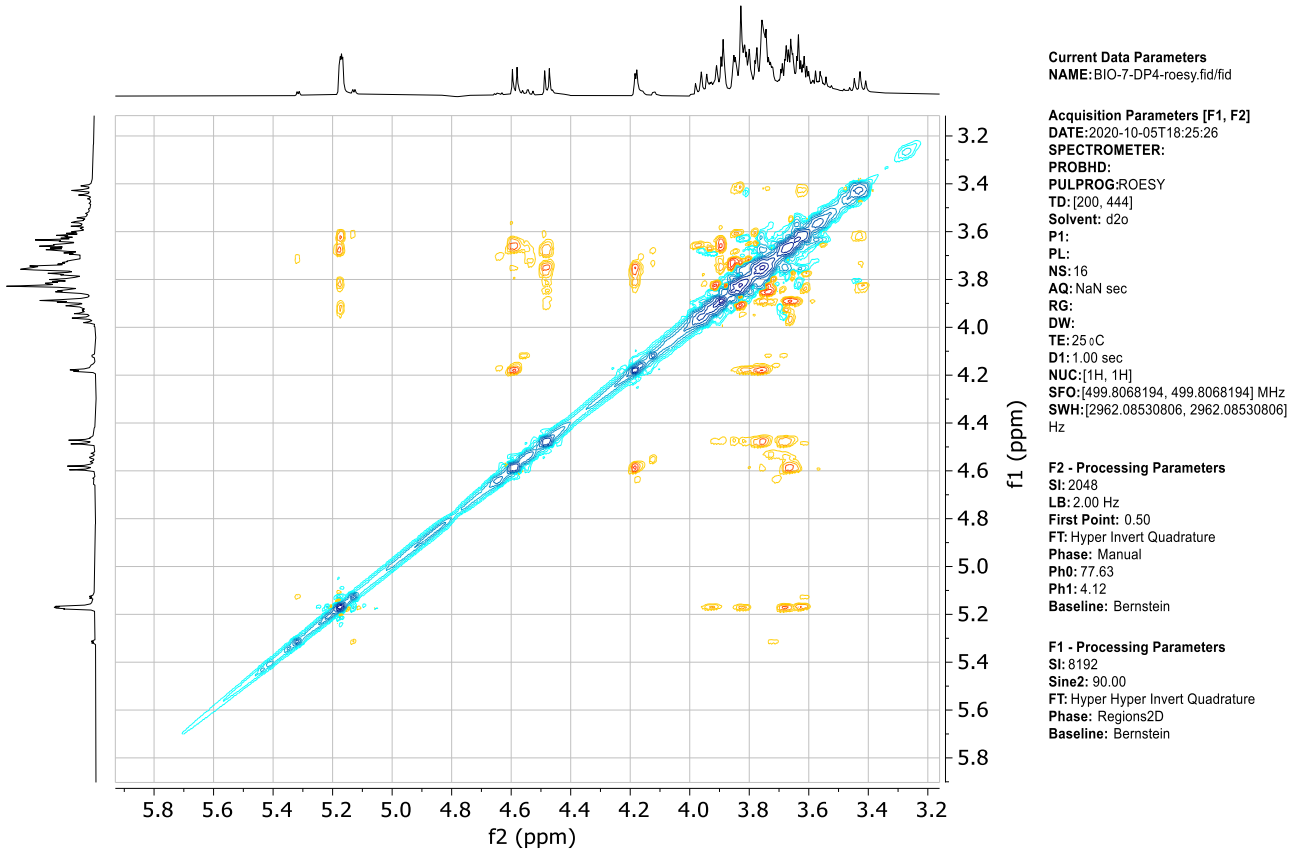

Figure S17. ROESY (500 MHz, D_2O) of tetrasaccharide **3** derived from trehalose.

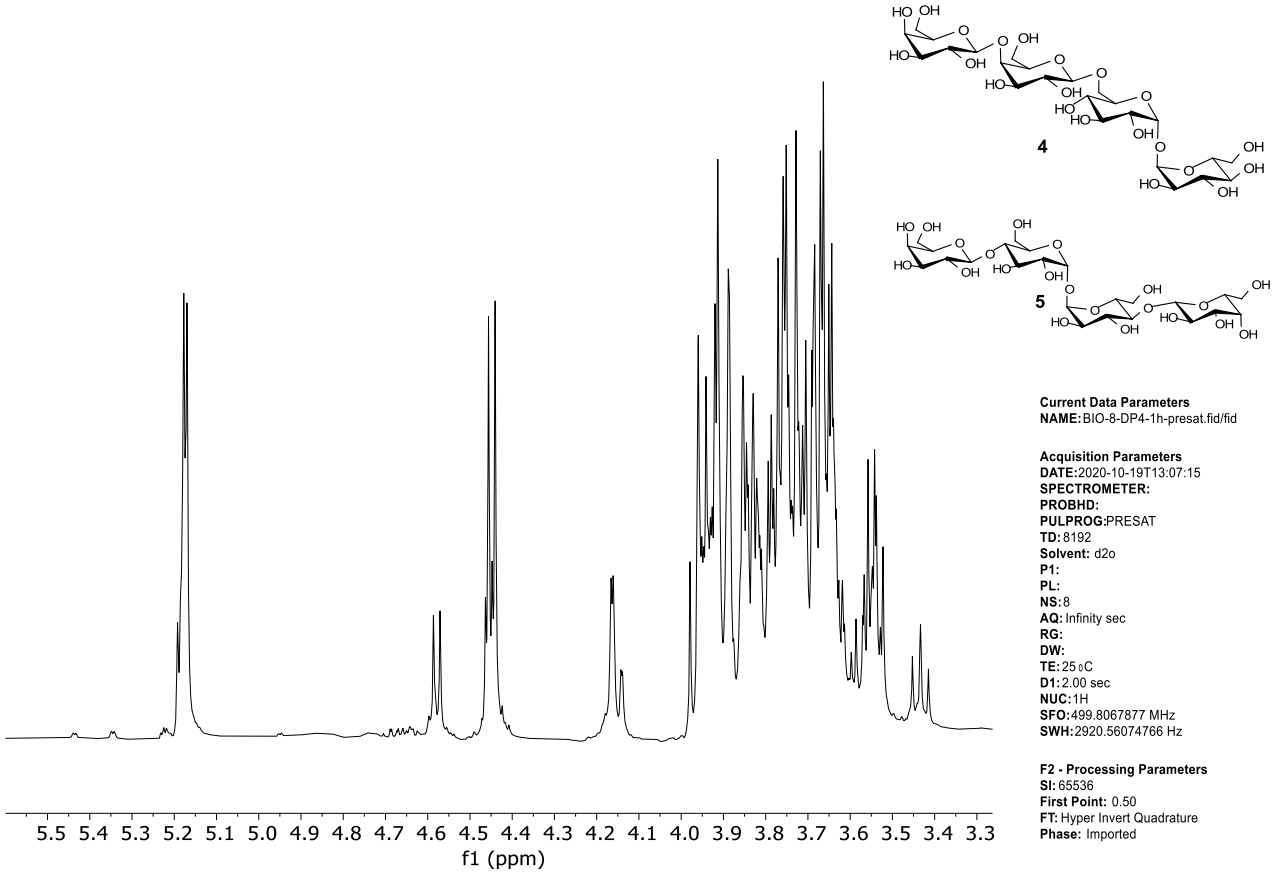

Figure S18. ^{1}H NMR (500 MHz, D_2O) for the mixture of tetrasaccharides **4** and **5** derived from trehalose.

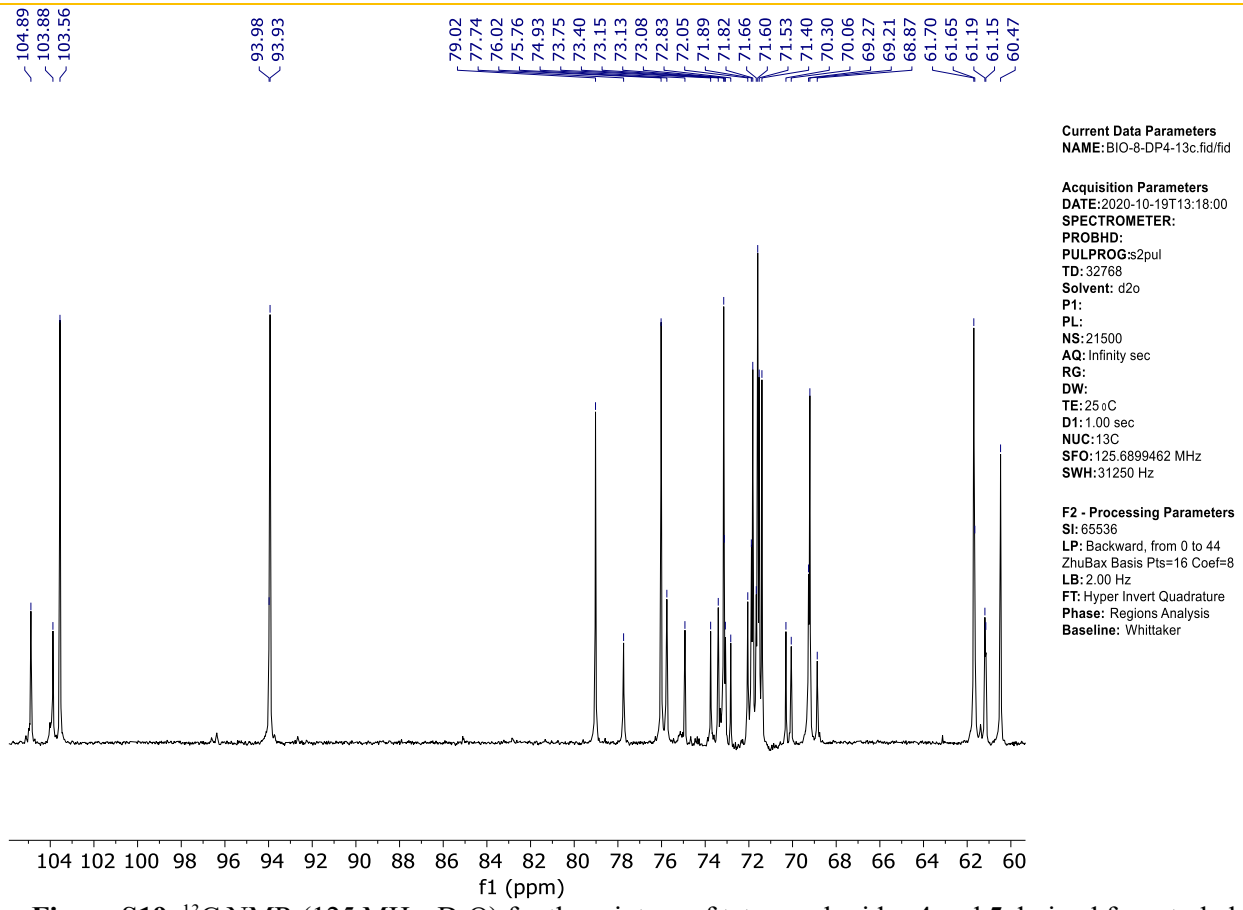

Figure S19. ^{13}C NMR (125 MHz, D_2O) for the mixture of tetrasaccharides **4** and **5** derived from trehalose.

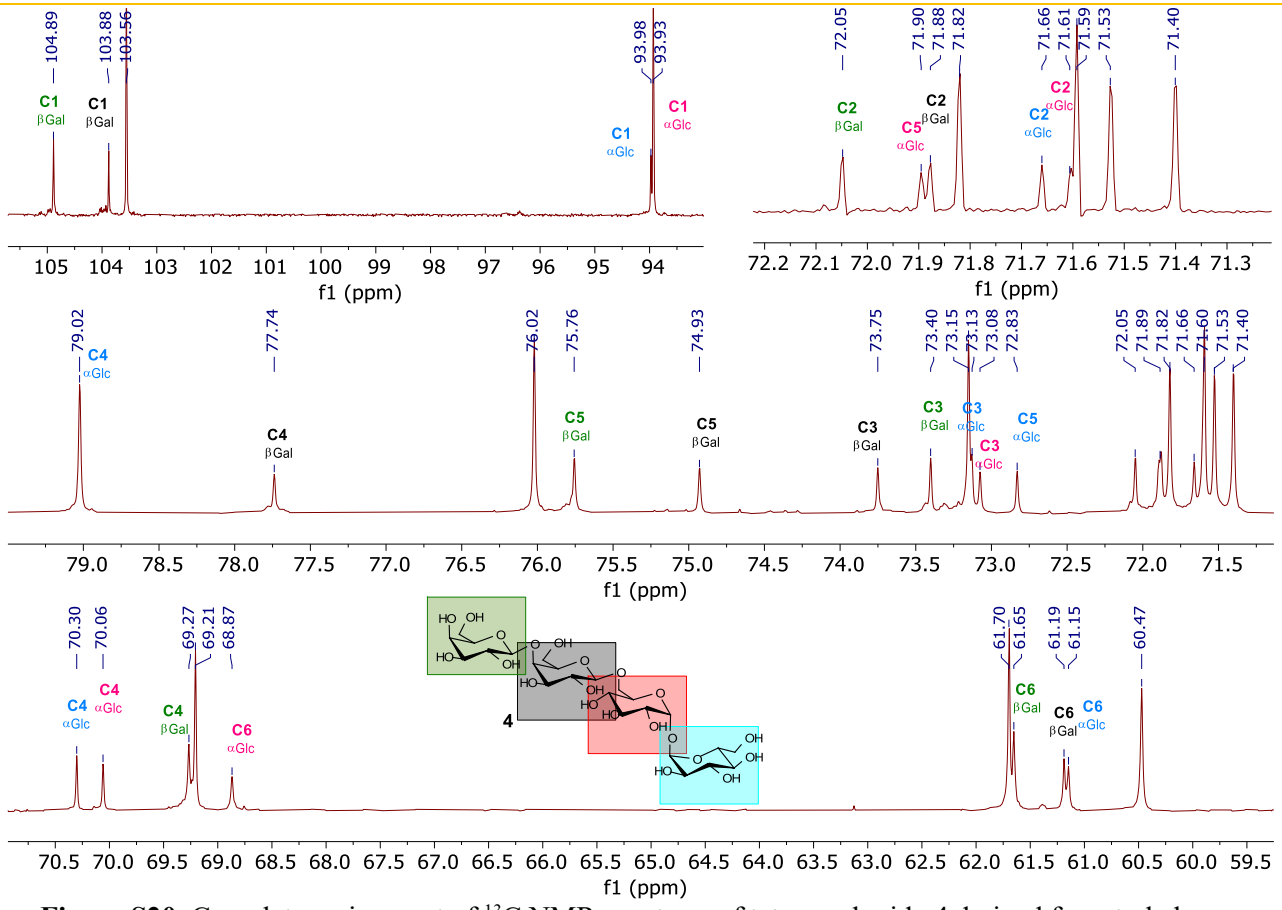

Figure S20. Complete assignment of ^{13}C NMR spectrum of tetrasaccharide **4** derived from trehalose.

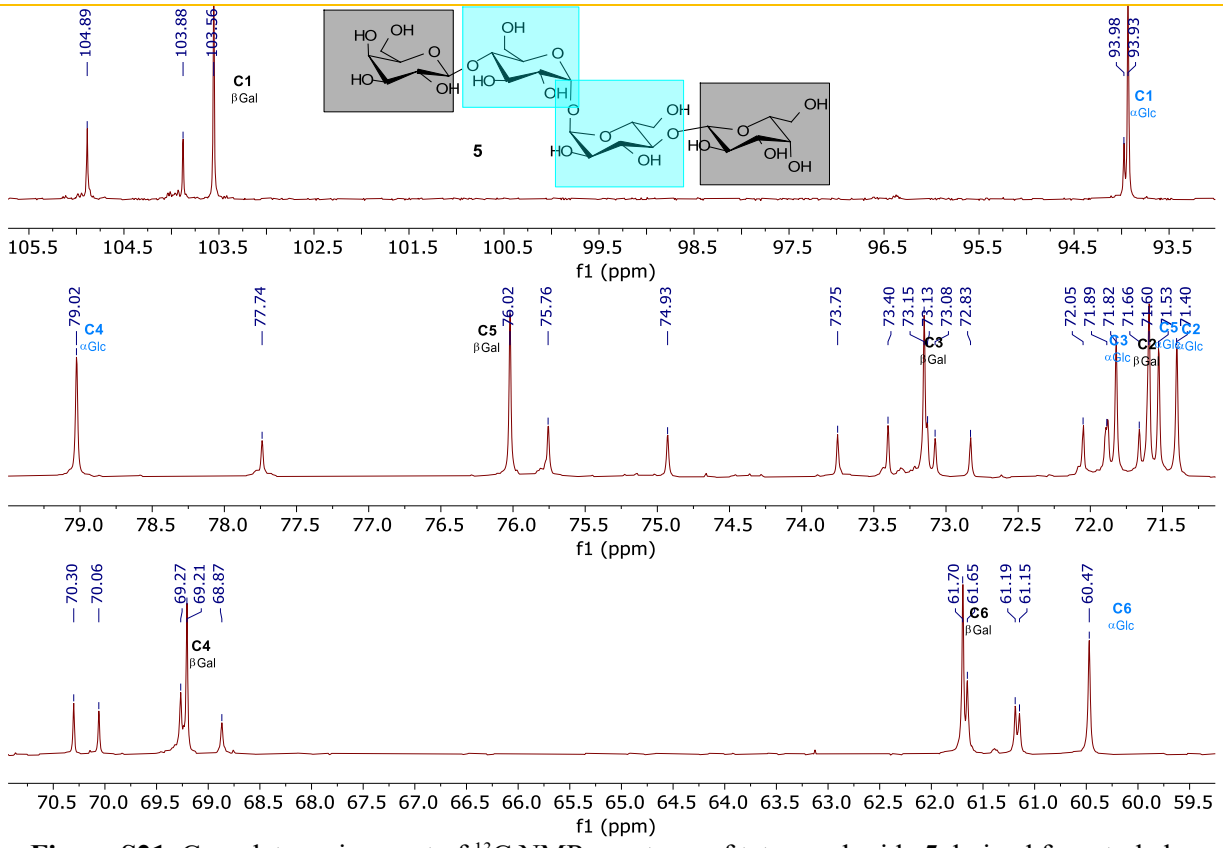

Figure S21. Complete assignment of ^{13}C NMR spectrum of tetrasaccharide **5** derived from trehalose.

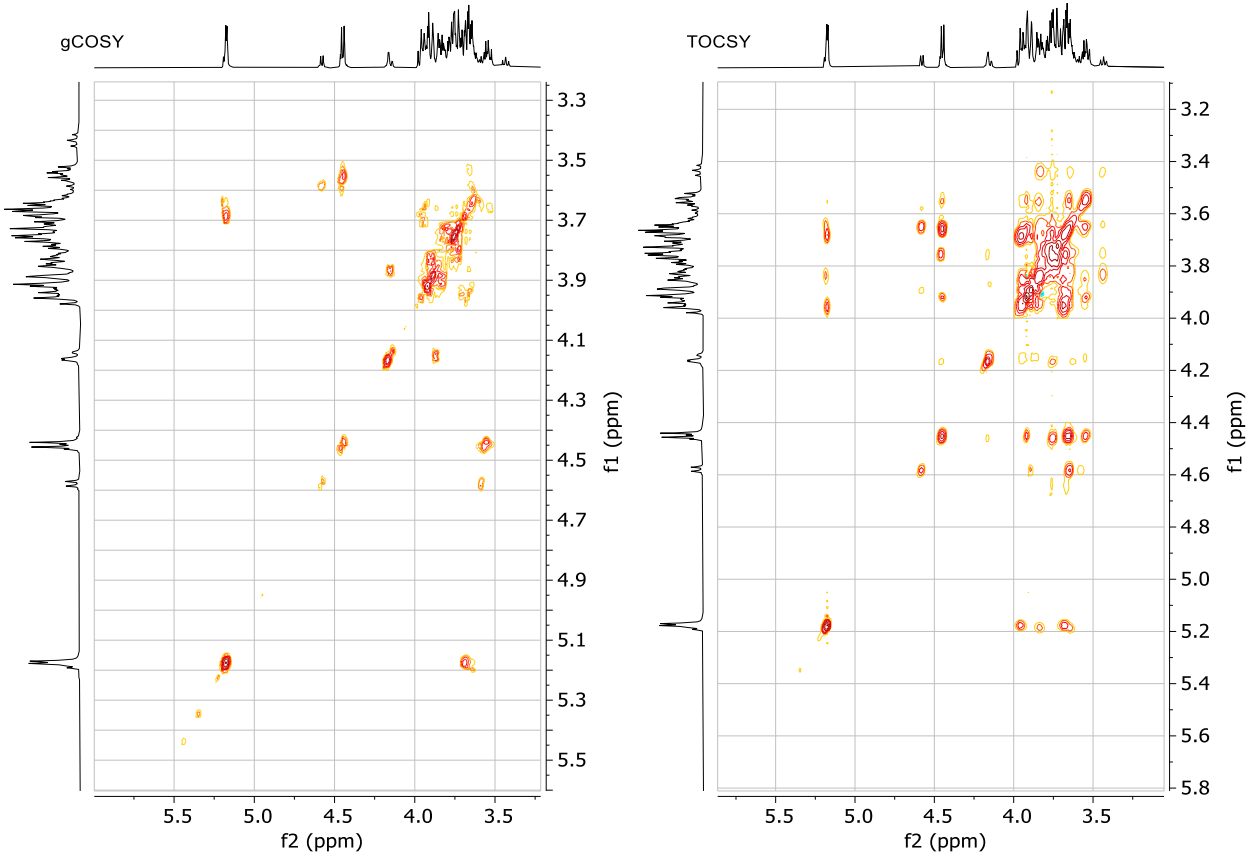

Figure S22. gCOSY and TOCSY (500 MHz, D_2O) for the mixture of tetrasaccharides **4** and **5** derived from trehalose.

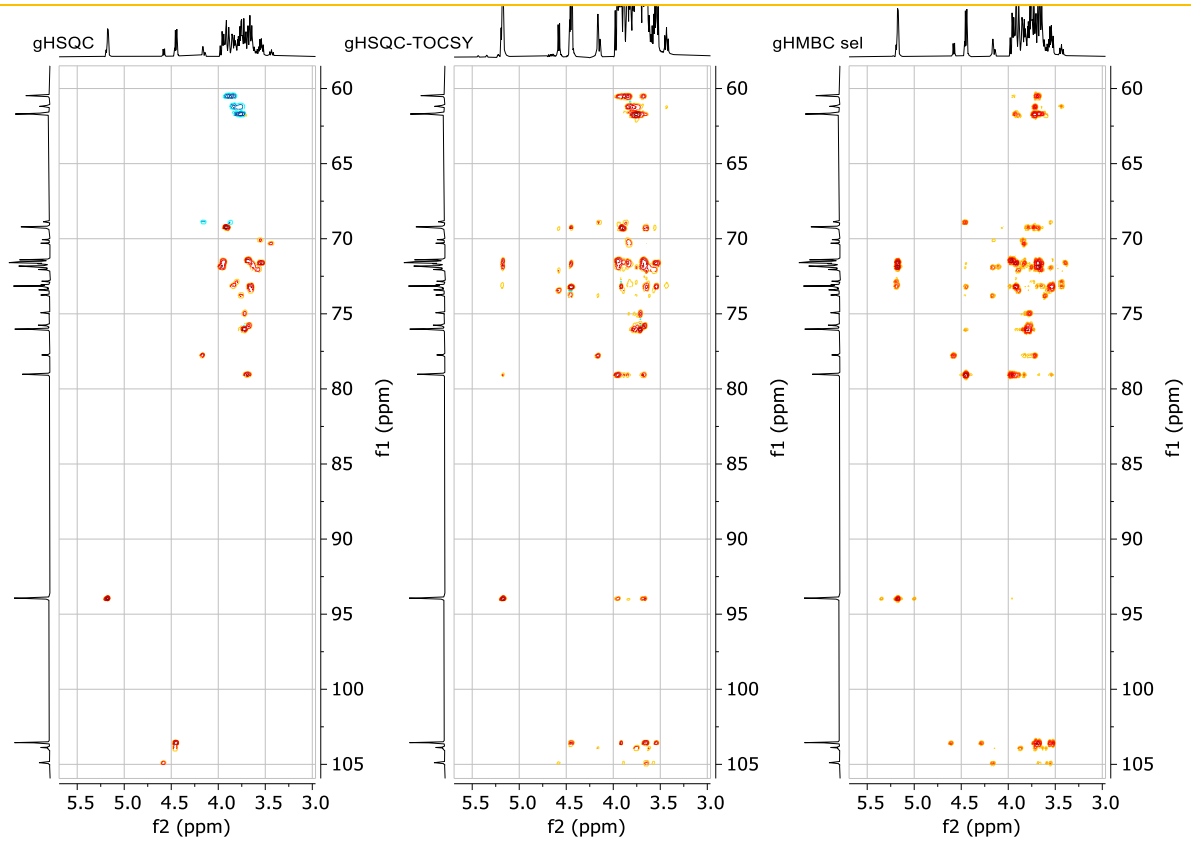

Figure S23. Multiplicity-edited gHSQC **(**methylene**:** blue cross peaks; methine**:** red cross peaks), gHSQC-TOCSY and gHMBC semiselective (500 MHz, D_2O) for the mixture of tetrasaccharides **4** and **5** derived from trehalose.

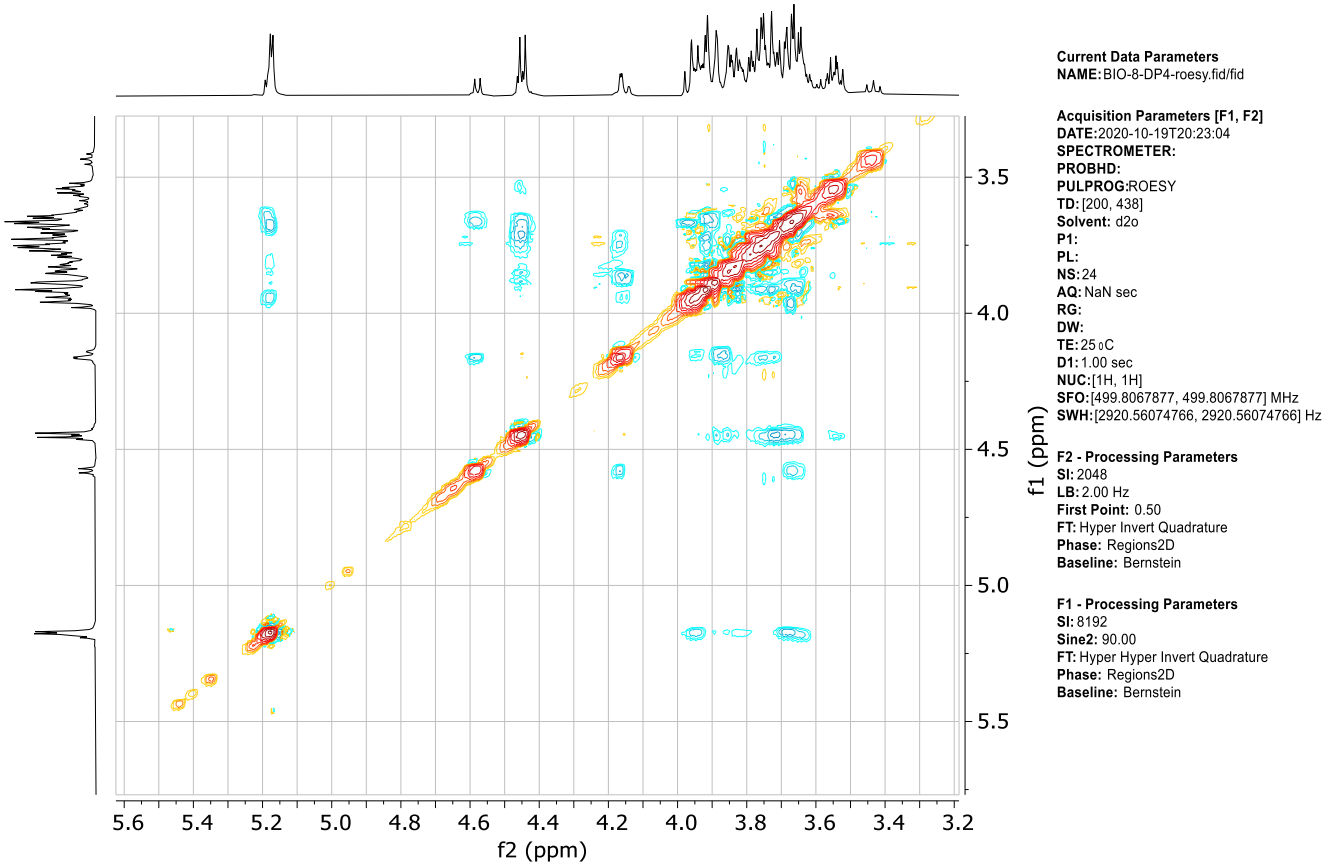

Figure S24. ROESY (500 MHz, D_2O) for the mixture of tetrasaccharides **4** and **5** derived from trehalose.

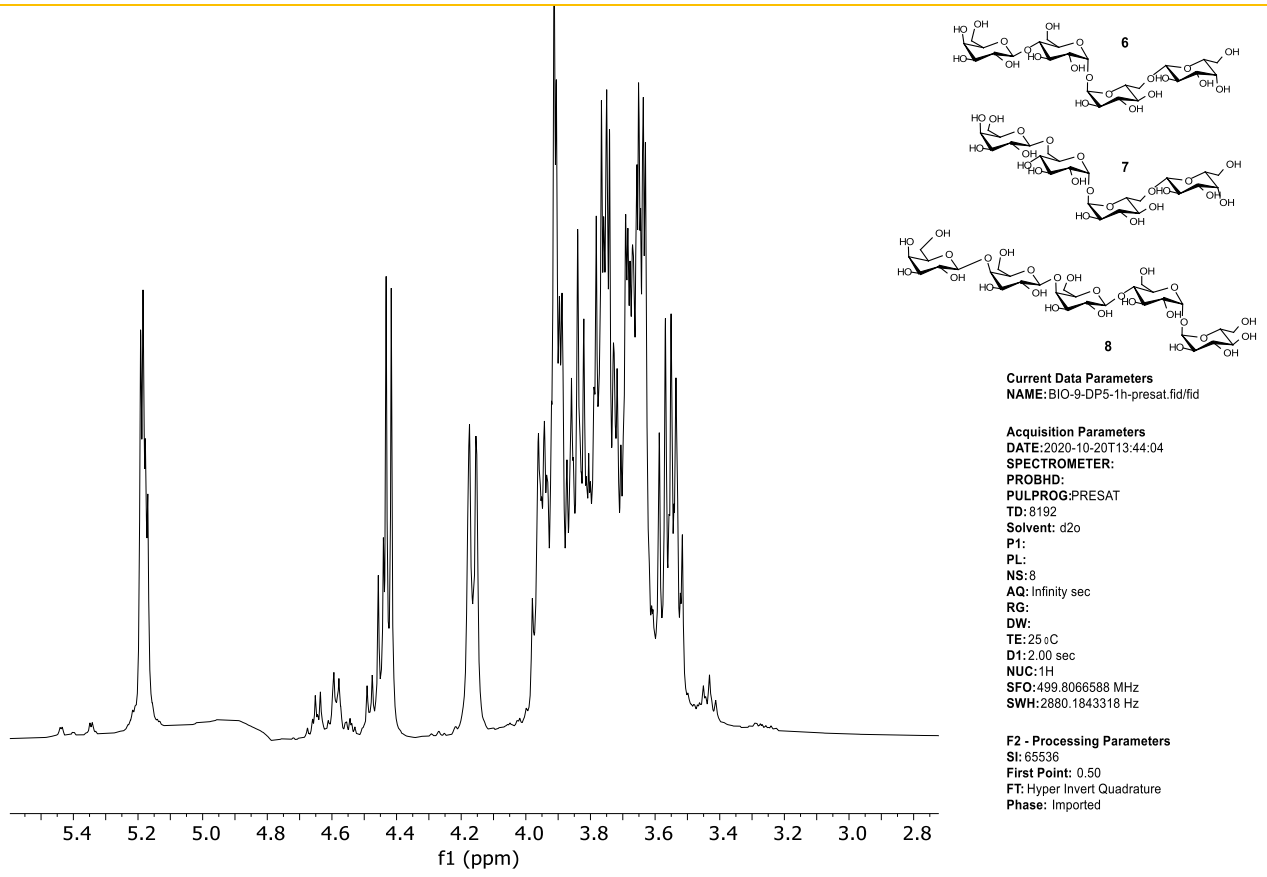

Figure S25. ^{1}H NMR (500 MHz, D_2O) for the mixture of tetrasaccharides **6** and **7**, and pentasaccharide **8** derived from trehalose.

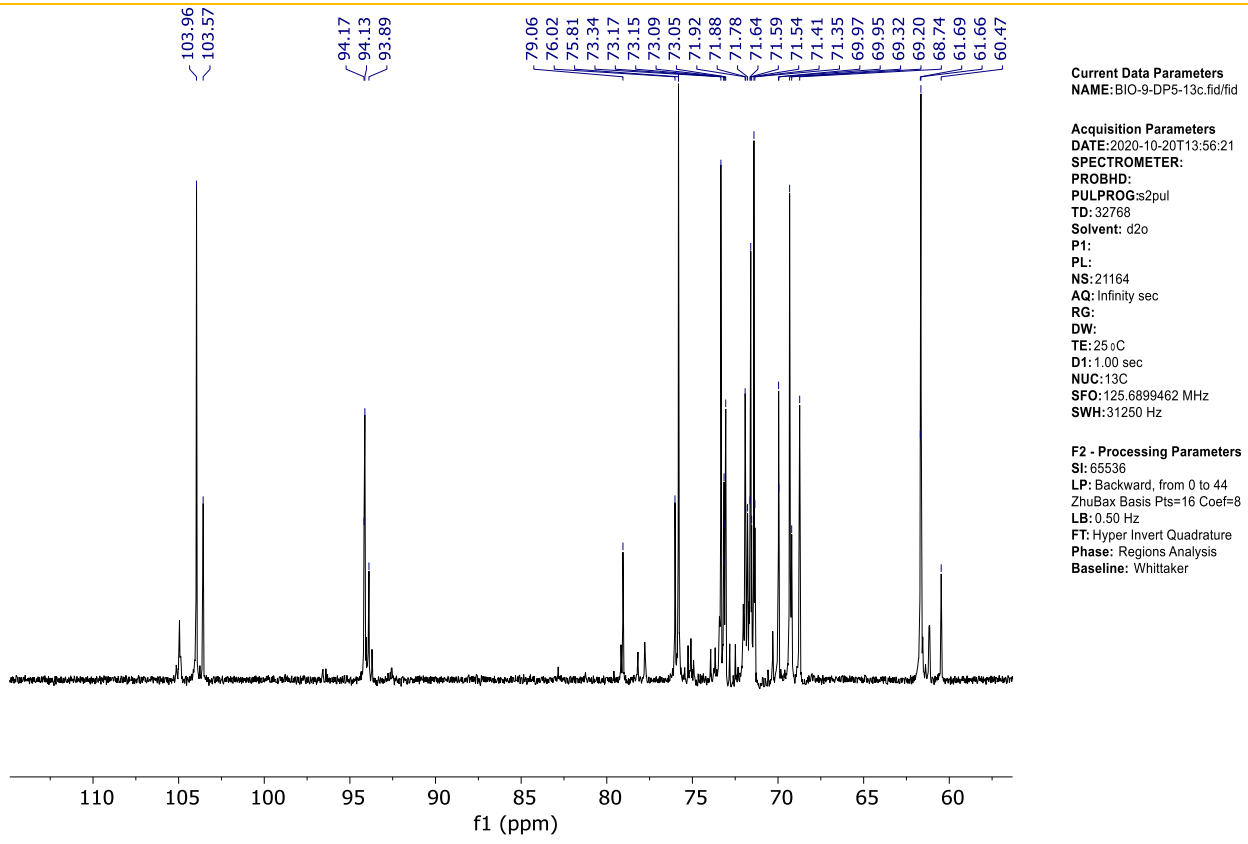

Figure S26. ^{13}C NMR (125 MHz, D_2O) for the mixture of tetrasaccharides **6** and **7**, and pentasaccharide **8** derived from trehalose.

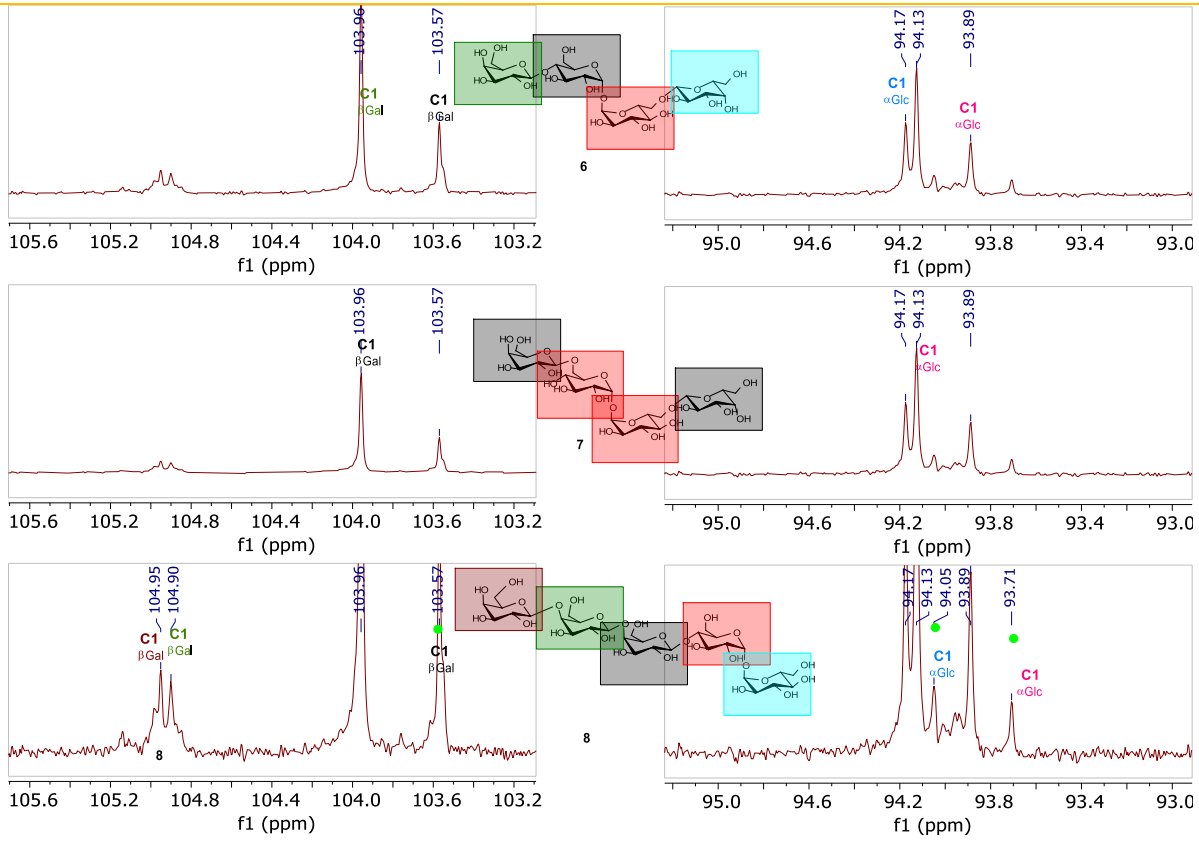

Figure S27. Complete assignment of anomeric region of ^{13}C spectrum NMR of tetrasaccharides **6** and **7**, and pentasaccharide **8** derived from trehalose.

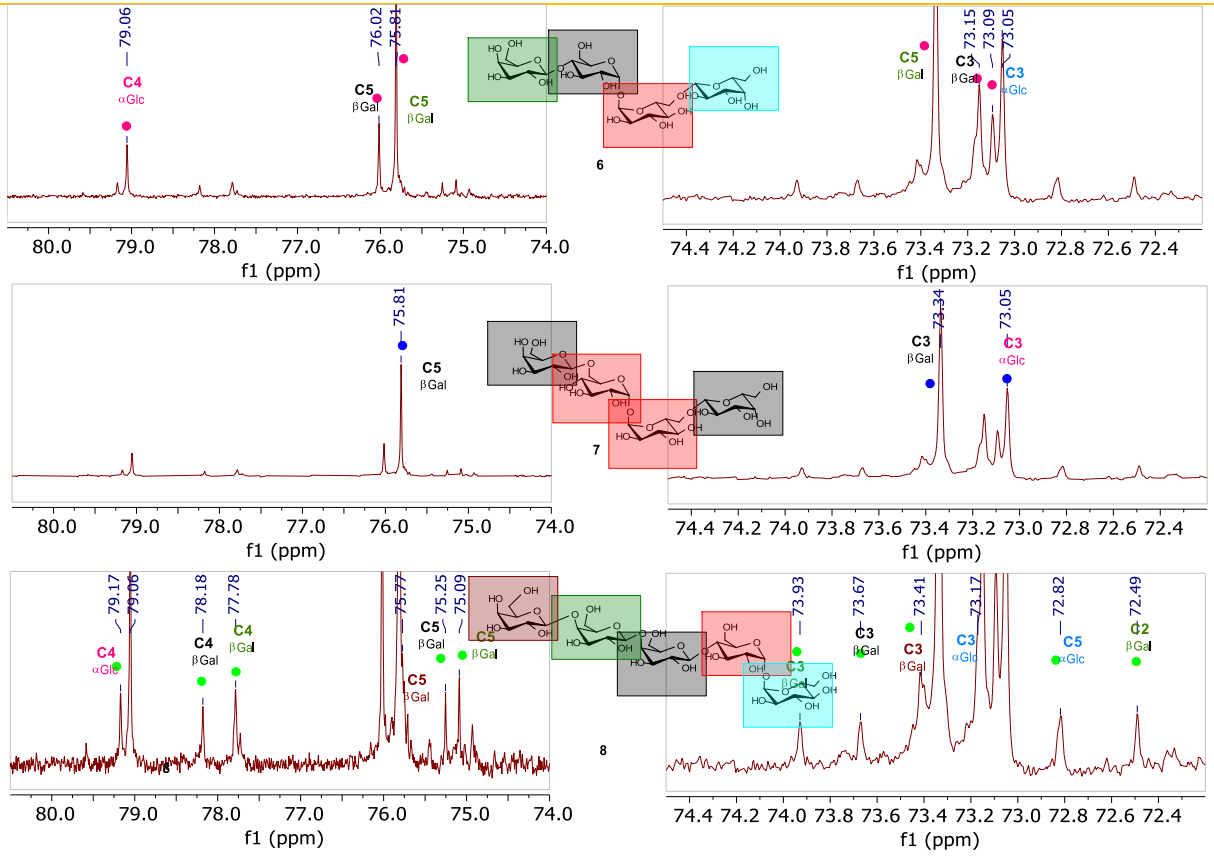

Figure S28. Complete assignment of 80-72 ppm region of ^{13}C spectrum NMR of tetrasaccharides **6** and **7**, and pentasaccharide **8** derived from trehalose.

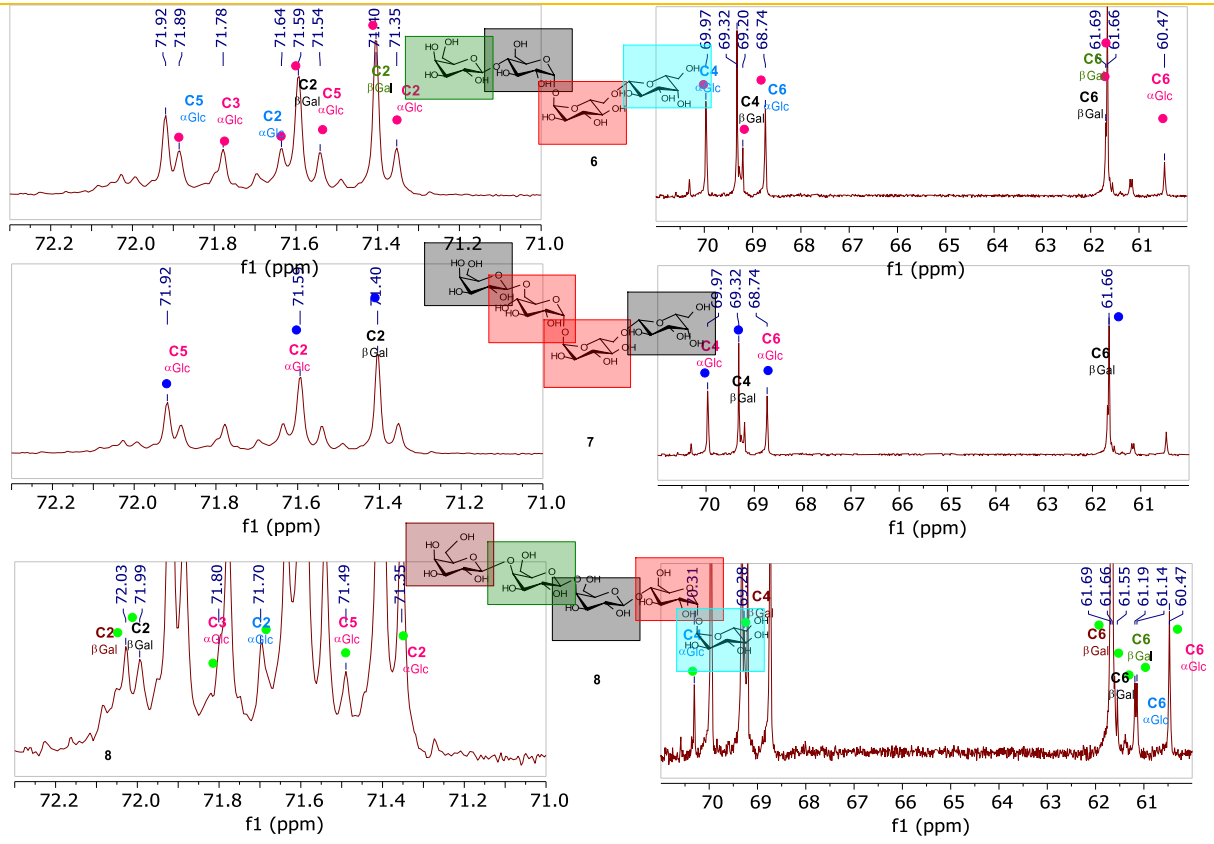

Figure S29. Complete assignment of 72-60 ppm region of ^{13}C spectrum NMR of tetrasaccharides **6** and **7**, and pentasaccharide **8** derived from trehalose.

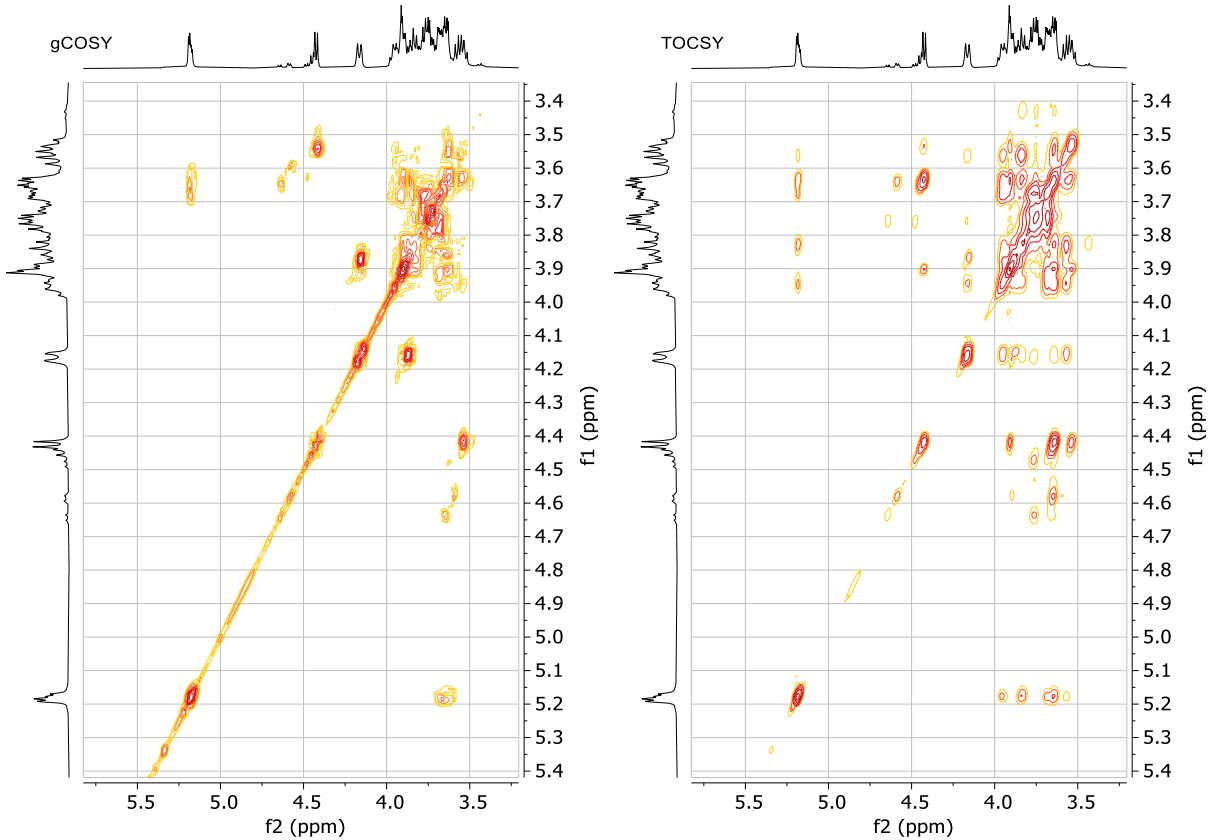

Figure S30. gCOSY and TOCSY (500 MHz, D_2O) for the mixture of tetrasaccharides **6** and **7**, and pentasaccharide **8** derived from trehalose.

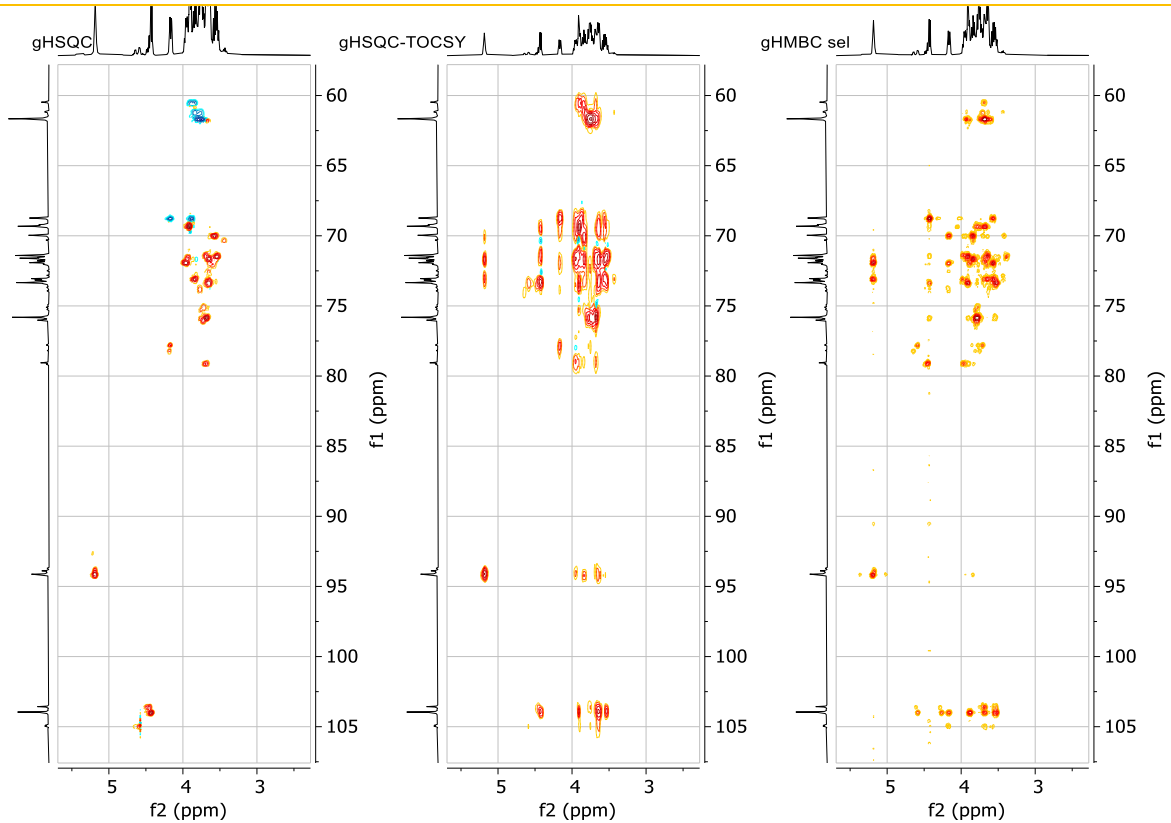

Figure S31. Multiplicity-edited gHSQC **(**methylene**:** blue cross peaks; methine**:** red cross peaks), gHSQC-TOCSY and gHMBC semiselective (500 MHz, D_2O) for the mixture of tetrasaccharides **6** and **7**, and pentasaccharide **8** derived from trehalose.

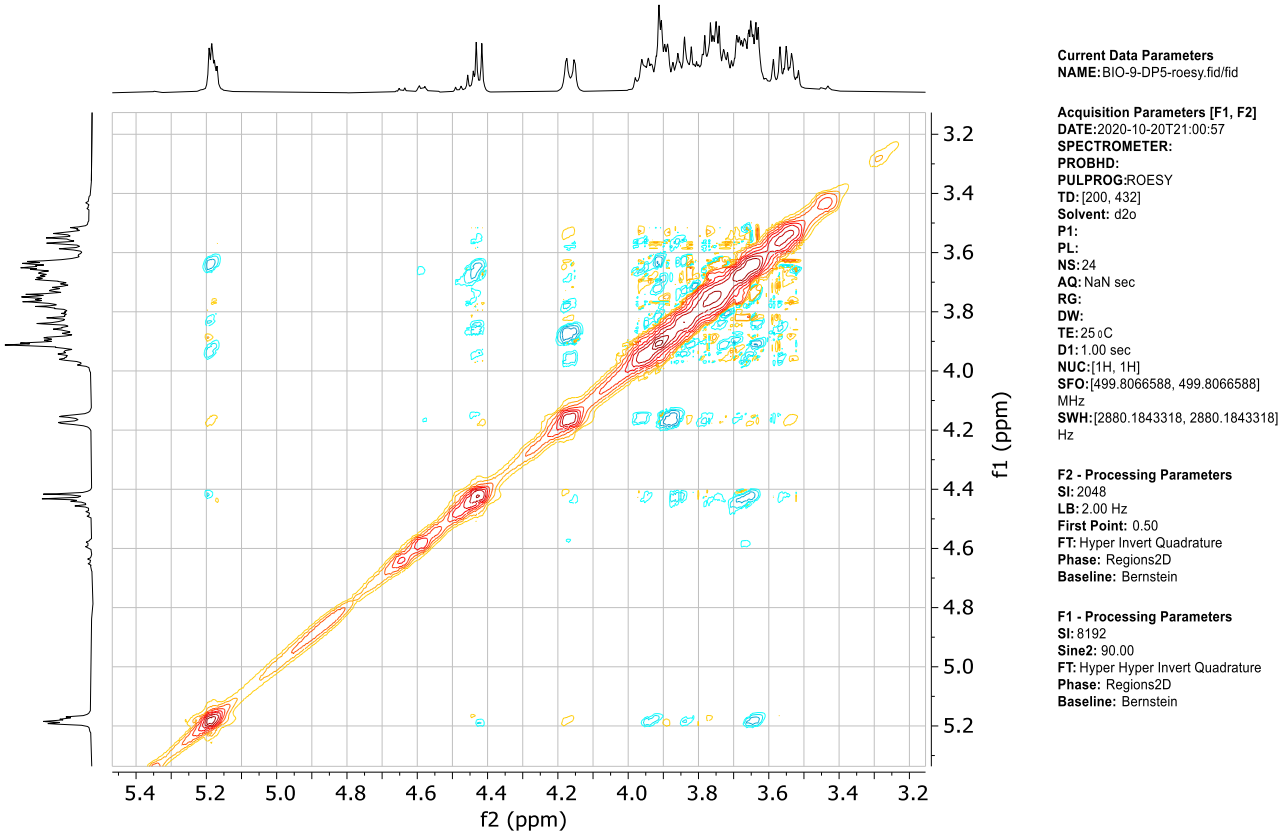

Figure S32. ROESY (500 MHz, D_2O) for the mixture of tetrasaccharides **6** and **7**, and pentasaccharide **8** derived from trehalose.

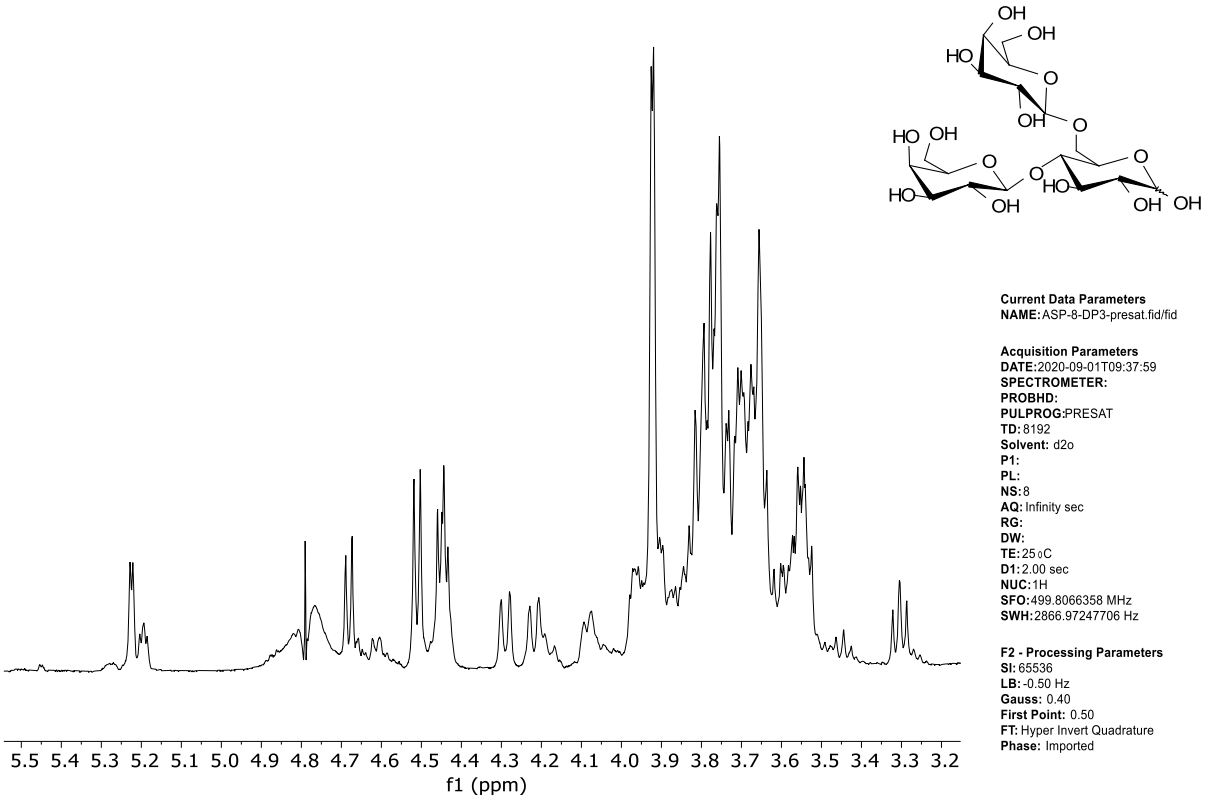

Figure S33. ^{1}H NMR (500 MHz, D_2O) of trisaccharide **9** derived from lactose.

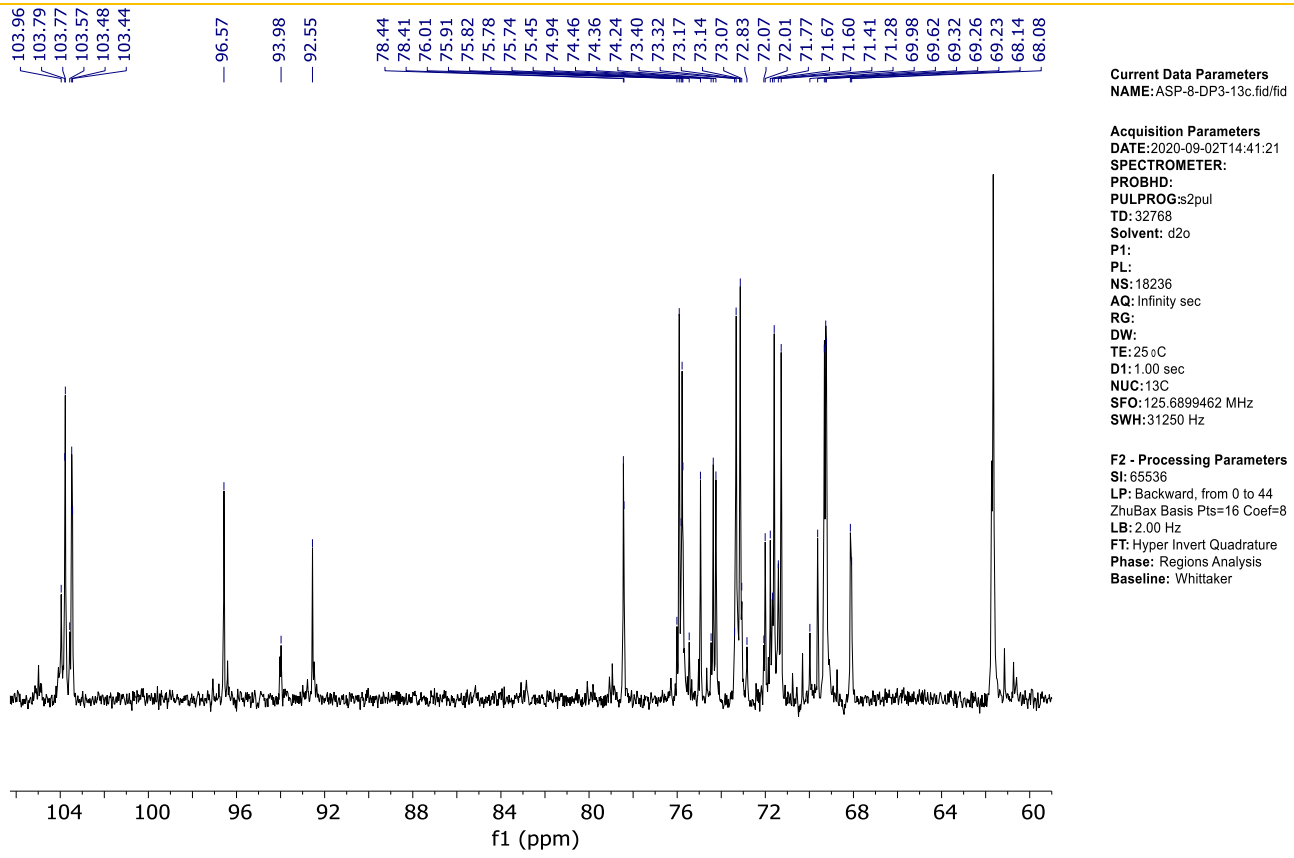

Figure S34. ^{13}C NMR (125 MHz, D_2O) of trisaccharide **9** derived from lactose.

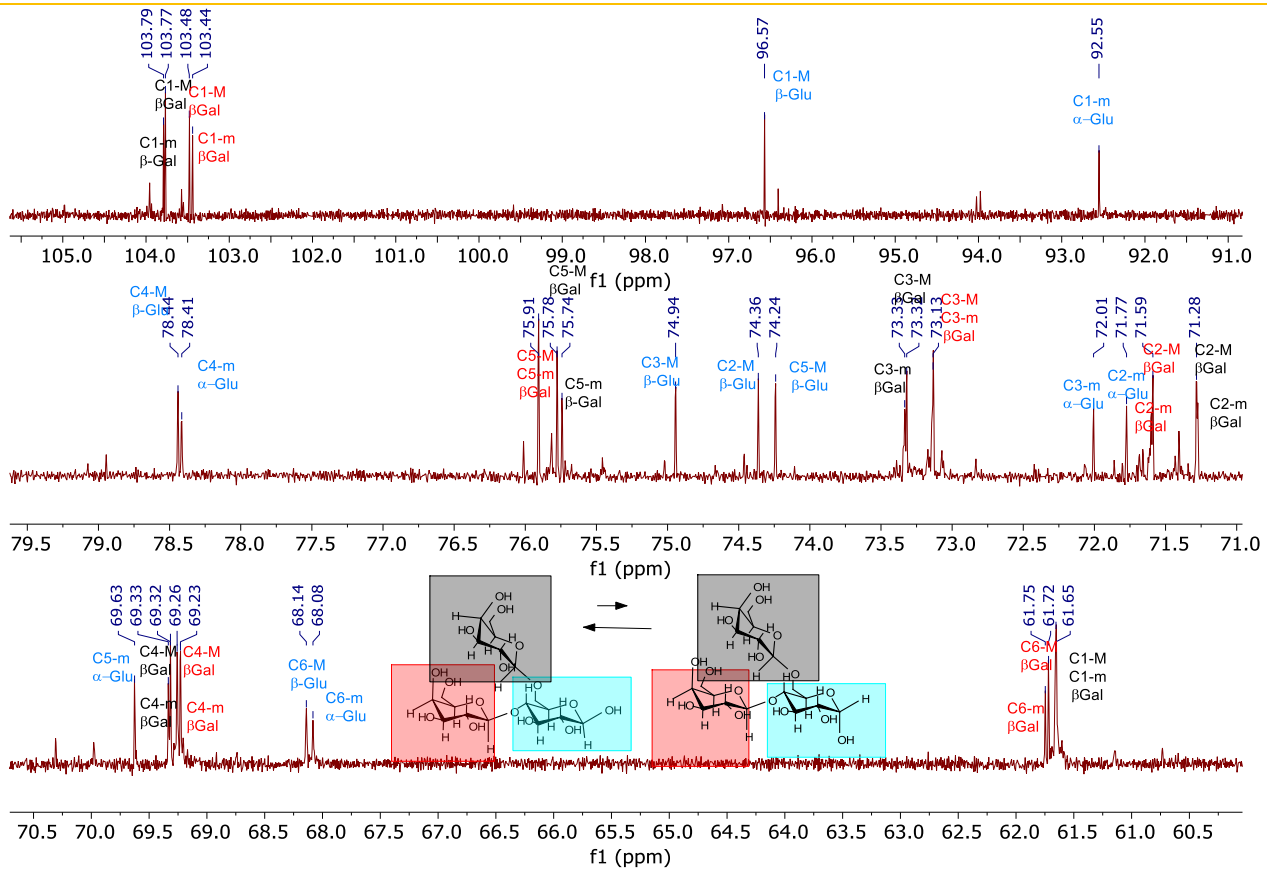

Figure S35. Complete assignment of ^{13}C NMR spectrum of trisaccharide **9** derived from lactose.

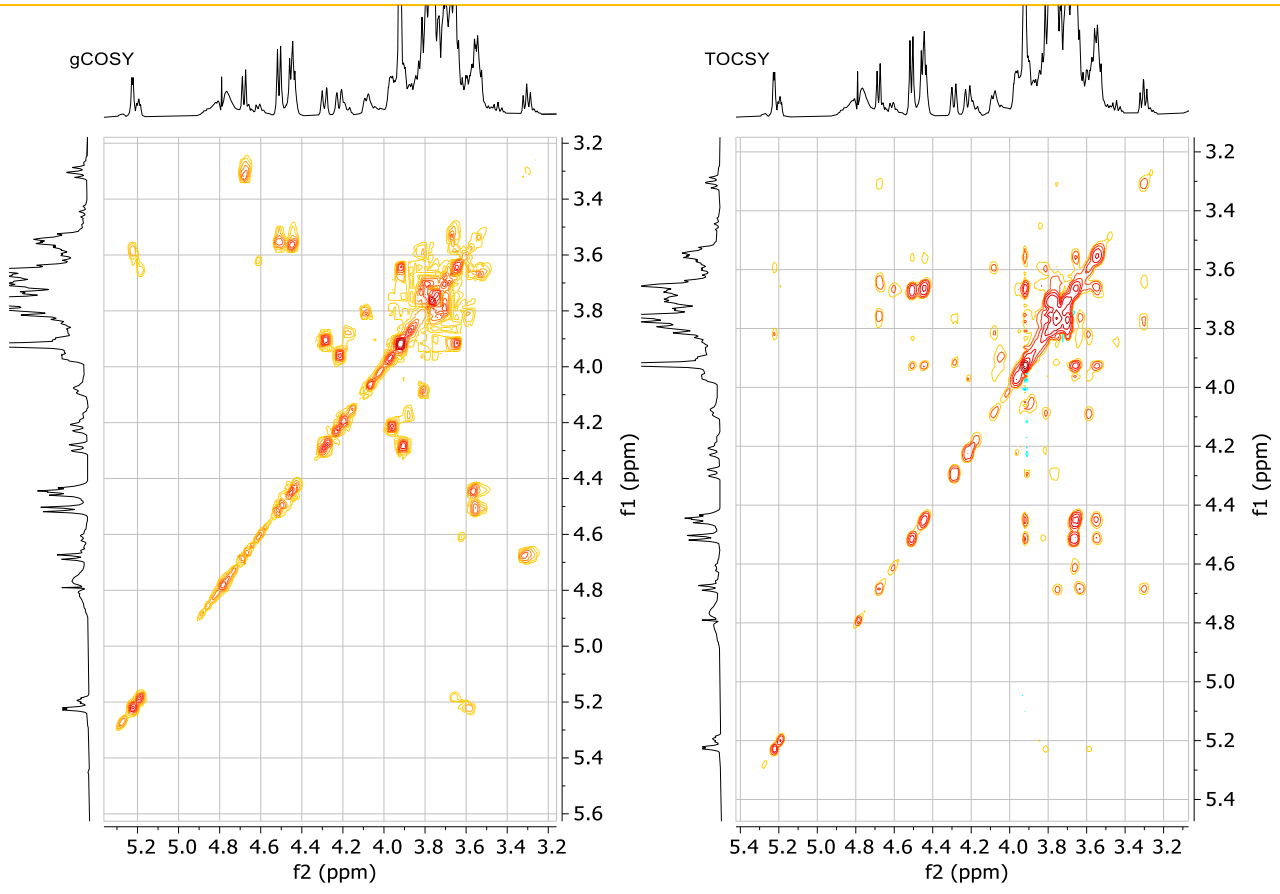

Figure S36. gCOSY and TOCSY (500 MHz, D_2O) of trisaccharide **9** derived from lactose.

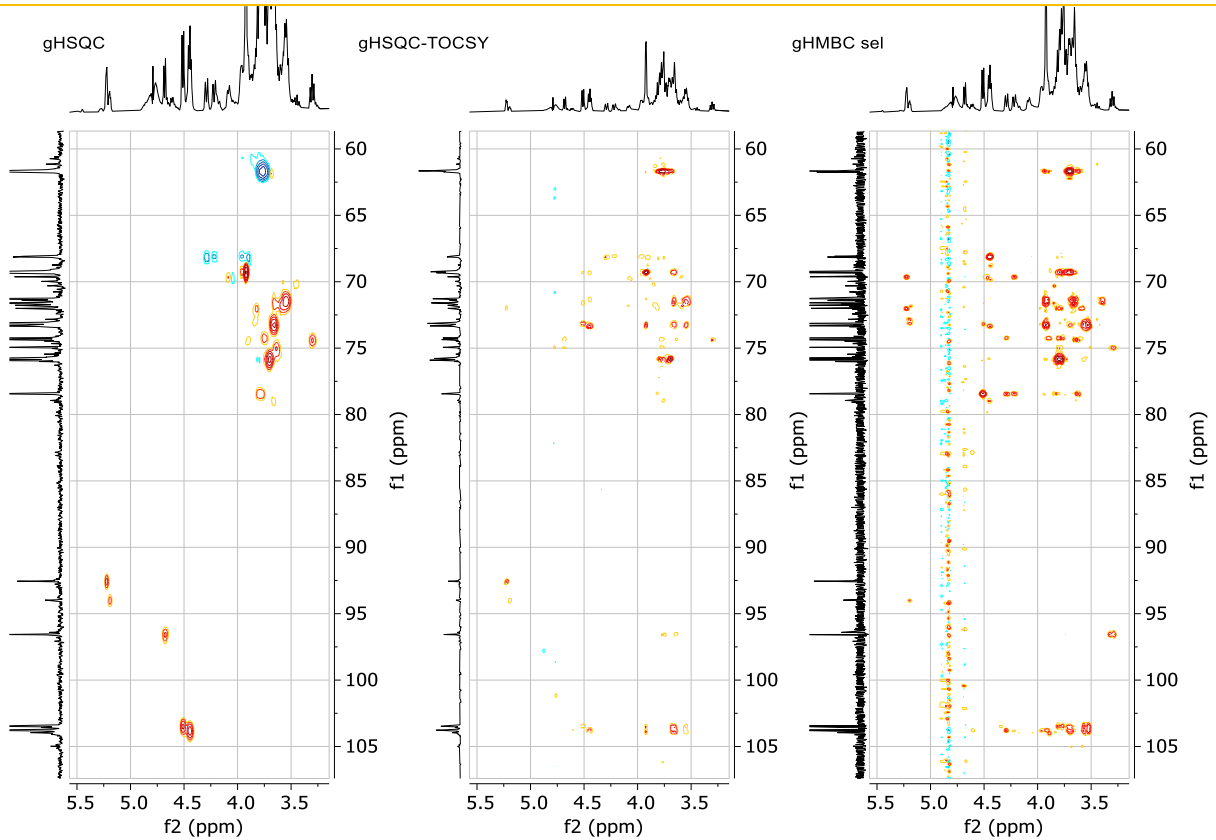

Figure S37. Multiplicity-edited gHSQC **(**methylene**:** blue cross peaks; methine**:** red cross peaks), gHSQC-TOCSY and gHMBC semiselective (500 MHz, D_2O) of trisaccharide **9** derived from lactose.

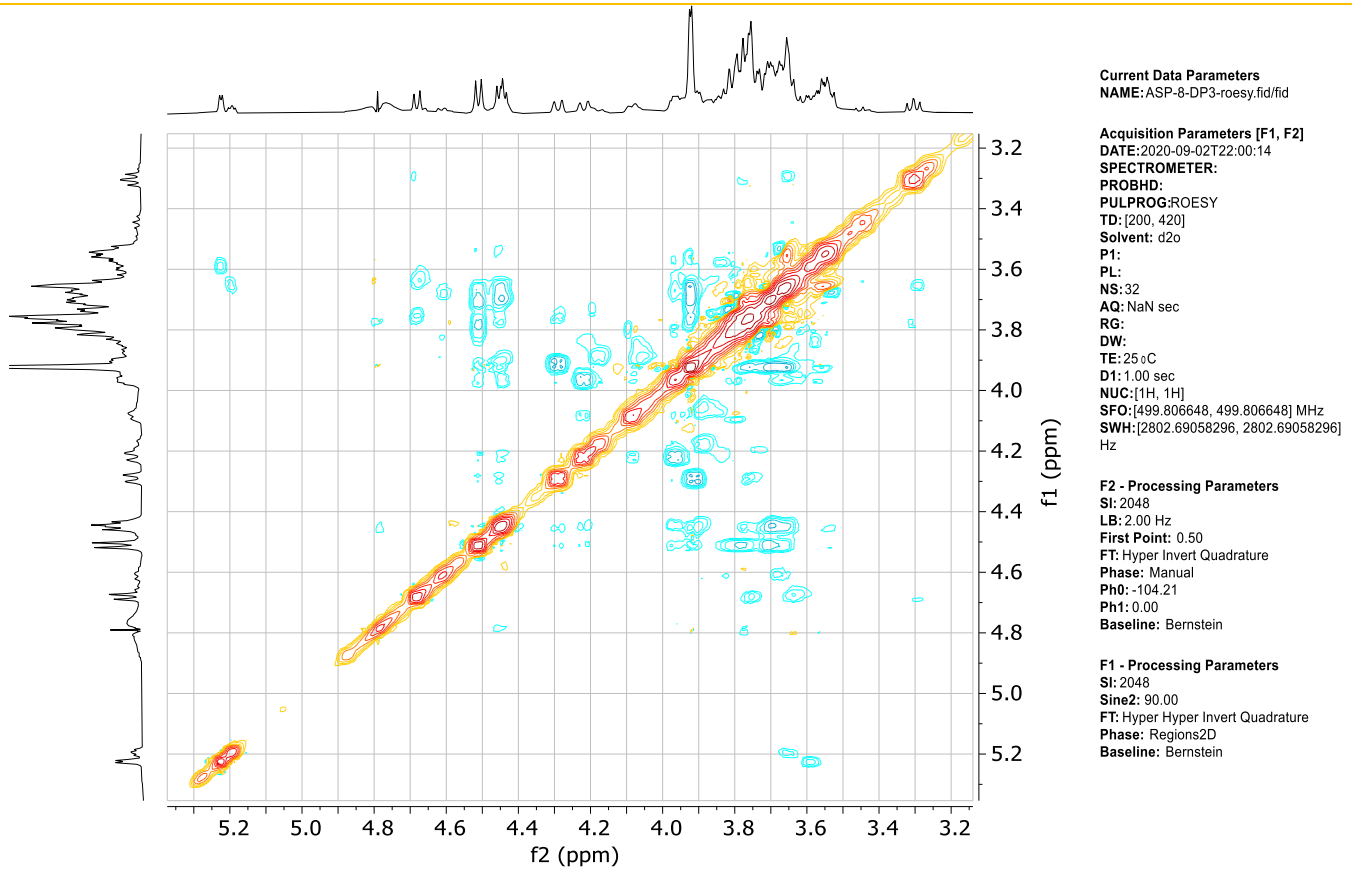

Figure S38. ROESY (500 MHz, D_2O) of trisaccharide **9** derived from lactose.

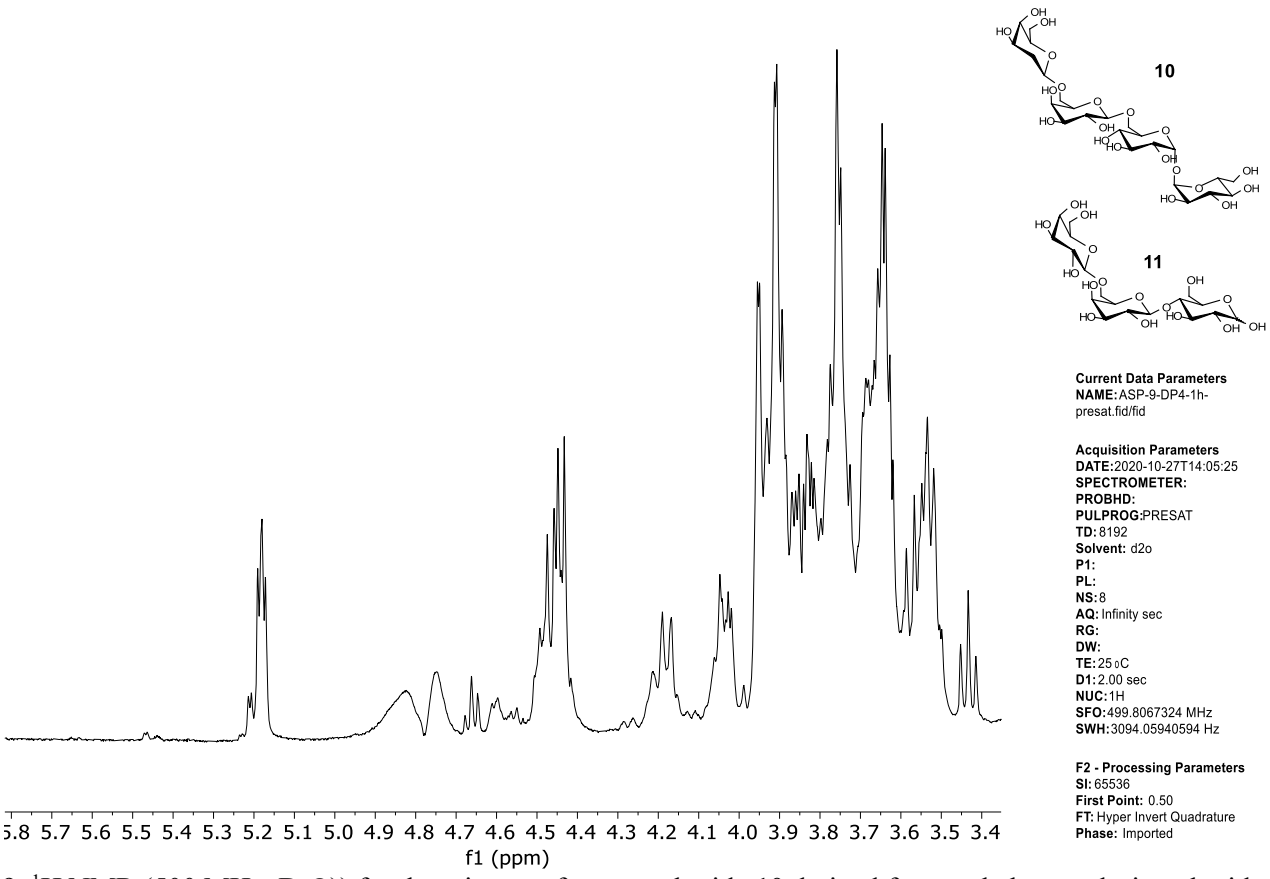

Figure S39. ^{1}H NMR (500 MHz, D_2O)) for the mixture of tetrasaccharide **10** derived from trehalose and trisaccharide **11** derived from lactose.

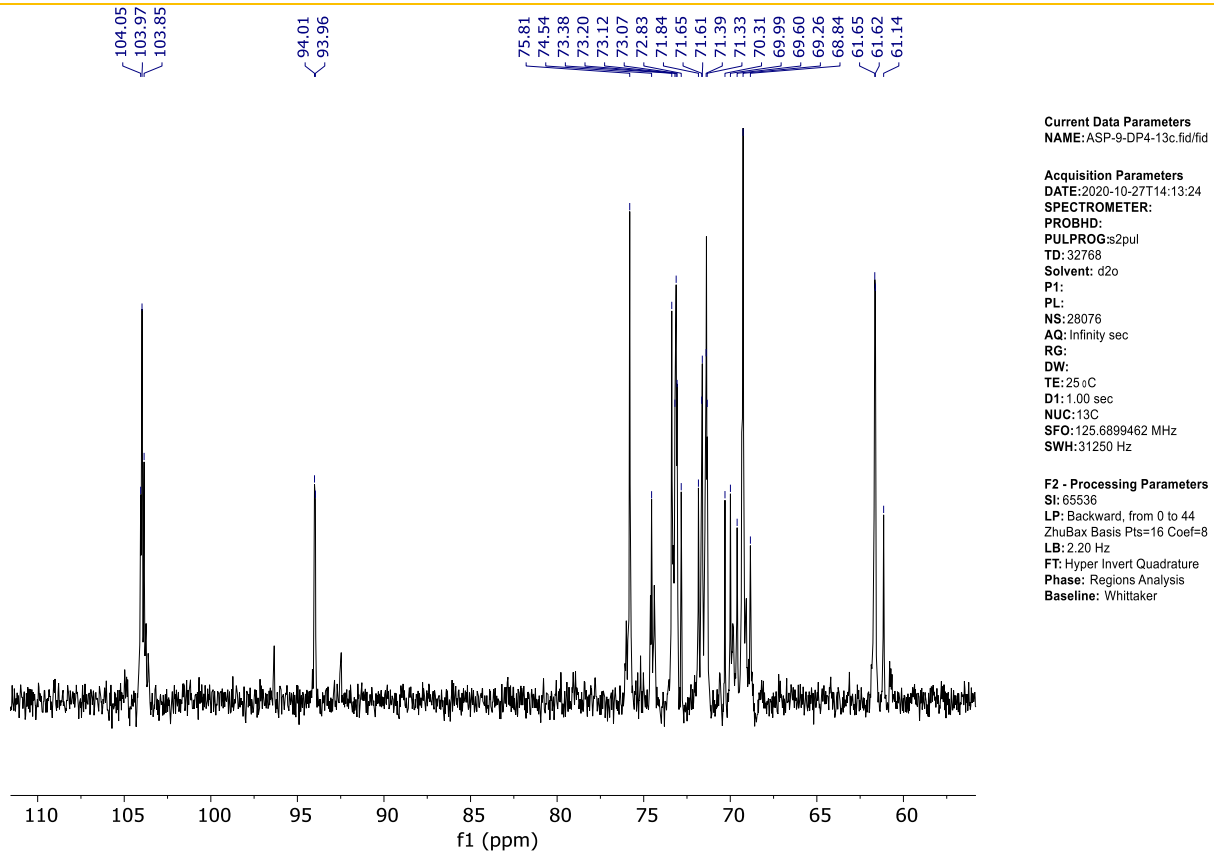

Figure S40. ^{13}C NMR (125 MHz, D_2O) for the mixture of tetrasaccharide **10** derived from trehalose and trisaccharide **11** derived from lactose.

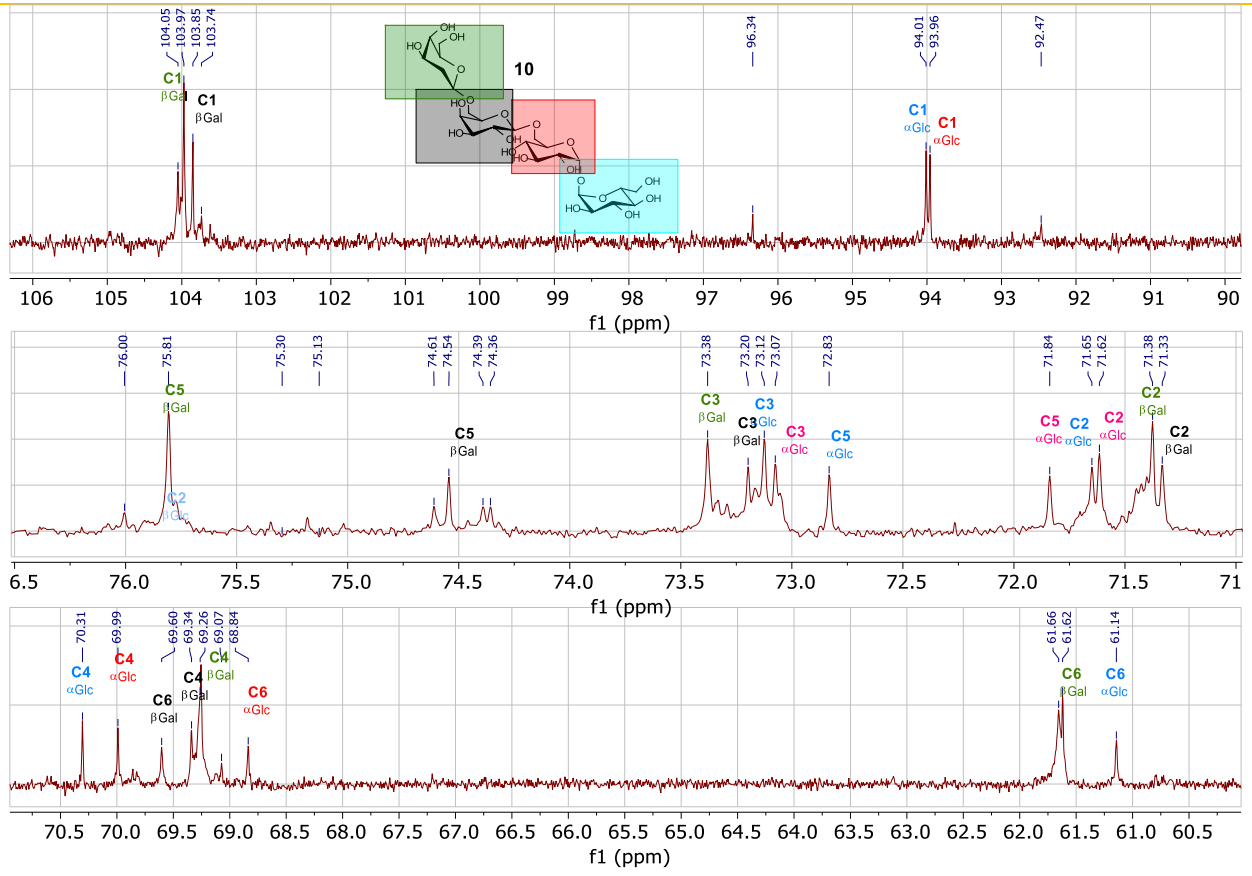

Figure S41. Complete assignment of ^{13}C NMR spectrum of tetrasaccharide **10** derived from trehalose.

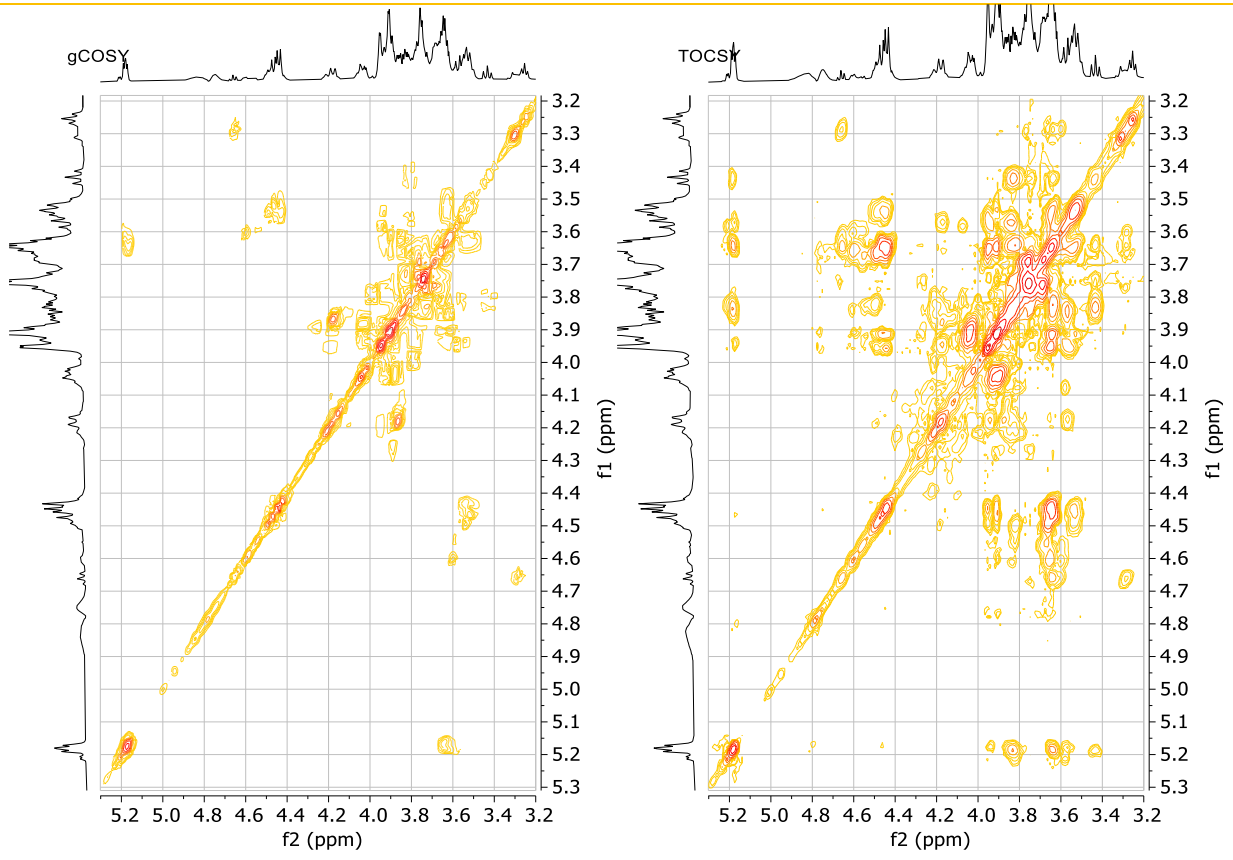

Figure S42. gCOSY and TOCSY (500 MHz, D_2O) for the mixture of tetrasaccharide **10** derived from trehalose. and trisaccharide **11** derived from lactose.

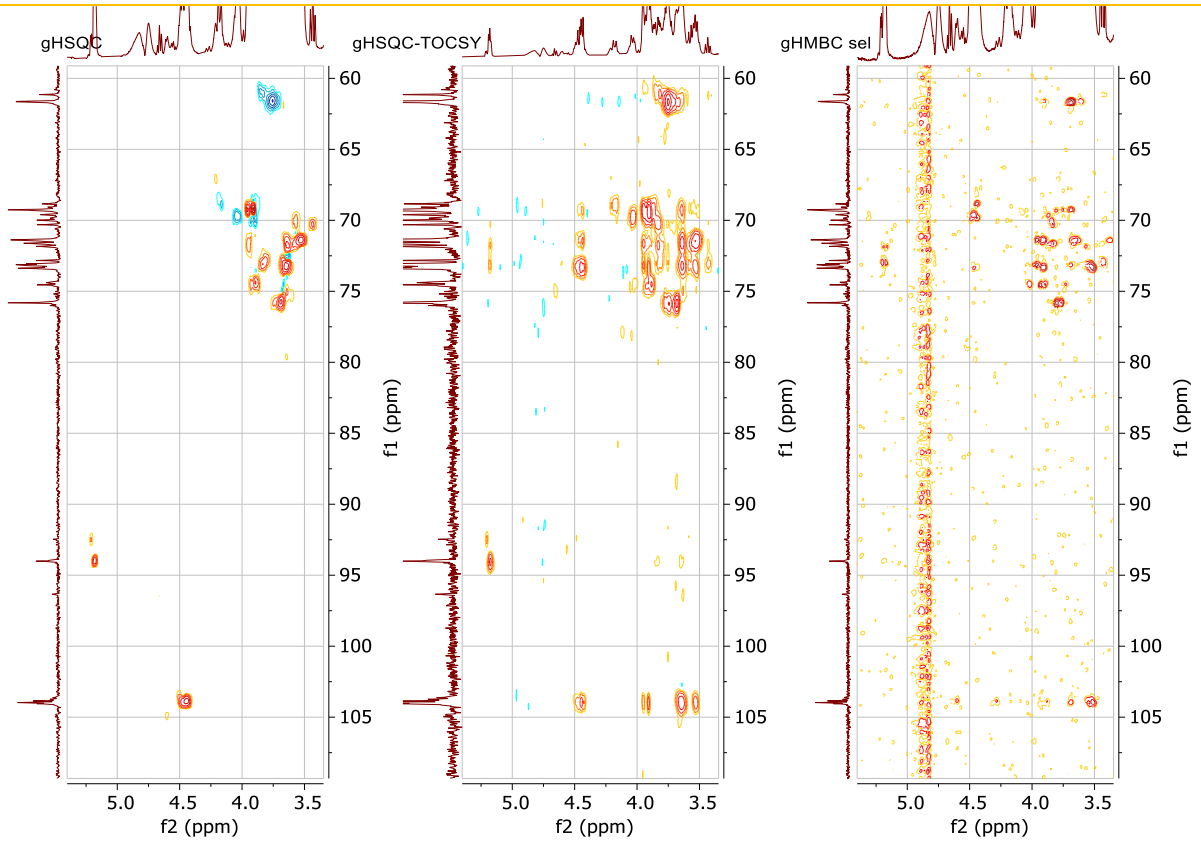

Figure S43. Multiplicity-edited gHSQC **(**methylene**:** blue cross peaks; methine**:** red cross peaks), gHSQC-TOCSY and gHMBC semiselective (500 MHz, D_2O) for the mixture of tetrasaccharide **10** derived from trehalose. and trisaccharide **11** derived from lactose.

ANEXO D

ARTÍCULOS CIENTÍFICOS PUBLICADOS

Capítulo 1: Kinetic study on the digestibility of lactose and lactulose using small intestinal glycosidases

Capítulo 2: Evaluation of the impact of a rat small intestinal extract on the digestion of four different functional fibers

Capítulo 3: *In vitro* digestion of polysaccharides: InfoGest protocol and use of small intestinal extract from rat

Capítulo 4: Behaviour of citrus pectin and modified citrus pectin in an azoxymethane/dextran sodium sulfate (AOM/DSS)-induced rat colorectal carcinogenesis model

Capítulo 5: Enzymatic synthesis and structural characterization of novel trehalose-based oligosaccharides.

Food Chemistry 316 (2020) 126326

Contents lists available at ScienceDirect

Food Chemistry

journal homepage: www.elsevier.com/locate/foodchem

Kinetic study on the digestibility of lactose and lactulose using small intestinal glycosidases

Pablo Gallego-Lobillo, Alvaro Ferreira-Lazarte, Oswaldo Hernandez-Hernandez*, Mar Villamiel

Instituto de Investigación en Ciencias de la Alimentación, CIAL (CSIC-UAM). C/Nicolás Cabrera, 9, Campus de la Universidad Autónoma de Madrid, 28049 Madrid, Spain

ARTICLE INFO

Chemical compounds studied in this article:
Lactose (PubChem CID:6134)
Lactulose (PubChem CID:11333)
D-galactose (PubChem CID: 6036)
D-glucose (PubChem CID: 5793)
Fructose (PubChem CID: 2723872)
Sucrose (PubChem CID: 5988)
Trehalose (PubChem CID: 7427)

Keywords:
Carbohydrates digestion
Prebiotics
Chemical structure
Hydrolysis kinetics

ABSTRACT

Lactose is mostly hydrolysed in the small intestine, whereas lactulose, recognised prebiotic carbohydrate, reaches the colon to be fermented by the intestinal microbiota. Digestibility of these substrates was investigated by an *in vitro* digestion model using a Rat Small Intestine Extract (RSIE). A kinetic study of lactose digestion showed levels of hydrolysis (82.8%) at 0.2 mg*mL^{-1} and the highest hydrolysis rate constant (k_{obs}). Considering these conditions, lactulose showed high resistance to intestinal digestion by RSIE, resulting in low hydrolysis degrees (20.4%) after 5 h reaction. These results underline the suitability of these intestinal extracts under the studied conditions, as a reliable tool to evaluate carbohydrate digestion and support the evidences towards the higher resistance of galactosyl-fructose linkages during its intestinal degradation.

1. Introduction

Lactose (β-D-galactopyranosyl-(1 → 4)-D-glucopyranose) is produced by the mammary gland in mammals, being the major carbohydrate in milk (4–7%) and the main source of nutrition until weaning. Lactose is hydrolysed in the small intestine and the resulting monosaccharides (glucose and galactose) are absorbed by the intestinal enterocytes in the blood-stream. Glucose is finally used as a source of energy, and galactose, in the liver, is converted into components of glycolipids and glycoproteins. The hydrolysis of lactose normally occurs in the initial part of the small intestine (jejunum) where the concentration of microorganisms is very low and hardly any amount of lactose is fermented. The hydrolysis of lactose is catalysed by the enzyme lactase-phlorizin hydrolase (β-galactosidase or lactase), located in the brush border of the intestinal villi. Most of the individuals are born with the capability to digest lactose, but this activity drops after weaning (around 75% of the world's inhabitants) to an undetectable concentration as a consequence of normal maturational down-regulation of lactase expression. The exceptions to this rule are descendants of people that by tradition practiced cattle domestication and keep the capacity to hydrolyse milk and other dairy foods during adulthood (Belitz, Grosch, & Schieberle, 2009; Di Rienzo et al., 2013).

When lactose is not well digested in the small intestine, different symptoms can take place, including abdominal pain, bloating, flatulence, and diarrhoea with a considerable intra-individual and inter-individual variability in severity. These symptoms are due to the increased osmotic load that raises the intestinal water content and the fermentation of lactose by the colonic microbiota leading to production of short chain fatty acids and gas (H_2, CO_2, and CH_4) (Bayless, Brown, & Paige, 2017). Taking into account these antecedents, it is of importance to know under which circumstances lactose is worse hydrolysed causing discomfort in the body.

Hardly any research has been done on the lactose hydrolysis during intestinal digestion. Recently, a reliable and simple *in vitro* method using Rat Small Intestine Extract (RSIE) has been developed for digestion of non-digestible and digestible carbohydrates, such as maltose, sucrose, and lactose. However, that study focused only on a ratio extract/substrate (20 mg/0.5 mg) and maximum time (2 h), obtaining lactose hydrolysis levels of no more than 56% (Ferreira-Lazarte, Olano, Villamiel, & Moreno, 2017). The aim of the present investigation is to carry out a kinetic study on the digestion of lactose with the RSIE in order to know the conditions that predicate the maximum level of

* Corresponding author.
E-mail addresses: p.gallego.lobillo@csic.es (P. Gallego-Lobillo), alvaro.ferreira@csic.es (A. Ferreira-Lazarte), o.hernandez@csic.es (O. Hernandez-Hernandez), m.villamiel@csic.es (M. Villamiel).

https://doi.org/10.1016/j.foodchem.2020.126326
Received 1 December 2019; Received in revised form 25 January 2020; Accepted 28 January 2020
Available online 01 February 2020

hydrolysis. Moreover, the use of these conditions on the digestion of the recognised prebiotic, lactulose is also intended in order to validate the method as well as to obtain more information of the structure/function of carbohydrates during digestion.

2. Materials and methods

2.1. Chemicals and reagents

In the present work, the following standards have been provided by Sigma-Aldrich (St. Louis, MO): D-galactose (Gal), D-glucose (Glc), sucrose (β-D-Fru-(2 → 1)-α-D-Glc), trehalose (α-D-Glc-(1 → 1)-α-D-Glc), lactulose (Lu) (β-D-Gal-(1 → 4)-D-Fru), phenyl-β-glucoside, *o*-nitrophenyl (*o*-NP), *p*-nitrophenyl (*p*-NP), *o*-nitrophenyl-β-D-glucopyranoside (*o*-NPG), *p*-nitrophenyl-α-glucopyranoside (*p*-NPG) and intestinal acetone powders from rat (RSIE), as well as standards for Bradford method (Bio-Rad Laboratories Gmbh, Múnich, Alemania) and for 3,5-dinitrosalicylic acid (DNS) method. Lactose (Lac) (β-D-Gal-(1 → 4)-D-Glc) was obtained from ACROS Organics (Geel, Belgium) and fructose (Fru) from Fluka Analytical (St. Gallen, Switzerland). All standards carbohydrates were of analytical grade (greater than 95%).

2.2. Rat small intestine Extract characterisation

A solution of RSIE (10 mg*mL^{-1}) was prepared in 0.05 M sodium phosphate buffer at 4 °C following the method of Olaokun et al. (Olaokun, McGaw, Eloff, & Naidoo, 2013), with minor changes. Subsequently, centrifugation at 6,000 rpm for 15 min was carried out and the supernatant was used for the complete characterisation of RSIE.

2.2.1. Protein content

Protein quantification was done through the Bradford method (1976). Bovine Serum Albumin (BSA) was used as standard and absorbance was measured at 595 nm.

2.2.2. β-galactosidase and maltase activities

The enzymatic activity was determined following the method of Ferreira-Lazarte et al. (2017) and Warmerdam, Zisopoulos, Boom and Janssen (2014). A spectrophotometer (Specord Plus, Analytik Jena) at 420 nm coupled to a temperature controller (Jumo dTRON 308, Jumo Instrument Co.) was used to obtain β-galactosidase activity of RSIE. Reactions of 1,900 μL of an *o*-NPG solution (0.5 mg*mL^{-1} in phosphate buffer, pH 7) and 100 μL of the solution of RSIE was monitored every 20 s, during 2 h at 37 °C. Then, specific enzymatic activities (U) of RSIE were calculated and expressed in μmol*min^{-1}*g protein^{-1} as the amount of enzyme which released 1 μmol of *o*-NP in 1 min of incubation (n = 3).

The same assay was done to obtain the maltase activity, except for the use of a *p*-NPG solution (0.5 mg*mL^{-1} in phosphate buffer, pH 6.8), measuring the release of *p*-NP during 2 h at 37 °C (n = 3).

2.2.3. Sucrase and trehalase activities

The determination of these enzymatic activities was carried out according to the method of Ferreira-Lazarte et al. (2017). Two solutions of sucrose and trehalose 5 mg*mL^{-1} (0.5%, *w/w*) in sodium phosphate buffer pH 6.8 were prepared. Independently, 500 μL of solution of sucrose and trehalose were mixed with 100 μL of enzymatic solution of RSIE (10 mg*mL^{-1}) and incubated for 2 h at 37 °C. Aliquots were taken at different times (blank, 5, 15, 30, 60, 90 and 120 min). Reaction was ended with the subsequent addition of 650 μL of DNS. The liberation of the reducing sugars was measured at 540 nm, following the DNS method thus calculating the specific enzymatic activity (U*g protein^{-1}) (n = 3).

2.3. In vitro digestion assays

Firstly, a preliminary assay was conducted to determine the lactose concentration, in which maximum hydrolysis existed, using RSIE. For this purpose, 10 mg*mL^{-1} RSIE solution was prepared in potassium phosphate buffer 50 mM at pH 6.8. Subsequently, different concentrations of lactose were added to the enzyme mixture: 5, 2, 1, 0.6, 0.2 and 0.1 mg*mL^{-1}. Digestion was carried out in agitation at 750 rpm and 37 °C for 5 h in a Thermomixer comfort Eppendorf®. Different aliquots were taken at different times (0, 0.5, 1, 2, 3, 4 and 5 h of digestion), which immediately afterwards were heated with boiling water for 5 min to stop the reaction. For the digestion of lactulose with RSIE (10 mg*mL^{-1}) the same procedure was performed being 0.2 mg*mL^{-1} the concentration of the disaccharide. In all cases, reaction blanks were performed with RSIE (10 mg*mL^{-1}) under the same conditions to avoid overestimation of the carbohydrate content.

In addition, lactose control digestions were carried out to confirm the total hydrolysis. Two enzymes were used: Lactozym® 6500 L HP G and Saphera® 2500 L. In the former, a solution of the enzyme at a concentration of 2 μL*mL^{-1} in potassium phosphate buffer 50 mM with 2 mM of $MgCl_2$ at pH 6.5 was prepared. In the case of Saphera® 2500 L, the concentration was 5 μL*mL^{-1} in potassium phosphate buffer 50 mM with 2 mM of $MgCl_2$ at pH 6.0. Lactose 0.2 mg*mL^{-1} was added to this mixture and the reaction was carried out on the Thermomixer at 750 rpm and 40 °C for 5 h. Aliquots were taken at the same time as above indicated for RSIE reactions.

2.4. Carbohydrate analysis using gas chromatography

GC-FID was used to analyse the fraction of carbohydrates in each digestion with intestinal extracts. Before the analysis, it was necessary to carry out the derivatisation, obtaining trimethylsilyl derivatives from oximes (TMSO) of carbohydrates, according to Ruiz-Matute et al. (Ruiz-Matute, Hernández-Hernández, Rodríguez-Sánchez, Sanz, & Martínez-Castro, 2011). Firstly, an aliquot of 500 μL of each intestinal digestion was taken (0.1 mg*mL^{-1} of carbohydrates) and 500 μL of the internal standard solution (β-phenyl-glucoside, 0.5 mg*mL^{-1}) were added and evaporated to dryness. Secondly, for carbohydrate oximes, 300 μL of hydroxylamine chloride (2.5%, *w/v*) in pyridine were added, incubated at 70 °C for 30 min. Subsequently, 300 μL of hexamethyldisylazan (HDMS) and 30 μL of trifluoroacetic acid (TFA) were added, allowing to be reacted for 30 min to 50 °C with agitation. Finally, the samples were centrifuged for 2 min at 10,000 rpm. The supernatant (1 μL) was injected into the gas chromatograph.

The analysis was performed on a gas chromatograph (GC7890A), coupled to a flame ionisation detector (FID) and an automatic injector 7693 (Agilent Technologies Ing., Palo Alto, CA). Separation was performed in a capillary column of molten silica DB-5HT (30 m × 0.32 mm × 0.10 m) (J&W Scientific, Folson, California, USA), using N_2 at a flow of 1 mL*min^{-1} as the carrier gas. The temperature of the injector and detector was 280 °C and 385 °C, respectively. The oven temperature was programmed from 150 °C to 380 °C with an increase of 3 °C*min^{-1}. The sample was injected in split mode 1:20.

Data processing and integration were carried out using an Agilent ChemStations software (Washington, DE, USA). Quantitative analysis was performed using the internal standard method calculating the response factors of the standard carbohydrates (D-fructose, D-galactose, D-glucose and lactose) previously injected at known concentrations (0.005 to 1 mg*mL^{-1}) with respect to the β-phenyl-glucoside.

2.5. Statistical analysis

The digestions were done in duplicate and the characterisation in triplicate by GC-FID. The results of the GC-FID analysis were statistically compared using variance analysis (ANOVA) for parametric testing in the SPSS software (IBM, Chicago, Il), whereby the values are

Table 1
Specific enzymatic activities of Rat Small Intestine Extract.

Enzymatic activity	Substrate	U (μmol*min^{-1} g protein^{-1})
β-galactosidase	*o*-NPG	24.76 ± 2.01^{b}
Maltase	*p*-NPG	40.37 ± 0.14^{c}
Sucrase	Sucrose	28.39 ± 2.31^{b}
Trehalase	Trehalose	15.48 ± 1.55^{a}

Protein content of RSIE: 6.1 ± 0.9% (*w/w*). $^{a-c}$ Different letters indicate statistical differences ($p < 0.05$). Values are expressed as means ± SD (n = 3).

considered to be statistically significant at $p < 0.05$.

3. Results and discussion

3.1. Enzymatic activities of the rat small intestine extract

Table 1 shows the enzymatic activities under the conditions described above. For the determination of the specific enzymatic activity (U*g protein^{-1}), the protein content of the extract was calculated being 6.1 ± 0.9% (*w/w*). Maltase was found to be the highest enzymatic activity, being twice the sucrase and β-galactosidase and 3-fold the trehalase activity. Similar trends were observed in previous reports by Ferreira-Lazarte et al. (2017) and Oku et al. (Oku, Tanabe, Ogawa, Sadamori, & Nakamura, 2011), where the difference between maltase and the other enzymes were almost four times higher. These dissimilarities may be ascribed to the great variability that exists between the different extracts of the small rat intestine. The sucrose activity was

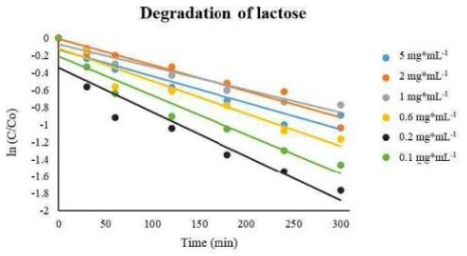

Fig. 2. Kinetics of lactose hydrolysis at the different concentrations during small intestinal digestion using RSIE at 37 °C, pH 6.8.

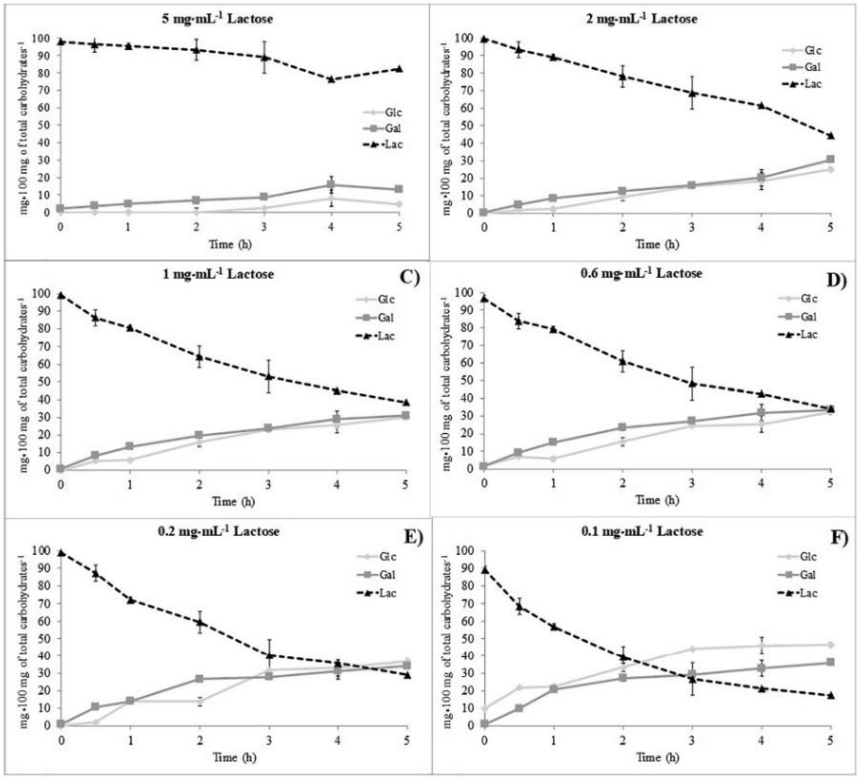

Fig. 1. Evolution of the carbohydrate content in the digestion of lactose at different concentrations: 5 (A), 2 (B), 1 (C), 0.6 (D), 0.2 (E) and 0.1 (F) mg mL^{-1} during 5 h of small intestinal digestion using RSIE at 37 °C, pH 6.8.

Table 2
Hydrolysis degree (%) of lactose at different concentrations and lactulose (0.2 mg mL^{-1}) using Rat Small Intestine Extract at 37 °C, pH 6.8.

Digestion time (h)	Lactose concentration						Lactulose concentration
	5 mg*mL^{-1}	2 mg*mL^{-1}	1 mg*mL^{-1}	0.6 mg*mL^{-1}	0.2 mg*mL^{-1}*	0.1 mg*mL^{-1}	0.2 mg*mL^{-1}*
0.5	1.48 ± 1.93	16.03 ± 1.81	11.15 ± 0.10	13.71 ± 0.75	42.95 ± 1.00	28.30 ± 0.01	2.05 ± 2.32
1	2.51 ± 1.00	18.13 ± 0.78	25.60 ± 5.70	42.90 ± 2.45	60.04 ± 5.31	47.25 ± 0.82	4.27 ± 3.70
2	4.74 ± 1.55	28.05 ± 6.68	35.07 ± 5.04	45.79 ± 3.51	64.61 ± 5.40	59.38 ± 0.81	10.20 ± 4.20
3	9.10 ± 1.60	40.62 ± 1.50	45.24 ± 3.20	53.99 ± 2.16	74.07 ± 5.92	64.88 ± 0.29	20.17 ± 0.01
4	22.09 ± 2.21	46.01 ± 0.20	51.98 ± 3.48	65.59 ± 2.63	78.54 ± 5.12	72.67 ± 0.44	19.32 ± 0.04
5	15.84 ± 0.10	64.44 ± 1.10	53.77 ± 2.54	68.96 ± 1.68	82.81 ± 4.99	76.95 ± 0.42	20.41 ± 0.09

*Digestion of lactulose was done in the conditions of the highest hydrolysis of lactose (0.2 mg mL^{-1}).
Values are expressed as means ± SD (n = 2).

Table 2b
Hydrolysis rate constants obtained (k_{obt}) and half-lives ($t_{1/2}$) after 2 and 5 h digestion at the different concentrations of lactose.

Lactose concentration (mg*mL^{-1})	2 h		5 h	
	k_{obt} (min^{-1})	$t_{1/2}$ (min)	k_{obt} (min^{-1})	$t_{1/2}$ (min)
5	4.7×10^{-3}	146.77	3.0×10^{-3}	234.05
2	2.7×10^{-3}	252.69	3.4×10^{-3}	201.10
1	3.6×10^{-3}	192.62	2.6×10^{-3}	269.51
0.6	5.1×10^{-3}	135.84	3.9×10^{-3}	177.74
0.2	8.7×10^{-3}	80.07	5.9×10^{-3}	118.09
0.1	7.5×10^{-3}	92.32	4.9×10^{-3}	141.71

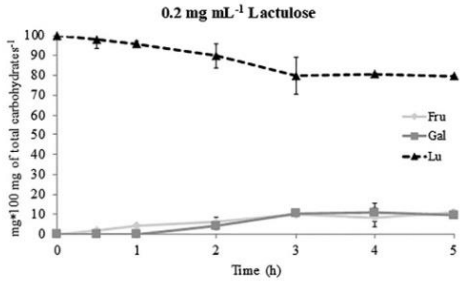

Fig. 3. Evolution in the carbohydrate content of lactulose during the intestinal digestion of lactulose at 0.2 mg*mL^{-1} during 5 h with RSIE at 37 °C, pH 6.8.

Table 3
Kinetics of the degradation of lactulose during the digestion of lactulose at during 2 and 5 h with RSIE at 37 °C, pH 6.8.

Lactulose concentration (mg*mL^{-1})	2 h		5 h	
	k_{obt} (min^{-1})	$t_{1/2}$ (min)	k_{obt} (min^{-1})	$t_{1/2}$ (min)
0.2	9.0×10^{-4}	772.89	7.6×10^{-4}	911.07

slightly higher than the activity of β-galactosidase, with no significant differences, as also evidenced by Oku et al. (2011) and Semenza and Auricchio (1965).

In the case of the β-galactosidase, the activity was very close to that found by Ferreira-Lazarte et al. (2017). The observed variability between the enzymatic activities of β-galactosidase could be due to the fact that these enzymes are gradually degraded with the age of the rat (Alexandre et al., 2013). The trehalase activity was the least active, showing significant differences with the rest of the disaccharidases ($p < 0.05$), similarly to data of Ferreira-Lazarte et al. (2017) and Oku et al. (2011).

3.2. Lactose and lactulose digestibility with RSIE

Firstly, digestions of control samples, based on the incubation of RSIE without carbohydrates, were performed under the same experimental conditions of digestions (5 h, pH 6.8, 37 °C, and 750 rpm). The results reflected a limited rise in fructose and galactose (data not shown), while glucose increased significantly during the 5 h digestion. These values were adequately considered to avoid overestimation of the content in monosaccharides.

Fig. 1 shows the evolution of lactose hydrolysis and, consequently, the release of galactose and glucose during intestinal digestion at the different substrate concentrations used (5, 2, 1, 0.6, 0.2, and 0.1 mg*mL^{-1} of lactose) with RSIE.

The ln (C/C_0) versus time plot of lactose (Fig. 2) gave straight lines at each concentration value, indicating the substrate-concentration dependence nature of the reaction, suggesting, therefore, that hydrolysis followed in the first- or pseudo-first- order kinetics (Logan, 1996):

$$C = C_0 e^{-k_{obt} t}$$

where t represents the incubation time in hours, C is the concentration of lactose at time t, C_0 is the initial concentration in mg 100*mg total carbohydrates^{-1} and k_{obt} (min^{-1}), the obtained rate constant of the reaction.

Hydrolysis percentages, as well as the hydrolysis rate constant (k_{obt}) and half-life ($t_{1/2} = \ln 0.5/k_{obt}$) values, obtained for lactose are shown in Table 2. Higher lactose hydrolysis values were correlated with lower initial contents of this substrate compared to enzymatic extract used (higher E:S ratio), which was maintained constant in all assays. In this sense, the maximum hydrolysis of lactose was 82.8% at a concentration of 0.2 mg*mL^{-1}, without reaching total carbohydrate degradation. The hydrolysis observed at the lowest concentration, 0.1 mg*mL^{-1}, was slightly lower (77%), indicating that the maximum RSIE activity was reached at 0.2 mg*mL^{-1} concentration. Additionally, k_{obt} determined after 2 and 5 h of digestion showed the highest values for the reaction with 0.2 mg*mL^{-1} and consequently the lowest $t_{1/2}$ at these conditions. Higher values of k_{obt} were observed after 2 h of digestion when compared to 5 h digestion, highlighting that the hydrolysis of the lactose was faster in the first stages of reaction due to higher presence of the disaccharide and lower concentration of monosaccharides that could inhibit the enzyme activity, which decreases over time.

Furthermore, lactose control digestions that were performed under the same conditions with *Kluyveromyces lactis* and *Bifidobacterium bifidum* commercial lactase (data not shown), showed a total degradation of lactose at 30 min of digestion in the case of *K. lactis*, and at 1 h in the case of *B. bifidum*, confirming its total hydrolysis, unlike the RSIE. Previous studies (Santibáñez, Fernández-Arrojo, Guerrero, Plou, & Illanes, 2016) have shown the high capacity of *K. lactis* and *B. bifidum* lactases to hydrolyse lactose, being used by the industry to obtain

Prieto, R. M., Ferrer, M., Rayó, J. M., & Tur, J. A. (1994). Disaccharidase activities in pregnant and lactating rats. *Comparative Biochemistry and Physiology –. Part A: Physiology, 109*(3), 741–747. https://doi.org/10.1016/0300-9629(94)90217-8.

Ruiz-Matute, A. I., Hernández-Hernández, O., Rodríguez-Sánchez, S., Sanz, M. L., & Martínez-Castro, I. (2011). Derivatization of carbohydrates for GC and GC-MS analyses. *Journal of Chromatography B: Analytical Technologies in the Biomedical and Life Sciences, 879*(17–18), 1226–1240. https://doi.org/10.1016/j.jchromb.2010.11.013.

Santibáñez, L., Fernández-Arrojo, L., Guerrero, C., Plou, F. J., & Illanes, A. (2016). Removal of lactose in crude galacto-oligosaccharides by β-galactosidase from *Kluyveromyces lactis*. *Journal of Molecular Catalysis B: Enzymatic, 133*, 85–91. https://doi.org/10.1016/j.molcatb.2016.07.014.

Semenza, G., & Auricchio, S. (1965). Multiplicity of human intestinal disaccharides. I. Chromatographic separation of maltases and two lactases. *Biochimica et Biophysica Acta, 96*, 487–497. https://doi.org/10.1016/0005-2787(65)90565-4.

Warmerdam, A., Zisopoulos, F. K., Boom, R. M., & Janssen, A. E. M. (2014). Kinetic characterization of galacto-oligosaccharide (GOS) synthesis by three commercially important β-galactosidases. *Biotechnology Progress, 30*(1), 38–47. https://doi.org/10.1002/btpr.1828.

Food & Function

ROYAL SOCIETY OF CHEMISTRY

PAPER

View Article Online
View Journal

Cite this: DOI: 10.1039/d0fo00236d

Evaluation of the impact of a rat small intestinal extract on the digestion of four different functional fibers

Pablo Gallego-Lobillo, Alvaro Ferreira-Lazarte, Oswaldo Hernández-Hernández, * Antonia Montilla and Mar Villamiel

The degree of digestion, modulated by rat small intestinal extract on different functional fibers was investigated. In general, inulin-type fructans and fructooligosaccharides were the most resistant to the enzymatic digestion. Results evidenced the high-resistance of fructosyl-fructose bonds. This fits well with the concept of prebiotic carbohydrates. However, the mixture of melibiose, manninotriose and verbascotetraose (α-GOS) from peas, with a considerably lower molecular weight (0.6 kDa) than the fructans studied, were highly digested (61.2%). Interestingly, the Gal-(1 → 6)-Gal bonds present into the manninotriose and verbascotetraose were more prone to be hydrolyzed than Gal-(1 → 6)-Glc (melibiose). However, when melibiose was the only disaccharide present in the reaction mixture, the hydrolysis was also high (67.7%). The use of small intestinal enzymatic preparations is a realistic approximation to evaluate the digestion of different carbohydrates, thus, showing that recognized non-digestible carbohydrates can also be partially digested.

Received 27th January 2020,
Accepted 20th April 2020

DOI: 10.1039/d0fo00236d

rsc.li/food-function

1. Introduction

The recommended daily allowances (RDAs) for total fiber consumption for healthy men and women (19–50 years old) are 38 g day^{-1} and 25 g day^{-1}, respectively, and these general needs can vary depending on the health status of the individual. Although fibers have revealed to possess numerous positive health effects on severe pathologies (obesity, diabetes, cardiovascular disease, among others), the mean daily intake for most people is much lower than the RDA. There is no superior acceptable amount for fiber consumption, although the tolerance depends mainly on the individual; bloating and abdominal pain being the most important consequences of excessive intake.[1,2]

In general, the total fiber consumption is the quantity of dietary fiber and functional fiber. Technically, dietary fiber is a complex group of carbohydrates and lignin, which are not digested nor absorbed, in the human body. They can be divided in two major groups: soluble and insoluble fiber according to their water solubility, both being indigestible in the small intestine.[3–5]

Functional fibers constitute a wide range of non-digestible carbohydrates that are either isolated or synthesized from natural sources mainly agro-food by-products. Once the functional fiber is produced is added to food during processing with the aim of providing beneficial effects on human health. Functional fibers include polysaccharides such as β-glucans, cellulose, chitins and chitosan, fructans, gums, pectin, polydextrose, polyols, resistant dextrins, resistant starches and oligosaccharides that are resistant to digestion.[2]

According to previous studies, these carbohydrates can reach intact the large intestine, where they are hydrolyzed and fermented by the intestinal microbiota, thus causing the production of short chain fatty acids (SCFAs) that exert a beneficial effect not only in the colon but also systemically.[6–8] However, few studies have been conducted on the digestive resistance of carbohydrates (also refereed as non-digestible carbohydrates), probably due to the lack of reliable digestion methods specifically designed for carbohydrates.

To date, the focus of the most common approach to simulate the small intestinal digestion is dedicated to proteins, lipids and starch, by using pancreatic enzymes from porcine origin, salivary enzymes and microbial enzymes, which could not reflex most of the carbohydrase activities of the whole small intestine.[9] The Association of Official Analytical Chemist (AOAC) developed an integrated determination method for dietary fiber, including non-digestible oligosaccharides (NDOs) and resistant starch, which was modified later in 2015 (AOAC 2009.01).[10,11] Other methods, as well as this method, are based on the use of isolated digestive enzymes. Porcine

Instituto de Investigación en Ciencias de la Alimentación, CIAL (CSIC-UAM). C/Nicolás Cabrera, 9, Campus de la Universidad Autónoma de Madrid, 28049 Madrid, Spain. E-mail: o.hernandez@csic.es; Tel: +34910017951

pancreatic α-amylase and a fungal amyloglucosidase from *Aspergillus niger* are used to produce the complete hydrolysis of digestible saccharides, and therefore, to distinguish between digestible and non-digestible carbohydrates. However, similar to the InfoGest protocol, these enzymes cannot completely hydrolyze digestible saccharides since they do not represent the fully complex enzymatic environment of the small intestine, mainly because of the absence of the brush border enzymes of the enterocytes. As a result, digestible saccharides that are not fully degraded are detected as non-digestible carbohydrates, which lead to an inaccurate determination of the digestion resistance of these carbohydrates.[12,13] Recently, a promising *in vitro* digestibility method of dietary carbohydrates using rat small intestinal extract (RSIE) has questioned the belief that recognized prebiotics oligosaccharides derived from lactose (GOS) and fructooligosaccharides (FOS) reach the distal portions of colon without alterations.[14–16] Therefore, with the aim of gain more insight on the benefits of non-digestible carbohydrates, in this work the digestibility of commercial functional fiber, such as α-galactooligosaccharides derived from peas and different types of fructans have been tested using a rat small intestine extract.

2. Materials and methods

2.1. Chemical and reagents

Fructose (Fru) standard was obtained from Fluka Analytical (St Gallen, Switzerland). Analytical standards of D-Galactose (Gal), D-glucose (Glc), maltose (α-D-Glc(1 → 4)-D-Glc), sucrose (β-D-Fru(2 → 1)-α-D-Glc), phenyl-β-D-glucoside, pullulan set (805–0.34 kDa), as well as the reagents for Bradford method (Bio-Rad Laboratory Gmbh, Munich, Germany) and intestinal acetone powders from rat (Rat Small Intestine Extract, RSIE) were provided by Sigma-Aldrich (St Louis, MO). Lactose (β-D-Gal(1 → 4)-D-Glc) standard was purchased from ACROS Organics (Geel, Belgium). Melibiose (α-D-Gal(1 → 6)-D-Glc) standard was obtained from Thermo Fisher Scientific (Kandel, Germany). Analytical standards of kestose (β-D-Fru(2 → 1)-β-D-Fru(2 → 1)-α-D-Glc) and nystose (β-D-Fru(2 → 1)-β-D-Fru(2 → 1)-β-D-Fru(2 → 1)-α-D-Glc) were supplied by FUJIFILM Wako Chemical Corporation (Neuss, Germany).

2.2. Prebiotic carbohydrates

Four types of commercial carbohydrates were used for the digestion assays: Orafti® GR (92% of inulin and 8% of FOS with a degree of polymerization (DP) up to 10), Raftiline® High Performance (inulin with an average DP up to 25), Raftilose® P95 (FOS; DP 3 to 7). These carbohydrates were obtained from Orafti S. A. (Oreye, Belgium). In addition, a commercial mixture of α-GOS with DP 2–4 (AlphaGOS® P) from Olygose (Venette, France) were tested.

2.3. Characterization of substrate by HPSEC-ELSD

The molecular weight (M_w) of each carbohydrate was obtained by High Performance Size Exclusion Chromatography (HPSEC) coupled to an Evaporative Light Scattering Detector (ELSD), following the method described by Muñoz-Almagro *et al.* (2018).[17] Analysis was carried out on a LC 1220 Infinity System (Agilent Technologies, Boebligen, Germany), using two TSK-GEL columns (G5000 PWXL, 7.8 × 300 mm, 10 μm; G2500 PWXL, 7.8 × 300 mm, 6 μm) linked with a TSK-Gel guard column (6.0 mm × 400 mm) (Tosoh Bioscience, Stuttgart, Germany). Diluted samples were filtered (0.45 μm) and eluted (20 μL) with 0.1 M $NH_4CH_3CO_2$, at a flow rate of 0.5 mL min^{-1} for 50 min at 30 °C. The detection was carried out on an ELSD System 1260 Infinity (Agilent Technologies, Boebligen, Germany). Pullulans of M_w 805, 200, 10, 1.3 and 0.34 kDa were used as calibration standards.

2.4. Enzymatic characterization of rat small intestine extract

2.4.1. Protein determination. Protein quantification was done through the Bradford method.[18] Bovine Serum Albumin (BSA) was used as a standard and absorbance was measured at 595 nm.

2.4.2. Enzymatic activities. Sucrase, melibiase and inulinase activities of RSIE were established by GC-FID. Firstly, solutions of sucrose, melibiose and inulin were incubated with RSIE (40 mg mL^{-1}) in distilled water (pH 6.8) during 180 min at 37 °C in an orbital Thermomixer comfort (Eppendorf®). Aliquots were taken in 0, 60, 120 and 180 min and inactivated in boiling water for 5 min.

The carbohydrate hydrolysis was measured through GC-FID as described below. Specific enzymatic activities (U) of RSIE were calculated and expressed in μmol per (min per g per protein). Each unit of specific enzymatic activity was defined as the amount of enzyme which released 1 μmol of the corresponding monosaccharides in 1 min of incubation (n = 4).

2.5. *In vitro* digestion of polysaccharides with RSIE

The digestibility of three types of inulin, a mixture of α-GOS and the corresponding blanks (no added carbohydrate sample) were digested with RSIE following the method used by Ferreira-Lazarte *et al.* (2017)[14] with slight changes. Initially, a solution of 0.5 mg mL^{-1} of prebiotic carbohydrate in distilled water was prepared, then 40 mg of RSIE was mixed with 1 mL of prebiotic solution and the mixture was incubated to perform the reactions. Digestions were carried out in an orbital Thermomixer comfort (Eppendorf®) at 37 °C during 3 h of reaction with continuous agitation (750 rpm). Duplicate of individual reactions were carried out for each time (0, 60, 120 and 180 min) in order to avoid any possible enzymes/substrate composition changes produced by taking aliquots, and reactions were stopped by heating in boiling water for 5 min.

2.6. Chromatographic analysis of carbohydrates

Gas chromatography, equipped with a flame ionization detector (GC-FID), was used to analyze the fraction of carbohydrates for each enzymatic characterization and digestion. Samples were derivatized, to obtain trimethylsilylated oximes (TSMO) of carbohydrates, according to the method of Brobst and Lott (1966).[19] Samples solutions were prepared with 500 μL of

digestion samples (0.25 mg of carbohydrates) and 250 μL of phenyl-β-D-glucoside (internal standard, 0.5 mg mL^{-1}), and were evaporated under vacuum. Three hundred μL of hydroxylamine chloride in pyridine (2.5%, w/v) were added to the samples and incubated at 70 °C for 30 min with agitation. Then, 300 μL of hexamethyldisilazane (HDMS) and 30 μL of trifluoroacetic acid (TFA) were added and heated at 50 °C for 30 min under continuous agitation. Finally, samples were centrifuged at 10 000 rpm for 3 min. Supernatants were injected in GC-FID.

GC-FID analysis was carried out in an Agilent Technologies 7820A gas chromatograph system. Separations of the compounds were achieved with a fused silica capillary column DB-5HT (5% phenyl methylpolysiloxane, 30 m × 0.25 mm × 0.1 μm, Agilent J&W Scientific, Folsom, CA, USA). The initial oven temperature was 150 °C, then increased at a rate of 3 °C min^{-1} to 380 °C. The carrier gas used was nitrogen at a flow rate of 1 mL min^{-1}. Injector and detector temperatures were set at 280 and 385 °C, respectively. Split mode 1 : 20 were used for the injections.

Interpretation and identification of the TMSO derivatives were performed using Agilent ChemStation software (Washington, DE, USA). Quantitative analysis was obtained through the internal standard method, thus calculating the response factors of standards solutions of carbohydrates (D-fructose, D-galactose, D-glucose, sucrose, lactose, kestose, nystose) at known concentrations (0.005 to 1 mg mL^{-1}).

2.7. Statistical analysis

All digestions were made in duplicate and two GC-FID analysis (n = 2). For the statistical analysis, comparisons were made using analysis of variance (ANOVA) and Tukey's *post hoc* test with SPSS software for Windows (SPSS Inc., Chicago, Il). Differences between content in carbohydrates were considered statistically significant when $p < 0.05$.

3. Results and discussion

3.1 Enzymatic characterization of RSIE

Table 1 shows the sucrase, inulinase and melibiase activities of RSIE analyzed by GC-FID in the same conditions of digestion. Sucrase activity (42.07 U) was the highest, being 2-fold higher than melibiase activity (26.56 U) and eight times higher than inulinase (5.46 U). Sucrase activity obtained was moderately higher than the values obtained in previous reports in rats by Ferreira-Lazarte *et al.* (2017)[14] (23.5 U). These differences could be due to the variability between the batches of commercial intestinal acetone powders from rat. Regarding inulinase and melibiase activity, no previous studies have reported these activities in these enzymatic substrates.

Table 1 Specific enzymatic activities and protein content of Rat Small Intestine Extract (RSIE) at 37 °C and pH 6.8

Activity	Substrate	U (μmol min^{-1} g^{-1})
Sucrase	Sucrose	42.1 ± 2.6[a]
Inulinase	Inulin	5.5 ± 0.1[a]
Melibiase	Melibiose	26.6 ± 7.1[b]

Protein content of RSIE was 6.9 ± 0.5% (w/w). Hydrolytic activities were calculated by measuring the carbohydrate evolution by GC-FID. [a] Increase of μmol of fructose. [b] Increase of μmol of galactose.

RSIE is a complex mixture of proteins, cells, lipids, enzymes and other carbohydrates contained in the small intestine. Sucrose (β-D-Fru(2 → 1)-α-D-Glc) and melibiose (α-D-Gal(1 → 6)-D-Glc) hydrolysis can be attributed to the sucrase-isomaltase complex.[20] Sucrase site splits glucose and fructose, while isomaltase site splits Glc–Glc α(1 → 4) and α(1 → 6) linkages, being one of the most common complexes in the small intestine.[21] Inulinase activity showed the lowest value, which could be related to the low digestibility of prebiotic fructans.[14,22]

3.2 Characterization of prebiotic carbohydrates

The chromatographic profiles corresponding to the molecular weight (M_w) distribution of carbohydrates used in the digestion assays are showed in Fig. 1. Raftiline HP had the highest M_w (3.4 kDa – 19 DP), followed by Inulin Orafti GR (2.6 kDa; 14.5 DP); Raftilose P95 and AlphaGOS P presented similar values (0.6 and 0.7 kDa and 3.3 and 4.0 DP, respectively); and melibiose the lowest (0.4 kDa; 2.2 DP). Raftiline HP is reported to be a polysaccharide composed of mainly inulin, with a high DP (10–60) and higher M_w.[23–26] A similar situation occurs with inulin Orafti GR, although a slightly lower M_w inulin was observed in this case.[26–28] Raftilose P95 and AlphaGOS P oligosaccharides showed the lowest M_w, 0.6 kDa (3.3 DP) and 0.7 kDa (4.0 DP), respectively.[23,24,28–30]

3.3 Digestion of prebiotic carbohydrates using RSIE

The digestibility of three recognized prebiotics (Inulin Orafti GR, Raftiline HP and Raftilose P95) and two potential prebiotic carbohydrates (AlphaGOS P and melibiose) were tested using RSIE. Blank samples of digestion without carbohydrates were also carried out to measure possible matrix effects of this complex mixture.[31]

Table 2 shows the individual composition of each carbohydrate incubated with RSIE, including mono-, di-, tri- and tetrasaccharide fractions. Before digestion treatments, Raftiline HP which is described as an inulin-type long-chain fructans, where DP below 10 is removed,[32] did not show any carbohydrate with DP < 4, apart from small amounts of fructose. On the other side, Inulin Orafti GR contains small amounts of FOS, detected as nystose, kestose and sucrose. Fructooligosaccharides (Raftilose P95) showed higher contents of small compounds (DP < 4) due to their oligosaccharide composition. Inulobiose (β-D-Fru(2 → 1)-β-D-Fru), inulotriose (β-D-Fru(2 → 1)-β-D-Fru(2 → 1)-β-D-Fru), inulotetraose (β-D-Fru(2 → 1)-β-D-Fru(2 → 1)-β-D-Fru(2 → 1)-β-D-Fru) and nystose were detected in Raftilose P95 samples, in agreement with the data reported by Montilla *et al.* (2006).[33] Interestingly, the analysis of AlphaGOS P showed that this commercial product contains melibiose (α-D-Gal(1 → 6)-D-Glc), manninotriose (α-D-Gal(1 →

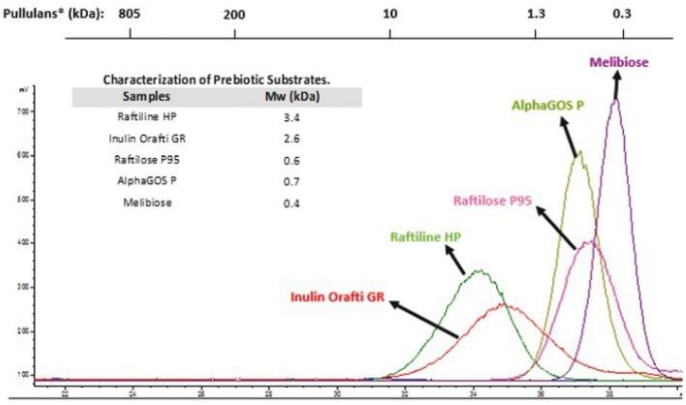

Fig. 1 Molecular weight (M_w) and chromatographic profiles by HPSEC-ELSD of prebiotic carbohydrates used in the digestion assays. *M_w of standards of pullulans is indicated above.

6)-α-D-Gal(1 → 6)-D-Glc) and verbascotetraose (α-D-Gal(1 → 6)-α-D-Gal(1 → 6)-α-D-Gal(1 → 6)-D-Glc), defructosylated derivatives from the α-galactosides raffinose, stachyose and verbascose, respectively, compounds naturally present in peas.[34] This different composition may be due to the fact that original α-galactosides could have been enzymatically treated with a fructosidase. Montilla *et al.* (2011),[35] previously, found that this enzyme, under appropriate conditions, is able to completely eliminate the fructose from stachyose, forming manninotriose.

The evolution in the content of di-, tri- and tetrasaccharides in the samples was highly dependent on the structure during the RSIE digestion treatment. Inulin based samples such as Raftiline HP and Inulin Orafti GR exhibited the lowest changes in their composition due to the resistance of these substrates to intestinal enzymes. A minimum increase of fructose was observed in Raftiline HP possibly produced by the hydrolysis of high M_w inulin species and no bigger structures (DP < 4) were detected. Regarding Inulin Orafti GR sample, slight degradations, but not significant, in the high M_w structures such as nystose (24 to 19.5 mg nystose per g of sample) was registered after the digestion process (Table 2), and increases in the trisaccharide fraction were observed. Sucrose was the most digested structure causing important increases in fructose content. A similar trend was observed by Ferreira-Lazarte *et al.* (2017)[14] after the digestion of FOS with RSIE exhibiting the tetrasaccharide structure the highest degradation (40%). The trisaccharide also increased, most likely, due to degradation of the tetrasaccharide. These changes are in line with the low inulinase activity measured in this extract (Table 1).

Regarding Raftilose P95, both tetrasaccharides detected showed slight but not significant degradations, being inulotetraose more hydrolyzed than nystose. A consequent increase in the corresponding trisaccharide (inulotriose) was observed after 120 min digestion, probably due to the degradation of the former. Moreover, the presence of higher DP compounds in the sample could also produce tri- and tetrasaccharides during the digestion treatment.[29] Increases in smaller structures such as disaccharides (inulobiose) and monosaccharides (fructose) were also observed due to the hydrolysis of the biggest compounds.

These results underline the relevance of the higher M_w composition in terms of digestibility.[16,36] Higher hydrolysis in Inulin Orafti GR was observed in the tetrasaccharide fraction after 180 min of digestion, supporting the data obtained in the *in vivo* and *in vitro* studies by Ferreira-Lazarte *et al.* (2017)[14] and Molis *et al.* (1996),[37] resulting in 12% and 11% of total digestion, respectively. In the case of Raftilose P95, a not significant decrease of tri- and tetrasaccharides was observed: hydrolysis being higher in the case of the linkage β(2 → 1) between fructose monomers (inulotriose and inulotetraose of Raftilose P95), when glucose is not present in the structure ending compared to sucrose oligosaccharides (kestose and nystose of Inulin Orafti GR) (Table 2). This could suggest the lower resistance of the β(2 → 1) bonds to the action of the digestive enzymes.[14]

With respect to oligosaccharides from galactose, chromatographic profiles by GC-FID of AlphaGOS P undigested and after digestion with RSIE are shown in Fig. 2. A decrease of verbascotetraose and manninotriose was observed (peaks 4 and 5) and, consequently, melibiose and galactose contents were increased after 180 min of digestion due to the degradation of the structures with higher M_w (Table 2). However, decreases in the melibiose levels were detected when a standard of only melibiose was digested, showing the highest hydrolysis values (67.7%) after 180 min of digestion. This degradation is in accordance with the considerable previous melibiase activity detected in the enzymatic extract, thus suggesting that the

Table 2 Carbohydrate evolution during the small intestinal digestion with Rat Small Intestine Extract (RSIE) at 37 °C, pH 6.8, determined by GC-FID analysis (mg g^{-1} of sample)

Digestion time (min)	Monosaccharides		Disaccharides			Trisaccharides			Tetrasaccharides			
	Fructose	Galactose	Sucrose	Inulobiose	Melibiose[a]	Kestose	Inulotriose	Maninotriose[a]	Nystose	Inulotetraose	Verbascotetraose[a]	Total OS[a,b]
Raftiline HP												
0	0.0 ± 0.0	—	—	—	—	—	—	—	—	—	—	—
60	20.2 ± 1.8	—	—	—	—	—	—	—	—	—	—	—
120	32.0 ± 1.2	—	—	—	—	—	—	—	—	—	—	—
180	44.1 ± 4.5	—	—	—	—	—	—	—	—	—	—	—
Inulin Orafti GR												
0	0.0 ± 0.0	—	42.5 ± 1.8	—	—	20.1 ± 0.5	—	—	24.0 ± 1.7	—	—	44.0 ± 1.0
60	39.7 ± 3.0	—	17.6 ± 1.0	—	—	31.7 ± 2.2	—	—	20.0 ± 1.6	—	—	51.7 ± 1.9
120	56.5 ± 2.5	—	12.1 ± 3.0	—	—	31.6 ± 1.3	—	—	19.8 ± 1.4	—	—	51.4 ± 1.4
180	66.1 ± 3.7	—	10.1 ± 0.2	—	—	26.2 ± 1.8	—	—	19.5 ± 1.2	—	—	45.7 ± 1.5
Raftilose P95												
0	45.6 ± 1.7	—	—	49.1 ± 4.5	—	—	199.6 ± 3.0	—	34.8 ± 2.2	121.0 ± 5.4	—	404.5 ± 3.8
60	81.6 ± 8.2	—	—	70.9 ± 6.8	—	—	226.2 ± 7.6	—	27.5 ± 1.7	98.8 ± 5.6	—	423.4 ± 5.4
120	85.5 ± 5.3	—	—	72.8 ± 4.7	—	—	215.7 ± 7.8	—	26.7 ± 1.6	97.3 ± 15.0	—	412.6 ± 7.3
180	117.6 ± 7.4	—	—	72.2 ± 2.0	—	—	172.3 ± 9.7	—	29.6 ± 0.9	100.6 ± 8.2	—	374.7 ± 5.2
AlphaGOS P												
0	—	0.0 ± 0.0	—	—	37.2 ± 0.2	—	—	538.4 ± 15.0 *(0%)*	—	—	377.6 ± 11.0 *(0%)*	953.2 ± 8.7 *(0%)*
60	—	158.2 ± 3.1	—	—	69.9 ± 1.3	—	—	338.9 ± 1.7 *(37.1%)*	—	—	150.1 ± 5.1 *(60.2%)*	558.9 ± 2.7 *(41.4%)*
120	—	213.3 ± 3.8	—	—	75.7 ± 2.6	—	—	275.5 ± 8.1 *(48.8%)*	—	—γ	110.2 ± 7.3 *(70.8%)*	461.4 ± 6.0 *(51.6%)*
180	—	246.0 ± 5.9	—	—	80.9 ± 6.9	—	—	215.7 ± 15.4 *(59.9%)*	—	—	73.4 ± 2.5 *(80.6%)*	370.0 ± 8.3 *(61.2%)*
Melibiose												
0	—	0.0 ± 0.0	—	—	1013.6 ± 32.0 *(0%)*	—	—	—	—	—	—	—
60	—	158.2 ± 4.6	—	—	492.8 ± 19.8 *(51.3%)*	—	—	—	—	—	—	—
120	—	231.6 ± 20.7	—	—	403.7 ± 11.0 *(60.2%)*	—	—	—	—	—	—	—
180	—	280.8 ± 6.0	—	—	327.3 ± 14.7 *(67.7%)*	—	—	—	—	—	—	—

Data are expressed as the mean ± SD (n = 4). [a] Hydrolysis degree (%) of isolated melibiose, maninotriose, verbascotetraose and total OS of AlphaGOS P are indicated in parentheses. [b] Total oligosaccharides was calculated by the sum of di-, tri- and tetrasaccharides of each carbohydrate.

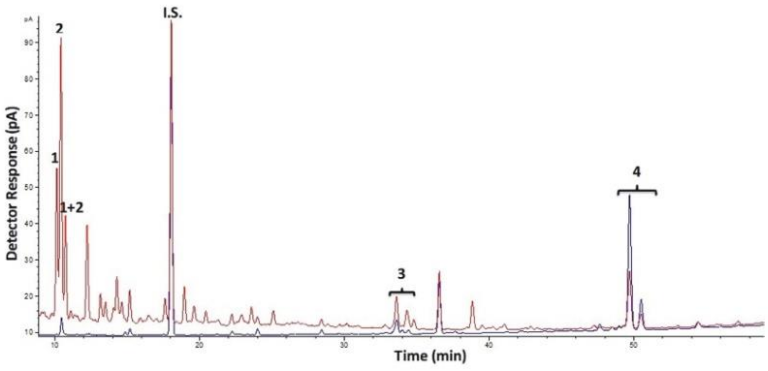

Fig. 2 Chromatographic profiles obtained by GC-FID of TMSO derivatives of oligosaccharides present in AlphaGOS P before (blue) and after 180 min of small intestinal digestion with RSIE (red). Peaks: 1. Galactose, 2: glucose, i.s.: internal standard, 3: melibiose, 4: maninotriose, 5: verbascotetraose.

intestinal enzymes probably are more prone to hydrolyze higher M_w structures present in the sample (manninotriose and verbascotetraose) rather than the disaccharide.

Increases in galactose levels also suggest that linkages between galactose monomers are being broken by digestive enzymes, similar to the degradation of β-GOS derived from lactose and lactulose observed during small intestinal digestion in previous works.[14,16,36,38,39] Beneficial effect of the α-GOS on the modulation of the intestinal microbiota is well-known.[40,41] Nevertheless, there is not enough information about their digestibility, even the expert scientific panel from the European Food Safety Authority (EFSA) claims that the α-GOS are non-digestible carbohydrates.[42] Considering the sum of total oligosaccharides of AlphaGOS P (manninotriose and verbascotetraose) the hydrolysis was considerably high (61.2%) (Table 2), despite the lack of pancreatic α-galactosidase in mammals.[43] However, Ferreira-Lazarte *et al.* (2019)[16] showed meaningful hydrolysis degree of prebiotic β-GOS (53% for linkages β(1 → 3)) using brush border membrane vesicles of small intestine of pig. A possible explanation for this fact could be the promiscuous multienzymatic complexes in the rat small intestine extract.[12] Carbohydrases of the small intestine, such as α-amylase, hydrolyze large starch structures, whereas complete digestion is done by the mucosal α-glucosidases.[44,45] In this sense, mucosal maltase-glucoamylase and sucrase-isomaltase complexes could hydrolyze to α(1 → 6) bonds between the monomers of both AlphaGOS P and melibiose.[20,21,46] These enzymatic structures could also have more versatility in terms of hydrolytic activity, as was showed elsewhere.[16,47] To the best of our knowledge, these data are the first evidence about digestibility of α-GOS with small intestine enzymes.

Some *in vivo* studies with rats have demonstrated a partial digestibility of prebiotic carbohydrates, showing a considerable high hydrolysis rate of β-GOS obtained from lactose and lactulose.[36,48] In the same way, an *in vitro* study with RSIE reported a hydrolysis degree of 12% of a mixture of FOS after 120 min of digestion.[14] These reported data are consistent with this work, highlighting the key role of the mammalian intestinal enzymes on the digestibility of carbohydrates.

4. Conclusions

Limitations of traditional digestibility methods of carbohydrates have been shown in several works.[12,13] Therefore, results obtained in this work confirmed the usefulness and effectiveness of the use of a RSIE to evaluate the digestion of polysaccharides. Moreover, similarities between small intestinal enzymes of rat and human emphasized the viability of this extract.[49] Raftiline HP, which is mainly constituted by inulin, showed the highest resistance to the gastrointestinal enzymes, with only a slight increase of fructose. Inulin Orafti GR also showed high resistance, with a small hydrolysis of tetrasaccharides, followed by Raftilose P95, thus supporting the role of these substrates as prebiotic compounds. Finally, AlphaGOS P and melibiose showed a considerable high hydrolysis degree (61.2 and 67.7%, respectively), remarking the effect of the chemical structure (M_w and type of linkage) of prebiotic oligosaccharides with respect to their resistance to digestibility. According to the obtained results, mucosal enzymes complexes have versatile hydrolytic activities and contribute to the digestion of different types of functional fiber which is belief to reach intact the distal colon to be fermented by the microbiota exerting its beneficial effects. Therefore, although more studies are required, including *in vivo* analysis, the results obtained underline the need to use specific methods for carbohydrates based on small intestinal extract of mammals, to test the resistance of these compounds to digestion.

In general, the well-known prebiotic activity of these fibers is aligned with their partial digestibility, since not all the carbohydrate fraction is digested. In consequence, it is important to highlight that not all prebiotic carbohydrates are non-digestible and can be partially digested, still exerting the beneficial effect in the large intestine, which, therefore, warrants a revision of the current assumption of non-digestibility of prebiotic carbohydrates, as recently was suggested by Hernandez-Hernandez (2019).[50]

Abbreviations used

DP	Degree of polymerization
FOS	Fructooligosaccharides
GC-FID	Gas chromatography with flame ionization detector
GOS	Galactooligosaccharides
HP	High performance
HPSEC-ELSD	High performance size exclusion cromatography with an evaporative light scattering detector
M_w	Molecular weight
NDOs	Non-digestible oligosaccharides
RDA	Recommended daily allowance
RSIE	Rat small intestine extract
TMSO	Trimethylsilylated oximes

Conflicts of interest

There are no conflicts to declare.

Acknowledgements

Authors acknowledge the finance of this work by the Spanish Ministry of Economy, Industry and Competitiveness (Project AGL2017-84614-C2-1-R) and the Spanish Ministry of Science, Innovation and Universities (Project RTI2018-101273-J-I00).

References

1 M. Van Hul and P. D. Cani, Targeting Carbohydrates and Polyphenols for a Healthy Microbiome and Healthy Weight, *Curr. Nutr. Rep.*, 2019, **8**, 307–316.
2 G. A. Soliman, Dietary Fiber, Atherosclerosis, and Cardiovascular Disease, *Nutrients*, 2019, **11**, 1155.
3 P. C. Champe and R. A. Harvey, *Biochemistry (Lippincott's illustrated reviews)*, Lippincott, 1994.
4 X. Qi, F. H. Al-Ghazzewi and R. F. Tester, Dietary Fiber, Gastric Emptying, and Carbohydrate Digestion: A Mini-Review, *Starch/Staerke*, 2018, **70**, 1700346.
5 A. Abdul-Hamid and S. L. Yu, Functional properties of dietary fibre prepared from defatted rice bran, *Food Chem.*, 2000, **68**, 15–19.
6 P. D. Cani and B. F. Jordan, Gut microbiota-mediated inflammation in obesity: a link with gastrointestinal cancer, *Nat. Rev. Gastroenterol. Hepatol.*, 2018, **15**, 671–682.
7 E. S. Chambers, T. Preston, G. Frost and D. J. Morrison, Role of gut Microbiota-Generated short-chain fatty acids in metabolic and cardiovascular health, *Curr. Nutr. Rep.*, 2018, **7**, 198–206.
8 P. Louis and H. J. Flint, Formation of propionate and butyrate by the human colonic microbiota, *Environ. Microbiol.*, 2017, **19**, 29–41.
9 A. Brodkorb, L. Egger, M. Alminger, P. Alvito, R. Assunção, S. Ballance, T. Bohn, C. Bourlieu-Lacanal, R. Boutrou, F. Carriere, A. Clemente, M. Corredig, D. Dupont, C. Dufour, C. Edwards, M. Golding, S. Karakaya, B. Kirkhus, S. Le Feunteun, U. Lesmes, A. Macierzanka, A. R. Mackie, C. Martins, S. Marze, D. J. McClements, O. Ménard, M. Minekus, R. Portman, C. N. Santos, I. Souchon, R. P. Singh, G. E. Vegarud, M. S. J. Wickhman, W. Weitschies and I. Recio, INFOGEST static in vitro simulation of gastrointestinal food digestion, *Nat. Protoc.*, 2019, **14**, 991–1014.
10 B. V. McCleary, J. W. De Vries, J. I. Rader, G. Cohen, L. Prosky, D. C. Mugford, M. Champ and K. Okuma, Determination of total dietary fiber (CODEX definition) by enzymatic-gravimetric method and liquid chromatography: Collaborative study, *J. AOAC Int.*, 2010, **93**, 221–233.
11 B. V. McCleary, N. Sloane and A. Draga, Determination of total dietary fibre and available carbohydrates: A rapid integrated procedure that simulates in vivo digestion, *Starch/Staerke*, 2015, **67**, 860–883.
12 A. Ferreira-Lazarte, *In vitro digestibility and fermentability of selected prebiotics and functional carbohydrates with prebiotic potential*, PhD Thesis, Universidad Autónoma de Madrid, 2019.
13 K. Tanabe, S. Nakamura and T. Oku, Inaccuracy of AOAC method 2009.01 with amyloglucosidase for measuring non-digestible oligosaccharides and proposal for an improvement of the method, *Food Chem.*, 2014, **151**, 539–546.
14 A. Ferreira-Lazarte, A. Olano, M. Villamiel and F. J. Moreno, Assessment of in vitro digestibility of dietary carbohydrates using rat small intestinal extract, *J. Agric. Food Chem.*, 2017, **65**, 8046–8053.
15 A. Ferreira-Lazarte, A. Montilla, A. I. Mulet-Cabero, N. Rigby, A. Olano, A. Mackie and M. Villamiel, Study on the digestion of milk with prebiotic carbohydrates in a simulated gastrointestinal model, *J. Funct. Foods*, 2017, **33**, 149–154.
16 A. Ferreira-Lazarte, P. Gallego-Lobillo, F. J. Moreno, M. Villamiel and O. Hernandez-Hernandez, In vitro digestibility of galactooligosaccharides: effect of the structural features on their intestinal degradation, *J. Agric. Food Chem.*, 2019, **67**, 4662–4670.
17 N. Muñoz-Almagro, F. Rico-Rodriguez, M. Villamiel and A. Montilla, Pectin characterisation using size exclusion chromatography: A comparison of ELS and RI detection, *Food Chem.*, 2018, **252**, 271–276.

18 M. M. Bradford, A rapid and sensitive method for the quantitation of microgram quantities of protein utilizing the principle of protein-dye binding, *Anal. Biochem.*, 1976, **72**, 248–254.
19 K. M. Brobst and C. E. Lott Jr., Determination of some components in corn syrup by gas-liquid chromatography of the trimethylsilyl derivatives, *Cereal Chem.*, 1966, **43**, 35–43.
20 J. Feher, *Digestion and absorption of the macronutrients, in Quantitative human physiology*, Academic Press, 2012, 731–743.
21 D. Hooton, R. Lentle, J. Monro, M. Wickham and R. Simpson, The secretion and action of brush border enzymes in the mammalian small intestine, in *Reviews of physiology, biochemistry and pharmacology*, Springer Cham, 2015, 168, 59–11.
22 R. A. Rastall, Functional oligosaccharides: application and manufacture, *Annu. Rev. Food Sci. Technol.*, 2010, **1**, 305–339.
23 A. Franck, Technological functionality of inulin and oligofructose, *Br. J. Nutr.*, 2002, **87**, S287–S291.
24 M. A. Mensink, H. W. Frijlink, K. van der Voort Maarschalk and W. L. Hinrichs, Inulin, a flexible oligosaccharide I: Review of its physicochemical characteristics, *Carbohydr. Polym.*, 2015, **130**, 405–419.
25 L. A. Schaller-Povolny, D. E. Smith and T. P. Labuza, Effect of water content and molecular weight on the moisture isotherms and glass transition properties of inulin, *Int. J. Food Prop.*, 2000, **3**, 173–192.
26 Á. Ávila-Fernández, E. Cuevas-Juárez, M. E. Rodríguez-Alegría, C. Olvera and A. López-Munguía, Functional characterization of a novel β-fructofuranosidase from Bifidobacterium longum, subsp. infantis ATCC 15697 on structurally diverse fructans, *J. Appl. Microbiol.*, 2016, **121**, 263–276.
27 *Product Sheet DOC.A4-03/001 Orafti ® GR, Beneo-Orafti S.A*, Tienen, Belgium, 2016.
28 K. H. Han, H. Tsuchihira, Y. Nakamura, K. I. Shimada, K. Ohba, T. Aritsuka, H. Uchino, H. Kikuchi and M. Fukushima, Inulin-type fructans with different degrees of polymerization improve lipid metabolism but not glucose metabolism in rats fed a high-fat diet under energy restriction, *Dig. Dis. Sci.*, 2013, **58**, 2177–2186.
29 C. Nobre, S. C. Sousa, S. P. Silva, A. C. Pinheiro, E. Coelho, A. A. Vicente, A. M. P. Gomes, M. A. Coimbra, J. A. Teixeira and L. R. Rodrigues, In vitro digestibility and fermentability of fructo-oligosaccharides produced by Aspergillus ibericus, *J. Funct. Foods*, 2018, **46**, 278–287.
30 C. Blecker, C. Fougnies, J. C. Van Herck, J. P. Chevalier and M. Paquot, Kinetic study of the acid hydrolysis of various oligofructose samples, *J. Agric. Food Chem.*, 2003, **50**, 1602–1607.
31 A. Pyner, H. Nyambe-Silavwe and G. Williamson, Inhibition of human and rat sucrase and maltase activities to assess antiglycemic potential: Optimization of the assay using acarbose and polyphenols, *J. Agric. Food Chem.*, 2017, **65**, 8643–8651.
32 G. Kelly, Inulin-type prebiotics–a review: part 1, *Altern. Med. Rev.*, 2008, **13**, 315–329.
33 A. Montilla, J. Van de Lagemaat, A. Olano and M. D. Del Castillo, Determination of oligosaccharides by conventional high-resolution gas chromatography, *Chromatographia*, 2006, **63**, 453–458.
34 N. Moussou, M. Corzo-Martínez, M. L. Sanz, F. Zaidi, A. Montilla and M. Villamiel, Assessment of Maillard reaction evolution, prebiotic carbohydrates, antioxidant activity and α-amylase inhibition in pulse flours, *J. Food Sci. Technol.*, 2017, **54**, 890–900.
35 A. Montilla, A. Olano, C. Martínez-Villaluenga and N. Corzo, Study of influential factors on oligosaccharide formation by fructosyltransferase activity during stachyose hydrolysis by Pectinex Ultra SP-L, *J. Agric. Food Chem.*, 2011, **59**, 10705–10711.
36 O. Hernández-Hernández, M. C. Marín-Manzano, L. A. Rubio, F. J. Moreno, M. L. Sanz and A. Clemente, Monomer and linkage type of galacto-oligosaccharides affect their resistance to ileal digestion and prebiotic properties in rats, *J. Nutr.*, 2012, **142**, 1232–1239.
37 C. Molis, B. Flourie, F. Ouarne, M. F. Gailing, S. Lartigue, A. Guibert, F. Bornet and J. P. Galmiche, Digestion, excretion, and energy value of fructooligosaccharides in healthy humans, *Am. J. Clin. Nutr.*, 1996, **64**, 324–328.
38 L. C. Julio-Gonzalez, O. Hernandez-Hernandez, F. J. Moreno, A. Olano, M. L. Jimeno and N. Corzo, Trans-β-galactosidase activity of pig enzymes embedded in the small intestinal brush border membrane vesicles, *Sci. Rep.*, 2019, **9**, 960.
39 Y. Shi, J. Liu, Q. Yan, X. You, S. Yang and Z. Jiang, In vitro digestibility and prebiotic potential of curdlan (1→3)-β-D-glucan oligosaccharides in Lactobacillus species, *Carbohydr. Polym.*, 2018, **188**, 17–26.
40 Q. Chen, M. Liu, P. Zhang, S. Fan, J. Huang, S. Yu, C. Zhang and H. Li, Fucoidan and galactooligosaccharides ameliorate high-fat diet–induced dyslipidemia in rats by modulating the gut microbiota and bile acid metabolism, *Nutrition*, 2019, **65**, 50–59.
41 S. Yousefi, S. H. Hoseinifar, H. Paknejad and A. Hajimoradloo, The effects of dietary supplement of galactooligosaccharide on innate immunity, immune related genes expression and growth performance in zebrafish (Danio rerio), *Fish Shellfish Immunol.*, 2018, **73**, 192–196.
42 EFSA Panel on Dietetic Products, Nutrition and Allergies (NDA), Scientific Opinion on the substantiation of a health claim related to AlphaGOS® and a reduction of post-prandial glycaemic responses pursuant to Article 13 (5) of Regulation (EC) No 1924/2006, *EFSA J.*, 2014, **12**, 3838.
43 J. G. LeBlanc, M. S. Garro, A. Silvestroni, C. Connes, J. C. Piard, F. Sesma and G. Savoy de Giori, Reduction of α-galactooligosaccharides in soyamilk by Lactobacillus fermentum CRL 722: in vitro and in vivo evaluation of fermented soyamilk, *J. Appl. Microbiol.*, 2004, **97**, 876–881.
44 B. H. Lee and B. R. Hamaker, Number of branch points in α-limit dextrins impact glucose generation rates by mam-

malian mucosal α-glucosidases, *Carbohydr. Polym.*, 2017, **157**, 207–213.
45 H. Shin, D. H. Seo, J. Seo, L. M. Lamothe, S. H. Yoo and B. H. Lee, Optimization of in vitro carbohydrate digestion by mammalian mucosal α-glucosidases and its applications to hydrolyze the various sources of starches, *Food Hydrocolloids*, 2019, **87**, 470–476.
46 A. C. Dona, G. Pages, R. G. Gilbert and P. W. Kuchel, Digestion of starch: In vivo and in vitro kinetic models used to characterise oligosaccharide or glucose release, *Carbohydr. Polym.*, 2010, **80**, 599–617.
47 B. H. Lee, D. R. Rose, A. H. M. Lin, R. Quezada-Calvillo, B. L. Nichols and B. R. Hamaker, Contribution of the individual small intestinal α-glucosidases to digestion of unusual α-linked glycemic disaccharides, *J. Agric. Food Chem.*, 2016, **64**, 6487–6494.
48 E. Jantscher-Krenn, C. Marx and L. Bode, Human milk oligosaccharides are differentially metabolised in neonatal rats, *Br. J. Nutr.*, 2013, **110**, 640–650.
49 T. Oku, K. Tanabe, S. Ogawa, N. Sadamori and S. Nakamura, Similarity of hydrolyzing activity of human and rat small intestinal disaccharidases, *Clin. Exp. Grastroenterol.*, 2011, **4**, 155–161.
50 O. Hernandez-Hernandez, In vitro Gastrointestinal Models for Prebiotic Carbohydrates: A Critical Review, *Curr. Pharm. Des.*, 2019, **25**, 3478–3483.

Food Research International 140 (2021) 110054

Contents lists available at ScienceDirect

Food Research International

journal homepage: www.elsevier.com/locate/foodres

In vitro digestion of polysaccharides: InfoGest protocol and use of small intestinal extract from rat

Pablo Gallego-Lobillo , Alvaro Ferreira-Lazarte , Oswaldo Hernández-Hernández , Mar Villamiel *

Institute of Food Science Research, CIAL (CSIC-UAM), C/Nicolás Cabrera, 9, Campus de la Universidad Autónoma de Madrid, 28049 Madrid, Spain

ARTICLE INFO

Keywords:
Prebiotics
Pectin
Starch
Dextran
Brush border enzymes
In vitro digestion method
Hydrolysis
InfoGest

ABSTRACT

Starch, dextran, pectin and modified citrus pectin were subjected to intestinal digestion following InfoGest protocol and a rat small intestine extract (RSIE) treatment. Gastric stage did not show any modification in the structure of the carbohydrates, except for modified pectin. Regarding intestinal phases, starch was hydrolyzed by different ways, resulting in a complementary behavior between InfoGest and RSIE. Contrarily, digestion of dextran was only observed using RSIE. Similar situation occurred in the case of pectins with RSIE, obtaining a partial hydrolysis, especially in the modified citrus pectin. However, citrus pectin was the less prone to hydrolysis by enzymes. The results demonstrated that InfoGest method underestimates the significance of the carbohydrates hydrolysis at the small intestine, thus indicating that RSIE is a very reliable and useful method for a more realistic study of polysaccharides digestion.

1. Introduction

Polysaccharides compose a wide group of carbohydrates that play different roles in the human body such as the storage of energy and the structural function in the cell, and these functions are determined by their digestibility in the small intestine (Hu, Nie, & Xie, 2018). Thus, polysaccharides can be considered as digestible or non-digestible depending on chemical structure as the most relevant factor (Li et al., 2020; Zhu et al., 2019). Among dietary polysaccharides, starch is the only one which can be hydrolyzed without the intervention of the intestinal microbiota (Cockburn & Koropatkin, 2016). Others, such as pectin could resist intestinal digestion and reach the colon to be fermented by the colonic bacteria, modulating intestinal metabolism. This effect on the microbiota is one of the reasons for that the interest toward pectin has aroused a great increase in recent years (Ferreira-Lazarte, Kachrimanidou, Villamiel, Rastall, & Moreno, 2018; Ferreira-Lazarte, Moreno, et al., 2019a; Holck, Hotchkiss, Meyer, Mikkelsen, & Rastall, 2014). In this context, the majority of research has been focused on the benefits of pectin as dietary fiber and modulator of the microbiota and limited information is available on its digestion. Recently, digestion of pectin has been studied in a complex dynamic gastrointestinal simulator (simgi®) (Ferreira-Lazarte, Moreno, et al., 2019a). With this method, based on the use of digestive fluids including pancreatin, hardly any changes were observed along the gastric and small intestinal phases, resulting in a hydrolysis degree of 12%.

Majority of the digestibility methods are focused on proteins or starch allowing to distinguish between resistant and rapidly absorbable starch (K. Englyst et al., 2018; Han, Xie, Wu, & Wu, 2018). The most common and accepted *in vitro* method for digestion is InfoGest protocol, developed in 2014 (Brodkorb et al., 2019; Minekus et al., 2014), and it is based on the use of simulated fluids of gastrointestinal enzymes. The Association of Official Analytical Chemist (AOAC) carried out another digestibility method for non-digestible carbohydrates, such as dietary fiber (McCleary et al., 2010). Nevertheless, the use of isolated enzymes of both methods does not reflect the complexity of the digestion of carbohydrates at the small intestine (Ferreira-Lazarte, Moreno, & Villamiel, 2020).

Beyond starch hydrolysis, there is a lack of standardized methods for carbohydrates digestion despite of their importance in human health (Hernandez-Hernández, 2019; Hernandez-Hernandez, Olano, Rastall, &

Abbreviations: CP, Citrus Pectin; DP, Degree of polymerization; GOS, Galactooligosaccharides; GalA, Galacturonic Acid; HG, Homogalacturonan; MCP, Modified Citrus Pectin; Mw, Molecular weight; RSIE, Rat Small Intestine Extract.

* Corresponding author at: Institute of Food Science Research (CIAL) (CSIC-UAM), C/Nicolás Cabrera 9, Campus de la Universidad Autónoma de Madrid, E-28049 Madrid, Spain.

E-mail addresses: p.gallego.lobillo@csic.es (P. Gallego-Lobillo), alvaro.ferreira@csic.es (A. Ferreira-Lazarte), o.hernandez@csic.es (O. Hernández-Hernández), m.villamiel@csic.es (M. Villamiel).

https://doi.org/10.1016/j.foodres.2020.110054
Received 13 July 2020; Received in revised form 16 December 2020; Accepted 17 December 2020

Moreno, 2019). Specifically, in the case of prebiotic carbohydrates is assumed that they are completely non-digestible (Hernandez-Hernández, 2019). However, it has been described that some well-known prebiotic carbohydrates are partially degraded during small intestinal digestion (Ferreira-Lazarte et al., 2020; Hernández-Hernández et al., 2012).

Ferreira-Lazarte, Olano, et al. (2017a) proposed a useful and simple *in vitro* method of digestibility using a rat small intestine extract (RSIE). A meaningful hydrolysis of β-galactooligosaccharides, previously considered as non-digestible with a degree of polymerization (DP) up to 4 was observed, similar to the *in vivo* results obtained by Hernández-Hernández et al. (2012). This GOS hydrolysis was not observed when InfoGest method was applied (Ferreira-Lazarte, Montilla, et al., 2017b). This could be ascribed to the lack of the disaccharidases present in the enterocyte brush border membranes in the InfoGest methodology (Hernandez-Hernández, 2019; Hooton, Lentle, Monro, Wickham, & Simpson, 2015). Indeed, it has been recently reported the hydrolysis of different kinds of dietary fiber such as non-fructosylated α-GOS and different types of inulin structures when RSIE was used (Gallego-Lobillo, Ferreira-Lazarte, Hernández-Hernández, Montilla, & Villamiel, 2020).

The reported data on carbohydrates digestion emphasized the advantages of using mammal small intestinal digestive enzymes, which permit reducing uncertainties about the behavior of carbohydrates during the gastrointestinal process, and about the effect of carbohydrate chemical structure and the type of linkage on their digestibility (Ferreira-Lazarte, Olano, et al., 2017a; Hernández-Hernández et al., 2012).

To the best of our knowledge, no investigation has been conducted on the impact of InfoGest protocol and subsequent application of RSIE for the evaluation of dietary polysaccharides. Thus, the aim of this work was to study the *in vitro* digestibility of polysaccharides by combining the standardized InfoGest protocol with the proposed digestion model using rat small intestine extract. The viability of these methods has been proven with starch and dextran as glucose-based polysaccharides, and pectin and modified citrus pectin, as pectic polysaccharides.

2. Materials and methods

2.1. Chemical and standards

The following analytical standards were supplied by Sigma-Aldrich (St. Louis, MO): D-galactose (Gal), D-glucose (Glc), D-arabinose (Ara), galacturonic acid (GalA), maltose (α-D-Glc-(1 → 4)-D-Glc), sucrose (β-D-Fru-(2 → 1)-α-D-Glc), maltotriose (α-D-Glc-(1 → 4)-α-D-Glc-(1 → 4)-D-Glc), phenyl-β-D-glucoside, as well as the intestinal acetone powders from rat (Rat Small Intestine Extract, RSIE). D-xylose (Xyl), L-rhamnose (Rha) and D-mannose (Man) standards were purchased from PanReac AppliChem (Darmstadt, Germany). Reagents for Bradford method were obtained from Bio-Rad Laboratory (Gmbh, Munich, Germany).

2.2. Polysaccharides studied

Two glucose-based polysaccharides were evaluated in this work: soluble starch and dextran from *Leuconostoc mesenteroides*, obtained from Sigma Aldrich. In addition, two commercial samples of pectin were also tested: commercial citrus pectin (CP) (Ceampectin®, ESS-4400), was supplied by CEAMSA (Porriño, Pontevedra, Spain); and a commercial pH-modified citrus pectin (MCP) was kindly provided by eco-Nugenics (Santa Rosa, CA). Monomeric composition of CP was (percentages of total carbohydrates): traces of xylose, 6.7% arabinose, 4.4% rhamnose, 22.5% galactose, traces of mannose, 2.4% glucose and 64.0% galacturonic acid; and average Mw was 472 kDa (Muñoz-Labrador, Moreno, Villamiel, & Montilla, 2018). On the other hand, monosaccharides content of MCP were (percentages of total carbohydrates): traces of xylose, 3.9% arabinose, 2.3% rhamnose, 8.9% galactose, traces of mannose, 1.0% glucose and 83.9% galacturonic acid; and average Mw was 3.1–0.7 kDa.

2.3. Characterization of rat small intestine extract

2.3.1. Protein content

RSIE protein content was determined through the Bradford method (Bradford, 1976). The absorbance was measured at 595 nm and the standard used was bovine serum albumin.

2.3.2. Enzymatic activities

RSIE maltase, sucrase and pectinase activities (U*g protein^{-1}) were evaluated by duplicate using GC-FID, according to the previously described methodology (Gallego-Lobillo et al., 2020). Incubation of RSIE (40 mg*mL^{-1}) with individual solutions of maltose, sucrose and citrus pectin in distilled water at pH 6.8 was carried out in an orbital Thermomixer comfort (Eppendorf®) at 37 °C for 0, 60, 120 and 180 min and then, heated in boiling water during 5 min to stop the reaction.

Evolution of the carbohydrate content was analyzed through GC-FID, as described below, in order to calculate the specific enzymatic activity.

2.4. In vitro digestions

Fig. 1 shows the scheme followed in this work. The InfoGest protocol was used according to the literature (Brodkorb et al., 2019). Digestions with RSIE were carried out following the method of Ferreira-Lazarte, Olano, et al. (2017a).

2.4.1. Gastrointestinal digestion by InfoGest

The model and the simulated fluids preparation for the gastric and intestinal phases were based on the standardized InfoGest protocol reported by Brodkorb et al. (2019).

First, solutions of each polysaccharide with a concentration of 30 mg*mL^{-1} (3%, w/w) in distilled water were prepared. For the stomach stage, solutions were mixed with an equal volume of simulated gastric fluid (SGF). Then, 2 mL of a porcine pepsin solution were added to obtain 2000 U*mL^{-1}. Then, 5 μL of $CaCl_2$ 0.3 M and the pH was adjusted to 3.0. The mixture was incubated in an orbital Thermomixer at 37 °C with continuous agitation. Samples were collected at 0 and 2 h, and the reaction was stopped by heating in boiling water for 5 min.

For the intestinal stage, solutions of the end of the gastric phase (Gastric Phase 2 h) of each carbohydrate were mixed with an equal volume of simulated intestinal fluid (SIF). Porcine pancreatin and bile salts were added to the digestion in order to achieve 100 U*mL^{-1} (trypsin activity) and 10 mM, respectively. Then, 40 μL of $CaCl_2$ 0.3 M were added and the pH was adjusted to 7.0. Digestions were carried out in an orbital Thermomixer at 37 °C with continuous agitation. Samples were taken at 0, 1 and 2 h of reaction, and inactivated in boiling water for 5 min. Samples of gastric and intestinal phases were analyzed by GC-FID.

2.4.2. Small intestinal digestion by RSIE

Samples of carbohydrates after Gastric Phase (2 h) and after 1 h of Intestinal Phase (InfoGest) (Fig. 1) were digested with RSIE according to the method of Ferreira-Lazarte, Olano, et al. (2017a) with minor changes, to evaluate the digestibility of digested samples with RSIE and with the combined methods (InfoGest + RSIE), respectively.

Firstly, a concentration of 0.5 mg*mL^{-1} of each carbohydrate was prepared and mixed with RSIE (40 mg*mL^{-1}). Reactions were performed in an orbital Thermomixer during 2 h at 37 °C and 750 rpm. Samples were collected at different times (0, 1 and 2 h for only RSIE digestion and after 1 h for InfoGest + RSIE digestion), stopping the digestion by heating. Analysis were carried out by GC-FID.

2.5. Assessment of digestion evolution by GC-FID

Gas chromatography coupled to a flame ionization detector (GC-FID) was used to analyze the evolution of polysaccharides in all digestion assays by means of the release of molecular species with lower

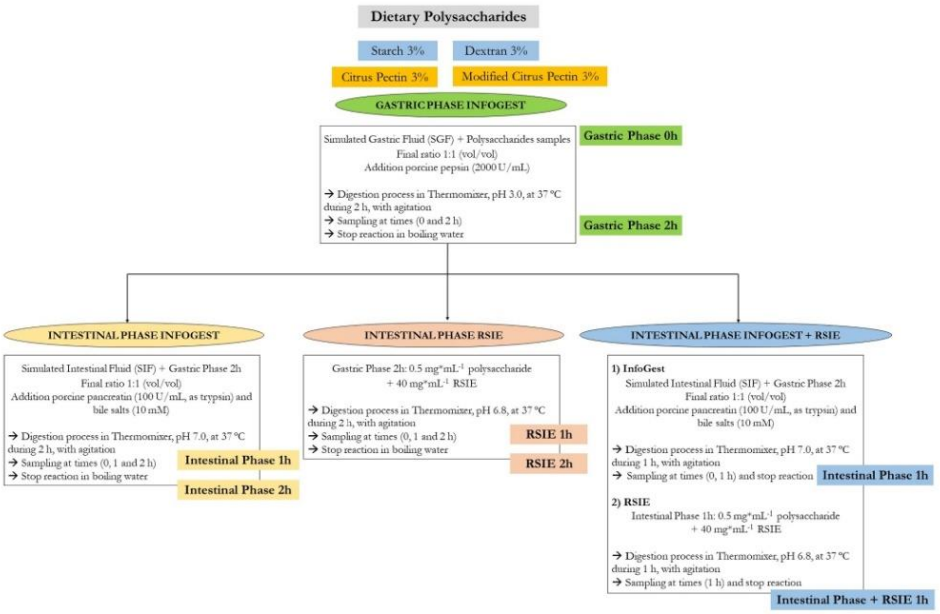

Fig. 1. Scheme of the digestion assays with InfoGest protocol and RSIE.

polymerization degree (monosaccharides and oligosaccharides). Firstly, a derivatization process to obtain trimethylsilylated oximes (TSMO) was done, according to Brobst and Lott (1966). For that, samples obtained after digestions were mixed with 400 μL of phenyl-β-D-glucoside (internal standard, 0.5 mg*mL^{-1}) and dried in a rotary evaporator (Büchi Labortechnik AG, Flawil, Switzerland). For the oxime formation, 300 μL of hydroxylamine chloride in pyridine (2.5%, w/v) were added, and the mixture was incubated at 70 °C during 30 min. Then, silylation was performed with the addition of 300 μL of hexamethyldisilazane (HDMS) and 30 μL of TFA and incubated at 50 °C for 30 min with agitation. Finally, TMSOs were centrifuged at 6,700 × *g* for 2 min, and the supernatants were injected into the GC-FID.

An Agilent Technologies 7820A gas chromatograph system was used for the analysis, equipped with a fused silica capillary column DB-5HT (5% phenyl methylpolysiloxane, 30 m × 0.25 mm × 0.1 μm, Agilent J&W Scientific, Folsom, CA, USA). Nitrogen was used as the carrier gas at 1 mL*min^{-1} of flow rate. Heat oven program started in 150 °C, and then, increased to 380 °C at a rate of 3 °C*min^{-1}. Injector and detector temperature was 280 °C and 385 °C, respectively. Samples were analyzed in split mode 1:20.

Quantification in the content of carbohydrates were done calculating the response factors of standards solutions of carbohydrates (xylose, arabinose, rhamnose, galactose, mannose, glucose, galacturonic acid, maltose and maltotriose) at known concentrations (0.005 to 2 mg*mL^{-1}). Data interpretation and integration were performed using Agilent ChemStation software (Washington, DE, USA).

2.6. Statistical analysis

All experiments were done in duplicate and two GC-FID analysis (n = 4). Statistical differences were analyzed using analysis of variance (ANOVA) and Scheffé's post hoc test, with the SPSS statistical package (Inc., Chicago, Il), considering significant values when $p \leq 0.05$.

3. Results and discussion

3.1. Enzymatic characterization of RSIE

Specific enzymatic activities of RSIE, measured under simulated physiological conditions (pH 6.8, 37 °C) are shown in Table 1. Maltase was found to be the major activity (126.6 U) with a value 9- and 160-fold higher as compared to sucrose and pectinase activities, respectively. The considerable difference between activities with respect to maltase is in agreement with previous studies using the same commercial extract (Ferreira-Lazarte, Olano, et al., 2017a; Ferreira-Lazarte, Gallego-Lobillo, et al., 2019b; Gallego-Lobillo et al., 2020; Oku, Tanabe, Ogawa, Sadamori, & Nakamura, 2011). Maltase activity, which is exerted by the maltase-glucoamylase and sucrase-isomaltase complexes present in the RSIE, is one of the main enzymes involved in the digestion of starch (Hooton et al., 2015; Whistler & Daniel, 2000). Sucrase activity (14.3 U) coming from the sucrase-isomaltase complex was slightly lower than the data obtained by Ferreira-Lazarte, Olano, et al. (2017a) and Gallego-

Table 1
Characterization of enzymatic activities in Rat Small Intestine Extract (RSIE).

Hydrolytic activity	Substrate	U*g protein^{-1}
Maltase	Maltose	126.6 ± 0.1[a]
Sucrase	Sucrose	14.1 ± 0.3[b]
Pectinase	Citrus pectin	0.8 ± 0.1[c]

Protein content of RSIE: 8.2 ± 0.5% (*w/w*).
Activities were calculated evaluating the content of monosaccharides by GC-FID:
[a] Release of glucose. [b] Release of fructose. [c] Release of galacturonic acid.
Data is expressed ± SD (n = 4).

Lobillo et al. (2020), probably, due to the variability among the different lot of intestinal extracts. Moreover, a low pectinase activity was also found in the RSIE (0.8 U), which can be explained by the resistance of this soluble fiber to digestion.

3.2. In vitro digestion assays

The effect of gastrointestinal digestion of four dietary polysaccharides (starch, dextran, CP and MCP) was evaluated using InfoGest and RSIE following the scheme indicated in Fig. 1.

Tables 2 and 3 indicate the quantitative evolution of the carbohydrate fraction in each polysaccharide analyzed during all the stages of the digestion process. Tables 2a and 2b are referred to the soluble starch and dextran, showing slight but no significant changes ($p \geq 0.05$) in the gastric digestion according to InfoGest protocol. Gastric juice contains hydrochloric acid and pepsin, with lack of carbohydrases (Feher, 2017). However, pepsin and acids can provoke alterations to the surface of the molecule of starch, as well as dextran, causing partial breakdown of the polysaccharide, with the consequent release of glucose (Fernandes, Madalena, Pinheiro, & Vicente, 2020; Pérez & Bertoft, 2010). This effect is not overly strong (Freitas, Le Feunteun, Panouillé, & Souchon, 2018).

Table 4 indicates the total hydrolysis degree of polysaccharides after each stage of digestion treatment. Low hydrolysis (1–2%) occurred during the gastric digestion of starch and dextran, which is in agreement

Table 2
Digestion of glucose-based polysaccharides. Evolution in the content of carbohydrates of starch and dextran via InfoGest protocol and RSIE, determined by GC-FID (mg*g of sample^{-1}).

		Glucose	Maltose	Maltotriose	Total CH
(a) Starch					
Gastric Phase InfoGest	0 h	18.3 ± 5.6^{a}	0.0 ± 0.0^{a}	0.0 ± 0.0^{a}	18.3 ± 5.6^{a}
	2 h	9.9 ± 3.6^{a}	0.0 ± 0.0^{a}	0.0 ± 0.0 ^{a}	9.9 ± 3.6^{a}
Intestinal Phase InfoGest	1 h	125.0 ± 4.7^{b}	325.5 ± 15.9^{b}	19.1 ± 1.1^{b}	469.6 ± 20.5^{b}
	2 h	178.5 ± 5.8^{c}	325.6 ± 22.1^{b}	45.4 ± 0.7^{c}	549.5 ± 27.7^{c}
Intestinal Phase RSIE	1 h	374.1 ± 20.3^{d}	0.0 ± 0.0^{a}	0.0 ± 0.0^{a}	374.1 ± 20.3^{d}
	2 h	584.7 ± 10.0^{e}	0.0 ± 0.0^{a}	0.0 ± 0.0^{a}	584.7 ± 10.0^{e}
Intestinal Phase InfoGest	1 h	125.0 ± 4.7^{b}	325.5 ± 15.9^{b}	19.1 ± 1.1^{b}	469.6 ± 20.5^{b}
Intestinal Phase InfoGest + RSIE	1 h	525.1 ± 15.0^{f}	0.0 ± 0.0^{a}	0.0 ± 0.0^{a}	525.1 ± 15.0^{c}
(b) Dextran					
Gastric Phase InfoGest	0h	7.6 ± 2.0^{a}	N.D.	N.D.	7.6 ± 2.0^{a}
	2h	10.8 ± 3.1^{a}	N.D.	N.D.	10.8 ± 3.1^{a}
Intestinal Phase InfoGest	1h	10.1 ± 0.1^{a}	N.D.	N.D.	10.1 ± 0.1^{a}
	2h	10.9 ± 0.6^{a}	N.D.	N.D.	10.9 ± 0.6^{a}
Intestinal Phase RSIE	1h	149.3 ± 8.0^{b}	N.D.	N.D.	149.3 ± 8.0^{b}
	2h	163.0 ± 10.6^{b}	N.D.	N.D.	163.0 ± 10.6^{b}
Intestinal Phase InfoGest	1h	10.1 ± 0.1^{a}	N.D.	N.D.	10.1 ± 0.1^{a}
Intestinal Phase InfoGest + RSIE	1h	205.9 ± 20.2^{c}	N.D.	N.D.	205.9 ± 20.2^{c}

Values are expressed as means as ± SD (n = 4). Total CH: Total carbohydrates (glucose + maltose + maltotriose). N.D.: Not detected.
$^{a-f}$Different letters indicate statistical differences between content of each column using ANOVA ($p \leq 0.05$).
LOD of Glc, Mal and Matotriose, respectively: 0.044, 0.043 and 0.059 mg.
LOQ of Glc, Mal and Maltotriose, respectively: 0.146, 0.144 and 0.195 mg.

Table 3
Digestion of pectic polysaccharides. Evolution in the content of carbohydrates of Citrus Pectin and Modified Citrus Pectin via InfoGest protocol and RSIE, determined by GC-FID (mg*g of sample^{-1}).

		Galactose	Galacturonic Acid	Total CH
(a) Citrus Pectin				
Gastric Phase InfoGest	0 h	0.0 ± 0.0^{a}	0.0 ± 0.0^{a}	0.0 ± 0.0^{a}
	2 h	0.7 ± 0.4^{a}	0.0 ± 0.0^{a}	0.7 ± 0.4^{a}
Intestinal Phase InfoGest	1 h	1.4 ± 0.1^{a}	0.0 ± 0.0^{a}	1.4 ± 0.1^{a}
	2 h	1.4 ± 0.1^{a}	0.0 ± 0.0^{a}	1.4 ± 0.1^{a}
Intestinal Phase RSIE	1 h	60.4 ± 4.1^{b}	43.9 ± 5.0^{b}	104.3 ± 6.5^{b}
	2 h	72.7 ± 5.5^{b}	56.4 ± 2.9^{b}	129.1 ± 6.3^{c}
Intestinal Phase InfoGest	1 h	1.4 ± 0.1^{a}	0.0 ± 0.0^{a}	1.4 ± 0.1^{a}
Intestinal Phase InfoGest + RSIE	1 h	148.2 ± 13.2^{c}	23.1 ± 3.2^{c}	172.3 ± 10.6^{d}
(b) Modified Citrus Pectin (MCP)				
Gastric Phase InfoGest	0h	2.2 ± 1.2^{a}	37.5 ± 4.1^{a}	39.7 ± 9.7^{a}
	2h	3.7 ± 1.7^{a}	86.6 ± 7.9^{b}	90.3 ± 10.2^{b}
Intestinal Phase InfoGest	1h	2.6 ± 0.1^{a}	103.9 ± 3.7^{c}	106.5 ± 3.6^{b}
	2h	3.0 ± 0.3^{a}	108.3 ± 5. 9^{c}	111.3 ± 5.9^{b}
Intestinal Phase RSIE	1h	53.4 ± 5.5^{b}	334.1 ± 7.8^{d}	387.5 ± 2.7^{c}
	2h	75.2 ± 7.0^{c}	341.1 ± 18.5^{d}	416.3 ± 7.5^{c}
Intestinal Phase InfoGest	1h	2.6 ± 0.1^{a}	103.9 ± 3.7^{c}	106.5 ± 3.6^{b}
Intestinal Phase InfoGest + RSIE	1h	81.6 ± 11.4^{c}	340.9 ± 29.1^{d}	422.5 ± 36.5^{c}

Values are expressed as means as ± SD (n = 4). Total CH: Total carbohydrates (galactose + galacturonic acid). N.D.: Not detected.
$^{a-d}$Different letters indicate statistical differences between content of each column using ANOVA ($p \leq 0.05$).
LOD of Gal and GalA, respectively: 0.038 and 0.032 mg.
LOQ of Gal and GalA, respectively: 0.126 and 0.106 mg.

Table 4
Total hydrolysis degree (%) of polysaccharides after digestion by treatment InfoGest protocol and RSIE.

		Starch	Dextran	Citrus Pectin	Modified Citrus Pectin
Gastric Phase InfoGest	0 h	1.8 ± 0.6^{a}	0.8 ± 0.2^{a}	0.0 ± 0.0^{a}	4.0 ± 0.9^{a}
	2 h	0.9 ± 0.3^{a}	1.1 ± 0.3^{a}	0.0 ± 0.0^{a}	9.0 ± 1.0^{b}
Intestinal Phase InfoGest	1 h	47.0 ± 2.1^{b}	1.0 ± 0.0^{a}	0.1 ± 0.0^{a}	10.7 ± 0.4^{b}
	2 h	55.0 ± 2.8^{c}	1.1 ± 0.0^{a}	0.1 ± 0.0^{a}	11.1 ± 0.6^{b}
Intestinal Phase RSIE	1 h	37.4 ± 2.0^{d}	14.9 ± 0.8^{b}	10.4 ± 0.7^{b}	38.8 ± 0.3^{c}
	2 h	58.5 ± 1.0^{e}	16.3 ± 0.2^{c}	12.9 ± 0.6^{c}	41.6 ± 0.8^{d}
Intestinal Phase InfoGest	1 h	47.0 ± 2.1^{b}	1.0 ± 0.0^{a}	0.1 ± 0.0^{a}	10.7 ± 0.4^{b}
Intestinal Phase InfoGest + RSIE	1 h	52.5 ± 1.5^{c}	20.6 ± 0.2^{d}	17.2 ± 1.1^{d}	42.3 ± 3.7^{d}

Values are expressed as means as ± SD (n = 4).
$^{a-e}$Different letters indicate statistical differences between content of each column using ANOVA ($p \leq 0.05$).

with Tamura, Singh, Kaur, and Ogawa (2016), who found no hydrolysis during gastric process using simulated digestion fluids.

On the other hand, Tables 3a and 3b show the content of pectic carbohydrates. In first instance, MCP had a considerable content in galacturonic acid (GalA) due to the process of manufacture of the modified pectin, which involved enzymes-catalyzed reactions in the structure of the pectin (Holck et al., 2014; Míguez, Gómez, Gullón, Gullón, & Alonso, 2016). Barely any hydrolysis was observed during gastric digestion of CP (Table 3a), highlighting their resistance to acidic gastric digestion. Nevertheless, a significant increase in GalA ($p \leq 0.05$) is observed in MCP (Table 3b), thus indicating the possible acidic hydrolysis effect in the lower Mw compounds (Holloway, Tasman-Jones, & Maher, 1983; Thibault, Renard, Axelos, Roger, & Crépeau, 1993). In addition, MCP is a de-esterified pectin, a simpler structure which permits an easier acidic-hydrolysis to the homogalacturonan (HG) backbone (Holck et al., 2014).

3.2.1. Small intestinal digestion of starch

As it is very well-known, starch is the major dietary glycemic carbohydrate. Glucose molecules of starch are linked by α-(1 → 4) bonds for the amylose, and α-(1 → 6) and α-(1 → 4) for the amylopectin. In the gastrointestinal digestion, soluble starch is completely hydrolyzed to glucose by the action of different α-amylases and α-glucosidases (Englyst, Kingman, & Cummings, 1992).

After gastric digestion, a high and significant ($p \leq 0.05$) starch hydrolysis was observed in the first hour of InfoGest intestinal digestion (Table 2a), resulting in a significant increase of maltotriose, maltose and glucose content. After 2 h, although in minor proportion, a significant increase was obtained in the digestion of starch resulting in increases of glucose, maltotriose and total carbohydrates observed with respect to 1 h. These data are in line with the traditional hydrolytic activity of α-amylase towards α-(1 → 4) linkages presented in the starch, providing a mixture of low-molecular weight carbohydrates to be digested in the mucous membrane of the small intestine (Feher, 2017; Freitas & Le Feunteun, 2019). Starch digestion after RSIE treatment (Table 2a), indicates a different behavior with respect to the InfoGest small intestine protocol. RSIE treatment produced no disaccharides or trisaccharides presence, registering only a high and significant ($p \leq 0.05$) increase in glucose level after two hours of digestion, being more pronounced in the first hour. This behavior is in agreement with the high maltase activity of RSIE observed (Table 1), underlining the action of the maltase-glucoamylase complex present in this extract (Ferreira-Lazarte, Olano, et al., 2017a; Hooton et al., 2015; Lin, Lee, & Chang, 2016). Recently, Seo et al. (2020), which carried out a digestion assay using a solution of RSIE, observed a higher hydrolytic activities of the enzymes present in the RSIE compared to other digestive enzyme solutions, which is in good agreement with the highest hydrolysis degree of starch (58.5%, Table 4) and glucose generation observed.

The combination of both *in vitro* methods, InfoGest and RSIE, was also investigated (Table 2a). The effects of the two types of methodologies were complementary as pancreatic α-amylase hydrolyzed intra α-(1 → 4) linkages, resulting in di- and trisaccharides, whereas brush border enzymes hydrolyze by the reducing end of the chains of starch and the resulting di- and trisaccharides, generating more quantity of glucose when compare with the individual digestibility protocols (Table 2a).

In terms of hydrolysis degree (Table 4), the highest and significant value ($p \leq 0.05$) was observed with RSIE assay (58.5%), underlining the high importance of the enterocytes brush border enzymes for carbohydrate digestion (Ferreira-Lazarte, Olano, et al., 2017a; Gallego-Lobillo et al., 2020; Lin et al., 2016; Lin, Hamaker, & Nichols, 2012). Hydrolysis degree of starch via the combination of methods was slightly lower (55%, Table 4). Similar values were obtained by Bustos, Vignola, Pérez, and León (2017) and Fernandes et al. (2020) using InfoGest, with a 44.5% of hydrolysis of rice starch and 40% degradation of wheat starch observed by Selma-Gracia, Laparra, and Haros (2020).

3.2.2. Small intestinal digestion of dextran

Dextran is a glucose polymer mainly formed by α-(1 → 6) linkages (Naessens, Cerdobbel, Soetaert, & Vandamme, 2005; Sims, Thomson, Hubl, Larsen, & Furneaux, 2001). Dextran contain short branches of two or three monomers of glucose linked by α-(1 → 3). No significant hydrolysis ($p \geq 0.05$) was observed during the intestinal digestion with InfoGest, compared to gastric digestion (Table 2b). This is consequence of the inability of α-amylase to hydrolyze α-(1 → 6) linkages (Whistler & Daniel, 2000).

Several works have reported a high resistance of dextran to the gastrointestinal digestion when simulated fluids are used, excluding the brush border enzymes (Fan, Yi, Zhang, Wen, & Zhao, 2017; Loyeau et al., 2018; Meng, Kang, Wang, Zhao, & Lu, 2018). In addition, Kothari, Tingirikari, and Goyal (2015) analyzed the behavior of the dextran used in this work with simulated digestion fluids, observing high resistance to digestion properties. Conversely, a significant increase of glucose ($p \leq 0.05$) was detected when RSIE was used, mainly after the first hour (Table 2b), reaching a total hydrolysis degree of 16.3% (Table 4). The α-(1 → 6) linkages were hydrolyzed by the sucrose-isomaltase complex, specifically, the isomaltase active site and also by the glucoamylase presented in the maltase-glucoamylase complex (Feher, 2017; Hooton et al., 2015), confirming the effect of the chemical structure and type of linkage in the intestinal digestion (Ferreira-Lazarte, Gallego-Lobillo, et al., 2019b; Hernández-Hernández et al., 2012). Lee et al. (2016) showed a hydrolysis rate of 24% of α-(1 → 6) disaccharides using rat enzymes, which was higher to the 16.3% observed in this study (Table 3), possibly due to the different methodology. In addition, these authors obtained 100% of hydrolysis of α-(1 → 4) carbohydrates (starch bonds), and a 52% for α-(1 → 3), emphasizing the effect of the glycosidic linkages and the capability of RSIE enzymes to hydrolyze different structures of carbohydrates (Gallego-Lobillo et al., 2020; Lee et al., 2016). Moreover, the considerable concentration of microorganisms in the small intestine, specially in the ileum (Kovatcheva-Datchary, Tremaroli, & Bäckhed, 2013), may also contribute to the hydrolysis of dextran. Thus, the complex environment of the small intestine concerns the activity of both types of enzymes: mammal and microbial. In this sense, Hernández-Hernández et al. (2012) reported a high *in vivo* ileal digestion of β-GOS, considering the complete behavior of the small intestine in terms of carbohydrate digestion.

Concerning digestion assay of both methods, no significant modifications were obtained after the first small intestinal InfoGest hour, followed by a remarkable and significant hydrolysis during RSIE process (10.1 to 208.9 mg carbohydrates*g of sample^{-1}, Table 2b; 20.6% hydrolysis degree, Table 4). Moreover, longer digestion times (6 h) with RSIE have demonstrated to reach higher degradation rates of dextran (44%) as observed in previous works (Poele et al., 2020). Therefore, dextran could be mostly hydrolyzed by small intestinal enzymes present in the extract, showing a slight and significant increase when both methods are combined.

3.2.3. Small intestinal digestion of pectin and modified citrus pectin

Regarding non-digestible carbohydrates, the CP content along the different treatments is shown in Table 3a. CP is a heteropolysaccharide with a high Mw (472 kDa), mainly composed of GalA and galactose, as the most abundant neutral sugar. No hydrolysis by InfoGest method was observed, because of the resistance of this soluble fiber to the InfoGest simulated gastrointestinal digestion (Míguez et al., 2016). The CP used in this study, had a degree of methylation of 70.7% (Muñoz-Labrador et al., 2018), which increases the difficulty of the simulated fluids to hydrolyze this complex polysaccharide (Carnachan, Bootten, Mishra, Monro, & Sims, 2012), although, some authors have also reported slight hydrolysis with digestive solutions (10%) (Chen et al., 2017), presumably due to the dynamic method used by them.

CP was partially hydrolyzed by RSIE, given a significant increase ($p \leq 0.05$) in GalA and galactose after the first hour of treatment (Table 4). These monomers are linked via α-(1 → 4) in the CP backbone. As

previously discussed, a complete ileal digestion with RSIE, regarding possible microbial and small intestine enzymes, might be able to hydrolyze α-(1 → 4) bonds with monomers different to glucose (Gallego-Lobillo et al., 2020; Hernández-Hernández et al., 2012; Lee et al., 2016; Marounek, Vovk, & Skřivanová, 1995), releasing GalA and galactose in significant proportions.

Digestion rate of the combined methods showed similar trend as these applied separately (Table 3a). Similarly, as occurred in dextran digestion with both methods, a higher and significant hydrolysis was observed in the combined method (20.6%, Table 4).

Galactose and galacturonic acid released in the digestion indicate the hydrolysis of the HG backbone and the lateral chains of galactose of RG-I (Ciriminna, Fidalgo, Delisi, Ilharco, & Pagliaro, 2016). Furthermore, hydrolysis is related to the low pectinase activity obtained for this extract (Table 1). Different studies showed the low capability of the simulated digestion fluids to hydrolyze polysaccharides similar in structure to citrus pectin, obtaining percentages of low hydrolysis rate (8–10%) and observing limited modifications in the Mw (Chen et al., 2017; Ferreira-Lazarte, Moreno, et al., 2019a; Huang et al., 2019). With the combination of both methods, hydrolysis obtained is higher (17.2%) than literature. It is plausible that the combination of InfoGest and RSIE provides a more realistic approach on the digestion of these carbohydrates, nonetheless, the effect of the ileal microbiota present in the small intestine of the rat should also be considered in future studies to understand the complete environment of the digestive system (Hernández-Hernández et al., 2012; Marounek et al., 1995).

Evolution of the carbohydrate fraction of MCP is shown in Table 3b. MCP which has a lower Mw (3.1–0.7 kDa) than CP, it is also composed mainly by lineal GalA structures. A slight but significant increase ($p \leq 0.05$) in the GalA was observed after the first hour during the intestinal stage by InfoGest with no changes in the content of galactose. Hydrolysis degree (11.1%, Table 4), observed in this structure was similar to results reported by Khodaei, Fernandez, Fliss, and Karboune (2016), who digest a pectic polysaccharide rich in galactose and GalA, obtaining 14% of hydrolysis. Surprisingly, the incubation with RSIE significantly increase the concentration of GalA and galactose, resulting in a 41.6% of hydrolysis degree (Table 4). As indicated above, MCP is a non-methylated structure in contrast to the high methylation of CP (70.7). Therefore, the digestive enzymes might have a better catalytic access to the HG backbone, providing a higher hydrolysis degree than in CP (Dongowski, Lorenz, & Proll, 2002). Furthermore, the better access may permit the intestinal enzymes, including the microbial and brush border complexes, to hydrolyze in major quantity the α-(1 → 4) bonds between GalA monomers, as it is observed in the higher and significant increase of this monosaccharide (Table 3b).

Concerning RSIE and the combination of InfoGest intestinal phase and RSIE, a significant increase in galactose and GalA was observed (Table 3b) and not significant differences between GalA concentration, resulting from these two methods, were found ($p \geq 0.05$). Similarly, the hydrolysis degree showed no statistical differences ($p \geq 0.05$) (42.3% InfoGest + RSIE vs. 41.6% RSIE, Table 4). In this context, the microbial enzymes present in the RSIE could also have an effect on the complete ileal carbohydrate digestion (Hernández-Hernández et al., 2012; Marounek et al., 1995). Thus, hydrolysis of MCP was higher than CP (Table 3), mainly due to the structural differences between the two types of pectins, such as the Mw and DP (Míguez et al., 2016; Morris, Belshaw, Waldron, & Maxwell, 2013).

Interestingly, in all samples, a more pronounced effect of intestinal digestion was observed after 1 h of InfoGest and RSIE treatment separately, while after 2 h digestion was lower. This fact also occurred in the combination (Intestinal Phase InfoGest + RSIE 1 h, Table 2, 3 and 4). An explanation for this fact might be the higher activity of pancreatic enzymes in their first approach, which is reduced in the second hour, probably reaching the maximum enzymatic activity (Freitas & Le Feunteun, 2019; Whistler & Daniel, 2000). Moreover, results in dextran and CP with the combination of InfoGest and RSIE are very similar in terms of hydrolysis degree (20.6% dextran vs. 17.2% CP, Table 4). These findings support the fact of the need of a complete method for the digestion of dietary polysaccharides.

According to these findings, the reliability of the RSIE as an *in vitro* digestion method is confirmed, showing meaningful differences with respect to InfoGest protocol as observed in previous reports. Although, the presence of small intestine microbial enzymes in the digestion process could provide a more realistic simulation of the real process, a purification process should be considered in further studies. Although InfoGest is recognized as an international digestion model, the lack of the brush border enzymes and the inaccuracy to distinguish between digestible, partial non-digestible and non-digestible carbohydrates suggests the need of a revision and obtainment of a better method for the digestibility of carbohydrates (Ferreira-Lazarte, 2019c; Hernandez-Hernández, 2019), including brush border enzymes as was already reported in some works (Egger et al., 2017; Ferreira-Lazarte, Gallego-Lobillo, et al., 2019b; Ferreira-Lazarte, Olano, et al., 2017a; Gallego-Lobillo et al., 2020; García-Campayo, Han, Vercauteren, & Franck, 2018; Mamone et al., 2015; Tanabe, Nakamura, Omagari, & Oku, 2015).

4. Conclusions

Digestibility of two glucose-based (starch and dextran) and two pectic polysaccharides (citrus pectin and modified citrus pectin) was investigated through the combination of two types of *in vitro* digestion methods: InfoGest protocol, method based on the use of simulated digestive fluids and RSIE, recently proposed as a useful model using a complete small intestine of rat. In the case of starch, the results confirmed the complementary effect of α-amylases and RSIE, with the hydrolysis rate higher than 50%. However, dextran was only hydrolyzed with RSIE. Citrus pectin was the least susceptible to the effect of digestive enzymes. In Modified Citrus Pectin, partial hydrolysis was observed, especially in the RSIE treatment and with the combination of the methods, resulting in a significant increase in GalA and galactose.

The data obtained in this work indicated the ineffectiveness of the InfoGest method as a versatile procedure for polysaccharides digestion. Although the presence of other enzymes different from α-amylase, including carbohydrases of the brush border enzymes of the enterocytes, is considered in this standardized method, they are still not used reducing the suitability of this method for carbohydrates digestion studies. Conversely, the reliability and usefulness of RSIE model has been proven. Going forward, standardized and specific methods for the digestibility of carbohydrates, realistically mimicking the environment of the small intestine, are needed to understand the digestibility of different carbohydrates in the gastrointestinal tract.

Funding

This work was supported by the Spanish Ministry of Economy, Industry and Competitiveness (Project AGL2017-84614-C2-1-R) and the Spanish Ministry of Science, Innovation and Universities (Project RTI2018-101273-J-I00).

CRediT authorship contribution statement

Pablo Gallego-Lobillo: Conceptualization, Data curation, Formal analysis, Investigation, Methodology, Writing - original draft. **Alvaro Ferreira-Lazarte:** Data curation, Formal analysis, Investigation, Software, Writing - original draft, Visualization. **Oswaldo Hernández-Hernández:** Funding acquisition, Resources, Software, Supervision, Validation, Visualization, Writing - review & editing. **Mar Villamiel:** Funding acquisition, Project administration, Resources, Supervision, Validation, Writing - review & editing.

Declaration of Competing Interest

The authors declare that they have no known competing financial interests or personal relationships that could have appeared to influence the work reported in this paper.

References

Bradford, M. M. (1976). A rapid and sensitive method for the quantitation of microgram quantities of protein utilizing the principle of protein-dye binding. *Analytical Biochemistry, 72*(1–2), 248–254.

Brobst, K. M., & Lott, C. E. J. (1966). Determination of some components in cron syrup by gas-liquid chromatography of the trimethylsilyl derivatives. *Cereal Chemistry, 43*, 35–43.

Brodkorb, A., Egger, L., Alminger, M., Alvito, P., Assunção, R., Ballance, S., … Recio, I. (2019). INFOGEST static *in vitro* simulation of gastrointestinal food digestion. *Nature Protocols, 14*(4), 991–1014.

Bustos, M. C., Vignola, M. B., Pérez, G. T., & León, A. E. (2017). *In vitro* digestion kinetics and bioaccessibility of starch in cereal food products. *Journal of Cereal Science, 77*, 243–250.

Carnachan, S. M., Bootten, T. J., Mishra, S., Monro, J. A., & Sims, I. M. (2012). Effects of simulated digestion *in vitro* on cell wall polysaccharides from kiwifruit (Actinidia spp.). *Food Chemistry, 133*(1), 132–139.

Chen, D., Chen, G., Wan, P., Hu, B., Chen, L., Ou, S., … Ye, H. (2017). Digestion under saliva, simulated gastric and small intestinal conditions and fermentation in vitro of polysaccharides from the flowers of Camellia sinensis induced by human gut microbiota. *Food and Function, 8*(12), 4619–4629.

Ciriminna, R., Fidalgo, A., Delisi, R., Ilharco, L. M., & Pagliaro, M. (2016). Pectin production and global market. *Agro Food Industry Hi-Tech, 27*(5), 17–20.

Cockburn, D. W., & Koropatkin, N. M. (2016). Polysaccharide degradation by the intestinal microbiota and its influence on human health and disease. *Journal of Molecular Biology, 428*(16), 3230–3252.

Dongowski, G., Lorenz, A., & Proll, J. (2002). The degree of methylation influences the degradation of pectin in the intestinal tract of rats and *In Vitro*. *The Journal of Nutrition, 132*(7), 1935–1944.

Egger, L., Schlegel, P., Baumann, C., Stoffers, H., Guggisberg, D., Brügger, C., … Portmann, R. (2017). Physiological comparability of the harmonized INFOGEST *in vitro* digestion method to *in vivo* pig digestion. *Food Research International, 102*, 567–574.

Englyst, H. N., Kingman, S. M., & Cummings, J. H. (1992). Classification and measurement of nutritionally important starch fractions. *European Journal of Clinical Nutrition, 46*(2), S33–S50.

Englyst, K., Goux, A., Meynier, A., Quigley, M., Englyst, H., Brack, O., & Vinoy, S. (2018). Inter-laboratory validation of the starch digestibility method for determination of rapidly digestible and slowly digestible starch. *Food Chemistry, 245*, 1183–1189.

Fan, Y., Yi, J., Zhang, Y., Wen, Z., & Zhao, L. (2017). Physicochemical stability and in vitro bioaccessibility of β-carotene nanoemulsions stabilized with whey protein-dextran conjugates. *Food Hydrocolloids, 63*, 256–264.

Feher, J. (2017). Digestion and Absorption of the Macronutrients. *Quantitative Human Physiology*, 821–833.

Fernandes, J. M., Madalena, D. A., Pinheiro, A. C., & Vicente, A. A. (2020). Rice *in vitro* digestion: Application of INFOGEST harmonized protocol for glycemic index determination and starch morphological study. *Journal of Food Science and Technology, 57*(4), 1393–1404.

Ferreira-Lazarte, A., Moreno, F. J., & Villamiel, M. (2020). Bringing the digestibility of prebiotics into focus: Update of carbohydrate digestion models. *Critical Reviews in Food Science and Nutrition*, 1–12.

Ferreira-Lazarte, A. (2019c). *In vitro digestibility and fermentability of selected prebiotics and functional carbohydrates with prebiotic potential (Doctoral Thesis)*. Universidad Autónoma de Madrid.

Ferreira-Lazarte, A., Gallego-Lobillo, P., Moreno, F. J., Villamiel, M., & Hernandez-Hernandez, O. (2019b). *In Vitro* digestibility of galactooligosaccharides: effect of the structural features on their intestinal degradation. *Journal of Agricultural and Food Chemistry, 67*(16), 4662–4670.

Ferreira-Lazarte, A., Kachrimanidou, V., Villamiel, M., Rastall, R. A., & Moreno, F. J. (2018). *In vitro* fermentation properties of pectins and enzymatic-modified pectins obtained from different renewable bioresources. *Carbohydrate Polymers, 199*, 482–491.

Ferreira-Lazarte, A., Montilla, A., Mulet-Cabero, A. I., Rigby, N., Olano, A., Mackie, A., & Villamiel, M. (2017b). Study on the digestion of milk with prebiotic carbohydrates in a simulated gastrointestinal model. *Journal of Functional Foods, 33*, 149–154.

Ferreira-Lazarte, A., Moreno, F. J., Cueva, C., Gil-Sánchez, I., & Villamiel, M. (2019a). Behaviour of citrus pectin during its gastrointestinal digestion and fermentation in a dynamic simulator (simgi®). *Carbohydrate Polymers, 207*(November 2018), 382–390.

Ferreira-Lazarte, A., Olano, A., Villamiel, M., & Moreno, F. J. (2017a). Assessment of *in vitro* digestibility of dietary carbohydrates using rat small intestinal extract. *Journal of Agricultural and Food Chemistry, 65*(36), 8046–8053.

Freitas, D., & Le Feunteun, S. (2019). Oro-gastro-intestinal digestion of starch in white bread, wheat-based and gluten-free pasta: Unveiling the contribution of human salivary α-amylase. *Food Chemistry, 274*, 566–573.

Freitas, D., Le Feunteun, S., Panouillé, M., & Souchon, I. (2018). The important role of salivary α-amylase in the gastric digestion of wheat bread starch. *Food and Function, 9*(1), 200–208.

Gallego-Lobillo, P., Ferreira-Lazarte, A., Hernández-Hernández, O., Montilla, A., & Villamiel, M. (2020). Evaluation of the impact of a rat small intestinal extract on the digestion of four different functional fibers. *Food and Function, 11*(5), 4081–4089.

Garcia-Campayo, V., Han, S., Vercauteren, R., & Franck, A. (2018). Digestion of food ingredients and food using an *in vitro* model integrating intestinal mucosal enzymes. *Food and Nutrition Sciences, 09*(06), 711–734.

Han, X., Xie, Y., Wu, Q., & Wu, S. (2018). A novel protein digestion method with the assistance of alternating current denaturation for high efficient protein digestion and mass spectrometry analysis. *Talanta, 184*, 382–387.

Hernandez-Hernández, O. (2019). *In vitro* gastrointestinal models for prebiotic carbohydrates: A critical review. *Current Pharmaceutical Design, 25*(32), 3478–3483.

Hernández-Hernández, O., Marín-Manzano, M. C., Rubio, L. A., Moreno, F. J., Sanz, M. L., & Clemente, A. (2012). Monomer and linkage type of galacto-oligosaccharides affect their resistance to ileal digestion and prebiotic properties in rats. *Journal of Nutrition, 142*(7), 1232–1239.

Hernandez-Hernandez, O., Olano, A., Rastall, R. A., & Moreno, F. J. (2019). *In vitro* digestibility of dietary carbohydrates: Toward a standardized methodology beyond amylolytic and microbial enzymes. *Frontiers in Nutrition, 6*(61), 1–5.

Holck, J., Hotchkiss, A. T., Meyer, A. S., Mikkelsen, J. D., & Rastall, R. A. (2014). Production and bioactivity of pectic oligosaccharides from fruit and vegetable biomass. In F. J. Moreno, & M. L. Sanz (Eds.), *Food Oligosaccharides: Production, Analysis and Bioactivity* (pp. 76–87). John Wiley & Sons, Inc.

Holloway, W. D., Tasman-Jones, C., & Maher, K. (1983). Pectin digestion in humans. *The American Journal of Clinical Nutrition, 37*(2), 253–255.

Hooton, D., Lentle, R., Monro, J., Wickham, M., & Simpson, R. (2015). The secretion and action of brush border enzymes in the mammalian small intestine. *Review in Physiological Biochemistry Pharmacology, 168*, 59–118.

Hu, J. L., Nie, S. P., & Xie, M. Y. (2018). Antidiabetic mechanism of dietary polysaccharides based on their gastrointestinal functions. *Journal of Agricultural and Food Chemistry, 66*(19), 4781–4786.

Huang, F., Liu, Y., Zhang, R., Bai, Y., Dong, L., Liu, L., … Zhang, M. (2019). Structural characterization and *in vitro* gastrointestinal digestion and fermentation of litchi polysaccharide. *International Journal of Biological Macromolecules, 140*, 965–972.

Khodaei, N., Fernandez, B., Fliss, I., & Karboune, S. (2016). Digestibility and prebiotic properties of potato rhamnogalacturonan I polysaccharide and its galactose-rich oligosaccharides/oligomers. *Carbohydrate Polymers, 136*, 1074–1084.

Kothari, D., Tingirikari, J. M. R., & Goyal, A. (2015). *In vitro* analysis of dextran from *Leuconostoc mesenteroides* NRRL B-1426 for functional food application. *Bioactive Carbohydrates and Dietary Fibre, 6*(2), 55–61.

Kovatcheva-Datchary, P., Tremaroli, V., & Bäckhed, F. (2013). The gut microbiota. In E. Rosenberg, E. F. DeLong, S. Lory, E. Stackebrandt, & F. Thompson (Eds.), *The Prokaryotes – Human Microbiology* (pp. 3–24). Heidelberg, Germany: Springer-Verlag.

Lee, B. H., Rose, D. R., Lin, A. H. M., Quezada-Calvillo, R., Nichols, B. L., & Hamaker, B. R. (2016). Contribution of the Individual Small Intestinal α-Glucosidases to Digestion of Unusual α-Linked Glycemic Disaccharides. *Journal of Agricultural and Food Chemistry, 64*(33), 6487–6494.

Li, X., Guo, R., Wu, X., Liu, X., Ai, L., Sheng, Y., … Wu, Y. (2020). Dynamic digestion of tamarind seed polysaccharide: Indigestibility in gastrointestinal simulations and gut microbiota changes in vitro. *Carbohydrate Polymers, 239*, 116194.

Lin, A. H. M., Hamaker, B. R., & Nichols, B. L. (2012). Direct starch digestion by sucrase-isomaltase and maltase-glucoamylase. *Journal of Pediatric Gastroenterology and Nutrition, 55*, S43–S45.

Lin, A. H. M., Lee, B. H., & Chang, W. J. (2016). Small intestine mucosal α-glucosidase: A missing feature of *in vitro* starch digestibility. *Food Hydrocolloids, 53*, 163–171.

Loyeau, P. A., Spotti, M. J., Vanden Braber, N. L., Rossi, Y. E., Montenegro, M. A., Vinderola, G., & Carrara, C. R. (2018). Microencapsulation of *Bifidobacterium animalis* subsp. *lactis* INL1 using whey proteins and dextrans conjugates as wall materials. *Food Hydrocolloids, 85*, 129–135.

Mamone, G., Nitride, C., Picariello, G., Addeo, F., Ferranti, P., & Mackie, A. (2015). Tracking the fate of pasta (T. Durum Semolina) immunogenic proteins by *in vitro* simulated digestion. *Journal of Agricultural and Food Chemistry, 63*(10), 2660–2667.

Marounek, M., Vovk, S. J., & Skřivanová, V. (1995). Distribution of activity of hydrolytic enzymes in the digestive tract of rabbits. *British Journal of Nutrition, 73*(3), 463–469.

McCleary, B. V., De Vries, J. W., Rader, J. I., Cohen, G., Prosky, L., Mugford, D. C., … Okuma, K. (2010). Determination of total dietary fiber (CODEX definition) by enzymatic-gravimetric method and liquid chromatography: Collaborative study. *Journal of AOAC International, 93*(1), 221–233.

Meng, J., Kang, T. T., Wang, H. F., Zhao, B. B., & Lu, R. R. (2018). Physicochemical properties of casein-dextran nanoparticles prepared by controlled dry and wet heating. *International Journal of Biological Macromolecules, 107*, 2604–2610.

Míguez, B., Gómez, B., Gullón, P., Gullón, B., & Alonso, J. L. (2016). Pectic oligosaccharides and other emerging prebiotics. In V. Rao, & L. G. Rao (Eds.), *Probiotics and Prebiotics in Human Nutrition and Health* (pp. 301–330). InTech.

Minekus, M., Alminger, M., Alvito, P., Ballance, S., Bohn, T., Bourlieu, C., … Brodkorb, A. (2014). A standardised static *in vitro* digestion method suitable for food-an international consensus. *Food and Function, 5*(6), 1113–1124.

Morris, V. J., Belshaw, N. J., Waldron, K. W., & Maxwell, E. G. (2013). The bioactivity of modified pectin fragments. *Bioactive Carbohydrates and Dietary Fibre, 1*(1), 21–37.

Muñoz-Labrador, A., Moreno, R., Villamiel, M., & Montilla, A. (2018). Preparation of citrus pectin gels by power ultrasound and its application as an edible coating in strawberries. *Journal of the Science of Food and Agriculture, 98*(13), 4866–4875.

Naessens, M., Cerdobbel, A., Soetaert, W., & Vandamme, E. J. (2005). Leuconostoc dextransucrase and dextran: Production, properties and applications. *Journal of Chemical Technology and Biotechnology, 80*(8), 845–860.

Oku, T., Tanabe, K., Ogawa, S., Sadamori, N., & Nakamura, S. (2011). Similarity of hydrolyzing activity of human and rat small intestinal disaccharidases. *Clinical and Experimental Gastroenterology, 4*(1), 155–161.
Pérez, S., & Bertoft, E. (2010). The molecular structures of starch components and their contribution to the architecture of starch granules: A comprehensive review. *Starch/Staerke, 62*(8), 389–420.
Poele, E., Corwin, S., Hamaker, B. R., Lamothe, L., Vafeiadi, C., & Dijkhuizen, L. (2020). Biotechnology and Biological Transformations Development of slowly digestible starch derived alpha-glucans with 4, 6-α-glucanotransferase and branching sucrase enzymes. *Journal of Agricultural and Food Chemistry, 8*(24), 6664–6671.
Selma-Gracia, R., Laparra, J. M., & Haros, C. M. (2020). Potential beneficial effect of hydrothermal treatment of starches from various sources on in vitro digestion. *Food Hydrocolloids, 103*, 105687.
Seo, J. M., Lamothe, L. M., Shin, H., Austin, S., Yoo, S. H., & Lee, B. H. (2020). Determination of glucose generation rate from various types of glycemic carbohydrates by mammalian glucosidases anchored in the small intestinal tissue. *International Journal of Biological Macromolecules, 154*, 751–757.
Sims, I. M., Thomson, A., Hubl, U., Larsen, N. G., & Furneaux, R. H. (2001). Characterisation of polysaccharides synthesised by Gluconobacter oxydans NCIMB 4943. *Carbohydrate Polymers, 45*(3), 285–292.
Tamura, M., Singh, J., Kaur, L., & Ogawa, Y. (2016). Impact of structural characteristics on starch digestibility of cooked rice. *Food Chemistry, 191*, 91–97.
Tanabe, K., Nakamura, S., Omagari, K., & Oku, T. (2015). Determination trial of nondigestible oligosaccharide in processed foods by improved AOAC Method 2009.01 using porcine small intestinal enzyme. *Journal of Agricultural and Food Chemistry, 63*(24), 5747–5752.
Thibault, J. F., Renard, C. M. G. C., Axelos, M. A. V., Roger, P., & Crépeau, M. J. (1993). Studies of the length of homogalacturonic regions in pectins by acid hydrolysis. *Carbohydrate Research, 238*, 271–286.
Whistler, R. L., & Daniel, J. R. (2000). Starch. In *Kirk-Othmer Encyclopedia of Chemical Technology* (p. 825). John Wiley & Sons, Inc.
Zhu, K., Yao, S., Zhang, Y., Liu, Q., Xu, F., Wu, G., … Tan, L. (2019). Effects of *in vitro* saliva, gastric and intestinal digestion on the chemical properties, antioxidant activity of polysaccharide from Artocarpus heterophyllus Lam. (Jackfruit) Pulp. *Food Hydrocolloids, 87*, 952–959.

International Journal of Biological Macromolecules 167 (2021) 1349–1360

Contents lists available at ScienceDirect

International Journal of Biological Macromolecules

journal homepage: http://www.elsevier.com/locate/ijbiomac

Behaviour of citrus pectin and modified citrus pectin in an azoxymethane/dextran sodium sulfate (AOM/DSS)-induced rat colorectal carcinogenesis model

Alvaro Ferreira-Lazarte [a,1], Javier Fernández [b,c,d,1], Pablo Gallego-Lobillo [a], Claudio J. Villar [b,c,d], Felipe Lombó [b,c,d], F. Javier Moreno [a], Mar Villamiel [a,*]

[a] Instituto de Investigación en Ciencias de la Alimentación, CIAL (CSIC-UAM), C/Nicolás Cabrera, 9, Campus de la Universidad Autónoma de Madrid, 28049 Madrid, Spain
[b] Research Unit "Biotechnology in Nutraceuticals and Bioactive Compounds-BIONUC", Departamento de Biología Funcional, Área de Microbiología, Universidad de Oviedo, Oviedo, Spain
[c] Instituto Universitario de Oncología del Principado de Asturias, Oviedo, Spain
[d] Instituto de Investigación Sanitaria del Principado de Asturias, Oviedo, Spain

ARTICLE INFO

Article history:
Received 25 June 2020
Received in revised form 11 November 2020
Accepted 12 November 2020
Available online 14 November 2020

Keywords:
Cancer
pH decrease
Intestinal microbiota
Gut
Dysbiosis
Lactic acid
Acetic acid

ABSTRACT

Large intestine cancer is one of the most relevant chronic diseases taking place at present. Despite therapies have evolved very positively, this pathology is still under deep investigation. One of the recent approaches is the prevention by natural compounds such as pectin. In this paper, we have assessed the impact of citrus pectin and modified citrus pectin on colorectal cancer in rats (*Rattus norvegicus* F344) to which azoxymethane and DSS were supplied. The lowest intake of food and body weight were detected in animals fed with citrus pectin, together with an increase in the caecum weight, probably due to the viscosity, water retention capacity and bulking properties of pectin. The most striking feature was that, neither citrus pectin nor modified citrus pectin gave rise to a tumorigenesis prevention. Moreover, in both, more than 50% of rats with cancer died, probably ascribed to a severe dysbiosis state in the gut, as shown by the metabolism and metagenomics studies carried out. This was related to a decrease of pH in caecum lumen and increase in acetate and lactic acid levels together with the absence of propionic and butyric acids. A relevant increase in *Proteobacteria* (*Enterobacteriaceae*) were thought to be one of the reasons for enteric infection that could have provoked the death of rats and the lack of cancer prevention. However, a reduction of blood glucose and triacylglycerides level and an increase of *Bifidobacterium* and *Lactobacillaceae* were found in animals that intake pectin, as compared to universal and modified citrus pectin feeding.

1. Introduction

Colorectal cancer (CRC) is the third most common malignancy in the world, being the second reason of cancer deaths in 2018 [1]. As it is known, CRC can imply severe health complications related to the illness itself and the side effects of surgery and/or therapy [2]. A recent study on the incidence and mortality of CRC in 39 countries has shown that the occurrence of colon and rectal cancers is increasing in countries with medium to high development degrees, mainly in the case of young people [3]; therefore, it is necessary to increase the early detection methods and to continue with the investigations that can shed light on the prevention and treatment of this pathology.

CRC usually is developed during several years when a sequence of genetic modifications (towards polyps, adenoma and carcinoma) gives rise to tumours that are more common in the distal large intestine, including the descending colon and rectum, as compared to the proximal sections. Although some CRC forms can be of genetic origin, most CRC cases have a relationship with the lifestyle and diet. In this sense, a diet based on dietary fiber and the use of cancer-therapeutic or cancer-preventive natural compounds are considered efficient and affordable approaches [4].

A plethora of scientific articles has linked a high fiber consumption with a lower frequency of large intestine cancer. Particular interest has been sparked in the case of pectin, mainly derived from citrus, that is used as important technological food ingredient and also for its bioactivity [5]. Experimental studies have also showed a limited consistency on the effects of pectin on CRC with results of inhibition, no effect, or even tumour augmentation [6–9]. Several factors related to pectin such as the source, extraction and purification methods can affect the effectiveness of the assays since the extracted pectin could have rather dissimilar structural features. This fact seems to play an important role in terms of molecular weight (Mw), methyl esterification degree (DM),

* Corresponding author.
E-mail address: m.villamiel@csic.es (M. Villamiel).
[1] Both authors have contributed to the article in equal mode.

https://doi.org/10.1016/j.ijbiomac.2020.11.089
0141-8130/

composition of galacturonic acid (GalA) and neutral sugars such as galactose and arabinose [8].

Pectin is a complex hetero-polysaccharide occurring in plant cell walls and its precise chemical structure is still under debate. The most recognised model combines the structural domains of homogalacturonan (HG), rhamnogalacturonan I (RG-I) and rhamnogalacturonan II (RG-II). HG corresponds to 65% of pectin molecules, with a linear backbone composed of α-(1,4)-D-galacturonic acid, partially methyl-esterified in the C6, or acetylated in O-3 and/or O-2. RG-I corresponds to 20–35% of pectin molecules; this chain is composed of hundreds of repeating disaccharides [→4)α-D-galacturonic acid and (1–2)α-L-rhamnose(1→]n, and may present side chains of molecules of L-arabinose and D-galactose. RG-II represents 10% of pectin molecules and it is a well-preserved and extremely complex molecule, where the main backbone is HG with four heteropolymer side chains with more than 17 rare monosaccharides and 20 different types of bonds [10].

Due to its highly branched complex, pectin is poorly soluble in water, limiting its use. Thus, Modified Citrus Pectin (MCP) has been developed by chemical, enzymatic or heat treatment of citrus pectin to produce a mixture of low Mw polysaccharides that could have a stronger therapeutic role against cancer as compared to full citrus pectin [11,12].

In colon cancer cell lines, several studies have demonstrated the efficiency of different citrus pectin and MCP, and their fractions, and even different mechanisms of action have been postulated [8]. Ai et al. assayed, against Caco-2 cells, different fractions obtained by an enzymatic treatment and subsequent ultrafiltration. Among the samples tested, the highest activity was found in the fraction of RG-II, probably due to its peculiar branched structure and low Mw [13]. In the case of Ramos do Prado et al., the production of MCP fractions was by heat treatment and ultrafiltration [14]. In HCT116 and HT29 colon cancer cells, the highest antiproliferative effect was observed when HG oligomers were de-esterified and enriched in arabinogalactan I and poor in RG-I.

On the contrary, the limited *in vivo* information available on the effect of citrus pectin on CRC shows contradictory results using different animal models, different types of modified pectin and carcinogen doses. Scarce attention has been considered to effects on the microbiota and the relationship with the pectin structure. Moreover, in some cases, the effect of citrus pectin is considered together with other bioactive compounds [8,15]. Ohkami et al. stated that the intake of 20% of citrus pectin in rats injected with azoxymethane (AOM) decreased the multiplicity of colon tumours and they hypothesised that a decrease of β-glucuronidase activity was the most important mechanism, although this effect was much higher in the case of apple pectin [16]. According to Jacobasch et al., who used a model of animals with a genetic predisposition for intestinal neoplasia (APCMin/$^{+}$ mice), pectins (with low and high DM) were ineffective for reduction of tumorigenesis in the small or large intestine and for suppressing COX-2 activity, an enzyme that plays a key role in the pathogenesis of tumour progression [7]. These results were in line with those earlier obtained by Jacobs and Lupton who stated in Sprawe-Dawley rats that the intake of pectin and other soluble fiber could increase proximal colon tumorigenesis [6]. However, Nangia-Makker et al. observed in BALB/c mice, with implanted tumours in the colon, that the daily oral administration of MCP reduced the growth of those implanted tumours and subsequent metastasis [17].

On the basis of this background, we have carried out an exhaustive study on the effect of commercial citrus pectin and Modified Citrus Pectin (MCP) in an animal model (*Rattus norvegicus* F344) developed for colorectal cancer using a combination of azoxymethane and DSS as carcinogenic compounds. Structural and physicochemical characteristics of both test substances have been considered in this animal model. Also, different tumorigenesis parameters (tumour size, number, area) have been analysed, together with metabolic data (short-chain fatty acids, glycemia, *etc.*), physiological (food intake, weight, number of hyperplastic Peyer's patches, caecum weight) and metagenomics of gut microbiota.

2. Materials and methods

2.1. Manufacturing and samples

Commercial citrus pectin (trade name Ceampectin, ESS-4400) was kindly provided by CEAMSA® (Porriño, Pontevedra, Spain). Modified Citrus Pectin (MCP) was kindly provided by Econugenics®, Inc. (Santa Rosa, CA, USA).

2.2. Physicochemical characterisation of substrates

A high Mw citrus pectin as well as MCP were used in this study. Physico-chemical characterisation of each substrate and the feed mixtures was carried out in samples before assays. Product composition was determined regarding carbohydrates, DM, Mw, water retention capacity (Wr) and pH (Table 1). Monomeric composition of pectins was analysed after acid hydrolysis with 2 M trifluoroacetic acid (TFA) at 110 °C during 4 h. The released monosaccharides were derivatised by the formation of trimethylsilyl oximes, following a previous method [18]. Then, samples were analysed by gas chromatography coupled to a flame ionisation detector (GC-FID) and equipped with a fused silica capillary column DB-5HT (5% phenyl methylpolysiloxane, 30 m × 0.25 mm × 0.1 μm, Agilent J&W Scientific, Folsom, CA, USA). Oven temperature program started in 150 °C and increased to 165 °C at 1 °C/min and up to 300 °C in a rate of 10 °C/min. Injector and detector temperature were 280 and 350 °C, respectively. Nitrogen was used as the carrier gas at 1 mL/min of flow rate. Samples were injected in split mode 1:5. Quantification was done through the internal standard method (β-phenylglucoside).

Estimation of the Mw was conducted by HPSEC-ELSD [19]. Samples were filtered (0.45 μm), analysed on a LC 1220 Infinity System (Agilent Technologies, Boebligen, Germany) and detected on an ELSD System 1260 Infinity (Agilent Technologies, Boebligen, Germany). Mobile phase used was 0.1 M $NH_4CH_3CO_2$, at a flow rate of 0.5 mL/min for 50 min at 30 °C. Pullulans of Mw 805, 200, 10, 3 and 0.3 kDa were used as standards.

DM of the samples was analysed by Fourier transform infrared spectroscopy (FTIR) [20]. The DM was determined as the average of the ratio of the peak area at 1747 cm^{-1} (COO-R) over the sum of the peaks 1747 cm^{-1} (COO-R) and 1632 cm^{-1} (COO^{-}).

Table 1
Physicochemical characterisation of pectin and modified citrus pectin used in this study.

Sample	Monosaccharides composition (%)							GalA:Rha	Ara:Rha	Gal:Rha	Wr (mL/mg)	Average Mw (kDa)	DM (%)
	Xyl	Ara	Rha	Gal	Man	Glc	GalA						
Citrus pectin	tr.	6.7 ± 0.4	4.4 ± 0.3	22.5 ± 0.5	tr.	2.4 ± 0.1	64.0 ± 0.9	14.6 ± 1.2	1.5 ± 0.1	5.1 ± 0.4	10 ± 0.0	472	70.7
Modified citrus pectin	tr.	3.9 ± 0.7	2.3 ± 0.1	8.9 ± 0.3	tr.	1.0 ± 0.0	83.9 ± 0.9	37.0 ± 1.1	1.7 ± 0.3	3.9 ± 0.2	0.7 ± 0.0	3.1–0.7	0

Analysis were carried out at least in duplicate ($n = 2$).
tr. = traces.

W_r was determined following the method of Chau & Huang [21]. Pectins were incubated with distilled water (1:10, w/v) for 24 h with continuous agitation. Then, samples were centrifuged at 1006 ×g for 30 min. W_r was expressed as mL of water held by 1 g of pectin. In addition, pH of samples was measured using a pH-meter FE20 (Mettler Toledo GmBH, Schwerzenbach, Switzerland).

2.3. Animal and experimental design

In the inducted colorectal cancer model a total of 30 male Fischer 344 rats were maintained in the Animal Facilities at the University of Oviedo (authorised facility No. ES330440003591). All rat assays were approved by the Ethics Committee of the Principality of Asturias (authorisation code PROAE 36/2018).

Rats (5 weeks old) were divided into 3 cohorts of 10 individuals each and fed *ad libitum* in individual cages. Cohort 1 was fed with universal feed (F cohort, 2014 Teklad Global 14% Protein Rodent Maintenance Harlan diet feed), which contained 6.7% protein, 5.8% fat, 53,6% carbohydrates, 20% fiber, 4.7% ashes (Table 2). Cohort 2 was fed with a mixture feed prepared from universal feed where cellulose (BW200) was substituted by citrus pectin (20%) (FP cohort) (Research Diets Inc., NJ, USA). In a similar way, cohort 3 was fed with a preparation where cellulose was substituted with the Modified Citrus Pectin (FMP cohort) (20%) (Research Diets Inc., NJ, USA).

2.4. Colorectal cancer induction and monitoring

The colorectal cancer inducing was carried out according to previously described methodology [22]. Assay took place one week after the animals arrived at the facility when the diets started. After one week of eating the corresponding diet, CRC was induced in eight rats from each cohort. The two other rats were kept free of CRC induction as absolute control animals. CRC induction was carried out in those eight rats of each cohort using azoxymethane (AOM, Sigma-Aldrich, Madrid, Spain) dissolved in sterile saline solution (0.9% NaCl) at a concentration of 2 mg/mL. This AOM solution was injected intraperitoneally at a final concentration of 10 mg per kg body weight. This AOM treatment was repeated seven days after the first injection (weeks 2 and 3). The absolute control animals received sterile saline in both injections.

In weeks 4 and 15, rats received drinking water during seven days' treatment, containing 3% and 2% dextran sodium sulfate (DSS, 40.000 g/mol, VWR), respectively. This ulcerative colitis step was repeated twice because it enhances the pro-carcinogenic effect caused by AOM administration.

Rats were sacrificed by pneumothorax 21 weeks after the first administration of AOM. Throughout the entire process, rats were monitored for body weight and stool consistency/rectal bleeding.

Table 2
Structural composition and characterisation of feed mixtures utilized in the experiment.

	Universal feed (F)	Universal feed + pectin (FP)	Universal feed + modified pectin (FMP)
Protein (%)	16.7	16.7	16.7
Lipids (%)	5.8	5.8	5.8
Carbohydrates (%)	53.6	53.6	53.6
Fiber (%)	20	20	20
Ashes (%)	4.7	4.7	4.7
Pectin or MCP content	–	20	20
pH	6.67	6.50	6.7
Water retention (mL/mg)	0.8	4.5	0.7
kcal/g	3.33	3.33	3.33

2.5. Weight measurements

Rats were weighed regularly during the 21 experimental weeks; at reception of the animals (week 1), at each of the AOM administrations (week 2 and 3), and at weeks 6, 10, 13, 18 and 21.

2.6. Blood and tissue samples

Before being sacrificed (bilateral pneumothorax) at week 21, rats were anesthetised (isoflurane) for the extraction of blood (2 mL) from the heart, which was then centrifuged at 3000 rpm for 15 min, in order to collect and freeze the plasma at −20 °C.

Small intestines were fresh removed and the hyperplastic Peyer's patches were counted. Their number in the experimental animals was calculated and compared with respect to the two absolute control animals from each cohort (animals 9 and 10). Weight and length of small intestines was also measured in all cohort individuals. Caecums were weighed immediately after sacrifice using a precision scale and then frozen at −20 °C.

Finally, the colon was opened longitudinally and washed with PBS (phosphate buffer saline) before keeping it in 4% formaldehyde at 4 °C. Fixed colons were meticulously examined with a caliper in order to count the number of polyps larger than 1 mm on the inner mucosa surface. The largest detected polyps were 10 mm in diameter. The shape of the polyps was identified as pedunculated (a disc connected *via* a peduncle to the colon mucosa), plane irregular, plane circular and spherical. Finally, the total polyp-affected area was calculated.

2.6.1. Plasma glucose and triacylglycerides analysis

Plasma glucose levels were measured using a Accutrend Plus and the reactive strips 11447475 (Roche, Barcelona, Spain). Plasma triacylglycerides levels were measured using the same equipment, but with reactive strips 11538144 (Roche, Barcelona, Spain).

2.7. HPLC-UV quantification of SCFA in caecum samples

Prior to HPLC analysis, short chain fatty acids (SCFA) were extracted from rat caecum, according to the method of Joseph et al. [23]. Caecum samples (0.2 g) were added to distilled water (1.6 mL) in order to get a final ratio of 1:8 (w/v). Then, extraction was performed by mixing powerfully in vortex for 1 min. Finally, samples were centrifuged for 10 min at 10,000 ×g and supernatant was filtered using a 0.22 μm syringe filter (Symta, Madrid, Spain). Samples were injected on a HPLC system (Agilent Technologies, Germany) equipped with a UV-975 detector. Separation was done through a Rezex ROA Organic Acids column (300 cm × 7.8 mm) (Phenomenex, Macclesfield, UK) at a flow rate of 0.5 mL/min (isocratic elution) at 50 °C. The mobile phase was 0.005 N H_2SO_4 and detection was performed at a wavelength of 210 nm. Identification and quantification of peaks were done through external standards solutions of SCFA (acetic, propionic, butyric, formic, lactic, valeric and isovaleric acid) in different concentrations (1–100 mM).

2.8. Genomic DNA extraction and 16S ribosomal RNA sequencing for metagenomics

Genomic DNA (gDNA) was extracted from 200 mg of frozen (−80 °C) caecum feces using E.Z.N.A.® DNA Stool kit (Omega BioTek Ref. D4015-02, VWR, Madrid, Spain) and provided 200 μL of genomic DNA. These gDNA samples were then quantified using a BioPhotometer® (Eppendorf, Madrid, Spain) and their concentrations diluted to 6 ng/μL. Diluted samples were used for performing polymerase chain reactions (PCR) amplification, following the protocol of the Ion 16™ Metagenomic kit (Thermo Fischer Scientific, Madrid, Spain).

PCR amplification products were utilised to create a library using the Ion Plus Fragment Library kit for AB Library Builder™ System (Cat. No. 4477597, Thermo Fischer Scientific), with sample indexing using the Ion

Xpress™ Barcode adapters 1–96 kit (Cat. No. 4474517, Thermo Fischer Scientific).

Template preparation was performed using the ION OneTouch™ 2 System and the ION PGM™ Hi-Q™ OT2 kit (Cat. No. A27739, Thermo Fischer Scientific). Metagenomics sequencing was performed using ION PGM™ Hi-Q™ Sequencing kit (Cat. No. A25592, Thermo Fischer Scientific) on the ION PGM™ System. The chips used were the ION 314™ v2, 316™ v2 or 318™ v2 Chips (Cat. No. 4482261, 4483188, 4484355, Thermo Fischer) with various barcoded samples per chip [24].

2.9. Phylogenetic analysis

The consensus excel table for each metagenomics sequencing was downloaded from ION Reporter 5.6 software (Life Technologies Holdings Pte Ltd., Singapore). This excel table includes the percentages for each taxonomic level and was used for comparing frequencies between rat individuals and cohorts.

Taxonomic adscription up to species level was conducted using the QIIME-2 (v.2017.6.0) open-source bioinformatics pipeline. Analysis of the microbiome community was carried out using R software (v3.2.4): non-supervised multivariate analysis (PCA). The reference library used was the Curated MicroSEQ(R) 16S Reference Library v2013.1; Curated Greengenes v13.5. The number of mapped reads (after the ignored ones due to less than 10 copies) per sample was always over 80.000. Total number of reads was always over 110.000. Counts were normalised by sum scaling [25].

2.10. Statistical methods

Data were expressed as the mean value ± S.E.M. Statistical analyses were conducted using ANOVA test when the quantitative data presented normality and the variances were assumed equal. Normality was analysed using Shapiro-Wilk. In the absence of normality, Kruskal-Wallis test was used. The graphical representation of all these data was generated using GraphPad Prism software (version 8, GraphPad Software, San Diego, CA, USA). In all cases, a p value < 0.05 was considered statistically significant ($^{*}p < 0.05$; $^{**}p < 0.005$; $^{***}p < 0.0005$; $^{****}p < 0.0001$) [25].

3. Results

3.1. Effect of pectin diets on body weight

Body weight was affected in all cohorts due to the different feeding after the AOM and DSS treatment. In general, all cohorts gained weight during the experiment after the DSS treatment maintaining a continuous gain along the experimental weeks. Rats with inducted CRC achieved a slightly lower weight values as compared to the control rats (Fig. 1A and B). It is noteworthy that cohort fed with pectin (FP) showed the lowest intake and body weights in all cohorts, followed by the cohort fed with modified pectin (FMP), whereas the cohort fed with the universal diet (F) showed the highest values.

Nevertheless, it should be noted that nine animals died during the assay; five in FP cohort and four in FMP cohort. They did not survive the DSS treatment, which was used to enhance the final production and size of the colon tumours, and died just after its administration. Five of them died during the next 10 days after finishing the first DSS treatment (mainly in FP cohort), three died one day after finishing the second DSS treatment and the last animal died 2 days before sacrifice day (mainly in FMP cohort).

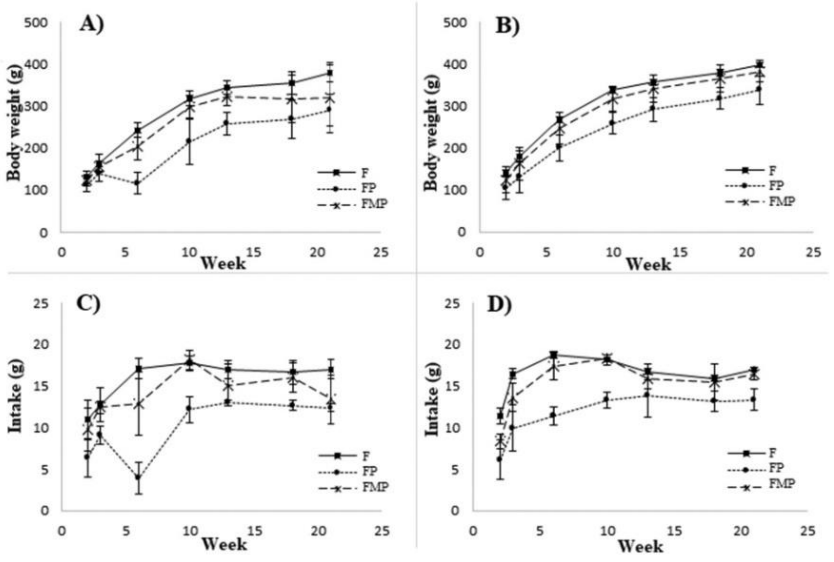

Fig. 1. A) Evolution of body weight throughout the experiment for the eight rats with colorectal cancer (CRC) induction in the three cohorts, F = universal feed cohort; FP = pectin + universal feed cohort; FMP = modified pectin + universal feed cohort. Body weight was measured at week 2, 3, 6, 10, 13, 18 and 21. When the animals were sacrificed, the mean value for the F cohort was 378.6 ± 20.4, and 290.7 ± 37, and 321.3 ± 63.2 g for FP and FMP cohorts, respectively. B) Evolution of body weight for the two rat controls (no CRC induction) in the three cohorts. The mean weight when the animals were sacrificed were 398.5 ± 6.4, 338.0 ± 33.9 and 383.5 ± 24.8 g for F, FP and FMP cohorts, respectively. C) Evolution of the intake of the feed by the rats throughout the experiments for the eight CRC rats. D) Intake evolution for the two rat controls (no CRC inducted).

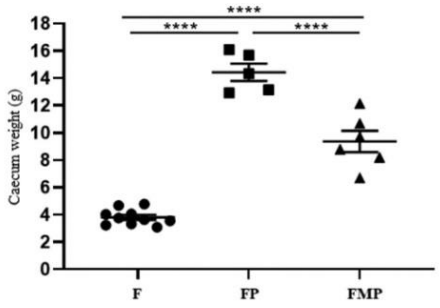

Fig. 2. Mean cecum weight in grams for each cohort (all rats included) in the chemically induced CRC animal model. F = universal feed cohort, FP = pectin + universal feed cohort, FMP = modified pectin + universal feed cohort.

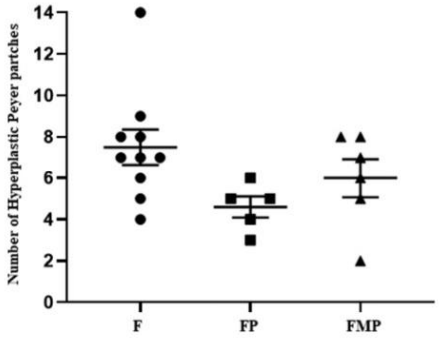

Fig. 3. Mean number of hyperplastic Peyer patches in the small intestine from each cohort (all rats included). Rats from F cohort with CRC induced showed a mean of **7.4** ± **0.9** compared with rat F controls 4.5 ± 0.7. Rats from FP cohort with CRC induced showed values of **4.7** ± **1.5** and 4.5 ± 0.7 for control FP rats. FMP cohort showed values of **5.3** ± **2.5** and 7.5 ± 0.7 for CRC induced and control rats, respectively. In general, no significant differences were observed along all cohorts. F = universal feed cohort, FP = pectin + universal feed cohort, FMP = modified pectin + universal feed cohort.

3.2. Effect of pectin diets on caecum weight

Statistically significant differences in the caecum weight values between the three different cohorts were observed (Fig. 2). Highest weight was detected in the FP cohort (14.4 ± 1.4 g) as compared to FMP (9.4 ± 1.9) and F (3.8 ± 0.6) cohorts.

3.3. Effect of pectin diets on hyperplastic Peyer's patches

The hyperplastic Peyer's patches in the small intestine was quantified when the animals were sacrificed. Peyer's patches contain high amounts of lymphocytes and are located in the mucosa layer of the small intestine. These lymphoid nodules can become hyperplastic and are, therefore, easily visible in the small intestine as rounded, protruding, white 2–3 mm ovals [24].

In this work, differences in the Peyer's patch mean values were not statistically significant between the universal feed cohort and pectin and modified pectin cohorts (Fig. 3).

3.4. Effect of pectin diets on number of polyps and tumour-affected area

After sacrifice, colonic mucosa of each animal was analysed for the number of polyps which diameter ranged from 1 to 10 mm. Statistically differences were not observed in the number of polyps between rats from the different cohorts (Fig. 4A). Moreover, the area of each polyp present in a given colon mucosa was calculated according to its shape and the total polyp area was computed for each animal. Highest tumour area was measured for F cohort (629.1 ± 270) with a reduction of 23.5% in FP cohort and 5% in FMP cohort, respectively; however, these reductions were not statistically significant (Fig. 4B).

3.5. Effect of pectin diets on SCFAs production and blood glucose and triacylglyceride levels

Caecal production of SCFA is important since these compounds show interesting antitumor properties regarding CRC prevention. As it could be expected, acetate, which is the main product of saccharolytic fermentation of polysaccharides, was the highest SCFA detected in all samples (Fig. 5A). F cohort showed the lowest values of acetate (22.6 mM ± 5.5) as compared to FP (33.71 mM ± 7.4) and FMP (35.0 mM ± 6.3), respectively. Slight levels of lactic acid were also detected in all cohorts (0.4 mM ± 0.3; 1.9 mM ± 0.1 and 2.8 mM ± 1.4 for F, FP and FMP, respectively) (Fig. 5B). Although lactate is not a SCFA, it is usually considered in the metabolism of bacteria as a product of saccharolytic

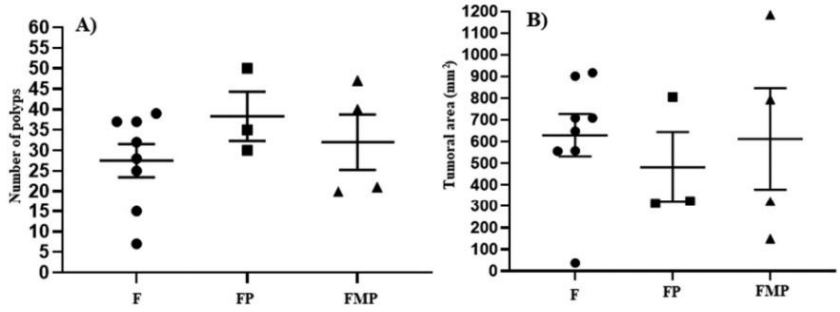

Fig. 4. A) Mean number of colon polyps from each cohort in the animal CRC model (rats 1 to 8 in the three groups). Control rats in each cohort showed zero colon polyps (rats 9 and 10 in each cohort). B) Mean value in mm^2 of the sum of polyp area from all polyps in all rats from each cohort. F = universal feed cohort, FP = pectin + universal feed cohort, FMP = modified pectin + universal feed cohort.

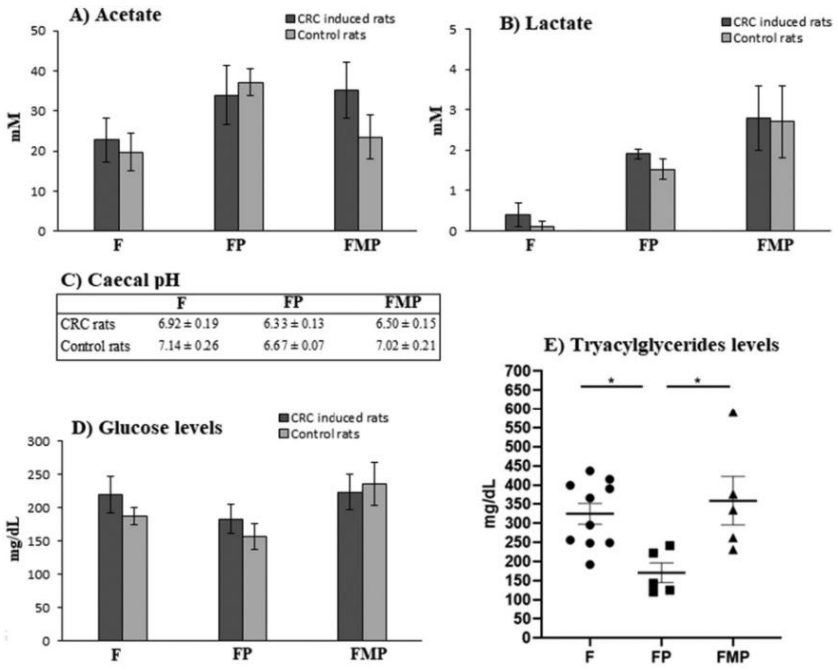

	F	FP	FMP
CRC rats	6.92 ± 0.19	6.33 ± 0.13	6.50 ± 0.15
Control rats	7.14 ± 0.26	6.67 ± 0.07	7.02 ± 0.21

Fig. 5. Caecal concentration of organic acids (A) acetate (B) lactate and pH measured in all three cohorts caecum (C). D) Glucose levels (mg/dL) measured in plasma of individuals in the three cohorts. E) Triacylglycerides levels in plasma for the three cohorts. F = universal feed cohort, FP = pectin + universal feed cohort, FMP = modified pectin + universal feed cohort.

fermentation. Regarding other SCFA, no quantifiably values were found in the samples with the chromatographic method used. In general, total organic acids observed (acetate and lactate) showed an increase in FP and FMP cohorts (in line with the lower pH observed in these groups; 6.33 ± 0.13 and 6.50 ± 0.15, respectively, *vs* F cohort 6.92 ± 0.19; Fig. 5C), although these increases did not show statistically significant differences.

Regarding glucose levels determined in plasma (Fig. 5D), citrus pectin presence in the FP cohort provided lower levels of glucose in the animals, which is in accordance with its relation of a better control of the caloric intake given its high resistance to intestinal digestion. Conversely, FMP, which is mainly composed of oligosaccharides (average Mw = 3.1 kDa) did not show any decrease in the glucose levels compared to the F cohorts. Nevertheless, all variations found in this analysis did not show any statistically significant differences.

Finally, plasma triacylglycerides levels showed a statistically significant reduction of this parameter in FP cohort (170.2 mg/dL ± 25.4) in comparison with F (324.7 mg/dL ± 27.3) and FMP (358.8 mg/dL ± 63.4) (Fig. 5E).

3.6. Effect of pectin diets on intestinal microbiota

Average phyla compositions showed important differences between the three animal cohorts with and without disease (Table 3). At this level, one of the main differences observed was the high increase in *Bacteroidetes* in the FP cohort with respect to F and FMP cohorts in both CRC and healthy rats. No-CRC rats showed higher increases in this phyla compared to CRC rats. Additionally, reduction in the *Firmicutes* levels was found in the FP cohort of CRC rats with respect to the F (20.7%) and FMP (19.9%) groups, where no-CRC animals showed decreases only in FP cohort, in a lesser extent, compared to F cohort (6.9%). Finally, the main difference observed in this level was the important increase in *Proteobacteria* in CRC rats, in FP (14.8%) and FMP (4.3%) groups compared to F group, whereas no-CRC animals showed a reduction of these bacteria, 3.1% and 2.3% reduction for FP and FMP cohorts compared to F, respectively.

At family level (Fig. 6, Table 4), in the F cohort, the most abundant families were *Clostridiaceae* (14.91%), *Lachnospiraceae* (13.60%),

Table 3
Average percentage composition of intestinal microbiota at phylum level for the three cohorts studied for CRC and no-CRC rats.

	CRC rats			No-CRC rats		
Percentage of:	F	FP	FMP	F	FP	FMP
Actinobacteria	0.06	0.27	0.42	0.02	0.18	0.03
Bacteroidetes	29.44	39.32	28.89	32.35	47.09	36.02
Deferribacteres	0.97	0.00	0.00	1.39	0.00	0.00
Firmicutes	51.51	30.78	50.72	42.94	36.02	46.49
Lentisphaerae	0.00	0.26	0.23	0.00	0.10	0.02
Nitrospinae	0.00	0.12	0.03	0.01	0.01	0.00
Proteobacteria	13.16	27.99	17.44	17.25	14.13	14.96
Spirochaetes	0.18	0.00	0.00	1.00	0.00	0.00
Synergistetes	0.06	0.02	0.02	0.10	0.04	0.04
Tenericutes	0.15	0.06	0.17	0.00	0.10	0.01
Verrucomicrobia	4.03	1.08	2.05	4.94	2.18	2.40
Unclasified bacteria	0.01	0.06	0.01	0.00	0.12	0.00
Firmicutes/Bacteroidetes	1.75	0.78	1.76	1.33	0.76	1.29

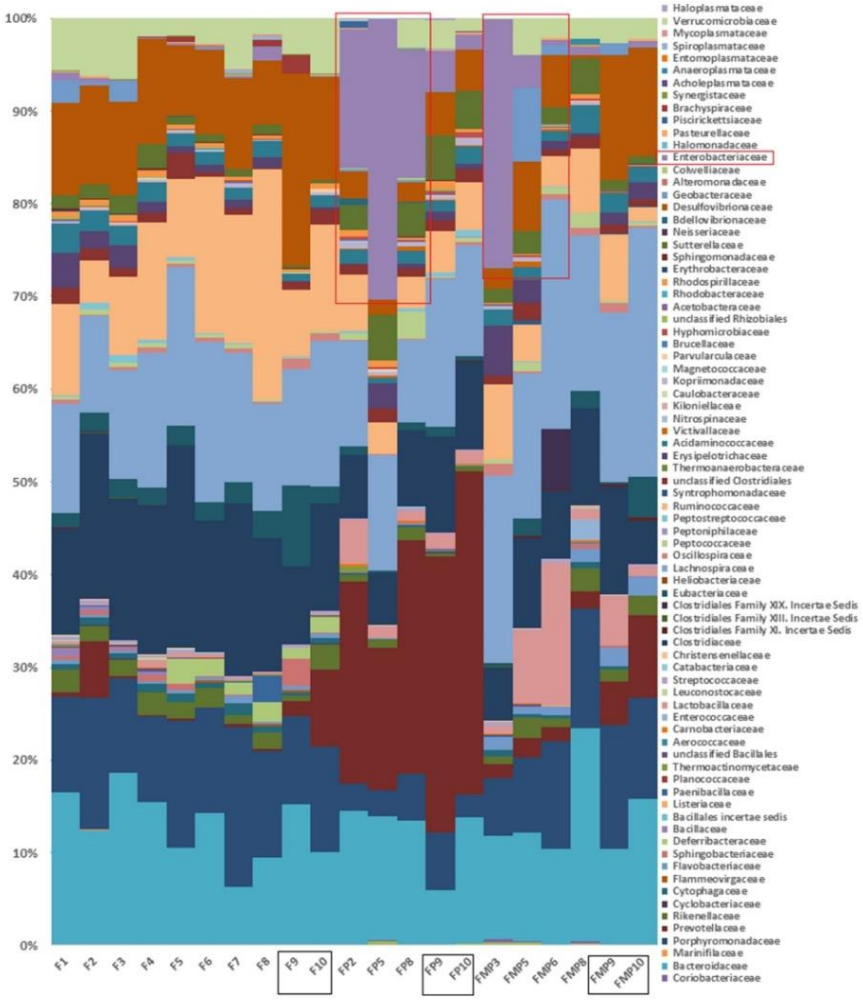

Fig. 6. Intestinal microbiota composition at the family level in rats belonging to all tree cohorts. Rectangles remark results obtained for the no-CRC control rats (black) and the high levels of *Enterobacteria* observed in FP and FMP CRC-rats (red).

Bacteroidaceae (12.78%), *Porphyromonadaceae* (11.86%), *Ruminococcaceae* (11.75%), and *Desulfovibrionaceae* (10.70%). In the case of FP cohort, the most abundant ones were *Prevotellaceae* (25.42%), *Enterobacteriaceae* (13.04%), *Lachnospiraceae* (12.12%), *Bacteroidaceae* (12.08%), and *Clostridiacea* (8.12%). Highest values found in FMP were for *Lachnospiraceae* (20.39%), *Bacteroidaceae* (13.74%), *Porphyromonadaceae* (10.49%), *Clostridiaceae* (8.28%), *Desulfovibrionaceae* (6.85%), *Enterobacteriaceae* (5.37%), *Lactobacillaceae* (5.25%) and *Ruminococcaceae* (5.17%).

At this level, different statistically significant increases can be observed compared to the F cohort. For example, *Lactobacillaceae* increased from 0.27% to 2.01% and 5.25% in FP and FMP cohorts, respectively. *Prevotellaceae* increased from 1.77% to 25.42% in FP group. *Enterobacteriaceae* showed high increase in FP individuals (13.04%) and FMP (5.37%) *vs* 0.35% in F group. *Suterellaceae* increased from 1.12% in F cohort to 4.05% in FP animals. *Lachnospiraceae* family showed an increase in FMP cohort (20.39%) in comparison with F (13.60%) and FP animals (12.12%).

Additionally, significant reductions were observed in *Porphyromonadaceae* (3.91% in FP, 11.86% in F and 10.49% in FMP). *Clostridiaceae* in FP (8.12%) and FMP (8.28%) *vs* 14.91% in F cohort and

Desulfovibrionaceae (3.18%, 6.85% for FP and FMP, *vs* 10.70% for F cohort). *Ruminococcaceae* showed a value of 4.48% in FP, 5.17% in FMP and 11.75% in F cohort (Table 4).

PCA analysis of gut microbiota composition at family level divided the animals in three clusters, indicating differences in the gut microbiota composition associated to these dietary interventions, where F and FMP animals are clustered closer than FP cohort (Fig. 7).

Tables 5 and 1S show the percent abundance of the genera and species with statistically significant differences between the three cohorts in the assay. The main differences are associated with a higher proportion of some genera (such as *Lactobacillus*) in the pectin administration diets (FP, FMP), some of them involved in SCFAs biosynthesis (*Bifidobacterium*, *Paraprevotella*, *Bacteroides*, *Eubacterium*, *Parasutterella*, *Blautia*), and a reduction in the populations of other genera in these cohorts (*Prevotella*, *Clostridium*, *Blautia*), including a significant reduction in some pro-inflammatory genera (*Ruminococcus* and *Bilophila*).

4. Discussion

Potential antitumor effects of commercial citrus pectin (CP) and Modified Citrus Pectin (MCP) were studied in an animal model where CRC was generated using AOM/DSS. Chemical composition of both test substrates demonstrated to be similar regarding the monomeric composition (Table 1). The higher Mw and methylation degree observed in pectin support the highly complex structure of this substrate with a high number of side chains, already observed in previous studies [26], whereas MCP was mainly composed of a galacturonic acid backbone and free mono- and oligosaccharides, showing a lack of methylation degree (0%). Pectin structure provides an important water retention capacity being almost 15-fold higher than that of MCP (10 mL/mg *vs* 0.7 mL/mg). In this sense, pectin, as well as other dietary fibers, is known to impact on satiety and satiation due to its properties of producing viscosity (satiety) and adding bulk to the food (satiation). Pectin has been shown to significantly delay gastric emptying time, hence increasing satiety [27–29], which can explain the lower intake of food observed in the FP cohort (Fig. 1C) and, therefore, the lower body weight observed in all individuals (Fig. 1A), although the important food intake reduction observed at week 6 was also associated to the secondary effects of the ulcerative colitis episode due to DSS administration. Conversely, MCP, with a lower Mw and DM than pectin and similar physicochemical properties to the universal feed regarding water retention capacity, showed higher intake values during the assay (FMP cohort), with almost similar responses to the universal feed individuals (F cohort) (Fig. 1C). In addition, bacterial pectate lyase has shown to hydrolyse preferably low DM pectin structures, such as MCP, contributing, therefore, to their high intake and absorption [7]. Thus, higher body weight was observed in the FMP cohort as compared to pectin being almost as high as the F cohort was.

Regarding glucose content at the end of the study, high plasma levels were observed in F and FMP cohorts (>200 mg/dL) (Fig. 5D), whereas, pectin intake decreased glucose levels showing the lowest values (FP cohort) of all studied groups. The anti-diabetic and hypoglycemic effects of dietary fiber and pectin have been widely reported in previous *in vivo* and *in vitro* studies [30–32]. In this sense, the European Food Safety Authority (EFSA) has recognised a direct cause and effect relationship between the consumption of pectins and a reduction of postprandial glycemic responses in adults [27,33]. Studies with rats have demonstrated the effectiveness of pectin in reducing glucose levels in type 1 and type 2 diabetic rats [34,35]. Conversely, the low Mw carbohydrates composition and low viscosity in FMP produced higher glucose levels, since it has been reported that a reduction in the viscosity of pectins can reduce significantly the effect on postprandial hyperglycaemia [36]. A plausible explanation for this is that glucose intake is reduced

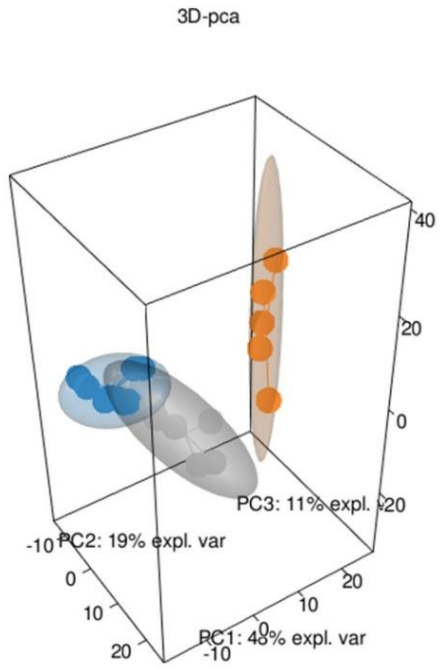

Fig. 7. Gut microbiota PCA cluster analysis, showing that animals belonging to each of the three compared diet cohorts show very distinctive characteristics. Blue dots = universal feed cohort, orange dots = pectin + universal feed cohort, grey dots = modified pectin + universal feed cohort.

Table 4
Average percentage composition of intestinal microbiota at family level for the three cohorts studied.

Percentage of:	F	FP	FMP	F-FP	F-FMP	FP-FMP
Bifidobacteriaceae	0.00	0.17	0.13	**	–	–
Porphyromonadaceae	11.86	3.91	10.49	****	–	***
Prevotellaceae	1.76	25.42	3.44	***	–	–
Rikenellaceae	1.80	0.79	1.64	*	–	–
Cytophagaceae	0.73	0.14	0.42	***	*	–
Flavobacteriaceae	0.40	0.03	1.41	***	*	**
Sphingobacteriaceae	0.56	0.03	0.12	*	–	–
Deferribacteraceae	1.04	0.00	0.00	–	–	*
Paenibacillaceae	0.31	0.00	0.05	–	–	–
Lactobacillaceae	0.27	2.01	5.25	**	**	–
Clostridiaceae	14.91	8.11	8.27	**	**	–
Clostridiales family XI	0.01	0.00	0.14	–	*	*
Eubacteriaceae	2.71	0.69	1.44	*	–	–
Lachnospiraceae	13.60	12.12	20.39	–	**	**
Oscillospiraceae	0.49	0.17	0.69	–	–	*
Ruminococcaceae	11.75	4.48	5.17	*	*	–
Victivallaceae	0.00	0.19	0.15	**	–	–
Kopriimonadaceae	0.16	0.43	0.16	*	–	*
Hyphomicrobiaceae	0.06	0.31	0.10	**	–	–
Rhodospirillaceae	0.49	0.54	0.16	–	*	*
Suterellaceae	1.12	4.05	1.89	****	–	**
Bdellovibrionaceae	0.03	0.15	0.00	–	*	–
Desulfovibrionaceae	10.70	3.17	6.84	**	–	–
Enterobacteriaceae	0.34	13.04	5.36	**	–	–
Verrumicrobiaceae	4.21	1.54	2.16	*	–	–

* Indicate statistically significant differences between each pairs of compared cohorts.

Table 5
Caecal microbiota composition (percentages) at the genus and species levels where statistically significant differences observed are marked as (*).

Genus	Species	F	FP	FMP	F-FP	F-FMP	FP-FMP
Bifidobacterium		0.000	0.174	0.135	**		
	animalis	0.000	0.090	0.007	*		
Bacteroides	*acidifaciens*	1.420	0.514	0.000		***	
	eggerthii	0.050	0.290	1.053		*	
	vulgatus	0.710	0.050	0.217	*		
Butyricimonas		0.342	0.138	0.278	*		
	virosa	0.157	0.048	0.090	**		
Parabacteroides		1.357	0.570	2.210			*
	merdae	0.200	0.116	0.662		**	**
Paraprevotella		0.001	0.306	0.358	**	**	
Prevotella		0.004	2.302	1.692	**		
Alistipes	*sp.*	0.072	0.010	0.158			*
Mucispirillum		1.049	0.000	0.000		*	
	schaedleri	1.049	0.000	0.000		*	
Lactobacillus		0.004	0.704	0.620	**	**	
Clostridium		4.296	3.000	2.643		*	
Eubacterium		0.015	0.274	0.055	*		
Anaerostipes		0.492	0.004	0.020	**	*	
Blautia		0.429	0.166	1.115			*
	producta	0.316	0.086	0.858			**
Dorea		0.145	0.008	0.037	*		
	Dorea	0.145	0.008	0.037	*		
Lachnoclostridium	*bolteae*	0.003	0.000	0.360		*	**
Stomatobaculum		0.195	0.000	0.007	**	**	
	longum	0.195	0.000	0.007	**	**	
Faecalibacterium	*prausnitzii*	1.345	0.338	0.565	**	*	
Ruminiclostridium		0.152	0.016	0.005	*	**	
Ruminococcus		2.503	0.342	0.242	*	**	
Bacteroides		0.000	0.366	0.000	***		***
Turicibacter		0.030	0.148	0.000			**
Victivallis		0.003	0.196	0.155	**		
	vadensis	0.003	0.196	0.155	**		
Parasutterella		1.123	4.058	1.895	****		**
	excrementihominis	1.026	3.370	1.657	****		**
Bilophila		9.832	3.042	6.687	*		
	wadsworthia	7.635	2.260	2.735	**	**	
Escherichia		0.004	0.552	0.197	**		
	coli	0.004	0.532	0.195	**		
Akkermansia		4.208	1.518	2.165	*		
	muciniphila	4.208	1.518	2.165	*		

with a high viscosity possibly due to a combination of delayed gastric emptying, reducing macronutrient absorption and preventing diffusion of glucose through the lumen to the epithelium [37,38]. In the same sense, plasma triacylglycerides showed a statistically significant reduction in the case of pectin cohort (FP) in comparison with the two other cohorts (Fig. 5E), due to a similar positive effect.

At the end of the experiment, all surviving animals were sacrificed. It has to be noted that FP diet caused the death of five CRC rats and four rats did not survive in the FMP cohort, whereas CRC control cohort rats (F) did not show any mortality. One possible explanation to this is the fact that these two diets based on pectins, caused a dysbiosis at the intestinal microbiota level, with higher percentages of pro-inflammatory taxons, especially in the *Proteobacteria* phylum, which was not observed in the no-CRC rats (Table 3). This dysbiosis is more extreme in the FP cohort (Fig. 7), where more animals' deaths took place, and also it took place during the first DSS challenge. However, dysbiosis in the FMP cohort is less accentuated and these animals' deaths took place closer to the last experimental weeks. DSS challenges are helpful for induction of a stronger CRC phenotype due to its ability to cause ulcerative colitis as pro-inflammatory trigger of CRC. This ulcerative colitis increases the intestinal permeability, enhancing the transfer of bacterial cells from lumen to intestinal submucosa tissue, inducing a pro-inflammatory status; and in FP and FMP animals this higher permeability is probably increasing the presence in intestinal submucosa of highly pro-inflammatory taxons (such as *E. coli*) (Tables 5, 1S, Fig. 6). Remarkably, those rats fed with either pectin or modified citrus pectin but that were also kept free of CRC induction did not exhibit any increase in pro-inflammatory taxons. In a mouse model, virulent *E. coli* was accumulated after antibiotic treatment and can disseminate systematically when the intestinal epithelial barrier is breached by DSS, thereby inducing lethal inflammasome activation [39]. In a similar way, DSS-induced intestinal inflammation markedly increased the proliferation of *Citrobacter rodentium* in the intestine [40]. Thus, the reduced barrier function, as could be taking place in our study, would enable more interaction with the epithelium, resulting in an increased delivery of mutagenic and/or proinflammatory metabolites produced by *Enterobacteriaceae* [41,42].

To assess the effect of the pectin diets on CRC, histological parameters such as caecum weight, number of hyperplastic Peyer's patches, number of colon tumours, and total tumour area in the colon mucosa were measured.

Caecum weight was significantly increased in individuals from FP cohort, and, to a lesser extent, in the FMP animals (Fig. 2). This effect could be ascribed to a higher stimulation of bacterial cell growth [43] in the case of pectin. However, the most plausible cause may be the physicochemical properties of pectin, such as the high viscosity, water retention capacity and bulking properties, which are higher in pectin in comparison with MCP [28].

Concerning hyperplastic Peyer's patches, no statistically significant differences were found between all three cohorts (Fig. 3). Peyer's patches are abundant in lymphocytes and become hyperplastic when alterations in the digestive tract, which affect the animal's immune condition, take place, as may occur in response to some chemicals, pathogens or toxins [44,45]. This parameter has been used as a marker of the general pro-inflammatory condition of the small intestine mucosa in all individuals in response to the CRC induction treatment [43,46].

However, in our case, the absence of significant differences revealed that pectin does not affect the presence of these mucosal structures in the experimental model used.

Regarding the last histological parameters measured, number of colon tumours and the total tumour area in the colon mucosa (Fig. 4), any significant difference between all cohorts were found.

The limited available *in vivo* information on the effect of citrus pectin on CRC and the contradictory results makes it difficult to elucidate the mechanism of action of these substrates, where most studies have been carried out in *in vitro* assays [8,47,48]. However, there are *in vivo* reports that do not support the chemopreventive effect of these pectins in line with our work. Jacobs et al. reported that different fiber such as oat bran, guar and citrus pectin could increase by 4.5 to 5 times the yield of proximal colonic adenocarcinomas, providing stimulus to cell proliferation in a 1,2-dimethylhydrazine (DMH) colonic cancer model in rats [6]. These authors attributed that a reduction in colonic luminal pH, similar to the observed in our work (≥0.3), while not providing any protection, may even enhance colon tumorigenesis. In addition, Jacobasch et al. found that citrus pectins (with high and low methylation degree, 70% and 37%, respectively) did not inhibit tumorigenesis regardless their DM in $APC^{Min/+}$ mice [7]. Moreover, those pectins seemed even to accelerate CRC carcinogenesis since all polyps found in pectin-fed animals were large adenocarcinomas whereas only 80% in control diet mice were large adenocarcinomas. As basic requirements for colorectal anticarcinogenic effect can be a sufficient high fermentative butyrate production and an adequate butyrate absorption. These authors attributed this behaviour to an insufficient butyrate supply, since fermentation of pectin delivered only low amounts of butyrate. This might lead to a deficient energy metabolism and an ineffective function of butyrate as a promoter of normal cell differentiation and inducer of apoptosis in tumour cells, which could also explain the obtained results in the present study.

Thus, changes in the luminal pH may affect the uptake of luminal compounds by colonocytes and their action on these cells; increasing tumorigenesis as observed in our results [49]. Decreases in the pH could increase hydrogen sulphide concentrations (pKa = 7.04) [50], which easily penetrates the biological membrane amplifying its deleterious and pro-inflammatory effect on colonocytes respiration at excessive concentration [51]. Moreover, modification of the luminal pH *per se* may affect colonic epithelial cell physiology where lower colonic luminal pH in patients with ulcerative colitis has been observed as compared to healthy patients [52]. Low external pH has been shown to dramatically increase the expression of p-glycoproteins, related with multidrug resistance, in human colon carcinoma cell lines [53], rendering these cells more resistant to chemotherapeutic agents.

Interestingly, an evaluation of the abilities to prevent colorectal cancer of different dietary fiber in an AOM rat model showed that pectin from green cincau (*Premna oblongifolia* Merr.) was able to increase butyrate levels, however, no antiproliferative properties were observed [9]. Despite the SCFA stimulation, feeding with pectin led to an increase in proliferation within the colon and an increase in preneoplastic lesions, thus, appeared to be acting more like a pro-carcinogen. These authors maintained that it was possible that more pectin (>5%) needed to be consumed by rats to act as a protective, which was not confirmed in our work (20%), or that pectin may need to be delivered with other nutrients or fiber source to be protective in AOM/DSS models as observed in other studies [54,55].

Analyses of organic acids showed important differences in acetate levels, as well in lactic acid amounts (Fig. 5A and B). Acetate has been previously reported as the main SCFA from pectin structures fermentation [56]. The high presence of this metabolite can be justified due to that acetate is generated by many bacterial groups that inhabit the colon, with approximately one-third of the product coming from reductive acetogenesis [57,58]. Absence of propionic and butyric acids in our study is in line with the no protective effect against tumorigenesis observed, since the presence of these metabolites have been widely correlated with the inhibition of growth of different CRC lines, induction of apoptosis of tumour cells and enhancement of anti-inflammatory properties [4,8,59], whereas low levels of these metabolites can increase the risks of CRC and inflammatory gut diseases [7,60,61]. Moreover, in line with our results, elevated concentrations of luminal lactic acid have been reported in active colitis and CRC cases [62,63], a factor that could explain again that more animals died in our study during DSS challenges.

Analysis of microbiota of survival animals at phylum level showed significant differences between FP cohort *versus* F and FMP cohorts (Table 3). The *Firmicutes*/*Bacteroidetes* coefficient, which has been described as a parameter associated with obesity and type II diabetes [64,65], was reduced in FP (0.78) when compared to F and FMP cohorts (1.75 and 1.76, respectively), due to the increase in *Bacteroidetes* and diminution in *Firmicutes*, supporting the hypoglycemic effect of high Mw citrus pectin.

Higher *Bacteroidetes* population in FP was mainly produced due to the significant increase in *Prevotellaceae* family (Fig. 6, Table 4). Species within genera *Bacteroides* and *Prevotella* are the primary pectin-degraders, possessing carbohydrate-active enzymes (CAZymes) within the polysaccharide utilization loci [66–68]. However, the decrease in families, such as *Porphyromonadaceae*, observed in FP cohort might contribute to the absence of propionate production since these families contain numerous genera involved in propionate production [4]. The marked reduction in *Firmicutes* phylum was mainly produced by the decrease of the *Ruminococcaceae*, *Clostridiaceae* and *Eubacteriaceae* families, as it was observed in previous *in vitro* studies with pectin [26,69]. The reduction observed in *Faecalibacterium* genus (especially *F. prausnitzii*, *Ruminococcaceae* family) could also contribute to the low anticarcinogenic properties observed in pectins cohorts, since its presence has been related with anti-inflammatory properties and it is described as a key bacteria species in promoting health [69,70].

Strikingly, a massive increase in *Proteobacteria* phylum was also observed in FP cohort due to the increase in *Enterobacteriaceae* family (13.04%) (Fig. 6). This family did not show any increase in a previous *in vitro* study with the same pectin [69]. Higher *Proteobacteria* populations and, particularly, *Enterobacteriaceae* family (including *E. coli*) are found in the gut microbiota of patients with IBD, which is a known risk factor for CRC [71]. In this sense, generally recognised pathogenic species, such as *E. coli*, *Salmonella* and *Serratia* increased in FP cohort compared to F cohort. This dysbiotic status has been correlated with various immune, metabolic and neurological disorders, in both intestinal and extra-intestinal sites [72]. As a consequence, susceptibility to enteric infection can be markedly increased. *Salmonella enterica* for example, poorly colonize the mouse intestine in the presence of commensal microbiota, however, it can proliferate and induce inflammation if the resident bacterial community is disrupted [73]. Thus, the presence of inflammation or an altered bacterial community facilitates the overgrowth of potentially harmful bacteria by decreasing the production of protective mucins and antimicrobial peptides.

In contrast, certain beneficial effect can also be identified when pectin is present such as the reduction of *Desulfovibrionaceae* family (*Proteobacteria* phylum), whose high levels have been associated with damages at the mucosal level caused by reduction of the mucin barrier [74].

High levels of *Prevotellaceae* family, as observed in our study in the FP cohort (25.42%) (Table 4), have also been associated in some studies with a healthier status [75,76]. In this study, it has been also observed a significant increase in *Bifidobacteriaceae* family (*Actinobacteria* phylum) in both FP and FMP cohorts, mainly due to the increase of *Bifidobacterium*; as well as in *Lactobacillaceae* family (*Lactobacillus* genus, *Firmicutes* phylum). Both families have been associated to several health benefits [72,77,78].

5. Conclusions

No previous studies have been carried out on the evaluation of the potential anticarcinogenic properties of citrus pectin and modified citrus pectin in *in vivo* models based on the use of azoxymethane/dextran sodium sulfate (AOM/DSS) to induce colorectal cancer in rats. Neither citrus pectin nor modified citrus pectin tested were able to inhibit tumorigenesis in this rat model. Of special relevance is the effect found in the intestinal microbiota. Strikingly, both pectins, particularly citrus pectin, seemed to induce a decrease of luminal pH of caecum and a huge dysbiosis degree in the CRC rats at the intestinal microbiota level, leading towards a potential proinflammatory status, even causing the death of five and four animals (of a total of eight) in pectin and modified pectin cohorts, respectively. Thus, a high increase in *Proteobacteria* (proinflammatory bacteria) and a reduction in *Faecalibacterium* genus were observed mainly in the former. These results were in line with the absence of butyric and propionic acids and the levels of lactic and acetic acid. On the other hand, citrus pectin demonstrated an important impact in the decrease of glucose and triacylglycerides in plasma, probably related to the lower feeding and body weight as compared to modified citrus pectin and universal feed cohorts. These results agree to the low *Bacteroidetes/Firmicutes* ratio. Citrus pectin and modified citrus pectin also demonstrated to stimulate the growth of other positive bacteria such as *Prevotellaceae, Bifidobacteriaceae and Lactobacillaceae* families. Summing up, the consumption of pectin such as citrus pectin and modified citrus pectin could not be beneficial in an inflammatory-tumour status due to an important worsening of the pathology related to a severe unbalance of the intestinal microbiota. However, in a status of health, these pectins have relevant benefits not only in the gut but also at systemic level. Although the results obtained under the conditions assayed in this investigation seems to indicate the ineffectiveness of commercial citrus pectin and modified citrus pectin to exert a benefit in the prevention of CRC, more research is needed with other animal models in order to understand the intricate behaviour of this polysaccharide in this severe pathology.

Supplementary data to this article can be found online at https://doi.org/10.1016/j.ijbiomac.2020.11.089.

Acknowledgements

Authors acknowledge the finance of this work by the Spanish Ministry of Economy, Industry and Competitiveness (Projects AGL2017-84614-C2-1-R and AGL2014-53445-R) and to the *Programa de Ayudas a Grupos de Investigación del Principado de Asturias* (IDI/2018/000120, Spain). Authors wish to thank Servicios Científico Técnicos from the University of Oviedo (Environmental Assays Unit, Sequencing Unit) and Biostatistical Unit from ISPA (Spain).

CRediT authorship contribution statement

Alvaro Ferreira-Lazarte: Conceptualization, Methodology, Investigation; Writing- Original draft preparation.
Javier Fernández: Conceptualization, Methodology, Investigation.
Pablo Gallego-Lobillo: Methodology, Data Curation.
Claudio J. Villar, Felipe Lombó, F. Javier Moreno: Reviewing.
Mar Villamiel: Writing- Reviewing and Editing.

References

[1] F. Bray, J. Ferlay, I. Soerjomataram, R.L. Siegel, L.A. Torre, A. Jemal, CA Cancer J. Clin. 68 (2018) 394–424.
[2] C.K.H. Wong, C.L.K. Lam, J.T.C. Poon, S.M. McGhee, W.L. Law, D.L.W. Kwong, J. Tsang, P. Chan, J. Eval. Clin. Pract. 18 (2012) 1203–1210.
[3] M. C. Wong, J. Huang, V. Lok, J. Wang, F. Fung, H. Ding and Z.-J. Zheng, Clin. Gastroenterol. Hepatol. DOI:https://doi.org/10.1016/j.cgh.2020.02.026.
[4] P. Louis, G.L. Hold, H.J. Flint, Nat. Rev. Microbiol. 12 (2014) 661–672.
[5] E.G. Maxwell, N.J. Belshaw, K.W. Waldron, V.J. Morris, Trends Food Sci. Technol. 24 (2012) 64–73.
[6] L.R. Jacobs, J.R. Lupton, Cancer Res. (1986) 1727–1734.
[7] G. Jacobasch, G. Dongowski, S. Florian, K. Müller-Schmehl, B. Raab, D. Schmiedl, J. Agric. Food Chem. 56 (2008) 1501–1510.
[8] W. Zhang, P. Xu, H. Zhang, Trends Food Sci. Technol. 44 (2015) 258–271.
[9] S.U. Nurdin, R.K. Le Leu, A. Aburto-medina, G.P. Young, J.C.R. Stangoulis, A.S. Ball, C.A. Abbott, Int. J. Mol. Sci. 19 (2018) 2593.
[10] F.R.B. Marenda, F. Mattioda, I.M. Demiate, A. de Francisco, C.L. de Oliveira Petkowicz, M.H.G. Canteri, R.D. de Mello Castanho Amboni, J. Polym. Environ. 27 (2019) 549–560.
[11] V.V. Glinsky, A. Raz, Carbohydr. Res. 344 (2009) 1788–1791.
[12] V.J. Morris, N.J. Belshaw, K.W. Waldron, E.G. Maxwell, Bioact. Carbohydrates Diet. Fibre 1 (2013) 21–37.
[13] L. Ai, Y.C. Chung, S.Y. Lin, K.C. Lee, P.F.H. Lai, Y. Xia, G. Wang, S.W. Cui, Food Hydrocoll. 83 (2018) 239–245.
[14] S.B.R. do Prado, T.M. Shiga, Y. Harazono, V.A. Hogan, A. Raz, N.C. Carpita, J.P. Fabi, Carbohydr. Polym. 211 (2019) 141–151.
[15] F. Odun-Ayo, J. Mellem, L. Reddy, Food Sci. Technol. 37 (2017) 478–482.
[16] H. Ohkami, K. Tazawa, I. Yamashita, T. Shimizu, K. Murai, K. Kobashi, M. Fujimaki, Japanese J. Cancer Res. 86 (1995) 523–529.
[17] P. Nangia-Makker, V. Hogan, Y. Honjo, S. Baccarini, L. Tait, R. Bresalier, A. Raz, J. Natl. Cancer Inst. 94 (2002) 1854–1862.
[18] K. M. Brobst and C. E. Lott Jr, Cereal Chem., 1966, 43, 35–43.
[19] N. Muñoz-Almagro, F. Rico-Rodriguez, M. Villamiel, A. Montilla, Food Chem. 252 (2018) 271–276.
[20] N. Muñoz-Almagro, A. Montilla, F.J. Moreno, M. Villamiel, Ultrason. Sonochem. 38 (2017) 807–819.
[21] C.F. Chau, Y.L. Huang, J. Agric. Food Chem. 51 (2003) 2615–2618.
[22] J. Fernández, F.J. Moreno, A. Olano, A. Clemente, C.J. Villar, F. Lombó, Front. Microbiol. 9 (2018) 1–14.
[23] N. Joseph, K. Vasodavan, N.A. Saipudin, B.N.M. Yusof, S. Kumar, S.A. Nordin, J. Funct. Foods 57 (2019) 103–111.
[24] J. Fernández, L. García, J. Monte, C. J. Villar and F. Lombó, Genes (Basel)., DOI:https://doi.org/10.3390/genes9030133.
[25] J. Fernández, V.G. De Fuente, M.T.F. García, J.G. Sánchez, B.I. Redondo, Lipids Health Dis. 19 (2020) 1–19.
[26] A. Ferreira-Lazarte, V. Kachrimanidou, M. Villamiel, R.A. Rastall, F.J. Moreno, Carbohydr. Polym. 199 (2018) 482–491.
[27] A. Mortensen, F. Aguilar, R. Crebelli, A. Di Domenico, B. Dusemund, M.J. Frutos, P. Galtier, D. Gott, U. Gundert-Remy, C. Lambré, J. Leblanc, O. Lindtner, P. Moldeus, P. Mosesso, A. Oskarsson, D. Parent-Massin, I. Stankovic, I. Waalkens-Berendsen, M. Wright, M. Younes, P. Tobback, S. Ioannidou, S. Tasiopoulou, R.A. Woutersen, EFSA J. 15 (2017) 4866.
[28] S. Christiaens, S. Van Buggenhout, K. Houben, Z. Jamsazzadeh Kermani, K.R.N. Moelants, E.D. Ngouémazong, A. Van Loey, M.E.G. Hendrickx, Crit. Rev. Food Sci. Nutr. 56 (2016) 1021–1042.
[29] C.D.I. Lorenzo, C.M. Williams, J.E. Valenzuela, Nutr. Rev. 47 (1989) 268–270.
[30] J. Cui, X. Gu, Q. Zhang, Y. Ou, J. Wang, Food Funct. 6 (2015) 1635–1642.
[31] Q. Chen, L. Zhu, Y. Tang, Z. Zhao, T. Yi and H. Chen, Ann. N. Y. Acad. Sci., 2017, 1–15.
[32] G. Grunberger, K.-L.C. Jen, J.D. Artiss, Diabetes Metab. Res. Rev. 32 (2014) 13–23.
[33] European Food Safety Authority, EFSA J. 8 (2010) 1462.
[34] Y. Liu, M. Dong, Z. Yang, S. Pan, Int. J. Biol. Macromol. 89 (2016) 484–488.
[35] D.C. Silva, A.L.P. Freitas, C.D.S. Pessoa, R.C.M. Paula, J.X. Mesquita, L.K.A.M. Leal, G.A.C. Brito, D.O. Gonçalves, G.S.B. Viana, J. Med. Food 14 (2011) 1118–1126.
[36] S.L. Brenelli, S.D.S. Campos, M.J.A. Saad, Brazilian J. Med. Biol. Res. 30 (1997) 1437–1440.
[37] S. Ou, K. Kwok, Y. Li, L. Fu, J. Agric. Food Chem. 49 (2001) 1026–1029.
[38] M.O. Weickert, A.F.H. Pfeiffer, J. Nutr. 138 (2008) 439–442.
[39] J.S. Ayres, N.J. Trinidad, R.E. Vance, C. Biology, Nat. Med. 18 (2012) 799–806.
[40] N. Kamada, Y.-G. Kim, H.P. Sham, B.A. Vallance, J.L. Puente, E.C. Martens, G. Núñez, Science (80). 336 (2012) 1325–1329.
[41] T. Secher, A. Samba-louaka, E. Oswald, J. Nougayrède, PLoS One 8 (2013) 1–17.
[42] J.C. Arthur, E. Perez-chanona, M. Mühlbauer, S. Tomkovich, J.M. Uronis, T. Fan, B.J. Campbell, T. Abujamel, B. Dogan, A.B. Rogers, J.M. Rhodes, A. Stintzi, K.W. Simpson, J. Jonathan, T.O. Keku, A.A. Fodor, C. Jobin, Science (80). 338 (2013) 120–123.
[43] J. Fernández, E. Ledesma, J. Monte, E. Millán, P. Costa, V.G. de la Fuente, M.T.F. García, P. Martínez-Camblor, C.J. Villar, F. Lombó, Sci. Rep. 9 (2019) 1–17.
[44] S. Mishra, A. Tripathi, B.P. Chaudhari, P.D. Dwivedi, H.P. Pandey, M. Das, Toxicol. Appl. Pharmacol. 279 (2014) 186–197.
[45] M. Bailey, F.J. Plunkett, H. Rothkötter, K. Haverson, C.R. Stokes, Proc. Nutr. Soc. 2001 (60) (2001) 427–435.
[46] C. Jung, J. Hugot, Int. J. Inflam (2010) 1–12.
[47] L. Ai, Y. Chung, S. Lin, K. Lee, P.F. Lai, Y. Xia, G. Wang, S.W. Cui, Food Hydrocoll. 83 (2018) 239–245.
[48] H. Cheng, S. Li, Y. Fan, X. Gao, M. Hao, J. Wang, X. Zhang, G. Tai, Y. Zhou, Med. Oncol. 28 (2011) 175–181.
[49] F. Blachier, M. Beaumont, M. Andriamihaja, A.M. Davila, A. Lan, M. Grauso, L. Armand, R. Benamouzig, D. Tomé, Am. J. Pathol. 187 (2017) 476–486.
[50] F. Blachier, A.M. Davila, S. Mimoun, P.H. Benetti, C. Atanasiu, M. Andriamihaja, R. Benamouzig, F. Bouillaud, D. Tomé, Amino Acids 39 (2010) 335–347.
[51] S. Mimoun, M. Andriamihaja, C. Chaumontet, C. Atanasiu, R. Benamouzig, J.M. Blouin, D. Tomé, F. Bouillaud, F. Blachier, Antioxid. Redox Signal. 17 (2012) 1–10.
[52] S. Nugent, D. Kumar, D. Rampton, D. Evans, Gut 48 (2001) 571–577.
[53] L.Y. Wei, P.D. Roepe, Biochemistry 33 (1994) 7229–7238.
[54] Y. Cho, N.D. Turner, L.A. Davidson, R.S. Chapkin, R.J. Carroll, J.R. Lupton, Exp. Biol. Med. 237 (2012) 1387–1393.

[55] F. Odun-ayo, J. Mellem, T. Naicker, L. Reddy, Anticancer Res. 4776 (2015) 4765–4775.
[56] B. Gómez, B. Gullón, R. Yáñez, H. Schols, J.L. Alonso, J. Funct. Foods 20 (2016) 108–121.
[57] T. L. Miller and M. J. Wolin, 1996, 62, 1589–1592.
[58] J. Fernández, S. Redondo-Blanco, I. Gutiérrez-del-Río, E.M. Miguélez, C.J. Villar, F. Lombó, J. Funct. Foods 25 (2016) 511–522.
[59] H. Zeng, World J. Gastrointest. Oncol. 6 (2014) 41–51.
[60] D.L. Topping, P.M. Clifton, Physiol. Rev. 81 (2001) 1031–1064.
[61] A. Wächtershäuser, J. Stein, Eur. J. Nutr. 39 (2000) 164–171.
[62] A.H. Uga, P. Loganathan, A. Habeeb, M. Oyeka, Ann. Clin. Case Reports 4 (2019) 3–4.
[63] H. Hove, P.B. Mortensen, Dig. Dis. Sci. 40 (1995) 1372–1380.
[64] C. De Filippo, D. Cavalieri, M. Di, M. Ramazzotti, J. Baptiste, Proc. Natl. Acad. Sci. 107 (2010) 14691–14696.
[65] R.E. Ley, P.J. Turnbaugh, S. Klein, J.I. Gordon, Nature 444 (2006) 1022–1023.
[66] N. Larsen, C. Bussolo de Souza, L. Krych, T. Barbosa Cahú, M. Wiese, W. Kot, K.M. Hansen, A. Blennow, K. Venema, L. Jespersen, Front. Microbiol. 10 (2019) 1–13.
[67] H.J. Flint, K.P. Scott, S.H. Duncan, P. Louis, E. Forano, Gut Microbes 3 (2012) 289–306.
[68] E.C. Martens, E.C. Lowe, H. Chiang, N.A. Pudlo, M. Wu, P. Nathan, D.W. Abbott, B. Henrissat, H.J. Gilbert, D.N. Bolam, J.I. Gordon, PLoS Biol. 9 (2011) 1–16.
[69] A. Ferreira-Lazarte, F.J. Moreno, C. Cueva, I. Gil-Sánchez, M. Villamiel, Carbohydr. Polym. 207 (2019) 382–390.
[70] S. Miquel, R. Martín, O. Rossi, L.G. Bermúdez-Humarán, J.M. Chatel, H. Sokol, M. Thomas, J.M. Wells, P. Langella, Curr. Opin. Microbiol. 16 (2013) 255–261.
[71] I. Mukhopadhya, R. Hansen, E. M. El-omar and G. L. Hold, Nat. Rev. Gastroenterol. Hepatol., DOI:https://doi.org/10.1038/nrgastro.2012.14.
[72] G.P. Donaldson, S.M. Lee, S.K. Mazmanian, Nat. Rev. Microbiol. 14 (2016) 20–32.
[73] K. Endt, B. Stecher, S. Chaffron, E. Slack, N. Tchitchek, A. Benecke, K. Endt, L. Van Maele, J. Sirard, A.J. Mueller, M. Heikenwalder, J. Andrew, R. Strugnell, C. Von Mering, W. Hardt, PLoS Pathog. 6 (2010) 1–18.
[74] H. Song, W. Wang, B. Shen, H. Jia, Z. Hou, P. Chen, Y. Sun, Cancer Sci. (2018) 666–677.
[75] B. Flemer, M. Herlihy, M.O. Riordain, Gut Microbes 0 (2018) 1–5.
[76] C. Ferrario, R. Statello, L. Carnevali, L. Mancabelli, C. Milani, M. Mangifesta, S. Duranti, G.A. Lugli, B. Jimenez, S. Lodge, A. Viappiani, G. Alessandri, M.D. Asta, D. Del Rio, A. Sgoifo, D. Van Sinderen, M. Ventura, F. Turroni, Front. Microbiol. 8 (2017) 1–11.
[77] C.M. Guinane, P.D. Cotter, Ther. Adv. Gastroenterol. Rev. (2013) 295–308.
[78] P. Louis, S.H. Duncan, Nat. Rev. Gastroenterol. Hepatol. 9 (2012) 577–589.

JOURNAL OF AGRICULTURAL AND FOOD CHEMISTRY

pubs.acs.org/JAFC Article

Enzymatic Synthesis and Structural Characterization of Novel Trehalose-Based Oligosaccharides

Pablo Gallego-Lobillo, Elisa G. Doyagüez, María Luisa Jimeno, Mar Villamiel,* and Oswaldo Hernandez-Hernandez

Cite This: *J. Agric. Food Chem.* 2021, 69, 12541−12553 Read Online

ACCESS | Metrics & More | Article Recommendations | Supporting Information

ABSTRACT: Trehalose, α-D-glucopyranosyl-(1↔1)-α-D-glucopyranoside, is a disaccharide with multiple effects on the human body. Synthesis of new trehalose derivatives was investigated through transgalactosylation reactions using β-galactosidase from four different species. β-galactosidases from *Bacillus circulans* (*B. circulans*) and *Aspergillus oryzae* (*A. oryzae*) were observed to be the best biocatalysts, using lactose as the donor and trehalose as the acceptor. Galactosyl derivatives of trehalose were characterized using nuclear magnetic resonance spectroscopy. Trisaccharides were the most abundant oligosaccharides obtained followed by the tetrasaccharide fraction (19.5% *vs* 8.2% carbohydrates). Interestingly, the pentasaccharide [β-Galp-(1→4)]^3-trehalose was characterized for the first time. Greater oligosaccharide production was observed using β-galactosidase from *B. circulans* than that obtained from *A. oryzae*, where the main structures were based on galactose monomers linked by β-(1→6) and β-(1→4) bonds with trehalose in the ending. These results indicate the feasibility of commercially available β-galactosidases for the synthesis of trehalose-derived oligosaccharides, which might have functional properties, excluding the adverse effects of the single trehalose.

KEYWORDS: *trehalose, oligosaccharide, β-galactosidase, prebiotic, transgalactosylation, GOS*

1. INTRODUCTION

Trehalose, α-D-glucopyranosyl-(1↔1)-α-D-glucopyranoside, is a nonreducing disaccharide with a wide range of applications as a food additive as well as in cosmetics and pharmaceutical sciences.[1,2] Trehalose can be found in multiple sources such as invertebrates, fungi, and bacteria, holding a protective function against dryness and stress.[1,3] This disaccharide was generally recognized as safe (GRAS) in 2000 by the Food & Drug Administration (FDA, USA), with an equivalent sweetness of 45% sucrose and being mainly used in the food industry as a sweetener, stabilizer, and moisturizer.[4] In this context, it is important to emphasize its high stability in terms of temperature and pH. In addition, its α-bond is not hydrolyzed by the pancreatic α-amylase, and it has considerable resistance to acids.[5,6]

Multiple functionalities of trehalose such as a decrease in the postprandial glucose level,[7,8] improvement of the insulin resistance,[8,9] prevention of adipocyte hypertrophy,[9,10] suppression of bone resorption,[11] and induction of autophagy[12] have been reported. Regarding the latter, it is of paramount importance in the case of neurodegenerative and metabolic diseases. Autophagy is a conserved degradation mechanism of the cell, which can be regulated by trehalose, due to the chemical chaperone properties.[6,13] This fact opens a new field in the development of some rare diseases, such as Huntington's and Parkinson's diseases.[14−16] Furthermore, the latest studies have found promising results of trehalose in amyotrophic lateral sclerosis (ALS).[17] All these beneficial properties occur in response to its absorption in the small intestine and then the transport to the target organs through the bloodstream.[6,14]

Enzymatic complexes of disaccharidases are placed in the brush border membranes of the enterocytes, including the enzyme trehalase, which hydrolyzes the trehalose into two molecules of glucose.[18] The content of trehalase in the small intestine is lower than other small-intestinal disaccharidases,[19] and a considerable amount of the disaccharide (~75 g) is necessary to observe a real benefit in the organism.[20,21] Then, a substantial quantity of the saccharide might not be hydrolyzed or absorbed in the small intestine, and therefore, it would reach the colon. This fact could become a drawback, especially due to the feeding of some species of pathogenic microorganisms, which can be present in the gut, such as *Clostridium difficile* (*C. difficile*).

Recent findings have shown the development of genetic mechanisms by *C. difficile* species to metabolize trehalose.[22,23] It has been observed that these bacteria could increase significantly the risk of death when they were fed with trehalose, causing strong diarrhea.[24] Trehalose does not induce bacterial growth; nevertheless, it seems to increase the production of toxins that could exacerbate the infection.[22] Synthesis of trehalose derivatives might be a solution to reduce the adverse effects of this carbohydrate. These derivatives would suppose a change in the chemical structure of the classic trehalose; therefore, their behavior in the human body would

Received: June 23, 2021
Revised: September 24, 2021
Accepted: September 28, 2021
Published: October 12, 2021

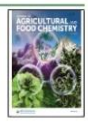

https://doi.org/10.1021/acs.jafc.1c03768
J. Agric. Food Chem. 2021, 69, 12541−12553

be different. In addition, these new compounds might have new beneficial properties.

Concerning the synthesis processes of new oligosaccharides, enzymatic procedures, such as the use of β-galactosidases (β-gal), are proven to be reliable, cost-effective, and environmentally friendly. β-Gal of *Escherichia coli* (*E. coli*) were used to produce trisaccharides from trehalose through transgalactosylation, obtaining structures such as β-Galp-(1→4)-trehalose and β-Galp-(1→6)-trehalose.[25] In previous works, β-gal activities from different microorganisms have shown an excellent ability to form lactose derivatives such as galactooligosaccharides (β-GOS);[26−29] however, to the best of our knowledge, few studies with trehalose as an acceptor have been carried out so far. A straightforward process of synthesis may permit the obtainment of new bioactive molecules from trehalose, avoiding the negative effects by *C. difficile*. Therefore, the aim of this work was to study the usefulness of four commercial β-gal to synthesize new oligosaccharides derived from trehalose, through transgalactosylation reactions. Different sources of the enzymes have been tested: *Bacillus circulans* (*B. circulans*), *Aspergillus oryzae* (*A. oryzae*), *Bifidobacterium bifidum* (*B. bifidum*), and *Kluyveromyces lactis* (*K. lactis*). Syntheses were studied with lactose (as a galactosyl donor) and trehalose (as an acceptor). Trehalose derivatives were characterized by nuclear magnetic resonance spectroscopy (NMR spectroscopy).

2. MATERIALS AND METHODS

2.1. Chemicals and Standards. Standards of D-galactose (Gal), D-glucose (Glc), trehalose, lactose, raffinose, nystose, phenyl-β-D-glucoside, and activated charcoal were purchased from Sigma-Aldrich (St. Louis, MO, USA). Lactose was supplied by ACROS Organics (Geel, Belgium). HPLC-grade acetonitrile and ethanol (96%) were obtained from VWR (Barcelona, Spain). All reagents were of analytical grade (purity of >95%). Standard GOS (3′-galactosyllactose, 4′-galactosyllactose, 6′-galactosyllactose, 3′-galactobiose, 4′-galactobiose, and 6′-galactobiose) were purchased from Biosynth Carbosynth (Reading, UK).

2.2. Commercial Enzyme Preparations. Four commercial β-gal preparations were evaluated in this work: Lactozym Pure 6500 L [*Kluyveromyces lactis* (6500 U g^{-1})] and Saphera 2600 L [*Bifidobacterium bifidum* (2600 U g^{-1})] were kindly provided by Novozymes A/S (Bagsvaerd, Denmark), biolactase [*Bacillus circulans* (1500 U g^{-1})] was supplied by Biocon (Barcelona, Spain), and β-gal from *Aspergillus oryzae* (111,000 U g^{-1}) was provided by Sigma-Aldrich (St. Louis, MO, USA).

2.3. Enzymatic Synthesis of Trehalose Derivatives. Enzymatic synthesis with *K. lactis* and *B. bifidum* β-gal was performed in 50 mM sodium phosphate buffer with 2 mM $MgCl_2$ at pH 6.5. *A. oryzae* and *B. circulans* β-gal assays were carried out in 50 mM sodium acetate buffer at pH 4.5. The enzymatic activity used for the four enzymes was 15 U mL^{-1}.

Transgalactosylation reactions were carried out in an orbital Thermomixer comfort (Eppendorf) at 50 °C and 750 rpm using trehalose (25% w/v), as an acceptor, and lactose (25% w/v), as a donor. Reactions were incubated during 24 h, taking aliquots at 0, 2, 4, 6, and 24 h. Assays were stopped by heating in boiling water for 5 min. In all cases, reaction blanks using only lactose were performed under the same conditions. Transgalactosylation reactions were monitored through gas chromatography coupled to a flame ionization detector (GC-FID), as described below. After GC-FID analysis, β-gal from *K. lactis* and *B. bifidum* did not show any formation of new trehalose derivatives. For this reason, analysis, isolation, and characterization were carried out using *A. oryzae* and *B. circulans* β-gal.

2.4. Analysis of the Carbohydrate Content by Gas Chromatography (GC-FID). Samples were derivatized to their corresponding trimethyl silylated oximes (TMSOs) according to Brobst and Lott.[30] Analysis was performed in an Agilent Technologies 7820A gas chromatograph system. Separation of the samples was carried out in a fused silica capillary column DB-5HT (5% phenyl methylpolysiloxane, 30 m × 0.25 mm × 0.1 μm) (Agilent J&W Scientific, Folsom, CA, USA). The oven temperature started at 150 °C and then increased to 380 °C at a rate of 3 °C min^{-1}. Injector and detector temperatures were 280 and 385 °C, respectively. Samples were analyzed in split mode 1:20 using nitrogen as the carrier gas at a 1 mL min^{-1} flow rate.

Data quantification was calculated through the internal standard method (phenyl-β-D-glucopyranoside, 0.5 mg mL^{-1}) and the corresponding response factors of standard solutions of carbohydrates (galactose, glucose, trehalose, lactose, raffinose, and nystose) at known concentrations (0.005−1 mg mL^{-1}). All analyses were carried out in triplicate.

2.5. Purification and Isolation of Trehalose Derivatives.

2.5.1. Activated Charcoal Treatment. With the objective to remove monosaccharides and concentrate the oligosaccharide fraction, synthesized samples after 6 (*A. oryzae*) and 24 h (*B. circulans*) were purified using activated charcoal according to Hernández et al.[31] First, 10 mL of the mixture of the reaction was mixed with 60 g of activated charcoal and 1 L of ethanol solution (5% v/v). This solution was incubated for 30 min at 25 °C under continuous agitation. Then, it was filtered through Whatman No.1 paper. The desorption of oligosaccharides was carried out by mixing the activated charcoal with ethanolic solution (50% v/v) during 30 min and filtering, and then, the ethanolic solution was evaporated for subsequent isolation.

2.5.2. Isolation by Semi-Preparative Chromatography. Trehalose-derived oligosaccharides were isolated by hydrophilic interaction liquid chromatography equipped with a refractive index detector (HILIC-RID), following the method of Julio-González et al.[32] Sample separation was carried out by a semi-preparative ZORBAX NH2 column (PrepHT cartridge 250 × 21.2 mm, 7 μm particle size) (Agilent), using acetonitrile/water (70:30, v/v) as a mobile phase, at a flow rate of 21 mL min^{-1} for 45 min at 25 °C. Two milliliters was repeatedly injected. The main synthesized compounds were collected, evaporated, and freeze-dried for characterization by NMR and GC−MS.

2.6. Structural Characterization of Trehalose Derivatives.

2.6.1. Gas Chromatography−Mass Spectrometry (GC−MS). Trehalose-derived oligosaccharides were also studied by GC−MS. Analysis was performed by a fused silica capillary column DB-5HT (5% phenyl methylpolysiloxane; 30 m × 0.25 mm × 0.10 μm) (Agilent) in a 6890 gas chromatograph system coupled to a 5973 quadrupole mass detector (Agilent). Helium was used as the carrier gas at a flow of 0.8 mL min^{-1}. The oven temperature program was 150 °C, increased to 300 °C at 3 °C min^{-1}, and maintained for 10 min. Injections were done in split mode (1:20). Electron impact (EI) mode was used at 70 eV in the mass spectrometer, considering a range of 35−700 *m*/*z*. Interface and source temperatures were 280 and 230 °C, respectively.

Identification of known structures of GOS was done by comparison of standard solutions and their respective mass spectra.

2.6.2. Nuclear Magnetic Resonance Spectroscopy (NMR Spectroscopy). Structure elucidation of the purified fractions was accomplished by nuclear magnetic resonance spectroscopy (NMR spectroscopy). NMR spectra were recorded at 298 K, using D_2O as a solvent, on an Agilent system 500 NMR spectrometer (^1H 500 MHz, ^{13}C 125 MHz) equipped with a 5 mm HCN cold probe. Chemical shifts of ^1H (δ_H) and ^{13}C (δ_C) in parts per million were determined relative to internal standards of sodium [2,2,3,3-$^2H_4$]-3-(trimethylsilyl)-propanoate in D_2O (δ_H 0.00) and 1,4-dioxane (δ_C 67.40) in D_2O, respectively. One-dimensional (1D) NMR experiments (^1H and $^{13}C\{^1H\}$) were performed using standard pulse sequences. Two-dimensional (2D) [^1H, ^1H] NMR experiments [gradient correlation spectroscopy (gCOSY), total correlation spectroscopy (TOCSY), and rotating-frame Overhauser effect spectroscopy (ROESY)] were carried out with the following parameters: a delay time of 1 s, a spectral width of 2800 Hz in both dimensions, 2048 complex points in t2, 4 transients (24 or 32 for ROESY) for each of 128 (200 for TOCSY and ROESY) time increments, and linear prediction to 512.

https://doi.org/10.1021/acs.jafc.1c03768
J. Agric. Food Chem. 2021, 69, 12541−12553

The mixing time used for ROESY was 0.3 ms. The data were zero-filled to 2048 × 2048 real points. 2D [^{1}H−^{13}C] NMR experiments [gradient heteronuclear single-quantum coherence (gHSQC), hybrid experiment gHSQC-TOCSY, and selective 2D bsgHMBC[33] used the same ^{1}H spectral window, a ^{13}C spectral window of 7541.5 Hz, 1 s relaxation delay, 1024 data points, and 128 or 200 time increments, with a linear prediction to 256. The data were zero-filled to 2048 × 2048 real points. Typical numbers of transients per increment were 4 and 16. A mixing time of 80 ms was used for gHSQC-TOCSY experiments.

3. RESULTS AND DISCUSSION

3.1. Transgalactosylation of Trehalose by β-Galactosidase from *Bacillus circulans*. The reaction conditions are different from those most commonly used for *Bacillus circulans* β-gal due to the major presence of the β-gal isoforms II and III in the Biolactase NTL Conc. Figure 1 shows the chromatographic GC-FID profile during the transgalactosylation assay after 24 h of reaction using lactose and trehalose and only lactose. In the first instance, a considerable amount of monosaccharides (peaks 1 and 2) was observed in the chromatogram due to the hydrolytic activity of the β-gal. Moreover, the transgalactosylation reaction was also observed (Figure 1A−D).

In the lactose assays, di- and trisaccharide β-GOS fractions (Figure 1A,B, red) were obtained and identified by GC−MS profiles (peaks 6−8, 10, and 11). These structures are known, as they were obtained by reactions with β-gal of different sources.[26,34] On the other hand, new oligosaccharides were synthesized using trehalose as a carbohydrate acceptor (Figure 1, blue). These compounds correspond to galactosylated trehalose (Figure 1B, peaks 9 and 12; Figure 1C, peaks 13, 14, 15, 16, and 17). Interestingly, although there was a low quantity, the pentasaccharide fraction was also observed in the chromatogram (Figure 1D, peak 18).

The kinetic behavior of the reaction mixtures, lactose/trehalose and lactose, is indicated in Figure 2A,B, respectively; moreover, quantitative data are shown in Table S1. After 24 h, 85.3 (Lac/Tre, Figure 2A) and 80.8% (Lac, Figure 2B) lactose was hydrolyzed, whereas trehalose decreased by 35.8% (Figure 2A). Regarding disaccharide synthesis, only β-GOS disaccharides derived from lactose were observed in both reactions, being produced in a higher amount using the lactose only mixture (23.3%, Figure 2B).

Trisaccharides were the main oligosaccharides generated during the lactose/trehalose reaction, especially those derived from trehalose (19.5% after 6 h), in contrast to those derived using only lactose (6.1%) (Figure 2A and Table S1). This result indicates that trehalose is a better acceptor than lactose. Just tetrasaccharides from trehalose were identified in the lactose/trehalose reaction (8.2%). A similar situation occurred with pentasaccharides, which were only formed in the trehalose/lactose mixture (Figure 2A; 1.4% after 24 h). The maximum formation of the trehalose derivatives occurred between 6 and 24 h of the incubation time (Figure 2A). These data support the efficiency and the suitability of the β-gal to produce trehalose derivatives. β-GOS tri- and tetrasaccharide productions were 21.0 and 6.5% after 24 h, respectively, using lactose as the sole donor and acceptor (Figure 2B), which is in line with previously reported β-GOS production.[27,35]

Tri-, tetra-, and pentasaccharide fractions were isolated by HILIC-RID and characterized by NMR. This characterization was accomplished by the combined use of 1D and 2D [^{1}H, ^{1}H] and [^{1}H, ^{13}C] NMR experiments (gCOSY, TOCSY, ROESY, multiplicity-edited gHSQC, bsgHMBC, and hybrid experiment gHSQC-TOCSY). ^{1}H and ^{13}C NMR chemical shifts were observed, and the structures of each compound are summarized and numbered in Tables 1−4. Full sets of spectra are available in the Supporting Information (Figures S1−S43).

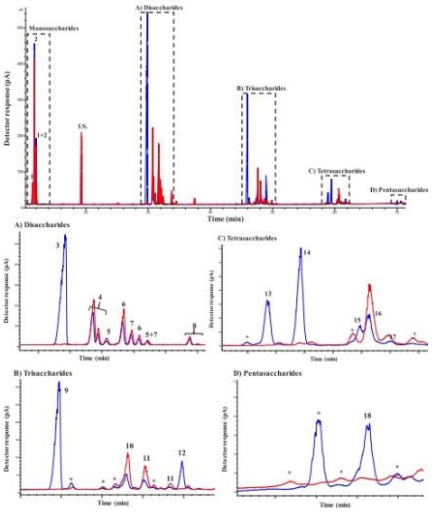

Figure 1. Chromatographic profiles obtained by GC-FID of TMSO derivatives of the transgalactosylation reaction after 24 h by β-galactosidase from *Bacillus circulans* using lactose/trehalose (blue) and lactose (red). Disaccharide (A), trisaccharide (B), tetrasaccharide (C), and pentasaccharide (D) fractions are shown for each reaction. Peaks: 1: galactose, 2: glucose, I.S.: internal standard, (A) 3: trehalose, 4: lactose, 5: β-D-galactopyranosyl-(1→4)-β-D-glucose, 6: β-D-galactopyranosyl-(1→3)-β-D-glucose, 7: β-D-galactopyranosyl-(1→2)-β-D-glucose, 8: β-D-galactopyranosyl-(1→6)-β-D-glucose, (B) 9: β-D-galactopyranosyl-(1→4)-D-trehalose, 10: β-D-galactopyranosyl-(1→4)-D-lactose, 11: β-D-galactopyranosyl-(1→6)-D-lactose, 12: β-D-galactopyranosyl-(1→6)-D-trehalose, (C) 13 and 15: β-D-galactopyranosyl-(1→4)-β-D-galactopyranosyl-(1→6)-D-trehalose or β-D-galactopyranosyl-(1→4)-α-D-glucopyranosyl-(1↔1)-[β-D-galactopyranosyl-(1→4)]-α-D-glucopyranoside, 14: β-D-galactopyranosyl-(1→4)-β-D-galactopyranosyl-(1→4)-D-trehalose, 16 and 17: β-D-galactopyranosyl-(1→4)-α-D-glucopyranosyl-(1↔1)-[β-D-galactopyranosyl-(1→6)]-α-D-glucopyranoside or β-D-galactopyranosyl-(1→6)-α-D-glucopyranosyl-(1↔1)-[β-D-galactopyranosyl-(1→6)]-α-D-glucopyranoside, and (D) 18: β-D-galactopyranosyl-(1→4)-β-D-galactopyranosyl-(1→4)-β-D-galactopyranosyl-(1→4)-D-trehalose. *Other saccharides with unknown structures.

Two compounds could be identified in the trisaccharide fraction (Figure 1B). Compound **1** (peak 12) was assigned as β-D-galactopyranosyl-(1→6)-α-D-glucopyranosyl-(1↔1)-α-D-glucopyranoside [β-D-galactopyranosyl-(1→6)-α,α-trehalose] (Table 1, compound **1**). The 1D ^{1}H NMR spectrum of this compound (see Supporting Information, Figure S1) showed three doublets in the anomeric region (δ 5.19, $^3J_{H1,H2}$ = 3.8 Hz, δ 5.18, $^3J_{H1,H2}$ = 3.8 Hz, and δ 4.43, $^3J_{H1,H2}$ = 8.1 Hz), corresponding to both α-glucoses and β-galactose, respectively. In addition, the 1D ^{13}C NMR spectrum showed signals corresponding to 18 carbons, including three anomeric carbons

https://doi.org/10.1021/acs.jafc.1c03768
J. Agric. Food Chem. 2021, 69, 12541−12553

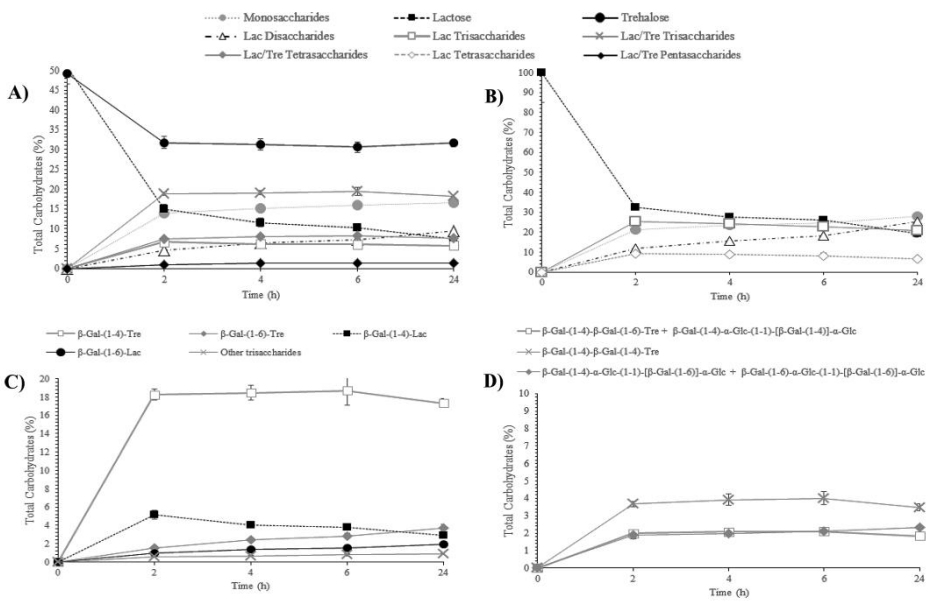

Figure 2. Evolution in the content of carbohydrates (%) during transgalactosylation reactions of lactose/trehalose (A) and lactose (B) solutions and evolution of tri- (C) and tetrasaccharides (D) (%) of the lactose/trehalose mixture. Reactions catalyzed by β-galactosidase from *Bacillus circulans* for 24 h at 50 °C, pH 4.5.

(δ 94.02, δ 93.97, and δ 103.95). A multiplicity-edited gHSQC spectrum was used to link the carbon signals to the corresponding proton resonances. It showed three anomeric carbons, 12 CH, and three methylene carbons. In addition, COSY, TOCSY, and gHSQC-TOCSY experiments supported the presence of two α-glucose units and one β-galactose unit. The position of glycosidic linkages was analyzed from the bsgHMBC spectrum. It showed correlations between the two α-Glc anomeric positions, confirming the presence of a trehalose unit. In addition, relevant correlation bands between the β-Gal-3-C1 anomeric carbon and α-Glc-2-H6 and between the α-Glc-2-C6 methylene carbon and the β-Gal-3-H1 anomeric proton could be found. These results confirmed the proposed structure. This compound has been previously characterized through NMR by Ajisaka and Fujimoto[36] and by Kim et al.[25] Some differences in chemical shifts are found, but in the first case, acetonitrile was used as an internal reference in D_2O, and in the second one, DMSO-d_6 was used as a solvent, which could explain these little changes.

Regarding compound **2** (peak 9, Figure 1B), it was assigned as β-D-galactopyranosyl-(1→4)-α-D-glucopyranosyl-(1↔1)-α-D-glucopyranoside [β-D-galactopyranosyl-(1→4)-α,α-trehalose] (Table 1, compound **2**). 1D and 2D spectra were analyzed as in the previous case (see Supporting Information, Figures S7−S11), and they also supported the presence of two α-glucose units and one β-galactose unit. All ^{1}H and ^{13}C signals could be assigned (Table 1). The results confirmed the structure as β-D-galactopyranosyl-(1→4)-α-D-glucopyranosyl-(1↔1)-α-D-glucopyranoside, and they are in accordance with other data from Ishii et al.[37]

In the case of tetrasaccharide fractions, we have been able to characterize two types of tetrasaccharides: two of them with a terminal trehalose in their structure (Table 2, compounds **3** and **4**) and three more where trehalose is situated in the center (Table 3, compounds **5**, **6**, and **7**).

Compound **3** (peak 14, Figure 1C) was assigned as β-D-galactopyranosyl-(1→4)-β-D-galactopyranosyl-(1→4)-α-D-glucopyranosyl-(1↔1)-α-D-glucopyranoside [β-D-galactopyranosyl-(1→4)-β-D-galactopyranosyl-(1→4)-α,α-trehalose] (Table 2, compound **3**). The 1D ^{1}H NMR spectrum (see Supporting Information, Figure S12 and Table 2) showed four doublets in the anomeric region (δ 5.17, $^3J_{H1,H2}$ = 3.7 Hz, δ 5.18, $^3J_{H1,H2}$ = 3.7 Hz, δ 4.48, $^3J_{H1,H2}$ = 7.8 Hz, and δ 4.59, $^3J_{H1,H2}$ = 7.8 Hz), corresponding to both α-glucoses from trehalose units and two β-galactoses. The 1D ^{13}C NMR spectrum showed signals corresponding to 24 carbons, including four anomeric carbons (δ 94.04, δ 93.70, δ 103.53, and δ 104.84). 2D spectra also supported the presence of two α-glucose and two β-galactose units. The position of glycosidic linkages was analyzed from the bsgHMBC spectrum. It showed correlations between the two α-Glc anomeric positions, confirming the presence of a trehalose unit, and in addition, relevant correlations between the β-Gal-3-C1 anomeric carbon and α-Glc-2-H4 and between α-Glc-2-C4 and β-Gal-3-H1 anomeric protons were found. Moreover, key correlations between the β-Gal-4-C1 anomeric carbon and β-Gal-3-H4 and between β-Gal-3-C4 and β-Gal-4-

https://doi.org/10.1021/acs.jafc.1c03768
J. Agric. Food Chem. 2021, 69, 12541−12553

Table 1. ^{1}H (500 MHz) and ^{13}C (125 MHz) NMR Chemical Shifts (δ, ppm) and Coupling Constants (J in Hz, in Parentheses) Determined by 1D and 2D NMR Spectroscopy of Trisaccharides 1 and 2

		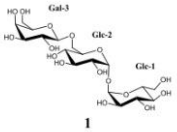 1 β-D-Gal*p*-(1→6)-α-D-Glc*p*-(1↔1)-α-D-Glc*p*		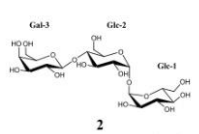 2 β-D-Gal*p*-(1→4)-α-D-Glc*p*-(1↔1)-α-D-Glc*p*	
		δ_C	δ_H(J, Hz)	δ_C	δ_H(J, Hz)
α-Glc-1	1	94.02	5.19 (3.8)	94.07	5.186 (3.8)
	2	71.61	3.64	71.70	3.64
	3	73.13	3.84	73.17	3.84
	4	70.31	3.44	70.31	3.44
	5	72.83	3.80	72.82	3.83
	6	61.15	3.85, 3.76	61.15	3.84, 3.76
α-Glc-2	1	93.97	5.18 (3.8)	93.74	5.188 (3.8)
	2	71.66	3.65	71.38	3.70
	3	73.07	3.85	71.81	3.97
	4	69.97	3.58	79.08	3.69
	5	71.86	3.95	71.50	3.94
	6	68.74	4.17,3.88	60.49	3.89,3.85
Gal-3	1	103.95	4.43 (8.1)	103.57	4.46 (8.1)
	2	71.40	3.54	71.60	3.55
	3	73.34	3.65	73.15	3.66
	4	69.32	3.91	69.21	3.92
	5	75.81	3.69	76.02	3.73
	6	61.66	3.79,3.75	61.69	3.79, 3.75

H1 anomeric protons showed a (1→4) linkage between two galactose units, confirming the proposed structure.

Compound **4** was obtained together with compound **5** by HILIC-RID, as a 1:1.5 mixture, but despite this, both compounds could be assigned by NMR unequivocally, differentiating signals of each one in the spectra (see Supporting Information, Figures S18−S24). Following the same procedure as before, compound **4** (peaks 13 and 15, Figure 1C) was assigned as β-D-galactopyranosyl-(1→4)-β-D-galactopyranosyl-(1→6)-α-D-glucopyranosyl-(1↔1)-α-D-glucopyranoside [β-D-galactopyranosyl-(1→4)-β-D-galactopyranosyl-(1→6)-α,α-trehalose] (Table 2, compound **4**). The position of glycosidic linkages was established, as in the previous case, with corresponding key correlations analyzed from bsgHMBC spectra. They showed a (1→4) linkage between the two galactose units, but in this case, the linkage between Gal-3 and the trehalose unit was (1→6).

As mentioned before, tetrasaccharides **5**, **6**, and **7** present a different structure, where the trehalose unit is situated in the center of the molecule. In these cases, every galactose unit is linked to a different glucose unit of the trehalose. Compound **5** (peaks 13 and 15, Figure 1C), assigned as β-D-galactopyranosyl-(1→4)-α-D-glucopyranosyl-(1↔1)-[β-D-galactopyranosyl-(1→4)]-α-D-glucopyranoside, is a symmetric compound, with a (1→4) linkage between every β-galactose and α-glucose (Table 3, compound **5**). Due to its symmetry, chemical shifts are the same for both galactoses and for both glucoses in the molecule. It showed two doublets in the anomeric region (δ 5.18, $^{3}J_{H1,H2}$ = 3.7 Hz and δ 4.45, $^{3}J_{H1,H2}$ = 7.8 Hz), corresponding to both α-glucoses from the trehalose unit and two β-galactoses, respectively. The 1D ^{13}C NMR spectrum showed signals corresponding to 12 carbons (due to the symmetry of the molecule), including two anomeric carbons (δ 93.93 and δ 103.56). 2D spectra, together with ^{13}C chemical shifts and intensity of the signals (see Supporting Information, Figures S19 and S21), supported the presence of two α-glucose and two β-galactose units. The (1→4) linkage between every β-galactose and α-glucose was determined by the bsgHMBC spectrum showing correlations between the β-Gal-C1 anomeric carbons and α-Glc-H4 and between α-Glc-C4 and β-Gal-H1 anomeric protons. Correlations between the two α-Glc anomeric positions supported the presence of the trehalose unit.

Compounds **6**, **7**, and **8** were part of the same fraction obtained by HILIC-RID, as a 3.5:2.7:1 mixture; however, all compounds could be assigned by NMR unequivocally, differentiating signals of each one in the spectra (see Supporting Information, Figures S25−S32).

In compound **6** (peaks 16 and 17, Figure 1C), assigned as β-D-galactopyranosyl-(1→4)-α-D-glucopyranosyl-(1↔1)-[β-D-galactopyranosyl-(1→6)]-α-D-glucopyranoside, three doublets in the anomeric region are shown (δ 5.19, $^{3}J_{H1,H2}$ = 3.7 Hz, δ 4.45, $^{3}J_{H1,H2}$ = 7.9 Hz, and δ 4.43, $^{3}J_{H1,H2}$ = 7.9 Hz). They corresponded to both α-glucoses from the trehalose unit and two β-galactoses (Table 3, compound **6**). The 1D ^{13}C NMR spectrum showed signals corresponding to 24 carbons, including four anomeric carbons (δ 94.17, δ 93.88, δ 103.55, and δ 103.95). 2D spectra also supported the presence of two α-glucose and two β-galactose units, and according to correlations shown in the bsgHMBC spectra, it could be affirmed that one galactose was linked to position 4 of one of the glucose units of the central trehalose, and the other galactose was linked to position 6 of the other glucose unit.

https://doi.org/10.1021/acs.jafc.1c03768
J. Agric. Food Chem. 2021, 69, 12541−12553

Table 2. ^{1}H (500 MHz) and ^{13}C (125 MHz) NMR Chemical Shifts (δ, ppm) and Coupling Constants (J in Hz, in Parentheses) Determined by 1D and 2D NMR Spectroscopy of Tetrasaccharides 3 and 4 and Pentasaccharide 8, with Terminal Trehalose

		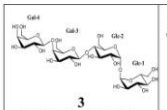 **3** β-D-Gal*p*-(1→4)-β-D-Gal*p*-(1→4)-α-D-Glc*p*-(1↔1)-α-D-Glc*p*		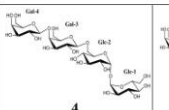 **4** β-D-Gal*p*-(1→4)-β-D-Gal*p*-(1→6)-α-D-Glc*p*-(1↔1)-α-D-Glc*p*		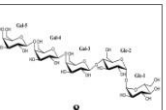 **8** β-D-Gal*p*-(1→4)-β-D-Gal*p*-(1→4)-β-D-Gal*p*-(1→4)-α-D-Glc*p*-(1↔1)-α-D-Glc*p*	
		δ_C	δ_H(J, Hz)	δ_C	δ_H(J, Hz)	δ_C	δ_H(J, Hz)
α-Glc-1	1	94.04	5.17 (3.7)	93.98	5.19 (3.7)	94.05	5.19 (3.7)
	2	71.69	3.63	71.66	3.64	71.70	3.65
	3	73.17	3.84	73.13	3.84	73.17	3.84
	4	70.31	3.43	70.30	3.44	70.31	3.45
	5	72.81	3.82	72.83	3.80	72.82	3.82
	6	61.14	3.85, 3.76	61.15	3.84, 3.75	61.14	3.84, 3.77
α-Glc-2	1	93.70	5.18 (3.7)	93.93	5.18 (3.7)	93.71	5.18 (3.7)
	2	71.33	3.68	71.61	3.62	71.35	3.68
	3	71.78	3.97	73.08	3.84	71.80	3.96
	4	79.14	3.67	70.06	3.54	79.17	3.68
	5	71.48	3.92	71.90	3.96	71.49	3.93
	6	60.44	3.88,3.85	68.87	4.15,3.87	60.47	3.90,3.85
Gal-3	1	103.53	4.48 (7.8)	103.88	4.46 (7.8)	103.57	4.49 (7.9)
	2	71.99	3.62	71.88	3.62	71.99	3.62
	3	73.58	3.77	73.75	3.75	73.67	3.77
	4	77.77	4.19	77.74	4.17	78.18	4.18
	5	75.16	3.75	74.93	3.72	75.25	3.76
	6	61.39	3.82, 3.80	61.19	3.83, 3.75	61.55	3.84, 3.77
Gal-4	1	104.84	4.59 (7.8)	104.89	4.58 (7.8)	104.90	4.65 (8.0)
	2	72.08	3.56	72.05	3.57	72.49	3.65
	3	73.45	3.66	73.40	3.65	73.93	3.77
	4	69.26	3.90	69.27	3.90	77.78	4.17
	5	75.77	3.67	75.76	3.67	75.09	3.71
	6	61.64	3.78, 3.75	61.65	3.78, 3.73	61.19	3.84, 3.77
Gal-5	1					104.95	4.59 (7.8)
	2					72.03	3.56
	3					73.41	3.65
	4					69.28	3.90
	5					75.77	3.68
	6					61.69	3.78, 3.75

Compound **7** (peaks 16 and 17, Figure 1C), assigned as β-D-galactopyranosyl-(1→6)-α-D-glucopyranosyl-(1↔1)-[β-D-galactopyranosyl-(1→6)]-α-D-glucopyranoside, is a symmetric compound, as compound **5**, and it was assigned following the same strategy (Table 3, compound **7**). This time, the bsgHMBC spectrum showed correlations between the β-Gal-C1 anomeric carbons and α-Glc-H6 and between α-Glc-C6 and β-Gal-H1 anomeric protons, besides correlations between the two α-Glc anomeric positions, supporting the proposed structure.

Compound **8** (peak 18, Figure 1D) was assigned as the pentasaccharide β-D-galactopyranosyl-(1→4)-β-D-galactopyranosyl-(1→4)-β-D-galactopyranosyl-(1→4)-α-D-glucopyranosyl-(1↔1)-α-D-glucopyranoside (β-D-galactopyranosyl-(1→4)-β-D-galactopyranosyl-(1→4)-β-D-galactopyranosyl-(1→4)-α,α-trehalose) (Table 2, compound **8**). In this case, the 1D ^{1}H NMR spectrum (see Supporting Information, Figure S25 and Table 2) showed five doublets in the anomeric region (δ 5.19, $^{3}J_{H1,H2}$ = 3.7 Hz, δ 5.18, $^{3}J_{H1,H2}$ = 3.7 Hz, δ 4.49, $^{3}J_{H1,H2}$ = 7.9 Hz, δ 4.65, $^{3}J_{H1,H2}$ = 8.0 Hz, and δ 4.59, $^{3}J_{H1,H2}$ = 7.8 Hz), corresponding to both α-glucoses from the trehalose unit and three β-galactoses. The 1D ^{13}C NMR spectrum showed signals corresponding to 30 carbons, including five anomeric carbons (δ 94.05, δ 93.71, δ 103.57, δ 104.90, and δ 104.95). 2D spectra also supported the presence of two α-glucose and three β-galactose units. In this case, trehalose is situated at the end of the chain, and the position of glycosidic linkages was analyzed from bsgHMBC spectra, being always (1→4) between every galactose unit and the next one of the chains and between galactose-3 and trehalose. Relevant correlations to support this affirmation were β-Gal-5-C1 anomeric carbon and β-Gal-4-H4, β-Gal-4-C4 and β-Gal-5-H1 anomeric protons, β-Gal-4-C1 anomeric carbon and β-Gal-3-H4, β-Gal-3-C4 and β-Gal-4-H1 anomeric protons, β-Gal-3-C1 anomeric carbon and α-Glc-2-H4, α-Glc-2-C4 and β-Gal-3-H1 anomeric protons, and between the two α-Glc anomeric positions, confirming the presence of a trehalose unit.

These results sustained the obtainment of two new trisaccharides derived from trehalose. The structure was confirmed to be as β-D-galactopyranosyl-(1→6)-D-trehalose (Table 1, compound **1**) and β-D-galactopyranosyl-(1→4)-D-trehalose (Table 1, compound **2**). β-Gal of *E. coli* was used by Kim et al.[25] to generate trehalose derivatives. That work revealed that the main products were β-gal-(1→4)-trehalose and β-gal-(1→6)-trehalose, which are in good agreement with the results of Figure 1. In addition, this type of linkage is very similar to the trisaccharides contained in commercial dietary β-GOS. Van Leeuwen et al.[38] compared the structure of different commercially available GOS trisaccharides, indicating that bonds β-(1→4) and β-(1→6) were the most abundant, depending on the microbial enzyme used in the synthesis. Specifically, Figure 2C shows the individual evolution of the

https://doi.org/10.1021/acs.jafc.1c03768
J. Agric. Food Chem. 2021, 69, 12541−12553

Table 3. ^{1}H (500 MHz) and ^{13}C (125 MHz) NMR Chemical Shifts (δ, ppm) and Coupling Constants (J in Hz, in Parentheses) Determined by 1D and 2D NMR Spectroscopy of Tetrasaccharides 5, 6, and 7, with Central Trehalose

		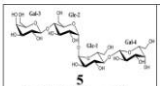 5 β-D-Galp-(1→4)-α-D-Glcp-(1↔1)-[β-D-Galp-(1→4)]-α- D-Glcp		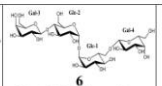 6 β-D-Galp-(1→4)-α-D-Glcp-(1↔1)- [β-D-Galp-(1→6)]-α-D-Glcp		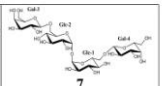 7 β-D-Galp-(1→6)-α-D-Glcp-(1↔1)-[β-D-Galp-(1→6)]-α-D-Glcp	
		δ_C	δ_H(J, Hz)	δ_C	δ_H(J, Hz)	δ_C	δ_H(J, Hz)
α-Glc-1	1	93.93	5.18 (3.7)	94.17	5.19 (3.7)	94.13	5.19 (3.7)
	2	71.40	3.68	71.64	3.65	71.59	3.65
	3	71.82	3.96	73.09	3.84	73.05	3.84
	4	79.02	3.69	69.97	3.57	69.97	3.57
	5	71.53	3.94	71.89	3.96	71.92	3.96
	6	60.47	3.89,3.85	68.74	4.17, 3.88	68.74	4.17, 3.88
α-Glc-2	1	93.93	5.18 (3.7)	93.88	5.19 (3.7)	94.13	5.19 (3.7)
	2	71.40	3.68	71.35	3.70	71.59	3.65
	3	71.82	3.96	71.78	3.96	73.05	3.84
	4	79.02	3.69	79.05	3.68	69.97	3.57
	5	71.53	3.94	71.54	3.93	71.92	3.96
	6	60.47	3.89,3.85	60.47	3.90,3.85	68.74	4.17, 3.88
Gal-3	1	103.56	4.45 (7.8)	103.55	4.45 (7.9)	103.96	4.43 (7.9)
	2	71.59	3.54	71.59	3.54	71.40	3.54
	3	73.15	3.66	73.15	3.65	73.34	3.65
	4	69.21	3.92	69.20	3.92	69.32	3.92
	5	76.02	3.72	76.02	3.72	75.81	3.68
	6	61.70	3.78, 3.74	61.69	3.78, 3.73	61.66	3.78,3.73
Gal-4	1	103.56	4.45 (7.8)	103.95	4.43 (7.9)	103.96	4.43 (7.9)
	2	71.59	3.54	71.40	3.54	71.40	3.54
	3	73.15	3.66	73.34	3.65	73.34	3.65
	4	69.21	3.92	69.32	3.92	69.32	3.92
	5	76.02	3.72	75.81	3.69	75.81	3.68
	6	61.70	3.78, 3.74	61.66	3.78, 3.73	61.66	3.78,3.73

trisaccharides synthesized in the lactose/trehalose reaction. The synthesis yield of each oligosaccharide increased with reaction time, observing the highest increase after 2 h of incubation and then reaching a plateau with a progressive synthesis of trisaccharides. The main product obtained was β-Gal-(1→4)-Tre (~18.7%) (Figure 2C). These results seem to indicate that β-gal from *Bacillus circulans* prioritize to join the galactose from lactose (used as a donor) in the trehalose with a linkage β-(1→4) and in a lesser extent β-(1→6). The same structures of trisaccharides derived from trehalose were also obtained by Ishii et al.[37] using *B. circulans* β-gal. This indicates the effectiveness of transgalactosylation mechanisms of β-gal of *B. circulans*.[39]

New tetrasaccharides were found in this work [β-D-galactopyranosyl-(1→4)-β-D-galactopyranosyl-(1→4)-D-trehalose and β-D-galactopyranosyl-(1→4)-β-D-galactopyranosyl-(1→6)-D-trehalose] (Table 2). These results followed the same pattern as the trisaccharides synthesized, where the galactose monomers of lactose have been driven to the acceptor molecule galactosyl-trehalose and linked by β-(1→6) and β-(1→4) bonds. Figure 2D indicates that similar quantities of the different tetrasaccharides were obtained. Therefore, quantitative results (Table S1) show a greater production after 6 h of reaction (8.2%). Remarkably, an interesting mixture of structures where the trehalose unit is situated in the center of the molecule was also synthesized (Table 3, compounds **5**, **6**, and **7**). In this case, the trehalose has been galactosylated in both terminal endings resulting in three different tetrasaccharides distinguished by both types of bonds. This fact could indicate that the trisaccharides β-Gal-(1→4)-Tre and β-Gal-(1→6)-Tre also acted as acceptors. Furthermore, the slight differences between these chemical structures may be important in a possible production in a major scale.

The majority of the studies based on the synthesis of trehalose derivatives focused on the synthesis of disaccharides analogues, such as lactotrehalose or mannotrehalose,[40,41] or trisaccharides, as the structures named above;[25,37] however, no tetra- or pentasaccharides were investigated. Chaube et al.[42] were the first to synthesize tetrasaccharides trehalose-derivatives from *Mycobacterium smegmatis* obtaining galactosyl and glucosyl structures linked by α-(1→6) and β-(1→6) to trehalose moieties, respectively. Nevertheless, the process of synthesis was arduous and complex, using organic solvents. On the other hand, Wessel and Niggemann[43] synthesized different types of trehalose oligosaccharides with glucose linked via β-(1→4) and DP up to 5. To the best of our knowledge, our data are the first evidence on the synthesis of tetra- and pentasaccharide trehalose galactosylated using commercially available enzymes.

3.2. Transgalactosylation by β-Galactosidase from *Aspergillus oryzae*. Figure 3 shows the GC-FID chromatogram during the transgalactosylation assay after 6 h of reaction using the lactose/trehalose mixture and only lactose by β-gal from *A. oryzae*. The GC-FID profile of *A. oryzae* (Figure 3) shows a less complex mixture than *B. circulans*, as a result of the less formation of disaccharides (Figure 3A), trisaccharides (Figure 3B), and tetrasaccharides (Figure 3C), including β-GOS and trehalose derivatives. In the lactose assay (Figure 3, red), β-GOS di- (peaks 5−7; Figure 3A) and trisaccharides (peaks 8−10, Figure 3B) were detected, in a higher level than the lactose/trehalose mixture. Tetrasaccharides were found in both reactions, in a substantially low level (multiple peaks labeled as 11 and *; Figure 3C). Remarkably, a series of unknown compounds were also detected in the lactose/trehalose mixture (Figure 3, blue): saccharides labeled as 10

https://doi.org/10.1021/acs.jafc.1c03768
J. Agric. Food Chem. 2021, 69, 12541−12553

Table 4. ^{1}H (500 MHz) and ^{13}C (125 MHz) NMR Chemical Shifts (δ, ppm) and Coupling Constants (J in Hz, in Parentheses) Determined by 1D and 2D NMR Spectroscopy of Oligosaccharides 9 and 10

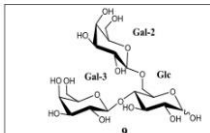

9
β-D-Gal*p*-(1→4)-[β-D-Gal*p*-(1→6)]-D-Glc*p*

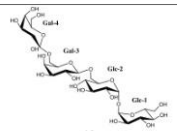

10
β-D-Gal*p*-(1→6)-β-D-Gal*p*-(1→6)-α- D-Glc*p*-(1↔1)-α-D-Glc*p*

		δ_C	δ_H(J, Hz)			δ_C	δ_H(J, Hz)
α-Glc	1	92.55	5.22 (3.8)	α-Glc-1	1	94.01	5.19 (3.9)
	2	71.77	3.60		2	71.65	3.64
	3	72.01	3.82		3	73.12	3.82
	4	78.41	3.79		4	70.31	3.44
	5	69.63	4.08		5	72.83	3.83
	6	68.08	4.21, 3.96		6	61.14	3.84,3.76
β-Glc	1	96.57	4.67 (8.0)	α-Glc-2	1	93.96	5.18 (3.9)
	2	74.36	3.31		2	71.62	3.64
	3	74.94	3.62		3	73.07	3.84
	4	78.44	3.79		4	69.99	3.57
	5	74.24	3.75		5	71.84	3.94
	6	68.14	4.29, 3.91		6	68.84	4.16,3.87
Gal-2(α) (1→6)	1	103.79	4.44 or 4.45 (7.8)	Gal-3	1	103.85	4.46 (7.9)
	2	71.28	3.54		2	71.33	3.53
	3	73.33	3.66		3	73.20	3.65
	4	69.33	3.92		4	69.34	3.95
	5	75.74	3.70		5	74.54	3.89
	6	61.65	3.78, 3.75		6	69.60	4.04,3.87
Gal-2(β) (1→6)	1	103.77	4.44 or 4.45 (7.8)	Gal-4	1	103.97	4.44 (7.9)
	2	71.28	3.54		2	71.38	3.53
	3	73.32	3.66		3	73.38	3.65
	4	69.32	3.92		4	69.26	3.91
	5	75.78	3.70		5	75.81	3.69
	6	61.65	3.78, 3.75		6	61.62	3.78,3.75
Gal-3(α) (1→4)	1	103.44	4.51 (7.8)				
	2	71.59	3.54				
	3	73.13	3.66				
	4	69.23 or 69.26	3.92				
	5	75.91	3.70				
	6	61.75	3.78, 3.75				
Gal-3(β) (1→4)	1	103.48	4.51 (7.8)				
	2	71.59	3.54				
	3	73.13	3.66				
	4	69.23 or 69.26	3.92				
	5	75.91	3.70				
	6	61.72	3.78, 3.75				

and 11 (Figure 3) were only synthesized when trehalose was present on the reaction.

The evolution in the content of carbohydrates for each reaction is observed in Figure 4A (lactose/trehalose) and Figure 4B (lactose). Table S2 shows the quantitative data of the assays. A progressive and complete hydrolysis of lactose after 24 h was observed in both reactions, while the corresponding monosaccharides increased (peaks 1 and 2, Figure 3A) with the incubation time. In the lactose/trehalose mixture (Figure 4A), the maximum formation of the di- and trisaccharides occurred between 2 and 6 h of reaction. As observed in the reaction with *B. circulans*, only disaccharides from lactose were synthesized, reaching a maximum of 14.1% after 6 h in the lactose mixture versus 6.3% obtained when lactose/trehalose was used. The presence of trehalose appeared to decrease the β-GOS formation in favor to giving rise to the new oligosaccharides. The less formation of disaccharides in Figure 4A was balanced for the synthesis of the trehalose trisaccharides (5.6% after 6 h). Trehalose levels were diminished in a lower degree than the *B. circulans* reaction (Figure 2A); therefore, the synthesis of trehalose-derived oligosaccharides was lower. It has been reported that the transgalactosylation properties of β-gal from *A. oryzae* are less effective than those of *E. coli* and *B. circulans* in terms of trehalose analogues.[36,37] Remarkably, despite the low quantity of tetrasaccharides (1.4%) observed in Figure 4A, new oligosaccharides were synthesized. The new oligosaccharides were isolated by HILIC-RID and characterized by NMR.

NMR characterization was accomplished as before by the combined use of 1D and 2D [^{1}H, ^{1}H] and [^{1}H, ^{13}C] NMR experiments (gCOSY, TOCSY, ROESY, multiplicity-edited gHSQC, bsgHMBC, and hybrid experiment gHSQC-TOCSY). ^{1}H and ^{13}C NMR chemical shifts observed are summarized in Tables 1 and 4. Full sets of spectra are available in the Supporting Information (Figures S1−S6 and S33−S43). Peak 10 (Figure 3B) was identified as compound **1** [β-D-galactopyranosyl-(1→6)-α,α-trehalose]. All NMR spectra were identical to those for the trisaccharide already described in the previous section.

https://doi.org/10.1021/acs.jafc.1c03768
J. Agric. Food Chem. 2021, 69, 12541−12553

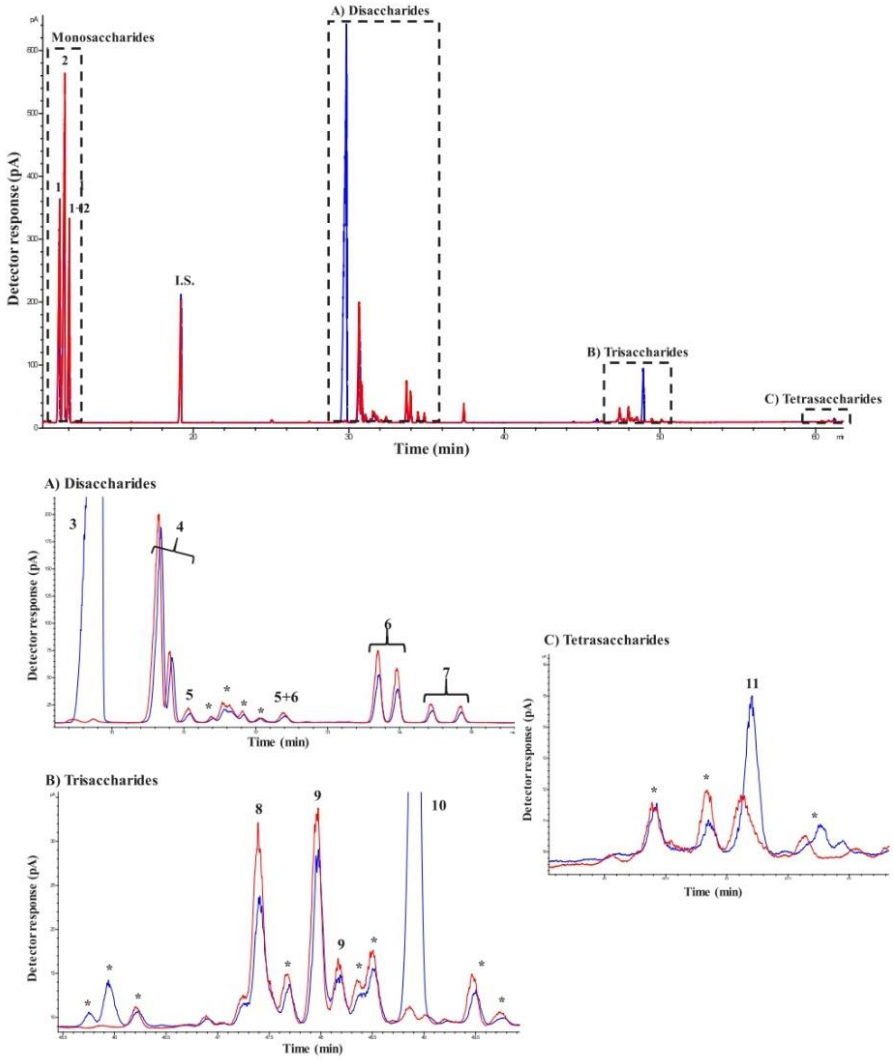

Figure 3. Chromatographic profiles obtained by GC-FID of TMSO derivatives of the transgalactosylation reaction after 6 h by β-galactosidase from *Aspergillus oryzae* using lactose/trehalose (blue) and lactose (red). Disaccharide (A), trisaccharide (B), and tetrasaccharide (C) fractions are shown for each reaction. Peaks: 1: galactose, 2: glucose, I.S.: internal standard, (A) 3: trehalose, 4: lactose, 5: β-D-galactopyranosyl-(1→4)-β-D-galactose, 6: β-D-galactopyranosyl-(1→6)-β-D-glucose, 7: β-D-galactopyranosyl-(1→6)-β-D-galactose, (B) 8: β-D-galactopyranosyl-(1→4)-[β-D-galactopyranosyl-(1→6)]-D-glucose, 9: β-D-galactopyranosyl-(1→6)-lactose, 10: β-galactopyranosyl-(1→6)-trehalose, and (C) 11: β-galactopyranosyl-(1→6)-β-galactopyranosyl-(1→6)-trehalose. *Other saccharides with unknown structures.

Interestingly, in the case of trisaccharide **9** (peak 8, Figure 3B), the α,α-trehalose moiety was not found. The 1D ^{1}H NMR spectrum (see Supporting Information, Figure S33 and Table 4) showed five doublets in the anomeric region. They

https://doi.org/10.1021/acs.jafc.1c03768
J. Agric. Food Chem. 2021, 69, 12541−12553

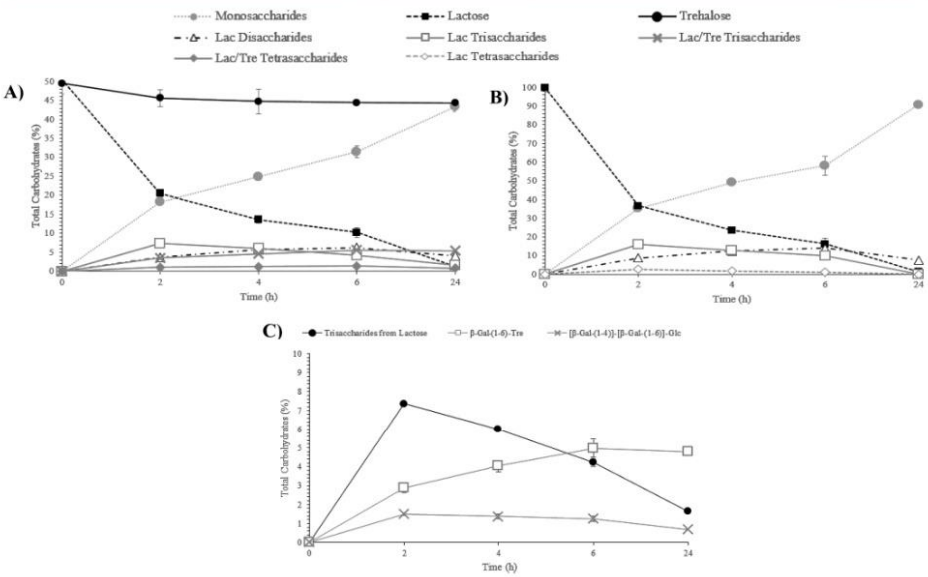

Figure 4. Evolution in the content of carbohydrates (%) during transgalactosylation reactions of lactose/trehalose (A) and lactose (B) solutions and (C) evolution in the content of trisaccharides (%) of the lactose/trehalose mixture. Reactions catalyzed by β-galactosidase from *Aspergillus oryzae* for 24 h at 50 °C, pH 4.

belong to two sets of signals, corresponding to an equilibrium of the α:β anomers of the terminal glucose (δ 5.22, $^3J_{H1,H2}$ = 3.8 Hz, δ 4.44 or 4.45, $^3J_{H1,H2}$ = 7.8 Hz, and δ 4.51, $^3J_{H1,H2}$ = 8.1 Hz for the α anomer and δ 4.67, $^3J_{H1,H2}$ = 8.0 Hz, δ 4.44 or 4.45, $^3J_{H1,H2}$ = 7.8 Hz, and δ 4.51, $^3J_{H1,H2}$ = 8.1 Hz for the β anomer). The 1D ^{13}C NMR spectrum showed signals corresponding to 31 carbons (five of them including two carbons in the same signal). The gHSQC spectrum was used to link the carbon signals to the corresponding proton resonances. It showed six anomeric carbons (δ 92.55, δ 96.57, δ 103.79, δ 103.77, δ 103.44, and δ 103.48), 20 CH (four pairs occur under the same signal), and five methylene carbons (two of them are under the same signal). In addition, COSY, TOCSY, and gHSQC-TOCSY experiments supported the presence of two β-galactose units and one glucose unit (α and β forms) for each trisaccharide of the pair. The position of glycosidic linkages was analyzed from bsgHMBC spectra. In this case, it showed correlations between the anomeric carbons of the two β-Gal units with protons in positions 4 and 6 of the same glucose unit for each anomeric form. Therefore, relevant correlation bands between the β-Gal-3-C1 anomeric carbon and α/β-Glc-H4 and between α/β-Glc-C4 carbon and the β-Gal-3-H1 anomeric proton could be found. Also, it showed correlations between β-Gal-2-C1 anomeric carbon and α/β-Glc-H6 methylene protons and between α/β-Glc-C6 methylene carbon and the β-Gal-2-H1 anomeric proton. These results confirmed the structure as β-D-galactopyranosyl-(1→4)-[β-D-galactopyranosyl-(1→6)]-D-glucopyranose (Table 4, compound **9**).

Carrying out a similar analysis, compound **10** (peak 11, Figure 3C) was assigned as β-D-galactopyranosyl-(1→6)-β-D-galactopyranosyl-(1→6)-α-D-glucopyranosyl-(1↔1)-α-D-glucopyranoside [β-D-galactopyranosyl-(1→6)-β-D-galactopyranosyl-(1→4)-α,α-trehalose] (see Supporting Information, Figures S39−S43 and Table 4, compound **10**). Key correlations in 2D spectra confirmed the presence of a trehalose unit and also the position of glycosidic linkages.

It should be noted that compound **10** was obtained together with compound **11**, in a 2:1 mixture. In this case, not all signals for compound **11** could be assigned, but signals observed in all spectra were consistent with the assignation of this compound as previously described,[44] the trisaccharide β-D-galactopyranosyl-(1→6)-β-D-galactopyranosyl-(1→4)-D-glucopyranose (see Supporting Information, Figures S39−S43).

The synthesis of the lactose/trehalose mixture promoted considerably the formation of two trisaccharides, reaching maximum yields at 6 h of reaction (Figure 4C). β-D-Galactopyranosyl-(1→4)-[β-D-galactopyranosyl-(1→6)]-D-glucopyranose (Table 4, compound **9**) was the main product obtained in the transgalactosylation assay; this β-GOS trisaccharide has been also found by Yin et al.[45] using lactose as a donor and acceptor. The other trisaccharide was the same as that obtained by *B. circulans*, β-Galp-(1→6)-Tre (Table 4, compound **1**), but in a lower quantity (Figure 4C). These data are in line with Urrutia et al.[46] who observed a high preference of β-gal of *A. oryzae* for the formation of β-(1→6) bonds, as well as for *B. circulans*. Moreover, the low level of production using the *A. oryzae* enzyme is in good agreement with Ajisaka and Fujimoto,[36] who carried out a total synthesis yield of 7%.

https://doi.org/10.1021/acs.jafc.1c03768
J. Agric. Food Chem. 2021, 69, 12541−12553

On the other hand, a new tetrasaccharide was obtained in the reaction, whose structure is shown in Table 4 (Compound **10**). As well as in *B. circulans*, these are the first data reported of galactosylated trehalose tetrasaccharides synthesized by commercial enzymes. In addition, Ferreira-Lazarte et al.[47] studied the digestibility of β-GOS with different types of bonds using brush border membrane vesicles from pig, which contains the disaccharidases responsible for the digestion of dietary sugars. Their findings revealed that the β-(1→6) linkage showed the highest resistance to digestion (12% after 3 h) followed by β-(1→4) (26%) and β-(1→3) (40%). This supports the hypothesis that the new trehalose tri- and tetrasaccharides could be less prone to hydrolysis.

The *B. circulans* enzyme seemed to have a greater production of potential new trehalose derivatives, including tri- and tetrasaccharides (19.5 and 8.2%, respectively). The main synthesized trisaccharides were β-Galp-(1→4)-Tre and β-Galp-(1→6)-Tre, obtained by both enzymes. On the other hand, tetrasaccharides were produced in a higher quantity while using the *B. circulans* enzyme and showed the most diverse structures. The *A. oryzae* enzyme only synthesized β-Galp-(1→6)-β-Galp-(1→6)-Tre in a lower amount. In addition, a tetrasaccharide was also found: β-Galp-(1→6)-β-Galp-(1→6)-Tre. β-(1→6) and β-(1→4) Galactosyl linkages are minimally digested in the small intestine; therefore, the virulence mediated by negative microorganisms, such as *C. difficile*, in the gut could be reduced. In addition, these new structures could have a key role in the proper beneficial effects of trehalose, such as autophagy or glycemic control. Data obtained in this wok could be useful to the production of trehalose derivatives in a major scale, concerning the selectivity of each β-gal from different sources. In this context, increasing the knowledge in terms of the digestibility of this new compound is necessary to understand the real behavior of this carbohydrate in the digestive system.

■ ASSOCIATED CONTENT

Supporting Information

The Supporting Information is available free of charge at https://pubs.acs.org/doi/10.1021/acs.jafc.1c03768.

Quantitative data of carbohydrate evolution during the transgalactosylation assays with lactose/trehalose and lactose solutions by β-galactosidase from *Bacillus circulans* (Table S1) and *Aspergillus oryzae* (Table S2) and full NMR spectra of each trehalose-based oligosaccharide (1 to 11) (Figures S1 to S43) (PDF)

■ AUTHOR INFORMATION

Corresponding Author

Mar Villamiel − *Institute of Food Science Research (CIAL), Spanish Council of Scientific Research, (CSIC)−Autonomous University of Madrid (UAM), Campus de la Universidad Autónoma de Madrid, Madrid E-28049, Spain;* orcid.org/0000-0001-6847-8359; Phone: +34 910017951; Email: m.villamiel@csic.es

Authors

Pablo Gallego-Lobillo − *Institute of Food Science Research (CIAL), Spanish Council of Scientific Research, (CSIC)−Autonomous University of Madrid (UAM), Campus de la Universidad Autónoma de Madrid, Madrid E-28049, Spain*

Elisa G. Doyagüez − *Centro de Química Orgánica "Lora Tamayo" (CSIC), Madrid E-28006, Spain;* orcid.org/0000-0002-3802-1726

María Luisa Jimeno − *Centro de Química Orgánica "Lora Tamayo" (CSIC), Madrid E-28006, Spain*

Oswaldo Hernandez-Hernandez − *Institute of Food Science Research (CIAL), Spanish Council of Scientific Research, (CSIC)−Autonomous University of Madrid (UAM), Campus de la Universidad Autónoma de Madrid, Madrid E-28049, Spain;* orcid.org/0000-0002-5670-4563

Complete contact information is available at: https://pubs.acs.org/10.1021/acs.jafc.1c03768

Funding

This work was supported by the Spanish Ministry of Economy, Industry and Competitiveness (Project AGL2017-84614-C2-1-R) and the Spanish Ministry of Science, Innovation and Universities (Project RTI2018-101273-J-I00). O.H.-H. has received funding from the European Union's Horizon 2020 research and innovation program under the Marie Skłodowska-Curie grant agreement no. 843950.

Notes

The authors declare no competing financial interest.

■ ABBREVIATIONS

β-Gal, β-galactosidase; bsgHMBC, band-selective gradient heteronuclear multiple bond correlation; DP, degree of polymerization; Gal, galactose; GC-FID, gas chromatography-flame ionization detector; GC−MS, gas chromatography−mass spectrometry; gHSQC, gradient heteronuclear single-quantum coherence; Glc, glucose; GOS, galactooligosaccharides; HILIC-RID, hydrophilic interaction liquid chromatography-refractive index detector; NMR, nuclear magnetic resonance; Tre, trehalose

■ REFERENCES

(1) Garcia, C. A.; Gardner, J. G. Bacterial α-diglucoside metabolism: perspectives and potential for biotechnology and biomedicine. *Appl. Microbiol. Biotechnol.* **2021**, *105*, 4033−4052.

(2) Acuña-Rodríguez, I. S.; Newsham, K. K.; Gundel, P. E.; Torres-Díaz, C.; Molina-Montenegro, M. A. Functional roles of microbial symbionts in plant cold tolerance. *Ecol Lett.* **2020**, *23*, 1034−1048.

(3) Mijailovic, N.; Nesler, A.; Perazzolli, M.; Aït Barka, E.; Aziz, A. Rare Sugars: Recent Advances and Their Potential Role in Sustainable Crop Protection. *Molecules* **2021**, *26*, 1720.

(4) Sokołowska, E.; Sadowska, A.; Sawicka, D.; Kotulska-Bąblińska, I.; Car, H. A head-to-head comparison review of biological and toxicological studies of isomaltulose, d-tagatose, and trehalose on glycemic control. *Crit. Rev. Food Sci. Nutr.* **2021**, 1−26.

(5) Peng, B.; Li, Y.; Ding, S.; Yang, J. Characterization of textural, rheological, thermal, microstructural, and water mobility in wheat flour dough and bread affected by trehalose. *Food Chem.* **2017**, *233*, 369−377.

(6) Khalifeh, M.; Barreto, G.; Sahebkar, A. Therapeutic potential of trehalose in neurodegenerative diseases: The knowns and unknowns. *Neural Regen. Res.* **2021**, *16*, 2026−2027.

(7) Yaribeygi, H.; Yaribeygi, A.; Sathyapalan, T.; Sahebkar, A. Molecular mechanisms of trehalose in modulating glucose homeostasis in diabetes. *Diabetes Metab. Syndr. Clin. Res. Rev.* **2019**, *13*, 2214−2218.

(8) Yoshizane, C.; Mizote, A.; Yamada, M.; Arai, N.; Arai, S.; Maruta, K.; Mitsuzumi, H.; Ariyasu, T.; Ushio, S.; Fukuda, S. Glycemic, insulinemic and incretin responses after oral trehalose ingestion in healthy subjects. *Nutr. J.* **2017**, *16*, 1−6.

(9) Arai, C.; Arai, N.; Mizote, A.; Kohno, K.; Iwaki, K.; Hanaya, T.; Arai, S.; Ushio, S.; Fukuda, S. Trehalose prevents adipocyte hypertrophy and mitigates insulin resistance. *Nutr. Res.* **2010**, *30*, 840−848.
(10) Arai, C.; Miyake, M.; Matsumoto, Y.; Mizote, A.; Yoshizane, C.; Hanaya, Y.; Koide, K.; Yamada, M.; Hanaya, T.; Arai, S.; Fukuda, S. Trehalose prevents adipocyte hypertrophy and mitigates insulin resistance in mice with established obesity. *J. Nutr. Sci. Vitaminol.* **2013**, *59*, 393−401.
(11) Nishizaki, Y.; Yoshizane, C.; Toshimori, Y.; Arai, N.; Akamatsu, S.; Hanaya, T.; Arai, S.; Ikeda, M.; Kurimoto, M. Disaccharide-trehalose inhibits bone resorption in ovariectomized mice. *Nutr. Res.* **2000**, *20*, 653−664.
(12) DeBosch, B. J.; Heitmeier, M. R.; Mayer, A. L.; Higgins, C. B.; Crowley, J. R.; Kraft, T. E.; Chi, M.; Newberry, E. P.; Chen, Z.; Finck, B. N.; Davidson, N. O.; Yarasheski, K. E.; Hruz, P. W.; Moley, K. H. Trehalose inhibits solute carrier 2A (SLC2A) proteins to induce autophagy and prevent hepatic steatosis. *Sci. Signaling* **2016**, *9*, ra21−ra21.
(13) Hosseinpour-Moghaddam, K.; Caraglia, M.; Sahebkar, A. Autophagy induction by trehalose: Molecular mechanisms and therapeutic impacts. *J. Cell. Physiol.* **2018**, *233*, 6524−6543.
(14) Emanuele, E. Can Trehalose Prevent Neurodegeneration? Insights from Experimental Studies. *Curr. Drug Targets* **2014**, *15*, 551−557.
(15) Khalifeh, M.; Barreto, G. E.; Sahebkar, A. Trehalose as a promising therapeutic candidate for the treatment of Parkinson's disease. *Br. J. Pharmacol.* **2019**, *176*, 1173−1189.
(16) Khalifeh, M.; Read, M. I.; Barreto, G. E.; Sahebkar, A. Trehalose against Alzheimer's Disease: Insights into a Potential Therapy. *BioEssays* **2020**, *42*, 1900195.
(17) Massenzio, F.; Peña-Altamira, E.; Petralla, S.; Virgili, M.; Zuccheri, G.; Miti, A.; Polazzi, E.; Mengoni, I.; Piffaretti, D.; Monti, B. Microglial overexpression of fALS-linked mutant SOD1 induces SOD1 processing impairment, activation and neurotoxicity and is counteracted by the autophagy inducer trehalose. *Biochim. Biophys. Acta - Mol. Basis Dis.* **2018**, *1864*, 3771−3785.
(18) Hooton, D.; Lentle, R.; Monro, J.; Wickham, M.; Simpson, R. The Secretion and Action of Brush Border Enzymes in the Mammalian Small Intestine. *Rev. Physiol. Biochem. Pharmacol.* **2015**, *168*, 59−118.
(19) Kluch, M.; Socha-Banasiak, A.; Paczeš, K.; Borkowska, M.; Czkwianianc, E. The role of disaccharidases in the digestion-diagnosis and significance of their deficiency in children and adults. *Pol. Merkur. Lekarski.* **2020**, *49*, 275−278.
(20) Higashiyama, T. Novel functions and applications of trehalose. *Pure Appl. Chem.* **2002**, *74*, 1263−1269.
(21) Tan, S.; Yang, S.; Chen, G.; Zhu, L.; Sun, Z.; Chen, S. Trehalose alleviates apoptosis by protecting the autophagy-lysosomal system in alveolar macrophages during human silicosis. *Life Sci.* **2020**, *257*, 118043.
(22) Collins, J.; Robinson, C.; Danhof, H.; Knetsch, C. W.; Van Leeuwen, H. C.; Lawley, T. D.; Auchtung, J. M.; Britton, R. A. Dietary trehalose enhances virulence of epidemic Clostridium difficile. *Nature* **2018**, *553*, 291−294.
(23) Halstead, F. D.; Ravi, A.; Thomson, N.; Nuur, M.; Hughes, K.; Brailey, M.; Oppenheim, B. A. Whole genome sequencing of toxigenic Clostridium difficile in asymptomatic carriers: insights into possible role in transmission. *J. Hosp. Infect.* **2019**, *102*, 125−134.
(24) Cao, H.; Wong, S. C. Y.; Yam, W. C.; Liu, M. C. J.; Chow, K. H.; Wu, A. K. L.; Ho, P. L. Genomic investigation of a sequence type 67 Clostridium difficile causing community-acquired fulminant colitis in Hong Kong. *Int. J. Med. Microbiol.* **2019**, *309*, 270−273.
(25) Kim, B. G.; Lee, K. J.; Han, N. S.; Park, K. H.; Lee, S. B. Enzymatic synthesis and characterization of galactosyl trehalose trisaccharides. *Food Sci. Biotechnol.* **2007**, *16*, 127−132.
(26) Cardelle-Cobas, A.; Villamiel, M.; Olano, A.; Corzo, N. Study of galacto-oligosaccharide formation from lactose using Pectinex Ultra SP-L. *J. Sci. Food Agric.* **2008**, *88*, 954−961.
(27) Martínez-Villaluenga, C.; Cardelle-Cobas, A.; Olano, A.; Corzo, N.; Villamiel, M.; Jimeno, M. L. Enzymatic synthesis and identification of two trisaccharides produced from lactulose by transgalactosylation. *J. Agric. Food Chem.* **2008**, *56*, 557−563.
(28) Hérnandez-Hérnandez, O. Desarrollo de nuevos métodos para la caracterización estructural de carbohidratos prebióticos y péptidos funcionales de interés alimentario. Estudio de su bioactividad (Doctoral Thesis). Autonumous University of Madrid, 2012.
(29) Chen, C. W.; Ou-Yang, C. C.; Yeh, C. W. Synthesis of galactooligosaccharides and transgalactosylation modeling in reverse micelles. *Enzyme Microb. Technol.* **2003**, *33*, 497−507.
(30) Brobst, K. M.; Lott, C. E. J. Determination of some components in cron syrup by gas-liquid chromatography of the trimethylsilyl derivatives. *Cereal Chem.* **1966**, *43*, 35−43.
(31) Hernández, O.; Ruiz-Matute, A. I.; Olano, A.; Moreno, F. J.; Sanz, M. L. Comparison of fractionation techniques to obtain prebiotic galactooligosaccharides. *Int. Dairy J.* **2009**, *19*, 531−536.
(32) Julio-González, L. C.; Hernández-Hernández, O.; Moreno, F. J.; Jimeno, M. L.; Doyagüez, E. G.; Olano, A.; Corzo, N. Hydrolysis and transgalactosylation catalysed by β-galactosidase from brush border membrane vesicles isolated from pig small intestine : A study using lactulose and its mixtures with lactose or galactose as substrates. *Food Res. Int.* **2020**, *129*, 108811.
(33) Gaillet, C.; Lequart, C.; Debeire, P.; Nuzillard, J.-M. Band-selective HSQC and HMBC experiments using excitation sculpting and PFGSE. *J. Magn. Reson.* **1999**, *139*, 454−459.
(34) Gänzle, M. G. Enzymatic synthesis of galacto-oligosaccharides and other lactose derivatives (hetero-oligosaccharides) from lactose. *Int. Dairy J.* **2012**, *22*, 116−122.
(35) Botvynko, A.; Bednářová, A.; Henke, S.; Shakhno, N.; Čurda, L. Production of galactooligosaccharides using various combinations of the commercial β-galactosidases. *Biochem. Biophys. Res. Commun.* **2019**, *517*, 762−766.
(36) Ajisaka, K.; Fujimoto, H. Regioselective syntheses of trehalose-containing trisaccharides using various glycohydrolases. *Carbohydr. Res.* **1990**, *199*, 227−234.
(37) Ishii, T.; Tanimoto, M.; Itagaki, Y.; Honda, Y.; Win, T. T.; Kawase, C.; Kita, A.; Onodera, S.; Ito, H.; Matsui, H.; Honma, M. Enzymatic synthesis of nonreducing trisaccharide containing lactose and trehalose as a part of the structure. *J. Appl. Glycosci.* **2000**, *47*, 193−196.
(38) Van Leeuwen, S. S.; Kuipers, B. J. H.; Dijkhuizen, L.; Kamerling, J. P. 1H NMR analysis of the lactose/β-galactosidase-derived galacto-oligosaccharide components of Vivinal® GOS up to DP5. *Carbohydr. Res.* **2014**, *400*, 59−73.
(39) Abdul Manas, N. H.; Md. Illias, R.; Mahadi, N. M. Strategy in manipulating transglycosylation activity of glycosyl hydrolase for oligosaccharide production. *Crit. Rev. Biotechnol.* **2018**, 272−293.
(40) Walmagh, M.; Zhao, R.; Desmet, T. Trehalose analogues: Latest insights in properties and biocatalytic production. *Int. J. Mol. Sci.* **2015**, *16*, 13729−13745.
(41) Zhang, Y.; Shaikh, N.; Ferey, J. L.; Wankhade, U. D.; Chintapalli, S. V.; Higgins, C. B.; Crowley, J. R.; Heitmeier, M. R.; Stothard, A. I.; Mihi, B.; Good, M.; Higashiyama, T.; Swarts, B. M.; Hruz, P. W.; Shankar, K.; Tarr, P. I.; DeBosch, B. J. Lactotrehalose, an Analog of Trehalose, Increases Energy Metabolism Without Promoting Clostridioides difficile Infection in Mice. *Gastroenterology* **2020**, *158*, 1402−1416.e2.
(42) Chaube, M. A.; Sarpe, V. A.; Jana, S.; Kulkarni, S. S. First total synthesis of trehalose containing tetrasaccharides from: Mycobacterium smegmatis. *Org. Biomol. Chem.* **2016**, *14*, 5595−5598.
(43) Wessel, H. P.; Niggemann, J. Synthesis of β-D-(1→4)-Substituted Trehalose Oligosaccharides. *J. Carbohydr. Chem.* **1995**, *14*, 1089−1100.
(44) Prakash, B. S.; Suyama, K.; Itoh, T.; Adachi, S. Structure Elucidation of Major Galacto Oligosaccharides Formed by Growing Culture of Trichoderma harzianum. *J. Agric. Food Chem.* **1989**, *37*, 334−337.

https://doi.org/10.1021/acs.jafc.1c03768
J. Agric. Food Chem. 2021, 69, 12541−12553

(45) Yin, H.; Bultema, J. B.; Dijkhuizen, L.; van Leeuwen, S. S. Reaction kinetics and galactooligosaccharide product profiles of the β-galactosidases from Bacillus circulans, Kluyveromyces lactis and Aspergillus oryzae. *Food Chem.* **2017**, *225*, 230−238.
(46) Urrutia, P.; Rodriguez-Colinas, B.; Fernandez-Arrojo, L.; Ballesteros, A. O.; Wilson, L.; Illanes, A.; Plou, F. J. Detailed analysis of galactooligosaccharides synthesis with β-galactosidase from Aspergillus oryzae. *J. Agric. Food Chem.* **2013**, *61*, 1081−1087.
(47) Ferreira-Lazarte, A.; Gallego-Lobillo, P.; Moreno, F. J.; Villamiel, M.; Hernandez-Hernandez, O. In Vitro Digestibility of Galactooligosaccharides: Effect of the Structural Features on Their Intestinal Degradation. *J. Agric. Food Chem.* **2019**, *67*, 4662−4670.

https://doi.org/10.1021/acs.jafc.1c03768
J. Agric. Food Chem. 2021, 69, 12541−12553